

MOLECULAR PHYSICS

VOLUME 1

8581

Printed and Published by

TAYLOR & FRANCIS LTD

RED LION COURT, FLEET STREET, LONDON, E.C.4

CONTENTS OF VOLUME 1

NUMBER 1—JANUARY 1958		Page
Editorial		1
Nuclear magnetic resonance and rotational isomerism in substituted ethanes. J. A. POPLÉ		3
Some considerations on the dipole moments of azines. H. F. HAMEKA and A. M. LIQUORI		9
The pressure-induced rotational absorption spectrum of hydrogen: I. J. P. COLPA and J. A. A. KETELAAR		14
Kritische Opaleszenz fester Lösungen. A. MÜNSTER und K. SAGEL ..		23
Electron-electron separation in molecular hydrogen. M. P. BARNETT, F. W. BIRSS and C. A. COULSON		44
On irreversible processes in quantum mechanics. I. PRIGOGINE and M. TODA		48
Transport of energy and momentum in a dense fluid of rough spheres. J. P. VALLEAU		63
Constant pressure ensembles in statistical mechanics. W. BYERS BROWN		68
One-dimensional multicomponent mixtures. H. C. LONGUET-HIGGINS		83
Thermodynamic properties of gas hydrates. J. C. PLATTEUW and J. H. van der WAALS		91
RESEARCH NOTE		
Dielectric properties of iodine in aromatic solvents at 9000 Mc/sec. G. W. NEDERBRAGT and J. PELLE		97

NUMBER 2—APRIL 1958

Wave functions for the methane molecule. IAN M. MILLS	99
Vibrational intensities in methane. IAN M. MILLS	107
The absorption spectra of aromatic carbonium ions in HF solution. G. DALLINGA, E. L. MACKOR and A. A. VERRIJN STUART	123
Concentration quenching in fluorescent acene solutions. A. DAMMERS-DE KLERK	141
Electronic spectra of alternant hydrocarbon di-negative ions. P. BALK, S. DE BRUIJN and G. J. HOIJTINK	151

CONTENTS OF VOLUME I

Page

Electron spin densities in alternant hydrocarbon mono-negative and mono-positive ions and in odd alternant hydrocarbon radicals. G. J. HOIJINK	157
A contribution to the theory of the exchange narrowing of spectral lines. R. A. SACK	163
The effect of quadrupole relaxation on nuclear magnetic resonance multiplets. J. A. POPLÉ	168
Molecular orbital theory of aromatic ring currents. J. A. POPLÉ	175
A molecular orbital treatment of the vinyl chloride molecule. M. SIMONETTA, G. FAVINI and S. CARRÀ	181
Open shell calculations for the two- and three-electron ions. R. P. HURST, J. D. GRAY, G. H. BRIGMAN and F. A. MATSEN	189

RESEARCH NOTE

Paramagnetism in molecular compounds. H. M. BUCK, J. H. LUPINSKI and L. J. OOSTERHOFF	196
---	-----

NUMBER 3—JULY 1958

Nuclear magnetic shielding of a hydrogen atom in an electric field. T. W. MARSHALL and J. A. POPLÉ	199
On the nuclear magnetic shielding in the hydrogen molecule. H. F. HAMEKA	203
Nuclear spin coupling by electron orbital polarization. J. A. POPLÉ ..	216
The effect of molecular interaction on magnetic shielding constants. M. J. STEPHEN	223
Hyperconjugation in the electron resonance spectra of free radicals. A. D. McLACHLAN	233
Structures of electron-transfer and related molecular complexes in the solid state. O. HASSEL	241
Proton magnetic resonance of aromatic carbonium ions. I. Structure of the conjugate acid. C. MACLEAN, J. H. VAN DER WAALS and E. L. MACKOR	247
On the Curie points and high temperature susceptibilities of Heisenberg model ferromagnetics. G. S. RUSHBROOKE and P. J. WOOD	257
Transport coefficients of dense fluids of molecules interacting according to a square well potential. H. C. LONGUET-HIGGINS and J. P. VALLEAU	284
A normal coordinate treatment of the plane symmetrical XY ₄ molecule. C. W. F. T. PISTORIUS	295

CONTENTS OF VOLUME I

RESEARCH NOTES		Page
Rotatory dispersion in hydrated cobaltous salts. M. J. STEPHEN ..		301
Evaluation of coulomb repulsion integrals from spectroscopic data. R. D. BROWN		304
Application of Brønsted's principle of congruence to n-alkane mixtures. J. HIJMAN		307

NUMBER 4—OCTOBER 1958

Ring currents and proton magnetic resonance in aromatic molecules. R. MCWEENY		311
Nuclear magnetic resonance spectra of compounds of the B-subgroup metals. L. E. ORGEL		322
Long range spin-spin interactions in high resolution nuclear magnetic resonance and the concept of hyperconjugation. R. A. HOFFMAN		326
High resolution hydrogen resonance spectra of trisubstituted benzenes. R. E. RICHARDS and T. SCHAEFER		331
The pressure-induced rotational absorption spectrum of hydrogen : II. J. P. COLPA and J. A. A. KETELAAR		343
The probabilities of triplet-singlet transitions in aromatic hydrocarbons and ketones. H. F. HAMEKA and L. J. OOSTERHOFF		358
Theory of the Renner effect in the NH ₂ radical. J. A. POPLE and H. C. LONGUET-HIGGINS		372
The π -electron spectra of the benzene N-heterocyclics. J. N. MURRELL		384
The infra-red spectra of some ferroelectric compounds with short hydrogen bonds. R. BLINC and D. HADŽI		391
Structure of the methyl radical. T. COLE, H. O. PRITCHARD, N. R. DAVIDSON and H. M. McCONNELL		406

RESEARCH NOTES

Ligand field bands of four-coordinated paramagnetic nickel (II) complexes. C. K. JØRGENSEN		410
Planarity of 1 : 2-4 : 5-tetrabromobenzene molecule. G. GAFNER and F. H. HERBSTEIN		412
Dipole interactions in fluids and fluid mixtures. J. S. ROWLINSON ..		414
Index of Authors (with the Titles of Papers)		416

EDITORIAL

THE subject of molecular physics occupies a key position in modern science. The frontier between physics and chemistry is disappearing as the methods of physics are brought to bear on the problems of chemistry. In this new development a primary focus of attention is the structure and properties of the molecule. The interest of molecules for the chemist naturally extends far beyond their purely physical properties; but these properties constitute the basis of chemical theory and are becoming increasingly important for an understanding of biology.

It is with these thoughts in mind that a group of scientists from different countries have decided to found *Molecular Physics*. A need is felt for bringing together papers on the physics of molecules, papers which might otherwise escape the notice of many interested readers.

Molecular Physics will, therefore, welcome scientific contributions on all aspects of the subject, and especially on the following topics :

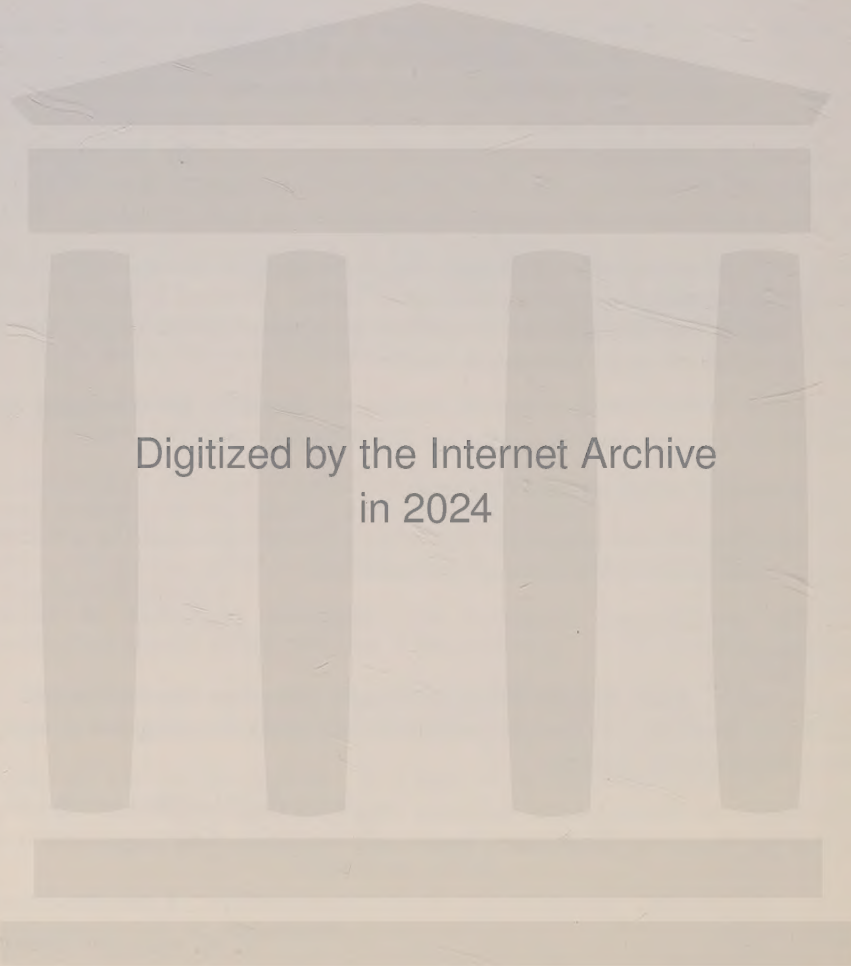
- (1) Molecular structure and dynamics.
- (2) The electric and magnetic properties of molecules, and the processes of molecular excitation, ionization and dissociation.
- (3) The equilibrium, transport and relaxation properties of molecular assemblies.

Such contributions may be either full length papers or research notes. It is intended also from time to time to publish review articles and reports of symposia on subjects of topical interest.

We thank our distinguished Editorial Board for their invaluable support, and trust that the future of *Molecular Physics* will vindicate their hopes and ours.

H. C. LONGUET-HIGGINS

J. H. VAN DER WAALS



Digitized by the Internet Archive
in 2024

Nuclear magnetic resonance and rotational isomerism in substituted ethanes

by J. A. POPLE

Department of Theoretical Chemistry, University of Cambridge

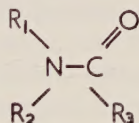
(Received 1 April 1957)

This paper deals with the classification of high-resolution nuclear magnetic resonance spectra of substituted ethanes and similar molecules. In particular, the forms of the spectra for individual rotational isomers of long lifetime are compared with those appropriate to rapid internal conversion. The use of nuclear resonance data to deduce information about the rate of internal rotation is discussed in detail.

1. INTRODUCTION

High-resolution nuclear magnetic resonance spectroscopy can be applied to the measurement of a number of molecular rate processes. The basic general principle is that the effective parameters (chemical shifts and spin-coupling constants) determining a spectrum are, in fact, averages over times short compared with the reciprocal of the breadth the spectrum would have without such averaging (energies being measured in cycles/sec). It may be possible, by inspection of a spectrum, to determine whether averaging is occurring and consequently to place some limit on the rate at which such a process takes place.

One of the most promising applications of this sort is to the rates of internal rotation in molecules. Phillips [1] and Gutowsky and Holm [2] have obtained a considerable amount of information on the rate of internal rotation about the C-N bond in amides,



by investigating whether signals from R₁ and R₂ appear separately, or are merged together into one average signal at various temperatures.

This paper is concerned with the general problem of investigating rotational isomerism in substituted ethanes by nuclear magnetic resonance methods. It is well known that the presence of different rotational isomers can be detected by infra-red spectroscopy and other physical means (Mizushima [3]), but rather less is known about the rates at which such isomers transform into one another. Some NMR data on substituted ethanes has recently been published by Anderson [4], Drysdale and Phillips [5] and Pople *et al.* [6].

Since rapid internal rotation leads to some averaging of magnetic screening and spin-coupling constants, the form of the proton spectrum (or that of other attached nuclei) may give some information about the rate of such rotation. There are three main possibilities.

1. Of the possible isomers of long lifetime, only one may exist in amounts large enough to be detected by NMR.

2. There may be a mixture of non-equivalent isomers in an equilibrium ratio, each isomer existing for a period long enough for its individual NMR spectrum to be present. The total spectrum will then be a superposition of these components.

3. It may be that internal rotation is occurring at a sufficiently rapid rate for the effective screening and spin-coupling constants to be averaged values.

Other intermediate possibilities exist. For example, it may happen that rapid interconversion takes place between two isomers but that a third is stable for a longer period.

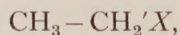
If the form of the spectrum appropriate to rapid internal rotation differs from that of individual rotational isomers, the NMR spectrum can be used to place an approximate lower limit on the rate of rotation (if the spectrum is of type (3)), or an upper limit (if it is of types (1) or (2)). In this paper we shall examine the changes that take place in various types of substituted ethanes on proceeding from 'slow' to 'rapid' rotation. It turns out that this does not always lead to a simplification and some care has to be exercised in using the spectra as evidence for hindered rotation. Even if a simplification is predicted in principle, of course, there may be accidental equalities or near-equalities of chemical shifts, which may lead to no difference in practice. In the final section, corresponding information derivable from temperature studies is discussed.

2. CLASSIFICATION OF NMR SPECTRA OF SUBSTITUTED ETHANES

It is generally accepted that the six hydrogens or other substituents in an ethane-type bond are in a 'staggered' configuration so that there are three possible rotational isomers between which interconversion is possible without actually inverting the configuration at either carbon atom. These isomers may or may not be equivalent as far as their physical properties are concerned.

We shall consider in detail the form of the proton spectrum of ethane-type molecules with some substituents X, Y, \dots with magnetically inactive nuclei. By magnetically inactive we mean nuclei which have no spins or do not couple effectively with the protons under investigation. Examples are halogen atoms (other than fluorine) and phenyl, the aromatic protons being well separated from the ethane bond under consideration.

Consider first a singly substituted molecule (e.g. ethyl chloride). We shall write this



H' referring to a hydrogen attached to the second carbon atom. If we label the methyl hydrogens H_1, H_2, H_3 and the methylene ones H_1', H_2' , the three possible isomers, between which rotational interconversion may occur, are as figure 1. These three are physically indistinguishable, of course. If the rotation is slow, the proton resonance will be typical of one structure. Thus in form I, the proton H_3 will have a different screening constant from the pair H_1, H_2 . The pair H_1', H_2' will not be separated. Thus, if the chemical shifts are large enough, the spectrum should show three types of proton, a single one and two pairs. In an obvious notation we shall refer to this as a spectrum of type AB_2C_2 . As there will be a considerable number of distinct coupling constants involved, the whole spectrum may be relatively complex.

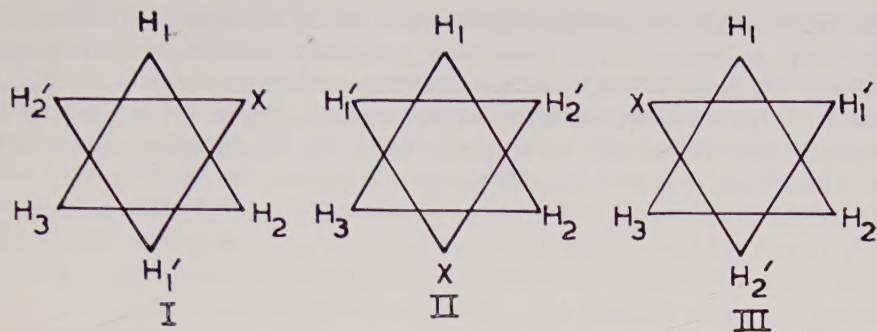


Figure 1.

If the rotation is rapid, on the other hand, the environment of any given proton has to be averaged over the three configurations I, II, and III (with equal weights). The screening constants of the three protons H_1 , H_2 and H_3 then become identical. Further the spin-coupling constants between any hydrogen on the CH_3 group (e.g. H_1) and the two protons on the other carbon atom H_1' and H_2' become equal. Thus

$$J_{H_1H_1'} = J_{H_1H_2'} \text{ (average).}$$

This follows since

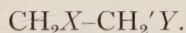
$$J_{H_1H_1'} \text{ (I)} = J_{H_1H_2'} \text{ (III)},$$

$$J_{H_1H_1'} \text{ (II)} = J_{H_1H_2'} \text{ (II)},$$

$$J_{H_1H_2'} \text{ (I)} = J_{H_1H_1'} \text{ (III)}.$$

Hence, for rapid rotation, the spectrum will become type A_2B_3 , with the further simplification that all AB coupling constants become equal. If the chemical shift between the H and H' groups is sufficiently large, it will appear as a 1-2-1 triplet and as a 1-3-3-1 quartet. If the chemical shift is of the same order as the spin-coupling constants there will be a rather complicated but still definite pattern. We conclude, therefore, that for a molecule CH_3-CH_2X , the form of the spectrum may give direct evidence about the rate of internal rotation.

As a second example, consider a 1, 2-disubstituted ethane



The three isomeric forms, interconvertible by internal rotation, are as figure 2. Of these, I (*trans*) is distinguishable from the other two (*gauche*). If the rotation is slow, the total spectrum will be a superposition of those of the *trans* and *gauche*

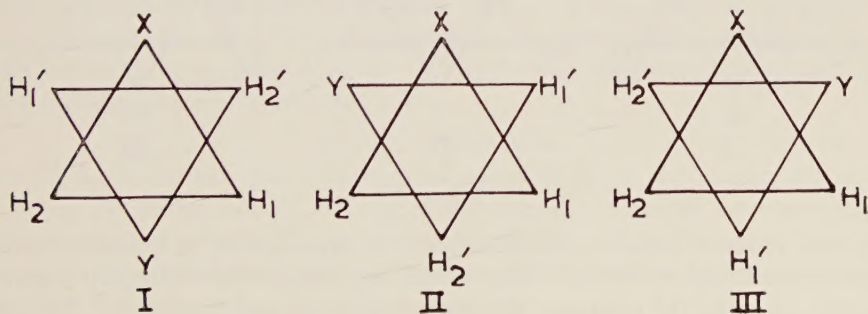


Figure 2.

forms, although the equilibrium population of one of them may be too small for its spectrum to appear. The *trans* form I consists of two equivalent pairs of nuclei H_1 , H_2 and H_1' , H_2' but the coupling constants $J_{H_1H_1'}$ and $J_{H_1H_2'}$ are different. This is a spectrum of type A_2B_2 (McConnell *et al.* [7], Pople *et al.* [6]. The *gauche* form (II or III) on the other hand, has four non-equivalent nuclei (type ABCD) and may give a highly complex spectrum.

If the rotation is rapid, the environment of each nucleus has to be averaged over I, II and III (although only II and III have equal weights). This means that the average screening constant for H_1 is the same as that for H_2 . A similar averaging occurs for H_1' and H_2' . However, even after averaging

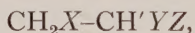
$$J_{H_1H_1'} \neq J_{H_1H_2'}$$

It follows that the spectrum of the rotating molecule has the same form as that of the *trans* isomer (A_2B_2) (i.e. depends on the same number and type of parameters). If the spectrum is observed to be of this type, two conclusions are possible. Either

1. rapid internal rotation is taking place, or
2. rotation is hindered but the molecules are mainly in the *trans* configuration.

It should be noted that the internal rotation need not take place in complete revolutions. Thus for CH_2X-CH_2Y , the three isomers are interconvertible without the bulkier X and Y groups having to pass an 'eclipsed' configuration where steric repulsion would increase the barrier.

As a third example, consider a tri-substituted ethane



for which the three forms are as figure 3. These three forms are physically distinct and may have different populations. In each individual isomer, there are three non-equivalent protons so, for slow rotation, the total spectrum will be a superposition of three of type ABC. But even if rotation is rapid, the average environment of H_1 will differ from that of H_2 so that once again the spectrum will appear to be that of three non-equivalent nuclei (ABC).

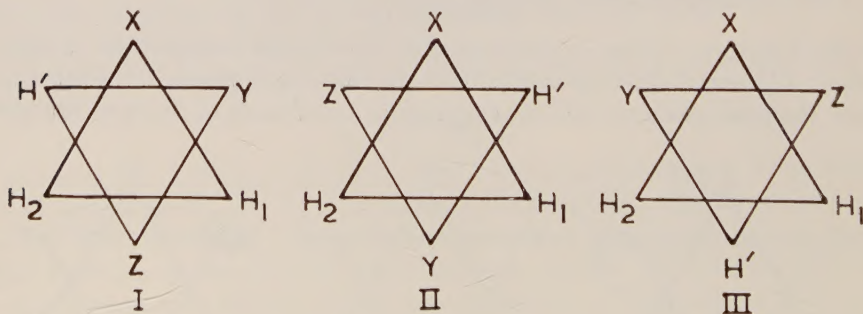


Figure 3.

Other types of substituted ethane can be investigated in a similar manner. A systematic tabulation of all forms containing at least two hydrogens is given in the table, showing the predicted spectra for slow and rapid rotation. The actual form of the spectrum can only be used as direct evidence for or against rapid

rotation if the form predicted for rapid rotation differs from that corresponding to any one of the individual isomers.

This discussion has all been in terms of proton spectra, but it is clear that similar conclusions apply to other nuclei, particularly fluorine. In fact the classification of spectra for unsymmetrically substituted molecules is unaltered if the hydrogens on one carbon are all replaced by fluorine. This is formally similar to spectra with a large chemical shift between hydrogens attached to different carbon atoms.

Compound	Form of spectrum	
	Slow rotation	Rapid rotation
$\text{CH}_3\text{--CH}_2'\text{X}$	AB_2C_2	A_2B_3 (all $J_{\text{HH}'}$ equal)
$\text{CH}_3\text{--CH}'\text{X}_2$	ABC_2	AB_3 (all $J_{\text{HH}'}$ equal)
$\text{CH}_3\text{--CH}'\text{XY}$	ABCD	AB_3 (all $J_{\text{HH}'}$ equal)
$\text{CH}_2\text{X--CH}_2\text{X}$	A_4 (<i>trans</i>) and A_2B_2 (<i>gauche</i>)	A_4
$\text{CH}_2\text{X--CH}_2'\text{Y}$	A_2B_2 (<i>trans</i>) and ABCD (<i>gauche</i>)	A_2B_2 (all $J_{\text{HH}'}$ not equal)
$\text{CH}_3\text{--CX}_3$	A_3	A_3
$\text{CH}_3\text{--CX}_2\text{Y}$	AB_2	A_3
$\text{CH}_3\text{--CXYZ}$	ABC	A_3
$\text{CH}_2\text{X--CHY}_2$	AB_2 and ABC	AB_2
$\text{CH}_2\text{X--CHYZ}$	Three ABC	ABC
$\text{CH}_2\text{U--CX}_3$	A_2	A_2
$\text{CH}_2\text{U--CX}_2\text{Y}$	A_2 and AB	A_2
$\text{CH}_2\text{U--CXYZ}$	Three AB	AB
$\text{CHX}_2\text{--CHX}_2$	Two A_2	A_2
$\text{CHX}_2\text{--CHY}_2$	Two AB	AB
$\text{CHX}_2\text{--CHYZ}$	Three AB	AB
CHXY--CHXY (Meso)	A_2 and AB	A_2
CHXY--CHXY (dl)	Three A_2	A_2
CHUV--CHXY	Six AB	Two AB (mixture of two isomers)

Proton resonance spectra for substituted ethanes.

3. TEMPERATURE EFFECTS

We have seen that for certain types of substituted ethane, any single measurement of the proton spectrum does not necessarily distinguish between slow and rapid rotation. The variation of the spectrum with temperature, however, may provide significant additional evidence. Thus, if the rotation is rapid, the various effective chemical shifts and coupling constants will be averages over the values for the three possible isomers. Thus the chemical shift parameter δ for a pair of nuclei will have an effective value

$$\delta = p_1\delta_1 + p_2\delta_2 + p_3\delta_3,$$

where δ_1 , δ_2 , δ_3 are the values corresponding to the separate isomers and p_1 , p_2 , and p_3 are weighting factors. If the three isomers are not all equivalent, these weighting factors will be temperature dependent. If we suppose that each isomer can be treated as a separate species with a distinct torsional vibration frequency, that ratio $p_1:p_2:p_3$ will be given by

$$p_1:p_2:p_3 = v_1(T) \exp(-E_1/kT) : v_2(T) \exp(-E_2/kT) : v_3(T) \exp(-E_3/kT)$$

where v_1 , v_2 and v_3 are the corresponding vibrational partition functions (which may be temperature-dependent if the torsional frequencies are of the order of kT/h). However, differences in vibrational partition functions are usually neglected. The mean value of δ is given by

$$\delta = \frac{\delta_1 v_1 \exp(-E_1/kT) + \delta_2 v_2 \exp(-E_2/kT) + \delta_3 v_3 \exp(-E_3/kT)}{v_1 \exp(-E_1/kT) + v_2 \exp(-E_2/kT) + v_3 \exp(-E_3/kT)}.$$

The spin-coupling constants will be averaged in a similar manner.

Thus, if the spectrum is such that the chemical shifts and spin-coupling constants are temperature-dependent, this is some evidence in favour of rapid rotation. However, the converse argument cannot be applied. If the spectrum is independent of temperature (and the molecule is such that the form for the rotating molecule is the same as that for one of the isomers), there are three main possibilities.

- (1) The molecules may exist almost entirely as one isomer, rotation being highly hindered.
- (2) The molecules may be rotating rapidly, but the energy differences between the isomeric forms may be so large that one of the weighting factors p_1 , p_2 , p_3 is much larger than the other two.
- (3) The energy differences may all be small so that temperature will not change the relative populations.

The author is indebted to Dr. N. Sheppard for discussions on this topic.

Le sujet de l'article est la classification des spectres de résonance nucléaire magnétique de haute résolution des éthanés substitués et des molécules pareilles. En particulier les formes des spectres pour les isomères individuels de rotation, ayant une longue période de vie, sont comparées avec la forme correspondante à une conversion interne rapide. On discute en détail l'emploi des données de résonance nucléaire pour obtenir de l'information sur la vitesse de rotation interne.

Der Aufsatz behandelt die Zuordnung der magnetischen Kernresonanzspektren hoher Auflösung für substituierte Äthane und ähnliche Moleküle. Insbesondere werden die Formen der Spektren für langlebige Rotationsisomere mit denjenigen verglichen, die einer schnellen inneren Umlagerung entsprechen. Es wird ausführlich dargelegt, welche Schlüsse über die innere Rotationsgeschwindigkeit aus den Daten der Kernresonanz gezogen werden können.

REFERENCES

- [1] PHILLIPS, W. D., 1955, *J. chem. Phys.*, **23**, 1363.
- [2] GUTOWSKY, H. S., and HOLM, C. H., 1956, *J. chem. Phys.*, **25**, 1228.
- [3] MIZUSHIMA, S., 1954, *Structure of Molecules and Internal Rotation* (New York: Academic Press).
- [4] ANDERSON, W. A., 1956, *Phys. Rev.*, **102**, 151.
- [5] DRYSDALE, J. J., and PHILLIPS, W. D., 1957, *J. Amer. chem. Soc.*, **79**, 319.
- [6] POPE, J. A., SCHNEIDER, W. G., and BERNSTEIN, H. J., 1957, *Canad. J. Chem.*, **35**, 1060.
- [7] MCCONNELL, H. M., MCLEAN, A. D., and REILLY, C. A., 1955, *J. chem. Phys.*, **23**, 1152.

Some considerations on the dipole moments of azines

by H. F. HAMEKA† and A. M. LIQUORI

Instituto di Chimica Farmaceutica
Centro di Strutturistica Chimica del C.N.R.
University of Rome, Italy

(Received 23 September 1957)

Some simplified calculations have been performed on the electric dipole moments of pyridine, pyrimidine, pyridazine, quinoline, isoquinoline and phthalazine on the assumptions that an important contribution to the total moment results from the hybridization of the lone pair electrons of the nitrogen atoms and that the π electron moment may be calculated with a simple LCAO calculation, taking the Coulomb integral of the nitrogen $\alpha_{NN} = \alpha_{CC} + 0.4\beta_{CC}$. The deviations between theoretical and experimental results are less than 6 per cent.

1. INTRODUCTION

The experimentally observed dipole moments of conjugated molecules containing nitrogen are generally ascribed to the greater electronegativity of the nitrogen atom with respect to carbon. This effect has been accounted for in two different ways. First it has been assumed that the Coulomb energy of a π electron with respect to the corresponding atom has a lower value for nitrogen than for carbon, so that the charge density is greater at the nitrogen atoms than at the carbon atoms. Secondly it is believed that there is a resulting dipole moment from the electron pair forming a C-N σ bond. Finally it is assumed that the total dipole moment μ is obtained by vector addition of the π and σ moments μ_π and μ_σ .

The π moment may be calculated with the aid of the well known LCAO method if the values of the Coulomb integral α_{NN} and the values of the exchange integrals β_{CN} and β_{NN} are known. It used to be customary to take $\beta_{CN} = \beta_{NN} = \beta_{CC} = \beta$ and to replace α_{NN} by $\alpha_{CC} + 2\beta$ (cf. [1], [2]). Orgel *et al.* [3] have suggested $\alpha_{NN} = \alpha_{CC} + \beta$, whereas Chalvet and Sandorfy [4] and Davies [5] proposed $\alpha_{NN} = \alpha_{CC} + 0.6\beta$.

In all these considerations the calculated π moment must be compared with an experimental value which is obtained by subtracting an appropriate μ_σ value from the total dipole moment μ . The σ moment which has been chosen for this purpose is the value which has been derived from the measured dipole moments for several organic compounds on the assumptions that the C-N and C-H bond moments in different compounds are equal (for instance, Orgel *et al.* [3] take C⁻-N⁺ equal to 0.45 D and C⁻-H⁺ equal 0.40 D) and that the total dipole moment may always be obtained by vector addition of these constant bond moments. It is our contention, however, that this procedure is not wholly adequate because the former assumption may be contested and because some important features of the calculation of dipole moments have been omitted.

† Present address: Department of Chemistry, Carnegie Institute of Technology, Pittsburgh, Pennsylvania, U.S.A.

It has been pointed out by Coulson [6] that the main contribution to the molecular dipole moment often arises from the moment of the lone pair electrons. If it is assumed, namely, that the lone pair electrons occupy a hybridized (sp^2) orbital

$$t_N = as_N + bp_{xN}, \quad (1)$$

the resulting dipole moment is

$$\mu_l = 4ab \int s_N x p_{xN} d\tau \quad (2)$$

which may reach values as great as 3 Debye units if the lone pair orbital is completely hybridized. In previous calculations [7] experimentally observed small deviations from 120° in the bond angles of heterocyclic compounds have been taken as evidence for the hybridization of the lone pair electrons of the nitrogen atoms. Consequently, an important contribution to the total dipole moment should be expected to result from the asymmetric charge distribution of these lone pair electrons. If this is indeed the case the assumption that in different compounds the C-N and C-H moments are equal may not make much sense because the degree of hybridization of the N atoms in different compounds need not necessarily be the same. Therefore, the dipole moment of the lone pair of the nitrogen atom has been calculated in combination with that of the opposite C-H bond on the assumption that the lone pair electrons occupy a hybrid (sp^2) orbital and that the wave functions of the electrons forming the C-H bond (which is taken to be purely covalent) may be constructed with the aid of the molecular orbital method from an (sp^2) hybrid orbital of the carbon atom and from a $1s$ orbital of the hydrogen.

In this way a rather large value (2.23 Debye units) has been found for the C^+-H^- moment only, which is generally believed to be practically zero. This value seems exceedingly great but, on the other hand, no decisive experimental evidence for any value of the C^+-H^- moment is available nowadays. If its magnitude is estimated from intensities of infra-red spectra it must be borne in mind that molecular vibrations strongly affect the degree of hybridization so that these considerations do not seem wholly acceptable.

The main contribution to the total dipole moment μ was found to be due to μ_r (3.56 D). The π moment has the same sign as the σ moment. Therefore, if our assumption should be correct and the general idea that the C-N bond has a polarity $C^+ N^-$ should be accepted, μ_σ would be very close to the total moment μ and μ_π would be extremely small. Alternatively the C-N bond moment may be considered to be practically zero whereas the value of μ_π is appreciable, although smaller than has been reported in previous calculations. This latter view seems more reasonable if other evidence such as the chemical reactivity of these molecules is taken into account. Therefore, it has been presumed that the greater electronegativity of the nitrogen atom with respect to carbon is accounted for by the behaviour of the π electrons only, so that the dipole moment of the C-N σ bond is zero. It will be shown that this conclusion actually implies that the C-N bond has a slightly C^--N^+ ionic character.

The π moment has then been calculated with the aid of the usual M.O. method and it was found that the best agreement between calculated and experimental dipole moments is obtained by taking $\alpha_{NN} = \alpha_{CC} + 0.4\beta$ and all exchange integrals equal. (A similar calculation was also performed with $\beta_{NN} = 1.2 \beta_{CC}$ and $\beta_{CN} = 1.1 \beta_{CC}$. It was found however that this change only slightly affected the results and in any case did not improve them.)

2. CALCULATIONS

The dipole moment of an electron lone pair occupying a hybrid (sp^2) orbital may be derived from (2). If a and b are taken as $(1/3)^{1/2}$ and $(2/3)^{1/2}$, respectively, and if s_N and p_{xN} are the atomic Slater functions

$$\begin{aligned}s_N &= (q_N^5/96\pi)^{1/2} \exp(-\tfrac{1}{2} q_N r) \\ p_{xN} &= (q_N^5/32\pi)^{1/2} x \exp(-\tfrac{1}{2} q_N r),\end{aligned}\quad (3)$$

then

$$\mu_l = 20\sqrt{2/3} q_N \sqrt{3}. \quad (4)$$

The dipole moment of the C-H bond may be calculated from

$$\mu_{CH} = (1 + \Delta_{CH})^{-1} \int (t_C + s_H)^2 x d\tau - r_{CH} \quad (5)$$

if the origin is taken as the nucleus of the carbon atom. From

$$t_C = (1/3)^{1/2} s_C + (2/3)^{1/2} p_{xC} \quad (6)$$

it is found that

$$\begin{aligned}\mu_{CH} &= (1 + \Delta_{CH})^{-1} \{ (10\sqrt{2}/3 q_C \sqrt{3}) + \Delta_{CH} r_{CH} - P \} \\ P &= (1/3)^{1/2} \int s_H x s_C d\tau + (2/3)^{1/2} \int s_H x p_{xC} d\tau\end{aligned}\quad (7)$$

if in the last integral the origin is taken as the hydrogen nucleus. With the aid of the tables of Mulliken *et al.* [8] it is found that $\mu_l = 3.56$ and $\mu_{CH} = 2.23$, because $q_N = 3.90$ and $q_C = 3.18$ (cf. [9], [10]). The resulting dipole moment is 1.33 Debye units.

The dipole moment of a C-N bond, which is represented by

$$\psi = (2 + 2\Delta_{CN})^{-1} \{ t_C(1) + t_N(1) \} \{ t_C(2) + t_N(2) \} \quad (8)$$

is

$$\mu_{CN} = (1 + \Delta_{CN})^{-1} [(10\sqrt{2}/3 q_C \sqrt{3}) - (10\sqrt{2}/3 q_N \sqrt{3}) + 2 \int t_C x t_N d\tau] \quad (9)$$

if in the latter integral the origin is taken as the centre of the C and N nuclei and the positive direction is from C to N. From (9) it is found that $\mu_{CN} = 0.39$ Debye units.

For μ_{CN} to be zero it has to be assumed that

$$\psi = (1 + 2\lambda\Delta_{CN} + \lambda^2)^{-1} \{ t_C(1) + \lambda t_N(1) \} \{ t_C(2) + \lambda t_N(2) \}. \quad (10)$$

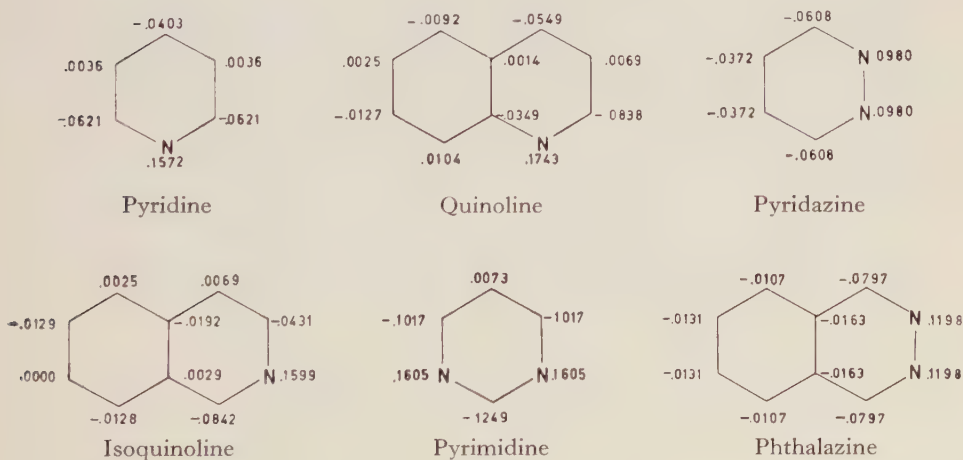


Figure 1.

It is then found that $\mu_{\text{CN}} = 0$ for $\lambda = 0.765$, so that the C-N bond has a slight C^--N^+ character.

The π moment μ_π may be obtained by solving for each molecule a secular equation in which $\alpha_{\text{NN}} = \alpha + 0.4\beta$, $\beta_{\text{CC}} = \beta_{\text{NN}} = \beta_{\text{CN}} = \beta_{\text{CC}} = \beta$. The charge densities found in this way are shown in figure 1.

For these calculations it has been assumed that in each molecule the carbon and nitrogen nuclei form one or two regular hexagons with bond distances of 1.38 \AA .

3. RESULTS AND DISCUSSION

The calculated and experimentally observed dipole moments are shown in table 1.

	μ_σ	$\mu_{\pi\parallel}$	$\mu_{\pi\perp}$	theor.	exp.
Pyridine	1.33	0.87	—	2.20	2.15 ± 0.05 [15]
Pyrimidine	1.33	0.86	—	2.19	2.10 ± 0.10 [11]
Pyridazine	2.30	1.50	—	3.80	3.94 [13]
Quinoline	1.33	0.88	0.09	2.22	2.16 [13]
Isoquinoline	1.33	1.00	0.48	2.38	2.54 [13]
Phthalazine	2.30	2.26	—	4.56	—

Table 1.

It should be observed that for some molecules there exist some discrepancies between the values of the dipole moment as reported by different authors. For instance, Schneider [12] reported 2.21 for pyridine, 2.42 for pyrimidine, 3.94 for pyridazine and 0.6 for pyrazine. It may be seen at once that the moment for pyrazine should be zero, which casts doubt on the accuracy of the other values. The values which are reported by Hückel and Salinger [11] for pyridine and pyrimidine, namely 2.1 ± 0.1 in both cases, seemed more acceptable. For pyridazine only the value of the dipole moment which has been reported by Schneider [12] is available. In the case of pyridine a value of 2.15 ± 0.05 has been derived by DeMore, Wilcox and Goldstein [15] from measurements on the microwave spectrum.

The fairly good agreement between the experimental data and the theoretical results must be regarded as fortuitous. First the assumption of the additivity of bond moments and of π and σ moments as well as a calculation of these quantities with the aid of a simple M.O. method forms an approach to the problem which is too crude to be expected to yield satisfactory results. Secondly, even if all these approximations should be permissible, there are several effects which have not been taken into account and which might affect the calculated dipole moments by an amount as great as 0.2 or 0.3 Debye units. For instance, in each molecule the bond angles are not exactly 120° , which may give rise to a resulting dipole moment of the C-H bonds, the overlap charges of the electrons have not been taken into account, etc.

On the other hand, it may quite well be that some of the deviations which result from these approximations are accounted for by the choice of the parameter α_{NN} , so that these calculations might be more reliable than they seem at first sight. The fact that this calculation contains only one adjustable parameter should be stressed. The satisfactory results which have been obtained in the case of the five

heterocyclic compounds for which the experimental values are known has encouraged us to believe that also for other compounds a similar procedure might yield results which are equally compatible with the experimental data.

The authors wish to express their gratitude towards Professor G. Giacomello for his stimulating interest, towards Professor H. C. Longuet-Higgins for helpful criticism; and towards the Istituto Nazionale per le Applicazioni del Calcolo and particularly Professor E. Aparo for solving the secular determinants with the F.I.N.A.C.

One of us (H. F. H.) wishes to thank the "Direzione Generale Relazioni Culturali" of the Italian Government and the Società Bombrini Parodi-Delfino for financial support.

On a fait quelques calculations simplifiées des moments dipolaires de la pyridine, pyrimidine, pyridazine, quinoléine, isoguinoléine et phthalazine, en supposant qu'une importante contribution au moment total provient de l'hybridisation des électrons "lone pair" des atomes d'azote, et que le moment de l'électron π peut être calculé par une simple calculcation LCAO, en admettant que l'intégrale coulombienne pour l'azote est $\alpha_{NN} = \alpha_{CC} + 0.4\beta_{CC}$. Les déviations entre les résultats théoriques et expérimentaux ne dépassent pas 6%.

Einige einfache Berechnungen der Dipolmomente des Pyridins, Pyrimidins, Pyridazins, Chinolins, Isochinolins und Phthalazins wurden ausgeführt und zwar unter der Voraussetzung, dass die Hybridisierung der "lone-pair"-Elektronen der Stickstoffatome zu den Gesamtmomentergebnissen einen wichtigen Beitrag liefert, und dass das π -Elektronen-Moment mit Hilfe der einfachen LCAO-Rechnung berechnet werden kann, wobei das Coulomb-Integral des Stickstoffs zu $\alpha_{NN} = \alpha_{CC} + 0.4\beta_{CC}$ angenommen ist. Die Abweichungen zwischen den theoretischen und experimentellen Ergebnissen sind $< 6\%$.

REFERENCES

- [1] WHELAND, G. W., and PAULING, L., 1935, *J. Amer. chem. Soc.*, **57**, 2086.
- [2] LONGUET-HIGGINS, H. C., and COULSON, C. A., 1947, *Trans. Faraday Soc.*, **43**, 87.
- [3] ORGEL, L. E., COTTRELL, T. L., DICK, W., and SUTTON, L. E., 1951, *Trans. Faraday Soc.*, **47**, 113.
- [4] CHALVET, O., and SANDORFY, C., 1949, *Compt. Rend.* **228**, 556.
- [6] DAVIES, D. W., 1954, *Trans. Faraday Soc.*, **50**, 449.
- [6] COULSON, C. A., 1953, *Valence*, Oxford,
- [7] HAMEKA, H. F., and LIQUORI, A. M., 1956, *Proc. Kon. Ac. Wet.*, Ser. B, **59**, 242.
- [8] MULLIKEN, R. S., RIEKE, C. A., ORLOFF, D., and ORLOFF, H., 1944, *J. chem. Phys.*, **17**, 1248.
- [9] ZENER, C., 1930, *Phys. Rev.*, **36**, 51.
- [10] SLATER, J. C., 1930, *Phys. Rev.*, **36**, 57.
- [11] HÜCKEL, W., and SALINGER, C. M., 1944, *Ber.* **77**, 810.
- [12] SCHNEIDER, W. C., 1948, *J. Amer. chem. Soc.*, **70**, 627.
- [13] RAU, G., and NARAYANASWAMY, B. N., 1934, *Z. phys. Chem.*, B, **26**, 23.
- [14] EVERARD, K. B., and SUTTON, L. E., 1949, *J. chem. Soc.*, 2318.
- [15] DE MORE, B. B., WILCOX, W. S., and GOLDSTEIN, J. H., 1954, *J. chem. Phys.*, **22**, 876.

The pressure-induced rotational absorption spectrum of hydrogen: I

by J. P. COLPA† and J. A. A. KETELAAR

Laboratory for General and Inorganic Chemistry of the University of Amsterdam, The Netherlands

(Received 7 October 1957)

The pressure-induced rotational absorption spectrum of hydrogen has been investigated at -60°C , 25°C and 80°C in pure hydrogen and in mixtures of hydrogen with helium, argon, nitrogen and carbon monoxide. The integrated absorption coefficients have been evaluated. In mixtures of hydrogen and carbon monoxide a simultaneous rotational-vibrational transition could be observed.

1. INTRODUCTION

The pure rotation and rotation-vibration spectra of homonuclear diatomic molecules are rigorously forbidden by the ordinary selection rules, because the dipole moments are zero by reasons of symmetry. However, it is known that the forbidden vibration spectra of such molecules can be observed in relatively thick layers of compressed gases. In 1949 Welsh and Crawford published the results of measurements on the vibrational absorption spectra of compressed hydrogen, oxygen and nitrogen [1]. A characteristic feature of their spectra is that the intensity is not proportional to the density of the gas but to the square of the density. Under the circumstances used in the experiments the ordinary selection rules, valid for isolated unperturbed molecules, break down. These rules are no longer valid for molecules in a compressed gas in which intermolecular interaction plays a part. In gases at moderate pressures one only needs to consider binary interactions. The number of interacting pairs with a certain intermolecular distance per unit of volume is proportional to the square of the density. The density dependence of the absorption intensity is explained by assuming these pairs to be responsible for the absorption. This is only possible if the intermolecular forces cause a certain change in the charge distribution of the molecules. This change can give rise to a resulting dipole moment and transition moment which need no longer be zero by symmetry requirements since the interacting molecules will generally be arbitrarily orientated.

We have quantitatively studied the pressure-induced pure rotational spectrum both in pure hydrogen and in mixtures of hydrogen with helium, argon, nitrogen and carbon monoxide in a pressure range from 20 to 150 atmospheres and at temperatures of -60°C , 25°C and 80°C . Compressed hydrogen absorbs in the infra-red from $8\text{--}24\mu$ contrary to other gases, e.g. O_2 and N_2 . Only the frequencies corresponding to the induced pure rotational transitions of hydrogen (and deuterium) are to be expected in the spectral region accessible with prism spectrometers. Pressure-induced rotational transitions for heavier molecules

† Present address : Koninklijke/Shell-Laboratorium, Amsterdam.

are to be expected in the microwave region (viz. the observations of Birnbaum *et al.* [2] on carbon dioxide).

In the literature about pressure-induced spectra several simultaneous transitions are described. In these transitions each molecule of a pair of interacting molecules undergoes a transition for which the pair absorbs only one photon and absorption maxima are found at frequencies that are the sum of characteristic frequencies of the individual molecules. Pressure-induced simultaneous transitions are described by Welsh *et al.* (in pure hydrogen) [3], by Fahrenfort and Ketelaar (in mixtures of carbon dioxide with hydrogen, nitrogen and oxygen) [4] and by Coulon *et al.* (in mixtures of hydrogen chloride and hydrogen) [5]. In these pressure-induced simultaneous transitions two vibrational transitions take part. In the spectrum of mixtures of carbon monoxide and hydrogen we found an absorption band due to a simultaneous transition in which the vibrational transition of carbon monoxide and a rotational transition of hydrogen are involved.

2. ROTATIONAL FREQUENCIES OF HYDROGEN. DISTRIBUTION OF THE MOLECULES OVER THE ROTATIONAL STATES

By an analysis of the ultra-violet and Raman spectra the energies associated with the rotational quantum states are known. For the vibrational ground state these energies, expressed as wave numbers in cm^{-1} , are given as a function of the rotational quantum number J by the following formula (cf. Herzberg [6]):

$$E(J) = 59.300J(J+1) - 0.04581J^2(J+1)^2 + 0.0000518J^3(J+1)^3.$$

As can be shown the selection rule for an induced transition in a homonuclear diatomic molecule is, just as in the Raman spectrum $\Delta J = \pm 2$ [7, 8].

From these data the frequencies of the bands to be expected in the spectrum of compressed hydrogen can be calculated (Table 1).

Rotational transition $J \rightarrow J+2$		Frequency in cm^{-1}
para H_2	$0 \rightarrow 2$	354.2
ortho H_2	$1 \rightarrow 3$	586.7
para H_2	$2 \rightarrow 4$	813.9
ortho H_2	$3 \rightarrow 5$	1034.1
para H_2	$4 \rightarrow 6$	1245.5

Table 1.

We measured the rotational spectrum at the following temperatures: -60°C , 25°C and 80°C . The distribution over the various ortho- and para-rotational states is calculated in the usual way (cf. Farkas [9]). In Table 2 are given the fractions $F(J)$ of molecules present in quantum state J . At the temperatures used the large majority of the molecules is in state $J=1$. Thus we can expect the strongest absorption to be due to the $J=1 \rightarrow J=3$ transition and to be found at about 587 cm^{-1} .

	$J=0$	$J=1$	$J=2$	$J=3$	$J=4$
60°C	0.171	0.718	0.079	0.032	—
25°C	0.129	0.658	0.118	0.091	0.003
80°C	0.111	0.616	0.131	0.132	0.009

Table 2. Fractions $F(J)$ of molecules, present in quantum state J .

3. EXPERIMENTAL

The spectra were obtained with a Perkin-Elmer 12C infra-red spectrometer. For the spectral range of 420–800 cm^{-1} we used a KBr prism and for the range of 700–1300 cm^{-1} a NaCl prism. Since the limit of a KBr prism is about 420 cm^{-1} we were not able to observe the band due to the $J=0 \rightarrow J=2$ transition at 354 cm^{-1} (Table 1). A spectral slit-width of about 5 cm^{-1} was maintained over the whole frequency range. Since this is very small in comparison with the half-width of the induced bands (about 140–200 cm^{-1}), the shape of these bands could be determined correctly. We used a gas cell with an optical path-length of 100 cm fitted with KBr windows. The pressure range used was 20–150 atm. The cell could be heated by an external electric heating tape and cooling was done by surrounding the cell with dry ice.

The gases used were carefully purified, e.g. by passage through cooling traps in liquid air. Pressures were read from calibrated manometers. In the case of mixtures, the hydrogen was let in first. On admission of the foreign gas mixing was rather rapid in the wide cell used. Spectra were taken only after sufficient time had elapsed, so that no subsequent changes were observed. For I_0 the transmitted energy was taken with the cell filled with nitrogen of 80 atm or with the cell filled at 1 atm with hydrogen or nitrogen; the differences between the values of I_0 obtained by these three methods were not significant.

4. EXPERIMENTAL RESULTS

The absorption coefficient is defined in the usual way

$$\alpha(\nu, T, n_{\text{H}_2}, n_X) = -\frac{1}{l} \ln \frac{I}{I_0} \quad (1)$$

(I/I_0 = transmission, l = optical path-length).

In the pressure-induced spectrum of hydrogen α will generally be a function of the wave number ν , the absolute temperature T , the density of the hydrogen gas n_{H_2} and the density of a foreign gas X added to hydrogen, n_X .

4.1. Induced absorption in pure hydrogen

For every wave number the absorption coefficient of the induced rotational spectrum of hydrogen appears to be strictly proportional to the square of the density of the gas, in the pressure range used, so that we can put:

$$\alpha(\nu, T, n_{\text{H}_2}) = n_{\text{H}_2}^2 \gamma_0(\nu, T), \quad (2)$$

with γ_0 the quadratic absorption coefficient. The half-widths of the induced bands are independent of the pressure; we only have pressure induction and no pressure broadening.

In figure 1 a graphical representation of γ_0 as a function of the wave number is given, referred to a density of 1 Amagat. (The density of hydrogen was calculated from the isotherms given by Michels and Goudekot [10].) The absorption band has a maximum at about 587 cm^{-1} and two shoulders at about 814 cm^{-1} and 1035 cm^{-1} . These three frequencies are characteristic for the $J=1\rightarrow J=3$, $J=2\rightarrow J=4$, and $J=3\rightarrow J=5$ transitions (Table 1, figure 1).

With increasing temperature at constant density of the gas the intensity of the band at 587 cm^{-1} decreases and the intensity in the region of the two shoulders increases. This is in accordance with the change of the distribution over the rotational levels with increasing temperature (Table 2).

The integrated specific absorption A_0 in pure hydrogen is defined by

$$A_0 = \int \alpha(\nu, T, n_{\text{H}_2}) d\nu = n_{\text{H}_2}^2 \int \gamma_0(T, \nu) d\nu = n_{\text{H}_2}^2 \Gamma_0; \quad (3)$$

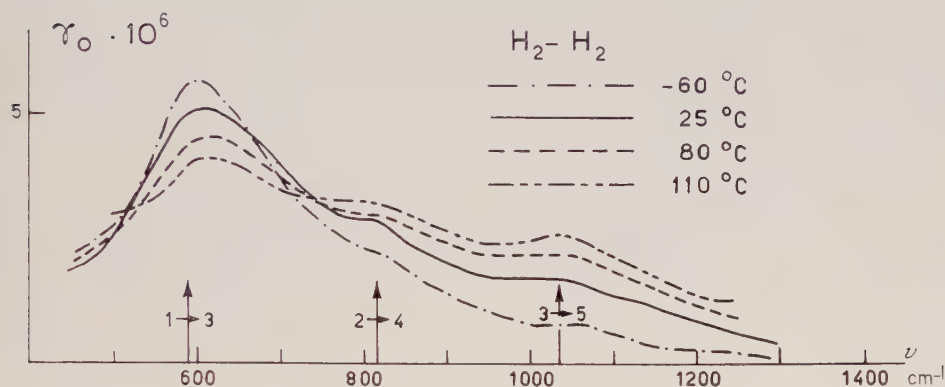


Figure 1. Pressure-induced rotational absorption spectrum in pure hydrogen at four temperatures. γ_0 =quadratic absorption coefficient in $10^{-6}\text{ cm}^{-1}\text{ Am}^{-2}$. ν =wave-number in cm^{-1} .

Γ_0 is the integrated quadratic absorption coefficient. At the temperatures used in our experiments the half-widths of the absorption bands are of the same order of magnitude as the spacings between the centres of the absorption bands. Thus a separation of the total intensity in intensities for the various bands observed was impossible without great arbitrariness. We have therefore extended the integration over the whole spectral range covering the three transitions $1\rightarrow 3$, $2\rightarrow 4$ and $3\rightarrow 5$.

The values of the overall integrated quadratic absorption coefficient $\Gamma_0 = A_0/n_{\text{H}_2}^2$, given in Table 3, are formally equivalent to the integrated quadratic absorption coefficient A_0 at a density of 1 Amagat. However, a reasonable estimate could be made of the half-width $\Delta\nu$ of the band at 587 cm^{-1} . These values are also shown in Table 3.

4.2. The rotational spectrum of hydrogen induced by foreign gases

The foreign gases we added to hydrogen were helium, argon, nitrogen and carbon monoxide. In a pure state none of these gases shows any absorption in the region of $420\text{--}1300\text{ cm}^{-1}$. When one of these gases is added to hydrogen, we see an increase of the absorption in the region of the rotational spectrum of hydrogen. At the densities used this increase is, at every frequency, proportional to the product of the density of the hydrogen originally present, and the density

of the foreign gas. In this part of the spectrum the density dependence of the absorption coefficient for mixtures of hydrogen and a foreign gas is given by the following equation

$$\left. \begin{aligned} \alpha(\nu, T, n_{\text{H}_2}, n_X) &= n_{\text{H}_2}^2 \gamma_0(\nu, T) + n_{\text{H}_2} \cdot n_X \gamma_m(\nu, T) \\ \Delta\alpha &= \alpha - n_{\text{H}_2}^2 \cdot \gamma_0 = n_{\text{H}_2} \cdot n_X \cdot \gamma_m \end{aligned} \right\} \quad (4)$$

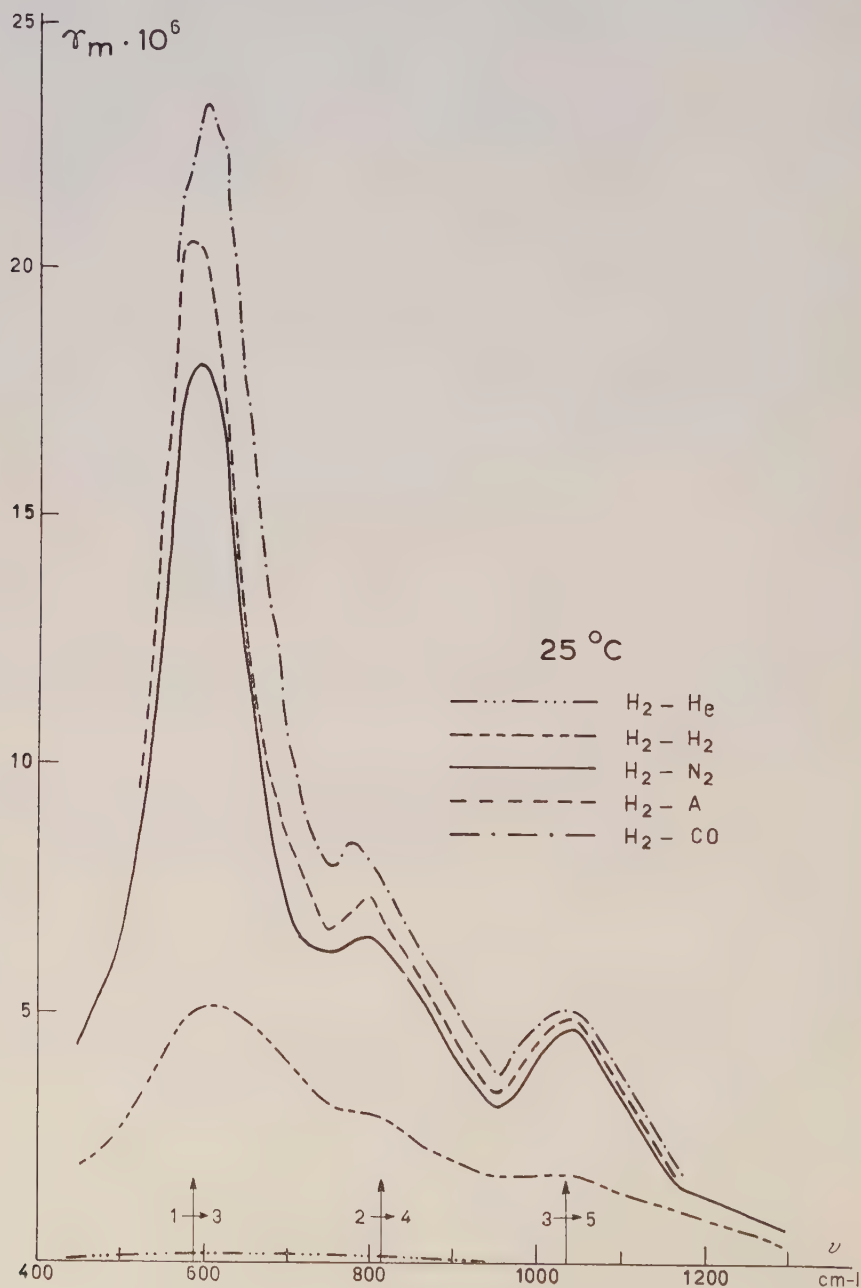


Figure 2. Pressure-induced rotational spectrum of hydrogen induced in mixtures of hydrogen with helium, argon, nitrogen and carbon-monoxide. γ_m = quadratic absorption coefficient in $10^{-6} \text{ cm}^{-1} \text{ Am}^{-2}$. ν = wavenumber in cm^{-1} .

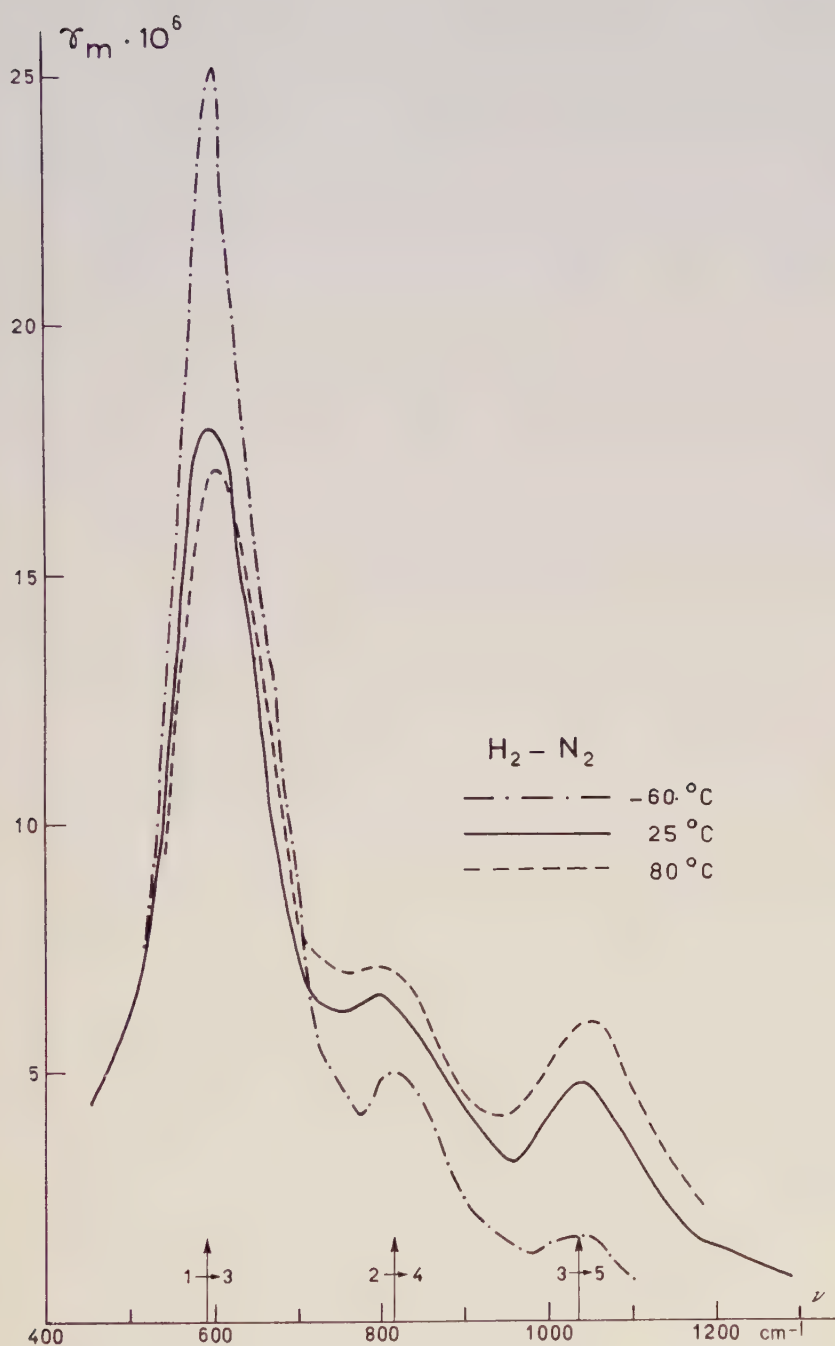


Figure 3. Pressure-induced rotational spectrum of hydrogen in mixtures of hydrogen and nitrogen. γ_m =quadratic absorption coefficient in $10^{-6} \text{ cm}^{-1} \text{ Am}^{-2}$. ν =wave-number in cm^{-1} .

The last term deals with the increase of the absorption caused by the addition of the foreign gas. This part, $\Delta\alpha$, we will call shortly the 'H₂-X spectrum'.

In figure 2 γ_m is given as a function of ν for several mixtures at 25°C. For a comparison also the spectrum of pure hydrogen, γ_0 is included.

In figure 3 the H₂-N₂ spectra (γ_m) at -60°C, 25°C and 80°C are given. For the other mixtures the spectra at different temperatures are very similar to those of the H₂-N₂ mixture; they will not be reproduced here. We see from figure 3 that the behaviour of the H₂-X spectra when the temperature of the gas is changed, is the same as for the spectrum of pure hydrogen (figure 1).

For the H₂-X spectra we define an integrated quadratic absorption coefficient Γ_m , analogous to the coefficient in equation (3)

$$A_m = \int \Delta\alpha \cdot d\nu = n_{\text{H}_2} \cdot n_X \int \gamma_m(\nu, T) d\nu = n_{\text{H}_2} \cdot n_X \cdot \Gamma_m. \quad (5)$$

As was done for pure hydrogen the integration is extended over the whole spectral range of three bands observed. In Table 3 these integrated intensities Γ_m are given. Also the half-widths of the band at 587 cm⁻¹ are given in this table. For a given spectrum the half-width $\Delta\nu$ appears to be very nearly proportional to the square root of the absolute temperature. For pure hydrogen the data for $\Delta\nu$ in Table 3 may be represented by $\Delta\nu_{\text{H}_2} = 11.6\sqrt{T}$; for induction by N₂, A or CO we find $\Delta\nu_m = 8.15\sqrt{T}$.

	H ₂		H ₂ -He		H ₂ -N ₂		H ₂ -A		H ₂ -CO	
	$\Delta\nu_0$	Γ_0	$\Delta\nu_m$	Γ_m	$\Delta\nu_m$	Γ_m	$\Delta\nu_m$	Γ_m	$\Delta\nu_m$	Γ_m
-60°C	171	1.64	—	—	120	4.0	120	4.6	—	—
25°C	200	1.88	—	~0.2	140	4.5	140	5.1	140	5.5
80°C	217	2.05	—	—	152	4.7	152	5.3	—	—

Table 3. Integrated quadratic absorption coefficient Γ_m in 10⁻³ cm⁻² Am⁻². Half-width $\Delta\nu$ of the $J = 1 \rightarrow J = 3$ band in cm⁻¹.

4.3. A simultaneous vibrational-rotational transition

Mixtures of hydrogen and carbon monoxide were also studied in the region of the vibrational frequencies (with a LiF prism in the spectrometer). At about 2730 cm⁻¹ a very weak and broad band was observed. In order to obtain better results two mirrors for multiple reflection were built in the pressure cell. In this way we got an effective optical path-length of 250 cm.

Since the observed band (figure 4) was not present in the spectrum of H₂ and CO, it could not be due to H₂, CO or impurities in these gases. As besides this band at 2730 cm⁻¹ and the bands of CO and H₂ no others were present in the spectrum, we could reject the possibility that the new band could be caused by the formation of a compound like H₂CO (formaldehyde). We interpreted this band as due to a simultaneous transition in which a vibrational transition of CO ($\nu = 2143$ cm⁻¹) and the $J = 1 \rightarrow J = 3$ rotational transition of H₂ ($\nu = 587$ cm⁻¹) take part. The sum of the corresponding wave numbers is 2730 cm⁻¹, as observed for the induced band. The integrated quadratic absorption coefficient Γ_m of this band is approximately 1.5×10^{-5} cm⁻² Am⁻².

In mixtures of nitrogen and hydrogen an analogous band could not be observed.

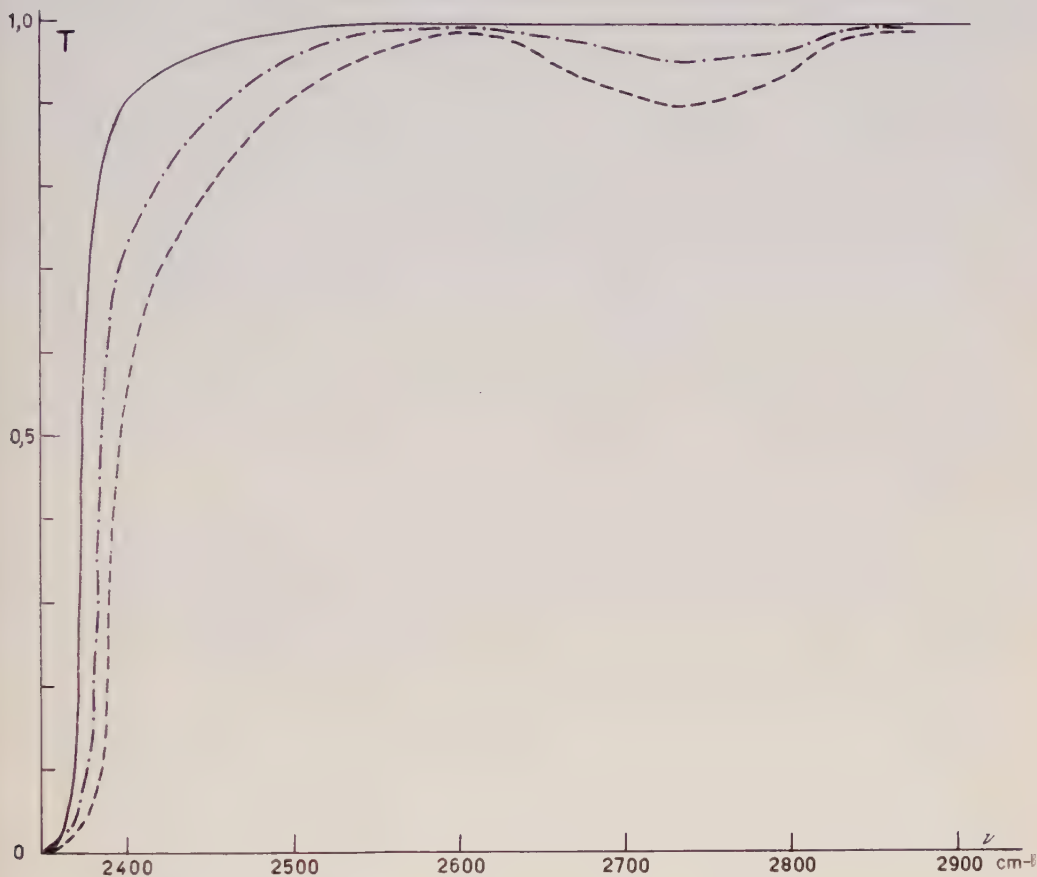


Figure 4. Simultaneous vibrational-rotational transition in mixtures of CO and H₂. Optical path-length 250 cm. Density of CO: 39 Am. Hydrogen is added to densities of 40 and 80 Am. Temperature 25°C. The absorption band at the lower frequencies is the (pressure broadened) fundamental of CO.

5. DISCUSSION

The absorptions in our spectra are proportional to $n_{\text{H}_2}^2$ for the self-induced absorption and to $n_{\text{H}_2} \cdot n_X$ for the foreign-induced absorption. For a given spectrum the half-width on the other hand, is independent of the density and depends only on the temperatures.

Both these properties are characteristic for a type of induction in which only binary interaction is of importance. (See e.g. Van Kranendonk [11].)

The absorption can take place only during the very short time of interaction of two molecules. Applying Heisenberg's uncertainty relation, we must expect the half-widths of these bands to be inversely proportional to the relative velocity of two molecules. The mean relative velocity of two molecules is proportional to \sqrt{T} and this explains why the half-widths of the induced bands are also proportional to \sqrt{T} .

From kinetic gas theory it follows that the mean relative velocity of a H_2 molecule and a N_2 (or A or CO) molecule is about 0.7 times as large as the mean relative velocity of two H_2 molecules. So the statement made about the proportionality of the half-width and the relative velocity also can explain why for a given temperature the half-width of the H_2-N_2 (H_2-A or H_2-CO) bands is 0.7 times the half-width of the band in pure hydrogen.

In Part II we will show that we can obtain a very good agreement between calculated and experimental values for the integrated quadratic absorption coefficients Γ_0 and Γ_m for the pressure-induced rotational spectra of hydrogen and of mixtures of hydrogen and foreign gases.

The authors wish to express their thanks to Mrs. J. P. Colpa-Boonstra, Mr. E. A. Th. Verdurmen and Mr. B. Stam for their valuable assistance with the measurements.

This work is part of the research programme of the "Stichting voor Fundamenteel Onderzoek der Materie" (Foundation for Fundamental Research on Matter, F.O.M.), and was made possible by financial support from the "Nederlandse Organisatie voor Zuiver-Wetenschappelijk Onderzoek" (Netherlands Organization for Pure Research, Z.W.O.).

Le spectre de rotation de l'hydrogène induit par pression a été étudié à $-60^\circ C$, $25^\circ C$ et $80^\circ C$ dans l'hydrogène pur et dans des mélanges de l'hydrogène avec l'hélium, l'argon, l'azote et le monoxyde de carbone. Les coefficients d'absorption intégrés ont été déterminés. Dans les mélanges de H_2 avec CO on observe une transition de combinaison entre la transition de vibration de CO et une transition de rotation de H_2 .

Das druckinduzierte Rotations-Absorptions-Spektrum von Wasserstoff wurde bei $-60^\circ C$, $25^\circ C$ und $80^\circ C$ in reinem Wasserstoff, sowie in Gemischen von Wasserstoff mit Helium, Argon, Stickstoff und Kohlenmonoxyd untersucht. Die integralen Absorptionskoeffizienten wurden ermittelt. In Mischungen von Wasserstoff und Kohlenmonoxyd konnte ein simultaner Rotations-Schwingungs-Übergang beobachtet werden, der aus einem Schwingungsübergang in CO und einem Rotationsübergang in H_2 zusammengesetzt ist.

REFERENCES

- [1] CRAWFORD, M. F., and WELSH, H. L., 1949, *Phys. Rev.*, **75**, 1607 ; WELSH, H. L., and CRAWFORD, M. F., 1949, *Phys. Rev.*, **76**, 580 ; CRAWFORD, M. F., WELSH, H. L., McDONALD, J. C. F. and LOCKE, J. L., 1950, *Phys. Rev.*, **80**, 469.
- [2] BIRNBAUM, G., MARYOTT, A. A., and WACKER, P. F., 1954, *J. chem. Phys.*, **22**, 1782.
- [3] WELSH, H. L., CRAWFORD, M. F., McDONALD, J. C. F. and CHISHOLM, D. A., 1951, *Phys. Rev.*, **83**, 1264.
- [4] FAHRENFORT, J., and KETELAAR, J. A. A., 1954, *J. chem. Phys.*, **22**, 1631 ; FAHRENFORT, J., 1955, *Thesis*, Amsterdam.
- [5] COULON, R., ROBIN, J., and VODAR, B., 1955, *Compt. Rend.*, **240**, 956.
- [6] HERZBERG, G., 1950, *Spectra of diatomic molecules* (New York : Van Nostrand).
- [7] COLPA, J. P., 1957, *Thesis*, Amsterdam.
- [8] GALATRY, L., and VODAR, B., 1956, *Compt. Rend.*, **242**, 1871.
- [9] FARKAS, A., 1935, *Ortho hydrogen, Para hydrogen and Heavy hydrogen*, Cambridge.
- [10] MICHELS, A., and GOUDEKET, H., 1941, *Physica*, **8**, 347, 353.
- [11] VAN KRANENDONK, J., 1952, *Thesis*, Amsterdam ; VAN KRANENDONK, J., and BIRD, R. B., 1951, *Physica*, **17**, 953 ; VAN KRANENDONK, J., 1957, *Physica*, **23**, 825.

Kritische Opaleszenz fester Lösungen

von A. MÜNSTER und K. SAGEL

Metall-Laboratorium der Metallgesellschaft A. G., Frankfurt/M

(Received 1 November 1957)

Durch Messung der diffusen Röntgenstreuung an dem System Al-Zn wird zum ersten Male gezeigt, dass die Erscheinung der kritischen Opaleszenz auch bei festen Lösungen auftritt. Die theoretischen Grundlagen, die experimentelle Technik und die Auswertungsmethode werden kurz beschrieben. Aus den experimentellen Streukurven werden die Korrelationsfunktionen berechnet und für die kritische Zusammensetzung die Reichweiten der Korrelation abgeschätzt. Etwa $0,5^\circ$ oberhalb der kritischen Temperatur beträgt dieselbe 31 \AA .

1. EINLEITUNG

Es ist seit langem bekannt, dass binäre flüssige Gemische in der Umgebung des kritischen Punktes der Entmischung eine starke Zunahme der Lichtstreuung zeigen, die als kritische Opaleszenz bezeichnet wird. Aus der Theorie der Lichtstreuung folgt, dass diese Erscheinung durch eine weitreichende statistische Ortskorrelation der Moleküle bedingt ist. Diese bewirkt, dass die Schwankungen in kleinen Volumenelementen (welche die normale Lichtstreuung erklären) nicht mehr als voneinander unabhängig betrachtet werden können. Die Reichweite dieser Schwankungskorrelation lässt sich nach der von Ornstein und Zernike [1] entwickelten Theorie aus den Messungen berechnen. Im kritischen Punkt erreicht dieselbe die Größenordnung der Lineardimension des Systems. Die inneren Schwankungen kompensieren sich dann nicht mehr bei der Mittelung über das Gesamtsystem, und für die Schwankungen des (als offen betrachteten) Gesamtsystems gilt nicht mehr, wie im homogenen Gebiet,

$$\frac{(N_i - \bar{N}_i)(N_j - \bar{N}_j)}{\bar{N}_i \bar{N}_j} = O(\bar{N}_j^{-1}) \quad (1)$$

sondern das relative Korrelationsmoment verschwindet asymptotisch von geringerer Ordnung [2, 3]. Nach der allgemeinen Schwankungstheorie [3] müssen dann gewisse thermodynamische Funktionen an dieser Stelle eine Singularität haben, indem etwa

$$\frac{\partial \bar{\rho}_i}{\partial \mu_j} \rightarrow \infty \quad (2)$$

gilt, wo ρ_i die mittlere molekulare Dichte der Komponente i , μ_j das chemische Potential der Komponente j ist.

Die Bedeutung der kritischen Opaleszenz liegt zunächst darin, dass sie einen direkten experimentellen Zugang zu dem schwierigen Problem der molekularen Deutung der kritischen Phasen darstellt. Darüber hinaus liefert sie ein Kriterium für die Anwendbarkeit der statistischen Mechanik im Hinblick auf die Frage der Einstellung innerer Gleichgewichte.

Über die Frage, ob die Erscheinung der kritischen Opaleszenz auch bei festen Lösungen auftritt, ist, soweit wir feststellen konnten, bisher nichts bekannt gewesen. Diese Frage ist nicht so trivial, wie es vielleicht zunächst scheinen mag. Bekanntlich führt die Mayer'sche Kondensationstheorie, ebenso wie ihre Verallgemeinerung für kondensierte binäre Systeme [3], auf erhebliche Schwierigkeiten, wenn man versucht, den kritischen Punkt etwa in der aus der van der Waals'schen Theorie bekannten Weise zu beschreiben. Mayer ist daher durch Überlegungen, die allerdings keine strengen Folgerungen aus der Theorie mehr sind, zu der Auffassung gelangt, dass die kritische Temperatur T_k nicht die Grenze des heterogenen Gebietes darstellt, sondern dass die Phasentrennung erst bei einer tieferen Temperatur T_m stattfindet. Zwischen T_k und T_m sollen die Isothermen horizontal, aber ohne eine Unstetigkeit der Steigung, verlaufen. Dies entspricht einer anomalen Umwandlung I. Ordnung, bei der alle benachbarten Phasen miteinander im Gleichgewicht sind. Dieser Umwandlungstyp liegt bei der Kondensation des idealen Bose-Einstein-Gases vor [4]. Aus dieser Auffassung folgt, dass die beobachtete Koexistenzkurve in ihrem obersten Teil über einen endlichen Konzentrationsbereich horizontal verlaufen muss. Wir sehen ab von der bisher ungeklärten Frage, ob die erwähnte Schwierigkeit durch ein ungelöstes mathematisches Problem der Mayer'schen Theorie bedingt ist. Die experimentellen Ergebnisse zeigen jedoch für fluide Systeme, die hinreichend genau untersucht worden sind (z. B. [5-8]), dass die Koexistenzkurve in der Umgebung des kritischen Punktes extrem flach, vielleicht sogar horizontal verläuft. Für die Kondensation von CO_2 und SF_6 zeigen neue Messungen von Wentorf [9], dass die Existenz der anomalen Umwandlung I. Ordnung über einen Bereich von wenigen Hundertstel Grad nicht auszuschliessen ist.

Wendet man aber die Mayer'sche Cluster-Methode auf das Gittermodell fester Lösungen an [10, 11], so kann man streng beweisen, dass hier der kritische Punkt der Entmischung in der herkömmlichen Weise durch die Gleichungen

$$\frac{\partial \mu_1}{\partial x_1} = 0, \quad \frac{\partial^2 \mu_1}{\partial x_1^2} = 0 \quad (3)$$

(wo x_1 der Molenbruch der Komponente 1 ist) beschrieben wird. Darüber hinaus scheinen die experimentellen Ergebnisse an zwei sorgfältig untersuchten Systemen [12, 13] zu zeigen, dass die Gestalt der Koexistenzkurve fester Lösungen in der Umgebung des kritischen Punktes charakteristisch von der flüssiger Gemische verschieden ist (Abb. 1). Die Annahme eines horizontalen oder auch nur extrem flachen Kurvenverlaufes am kritischen Punkt ist für die ersteren sehr unwahrscheinlich.

Unter diesen Umständen wäre es denkbar, dass die spezielle molekulare Struktur, welche die kritische Opaleszenz verursacht, bei festen Lösungen überhaupt nicht auftritt, dass sie also weniger eine Eigenschaft der kritischen Phasen als der fluiden Phasen darstellt.

Die Analyse der kritischen Opaleszenz flüssiger Gemische zeigt, dass hier in einem sehr engen Temperaturbereich extrem starke Verschiebungen des inneren Gleichgewichtes auftreten. Sie kann daher nur beobachtet werden, wenn diese Gleichgewichte sich innerhalb der Versuchszeiten einstellen. Für feste Lösungen ist dies keineswegs selbstverständlich; tatsächlich wurde schon unter diesem Gesichtspunkt der Versuch, den Effekt nachzuweisen, für hoffnungslos gehalten [14]. Die Entscheidung dieser Frage ist von grundsätzlicher Bedeutung,

weil beim Fehlen von definierten Hemmungen die statistische Mechanik nur anwendbar ist, wenn die Einstellung des inneren Gleichgewichtes innerhalb der Versuchszeiten vorausgesetzt werden kann.

Es ist uns jetzt gelungen, am System Aluminium-Zink, dessen Phasendiagramm Abb. 2 zeigt, erstmalig die kritische Opaleszenz fester Lösungen nachzuweisen [15]. Im folgenden berichten wir über Methoden und Ergebnisse dieser Messungen.

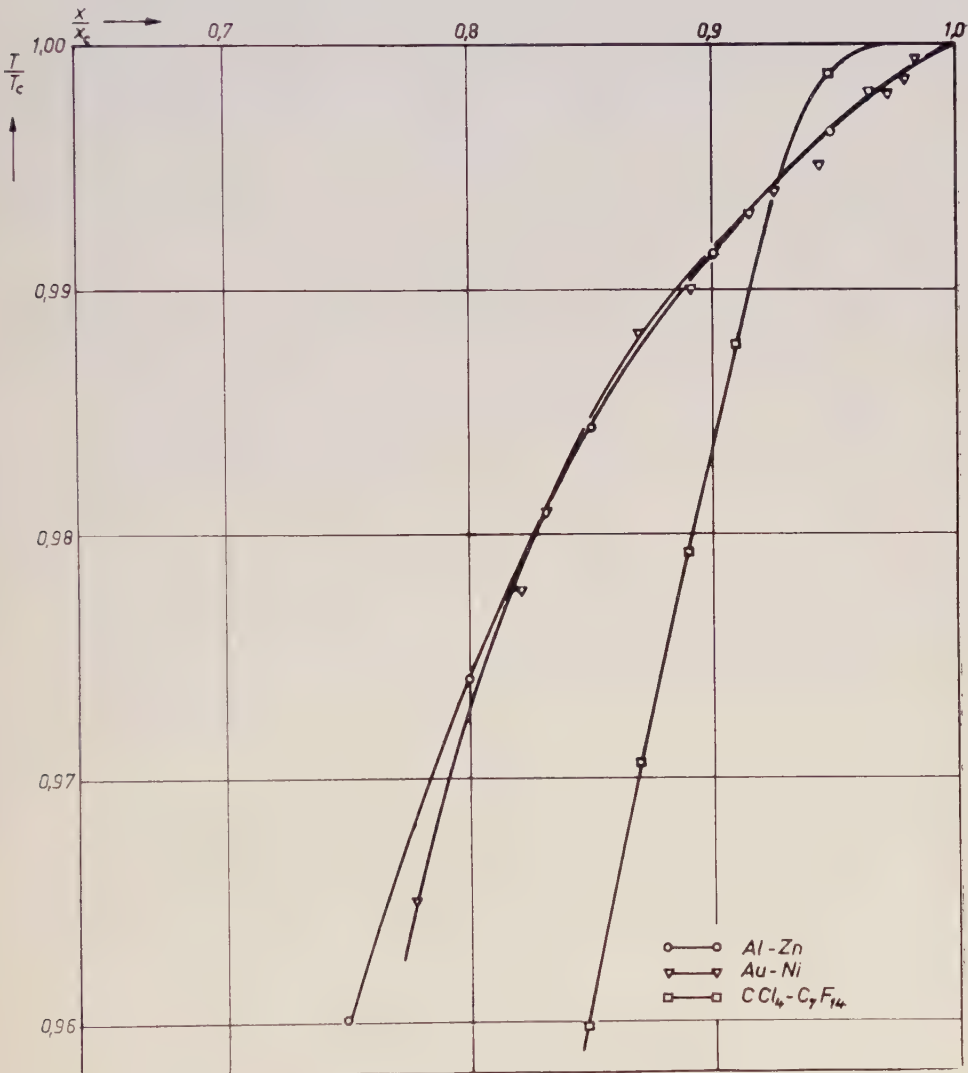


Abb. 1. Entmischungskurven binärer Systeme.

2. THEORETISCHE GRUNDLAGEN

Bei metallischen festen Lösungen ist ein Nachweis der kritischen Opaleszenz naturgemäss nur mit Hilfe von Röntgenstrahlen möglich. Da wir die Theorie

der diffusen Röntgenstreuung binärer Legierungen kürzlich an anderer Stelle [16] ausführlich entwickelt haben, beschränken wir uns hier auf eine Zusammenstellung der für das Folgende wesentlichen Resultate. Für die Formulierung der Theorie benutzen wir die aus der statistischen Mechanik bekannten molekularen Verteilungsfunktionen (molecular distribution functions) [3].

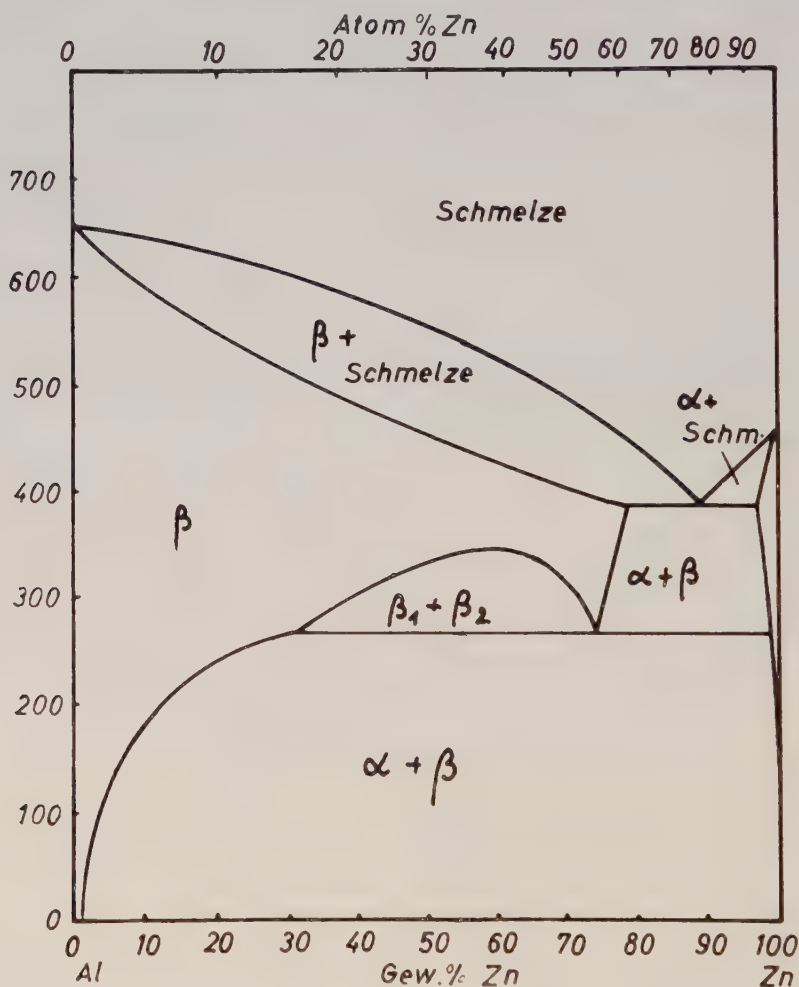


Abb. 2. Zustandsdiagramm des Systems Al-Zn.

Es ist also

$$\rho^{(n)} = \Pi \left(\frac{N_i}{V} \right)^{n_i} g^{(n)}, \quad (\sum n_i = n) \quad (4)$$

die Wahrscheinlichkeitsdichte, n Moleküle bei dem Koordinatensatz $\mathbf{q}^{(n)}$ zu finden. Dabei gilt

$$\lim_{V \rightarrow \infty} \left[\frac{1}{V^n} \int g^{(n)} d\mathbf{q}^{(n)} \right] = 1. \quad (5)$$

Wir setzen nun voraus, dass das betrachtete System ein Einkristall von bekannter

Orientierung ist und dass die Gitterplätze von Atomen der Sorten 1 und 2 besetzt sind. Dann ist

$$\rho_1^{(1)} = \frac{N_1}{V} g_1^{(1)}, \quad \rho_2^{(1)} = \frac{N_2}{V} g_2^{(1)} \quad (6)$$

wo $g_1^{(1)}$ und $g_2^{(1)}$, im Gegensatz zu fluiden Phasen, dreifach periodische Funktionen sind. Für die Paar-Verteilungsfunktionen gilt

$$\rho_{ij}^{(2)} = \frac{N_i N_j}{V^2} g_{ij}^{(2)}. \quad (7)$$

Die Wahrscheinlichkeitsdichte, dass ein Atom j an der Stelle \mathbf{q}_j gefunden wird, wenn bekannt ist, dass ein Atom i sich an der Stelle \mathbf{q}_i befindet, ist

$$\phi_{ij}^* = \frac{\rho_{ij}^{(2)}}{\rho_i^{(1)}} = \frac{N_j}{V} \frac{g_{ij}^{(2)}}{g_i^{(1)}}. \quad (8)$$

Diese Funktionen hängen von den Vektoren

$$\mathbf{r}_{ij} = \mathbf{q}_i - \mathbf{q}_j \quad (9)$$

und \mathbf{q}_i ab. Um die Abhängigkeit von \mathbf{q}_i zu beseitigen, mitteln wir ϕ_{ij} mit Hilfe der molekularen Verteilungsfunktion $g_i^{(1)}$ über alle Lagen des Atoms i und definieren

$$\phi_{ij} = \frac{1}{V} \int g_i^{(1)} \phi_{ij}^* d\mathbf{q}_i \quad (10)$$

wo \mathbf{r}_{ij} für die Integration ein konstanter Parameter ist. Setzen wir in nullter Näherung

$$g_i^{(1)} = \sum_{l=1}^N \delta(\mathbf{q}_l - \mathbf{q}_i^*) \quad (11)$$

wo $\delta(\mathbf{q}_l - \mathbf{q}_i^*)$ die dreidimensionale Delta-Funktion und \mathbf{q}_i^* der Ortsvektor des l -ten Gitterpunktes ist, so ist ϕ_{ij} die Wahrscheinlichkeit, im vektoriellen Abstand \mathbf{r}_{ij} von einem Atom i , das sich auf einem Gitterplatz befindet, ein Atom j anzutreffen. Aus der Definition (10) folgt

$$\phi_{ij} = 0 \quad \text{für} \quad r_{ij} = 0. \quad (12)$$

Setzen wir voraus, dass

$$\lim_{r_{ij} \rightarrow \infty} g_i^{(1)} \phi_{ij}^* = \frac{N_j}{V} g_i^{(1)} g_j^{(1)} \quad (13)$$

existiert und dass $g_i^{(1)} \phi_{ij}^*$ in dem einer Elementarzelle entsprechenden Bereich der Variablen \mathbf{q}_i gleichmässig gegen diesen Limes konvergiert, so wird

$$\lim_{r_{ij} \rightarrow \infty} \phi_{ij} = \frac{N_j}{V} g_j^{(1)}. \quad (14)$$

Ferner leitet man aus Gl. (10) die Normierungsrelation

$$\lim_{V \rightarrow \infty} \int \phi_{ij} d\mathbf{q}_j = N_j/V \quad (15)$$

ab.

Bei Messungen an polykristallinem Material (wie wir sie ausschliesslich durchgeführt haben) ist für ein beliebig herausgegriffenes Atom i nichts über die Orientierung des entsprechenden Kristalliten bekannt. Eine solche Messung kann daher nur eine über alle Orientierungen gemittelte Funktion ϕ_{ij} liefern.

Dabei setzen wir der Einfachheit halber voraus, dass keine bevorzugten Orientierungen auftreten. Die so definierte Funktion $\overline{\phi}_{ij}$ hängt dann nur noch von dem skalaren Abstand r_{ij} ab. Sie stellt die Wahrscheinlichkeitsdichte dar, im Abstand r_{ij} von einem beliebig herausgegriffenen Atom i ein Atom j zu finden. Im Hinblick auf die Gl. (8) und (10) können wir setzen

$$\overline{\phi}_{ij} = \frac{N_j}{V} \overline{g_{ij}^{(2)}}. \quad (16)$$

Die dadurch definierten Funktionen $\overline{g_{ij}^{(2)}}$ bezeichnen wir als die mittleren radialen Verteilungsfunktionen des Mischkristalls. Es ist

$$\overline{g_{ij}^{(2)}} = 0 \quad \text{für} \quad r_{ij} = 0 \quad (17)$$

und

$$\lim_{V \rightarrow \infty} \frac{1}{V} \int \overline{g_{ij}^{(2)}} d\mathbf{q}_j = 1. \quad (18)$$

Die Mittelung über alle Orientierungen lässt sich auch für die Funktion $\overline{g_j^{(1)}}$ durchführen, wenn wir den Koordinatenursprung in einen Gitterplatz legen und den Kristall um den Ursprung rotieren lassen. Für den Einkristall ergibt dann die so definierte Funktion $\overline{g_j^{(1)}}$ nach Multiplikation mit N_j/V die Wahrscheinlichkeitsdichte, im Abstand q_j vom Ursprung ein j -Atom zu finden. Für ein polykristallines System als Ganzes hat die Funktion keine anschauliche Bedeutung. Sie muss als Superposition der entsprechenden Funktionen der Kristallite betrachtet werden (was naturgemäss auch für $\overline{g_{12}^{(2)}}$ möglich ist). Für diese Funktion gilt

$$\lim_{V \rightarrow \infty} \frac{1}{V} \int \overline{g_j^{(1)}} d\mathbf{q}_j = 1 \quad (19)$$

und

$$\lim_{r_{ij} \rightarrow \infty} \overline{g_{ij}^{(2)}} = \overline{g_j^{(1)}}. \quad (20)$$

Die Gleichung für die kohärente Röntgenstreuung einer polykristallinen binären Legierung lässt sich auf die Form bringen

$$I = I_D + I_T + I_B. \quad (21)$$

Hier ist

$$I = \frac{I_\vartheta R^2}{I_0 a^2 p^2} \quad (22)$$

I_0 bezeichnet die Intensität des Primärstrahls, I_ϑ die im Abstand R von dem streuenden Präparat gemessene Strahlung,

$$a = e^2/mc^2 \quad (23)$$

den Thomson-Faktor und p den Polarisationsfaktor. Der Term I_B in Gl. (21) stellt die scharfen Bragg-Reflexe dar, I_T die Temperatur-Streuung um die Bragg-Reflexe, während I_D die hier interessierende diffuse Kleinwinkelstreuung ist. Es ergibt sich

$$I_D = N \left[x_1 x_2 (f_1 - f_2)^2 4\pi\rho \int_0^\infty (\overline{g_2^{(1)}} - \overline{g_{12}^{(2)}}) \frac{\sin ur}{ur} r^2 dr \right]. \quad (24)$$

Hier sind x_1 und x_2 die Atombrüche, f_1 und f_2 die Fourier-Transformierten der

auf den Kern als Ursprung bezogenen Elektronendichten eines 1- bzw. 2-Atoms,

$$u = \frac{4\pi}{\lambda} \sin \frac{\vartheta}{2} \quad (25)$$

und $\rho = \rho_1 + \rho_2 = N/V$. Die Funktion $\overline{g_2^{(1)}}$ wird eingeführt durch die Approximation

$$\sum_{l=0} z_l \frac{\sin ur_l}{ur_l} \simeq 4\pi\rho \int r^2 \overline{g_2^{(1)}} \frac{\sin ur}{ur} dr \quad (26)$$

wo z_l die Koordinationszahl und r_l der Radius der l -ten Koordinationsschale ist. Da $\overline{g_2^{(1)}}$ in dem gesamten Integrationsbereich beschränkt ist, wird die Konvergenz des rechts stehenden Integrals durch die bekannten Konvergenz Integrals

$$\frac{4\pi}{V} \int r^2 \frac{\sin ur}{ur} dr \quad (27)$$

gesichert.

Definieren wir eine neue Funktion

$$i(u) = 4\pi\rho \int (\overline{g_2^{(1)}} - \overline{g_{12}^{(2)}}) \frac{\sin ur}{ur} r^2 dr \quad (28)$$

so ist nach Gl. (24)

$$i(u) = \frac{I_D}{N x_1 x_2 (f_1 - f_2)^2}. \quad (29)$$

Die Funktion $i(u)$ kann daher aus den experimentellen Daten bestimmt werden. Dann ergibt sich aus Gl. (27) durch Fourier-Transformation

$$r (\overline{g_2^{(1)}} - \overline{g_{12}^{(2)}}) = \frac{1}{2\pi^2\rho} \int_0^\infty u i(u) \sin(ur) dr. \quad (30)$$

Die röntgenographisch bestimmbare Funktion $\overline{g_2^{(1)}} - \overline{g_{12}^{(2)}}$ beschreibt die Ortskorrelation zwischen den 1- und 2-Atomen soweit dieselbe nicht schon durch die Gitterstruktur als solche bedingt ist†. Da wir in dem hier untersuchten System Aluminium-Zink cluster-Bildung haben, ist an der Stelle der ersten Koordinationsschale ($r = r_1$) stets $\overline{g_2^{(1)}} - \overline{g_{12}^{(2)}} > 0$. Als Reichweite der Korrelation definieren wir den Wert $r_c > r_1$, für den erstmalig $\overline{g_2^{(1)}} - \overline{g_{12}^{(2)}} < 0$ wird. Abb. 3 zeigt die nach Gl. (24) für verschiedene Reichweiten der Korrelation berechneten Streukurven. Man sieht, dass mit zunehmender Reichweite der Korrelation die Intensität im Gebiete kleiner Streuwinkel sehr stark ansteigt.

3. STOFFE UND MESSMETHODEN

Als Ausgangsmaterialien dienten elektrolytisch raffiniertes Aluminium der Vereinigten Leichtmetallwerke GmbH., Bonn, und Feinzink der Berzelius Metallhütten-G.m.b.H., Duisburg-Wanheim. Die Analysen† sind in Tabelle 1 zusammengestellt. Die Herstellung der Legierungen und ihre Verarbeitung zu Presstangen ist in einer früheren Arbeit [12] ausführlich beschrieben worden. Aus den Presstangen wurden durch Walzen Folien von 20–30 μ Dicke hergestellt, die für die Messungen verwendet wurden. Die Dicke der Folien wurde mit Hilfe eines Leitz'schen Optimeters bestimmt. Die Zusammensetzung der Legierungen

† Im Folgenden gebrauchen wir den Ausdruck Ortskorrelation nur in diesem eingeschränkten Sinne.

‡ Für die Durchführung der Analysen haben wir Herrn Prof. J. Fischer zu danken.

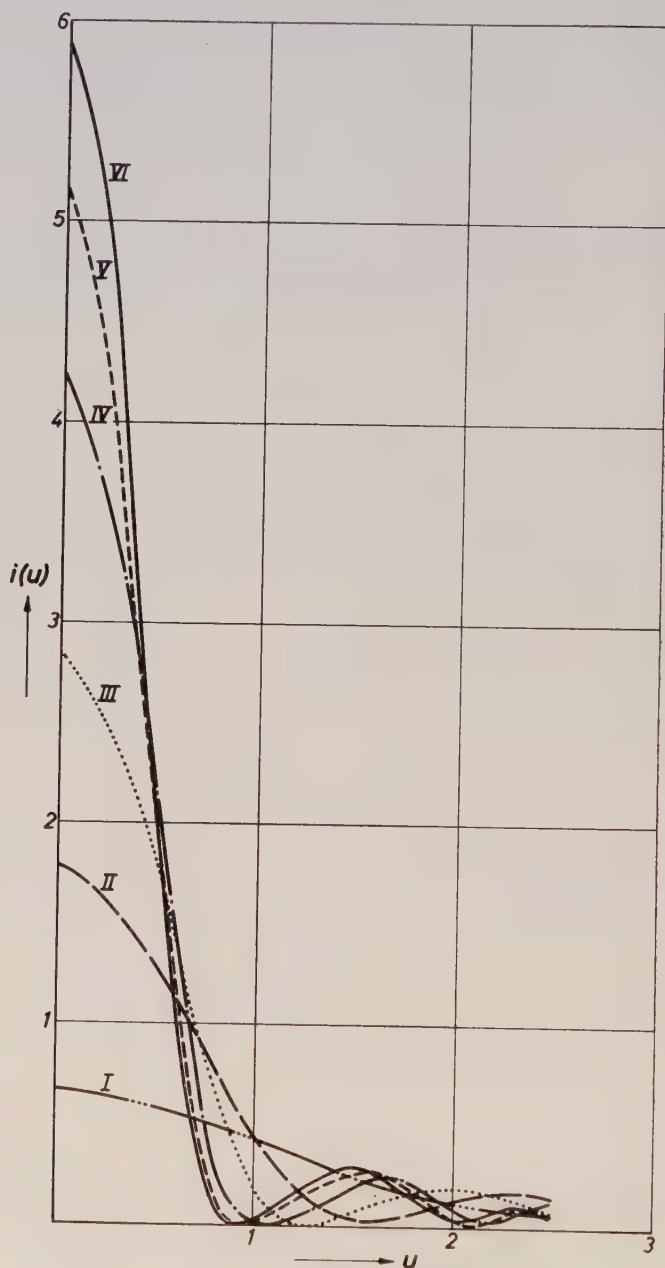


Abb. 3. Berechnete Streukurven.

- I. Keine Korrelation.
- II. Korrelation bis zur 1. Koordinationsschale.
- III. Korrelation bis zur 2. Koordinationsschale.
- IV. Korrelation bis zur 3. Koordinationsschale.
- V. Korrelation bis zur 4. Koordinationsschale.
- VI. Korrelation bis zur 5. Koordinationsschale.

wurde analytisch vor und in einigen Fällen nach der Messung kontrolliert. Die Änderung der Zusammensetzung während der Messung lag innerhalb der Fehlergrenzen der Analysenmethode ($\pm 0,2$ Gewichtsprozent Zn). Die Verunreinigungen der Legierungen zeigten keine wesentlichen Abweichungen von denen der Ausgangsmaterialien.

	Fe	Cu	Mg	Si	Pb	Cd
Al	0,001–0,002	0,001	0,001	0,001	—	—
Zn	0,001–0,002	0,001	0,001	—	0,002	0,001

Tabelle 1. Verunreinigungen der Ausgangsmaterialien Al und Zn in Gewichts-%.

Die Proben wurden zur Homogenisierung in der Apparatur zunächst 2h bei 380°C geglüht und dann jeweils vor Beginn einer Messung 1–2 Stunden auf der Messtemperatur gehalten.

Zur Messung der diffusen Röntgenstreuung diente ein nach dem Prinzip der Guinier'schen Anordnung gebautes Zählrohr-Goniometer mit Quarz-Monochromator, dessen Schema in Abb. 4 dargestellt ist. Die Probe befindet sich in einem Öfchen aus Silber. Die für den Strahlendurchgang freie Fläche des Präparates ist $1 \times 14 \text{ mm}^2$. Die Temperatur wird mit zwei Thermoelementen, deren Lötstellen sich unmittelbar neben der durchstrahlten Präparatfläche befinden, gemessen und

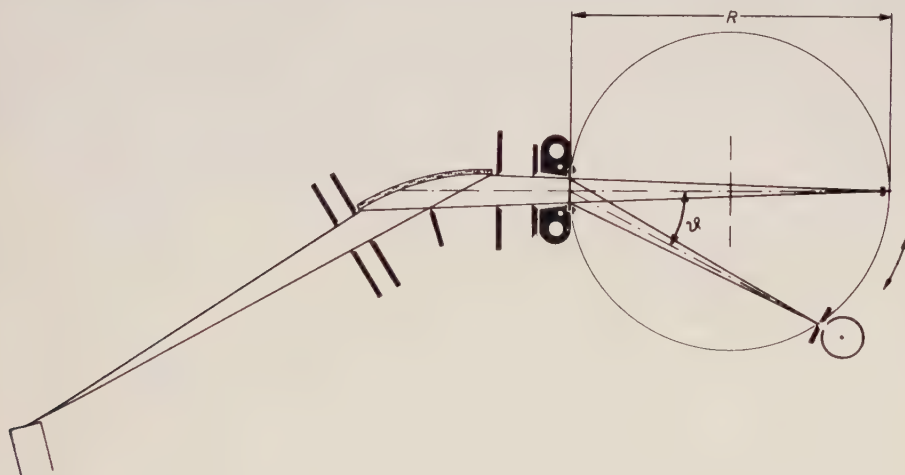


Abb. 4. Schema des Zählrohrgoniometers.

geregelt. Der Primärstrahl wird im Fokussierungspunkt durch einen 1,2 mm breiten Kupfersteg zum grössten Teil absorbiert. Die hindurchgehende Intensität dient als Grundlage der Normierung. Bei einem Öffnungswinkel des Primärstrahles von 20 Minuten und einer Spaltöffnung des Zählrohres von 0,3–0,6 mm beträgt der kleinste mit dieser Anordnung zugängliche Streuwinkel ca. 15–20 Minuten. Alle Messungen wurde nmit Co-K_{α} -Strahlung ausgeführt.

Um die sehr störende Luftstreuung ausschliessen zu können, befand sich das gesamte Goniometer in einem vakuumdichten Gefäss. Da bei den Messtemperaturen das Zink im Vakuum sehr rasch verdampft (Bei 400°C ist nach 1 Stunde in

einer Legierung von ursprünglich 35 Atom-% Zn praktisch kein Zink mehr vorhanden), wurde das Gefäss mit Wasserstoff von Normaldruck gefüllt und die experimentell ermittelte Streuung des Wasserstoffs von den Messresultaten abgezogen.

Die Zählrohr-Impulse wurden mit Hilfe eines Philips-Zählwerkes direkt gezählt. Durch geeignete Wahl der Messzeit konnten die statistischen Schwankungen hinreichend niedrig gehalten werden. Die Primär-Intensität wurde im Laufe jeder Messung häufiger kontrolliert. Die grössten Schwierigkeiten machte die Kontrolle der Temperatur, deren Unsicherheit (in relativer Skala) etwas grösser als $\pm 0,5^\circ$ angenommen werden muss.

4. AUSWERTUNG DER MESSUNGEN

Da bei unserer Anordnung R sich mit ϑ ändert, müssen die gemessenen Intensitäten zunächst mit einem geometrischen Korrekturfaktor $\cos \vartheta$ multipliziert werden [17]. Weiter muss für die Absorption korrigiert und durch den Polarisationsfaktor dividiert werden. Um die so erhaltenen Werte auf Elektroneneinheiten umzurechnen, wurde in der gleichen Anordnung die Streuung von glasigem SiO_2 bei grossen Streuwinkeln gemessen und durch Vergleich mit den berechneten Werten der Umrechnungsfaktor bestimmt. Schliesslich wurde von der auf diese Weise korrigierten experimentellen Streuung die berechnete Compton-Streuung abgezogen.

Die auf diese Weise erhaltene Intensitätskurve ist noch durch einen von dem endlichen Querschnitt des Primärstrahles herrührenden Kollimationsfehler verschmiert [18]. Dieser Fehler muss korrigiert werden, wenn die Linearabmessungen des Strahlquerschnittes gegen den (in unserer Anordnung) auf dem Fokussierungskreis gemessenen Abstand des ersten Messpunktes vom Primärstrahl nicht vernachlässigt werden können. Der Querschnitt des Primärstrahles ist bei unserer Anordnung $0,5 \times 14 \text{ mm}^2$, der Abstand des ersten Messpunktes vom Primärstrahl ca. 1 mm. Es ist daher zu erwarten, dass die Korrektur für die Höhe des Primärstrahles eine sehr wichtige Rolle spielt, während die für die Breite verhältnismässig geringfügig sein wird. Diese Erwartung wird durch unsere Rechnungen bestätigt. Wir haben die Entschmierung für die Höhe nach der Methode von Guinier und Fournet [19] in der von Kratky u.M.[20] angegebenen modifizierten Form für alle Intensitätskurven durchgeführt, dagegen die Entschmierung für die Breite im Hinblick auf die experimentellen Unsicherheiten vernachlässigt.

Bei der Durchführung der Fourier-Transformation Gl. (28) tritt die Schwierigkeit auf, dass experimentelle Werte nur für den Bereich $0 < u < 4\pi/\lambda$ vorliegen können. Dadurch treten in der Transformierten zusätzliche Maxima und Minima auf, die das Bild der radialen Verteilung erheblich verfälschen können. Man kann diese Schwierigkeit dadurch umgehen, dass man die gemessene Intensitätskurve extrapoliert. Dieses für die Streuung von sichtbarem Licht mit Erfolg angewandte Verfahren [21] ist in unserem Falle mit einer erheblichen Willkür behaftet und daher von uns nicht benutzt worden. Die zweite Möglichkeit besteht darin, dass man die Funktion $i(u)$ vor der Fourier-Transformation mit einem 'künstlichen Temperaturfaktor' (modification function) $M(u)$ multipliziert derart, dass der Integrand jenseits der Stelle u_0 , bis zu der die experimentellen Daten reichen, praktisch verschwindet. Dieses Verfahren

erscheint für unsere Zwecke besonders angemessen, weil die Messung der diffusen Streuung bei etwas grösseren Winkeln ($u > 2$) wegen der Überlagerung mit den Bragg-Reflexen mit einer erheblichen Unsicherheit behaftet ist, und daher bei der Auswertung ein geringeres Gewicht erhalten muss. Diese Methode ist kürzlich in allgemeiner Form von Waser und Schomaker [22] und in Zusammenhang mit dem hier interessierenden Streuproblem von Averbach u.M. [23] erörtert worden. Der künstliche Temperaturfaktor bewirkt naturgemäss neben der Beseitigung der ‚falschen‘ Maxima und Minima eine gewisse Verzerrung der Transformierten, deren wesentliche Züge sich leicht übersehen lassen. Bezeichnen wir die Cosinus-Transformierte von $M(u)$ mit $T(r)$ und mit $(\overline{g_2^{(1)}} - \overline{g_{12}^{(2)}})^*$ die mit Hilfe des künstlichen Temperaturfaktors erhaltene Verteilungsfunktion, so folgt aus dem Faltungssatz der Fourier-Transformation

$$r (\overline{g_2^{(1)}} - \overline{g_{12}^{(2)}})^* (r) = (2\pi)^{-1/2} \int_{-\infty}^{+\infty} (\overline{g_2^{(1)}} - \overline{g_{12}^{(2)}})(x) T(r-x) dx. \quad (31)$$

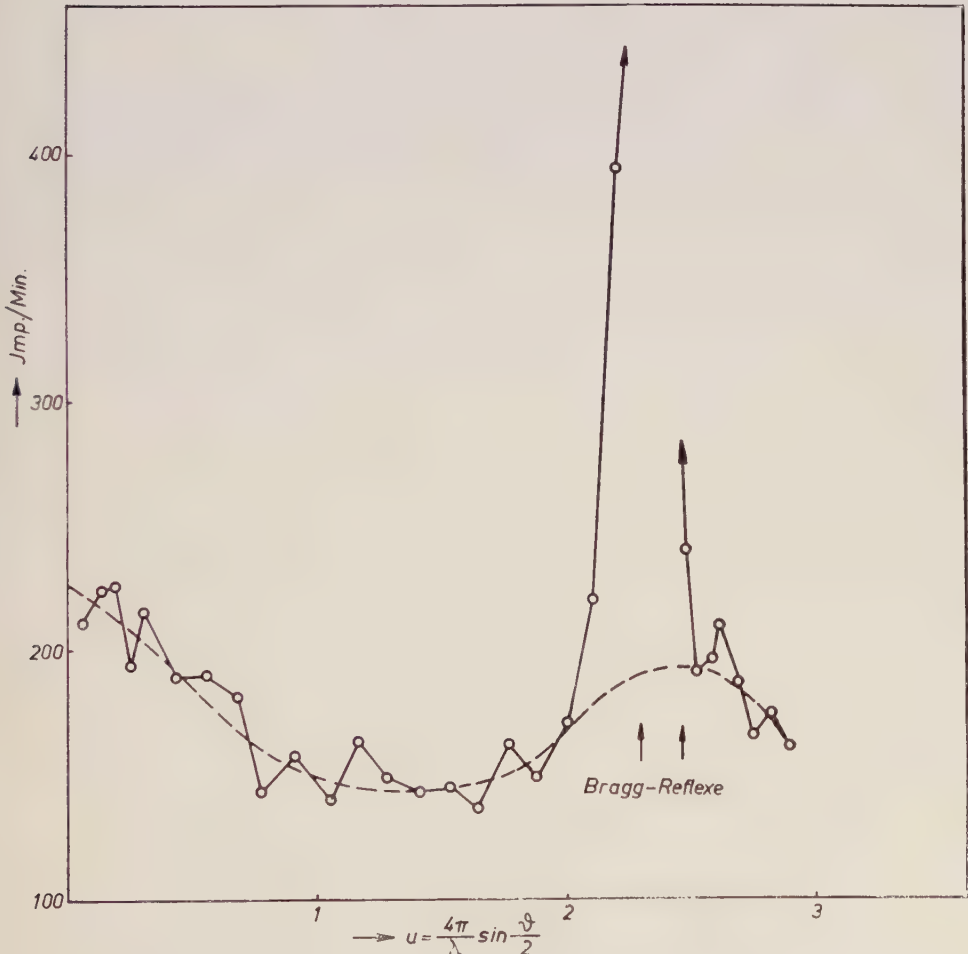


Abb. 5. Experimentelle Streukurve einer Al-Zn-Legierung mit 39,5 Atom-% Zn bei 360°C.

Dabei ist vorausgesetzt, dass $ui(u)$ eine ungerade, $M(u)$ eine gerade Funktion ist. Wir werden die von zahlreichen Autoren benutzte Funktion

$$M(u) = \exp(-a^2 u^2), \quad T(r) = C \exp(-r^2/4a^2) \quad (32)$$

verwenden, die den bei grösseren Winkeln gemessenen Intensitäten das kleinste Gewicht zuteilt. Man sieht nun leicht, dass die ‚wahren‘ Maxima von $(\overline{g_2^{(1)}} - \overline{g_{12}^{(2)}})$ durch die Faltung mit $T(r)$ umso weniger berührt werden, je kleiner a ist, dass andererseits die ‚falschen‘ Maxima umso besser unterdrückt werden, je grösser a ist. Man muss daher durch Probieren den günstigsten Wert von a ermitteln. Dabei sind auch andere Gesichtspunkte von Nutzen, insbesondere die Normierungsbedingungen (18) und (19) und die Forderung, dass die Maxima von $(\overline{g_2^{(1)}} - \overline{g_{12}^{(2)}})$ annähernd mit den aus den Bragg-Reflexen berechneten Radien der Koordinationsschalen zusammenfallen müssen. Wir haben bei unseren Rechnungen nach einigem Probieren $au_0 = 2$ gesetzt. Damit werden die sekundären Maxima weitgehend (wenn auch nicht vollständig) unterdrückt, während die wesentlichen Züge der Funktion erhalten bleiben. Die Fourier-Transformationen wurden mit Hilfe des Fourier-Synthetisators nach Hoppe [24, 25] durchgeführt.

5. ERGEBNISSE

Zur Veranschaulichung der eigentlichen experimentellen Grundlagen zeigt Abb. 5 die Impulszahlen in Abhängigkeit von u (nach Abzug der Wasserstoff-Streuung) für eine Legierung mit 39,5 Atom-% Zn bei 360°C. Die Abbildungen

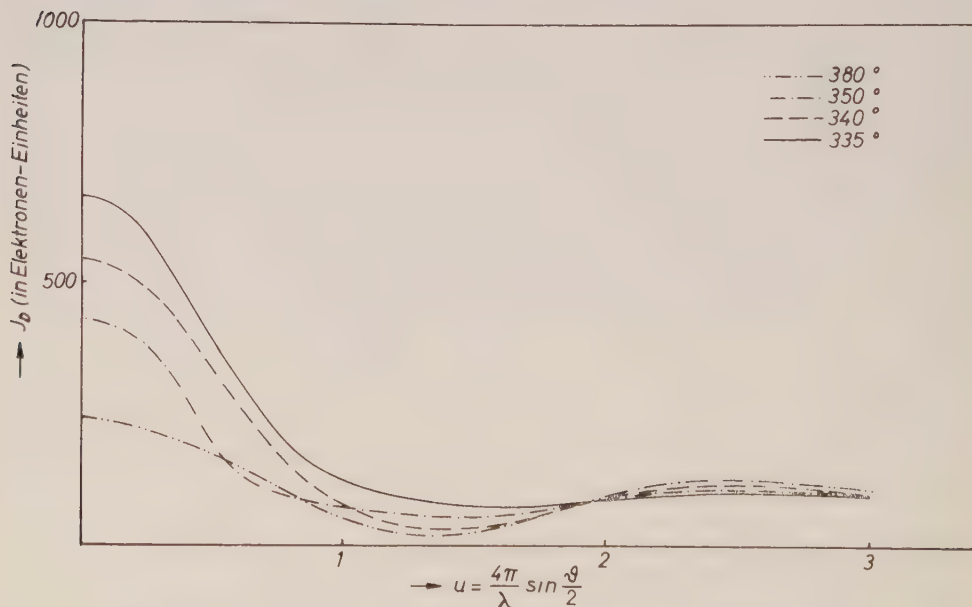


Abb. 6. Auskorrigierte Streukurven der Legierung mit 28,8 Atom-% Zn.

6–8 zeigen für verschiedene Konzentrationen die vollständig auskorrigierten Streukurven für verschiedene Temperaturen. Die der Abb. 8 entsprechende Konzentration ist nach früheren Untersuchungen [12] die kritische Konzentration $x_k = 0,395$. Die zugehörige kritische Temperatur ist $t_k = 351,5 \pm 0,4^\circ\text{C}$. Der kleinste Abstand vom kritischen Punkt beträgt somit ca. $0,5^\circ\text{C}$, doch ist dieser

Wert ziemlich ungenau. Die kritische Temperatur ist jedoch nicht unterschritten worden, da in diesem Falle die Streukurve einen völlig andersartigen Verlauf zeigt.

In Abb. 9–11 sind die durch Fourier-Transformation erhaltenen Funktionen $(\overline{g_2^{(1)}} - \overline{g_{12}^{(2)}})$ für einige der untersuchten Legierungen dargestellt.

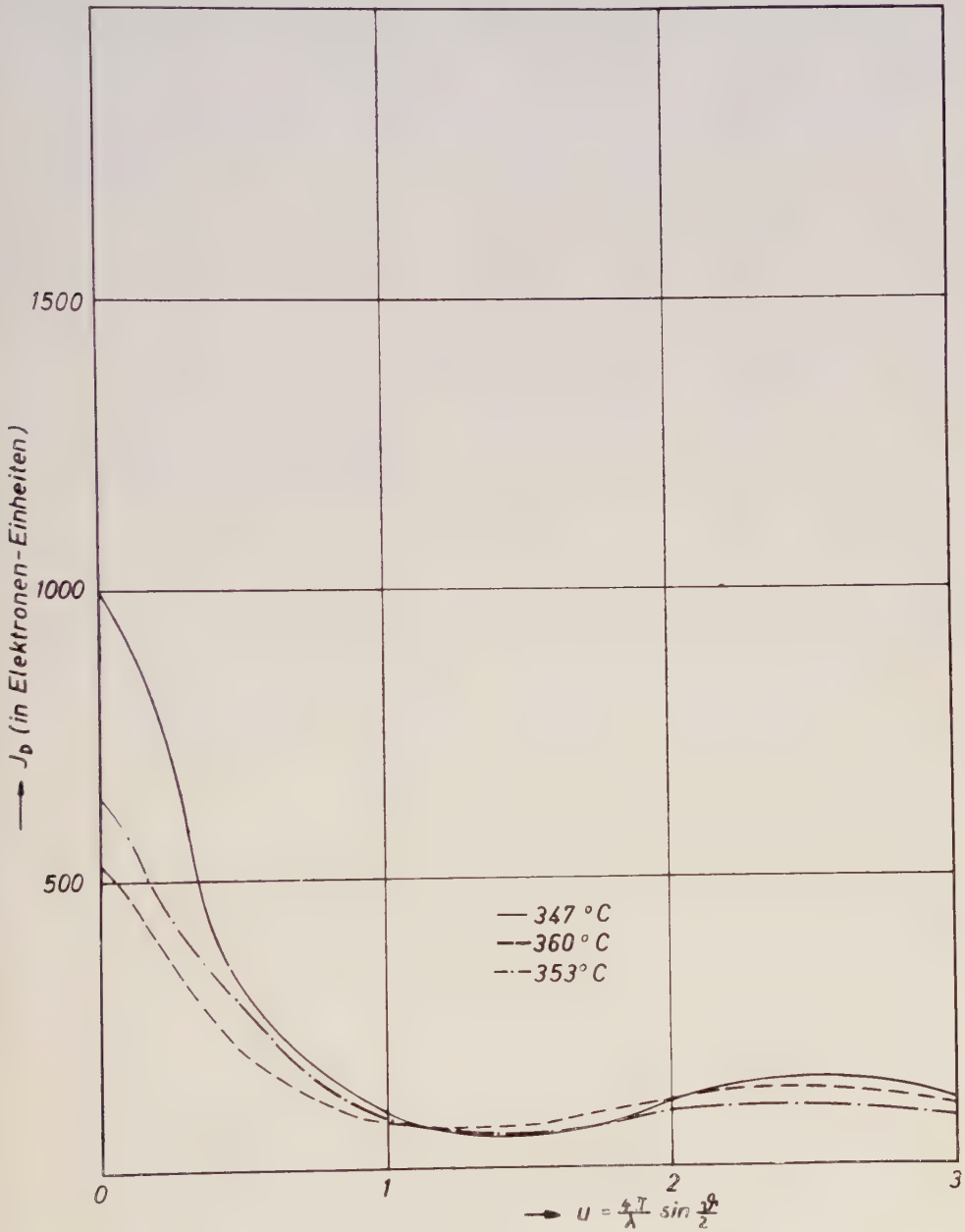


Abb. 7. Auskorrigierte Streukurven der Legierung mit 33 Atom-% Zn.

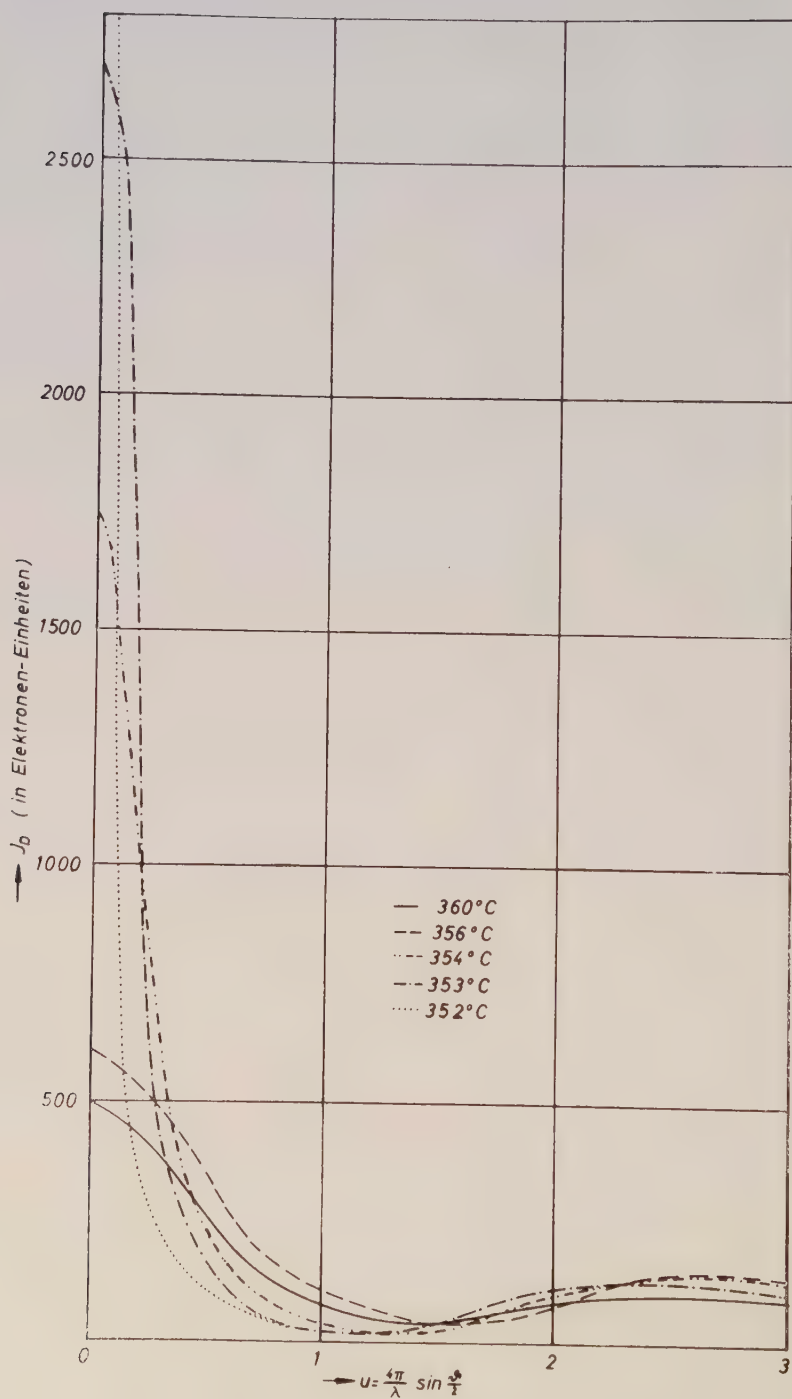


Abb. 8, Auskorrigierte Streukurven der Legierung mit 39,5 Atom-% Zn.

6. DISKUSSION

Die Abb. 6–8 zeigen, dass die Erscheinung der kritischen Opaleszenz bei dem kristallinen System Aluminium-Zink in ganz analoger Weise auftritt wie bei flüssigen Gemischen [5, 21]. Die Zunahme der Streuintensität im Gebiete sehr kleiner Streuwinkel bei der Annäherung an die kritische Temperatur und das Abklingen des Effektes zu beiden Seiten der kritischen Konzentration zeigen für beide Fälle einen ähnlichen Verlauf. Der einzige charakteristische Unterschied besteht darin, dass die kritische Opaleszenz flüssiger Gemische bei Verwendung

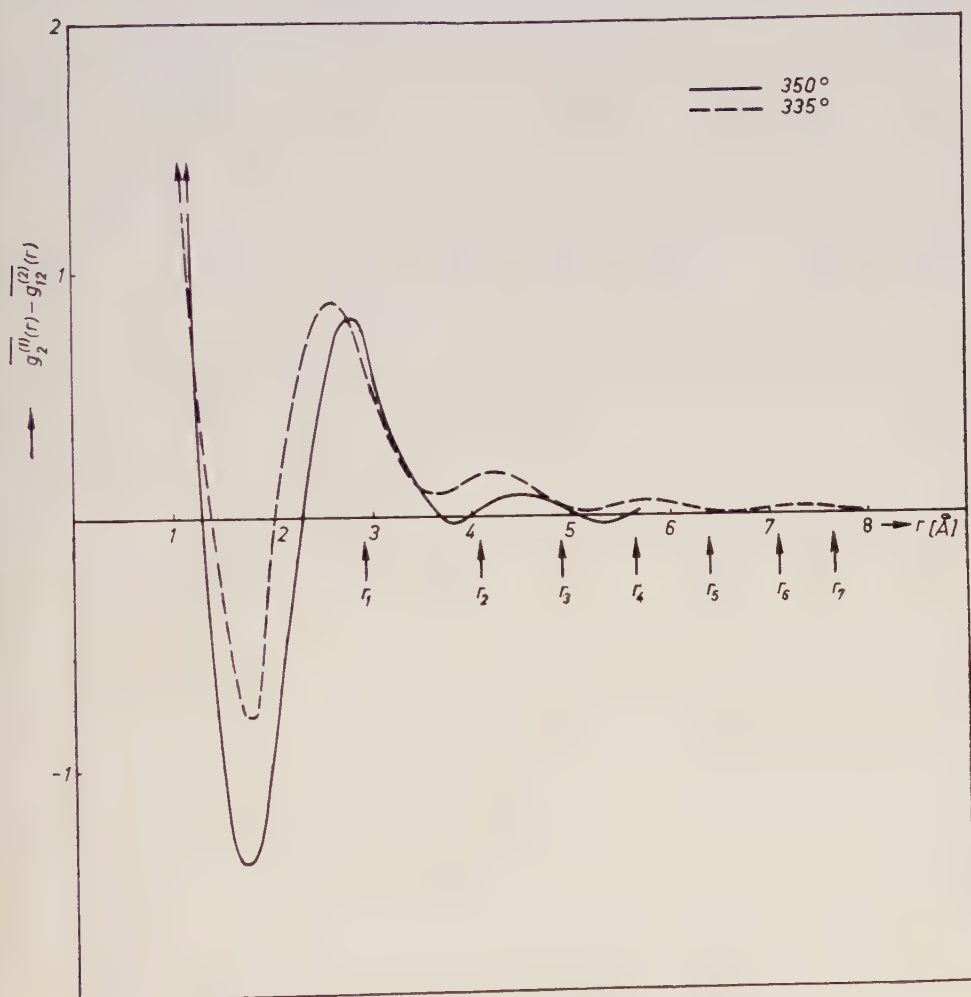


Abb. 9. Korrelationsfunktionen $\overline{g_2^{(1)}} - \overline{g_{12}^{(2)}}$ der Legierung mit 28,8 Atom-% Zn.

von sichtbarem Licht schon 0,5–1°C oberhalb der kritischen Temperatur kaum noch nachzuweisen ist, während sie in unserem Falle noch in einem Abstand von 2–3°C deutlich ist. Dieser Unterschied erklärt sich einfach dadurch, dass Röntgenstrahlen eine wesentlich empfindlichere ‚Sonde‘ für submikroskopische Inhomogenitäten darstellen als sichtbares Licht. Der Verlauf der Streukurven entspricht weitgehend den theoretisch berechneten Kurven der Abb. 3.

Die experimentellen Ergebnisse zeigen eindeutig, dass in der molekularen Struktur der kritischen Phasen kein grundsätzlicher Unterschied zwischen fluiden und kristallinen Systemen besteht. Man muss weiter schliessen, dass in Bezug auf die räumliche Verteilung der Atome sich das innere Gleichgewicht innerhalb der Versuchszeiten bei unseren Messungen vollständig einstellt. Die Anwendung der statistischen Mechanik auf das Problem wird damit unmittelbar gerechtfertigt.

Die in Abb. 9–11 dargestellten Kurven zeigen, dass an der Stelle der ersten Koordinationsschale stets $(\overline{g_2^{(1)}} - \overline{g_{12}^{(2)}}) > 0$ ist. Wir haben somit hier durchweg

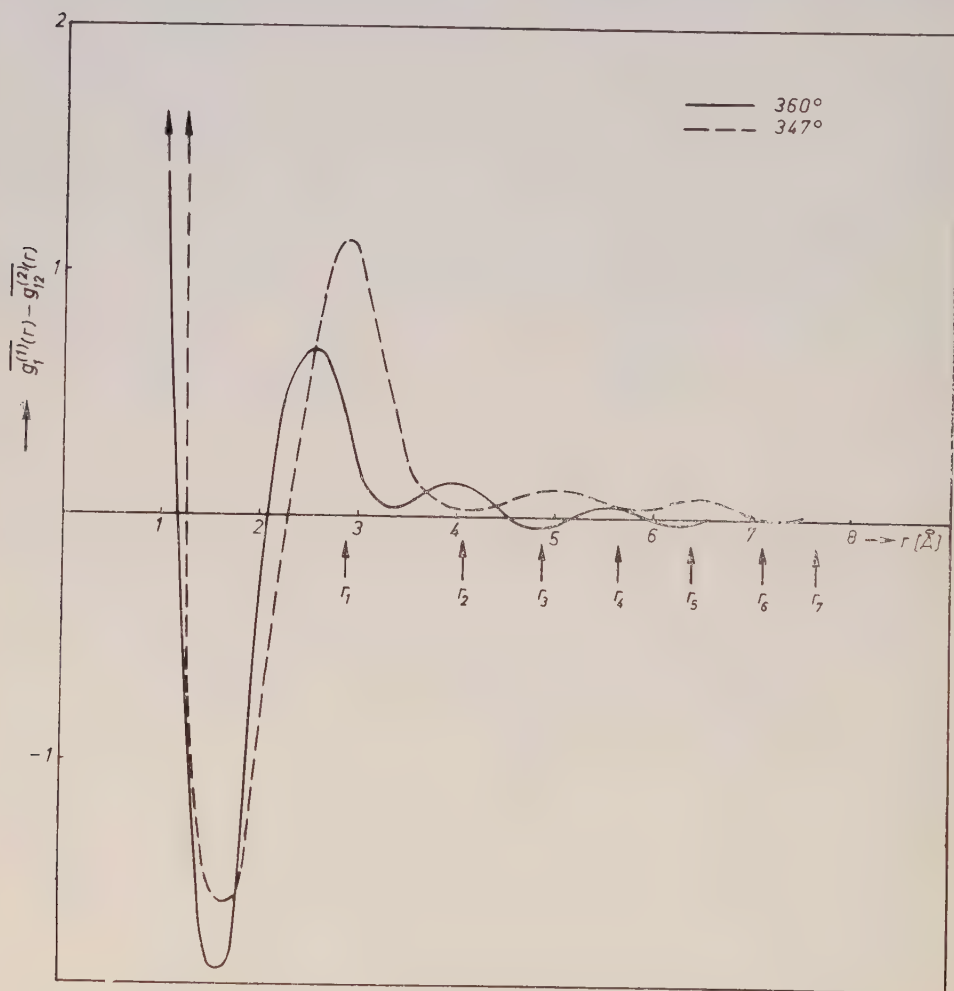


Abb. 10. Korrelationsfunktionen $\overline{g_2^{(1)}} - \overline{g_{12}^{(2)}}$ der Legierung mit 33 Atom-% Zn.

eine Korrelation im Sinne einer cluster-Bildung. Es liegt in der Natur der Sache, dass jeder Versuch, die Reichweite dieser Korrelation exakt zu definieren, innerhalb gewisser Grenzen willkürlich ist. Die von Ornstein und Zernike [1] sowie Fürth [21] vorgeschlagenen Definitionen knüpfen an bestimmte analytische Darstellungen der Korrelationsfunktion an und setzen überdies einen monotonen Abfall voraus. Sie sind daher für unsere Zwecke nicht geeignet. Wir werden

deshalb die Reichweite der Korrelation durch den Wert $r_c \rightarrow r_1$ definieren, für den erstmalig $(\overline{g_2^{(1)}} - \overline{g_{12}^{(2)}}) \approx 0$ wird. Man muss annehmen, dass für $r > r_c$ die Funktion tatsächlich praktisch gleich Null ist, dass aber die aus den Messungen berechnete Kurve in diesem Bereich durch die nicht völlig unterdrückten, 'falschen' Maxima

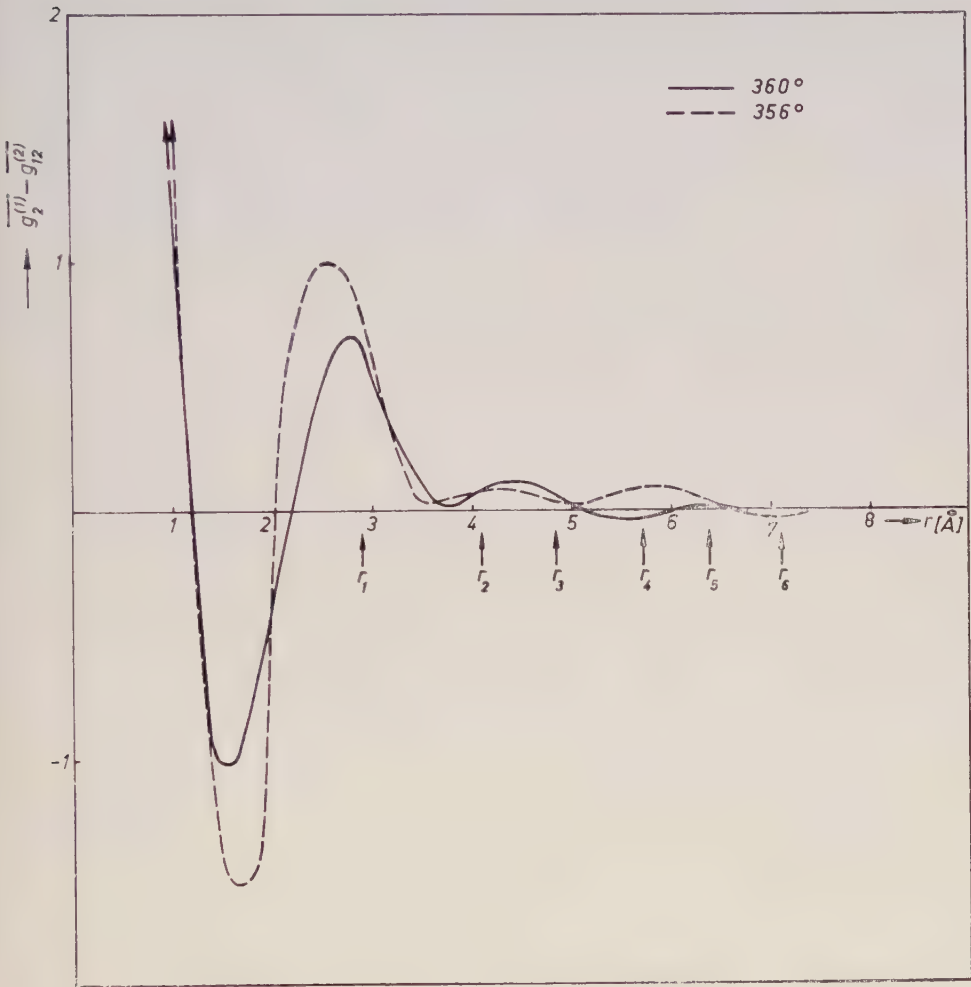


Abb. 11 (a). Korrelationsfunktionen $\overline{g_2^{(1)}} - \overline{g_{12}^{(2)}}$ der Legierung mit 39,5 Atom-% Zn.

ΔT (°C)	r_c (Å)
8,5	5
4,5	7
2,5	10
1,5	14
0,5	31

Tabelle 2. Reichweiten der Korrelation für die kritische Zusammensetzung von Al-Zn.

und Minima bestimmt wird. Dafür spricht insbesondere, dass diese Oszillationen keinerlei Beziehungen zur Gitterstruktur zeigen. In Tabelle 2 sind Korrelationsbereiche r_c für verschiedene Abstände von der kritischen Temperatur ΔT nach unseren Messungen an Aluminium-Zink zusammengestellt.

Bei flüssigen Gemischen wird die untere Grenze der lichtoptischen Nachweisbarkeit, die etwa bei $r_c = 100 \text{ \AA}$ liegt, für $\Delta T = 0,5\text{--}1,0^\circ\text{C}$ erreicht [5, 21]. Man sieht, dass in der Größenordnung ein vernünftiger Zusammenhang mit unseren Ergebnissen besteht.

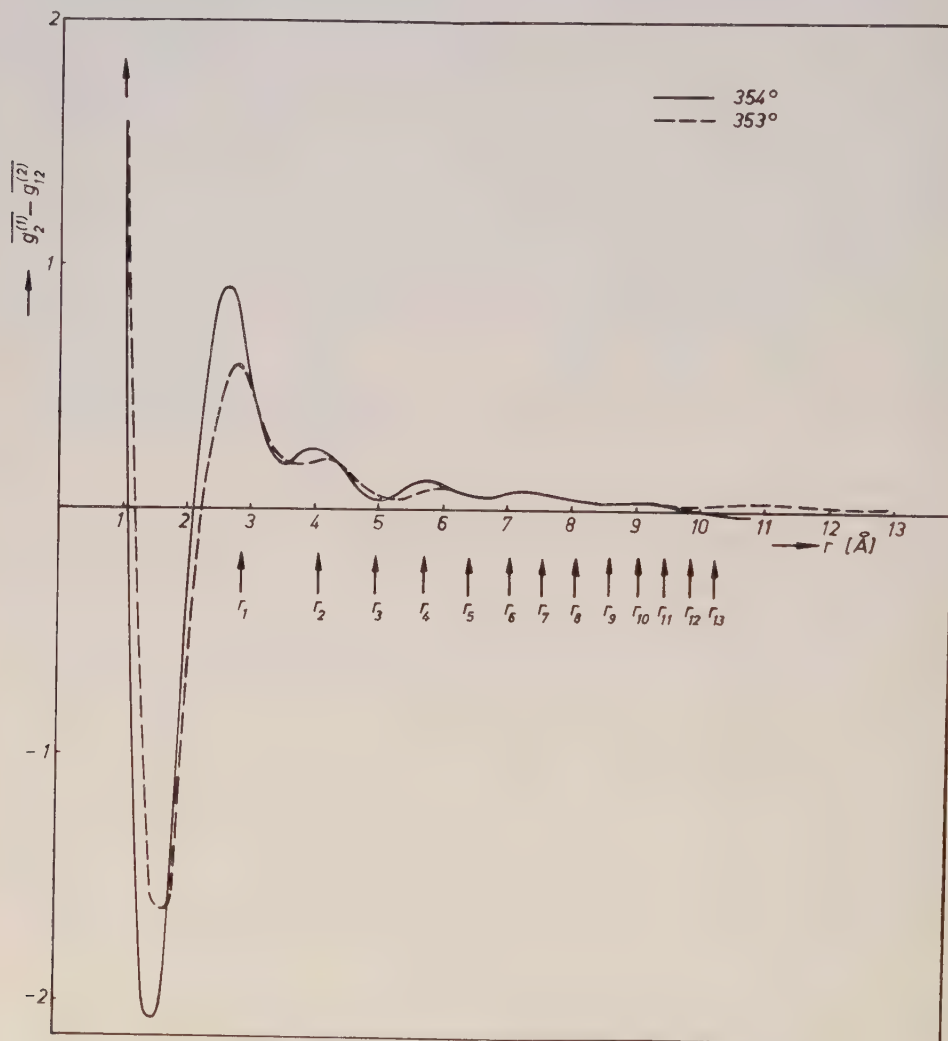


Abb. 11 (b). Korrelationsfunktionen $\overline{g_2^{(1)}} - \overline{g_{12}^{(2)}}$ der Legierung mit 39,5 Atom-% Zn.

Für die Streuung von sichtbarem Licht ist der Begriff der Reichweite der Korrelation aus der Schwankungstheorie entwickelt worden, während wir von den molekularen Verteilungsfunktionen ausgegangen sind. Wir wollen daher zum Schluss noch kurz den Zusammenhang der beiden Konzepte erörtern[†]. Es seien $\delta\rho_1$ und $\delta\rho_2'$ die lokalen Schwankungen der molekularen Dichten in zwei

[†] Die Behandlung dieses Problems bei Fürth und Williams [21] ist nicht korrekt.

Volumenelementen ΔV und $\Delta V'$ im Abstand r . Dann ist die Korrelationsfunktion der Schwankungen

$$g_c^{1,2}(r) = \frac{\overline{(\delta\rho_1\delta\rho_2')}}{(\overline{\delta\rho_1})^2}. \quad (33)$$

Dabei sind die Volumenelemente ΔV und $\Delta V'$ als so gross anzunehmen, dass der

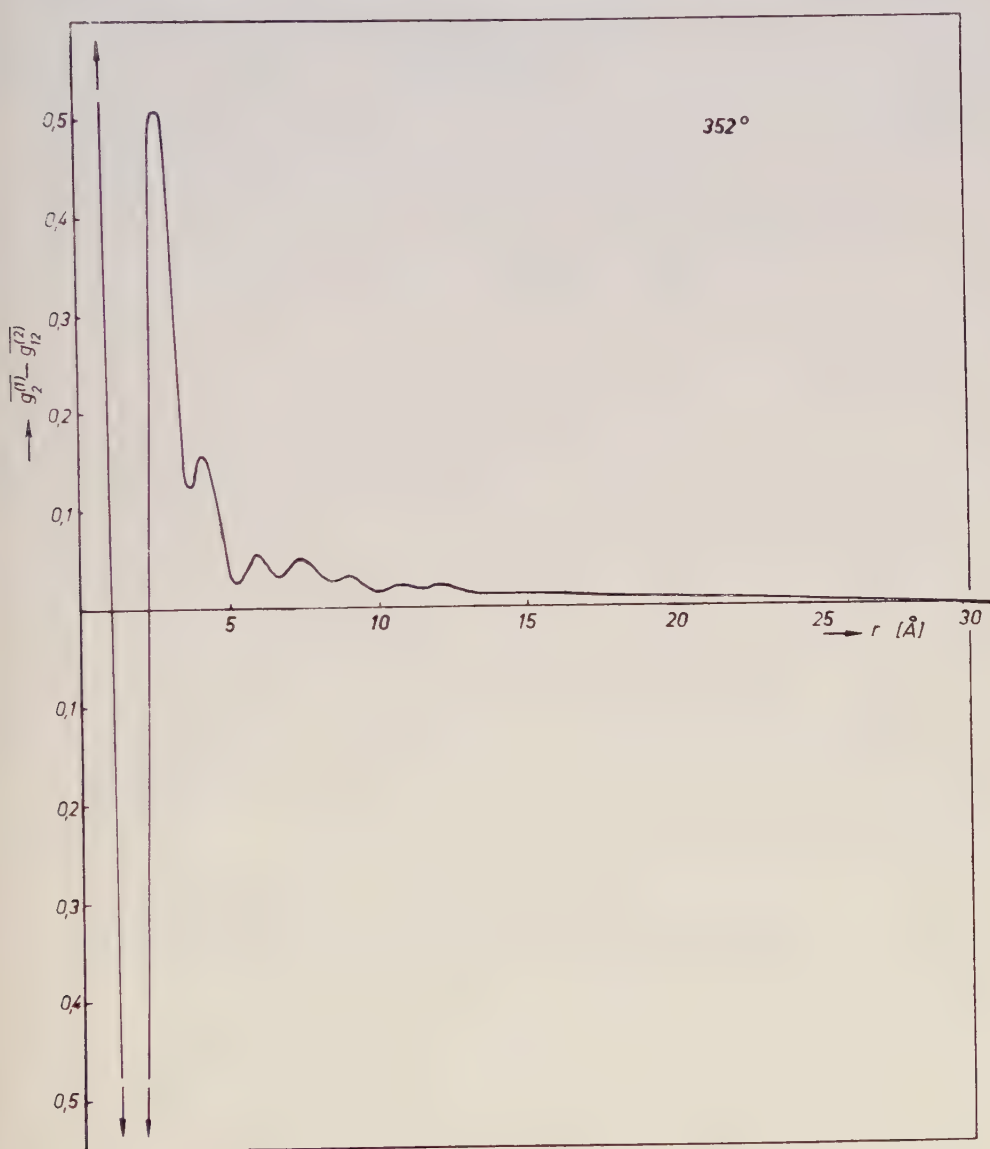


Abb. 11 (c). Korrelationsfunktionen $\overline{g_2^{(1)}} - \overline{g_{12}^{(2)}}$ der Legierung mit 39,5 Atom-% Zn.

Schwankungsbegriff noch einen Sinn hat. Die Wahrscheinlichkeit, ein 1-Atom in ΔV und gleichzeitig ein 2-Atom in $\Delta V'$ zu finden, ist nach Gl. (7), (8) und (10)

$$W_{12} = \int_{\Delta V} \int_{\Delta V'} \rho_1^{(1)} \phi_{12}^* d\mathbf{q}_1 d\mathbf{q}_2' = \rho_1 \Delta V \int_{\Delta V'} \phi_{12} d\mathbf{q}_2. \quad (34)$$

Mitteln wir ϕ_{12} über das Volumen $\Delta V'$, so erhalten wir

$$W_{12} = \rho_1 \Delta V \Delta V' \langle \phi(r) \rangle = \rho_1 \rho_2 \Delta V \Delta V' \langle g_{12}^{(2)}(r) \rangle \quad (35)$$

wobei $r \gg (\Delta V')^{1/3}$ vorausgesetzt ist. Bei gegebener Konfiguration des Systems können wir für die momentanen Dichten in den Volumenelementen ΔV und $\Delta V'$ schreiben

$$\rho_1^* = \rho_1 + \delta\rho_1, \quad \rho_2^{*'} = \rho_2 + \delta\rho_2'. \quad (36)$$

Wegen

$$\overline{\delta\rho_1} = \overline{\delta\rho_2'} = 0 \quad (27)$$

wird dann

$$W_{12} = \rho_1 \rho_2 \Delta V \Delta V' \left[1 + \frac{(\overline{\delta\rho_1 \delta\rho_2'})}{\rho_1 \rho_2} \right]. \quad (38)$$

Aus Gl. (35) und (38) folgt, da

$$\frac{1}{\Delta V'} \int_{\Delta V'} \overline{g_2^{(1)}} d\mathbf{q}_2' = \langle g_2^{(1)} \rangle = 1 \quad (39)$$

ist

$$\langle g_{12}^{(2)} \rangle - \langle g_2^{(1)} \rangle = \frac{\overline{\delta\rho_1 \delta\rho_2'}}{\rho_1 \rho_2}. \quad (40)$$

Die auf der linken Seite stehende Funktion unterscheidet sich, wie man aus Gl. (33) sieht, lediglich durch einen (für gegebene Zustandsgrößen) konstanten Faktor von $g_c^{1,2}(r)$. Dieser Faktor kann hier ausser Betracht bleiben, da er praktisch durch die Normierung bestimmt wird [21]. Es ergibt sich dann, dass die Korrelationsfunktion der Schwankungen im wesentlichen mit unserer Korrelationsfunktion $(\overline{g_2^{(1)}} - \overline{g_{12}^{(2)}})$ identisch ist, wenn diese über die Feinheiten der molekularen Struktur (d.h. in unserem Falle der Gitterstruktur) gemittelt wird und $r \gg \Delta V'^{1/3}$ ist. Unter dieser Voraussetzung erhält man aus beiden Formulierungen die gleiche Reichweite der Korrelation. Bei kleineren r_c -Werten ist die Schwingungstheorie nicht mehr anwendbar, aber mit Hilfe der molekularen Verteilungsfunktionen lässt sich auch hier die gleiche Grösse r_c definieren. Die aus Lichtstreuungs- und Röntgenmessungen erhaltenen Zahlen lassen sich daher unmittelbar zueinander in Beziehung setzen.

Herrn O. Häfner und Frau E. Giehl danken wir für Hilfe bei der Durchführung der Messungen, Frau E. Krämer und Frau I. Penndorf für die Durchführung der numerischen Rechnungen.

By measuring the intensity of diffuse x-ray scattering of the system Al-Zn it is shown for the first time that solid solutions exhibit the phenomenon of critical opalescence as well as liquid solutions and condensing gases. An outline is given of the theoretical background, the experimental technique and the method of evaluation. The correlation functions are calculated from the experimental scattering curves. An estimate is made of the correlation range for the critical composition. About 0.5°C above the critical temperature a value of 31 Å has been found.

En mesurant l'intensité de la diffusion des rayons x aux petits angles dans le système Al-Zn on a démontré pour la première fois l'existence du phénomène d'opalescence critique pour les solutions solides. Un résumé de la théorie est donné. Le dispositif expérimental et les méthodes de calcul sont décrites. Les fonctions de corrélation sont déterminées à

partir des courbes expérimentales corrigées. Les distances de corrélation sont estimées pour l'alliage critique. On trouve une valeur de 31 Å pour une température d'environ 0,5°C au dessus de la température critique.

REFERENCES

- [1] ORNSTEIN, L. S., und ZERNIKE, F., 1918, *Phys. Z.*, **19**, 134; *Ibid.*, **27**, 761, 1926.
- [2] MÜNSTER, A., 1953, *Z. Phys.*, **136**, 179.
- [3] MÜNSTER, A., 1956, *Statistische Thermodynamik* (Berlin).
- [4] MÜNSTER, A., 1956, *Z. Phys.*, **144**, 197.
- [5] ZIMM, B. H., 1950, *J. phys. Chem.*, **54**, 1306.
- [6] RICE, O. K., 1955, *J. chem. Phys.*, **23**, 164.
- [7] GOPAL, R., und RICE, O. K., 1955, *J. chem. Phys.*, **23**, 1614.
- [8] KOHLER, F., und RICE, O. K., 1957, *J. chem. Phys.*, **26**, 1614.
- [9] WENTORF, R. H., 1956, *J. chem. Phys.*, **24**, 607.
- [10] FUCHS, K., 1942, *Proc. roy. Soc. A*, **179**, 340.
- [11] MÜNSTER, A., und SAGEL, K., 1956, *Z. phys. Chem.*, **7**, 267.
- [12] MÜNSTER, A., und SAGEL, K., 1956, *Z. phys. Chem.*, **7**, 296.
- [13] MÜNSTER, A., und SAGEL, K., 1958, *Z. phys. Chem.* (im Druck).
- [14] WAGNER, C. (Privatmitteilung).
- [15] Vorläufige Mitteilung, *Naturwissenschaften*, 1957, **44**, 535.
- [16] MÜNSTER, A., und SAGEL, K., 1957, *Z. phys. Chem.*, **12**, 145.
- [17] SAGEL, K., 1958, *Tabellen zur Röntgenstrukturanalyse* (im Druck).
- [18] YUDOWITCH, K. L., 1949, *J. appl. Phys.*, **20**, 1232.
- [19] GUINIER, A., und FOURNET, G., 1947, *J. Phys. Radium*, **8**, 345.
- [20] KRATKY, O., POROD, G., und KOHOVEC, L., 1951, *Z. Elektrochem.*, **55**, 53.
- [21] FÜRTH, R., und WILLIAMS, C. L., 1954, *Proc. roy. Soc. A*, **224**, 104.
- [22] WASER, J., und SCHOMAKER, V., 1953, *Rev. mod. Phys.*, **25**, 671.
- [23] FLINN, P. A., AVERBACH, B. L., und RUDMAN, P. S., 1954, *Acta cryst.*, **7**, 153.
- [24] HOPPE, W., und PANNKE, K., 1956, *Z. Kristallogr.*, **107**, 451.
- [25] Hersteller : Dr. Ing. K. PANNKE, *Apparatebau* (Karlsruhe-Durlach).

Electron-electron separation in molecular hydrogen

by M. P. BARNETT

I.B.M. United Kingdom Limited, 101 Wigmore Street, London, W.1

F. W. BIRSS and C. A. COULSON
Mathematical Institute, Oxford

(Received 31 January 1957)

Calculations of the mean distance and mean inverse distance between the electrons in the hydrogen molecule show that a Heitler-London wave function exhibits more correlation and a molecular orbital function less correlation than a covalent-ionic wave function. Introduction of an atomic screening constant decreases the mean distance between the electrons.

It is well recognized that in the Heitler-London treatment of the hydrogen molecule, the two electrons are kept too far apart, and in the molecular-orbital treatment they are allowed to come too close together. This could be described by saying that there is too much electron correlation in the former case, and too little (in fact none at all) in the latter. There are two simple ways in which these defects may be partly remedied. In the first we introduce covalent-ionic resonance in the manner of Weinbaum [1], writing for the molecular wave function the familiar expression

$$\psi = N\{[a(1)b(2) + b(1)a(2)] + k[a(1)a(2) + b(1)b(2)]\} \quad (1)$$

where N is a normalizing factor, $a(1)$ and $b(2)$ are $1s$ atomic orbitals of electrons 1 and 2 around nuclei A and B, and k is a parameter. Different values of k lead to various familiar wave functions. Thus

$k=0$ gives the simple Heitler-London functions;

$k=1$ gives the simple molecular-orbital function;

$k=\infty$ gives a pure-ionic function;

$k=\frac{1}{4}$ gives approximately the 'best' energy at the observed equilibrium separation $R=1.4a_0$.

Now Coulson and Fischer [2] have shown that (1) can be rearranged in the form

$$\psi = N'\{[a(1) + b(1)][a(2) + b(2)] + k'[a(1) - b(1)][a(2) - b(2)]\} \quad (2)$$

which is another way of saying that covalent-ionic resonance can be regarded as being formally equivalent to configuration interaction. Here the conventional description of (2) is

$$\psi = C_1(\sigma 1s)^2 + C_2(\sigma^* 1s)^2 \quad (3)$$

where $(\sigma 1s)$ and $(\sigma^* 1s)$ are the lowest bonding and anti-bonding molecular orbitals.

The second way in which the incorrect electron correlation in the H.L. and m.o. theories may be improved is due to Frost and Braunstein [3] who used a "correlated molecular orbital wave function" of the form

$$\psi = N''[a(1) + b(1)][a(2) + b(2)](1 + pr_{12}) \quad (4)$$

where the parameter p has a value about 0.28 in the equilibrium condition, atomic units being used for distance. This relatively large value of p shows how important this electron correlation is. Its presence in (4) clearly has the effect of increasing the mean electron-electron separation $\overline{r_{12}}$, since it emphasizes those parts of the wave function for which r_{12} is large.

In table 1 we report calculations of three quantities, all of which illustrate the effect of k in (1) on electron correlation. The first row shows the mean inter-electron distance $\overline{r_{12}}$, the second row shows the mean inverse distance $(1/r_{12})$, and the third row shows the value of P , where P denotes the probability that one electron is on one side of the plane bisecting AB and the other electron is on the other side. Thus P measures the extent to which the two electrons are separated into the two halves of the molecule; it is an obvious generalization of some quantities introduced by Daudel *et al.* [4]. All the values of table 1 relate to $R = 1.40a_0$.

$k =$ type of function	0 Heitler- London	0.25 Covalent-ionic resonance (eqm.)	0.5	1.0 molecular- orbital	∞ pure ionic	Frost- Braunstein function (4)
$\overline{r_{12}}$ (a) (b)	2.49 2.20	2.44 2.14	2.40 2.10	2.37 2.04	2.25 1.90	
$(1/r_{12})$ (a) (b)	0.529 0.593	0.544 0.617	0.553 0.634	0.566 0.656	0.606 0.721	0.479 (c) 0.540 (c)
P (a) (b)	0.608 0.647	0.565 0.591	0.537 0.551	0.500 0.500	0.392 0.353	

Table 1. Mean values when $R = 1.40a_0$.

- (a) Using atomic orbitals e^{-r} with no screening constants;
- (b) using atomic orbitals e^{-cr} with exponent $c = 1.193$ (Weinbaum [1]);
- (c) taking $p = 0.28$ for both cases (a) and (b).

Table 1 shows that configuration interaction in the m.o. form (3) does increase the mean electron separation by about 4 per cent, an increase which reduces the corresponding potential energy by as much as 0.62 ev. But it would appear from the last column as if even then the restricted form of configuration interaction represented by (3) is not sufficiently effective in separating the electrons. It is also clear from table 1 that introducing a screening constant $c = 1.193$ in the atomic orbitals reduces the mean inter-electronic distance by about $0.3a_0$. In fact the whole charge cloud becomes decidedly more compact.

At first sight it is a little strange that P has such a relatively small value. Even with the Heitler-London type of function the separation of the two electrons into distinct halves of the molecule is very far from complete. But a closer inspection shows that P must not be too large since then there would be no build-up of charge between the nuclei; nor must it be too small since then the two electrons would be able to approach near to each other sufficiently often to give too big an electron-electron repulsion energy $(1/r_{12})$. For this reason it seems doubtful whether the quantity P , as here defined, is a very good one for molecular purposes.

We have made calculations similar to those of table 1 for a variety of internuclear distances R . Table 2 shows some of our results for $\overline{r_{12}}$, supposing always (case (a) of table 1) that the screening parameter $c=1$. The situation previously found at the equilibrium distance $R=1.4a_0$ is found in a similar way for the other R -values considered.

$k=$	0	0.25	0.5	1.0	∞
$R = 1.20$	2.41	2.38	2.35	2.32	2.24
1.40	2.49	2.44	2.41	2.37	2.25
1.80	2.70	2.61	2.55	2.47	2.27
2.00	2.80	2.70	2.62	2.53	2.26
2.50	3.15	2.99	2.86	2.70	2.26

Table 2. Mean values of r_{12} in a_0 .

The chief conclusions from these calculations can be stated very briefly. The H.L. function shows more correlation and the m.o. function shows less correlation than the covalent-ionic (=configuration interaction) function. The introduction of a screening parameter in the component atomic orbitals decreases the mean inter-electron distance by about $0.3a_0$.

APPENDIX

With the normalized wave function (1)

$$N^{-2} = 2(1+k^2)(1+S_{ab}^2) + 8kS_{ab}$$

where

$$S_{ab} = \int a(1)b(1)d\tau_1.$$

Also

$$\overline{r_{12}} = 2N^2\{C_0^1 + k^2D_0^1 + (1+k^2)E_0^1 + 4kM_0^1\}$$

and

$$\overline{(1/r_{12})} = 2N^2\{C_0^{-1} + k^2D_0^{-1} + (1+k^2)E_0^{-1} + 4kM_0^{-1}\}$$

where

$$D_0^1 = 2.1875/c, \quad D_0^{-1} = 5c/8.$$

C_0^1 , E_0^1 and M_0^1 are integrals evaluated by Frost and Braunstein [3]; C_0^{-1} , E_0^{-1} and M_0^{-1} (in the notation of Frost and Braunstein) are molecular integrals given by Kotani *et al.* [5], Roothaan [6] and Linnett and Hirschfelder [7].

The formula for the correlation factor P is

$$P = \frac{1}{2} + N^2(1-k^2)(1-2q)^2$$

where

$$q = 1 - \frac{1}{4}(2+cR)\exp(-cR).$$

This expression is found at once from the definition of P as

$$P = 2 \int_{V_1} \int_{V_2} \psi^2(1, 2) d\tau_1 d\tau_2$$

where V_1 is the 'half' of space associated with nucleus A, and V_2 is the 'half' associated with nucleus B.

Le calcul de la distance moyenne et de la distance inverse moyenne entre les électrons de la molécule d'hydrogène prouve que la fonction d'onde Heitler-London montre une corrélation plus grande, tandis qu'une fonction orbitale moléculaire montre une corrélation plus petite que la fonction d'onde covalente-ionique. L'introduction d'une fonction atomique de l'effet d'écran réduit la distance moyenne entre les électrons.

Berechnungen des durchschnittlichen Abstandes und des durchschnittlichen reziproken Abstandes zwischen den Elektronen in einem Wasserstoff-Molekül zeigen, dass die Heitler-London-Wellenfunktion mehr Korrelation, und die *molecular orbital*-Funktion weniger Korrelation aufweist als die kovalent-ionische Wellenfunktion. Durch die Einführung der atomaren Abschirmungskonstante wird der durchschnittliche Abstand zwischen den Elektronen verringert.

REFERENCES

- [1] WEINBAUM, S., 1933, *J. chem. Phys.*, **1**, 593.
- [2] COULSON, C. A., and FISCHER, Miss I., 1949, *Phil. Mag.*, **40**, 386.
- [3] FROST, A. A., and BRAUNSTEIN, J., 1951, *J. chem. Phys.*, **19**, 1133.
- [4] DAUDEL, R., ODIOT, Mlle S., and BRION, Mme H., 1954, *J. chim. Phys.*, **51**, 74.
- [5] KOTANI, M., AMEMIYA, A., ISHIGURO, E., and KIMURA, T., 1955, *Table of Molecular Integrals* (Tokyo : Maruzen).
- [6] Roothaan, C. C. J., 1955, University of Chicago Technical Report, *Table of Two-center Coulomb Integrals*.
- [7] LINNETT, J. W., and HIRSCHFELDER, J. O., 1950, *J. chem. Phys.*, **18**, 130.

On irreversible processes in quantum mechanics†

by I. PRIGOGINE and M. TODA‡

Faculté des Sciences, Université Libre de Bruxelles

The methods developed by Prigogine and his colleagues are applied to the study of quantum mechanical systems. The density matrix is divided into a slowly varying and an oscillatory part, and asymptotic equations are established for the elements of this matrix. In the representation in which the unperturbed hamiltonian is diagonal, these equations take a particularly simple form for weakly coupled systems: the matrix elements lying on diagonals parallel to the principal diagonal undergo separate transformations. A particular case is that of the diagonal elements themselves; for these the well-known Pauli equations are obtained. As an illustrative example the problem of the frictional forces on an oscillator immersed in a thermostat is considered in detail. The frictional forces introduced by Langevin and Lorentz are special cases of this.

1. INTRODUCTION

In recent papers [1, 2, 3, 4] Prigogine and his co-workers have developed a general theory of irreversible processes in weakly coupled systems based on classical mechanics. The distribution function in phase space is expanded in Fourier series in angle-action space,

$$\rho = \sum_{\{n\}} \rho_{\{n\}}(J_1, \dots, J_N, t) \exp \{i[\sum_k n_k(\alpha_k - \omega_k t)]\}. \quad (1.1)$$

It was then shown that for weakly coupled systems each Fourier coefficient $\rho_{\{n\}}$ satisfies separately an equation of the Fokker-Planck type in the space of the action variables. Some basic properties of the solution of these equations have been obtained. For example it has been shown that

$$\lim_{t \rightarrow \infty} \rho_{\{n\}}(J_1, \dots, J_N, t) = 0, \quad \{n\} \neq \{0\}. \quad (1.2)$$

This permits us the formulation of a limit theorem which generalizes the classical H-theorem: whatever the initial values of the Fourier coefficients, the asymptotic state corresponds to an equilibrium distribution of the action variables and to *spatial homogeneity* (in the absence of external forces). In view of the well-known correspondence between matrix elements and Fourier coefficients one might think that similar results could also be obtained in quantum mechanics. The object of this paper is to show that this is indeed so.

In §2 we summarize the averaging procedure we shall use. It is identical to that we have used for classical mechanics. This averaging procedure is really an extension of the methods of non-linear mechanics for a finite number of degrees of freedom developed mainly by Krylov and Bogolioubov [5]. The main result is that the elements of the density matrix which lie on a parallel to the main diagonal satisfy separate sets of equations. A special case is that of the elements on the main diagonal itself. In this case the well-known Pauli equation is obtained.

† Number 12 of a series of papers devoted to the Statistical Mechanics of Irreversible Processes.

‡ On leave from the Tokyo University of Education, Japan,

In §3 we show that in the classical limit the equations derived by Prigogine and his co-workers are indeed recovered. By a simple correspondence argument it is then possible to show that asymptotically all non-diagonal elements of the density matrix vanish.

In §4 we indicate briefly how our method may be extended to higher orders in the interaction constant.

The rest of the paper is devoted to a simple application: the problem of 'friction' in brownian motion. We apply our procedure to a system consisting of a thermostat which is assumed to be in thermodynamic equilibrium and a small subsystem which in §§ 5–6 is assumed to be an oscillator. We then calculate the relation between the form of the potential energy and the form of the friction due to the coupling with the thermostat. If the coupling is proportional to the coordinate of the oscillator, the friction is proportional to the average velocity ('Langevin force'). On the other hand if the coupling is proportional to the momentum of the oscillator we obtain the Lorentz damping force proportional to the third time derivative of the displacement.

We consider in some detail the effect of a periodic force on the oscillator. This is an example of a simple system in which the 'interference' terms between the external force and the 'collisions' may be exactly calculated.

Another situation to which our method clearly applies is spin relaxation. This will however be treated in a separate paper.

Finally we wish to stress that the considerations developed in this paper apply strictly only to collections of oscillators. In other cases, such as weakly coupled gases, new supplementary terms arise which are of a special interest because they are closely related to the problem of quantum hydrodynamics. But we shall not treat this problem here.

2. AVERAGING PROCEDURE AND LONG TIME EQUATIONS TO ORDER λ^2

Let us start with the well-known equation for the density matrix

$$i\hbar \frac{\partial \rho}{\partial t} = \mathcal{H} \rho - \rho \mathcal{H}, \quad (2.1)$$

where

$$\mathcal{H} = H + \lambda V. \quad (2.2)$$

If we make use of the interaction representation

$$\rho_{\text{in}} = A^{-1} \rho A, \quad V_{\text{in}} = A^{-1} V A, \quad (2.3)$$

with

$$i\hbar \frac{\partial A}{\partial t} = H A, \quad (2.4)$$

we obtain

$$i\hbar \frac{\partial \rho_{\text{in}}}{\partial t} = \lambda (V_{\text{in}} \rho_{\text{in}} - \rho_{\text{in}} V_{\text{in}}). \quad (2.5)$$

More explicitly, in a continuous formalism,

$$\begin{aligned} i\hbar \frac{\partial \rho_{\text{in}}(i, j)}{\partial t} = & \lambda \int dk \{ \exp[-iE(i)t/\hbar] V(i, k) \exp[iE(k)t/\hbar] \rho_{\text{in}}(k, j) \\ & - \rho_{\text{in}}(i, k) \exp[-iE(k)t/\hbar] V(k, j) \exp[iE(j)t/\hbar] \}. \end{aligned} \quad (2.6)$$

This equation replaces relation (2.1) of Brout and Prigogine [1]. We shall also write it

$$\frac{\partial \rho_{in}(i, j, t)}{\partial t} = \lambda X(i, j, \{\rho_{in}\}, t), \quad (2.7)$$

where X is a functional of the whole set of matrix elements ρ_{in} . This is stressed by the bracket notation.

We shall now transform the set of N^2 equation (2.7) into equations which no longer involve the time in a fluctuating way but only in a systematic manner.

2.1. First Order Terms

Let us write

$$\rho_{in}(i, j, t) = \tilde{\rho}_{in}(i, j, t) + \lambda P(i, j, \{\tilde{\rho}_{in}\}, t), \quad (2.8)$$

where $\tilde{\rho}_{in}$ satisfies an equation of the form

$$\frac{\partial \tilde{\rho}_{in}(i, j, t)}{\partial t} = \lambda \Phi(i, j, \{\tilde{\rho}_{in}\}). \quad (2.9)$$

The important point is that $\Phi(i, j, \{\tilde{\rho}_{in}\})$ does not depend explicitly on time. The decomposition (2.7) corresponds therefore to a separation into a systematic and a fluctuating part. Let us introduce (2.9) into (2.5)–(2.6). We then obtain the following simple equation for both Φ and P :

$$\Phi(i, j, \{\tilde{\rho}_{in}\}) + \partial P(i, j, \{\tilde{\rho}_{in}\}, t) / \partial t = X(i, j, \{\tilde{\rho}_{in}\}, t). \quad (2.10)$$

We now identify Φ with the time average of the right-hand side. This time average is taken at constant $\tilde{\rho}_{in}$ and over long times on the scale t .

We shall therefore write

$$\begin{aligned} \Phi(i, j, \{\tilde{\rho}_{in}\}) &= \frac{1}{T} \int_0^T dt X(i, j, \{\tilde{\rho}_{in}\}, t) \\ &= \frac{1}{i\hbar T} \int_0^T dt \int dk \{ \exp[-iE(i)t/\hbar] V(i, k) \exp[iE(k)t/\hbar] \tilde{\rho}_{in}(k, j) \\ &\quad - \tilde{\rho}_{in}(i, k) \exp[-iE(k)t/\hbar] V(k, j) \exp[iE(j)t/\hbar] \} \\ &= \frac{\pi}{i\hbar T} \int dk \left[\delta\left(\frac{E_i - E_k}{\hbar}\right) V(i, k) \tilde{\rho}_{in}(k, j) - \tilde{\rho}_{in}(i, k) \delta\left(\frac{E_k - E_j}{\hbar}\right) V(k, j) \right]. \end{aligned} \quad (2.11)$$

The integral in the right-hand side is finite. For sufficiently long times (2.11) becomes as small as we want. Therefore

$$\Phi(i, j, \{\tilde{\rho}_{in}\}) = 0. \quad (2.12)$$

There exists no systematic first order term. Formula (2.10) gives

$$\begin{aligned} P(i, j, \{\tilde{\rho}_{in}\}, t) &= \frac{1}{i\hbar} \int dk \left\{ \frac{\exp[-i(E_i - E_k)t/\hbar]}{(i/\hbar)(E_i - E_k)} V(i, k) \tilde{\rho}_{in}(k, j) \right. \\ &\quad \left. - \frac{\exp[-i(E_k - E_j)t/\hbar]}{(i/\hbar)(E_k - E_j)} \tilde{\rho}_{in}(i, k) V(k, j) \right\}. \end{aligned} \quad (2.13)$$

2.2. Second Order Terms

We now retain in (2.8) the second order term in λ and write

$$\rho_{\text{in}}(i, j, t) = \tilde{\rho}_{\text{in}}(i, j, t) + \lambda P(i, j, \{\tilde{\rho}_{\text{in}}\}, t) + \lambda^2 Q(i, j, \{\tilde{\rho}_{\text{in}}\}, t) \quad (2.14)$$

with

$$\partial \tilde{\rho}_{\text{in}}(i, j, t) / \partial t = \lambda^2 \Psi(i, j, \{\tilde{\rho}_{\text{in}}\}). \quad (2.15)$$

Again Ψ does not depend explicitly on time.

We now proceed as before to obtain

$$\begin{aligned} \Psi(i, j, \{\tilde{\rho}_{\text{in}}\}) + \partial Q(i, j, \{\tilde{\rho}_{\text{in}}\}, t) / \partial t = & \frac{1}{i\hbar} \int dk [V_{\text{in}}(i, k) P(k, j, \{\tilde{\rho}_{\text{in}}\}, t) \\ & - P(i, k, \{\tilde{\rho}_{\text{in}}\}, t) V_{\text{in}}(k, j)]. \end{aligned} \quad (2.16)$$

Let us again identify Ψ with the time average of the right-hand side

$$\begin{aligned} \Psi(i, j, \{\tilde{\rho}_{\text{in}}\}) = & \frac{1}{(i\hbar)^2 T} \int_0^T dt \iint dk dk' \left\{ \frac{\exp[-i(E_i - E_{k'})t/\hbar]}{i(E_{k'} - E_k)/\hbar} \right. \\ & \times V(i, k) V(k, k') \tilde{\rho}_{\text{in}}(k', j) - \exp[-i(E_i - E_k)t/\hbar] V(i, k) \tilde{\rho}_{\text{in}}(k, k') V(k', j) \\ & \times \frac{\exp[-i(E_{k'} - E_j)t/\hbar]}{i(E_{k'} - E_j)/\hbar} - \frac{\exp[-i(E_i - E_{k'})t/\hbar]}{i(E_{k'} - E_i)/\hbar} V(i, k') \tilde{\rho}_{\text{in}}(k', k) V(k, j) \\ & \left. \times \exp[-i(E_k - E_j)t/\hbar] + \tilde{\rho}_{\text{in}}(i, k') \frac{\exp[-i(E_{k'} - E_j)t/\hbar]}{i(E_{k'} - E_k)/\hbar} V(k', k) V(k, j) \right\}. \end{aligned} \quad (2.17)$$

Using asymptotic expressions for the oscillating exponentials, Ψ generally vanishes for the same reason as Φ . However, the situation changes radically if the system has a sufficient large number of degrees of freedom to use singularity conditions in the sense of Van Hove [6]. The diagonal singularity condition of Van Hove [6] is that

$$\int dk' V(i, k') A(k') V(k', k) = \delta(i - k) F(k) + \text{non-singular part}. \quad (2.18)$$

If we introduce this condition into the first and the fourth term of the right-hand side of (2.17) we see that the singular part of (2.17) gives a non-vanishing contribution to Ψ while the non-singular part does not.

Let us consider an integral of the form

$$\int d\mu V(i, i + \mu) M(i + \mu, i' + \mu + \mu') V(i' + \mu + \mu', i'). \quad (2.19)$$

The difference between (2.19) and (2.18) is that a non-diagonal element is 'sandwiched' between the two matrix elements of V in (2.19), while a diagonal element appears in (2.18). Proceeding as for (2.18) one sees that for all situations in which (2.18) has a diagonal δ singularity (2.19) also has a δ singularity but for $\mu' = 0$. Hence for all μ such that $V(i, i + \mu)$ is different from zero, $V(i' + \mu, i')$ will also be different from zero. On the other hand if μ' is different from zero the number of intermediate states will be less by a factor of order N^\dagger . We may therefore write instead of (2.18),

$$\begin{aligned} \int d\mu V(i, i + \mu) M(i + \mu, i' + \mu + \mu') V(i' + \mu + \mu', i') \\ = \delta(\mu') F(i, i') + \text{non-singular part}. \end{aligned} \quad (2.20)$$

[†] It is easy to verify these statements in the case of interaction between harmonic oscillators.

If we substitute these expressions in (2.17) we obtain (for harmonic oscillators $E_k \sim k$)

$$\begin{aligned} \Psi(i, j, \{\tilde{\rho}_{\text{in}}\}) = & \frac{1}{(i\hbar)^2} \frac{1}{T} \int_0^T dt \int dk \left[\frac{1}{i(E_i - E_k)/\hbar} |V(i, k)|^2 \tilde{\rho}_{\text{in}}(i, j) \right. \\ & - 2 \frac{V(i, k)}{i(E_k - E_i)/\hbar} \tilde{\rho}_{\text{in}}(k, k+j-i) V(k+j-i, j) \\ & \left. + \frac{1}{i(E_j - E_k)/\hbar} \tilde{\rho}_{\text{in}}(i, j) |V(j, k)|^2 \right]. \end{aligned} \quad (2.21)$$

Using a well-known asymptotic formula for $\lim_{\sigma \rightarrow 0} 1/(x - i\sigma)$ we therefore have the second-order equations

$$\begin{aligned} \partial \tilde{\rho}_{\text{in}}(i, j)/\partial t = & - \frac{\lambda^2 \pi}{\hbar^2} \int dk [\delta((E_i - E_k)/\hbar) |V(i, k)|^2 \\ & + \delta((E_j - E_k)/\hbar) |V(j, k)|^2] \tilde{\rho}_{\text{in}}(i, j) \\ & + 2 \frac{\lambda^2 \pi}{\hbar^2} \int dk \delta((E_i - E_k)/\hbar) V(i, k) \tilde{\rho}_{\text{in}}(k, k+j-i) \\ & \times V(k+j-i, j). \end{aligned} \quad (2.22)$$

Let us use the notation

$$\tilde{\rho}_{\text{in}}(i, j, t) = \tilde{\rho}_{\text{in}}(i|l; t) \quad \text{with} \quad l = j - i.$$

We see that (2.22) may also be written

$$\begin{aligned} \partial \tilde{\rho}_{\text{in}}(i|l)/\partial t = & - \frac{\lambda^2 \pi}{\hbar^2} \int dk [\delta((E_i - E_k)/\hbar) |V(i, k)|^2 + \delta((E_j - E_k)/\hbar) |V(j, k)|^2] \tilde{\rho}_{\text{in}}(i|l) \\ & + 2 \frac{\lambda^2 \pi}{\hbar^2} \int dk \delta((E_i - E_k)/\hbar) V(i, k) \tilde{\rho}_{\text{in}}(k|l) V(k+l, l+i). \end{aligned} \quad (2.23)$$

The remarkable fact is that the elements of the density matrix which lie on a parallel to the main diagonal (that is all elements with a given l) satisfy separate sets of equations. Each set corresponds to a given value of l . A special case is $l=0$. Then (2.23) reduces to the Pauli equation for the diagonal elements of the density matrix, namely:

$$\begin{aligned} \partial \tilde{\rho}_{\text{in}}(i|0)/\partial t = & - 2 \frac{\lambda^2 \pi}{\hbar^2} \int dk \delta((E_i - E_k)/\hbar) |V(i, k)|^2 \tilde{\rho}_{\text{in}}(i|0) \\ & + 2 \frac{\lambda^2 \pi}{\hbar^2} \int dk \delta((E_i - E_k)/\hbar) \tilde{\rho}_{\text{in}}(k|0) |V(i, k)|^2. \end{aligned} \quad (2.24)$$

Therefore instead of N^2 equations for the N^2 elements of the density matrix we have N separate sets of equations containing each N unknowns. This is the quantum analogue of the diagonal equations for the Fourier components of the density function obtained by one of us and his collaborators [3, 4].

A further important point is that the equations (2.23) are self-adjoint. If we write them in a discrete notation we obtain

$$\frac{d \tilde{\rho}_{\text{in}}(i|l)}{dt} = \sum_{i'} B_{ii'}^{(l)} \tilde{\rho}_{\text{in}}(i'|l), \quad (2.25)$$

with

$$B_{ii'}^{(l)} = \frac{2\pi\lambda^2}{\hbar^2} \delta_{B_i - E_{i'}} V(i, i') V(i' + l, l + i) = B_{i'i}^{(0)*}, \quad (i \neq i'). \quad (2.26)$$

The approach towards the asymptotic values is therefore described by a real spectrum.

Let us now consider more closely the classical limit of the equations (2.23).

3. CLASSICAL LIMIT—ASYMPTOTIC BEHAVIOUR

For convenience we shall write (2.23) in the form

$$\frac{\hbar^2}{\pi\lambda^2} \frac{d\tilde{\rho}_{\text{in}}(i, j)}{dt} = - \sum_k [\delta(\omega_{ik})|V_{ik}|^2 + \delta(\omega_{jk})|V_{jk}|^2] \tilde{\rho}_{\text{in}}(i, j) + 2 \sum_k \delta(\omega_{ik}) V_{ik} \tilde{\rho}_{\text{in}}(k, k+j-i) V_{k+j-i, j}^* \quad (3.1)$$

It is well known that the classical analogue of every matrix element $A_{KK'}$ is the Fourier component $A_{K-K'}(K')$.† For example the matrix element $\tilde{\rho}_{\text{in}}(i, j)$ becomes the Fourier component $\tilde{\rho}_{\text{in}; i-j}(j)$. Moreover we may in this approximation label the states by the action variables $J_1 \dots J_N$ which are quantized (cf. Brout [7]) according to

$$J_k = n_k \hbar. \quad (3.2)$$

$$(A_{KK'})_s = \frac{1}{2} [A_{K-K'}(K') + A_{K'-K}(K)].$$

The Fourier component V_μ of the potential introduces transitions from $J_1 \dots J_N$ to $J_1 + n_1 \hbar, J_2 + n_2 \hbar, \dots, J_N + n_N \hbar$.

We may therefore write the first term of (3.1) in the form

$$\sum' V_{ik} V_{ki} = \sum_\mu' V_{-\mu}(j+n+\mu) V_\mu(j+n) \quad (\text{with } \mu = k-i, n=i-j) \quad (3.3)$$

$$= \sum_\mu' V_{-\mu}(J+(n+\mu)\hbar) V_\mu(J+n\hbar), \quad (3.4)$$

where the summation is extended over all states conserving energy. We shall now develop (3.3) in the neighbourhood of j . As shown by (3.4) this introduces powers of \hbar . As we are interested only in the classical limit, we may limit ourselves to \hbar^2 . This gives

$$\begin{aligned} \sum_\mu' V_{-\mu}(j+n+\mu) V_\mu(j+n) &= \sum_\mu' \left\{ V_{-\mu}(j) V_\mu(j) + (n+\mu) \left(\frac{\partial V_{-\mu}}{\partial j} V_\mu \right)_s \right. \\ &\quad + n \left(V_{-\mu} \frac{\partial V_\mu}{\partial j} \right)_s + \frac{(n+\mu)^2}{2} \left(\frac{\partial^2 V_{-\mu}}{\partial j^2} V_\mu \right)_s \\ &\quad \left. + \frac{n^2}{2} \left(V_{-\mu} \frac{\partial^2 V_\mu}{\partial j^2} \right)_s + (n+\mu)n \frac{\partial V_{-\mu}}{\partial j} \frac{\partial V_\mu}{\partial j} \right\}. \end{aligned} \quad (3.5)$$

The subscript s indicates the combinations

$$\left(\frac{\partial V_{-\mu}}{\partial j} V_\mu \right)_s = \frac{1}{2} \left(\frac{\partial V_{-\mu}}{\partial j} V_\mu + \frac{\partial V_\mu}{\partial j} V_{-\mu} \right), \quad (3.6)$$

which appear because in (3.3) we have to add to the right-hand side the complex conjugate.

We proceed in exactly the same way for the other terms of (3.1). Adding and then dividing by \hbar^2 we obtain easily

$$\begin{aligned} \frac{\partial \tilde{\rho}_{\text{in}; \{n\}}(J_1, \dots, J_N, t)}{\partial t} &= \pi\lambda^2 \sum_{\{\mu\}} \sum_k \mu_k \mu_{k'} \frac{\partial V_{\{-\mu\}}}{\partial J_k} V_{\{\mu\}} \delta(\sum \mu_k \omega_k) \\ &\quad \times \frac{\partial}{\partial J_{k'}} \tilde{\rho}_{\text{in}; \{n\}}(J_1, \dots, J_N, t) - \pi\lambda^2 \sum_{\{\mu\}} \\ &\quad \times \left(\sum_k n_k \frac{\partial V_{\{-\mu\}}}{\partial J_k} \right) \left(\sum_{k'} n_{k'} \frac{\partial V_{\{\mu\}}}{\partial J_{k'}} \right) \\ &\quad \times \delta(\sum \mu_k \omega_k) \tilde{\rho}_{\text{in}; \{n\}}(J_1, \dots, J_N, t). \end{aligned} \quad (3.7)$$

† It is often more convenient to use the symmetrical formula.

These relations are identical with the equation derived in the classical case by Prigogine and Philippot [3]. They are of the form

$$\frac{\partial \tilde{\rho}_{\{n\}}}{\partial t} = \lambda^2 \Omega \tilde{\rho}_{\{n\}} - \lambda^2 M_{\{n\}}^2 \tilde{\rho}_{\{n\}}, \quad (3.8)$$

where Ω is the differential operator independent of $\{n\}$ which appears in (3.7) and $M_{\{n\}}^2$ a positive function of the actions (with $M_{\{n\}}^2 = M_{\{-n\}}^2$). From (3.8) follows directly the basic theorem that (cf. Prigogine and Philippot [3])

$$\tilde{\rho}_{\{n\}} \rightarrow 0, \quad t \rightarrow \infty \quad \text{for} \quad \{n\} \neq 0. \quad (3.9)$$

This asymptotic theorem is also valid in the quantum case. We may proceed in the following way. A direct proof obtained by Philippot will be published elsewhere.

We may write equation (3.1) in the form

$$\hbar^2 \frac{d\tilde{\rho}_{\{n\}}}{dt} = O_{\{n\}} \tilde{\rho}_{\{n\}}. \quad (3.10)$$

The operator $O_{\{n\}}$ being self-adjoint we have an asymptotic solution for $t \rightarrow \infty$. We now expand both $\rho_{\{n\}}$ and $O_{\{n\}}$ in powers of \hbar

$$\tilde{\rho}_{\{n\}} = \sum \hbar^m \rho_{\{n\}}^{(m)}, \quad O_{\{n\}} = \hbar^2 \sum \hbar^m O_{\{n\}}^{(m)}. \quad (3.11)$$

Substituting in (3.10) we obtain the set of equations:

$$\frac{d\rho_{\{n\}}^{(k)}}{dt} = O_{\{n\}}^{(0)} \rho_{\{n\}}^{(k)} + O_{\{n\}}^{(1)} \rho_{\{n\}}^{(k-1)} + \dots \quad (3.12)$$

Using repeatedly the limit property (3.9) corresponding to the operator $O_{\{n\}}^{(0)}$ we see that $\rho_{\{n\}}^{(m)}$ must vanish for all (m) . We conclude that $\tilde{\rho}_{\{n\}}$ itself vanishes. This proof presupposes the convergence of the expansions (3.11).

As in the classical case, the rate of disappearance of the matrix elements $\tilde{\rho}_{i,j}$ increases rapidly with $(j-i)$.

4. LONG TIME EQUATION TO HIGHER ORDER IN λ

The averaging procedure used in §2 may be extended to every order in λ . For example if we want to retain the third order terms in (2.13)–(2.14) we have to write

$$\rho_{\text{in}}(i, j, t) = \tilde{\rho}_{\text{in}}(i, j, t) + \lambda P(i, j, \{\tilde{\rho}_{\text{in}}\}, t) + \lambda^2 Q(i, j, \{\tilde{\rho}_{\text{in}}\}, t) + \lambda^3 R(i, j, \{\tilde{\rho}_{\text{in}}\}, t), \quad (4.1)$$

with

$$\partial \tilde{\rho}_{\text{in}}(i, j, t) / \partial t = \lambda^2 \psi(i, j, \{\tilde{\rho}_{\text{in}}\}) + \lambda^3 \chi(i, j, \{\tilde{\rho}_{\text{in}}\}). \quad (4.2)$$

Using the same recurrence method as in §2 we successively determine R and χ . We shall not go into details because the procedure is identical with that developed for the classical case by Prigogine and Henin [4]. We shall therefore only indicate a few general results and briefly discuss an example.

The system (4.2) (even including higher orders in λ) is self-adjoint and admits the same asymptotic solution whatever the order λ retained. Therefore

$$\tilde{\rho}_{\text{in}}(i, j, t) \underset{t \rightarrow \infty}{=} 0, \quad (i \neq j). \quad (4.3)$$

The only difference is that now all matrix elements are mixed as time progresses. The set of equations (4.2) is no longer diagonal in the difference $i-j$. Also the use of factorized distributions clearly becomes impossible because even the

equilibrium distribution contains correlations. Once $\tilde{\rho}_{\text{in}}$ is obtained from the 'systematic' equation (4.2), we have to use (4.1) to obtain the density matrix ρ .

Let us illustrate this procedure by an example. We calculate the non-diagonal elements of the density matrix using (4.1). We have, neglecting higher orders in λ ,

$$\rho_{\text{in}}(i, j, t) = \tilde{\rho}_{\text{in}}(i, j) + \lambda P(i, j, \{\tilde{\rho}_{\text{in}}\}, t), \quad (4.4)$$

where $\tilde{\rho}_{\text{in}}$ is the asymptotic solution of (4.2) satisfying (4.3). This gives (cf. (2.13))

$$\rho_{\text{in}}(i, j, t) = \lambda \frac{\exp[-i(E_i - E_j)t/\hbar]}{E_j - E_i} V_{ij}(\tilde{\rho}_{jja} - \tilde{\rho}_{iia}) \quad (i \neq j) \quad (4.5)$$

and (cf. (2.3))

$$\rho(i, j, t) = \lambda V_{ij} \frac{\tilde{\rho}_{jja} - \tilde{\rho}_{iia}}{E_j - E_i} \quad (i \neq j) \quad (4.6)$$

$$= \lambda V_{ij} \frac{\rho_{jj} - \rho_{ii}}{E_j - E_i} \quad (4.7)$$

Here ρ_{jj} , ρ_{ii} are the equilibrium values of the i th and j th diagonal elements. Now the right-hand side of (4.7) is precisely the equilibrium value of $\rho(i, j)$ correct to the first order in λ . To verify this we may take a canonical distribution. Then

$$\rho_{jj} = \exp(-E_j/kT), \quad \rho_{ii} = \exp(-E_i/kT) \quad (4.8)$$

and†

$$\begin{aligned} \rho_{ij} &= \{\exp[-(H_0 + \lambda V)/kT]\}_{ij} = \lambda V_{ij} \frac{\exp(-E_j/kT) - \exp(-E_i/kT)}{E_j - E_i} \\ &= \lambda V_{ij} \frac{\rho_{jj} - \rho_{ii}}{E_j - E_i} \end{aligned} \quad (4.9)$$

in agreement with (4.7).

In conclusion, we may say that one of the advantages of taking $\tilde{\rho}$ as the fundamental quantity is its simple asymptotic behaviour,

$$\tilde{\rho}_{\text{in}} \xrightarrow{t \rightarrow \infty} \begin{bmatrix} [f(H_0)]_{11} & 0 & 0 & \cdot & \cdot \\ 0 & [f(H_0)]_{22} & 0 & \cdot & \cdot \\ \cdot & \cdot & \cdot & \cdot & \cdot \\ \cdot & \cdot & \cdot & \cdot & \cdot \\ \cdot & \cdot & \cdot & \cdot & \cdot \end{bmatrix}, \quad (4.10)$$

in contrast to the more complicated behaviour of the density matrix itself

$$\rho_{\text{in}} \xrightarrow{t \rightarrow \infty} \begin{bmatrix} [f(H)]_{11} & [f(H)]_{12} & \cdot & \cdot & \cdot \\ [f(H)]_{21} & [f(H)]_{22} & \cdot & \cdot & \cdot \\ \cdot & \cdot & \cdot & \cdot & \cdot \\ \cdot & \cdot & \cdot & \cdot & \cdot \\ \cdot & \cdot & \cdot & \cdot & \cdot \end{bmatrix}, \quad (4.11)$$

where $f(H)$ is an arbitrary function of the unperturbed Hamiltonian H_0 in (4.10) and of the complete Hamiltonian H in (4.11).

5. THE PROBLEM OF FRICTION IN BROWNIAN MOTION

Let us consider an oscillator in interaction with a thermostat. We shall write the Hamiltonian in the form (cf. (2.2))

$$\mathcal{H} = H + H' + \lambda V, \quad (5.1)$$

† For similar calculations see, i.e. Chester [8].

where H is the Hamiltonian of the oscillator (including even any external forces), H' of the thermostat and λV the interaction. We may assume without loss of generality that V is of the form

$$V = X(x, p)Q, \quad (5.2)$$

where X is a function of the coordinate and momentum of the oscillator and Q of those of the thermostat.

We shall also assume that the thermostat is at every moment in thermodynamical equilibrium. This is consistent with the weak coupling approximation to which we restrict ourselves here. We shall therefore write

$$\tilde{\rho}_{\text{in}}; n n' N N' = f_{nn'} R_N \delta_{NN'}, \quad (5.3)$$

where n, n' are quantum numbers corresponding to the oscillator and N, N' to the thermostat.

We shall study the time dependence of the average value $\langle x \rangle$ of the coordinate of the oscillator

$$\langle x \rangle = \text{Tr } x \rho = \text{Tr } x_{\text{in}} \rho_{\text{in}}, \quad (5.4)$$

where x_{in} is defined in accordance with (2.3) by

$$x_{\text{in}} = A^{-1} x A. \quad (5.5)$$

The equation of motion for $\langle x \rangle$ may be written

$$d^2 \langle x \rangle / dt^2 + \omega^2 \langle x \rangle = f(t)/m + Y, \quad (5.6)$$

where $f(t)$ is the external force. Relation (5.6) defines the friction Y which we want to study in more detail.

Let us give first some purely mechanical relations. We have here (cf. (2.4))

$$A = \alpha \beta, \quad (5.7)$$

with

$$\left. \begin{aligned} i\hbar \partial \alpha / \partial t &= H \alpha, & -i\hbar \partial \alpha^{-1} / \partial t &= \alpha^{-1} H, \\ i\hbar \partial \beta / \partial t &= H' \beta, & -i\hbar \partial \beta^{-1} / \partial t &= \beta^{-1} H', \end{aligned} \right\} \quad (5.8)$$

and

$$[\alpha, \beta] = 0. \quad (5.9)$$

Also,

$$V_{\text{in}} = X_{\text{in}} Q_{\text{in}}, \quad X_{\text{in}} = \alpha^{-1} X \alpha, \quad Q_{\text{in}} = \beta^{-1} Q \beta, \quad (5.10)$$

$$\partial \rho_{\text{in}} / \partial t = \lambda [X_{\text{in}} Q_{\text{in}}, \rho_{\text{in}}] = (\lambda / i\hbar) \cdot (X_{\text{in}} Q_{\text{in}} \rho_{\text{in}} - \rho_{\text{in}} X_{\text{in}} Q_{\text{in}}). \quad (5.11)$$

Some important relations may be derived by the use of the commutation relations

$$\left. \begin{aligned} \text{Tr } x_{\text{in}} \partial \rho_{\text{in}} / \partial t &= \lambda \text{Tr} [(\partial X_{\text{in}} / \partial p_{\text{in}}) Q_{\text{in}} \rho_{\text{in}}] \\ \text{Tr } p_{\text{in}} \partial \rho_{\text{in}} / \partial t &= -\lambda \text{Tr} [(\partial X_{\text{in}} / \partial x_{\text{in}}) Q_{\text{in}} \rho_{\text{in}}] \end{aligned} \right\}. \quad (5.12)$$

In particular,

$$X = x: \text{Tr } (x_{\text{in}} \partial \rho_{\text{in}} / \partial t) = 0, \quad \text{Tr } (p_{\text{in}} \partial \rho_{\text{in}} / \partial t) = -\lambda \text{Tr } (Q_{\text{in}} \rho_{\text{in}}). \quad (5.13)$$

$$X = p: \text{Tr } (x_{\text{in}} \partial \rho_{\text{in}} / \partial t) = \lambda \text{Tr } (Q_{\text{in}} \rho_{\text{in}}), \quad \text{Tr } (p_{\text{in}} \partial \rho_{\text{in}} / \partial t) = 0. \quad (5.14)$$

In both cases

$$\text{Tr } X_{\text{in}} \partial \rho_{\text{in}} / \partial t = 0, \quad \text{Tr } Q_{\text{in}} \partial \rho_{\text{in}} / \partial t = 0. \quad (5.15)$$

Consider the case in which the subsystem is under an external force (forced oscillation). If the force is $f(t)$

$$H = H^0 - x f(t), \quad H^0 = p^2 / 2m + V(x). \quad (5.16)$$

With this Hamiltonian we get

$$i\hbar\partial\alpha/\partial t = (H^0 - xf(t))\alpha = (p^2/2m + U(x) - xf(t))\alpha(t). \quad (5.17)$$

Time-differentiation yields $([x, p] = 1, [x, p^2] = 2p)$,

$$dx_{\text{in}}/dt = \frac{\partial\alpha^{-1}}{\partial t} x\alpha + \alpha^{-1}x \frac{\partial\alpha}{\partial t} = \alpha^{-1} \left[x, \frac{p^2}{2m} \right] \alpha = \frac{1}{m} \alpha^{-1} p \alpha = \frac{p_{\text{in}}}{m}, \quad (5.18)$$

$$dp_{\text{in}}/dt = \alpha^{-1} [p, U(x) - xf(t)] \alpha = -\alpha^{-1} \frac{\partial U}{\partial x} \alpha + f(t)1, \quad (5.19)$$

so that if $X=x$ (cf. (5.13))

$$\frac{d}{dt} \langle x \rangle = \text{Tr} \left(\frac{dx_{\text{in}}}{dt} \rho_{\text{in}} + x_{\text{in}} \frac{\partial \rho_{\text{in}}}{\partial t} \right) = \text{Tr} \frac{p_{\text{in}}}{m} \rho_{\text{in}}, \quad (5.20)$$

$$\frac{d^2}{dt^2} \langle x \rangle = \frac{1}{m} \text{Tr} \left(\frac{dp_{\text{in}}}{dt} \rho_{\text{in}} + p_{\text{in}} \frac{\partial \rho_{\text{in}}}{\partial t} \right) = -\text{Tr} \left(\alpha^{-1} \frac{\partial U}{\partial x} \alpha \rho_{\text{in}} \right) / m + \frac{f(t)}{m} - \frac{\lambda}{m} \text{Tr} Q_{\text{in}} \rho_{\text{in}}. \quad (5.21)$$

On the other hand if $X=p$ (cf. (5.14))

$$\frac{d\langle x \rangle}{dt} = \text{Tr} \left(\frac{p_{\text{in}}}{m} \rho_{\text{in}} \right) + \lambda \text{Tr} Q_{\text{in}} \rho_{\text{in}}, \quad (5.22)$$

$$\begin{aligned} \frac{d^2\langle x \rangle}{dt^2} &= \frac{1}{m} \text{Tr} \left(\frac{dp_{\text{in}}}{dt} \rho_{\text{in}} + p_{\text{in}} \frac{\partial \rho_{\text{in}}}{\partial t} \right) + \lambda \text{Tr} \left(\frac{\partial Q_{\text{in}}}{\partial t} \rho_{\text{in}} + Q_{\text{in}} \frac{\partial \rho_{\text{in}}}{\partial t} \right) \\ &= -\frac{1}{m} \text{Tr} \left(\alpha^{-1} \frac{\partial U}{\partial x} \alpha \rho_{\text{in}} \right) + \frac{f(t)}{m} + \lambda \text{Tr} \left(\frac{\partial Q_{\text{in}}}{\partial t} \rho_{\text{in}} \right). \end{aligned} \quad (5.23)$$

Irrespective of these special cases

$$\alpha^{-1} \frac{\partial U}{\partial x} \alpha = \frac{\partial U(x_{\text{in}})}{\partial x_{\text{in}}} \quad \text{and} \quad m \frac{d^2 x_{\text{in}}}{dt^2} = -\frac{\partial U(x_{\text{in}})}{\partial x_{\text{in}}} + f(t) \cdot 1. \quad (5.24)$$

Solving this equation of motion we can get x_{in} without calculating the transformation matrix α . The initial condition is, for $t=0$, $\alpha(0)=1$

$$x_{\text{in}}(t=0) = x, \quad (dx_{\text{in}}/dt)_{t=0} = p. \quad (5.25)$$

We consider the case where the subsystem is a harmonic oscillator with proper frequency ω . Then

$$H^0 = \frac{p^2}{2m} + \frac{1}{2} m \omega^2 x^2, \quad (5.26)$$

$$m \frac{d^2 x_{\text{in}}}{dt^2} + m \omega^2 x_{\text{in}} = f(t) \cdot 1. \quad (5.27)$$

Thus

$$x_{\text{in}} = x \cos \omega t + p \frac{\sin \omega t}{m\omega} + \frac{1}{m\omega} \int_0^t f(t') \sin \omega(t-t') dt' \cdot 1, \quad (5.28)$$

$$p_{\text{in}} = -m\omega \sin \omega t + p \cos \omega t + \int_0^t f(t') \cos \omega(t-t') dt' \cdot 1. \quad (5.29)$$

In general $p_{nn'} = (i/\hbar)n(E_n - E_{n'})x_{nn'}$, so that for harmonic oscillators

$$p_{n, n+1} = -im\omega x_{n, n+1}, \quad p_{n, n-1} = im\omega x_{n, n-1}, \quad (5.30)$$

with

$$x_{n, n+1} = \sqrt{\left[\frac{\hbar}{2m\omega} (n+1) \right]}, \quad x_{n, n-1} = \sqrt{\left(\frac{\hbar}{2m\omega} n \right)}. \quad (5.31)$$

We may write

$$x_{in,nn'} = \exp[i(n-n')\omega t]x_{nn'} + \frac{1}{m\omega} \int_0^t f(t') \sin \omega(t-t') dt' \delta_{nn'}, \quad (5.32)$$

$$\frac{1}{m} p_{in,nn'} = i(n-n')\omega \exp[i(n-n')\omega t]x_{nn'} + \frac{1}{m} \int_0^t f(t') \cos \omega(t-t') dt' \delta_{nn'}. \quad (5.33)$$

We are now ready for the statistical treatment. This amounts to finding the explicit expression for $\text{Tr } Q_{in}\rho_{in}$ or for $\text{Tr } [(\partial Q_{in}/\partial t)\rho_{in}]$ in (5.21) or (5.23).

6. STATISTICAL TREATMENT OF THE FRICTION FORCE

Let us use the expansion (2.7) as well as (5.3) in the relations (5.21) or (5.23). We may safely assume that Q_{in} does not contain diagonal elements. Therefore the first term in

$$\text{Tr } Q_{in}\rho_{in} = \text{Tr } Q_{in}\tilde{\rho}_{in} + \lambda \text{Tr } Q_{in}P \quad (6.1)$$

vanishes. The first contribution to the friction comes from the oscillatory part P in the density matrix. Using (2.13) we have here in the absence of external forces,

$$P_{nn'NN''} = \frac{1}{i\hbar} \sum_{n''N'''} \left\{ \frac{\exp[it(\omega_{nn''} + \omega_{NN''})]}{i(\omega_{nn''} + \omega_{NN''})} X_{nn''} Q_{NN''} \tilde{\rho}_{in}; n''n'N''N''' \right. \\ \left. - \tilde{\rho}_{in}; n''n'N''N''' X_{n''n'} Q_{N''N'''} \frac{\exp[it(\omega_{n''n'} + \omega_{N''N''})]}{i(\omega_{n''n'} + \omega_{N''N''})} \right\} \quad (6.2)$$

and

$$\text{Tr } Q_{in}P = \frac{1}{i\hbar} \sum \left\{ \frac{\exp(it\omega_{nn'})}{i(\omega_{nn'} + \omega_{N'N})} X_{nn'} Q_{NN'} Q_{N'N} \tilde{\rho}_{in}; n'nNN \right. \\ \left. - \tilde{\rho}_{in}; n'nN'N' X_{n'n} Q_{NN'} Q_{N'N} \frac{\exp(it\omega_{n'n})}{i(\omega_{n'n} + \omega_{N'N})} \right\} + 0(\lambda). \quad (6.3)$$

Let us use (5.3) and assume that

$$Q = \sum C_\nu Q_\nu, \quad Q_{N_\nu, N_\nu+1}^\nu = \sqrt{(N_\nu+1)}, \quad Q_{N_\nu, N_\nu-1}^\nu = \sqrt{N_\nu}. \quad (6.4)$$

For $X_{nn'}$ we shall also assume that $X_{nn'}$ differs from zero only for $n' = n \pm 1$.

Introducing the asymptotic formula

$$\text{Re} \left\{ \lim_{\eta \rightarrow 0} \frac{1}{\eta + i\epsilon} \right\} = \pi \delta(\epsilon), \quad (6.5)$$

we then have

$$\text{Tr } Q_{in}P = \frac{1}{2i\hbar} \sum_\nu C_\nu^2 \sum_{N_\nu n} \{ (N_\nu+1) \exp(-it\omega) X_{n,n+1} f_{n+1,n} \\ + N_\nu \exp(it\omega) X_{n,n-1} f_{n-1,n} - (N_\nu+1) \exp(it\omega) X_{n,n-1} f_{n-1,n} \\ - N_\nu \exp(-it\omega) X_{n,n+1} f_{n+1,n} \} R_N \\ = \frac{1}{2i\hbar} C_\nu^2 g_\nu \sum_n [\exp(-it\omega) X_{n,n+1} f_{n+1,n} - \exp(it\omega) X_{n,n-1} f_{n-1,n}] \quad (6.6)$$

in which we have made use of the relation $\sum_{(N_\nu)} R_N = 1$, and g_ν is the number of external oscillators of frequency ν .

We shall limit ourselves to two cases:

(1) $X = x$.

The friction term is then

$$Y = -\frac{\lambda}{m} \text{Tr} (Q_{in}\rho_{in}) = -\frac{\lambda^2}{m} \text{Tr} (Q_{in}P) \\ = -\frac{\lambda^2 C_\nu^2 g_\nu}{2\hbar} [-i \exp(-it\omega) x_{n,n+1} f_{n+1,n} + i \exp(it\omega) x_{n,n-1} f_{n-1,n}]. \quad (6.7)$$

However, neglecting higher order terms of λ

$$\frac{d\langle x \rangle}{dt} = \text{Tr} \left(\frac{p}{m} \rho_{\text{in}} \right) = -i\omega \exp(-i\omega t) x_{n, n+1} f_{n+1, n} + i\omega \exp(i\omega t) x_{n, n-1} f_{n-1, n}. \quad (6.8)$$

Therefore the friction is proportional to the average velocity

$$Y = -\gamma \frac{d\langle x \rangle}{dt}, \quad (6.9)$$

with

$$\gamma = \frac{\lambda^2 C_v^2 g_v}{m 2\hbar \omega}. \quad (6.10)$$

The equation of motion is then

$$\frac{d^2\langle x \rangle}{dt^2} + \gamma \frac{d\langle x \rangle}{dt} + \omega^2 \langle x \rangle = 0. \quad (6.11)$$

$$(2) X = p, \quad V = \lambda_1 p Q.$$

The friction term in this case is

$$\begin{aligned} Y_1 &= \lambda_1 \frac{d}{dt} \text{Tr} Q_{\text{in}} \rho_{\text{in}} \\ &= \lambda_1^2 \frac{C_v^2 g_v}{2\hbar} \{ -\omega \exp(-i\omega t) p_{n, n+1} f_{n+1, n} - \omega \exp(i\omega t) p_{n, n-1} f_{n-1, n} \}. \end{aligned} \quad (6.12)$$

For a radiation field interacting with a charged oscillator

$$\lambda_1^2 = \frac{4\pi}{3} \left(\frac{e}{mc} \right)^2, \quad C_v = c \sqrt{\frac{\hbar}{4\pi\nu}}, \quad g_v = \frac{8\pi\nu^2}{c^3},$$

where c is the velocity of light, so that

$$\frac{\lambda_1^2 C_v^2 g_v}{2\hbar} = \frac{2e^2 \omega}{3c^3 m^2}. \quad (6.13)$$

Therefore

$$Y_1 = +\gamma_1 \frac{d^3\langle x \rangle}{dt^3},$$

with

$$\gamma_1 = \frac{2e^2}{3c^3}. \quad (6.14)$$

Hence in this case we have

$$\begin{aligned} \frac{d^3\langle x \rangle}{dt^3} &= \frac{1}{m} \frac{d^2}{dt^2} \langle p \rangle + 0(\lambda^2) = -\frac{\omega^2}{m} \{ \exp(-i\omega t) p_{n, n+1} f_{n+1, n} \\ &\quad + \exp(i\omega t) p_{n, n-1} f_{n-1, n} \} + 0(\lambda^2). \end{aligned} \quad (6.15)$$

The equation of motion is therefore

$$\frac{d^2\langle x \rangle}{dt^2} - \gamma_1 \frac{d^3\langle x \rangle}{dt^3} + \omega^2 \langle x \rangle = 0. \quad (6.16)$$

While in the first case the damping is described by the usual 'Langevin' force of the theory of brownian motion, we recover in the second case the Lorentz damping force.

7. INFLUENCE OF EXTERNAL FORCES

We may repeat in the case of external forces the derivation of §6 using the full expressions of the interaction representation (5.32)–(5.33). We shall limit ourselves to the case

$$X = x; \quad (7.1)$$

the extension to other cases is trivial.

Let us write (5.32) in the form

$$x_{in}; n, n' = \exp(i\omega_{nn'}t)x_{nn'} + \sum_w a_w \exp(i\omega t)\delta_{nn'}. \quad (7.2)$$

The supplementary term due to the external forces modifies the value of P which now becomes (in the case where the thermostat is out of equilibrium)

$$\begin{aligned} P_{nn'NN'} = & \frac{1}{i\hbar} \sum_{n''N''} \left[\left\{ \frac{\exp[it(\omega_{nn''} + \omega_{NN''})]}{i(\omega_{nn''} + \omega_{NN''})} x_{nn''} Q_{NN''} \right. \right. \\ & + \sum_w \frac{\exp[it(\omega + \omega_{NN''})]}{i(\omega_{nn''} + \omega_{NN''})} a_w \delta_{nn''} Q_{NN''} \left. \right\} \tilde{\rho}_{in, n''n'N''N'} - \tilde{\rho}_{in, nn''NN''} \\ & \times \left\{ \frac{\exp[it(\omega_{n''n'} + \omega_{N''N'})]}{i(\omega_{n''n'} + \omega_{N''N'})} x_{n''n'} Q_{N''N'} \right. \\ & \left. \left. + \sum_w \frac{\exp[it(\omega + \omega_{N''N'})]}{i(\omega + \omega_{N''N'})} a_w \delta_{n''n'} Q_{N''N'} \right\} \right]. \quad (7.3) \end{aligned}$$

The external forces therefore introduce supplementary terms into the friction constant (6.7). However the same terms appear also in the average velocity $d\langle x \rangle/dt$, and one obtains the simple equation of motion (cf. (5.21))

$$d^2\langle x \rangle/dt^2 + \gamma d\langle x \rangle/dt + \omega^2\langle x \rangle = f(t)/m. \quad (7.4)$$

Similarly, in the case $X = p$

$$d^2\langle x \rangle/dt^2 - \gamma_1 d^3\langle x \rangle/dt^3 + \omega^2\langle x \rangle = f(t)/m. \quad (7.5)$$

The change of the average value $\langle x \rangle$ is therefore described by the usual equation for forced oscillators with a damping term.

An alternative method is to use

$$P = \frac{1}{i\hbar} \left[\tilde{\rho}_{in}, \int^t X_{in}(t') Q_{in}(t') dt' \right]$$

in calculating the friction. In the special case $X = x$ we get

$$Y = -\frac{i\lambda^2}{\hbar m} \text{Tr} \left\{ \int^t dt' x_{in}(t') [Q_{in}(t') Q_{in}(t) - Q_{in}(t) Q_{in}(t')] \tilde{\rho}_{in}(t) \right\}.$$

But

$$(Q_{in}(t') Q_{in}(t) - Q_{in}(t) Q_{in}(t'))_{NN'} = \frac{c\hbar}{2\pi i} \sum \sin\{2\pi\nu(t' - t)\}/\nu$$

has a δ -character, which enables us to reach (6.11) or (7.4) immediately. The same applies to the case $X = p$.

A more complicated problem is to investigate how the matrix elements themselves $\rho_{in; n''n'N''N'}$ are modified in the presence of external forces, and to investigate the stationary state of our oscillator coupled to the thermostat in such situations. This amounts to calculating the 'interference terms' between collisions and external forces. Such a calculation has already been published by one of us (I. P.) and F. Hénin for classical systems [4]. We shall however reconsider briefly the situation because for the simple case (7.1) it is possible to solve the problem in closed form.

We have to repeat here the calculation of §2. However, new terms are introduced because of the second term of (7.2). We now have, instead of (2.16) (we drop the term $\partial Q/\partial t$),

$$\begin{aligned} \Psi(i, j, \{\tilde{\rho}_{in}\}) = & \frac{1}{i\hbar} \sum_{n''N''} \{ [\exp(it\omega_{nn''})x_{nn''} + \sum_w a_w \exp(i\omega t)\delta_{nn''}] \exp(it\omega_{NN''}) \\ & \times Q_{NN''} P_{n''n'N''N'} - P_{nn''NN''} [\exp(it\omega_{n''n'})x_{n''n'} + \sum_w a_w \exp(i\omega t)\delta_{n''n'}] \\ & \times \exp(it\omega_{N''N'}) Q_{N''N'} \}, \quad (7.6) \end{aligned}$$

with $P_{nn'NN'}$ given by (7.3).

Instead of the four terms of (2.17) we now have 16 expressions. Each of them is reduced using Van Hove's singularity condition (2.18)–(2.19). The calculations are somewhat lengthy but elementary and will not be reproduced.

In the brownian motion case (5.3) the final equation for $f_{nn'}$ is (for $f=f_0 \sin \Omega t$):

$$\begin{aligned} \frac{1}{\gamma} \frac{df_{nn'}}{dt} = & -\frac{1}{2} \{ (n+1) \bar{N}_\nu + n(\bar{N}_\nu + 1) + (n' + 1) \bar{N}_\nu + n'(\bar{N}_\nu + 1) \} f_{nn} \\ & + \sqrt{(nn')} \bar{N}_\nu f_{n-1, n'-1} + (n+1)^{1/2} (n' + 1)^{1/2} (\bar{N}_\nu + 1) f_{n+1, n'+1} \\ & + \frac{f_0 \Omega}{2im\omega(\omega^2 - \Omega^2)} \sqrt{\left(\frac{m\omega}{2\hbar}\right)} \\ & \times \{ (n')^{1/2} f_{n, n'-1} + (n' + 1)^{1/2} f_{n, n'+1} - (n)^{1/2} f_{n-1, n'} - (n+1)^{1/2} f_{n+1, n'} \}. \end{aligned} \quad (7.7)$$

In our special case there occur no terms of higher order in f_0 . This is mainly due to the fact that we considered a harmonic oscillator and chose the simple form (7.1) for the interaction.

The new term in (7.7) is really an 'interference term' between collisions and external forces. It is both proportional to λ^2 (through γ) and to f_0 . It should also be noticed that in (7.7) the change of the matrix element n, n' no longer depends only on the other matrix elements hh' for which $n - n' = h - h'$. The 'diagonal character' of the equation is destroyed.

We see by this example how the method we have developed in §§ 2–4 may be extended to more complicated situations.

The research reported in this paper has been made possible by the support and sponsorship of the Air Research and Development Command, through its European Office.

Les méthodes développées par Prigogine et ses collaborateurs sont appliquées à l'étude des systèmes quantiques. La matrice de densité est décomposée en une partie systématique et une partie oscillatoire. Des équations asymptotiques sont établies pour les éléments de cette matrice. Dans la représentation dans laquelle l'hamiltonien non perturbé est diagonal, ces équations prennent une forme particulièrement simple pour des systèmes faiblement couplés. Alors les éléments de la matrice qui sont parallèles à la diagonale principale se transforment entre eux. Un cas particulier est celui des éléments diagonaux eux-mêmes. Pour ces derniers les équations de Pauli sont obtenues.

À titre d'exemple le problème de la friction d'un oscillateur dans un thermostat est considéré en détail. Les forces de friction de Langevin et de Lorentz sont les cas particuliers de ce problème.

Die von Prigogine und Mitarbeitern entwickelten Verfahren werden zum Studium der quantenmechanischen Systeme angewandt. Die Dichtematrix wird in einen langsam variierenden und einen oszillatorischen Teil zerlegt, und asymptotische Gleichungen werden für die Elemente dieser Matrix aufgestellt. In der Darstellung, wo der ungestörte Hamiltonian die Diagonale bildet, nehmen diese Gleichungen für schwachgekoppelte Systeme eine besonders einfache Form an: die auf zur Hauptdiagonale parallelen Diagonalen liegenden Matrixelemente werden getrennten Transformationen unterworfen. Der Fall der Diagonalelemente ist ein Sonderfall, und es werden für diese Elemente die bekannten Pauli-Gleichungen erhalten. Als ein erläuterndes Beispiel wird das Problem der Reibungskräfte für einen in ein Thermostatbad getauchten Oszillator ausführlich erörtert. Die von Langevin und Lorentz eingeführten Reibungskräfte bilden Sonderfälle dieses Beispiels.

REFERENCES

- [1] BROUT, R., and PRIGOGINE, I., 1956, *Physica*, **22**, 621.
- [2] PRIGOGINE, I., and BALESCU, R., 1957, *Physica*, **23**, 555.
- [3] PRIGOGINE, I., and PHILIPPOT, J., 1957, *Physica*, **23**, 569.
- [4] PRIGOGINE, I., and HÈNIN, F., 1957, *Physica*, **23**, 585.
- [5] BOGOLIUBOV, N., and MITROPOLSKI, J., 1955, *Asymptotic Methods in the Theory of Non-Linear Vibrations* (in Russian), Moscow.
- [6] VAN HOVE, L., 1957, *Physica*, **21**, 517.
- [7] BROUT, R., 1957, *Physica*, **23** (to be published).
- [8] CHESTER, G. V., 1954, *Phys. Rev.*, **93**, 606.

Transport of energy and momentum in a dense fluid of rough spheres

by J. P. VALLEAU

Department of Theoretical Chemistry, University of Cambridge

(Received 15 January 1957; in final form 23 October 1957)

Theoretical values are obtained for the thermal conductivity and the viscosity of a dense fluid of perfectly rough elastic spheres, on the basis of simple assumptions about the pair distribution functions. In this fluid angular momentum may be transferred from the bulk motion of the fluid to the rotations of the individual spheres. The rate of this transfer is given by an anti-symmetric component in the pressure tensor, and involves a coefficient of 'rotational viscosity', analogous to the shear viscosity arising from the symmetric component. The thermal conductivity is found to be twice as great as that for perfectly smooth spheres, while the viscosities involve the moment of inertia of the spheres as well as their mass and radius.

1. INTRODUCTION

Theoretical values have recently been obtained for transport coefficients of fluids of smooth hard spheres, on the basis of simple assumptions as to the pair distribution functions [1, 2, 3]. One of the shortcomings of the smooth sphere model is the neglect of the internal modes of motion available to real molecules; the most important of these, for small molecules, is rotation. A simple model including rotational transfer in collisions was suggested by Bryan [4] in 1894: the particles are again assumed to be hard spheres, but with an 'infinitely rough' surface, such that all components of the relative velocity of the points of contact reverse on collision. Using this 'rough sphere' model we shall here determine, for a dense fluid, the heat flux as a function of the temperature gradient and the pressure tensor as a function both of the rates of strain and of the mean molecular angular velocity.

The basic assumption of these calculations, an extension of that used with the smooth sphere model, is that the two-particle distribution function is given by

$$f_{\alpha\beta} \equiv f(\mathbf{r}_\alpha, \mathbf{v}_\alpha, \mathbf{w}_\alpha; \mathbf{r}_\beta, \mathbf{v}_\beta, \mathbf{w}_\beta) = n^0(\mathbf{r}_\alpha, \mathbf{r}_\beta) \phi_\alpha(\mathbf{v}_\alpha, \mathbf{w}_\alpha) \phi_\beta(\mathbf{v}_\beta, \mathbf{w}_\beta), \quad (1.1)$$

where

(i) $n^0(\mathbf{r}_\alpha, \mathbf{r}_\beta) d\mathbf{r}_\alpha d\mathbf{r}_\beta$ is the probability of finding simultaneously a molecule in $d\mathbf{r}_\alpha$ at \mathbf{r}_α and another in $d\mathbf{r}_\beta$ at \mathbf{r}_β for the fluid in equilibrium. This function will be just that applicable to the smooth sphere model.

(ii) $\phi_\alpha(\mathbf{v}_\alpha, \mathbf{w}_\alpha)$ is the Maxwell-Boltzmann distribution function

$$\phi_\alpha(\mathbf{v}_\alpha, \mathbf{w}_\alpha) = \frac{m^{3.2} I^{3.2}}{(2\pi kT)^3} \exp \left\{ -\frac{m(\mathbf{v}_\alpha - \bar{\mathbf{v}})^2}{2kT} \right\} \exp \left\{ -\frac{I(\mathbf{w}_\alpha - \bar{\mathbf{w}})^2}{2kT} \right\}, \quad (1.2)$$

determined by the local hydrodynamic velocity $\bar{\mathbf{v}}$, the local average molecular angular velocity $\bar{\mathbf{w}}$, and the local temperature T , at the point \mathbf{r}_α . No account is taken of correlation between translational and angular velocities, or between the velocities or angular velocities of neighbouring molecules.

The shortcomings of such distribution functions have previously been pointed out [1, 2, 3], but they have the advantages of being physically clear and of leading directly to explicit values for the transport coefficients.

2. THERMAL CONDUCTION

Acceptance of the distribution function (1.1) involves neglecting, under a temperature gradient, the flux of heat due to a convective mechanism; this is clear from the isotropy of the velocity distribution function. Heat will flow owing to the instantaneous transfer of energy from mass-centre to mass-centre during collisions, however. Consider a small but finite volume ΔV in the fluid, and a short time interval Δt . We define a function $\Delta_{\alpha\beta}$ to be unity if two spheres, initially at $\mathbf{r}_\alpha, \mathbf{v}_\alpha, \mathbf{w}_\alpha$ and $\mathbf{r}_\beta, \mathbf{v}_\beta, \mathbf{w}_\beta$, will collide with each other inside ΔV during the time interval Δt , and otherwise zero. Then, if $\epsilon_{\alpha\beta}$ is the energy passed from the former to the latter during collision, we can write the energy flux [2] as

$$J = \lim_{\Delta t \rightarrow 0} \frac{1}{\Delta V \Delta t} \cdot \frac{1}{2} \int \dots \int f_{\alpha\beta} \Delta_{\alpha\beta} \epsilon_{\alpha\beta} \cdot 2a \mathbf{l} \cdot d\mathbf{r}_\alpha \dots d\mathbf{w}_\beta, \quad (2.1)$$

where $f_{\alpha\beta}$ is our distribution function (1.1), a is the radius of each sphere, and \mathbf{l} is the unit vector along the line of centres ($\alpha \rightarrow \beta$) at collision. The quantity $\epsilon_{\alpha\beta}$ may be determined as a function of $\mathbf{v}_\alpha, \mathbf{w}_\alpha, \mathbf{v}_\beta, \mathbf{w}_\beta$ and \mathbf{l} by an elementary dynamical calculation based on the above definition of 'infinite roughness'. The result is

$$\epsilon_{\alpha\beta} = \frac{m}{2} \left[\frac{I}{I + ma^2} \{(\mathbf{v}_\alpha + a\mathbf{w}_\alpha \times \mathbf{l})^2 - (\mathbf{v}_\beta - a\mathbf{w}_\beta \times \mathbf{l})^2\} + \frac{ma^2}{I + ma^2} \{(\mathbf{v}_\alpha \cdot \mathbf{l})^2 - (\mathbf{v}_\beta \cdot \mathbf{l})^2\} \right]. \quad (2.2)$$

The integral (2.1) can be evaluated by methods described previously [2]. This involves considering the conditions necessary for $\Delta_{\alpha\beta}$ to be non-zero, and finding the value of $n^0(\mathbf{r}_\alpha, \mathbf{r}_\beta)$ for $|\mathbf{r}_\alpha - \mathbf{r}_\beta|$ close to $2a$ —these are in no way different from the case of smooth spheres. The velocity distribution functions are expressed in terms of the temperature gradients, taking the mean temperature at the point of contact of the collision to be T , when the integrations may be carried out to any order in $\text{grad } T$. When this is done to the first order, and the result divided by $-\text{grad } T$, it gives the thermal conductivity

$$\lambda = 4an\chi k \sqrt{\frac{kT}{m\pi}}, \quad (2.3)$$

where n is the number density, m the mass of the spheres, and $\chi = P/nkT - 1$. This is just twice the thermal conductivity of fluids of smooth spheres [1]. It is interesting that this result is independent of the moment of inertia of the spheres.

3. ROTATIONS AND SHEARS

If the fluid is in motion there will be, in general, two contributions to its total angular momentum—that due to the bulk motion of the fluid and that due to the rotations of the molecules. It is evident that angular momentum may be transferred between these two modes. This leads, as was pointed out by Frenkel [5], to an anti-symmetric component in the pressure tensor, in addition to the familiar symmetric component due to the shearing of the fluid.

Suppose that in the fluid there are gradients, $\partial \bar{v}_x / \partial y$ and $\partial \bar{v}_y / \partial x$, of the x and y components of the hydrodynamic velocity, and that the average of the z components of the molecular angular velocities is Ω_z . The velocity gradients may be resolved into a symmetric part $\sigma_z = (\partial \bar{v}_y / \partial x + \partial \bar{v}_x / \partial y) / 2$, and an anti-symmetric part $w_z = (\partial \bar{v}_y / \partial x - \partial \bar{v}_x / \partial y) / 2$; these are, respectively, the pure shear of the fluid and its angular velocity. If P_{xy} is the rate of flow of x -momentum in the y -direction we can write, for small σ_z , w_z , and Ω_z ,

$$P_{xy} = \frac{\partial P_{xy}}{\partial \sigma_z} \sigma_z + \frac{\partial P_{xy}}{\partial w_z} w_z + \frac{\partial P_{xy}}{\partial \Omega_z} \Omega_z. \quad (3.1)$$

From symmetry it may be seen that

$$\frac{\partial P_{xy}}{\partial \sigma_z} - \frac{\partial P_{yx}}{\partial \sigma_z} = 0, \quad (3.2)$$

$$\frac{\partial P_{xy}}{\partial w_z} + \frac{\partial P_{yx}}{\partial w_z} = 0, \quad (3.3)$$

$$\frac{\partial P_{xy}}{\partial \Omega_z} + \frac{\partial P_{yx}}{\partial \Omega_z} = 0. \quad (3.4)$$

Accordingly we write the symmetric and anti-symmetric components of the pressure tensor as

$$P_{xy} + P_{yx} = 4\eta\sigma_z, \quad (3.5)$$

$$P_{xy} - P_{yx} = nI\dot{\Omega}_z = 4\mu(\Omega_z - w_z), \quad (3.6)$$

in which η is the ordinary shear viscosity, and μ is another quantity[†] of the same dimensions, but describing the rate of transfer of angular momentum between its two modes—a 'rotational viscosity'. The first equality of (3.6) just expresses the conservation of angular momentum, for $P_{yx} - P_{xy}$ and $nI\dot{\Omega}_z$ are the rates of increase, per unit volume, of the angular momenta due to bulk motion and molecular rotations, respectively. One could consider including another term $4\mu'(\Omega_z + w_z)$ in the final member of (3.6), but we suppose, with Frenkel, that the angular velocities Ω_z and w_z will tend to approach one another; this is confirmed by the calculation below.

To obtain η and μ we first calculate P_{xy} when the fluid is subjected to arbitrary rates of shear $\partial \bar{v}_x / \partial y$ and $\partial \bar{v}_y / \partial x$, and the average z component of molecular angular velocity, Ω_z , is non-zero. This may be written (cf. (2.1))

$$P_{xy} = \lim_{\Delta t \rightarrow 0} \frac{1}{\Delta V \Delta t} \cdot \frac{1}{2} \int \dots \int f_{\alpha\beta} \Delta_{\alpha\beta} M_{\alpha\beta} \cdot d\mathbf{r}_\alpha \dots d\mathbf{w}_\beta, \quad (3.7)$$

where $M_{\alpha\beta}$ is the transport of x -momentum in the y -direction during the collision of molecules at \mathbf{r}_α , \mathbf{v}_α , \mathbf{w}_α and \mathbf{r}_β , \mathbf{v}_β , \mathbf{w}_β . The quantity $M_{\alpha\beta}$ may, like $\epsilon_{\alpha\beta}$, be obtained by a dynamical calculation; the result is

$$M_{\alpha\beta} = 2am\mathbf{l} \cdot \mathbf{j} \left[\frac{I}{I + ma^2} \{ (\mathbf{v}_\alpha + a\mathbf{w}_\alpha \times \mathbf{l}) \cdot \mathbf{i} - (\mathbf{v}_\beta - a\mathbf{w}_\beta \times \mathbf{l}) \cdot \mathbf{i} \} \right. \\ \left. + \frac{ma^2}{I + ma^2} \{ (\mathbf{v}_\alpha \cdot \mathbf{l} - \mathbf{v}_\beta \cdot \mathbf{l})(\mathbf{l} \cdot \mathbf{i}) \} \right] \quad (3.8)$$

where \mathbf{i} and \mathbf{j} are unit vectors in the x and y directions.

[†] Our coefficient μ , defined by analogy with the shear viscosity, is one-quarter of that defined in Frenkel's discussion.

The velocity distribution functions can be written in terms of the rates of shear and the average molecular angular velocity, when (3.7) can be integrated as before [2]. Keeping only the first order term in each 'force', we obtain

$$P_{xy} = -\frac{2an\chi}{5} \left[\left(\frac{6I+2ma^2}{I+ma^2} \right) \frac{\partial \bar{v}_x}{\partial y} + \left(\frac{I+2ma^2}{I+ma^2} \right) \frac{\partial \bar{v}_y}{\partial x} + \left(\frac{5I}{I+ma^2} \right) \Omega_z \right] \left(\frac{mkT}{\pi} \right)^{1/2}. \quad (3.9)$$

Writing down the corresponding expression for P_{yx} , we can easily confirm the forms of (3.5) and (3.6) and obtain the shear viscosity

$$\eta = \frac{an\chi}{5} \left\{ \frac{7I+4ma^2}{I+ma^2} \right\} \sqrt{\frac{mkT}{\pi}}, \quad (3.10)$$

and the rotational viscosity

$$\mu = an\chi \left\{ \frac{I}{I+ma^2} \right\} \sqrt{\frac{mkT}{\pi}}. \quad (3.11)$$

Unlike the thermal conductivity (2.3), the shear viscosity approaches that for dense fluids of smooth spheres if the moment of inertia of the spheres becomes very small relative to ma^2 . The rotational viscosity, which cannot attain values greater than about half the shear viscosity, must of course vanish for small molecular moments of inertia.

It is not difficult to see that the observable effects of rotational viscosity will be very small indeed for small molecules, for two reasons. First, the average angular velocity of a small molecule at ordinary temperatures is of the order of 10^{10} cycles/sec, while the maximum hydrodynamic angular velocity obtainable in practically realizable flows is 10^7 sec^{-1} †. Hence the energy which can be dissipated by rotational viscosity will be a very small fraction of the total angular kinetic energy. Secondly, the time constant for rotational relaxation is given by

$$\tau = \frac{\Omega_z - w_z}{\dot{\Omega}_z} = \frac{nI}{4\mu} = \frac{I+ma^2}{4a\chi} \left(\frac{\pi}{mkT} \right)^{1/2} = \frac{n}{\eta} \left[\frac{7I+4ma^2}{20} \right].$$

This is of the order of the time between successive collisions of individual molecules, and may be as short as 10^{-12} sec or less.

The author takes pleasure in thanking Professor H. C. Longuet-Higgins for suggesting the problem and for his valuable advice. A scholarship awarded by the National Research Council of Canada is gratefully acknowledged.

En se basant sur de simples suppositions concernant les fonctions de distribution des paires, on obtient des valeurs théoriques pour la conductivité thermique et la viscosité d'un fluide dense consistant en des sphères élastiques parfaitement rugueuses. Dans ce fluide le moment angulaire peut être transféré du mouvement dans la masse du fluide aux rotations des sphères individuelles. La vélocité de ce transport est donnée par une composante antisymétrique du tenseur de la pression et contient un coefficient de la viscosité de rotation, par analogie avec la viscosité de cisaillement qui provient de la composante symétrique. On trouve que la conductivité thermique est deux fois plus grand que pour des sphères parfaitement lisses, tandis que les viscosités contiennent le moment d'inertie des sphères, ainsi que leur masses et rayons.

Von einfachen Annahmen über die Paarverteilungsfunktionen ausgehend, werden theoretische Werte für Wärmeleitfähigkeit und Viskosität eines dichten, aus vollkommen rauhen elastischen Kugeln bestehenden Fluidums (Flüssigkeit) erhalten. Das Winkel-drehmoment kann in dieser Flüssigkeit von der Hauptmassenbewegung der Flüssigkeit zu

† I am indebted to Professor M. J. Lighthill, F.R.S., for this estimate.

Drehungen von Einzelkugeln übertragen werden. Die Übertragungsgeschwindigkeit kann durch eine antisymmetrische Komponente des Drucktensors gegeben werden; sie enthält einen "Drehungviskositätskoeffizienten", ähnlich wie die Scherviskosität aus der symmetrischen Komponente entsteht. Es wurde gefunden, dass die Wärmeleitfähigkeit doppelt so gross ist wie für vollkommen glatte Kugeln, während die Viskositäten sowohl das Trägheitsmoment der Kugeln als auch deren Masse und Radius enthalten.

REFERENCES

- [1] LONGUET-HIGGINS, H. C., and POPLE, J. A., 1956, *J. chem. Phys.*, **25**, 884.
- [2] LONGUET-HIGGINS, H. C., POPLE, J. A., and VALLEAU, J. P., 1956, *Coll. Int. sur les Phénomènes Irreversibles, Brussels* (New York: Interscience Publishers, Inc., in press).
- [3] LONGUET-HIGGINS, H. C., and VALLEAU, J. P., 1956, *Disc. Faraday Soc.*, **22**, 47.
- [4] BRYAN, G. H., 1894, *Brit. Assoc. Reports*, p. 83.
- [5] FRENKEL, J., 1946, *Kinetic Theory of Liquids* (Oxford: University Press), pp. 286 f.

Constant pressure ensembles in statistical mechanics

by W. BYERS BROWN

Department of Chemistry, University of Manchester

(Received 11 May 1957)

A new statistical procedure is described for obtaining the thermodynamic properties of a molecular system directly as functions of the pressure. This procedure differs in principle from that suggested by Guggenheim [3] in that the members of the representative ensemble are envisaged as being in constant mechanical equilibrium with the exterior. The quantal and classical theories of petit micro-canonical and canonical ensembles of systems at constant pressure are presented, and shown to lead to the established results for perfect and imperfect gases, and for a hypothetical one-dimensional system. The conclusion that the statistical compressibility of a molecular system is essentially positive follows directly from the theory. An alternative procedure which leads to a more satisfactory form of Guggenheim's equation is also described, and its relation to the new approach is shown.

1. INTRODUCTION

The members of the ensembles introduced by Gibbs [1] to discuss the statistical mechanics of molecular systems are all supposed to have the same volume V , so that V appears as an independent variable in the fundamental equations. These constant volume ensembles may be characterized by their independent variables as the UVN -ensemble (petit micro-canonical), the TVN -ensemble (petit canonical) and the $TV\mu$ -ensemble (grand canonical). If a particular ensemble is thought of as chosen to represent a physical system because its independent variables are those which it is natural to use to describe the thermodynamic state of the system, then one would expect to be able to set up ensembles in which the pressure P appears as an independent variable instead of the volume; namely, HPN -, TPN - and $TP\mu$ -ensembles. For example, in physical chemistry it is usually more convenient to use the pressure to describe the state of liquids and their mixtures than to use the volume.

Even apart from this logical requirement, since most of the difficulties encountered in applying statistical mechanics are of a mathematical nature, one might hope that the fundamental equations of constant pressure ensembles would prove to be mathematically more tractable than those in which the volume is constant. This is suggested by the well known fact that the treatment of many problems is easier with the $TV\mu$ -ensemble than with the TVN -ensemble, and that in turn this is always easier to handle than the UVN -ensemble. Indeed, this expectation is already borne out in the particular case of a hypothetical one-dimensional system, which has been solved exactly by using what is, in effect, a TPN -ensemble.

It is also worth mentioning a practical argument in support of the use of constant pressure ensembles [2]. In favour of the TVN -ensemble as against the more elementary UVN -ensemble it has been argued that experimentally it is

impossible to realize the complete thermal isolation implied by the latter, and that furthermore the temperature of such a system could not be measured. Similarly, it can be argued that the *TPN*-ensemble is more realistic than the *TVN*-ensemble, since it is impossible to make a vessel with completely rigid walls, and that in any case, in order to measure the pressure of a system it must be provided with a movable wall.

The first discussion of constant pressure ensembles was given by Guggenheim [3], who suggested, by analogy with the relations between the constant volume ensembles, that the fundamental equation for the *TPN*-ensemble should be

$$\exp(-G/kT) = \sum_n \sum_m \exp\{-E_n(V_m)/kT\} \exp(-PV_m/kT), \quad (1.1)$$

where $G(T, P, N)$ is the Gibbs function, $E_n(V)$ is the energy of the n th eigenstate of a system of volume V , and the summations are over all volumes and all eigenstates. However, this equation is meaningless as it stands, since there is no reason for supposing that the volume of a system is not continuously variable, in which case the summation over the volume suffix m diverges. Even if discrete volumes are allowed, an arbitrary elementary unit of volume Λ^3 , whose physical significance is obscure, must be introduced when the transition is made to the integral form. This method is adopted by Hill [4], who is content to note that as long as the elementary length Λ is small but not zero, its exact magnitude is irrelevant when dealing with systems containing large numbers of molecules. Another unsatisfactory feature of the formal method of proceeding by analogy is that none of the authors [3, 4, 5] who have used it to discuss constant pressure ensembles are able to deal with the most elementary of these, the *HPN*-ensemble. The formal similarity between the intensive variables T, P and μ , upon which the method is based, obscures the fact that whereas the thermal and material potentials T and μ have necessarily a statistical character, being foreign to mechanics, the pressure P is a mechanical quantity, and can be introduced prior to any statistical considerations.

The object of this paper is to present a more fundamental conception of constant pressure ensembles which is based on the mechanical nature of the pressure. At the end of the paper an alternative treatment, similar to that of Guggenheim, is outlined, and the relation between the two methods shown.

2. QUANTAL THEORY

The quantal version of the petit canonical or *TVN*-ensemble consists of a large number of identical systems each containing N molecules confined to the same volume V , which are distributed among all the possible eigenstates in such a way that the probability of a system being in the n th eigenstate with energy $E_n(V)$ is proportional to $\exp\{-E_n(V)/kT\}$. The fundamental equation for the thermodynamic properties of the physical system which the ensemble represents is

$$\exp(-F/kT) = \sum_n \exp\{-E_n(V)/kT\}, \quad (2.1)$$

where $F(T, V, N)$ is the statistical analogue of the Helmholtz free-energy function, and the summation is over all eigenstates.

In the conception proposed for the corresponding constant pressure ensemble, the systems of N molecules are again distributed over all possible eigenstates, but

instead of having the same volume V , each system is in mechanical equilibrium with the exterior at constant pressure P . The pressure on the envelope of a system of volume V in the n th eigenstate is

$$P_n = - \frac{dE_n(V)}{dV}, \quad (2.2)$$

so that the 'eigen-pressures' for constant volume V will in general be different for each eigenstate. It is possible, however, for the quantum-mechanical pressure P to be the same for every system if the volume of a system depends on its eigenstate. The 'eigen-volume' of the n th eigenstate, V_n , for constant pressure P is given by the solution of the equation

$$P = - \frac{dE_n(V_n)}{dV_n}. \quad (2.3)$$

An eigen-enthalpy for pressure P , whose derivative is equal to the eigen-volume $V_n(P)$, can then be defined by

$$H_n(P) = E_n[V_n(P)] + PV_n(P). \quad (2.4)$$

The canonical distribution of the TPN -ensemble is therefore such that the probability of finding a system in the n th eigenstate is proportional to $\exp \{-H_n(P)/kT\}$, and the fundamental equation is evidently

$$\exp(-G/kT) = \sum_n \exp\{-H_n(P)/kT\}, \quad (2.5)$$

where $G(T, P, N)$ is the Gibbs' function, and the summation is over all eigenstates, as in equation (2.1). The 'quantization' of the volume, which is arbitrary in Guggenheim's equation (1.1), is thus secured naturally here, and furthermore it is not necessary to sum separately over eigen-energies and eigen-volumes.

The volume $V(T, P, N)$ of an actual system is now a statistical average over all the members of the ensemble, $(\overline{V_n})$, given by

$$V = \left(\frac{\partial G}{\partial P} \right)_{T, N} = \sum_n V_n \exp \{(G - H_n)/kT\}. \quad (2.6)$$

Differentiation of this equation with respect to P gives

$$\left(\frac{\partial V}{\partial P} \right)_{T, N} = \left(\frac{dV_n}{dP} \right) - \frac{(V_n - V)^2}{kT}, \quad (2.7)$$

so that

$$\frac{(\overline{V_n - V})^2}{V^2} = \frac{kT}{V^2} (\beta V - \overline{\beta_n V_n}), \quad (2.8)$$

where $\beta(T, P, N)$ is the thermodynamic isothermal compressibility, and $\beta_n(P, N)$ is the mechanical compressibility of a system in the n th eigenstate. Since β is in general of order V/NkT , the right-hand side of (2.8) is of order $1/N$. Fluctuations in the volume are therefore negligible in general, but will become indefinitely large for two-phase and critical states of the system, as the compressibility β of these states is infinite. Since all the eigenstates are presumably mechanically stable†, it follows from equation (2.8) that

$$\beta \geq \overline{\beta_n V_n} / V \geq 0. \quad (2.9)$$

† This assumption is implicit in the present treatment, but its truth has yet to be established.

The enthalpy $H(T, P, N)$ of an actual system is likewise simply the average enthalpy $\overline{(H_n)}$ of the ensemble, and the fluctuation in enthalpy, which is related to the isobaric heat capacity C_P by

$$C_P = \left(\frac{\partial H}{\partial T} \right)_{P, N} = \overline{(H_n - H)^2} / kT^2, \quad (2.10)$$

is also negligible except for two-phase and critical states of the system. The isobaric thermal expansivity $\alpha(T, P, N)$ is related to the cross fluctuation of volume and enthalpy by the equation

$$\alpha = \overline{(V_n - V)(H_n - H)} / kT^2 V. \quad (2.11)$$

It is interesting to show how equation (2.5) leads to the same expression for the Gibbs' function of a perfect gas as equation (2.1). The eigenstates of a system of N non-interacting particles of mass m confined to a cubical box of volume V have energies

$$E_n(V) = \frac{h^2 n^2}{8mV^{2/3}}, \quad (2.12)$$

where

$$n^2 = \sum_{i=1}^{3N} n_i^2, \quad (2.13)$$

and the n_i are any positive integers (classical statistics). The eigen-volumes for pressure P , defined by equation (2.3), are therefore given by

$$V_n = \left(\frac{h^2 n^2}{12Pm} \right)^{3/5}, \quad (2.14)$$

and the eigen-enthalpies, defined by equation (2.4), by

$$H_n = \frac{5}{2} PV_n. \quad (2.15)$$

Equation (2.5) then becomes

$$\exp(-G/kT) = \sum_n \Omega_n \exp\{-(n/c)^{6/5}\}, \quad (2.16)$$

where Ω_n is the degeneracy of the n th eigenstate with energy E_n , and c is given by

$$c^3 = \left(\frac{kT}{P\lambda^3} \right) \left(\frac{2}{\sqrt{\pi}} \right)^3 \frac{(3/2)^{3/2}}{(5/2)^{5/2}}, \quad (2.17)$$

where

$$\lambda = h/\sqrt{(2\pi mkT)}. \quad (2.18)$$

It is not possible to evaluate the sum in equation (2.16) exactly, but when c is large the sum can be replaced by an integral, and the following approximation, valid for large n , used for the degeneracy Ω_n :

$$\Omega_n = \frac{d}{dn} \left[\frac{(n\sqrt{\pi}/2)^{3N}}{N!(3N/2)!} \right]. \quad (2.19)$$

This leads to the expression,

$$\begin{aligned} \exp(-G/kT) &= \frac{(\sqrt{\pi}/2)^{3N}}{N!(3N/2)!} \int_0^\infty \exp\{-(n/c)^{6/5}\} d(n^{3N}), \\ &= \frac{(c\sqrt{\pi}/2)^{3N} (5N/2)!}{N!(3N/2)!}. \end{aligned} \quad (2.20)$$

When equation (2.17) is substituted for c and Stirling's formula for large factorials is used, the following well known equation for the Gibbs' function is obtained:

$$G = NkT \log (P\lambda^3/kT). \quad (2.21)$$

3. CLASSICAL THEORY

In this section it will be supposed that the system whose statistical properties are being considered consists of N identical molecules each possessing ν degrees of freedom, and that the phase of the system is described by the $2n$ coordinates $p_1, \dots, p_n, q_1, \dots, q_n$ ($n = \nu N$). The fundamental classical equation for a petit canonical or TVN -ensemble of such systems confined within a rigid envelope of volume V is

$$\exp(-F/kT) = \frac{1}{h^n N!} \int \dots \int_{\text{phases}}^{all} (2n) \dots \exp(-\mathcal{H}_V/kT) dp_1 \dots dq_n. \quad (3.1)$$

The classical Hamiltonian $\mathcal{H}_V(p_1, \dots, q_n)$ occurring in this equation is given by

$$\mathcal{H}_V = \mathcal{E} + \mathcal{W}_V, \quad (3.2)$$

where $\mathcal{E}(p_1, \dots, q_n)$ is the Hamiltonian for the molecules in the absence of the enclosing envelope, and $\mathcal{W}_V(q_1, \dots, q_n)$ is the potential energy of interaction of the molecules with the envelope. The latter term is effectively given by

$$\left. \begin{aligned} \mathcal{W}_V &= 0 \text{ if all molecules inside } V, \\ \mathcal{W}_V &= +\infty \text{ if any molecule outside } V, \end{aligned} \right\} \quad (3.3)$$

and therefore restricts the integration over spatial coordinates to configurations within the volume V .

The classical conception of the TPN -ensemble, corresponding to that proposed in § 2, is of systems of molecules in all possible phases, each subject to the condition of mechanical equilibrium with the exterior at constant pressure P . Whereas in the quantal version of this ensemble the pressure P is a quantum-mechanical average for the motion of the molecules confined within a *fixed* volume, in the classical version the movable part of the envelope can be imagined as having no inertia, so that it follows the motion of any molecule with which it is in contact. If the volume enclosed by the envelope when the system is in configuration q_1, \dots, q_n is $\mathcal{V}(q_1, \dots, q_n)$, then the Hamiltonian for the system under constant external pressure P is

$$\mathcal{H}_P = \mathcal{E} + P\mathcal{V}, \quad (3.4)$$

and the canonical distribution function for an isobaric ensemble is proportional to $\exp(-\mathcal{H}_P/kT)$. The fundamental classical equation for the TPN -ensemble is therefore

$$\exp(-G/kT) = \frac{1}{h^n N!} \int \dots \int_{\text{phases}}^{all} (2n) \dots \exp(-\mathcal{H}_P/kT) dp_1 \dots dq_n. \quad (3.5)$$

There remains the problem of determining the form of the *extension function* \mathcal{V} . It may be supposed that the envelope has only one moveable part, and that it encloses a volume $v(\mathbf{q})$ when in contact with a molecule whose configuration is described by the set of ν coordinates \mathbf{q} . The extension function \mathcal{V} is then equal to the largest of the quantities $v(\mathbf{q}_1), \dots, v(\mathbf{q}_N)$ (where $\mathbf{q}_1, \dots, \mathbf{q}_N \equiv q_1, \dots, q_n$). This may be expressed analytically by the formula

$$\mathcal{V}(q_1, \dots, q_n) = \sum_{i=1}^N v_i \prod_{j=1}^N \Delta(v_i - v_j), \quad (3.6)$$

where $v_i = v(\mathbf{q}_i)$, and $\Delta(t)$ is the Heaviside unit-step function, defined by

$$\Delta(t) = \begin{cases} 0 & \text{if } t < 0 \\ 1 & \text{if } t \geq 0 \end{cases}. \quad (3.7)$$

The above arguments leading to equations (3.6) and (3.4) for the extension function and the Hamiltonian for constant pressure are directly physical, and are not immediately related to the transformation used in the quantal version of the ensemble. However, it will now be shown that the same expressions are obtained by following strictly the method of § 2.

The mechanical pressure exerted by the system in phase p_1, \dots, p_n on the containing envelope of volume V is

$$\begin{aligned} \mathcal{P}_V &= - \frac{\partial \mathcal{H}_V}{\partial V}, \\ &= - \frac{\partial \mathcal{W}_V(q_1, \dots, q_n)}{\partial V}. \end{aligned} \quad (3.8)$$

If this pressure is equal to P for all phases of the system, then the extension \mathcal{V} will be a function of the configuration given by the solution of the equation

$$P = - \left(\frac{\partial \mathcal{W}_V}{\partial V} \right)_{V=\mathcal{V}}. \quad (3.9)$$

The mechanical enthalpy or Hamiltonian for constant pressure is then given by

$$\mathcal{H}_P = \mathcal{E} + \mathcal{W}_P + P\mathcal{V}. \quad (3.10)$$

In order to arrive at a definite expression for the extension function \mathcal{V} it is necessary to replace the discontinuous envelope energy function \mathcal{W}_V by a differentiable function which has the same behaviour for a limiting value of some parameter. Since the interactions of the molecules with the envelope may be assumed to be additive, a convenient form is

$$\mathcal{W}_V(q_1, \dots, q_n) = W \sum_{i=1}^N \exp \{ (v_i - V)/\omega \}, \quad (3.11)$$

where W is an arbitrary positive energy constant and ω is a positive volume parameter; this expression has the required behaviour for $\omega > 0$. Differentiation with respect to V gives

$$\mathcal{P}_V = \frac{W}{\omega} \sum_{i=1}^N \exp \{ (v_i - V)/\omega \}; \quad (3.12)$$

therefore the extension function \mathcal{V} at pressure P , defined by (3.9), is given by

$$\mathcal{V} = \omega \log \left[\sum_{i=1}^N \exp (v_i/\omega) \right] - \omega \log (P\omega/W),$$

the limiting value of which is

$$\mathcal{V} = \lim_{\omega \rightarrow 0} \left\{ \omega \log \left[\sum_{i=1}^N \exp (v_i/\omega) \right] \right\}. \quad (3.13)$$

This is easily seen to be equal to the largest volume of the set v_1, \dots, v_N , and is therefore given by the equation (3.6), which was put forward above on directly physical grounds. Since the limiting value of the function \mathcal{W}_P occurring in equation (3.10) is given by

$$\mathcal{W}_P = \lim_{\omega \rightarrow 0} \{ P\omega \} = 0, \quad (3.14)$$

the mechanical enthalpy function defined by that equation is identical with that of equation (3.4).

As in the quantal version of the ensemble, the volume V of an actual system is equal to the average value $\overline{\mathcal{V}}$ of the extension function, and the enthalpy H is the average $\overline{\mathcal{H}_P}$ of the Hamiltonian for constant pressure. The compressibility is given by the equation

$$\beta = -\frac{1}{V} \left(\frac{\partial V}{\partial P} \right)_{T, N} = \overline{(\mathcal{V} - \overline{\mathcal{V}})^2} / kTV, \quad (3.15)$$

which differs in form from the quantal formula derivable from equation (2.7), but is likewise always positive. The isobaric heat capacity is similarly related to the fluctuation of the mechanical enthalpy by

$$C_P = \overline{(\mathcal{H}_P - \overline{\mathcal{H}_P})^2} / kT^2, \quad (3.16)$$

as in the quantal formula (2.10).

For systems with central molecular interactions, the free Hamiltonian \mathcal{E} can be written as

$$\mathcal{E} = \sum_{i=1}^N (\mathbf{p}_i^2 / 2m + \epsilon_i) + \mathcal{U}(\mathbf{r}_1, \dots, \mathbf{r}_N), \quad (3.17)$$

where $\mathbf{p}_1, \dots, \mathbf{p}_N$ and $\mathbf{r}_1, \dots, \mathbf{r}_N$ are the momenta and positions of the centres of mass of the N molecules of mass m , ϵ_i is the Hamiltonian for the internal motion of the i th molecule, and \mathcal{U} is the total intermolecular potential energy of the system. When (3.17) is substituted into equation (3.5), the integrations over translational momenta and internal degrees of freedom can be performed to give

$$\exp(-G/kT) = \frac{\phi^N}{\lambda^{3N} N!} \int \dots \overset{\text{all}}{(N)} \dots \int \exp\{-(\mathcal{U} + P\mathcal{V})/kT\} d^3\mathbf{r}_1 \dots d^3\mathbf{r}_N, \quad (3.18)$$

where λ is defined by equation (2.18) and $\phi(T)$ is the internal partition function for a single molecule. In principle, the equilibrium properties of simple classical fluids can now be obtained by evaluating this configuration integral for constant pressure, as an alternative to the well known configuration integral based on the TVN -ensemble. It should be noticed, however, that no use can be made initially of the condition $P=0$ to simplify the treatment of condensed phases, since the integral then diverges†; this is also true of the sum in the quantal equation (2.5). The extension of equation (3.18) to multi-component systems is obvious.

4. APPLICATION TO GASES

It is interesting to show how the classical equation (3.5) leads to the correct formula for the Gibbs' function of a perfect gas. In this case the potential energy function \mathcal{U} vanishes for all configurations so that equation (3.18) becomes

$$\exp(-G/kT) = \frac{\phi^N}{\lambda^{3N} N!} \int_0^\infty \dots (N) \dots \int_0^\infty \exp(-P\mathcal{V}/kT) dv_1, \dots, dv_N. \quad (4.1)$$

Since \mathcal{V} is homogeneous and of the first degree in the volumes v_i , this equation can be transformed to give

$$\exp(-G/kT) = \frac{(\phi kT/P\lambda^3)^N}{N!} \int_0^\infty \exp(-V) d\Phi(V), \quad (4.2)$$

† This was pointed out to the author by Professor J. de Boer.

where

$$\begin{aligned}\Phi(V) &= \int \dots (N) \dots \int_{0 \leq \mathcal{V} \leq V} dv_1 \dots dv_N, \\ &= V^N.\end{aligned}\quad (4.3)$$

Hence

$$\exp(-G/kT) = (\phi kT/P\lambda^3)^N, \quad (4.4)$$

which for a system of particles (monatomic molecules) is the same as equation (2.21).

The imperfect gas theory of Ursell and Mayer can also be developed using the TPN -ensemble, but the mathematics is slightly more complicated. It is necessary to assume that the well known reducible cluster integrals $b_l(T, V)$ are independent of the volume V whether this is large or small, and this leads to the expansion

$$\exp(-G/kT)(\lambda^3/\phi)^N = \sum_{\{n_l\}} \left(\sum_{l=1}^N n_l \right)! \prod_{l=1}^N \frac{(b_l kT/P)^{n_l}}{n_l!}, \quad (4.5)$$

where the summation over the cluster distribution numbers n_l is subject to the usual condition

$$\sum_{l=1}^N l n_l = N.$$

The method of approximating the sum by its largest term leads naturally to the familiar expansion for the pressure in powers of the activity z :

$$P = kT \sum_{l=1}^N b_l z^l, \quad (4.6)$$

where z is defined by

$$G = NkT \log(z\lambda^3/\phi). \quad (4.7)$$

It is of interest to note, in connection with the $TP\mu$ -ensemble which is discussed in § 9, that the right-hand side of equation (4.5) is the coefficient of z^N in the expansion of

$$P/(P - kT \sum_{l=1}^{\infty} b_l z^l).$$

This promising relationship cannot, however, be easily exploited, and the deduction of equation (4.6) from it requires a careful discussion.

5. MOLECULAR DISTRIBUTION FUNCTIONS

The generic configurational distribution function for a TPN -ensemble of systems with central molecular interactions is

$$\rho^{(N)}(\mathbf{r}_1, \dots, \mathbf{r}_N; T, P, N) = \exp \left\{ \frac{G_* - \mathcal{U} - P\mathcal{V}}{kT} \right\}, \quad (5.1)$$

where $G_*(T, P, N)$ is the configurational Gibbs' function, defined by the normalizing condition

$$\int_{\text{configs}}^3 \dots (N) \dots \int^3 \rho^{(N)} d^3\mathbf{r}_1 \dots d^3\mathbf{r}_N = N!. \quad (5.2)$$

The configurational distribution function for a group of l molecules, $\rho^{(l)}(\mathbf{r}_1, \dots, \mathbf{r}_l)$, can be obtained in the usual way by integrating $\rho^{(N)}$ over all configurations of the remaining $N-l$ molecules, and is normalized to $N!/(N-l)!$. These molecular distribution functions differ markedly from those defined for a TVN -ensemble in

that they are all small for configurations in which any molecule is far from the point or points for which $v(\mathbf{r})=0$, but do not vanish unless one or more molecules is infinitely far removed from this position or surface. Thus even for a perfect gas they are not independent of the configuration, and it can be shown that $\rho^{(l)}$ has the Poisson-like form

$$\begin{aligned}\rho^{(l)} &= (P/kT)^l \exp(-P\mathcal{V}_l/kT) \sum_{m=0}^{N-l} \frac{(P\mathcal{V}_l/kT)^m}{m!}, \\ &= (P/kT)^l \left[1 - \sum_{m=N-l+1}^{\infty} \frac{(P\mathcal{V}_l/kT)^m}{m!} \exp(-P\mathcal{V}_l/kT) \right],\end{aligned}\quad (5.3)$$

where $\mathcal{V}_l(\mathbf{r}_1, \dots, \mathbf{r}_l)$ is the extension function for a group of l molecules, and may be defined by the equation, similar to (3.6),

$$\mathcal{V}_l = \sum_{i=1}^l v_i \prod_{j=1}^{l'} \Delta(v_i - v_j). \quad (5.4)$$

It can be seen from equation (5.3) that for configurations for which \mathcal{V}_l vanishes or is small,

$$\rho^{(l)} = (P/kT)^l = \rho^l, \quad (5.5)$$

where $\rho = N/V$ is the molecular density for the average volume V ; this result agrees with that derived from the TVN -ensemble. For small groups of molecules $\rho^{(l)}$ will be almost constant and equal to ρ^l for configurations within the average volume $V = \mathcal{V}$, but will fall off fairly rapidly for more extended configurations.

6. APPLICATION TO ONE-DIMENSIONAL SYSTEM

It can be seen from § 4 that the treatment of perfect and imperfect gases is more awkward with the TPN -ensemble than with the TVN -ensemble, in so far as it involves multiple integrals of the irreducible kind one usually tries to avoid. The only case in which the TPN -ensemble has so far been shown to give a simpler result than the TVN -ensemble is that of a one-dimensional system of N particles with an arbitrary nearest-neighbour interaction potential $u(r)$. The simple formula for the Gibbs' function was originally obtained by the mathematical device of a Laplace transform (see Münster [5]), but the same result can be obtained directly from equation (3.5), as will now be shown.

Let the N particles be free to move on a semi-infinite straight line, and let their coordinates be x_1, \dots, x_N . Equation (3.5) then takes the form

$$\exp(-G/kT) = \frac{1}{\lambda^N N!} \int_0^\infty \dots (N) \dots \int_0^\infty \exp\{-(\mathcal{U} + P\mathcal{V})/kT\} dx_1 \dots dx_N, \quad (6.1)$$

where the potential energy $\mathcal{U}(x)$ contains $N-1$ terms of the type $u(|x_i - x_j|)$ for the interaction of adjacent particles, and the extension function $\mathcal{V}(x)$ is given by equation (3.6) with $v_i = x_i$ ($i = 1, \dots, N$). Now it is possible to divide the integral into $N!$ equal parts, in each of which the coordinates x are confined to definite ranges between neighbouring coordinates; equation (6.1) can therefore be written

$$\exp(-G/kT) = \frac{1}{\lambda^N} \int_{0 \leq x_1 \leq x_2 \leq \dots \leq x_N \leq \infty} \dots (N) \dots \int \exp\{-(\mathcal{U} + P\mathcal{V})/kT\} dx_1 \dots dx_N. \quad (6.2)$$

To reduce this integral further it is convenient to introduce a new set of N positive coordinates ξ , defined by

$$\xi_1 = x_1, \quad \xi_i = x_i - x_{i-1} \quad (i = 2, 3, \dots, N),$$

so that the potential energy and extension are now

$$\mathcal{U}(\xi) = \sum_{i=2}^N u(\xi_i) \quad \text{and} \quad \mathcal{V}(\xi) = \sum_{i=1}^N \xi_i. \quad (6.3)$$

Equation (6.2) is therefore given by

$$\exp(-G/kT) = \psi^{N-1} kT / P\lambda, \quad (6.4)$$

where

$$\psi(T, P) = \frac{1}{\lambda} \int_0^\infty \exp\{-[u(\xi) + P\xi]/kT\} d\xi; \quad (6.5)$$

the perfect gas factor ($kT/P\lambda$) arises because the centre of mass of the particles is only subject to the force P . For large numbers of particles the Gibbs' function is given effectively by

$$G = -NkT \log \psi, \quad (6.6)$$

as found by other authors.

7. VIRIAL EQUATION

The classical virial equation is very simple to derive for a molecular system subject to constant pressure. This equation is based on Clausius' virial theorem, which states that the average value of the time derivative of the phase function

$$\mathcal{A} = \frac{1}{2} \sum_{i=1}^N \mathbf{p}_i \cdot \mathbf{r}_i \quad (7.1)$$

for a bound system of N particles vanishes; whether this average is a temporal one or over an ensemble need not be specified. The theorem leads directly to the equation

$$\overline{\mathcal{K}} = \frac{1}{2} \sum_{i=1}^N \overline{\mathbf{r}_i \cdot \frac{\partial \mathcal{H}}{\partial \mathbf{r}_i}}, \quad (7.2)$$

where \mathcal{K} is the translational kinetic energy of the system and \mathcal{H} is the Hamiltonian. For a system confined within a movable envelope subject to constant pressure P the Hamiltonian is \mathcal{H}_P , given by equation (3.4), and the free Hamiltonian \mathcal{E} is given by (3.17), so that equation (7.2) becomes

$$\overline{\mathcal{K}} = \frac{1}{2} P \sum_{i=1}^N \overline{\mathbf{r}_i \cdot \frac{\partial \mathcal{V}}{\partial \mathbf{r}_i}} + \frac{1}{2} \overline{\dot{\mathcal{U}}}, \quad (7.3)$$

where

$$\dot{\mathcal{U}}(\mathbf{r}_1, \dots, \mathbf{r}_N) = \sum_{i=1}^N \mathbf{r}_i \cdot \frac{\partial \mathcal{U}}{\partial \mathbf{r}_i}. \quad (7.4)$$

Since the extension function $\mathcal{V}(\mathbf{r}_1, \dots, \mathbf{r}_N)$ is homogeneous and of the third degree in the position coordinates \mathbf{r}_i ,

$$\sum_{i=1}^N \mathbf{r}_i \cdot \frac{\partial \mathcal{V}}{\partial \mathbf{r}_i} = 3\mathcal{V}. \quad (7.5)$$

Hence

$$PV = \frac{1}{3} (2\overline{\mathcal{K}} - \overline{\dot{\mathcal{U}}}), \quad (7.6)$$

where $V = \overline{\mathcal{V}}$ is the average volume; this is the usual form of the virial equation.

Equation (7.6) can also be deduced directly from the fundamental equation (3.5) of the TPN -ensemble (although the use of the virial is really superfluous when working with this ensemble). The deduction is simple because the Gibbs' function is independent of the scale of the coordinates used to describe a configuration.

Therefore in equation (3.18) $\mathbf{r}_1, \dots, \mathbf{r}_N$ can be replaced everywhere by $\gamma\mathbf{r}_1, \dots, \gamma\mathbf{r}_N$, where γ is an arbitrary dimensionless parameter, to give

$$\exp(-G/kT) = \frac{\phi^N}{\lambda^3 N!} \int^3 \dots \overset{\text{all}}{(N)} \dots \int^3 \gamma^{3N} \exp \left\{ \frac{-\mathcal{U}(\gamma\mathbf{r}) - \gamma^3 P \mathcal{V}(\mathbf{r})}{kT} \right\} d^3\mathbf{r}_1 \dots d^3\mathbf{r}_N. \quad (7.7)$$

Equation (7.6) is obtained by differentiating this integral with respect to γ , and setting γ equal to unity.

It is interesting to compare the formula obtained by differentiating equation (7.7) twice with respect to γ with the analogous formula obtained from the fundamental equation of the *TVN*-ensemble, since both formulae involve the compressibility. That derived from (7.7) is

$$-P^2 \left(\frac{\partial V}{\partial P} \right)_T = PV + \frac{1}{9} \overline{\ddot{\mathcal{U}}} + \overline{(\dot{\mathcal{U}} - \overline{\dot{\mathcal{U}}})^2} / 9kT, \quad (7.8)$$

where

$$\ddot{\mathcal{U}}(\mathbf{r}_1, \dots, \mathbf{r}_N) = \sum_{i=1}^N \mathbf{r}_i \cdot \frac{\partial \dot{\mathcal{U}}}{\partial \mathbf{r}_i}; \quad (7.9)$$

the compressibility for the *TPN*-ensemble is also given by the simple equation (3.15), and is therefore always positive. The formula derived from the *TVN* ensemble is

$$-V^2 \left(\frac{\partial P}{\partial V} \right)_T = PV + \frac{1}{9} \overline{\ddot{\mathcal{U}}} - \overline{(\dot{\mathcal{U}} - \overline{\dot{\mathcal{U}}})^2} / 9kT, \quad (7.10)$$

where the bar now denotes the average over a *TVN*-ensemble; in this case there is no alternative equation for the compressibility, and it is far from obvious that it must be positive.

8. PERTURBATION THEORY

As mentioned in § 1, it is frequently convenient to employ a statistical equation in which the temperature and pressure are independent variables. This is particularly the case when developing perturbation treatments to be applied to liquids. A general equation for calculating the thermodynamic effects of perturbations in molecular interactions can easily be obtained from the classical equation (3.5). If the total intermolecular potential energy function of the unperturbed system is \mathcal{U} , and that of the perturbed system is $\mathcal{U} + \delta\mathcal{U}$, the change δG in the Gibbs' function at constant temperature and pressure can be expanded by the method of cumulants to give

$$\delta G = \overline{\delta\mathcal{U}} - \overline{(\delta\mathcal{U} - \overline{\delta\mathcal{U}})^2} / 2kT + \overline{(\delta\mathcal{U} - \overline{\delta\mathcal{U}})^3} / 6(kT)^2 - \dots, \quad (8.1)$$

where the bar denotes the average over the *TPN*-ensemble of unperturbed systems. Particular cases in which this method could have been used to advantage instead of the *TVN*-ensemble analogue are the theory of conformal solutions [6, 7] and the theory of ordering in mixtures of Lennard-Jones molecules [8].

9. OTHER CONSTANT PRESSURE ENSEMBLES

It was pointed out in § 1 that the most elementary of the constant pressure ensembles, the *HPN*-ensemble, is notably absent from the lists of ensembles given by Guggenheim [3], by Hill [4] and by Münster [5]. This micro-canonical ensemble is readily described by using the conception of constant pressure ensembles introduced in this paper. It consists of systems of N molecules

subject to the same external pressure P , and having their enthalpies distributed in a small range ΔH about some value H . In the quantal version the fundamental equation is simply

$$\exp(S/k) = \Omega, \quad (9.1)$$

where Ω is the degeneracy of the eigenstate with volume V and energy $E(V, N)$, such that

$$-\frac{dE}{dV} = P \quad \text{and} \quad E + PV = H; \quad (9.2)$$

the degeneracy Ω can then be regarded as a function of the variables H, P, N instead of the usual set $U(=E), V, N$. In the classical theory the situation is formally similar: the distribution in phase is proportional to the Dirac delta function $\delta(H - \mathcal{H}_P)$ where \mathcal{H}_P is the Hamiltonian for constant pressure P , given by equation (3.4), and the fundamental equation is (9.1) where Ω is now the extension in phase (in units of the quantum h) for enthalpies in the range ΔH ; that is

$$\Omega = \frac{1}{h^n N!} \int \dots \overset{\text{all}}{(2n)} \dots \int \delta\left(\frac{H - \mathcal{H}_P}{\Delta H}\right) dp_1 \dots dq_n. \quad (9.3)$$

This HPN -ensemble is evidently related to the TPN -ensemble in exactly the same way that the UVN - and TVN -ensembles are related.

The only other constant pressure ensemble of interest is the $TP\mu$ -ensemble, which corresponds to Gibbs' grand canonical or $TV\mu$ -ensemble. The fundamental equation for an ensemble of this type, involving a triple summation over energy, volume and molecular content, was proposed by Guggenheim [3] but was later criticized by Prigogine [9]. The criticism is essentially that there is nothing to limit the extent of the systems of the ensemble, since the distribution parameters T, P and μ are all intensive variables, and the summation in the proposed fundamental equation is therefore bound to diverge. This criticism renders impossible any straightforward treatment of the $TP\mu$ -ensemble, whether it is developed from Guggenheim's TPN -ensemble or from that of the present paper. Hill [4] has attempted to re-instate this 'generalized ensemble' by restricting the summation, but this complication destroys the only advantage in the use of the ensemble, namely, its simplicity. The method of the present paper suggests a simple $TP\mu$ -ensemble in which the extent V and molecular content N of each system are adjusted to its eigenstate so that its pressure is equal to P and its molecular potential is equal to μ ; the fundamental equation would therefore only involve a single summation over all eigenstates. This idea cannot be carried through, however, because the transition from a system of N molecules to one with $N+1$ molecules, or vice versa, cannot be made 'adiabatic', and therefore the molecular potential μ cannot be defined mechanically. It seems preferable to obtain the relation between T, P and μ from the TPN -ensemble by putting $G = N\mu$ and taking the limit $N \rightarrow \infty$ (or alternatively by taking the limit $V \rightarrow \infty$ with the $TV\mu$ -ensemble). In the case of multi-component systems a 'petit-grand' ensemble can be used, in which the total number of molecules in each system is the same, but systems with every possible composition are present. The fundamental equation is evidently

$$\sum_{N_1+N_2+\dots=N} \sum \dots \sum \exp(N_1\mu_1/kT) \exp(N_2\mu_2/kT) \dots \sum_n \exp\{-H_n(P; N_1, N_2, \dots)/kT\} = 1, \quad (9.4)$$

and the relation between $T, P, \mu_1, \mu_2, \dots$ can again be obtained by going to the limit

$N \rightarrow \infty$. An example of a case in which this method can be used successfully is the treatment of a multi-component one-dimensional system [10].

10. ALTERNATIVE TREATMENT

An alternative view of constant pressure ensembles is possible which leads to a fundamental equation for the TPN -ensemble which is effectively the same as that of Guggenheim, but is free from the objections made in § 1. In this alternative approach† the systems of the ensemble are supposed to consist of N molecules of mass m possessing ν degrees of freedom enclosed in a vessel with a movable wall (for example, a cylinder closed by a piston) which is subject to a constant external pressure P and is considered to be part of the system. The movable wall of mass M may be supposed for convenience to have three degrees of freedom, so that its position and momentum can be described by vectors \mathbf{r} and \mathbf{p} ; the volume accessible to the molecules when the wall is in position \mathbf{r} will be denoted by $V(\mathbf{r})$. The quantum mechanics of such a system with $\nu N + 3$ degrees of freedom follows from its Hamiltonian

$$\mathcal{H} = \mathcal{E} + \mathcal{W}_r + \mathbf{p}^2/2M + PV, \quad (10.1)$$

where \mathcal{E} and \mathcal{W}_r are the functions defined in § 3. Since the movable wall is of macroscopic mass ($M \gg m$), the Born-Oppenheimer approximation can be used to simplify the Schrödinger equation for the eigenstates of the total system. This leads first of all to the eigen-energies $E_n(\mathbf{r})$ for the motion of the molecules with the wall fixed in position \mathbf{r} . These eigen-energies can then be substituted into the equation for the motion of the wall, whose potential energy in position \mathbf{r} is $[E_n(\mathbf{r}) + PV(\mathbf{r})]$, to find the approximate eigenvalues $H_{nm}(P)$ for the Hamiltonian of the total system. One can now imagine an ensemble whose fundamental equation is

$$\exp(-G/kT) = \sum_n \sum_m \exp(-H_{nm}/kT), \quad (10.2)$$

where the function $G(T, P, N)$ can be identified with the Gibbs' function of the N molecules at temperature T and pressure P .

The similarity between equations (1.1) and (10.2) becomes evident if the latter is written in the form

$$\exp(-G/kT) = \sum_n \sum_m \exp\{-E_n(V_{nm})/kT\} \exp(-PV_{nm}/kT), \quad (10.3)$$

where the volumes V_{nm} satisfy the equation

$$E_n(V) + PV = H_{nm}(P). \quad (10.4)$$

It should be noticed, however, that the 'eigen-volumes' V_{nm} are not uniquely defined by equation (10.4), since this will in general be satisfied by two values of V ; the fundamental equation is therefore more properly written in the form (10.2) than in the form (10.3).

Since the mass M of the movable wall is macroscopic, its motion can always be treated by classical mechanics, and the fundamental equation can be written in the partly classical form

$$\exp(-G/kT) = \frac{1}{h^3} \int^3 \int^3 \exp\left\{\frac{-\mathbf{p}^2/2M - F(\mathbf{r}) - PV(\mathbf{r})}{kT}\right\} d^3\mathbf{p} d^3\mathbf{r}, \quad (10.5)$$

$$= \frac{1}{\Lambda^3} \int_0^\infty \exp(-F/kT) \exp(-PV/kT) dV, \quad (10.6)$$

†The author is indebted to Professor L. Rosenfeld for the idea developed in this section.

where

$$\Lambda = h/\sqrt{(2\pi MkT)}, \quad (10.7)$$

and $F(T, V, N)$ is the Helmholtz free energy of the N molecules, given by equation (2.1). Equation (10.5) is interesting, and may be interpreted as follows: since the mass of the wall is so much greater than that of the molecules, the latter are in statistical equilibrium at temperature T for each position of the wall. The work function for the movement of the wall is therefore $(F + PV)$, so that equation (10.5) is the phase integral for a canonical ensemble of systems with movable walls possessing three degrees of freedom. The Gibbs' function defined by (10.6) will always contain a term $kT \log (P\Lambda^3/kT)$, but for macroscopic values of M (of the order of Nm) this is entirely negligible when N is large.

The advantages of including the movable wall in the treatment are therefore that the 'quantization' of the volume in equation (10.3) arises naturally, and that the elementary unit of length Λ in equation (10.6) is not arbitrary but follows in a straightforward manner. It should also be pointed out that this approach allows a micro-canonically distributed ensemble to be described, whereas the method used by Guggenheim gives no clue as to how this might be done.

It remains to show the relation between the fundamental equations (2.5) and (10.2). This can be done by the well known technique of picking out the maximum term in a sum-over-states, in this case the sum over the suffix m in equation (10.2). If H_{nm} is written in the form (10.4), then for a variation of m

$$\delta H_{nm} = \left[\frac{dE_n}{dV} + P \right] \delta V_{nm} = 0, \quad (10.8)$$

so that the value of V which maximizes $\exp(-H_{nm}/kT)$ with respect to the suffix m is given by equation (2.3). The minimum value of H_{nm} is therefore given by equation (2.4), and the approximation for the fundamental equation (10.2) is identical with equation (2.5). The main difference between the two methods is that in the genuine constant pressure ensemble of §§ 2 and 3, all the systems are in actual mechanical equilibrium with the exterior at pressure P , whereas in the ensemble of the present section, the systems are not in general exerting pressure P , but exert all possible pressures, depending on the eigenstate and the position of the wall.

11. CONCLUSIONS

Of the two types of TPN -ensemble described in this paper, only that introduced in § 2 can properly be called a constant pressure ensemble, and it alone offers a statistical treatment possessing new features; to obtain the Gibbs' function from Guggenheim's equation (1.1) or equation (10.6) it will usually be necessary first to find the Helmholtz free-energy function from the fundamental equation of the TVN -ensemble. With regard to the utility of the new procedure, the TPN -ensemble is undoubtedly convenient to work with in formal investigations of the kind mentioned in § 8, when the natural independent variables are those of the ensemble; but whether it will prove useful in the task of developing approximate methods for calculating thermodynamic functions remains to be seen. It is significant, however, that although the treatment of a system of *non-interacting* molecules (i.e. a perfect gas) is slightly more complicated with the TPN - than with the TVN -ensemble, the reverse is true for the hypothetical one-dimensional system of *interacting* particles treated in § 6. This suggests that the configuration integral (3.18) may be of value in developing the statistical theory of liquids.

As shown in §§ 2 and 3, it follows directly from the fundamental equation that the isothermal compressibility of a system represented by a *TPN*-ensemble can never be negative. Since there does not seem to be any *a priori* reason for preferring the *TVN*- to the *TPN*-ensemble, this provides a simple and satisfactory proof of the now well-established result that no loop can exist in the *PV*-isotherms derived from statistical mechanics.

Although the equations of this paper are confined exclusively to the case in which the volume is the only external parameter describing a system, the idea is easily extended to include other external parameters. The essential step is the Legendre-type transformation of the eigen-energies for constant parameters (external forces do no work) to the eigen-enthalpies for constant generalized forces. The fundamental equations for ensembles of systems subject to constant forces can then be found by analogy with the constant pressure case discussed in §§ 2, 3 and 9.

On décrit un nouveau procédé statistique pour obtenir les propriétés thermodynamiques d'un système moléculaire directement en fonction de la pression. Ce procédé diffère en principe de celui proposé par Guggenheim [3] en ce que les éléments de l'ensemble représentatif sont considérés comme se trouvant en état d'équilibre mécanique constant avec le milieu extérieur. On donne les théories quantiques et classiques de 'petits' ensembles micro-canoniques et canoniques des systèmes à pression constante, et l'on montre que ces théories conduisent aux résultats connus pour les gaz parfaits et imparfaits, ainsi que pour un système hypothétique à une seule dimension. On conclut directement de la théorie, que la compressibilité statistique d'un système moléculaire est essentiellement positive. On décrit aussi un procédé alternatif qui conduit à une forme plus satisfaisante de l'équation de Guggenheim, et l'on en montre la relation avec le procédé nouveau ci-dessus mentionné.

Ein neues statistisches Verfahren wird beschrieben, um die thermodynamischen Eigenschaften eines molekularen Systems direkt als Druckfunktionen zu erhalten. Dieses Verfahren unterscheidet sich von dem von Guggenheim [3] vorgeschlagenen grundsätzlich dadurch, dass die Glieder des repräsentativen Ensemble als mit dem Aussenraum in konstantem mechanischem Gleichgewicht bestehend angesehen werden. Die Quanten- und klassischen Theorien der 'petit' mikrokanonischen und kanonischen Ensembles von Systemen unter konstantem Druck werden entwickelt, und es wird gezeigt, dass dieselben zu den festgesetzten Ergebnissen für vollkommene und nicht vollkommene Gase sowie für ein hypothetisches eindimensionales System führen. Der Schluss, dass die statische Kompressibilität eines molekularen Systems im wesentlichen positiv ist, folgt direkt aus der Theorie. Ein alternatives Verfahren, dass zu einer befriedigendere Form der Guggenheimschen Gleichung führt, wird ebenfalls beschrieben, sowie die Beziehung zwischen diesem und dem neuen Verfahren.

REFERENCES

- [1] GIBBS, J. W., 1948, *Elementary Principles in Statistical Mechanics: Collected Works*, 2 (Yale University Press).
- [2] SCHRÖDINGER, E., 1946, *Statistical Thermodynamics* (Cambridge: University Press), see footnote to chap. 2.
- [3] GUGGENHEIM, E. A., 1939, *J. chem. Phys.*, **7**, 103.
- [4] HILL, T. L., 1956, *Statistical Mechanics* (New York: McGraw-Hill).
- [5] MÜNSTER, A., 1956, *Statistische Thermodynamik* (Berlin: Springer).
- [6] LONGUET-HIGGINS, H. C., 1951, *Proc. roy. Soc. A*, **205**, 247.
- [7] BROWN, W. B., 1957, *Proc. roy. Soc. A*, **240**, 561.
- [8] BROWN, W. B., 1957, *Phil. Trans. A*, **250**, 221.
- [9] PRIGOGINE, I., 1950, *Physica*, **16**, 133.
- [10] LONGUET-HIGGINS, H. C., 1957, *Mol. Phys.*, **1**, 83.

One-dimensional multicomponent mixtures

by H. C. LONGUET-HIGGINS

Department of Theoretical Chemistry, University of Cambridge

(Received 1 February 1957)

It is shown that a one-dimensional multicomponent mixture with nearest neighbour interactions $u_{ij}(r)$ obeys the implicit equation of state

$$\Delta(\lambda_A, \lambda_B, \dots; T, P) \equiv |\lambda_i \eta_{ij} - \delta_{ij}| = 0$$

where λ_i is the absolute activity of species i (divided by a kinetic factor) and

$$\eta_{ij}(T, P) = \int_0^\infty \exp[-\{\mu_{ij}(r) + Pr\}/kT] dr.$$

The concentration of species i is thence determined as

$$-\lambda_i \frac{\partial \Delta}{\partial \lambda_i} \bigg/ kT \frac{\partial \Delta}{\partial P}.$$

A one-dimensional solution is ideal if, and only if, the matrix $[\eta_{ij}]$ is of rank unity. The excess free energy of a nearly ideal solution is found to be

$$(\Delta^*G)_{T,P} = \sum_{i < j} x_i x_j (G_{ij} + G_{ji} - G_{ii} - G_{jj})$$

where $G_{ij}(T, P)$ is the (configurational) molar Gibbs free energy of a 'hybrid' species with interaction potential $u_{ij}(r)$.

1. INTRODUCTION

The purpose of this paper is to obtain the thermodynamic equations of state of a one-dimensional fluid mixture of any number of components on the assumption that only nearest neighbours interact. The one-dimensional one-component fluid has been discussed by various authors: Takahasi [1] derived the equation of state for the case of nearest neighbour interactions, and in a more comprehensive investigation Van Hove [2] showed that no phase transition can occur if the particles have a finite radius of incompressibility and a finite range of interaction. The two-component mixture has been discussed by Prigogine and Lafleur [3] and by Kikuchi [4], who obtained explicit expressions for the free energy of mixing; the theoretical methods used by these authors are not, however, suitable for the treatment of mixtures of more than two components. As far as the writer is aware, the only paper dealing with a one-dimensional assembly of any number of components is that of Rushbrooke and Ursell [5]. These authors gave a full account of the multicomponent 'regular assembly', in which the particles are restricted to a one-dimensional lattice, and showed that provided interaction is restricted to groups of p neighbouring particles, where p is finite, no phase transitions are possible.

In this paper we consider the multicomponent assembly in which the interaction potential is the sum of nearest neighbour interactions but the distances between the particles are variable. The analysis follows largely the elegant paper of Rushbrooke and Ursell, but differs from it in requiring the use of an unusual

type of grand partition function described in § 3. The final results include those of Prigogine and Lafleur and of Kikuchi as a special case, but are presented in a form which seems more suitable for (cautious) application to real, three-dimensional, solutions.

2. THE CONSTANT PRESSURE PARTITION FUNCTION

Let us begin by considering briefly the one-component linear assembly, of N identical particles. For convenience we arrange the particles on a circle of circumference V , and denote the distances between neighbours by r_1, r_2, \dots, r_N . (We assume that at least one particle is present.) Ignoring the kinetic energy of the particles, we may then obtain the Helmholtz free energy $F(N, T, V)$ from the equation

$$\exp(-F/kT) = \int \dots \int \exp \left[- \sum_{k=1}^N u(r_k)/kT \right] dr_1 \dots dr_N \quad (2.1)$$

where $u(r)$ is the interaction energy between adjacent particles at a distance r , and the range of integration is determined by the restrictions

$$0 \leq r_1, r_2, \dots, r_N; \quad r_1 + r_2 + \dots + r_N = V. \quad (2.2)$$

The latter restriction is awkward but may be evaded by passing on to the constant pressure partition function, namely [9]

$$Q \equiv \int_0^\infty \exp [-(F + PV)/kT] dV = \exp(-G/kT) \quad (2.3)$$

where $G(N, T, P)$ is the Gibbs free energy. Substitution into (2.1) leads immediately to the relation

$$Q = \prod_{l=1}^N \int_0^\infty \exp [- \{ u(r_l) + Pr_l \} / kT] dr_l. \quad (2.4)$$

Defining

$$\eta(T, P) = \int_0^\infty \exp [- \{ u(r) + Pr \} / kT] dr, \quad (2.5)$$

and recalling that

$$G = N\mu, \quad \mu = kT \ln \lambda, \quad (2.6)$$

where μ is the chemical potential and λ the absolute activity, we conclude that

$$\mu = -kT \ln \eta, \quad \lambda = \eta^{-1}. \quad (2.7)$$

This result was obtained by Takahasi [1], and has been used by some of the authors already mentioned.

Next let us consider an assembly composed of N_A molecules of type A, N_B of type B etc., where

$$N_A + N_B + \dots = N. \quad (2.8)$$

Let the interaction potential between a particle of species i and one of species j at a (clockwise) distance r be $u_{ij}(r)$. (We allow the possibility that $u_{ij}(r) \neq u_{ji}(r)$.) Then, by an obvious extension of the argument of the preceding paragraph, it may be shown that

$$Q(N_A, N_B, \dots; T, P) = \exp(-G/kT) = \sum^{(N_A, N_B, \dots)} \prod_i \prod_j \eta_{ij}^{N_{ij}} \quad (2.9)$$

where

$$\eta_{ij}(T, P) = \int_0^\infty \exp[-\{u_{ij}(r) + Pr\}/kT] dr \quad (2.10)$$

and the summation $\sum_{(N_A, N_B, \dots)}$ is over all distinguishable orderings of N_A molecules of type A, etc., N_{ij} being the number of (clockwise) ij neighbour pairs in a particular ordering of the molecules on the circle. The evaluation of this sum presents rather a cumbersome combinatorial problem which will be circumvented later; but at this stage certain useful deductions may be made.

In the first place, Q as defined by (2.9) is a function of the independent variables N_i , η_{ij} and no others. Therefore differentiating with respect to η_{AB} , say, keeping all the other variables constant, we obtain

$$\eta_{AB} \frac{\partial \ln Q}{\partial N_{AB}} = \frac{\sum_{(N_A, N_B, \dots)} N_{AB} \prod_i \prod_j \eta_{ij}^{N_{ij}}}{\sum_{(N_A, N_B, \dots)} \prod_i \prod_j \eta_{ij}^{N_{ij}}} = \bar{N}_{AB} \quad (2.11)$$

for the expectation number of clockwise AB neighbour pairs. Therefore

$$d \ln Q = \sum_i \frac{\partial \ln Q}{\partial N_i} dN_i + \sum_i \sum_j \bar{N}_{ij} \frac{d\eta_{ij}}{\eta_{ij}}. \quad (2.12)$$

But Q is related to the absolute activities by the equation

$$Q = \prod_i \lambda_i^{-N_i}; \quad (2.13)$$

hence

$$d \ln Q = - \sum_i \ln \lambda_i dN_i - \sum_i N_i \frac{d\lambda_i}{\lambda_i}. \quad (2.14)$$

Therefore for any small changes in the η_{ij} , the related changes in the λ_i satisfy

$$\sum_i N_i \frac{d\lambda_i}{\lambda_i} + \sum_i \sum_j \bar{N}_{ij} \frac{d\eta_{ij}}{\eta_{ij}} = 0. \quad (2.15)$$

Finally, if we define

$$\mu_{ij} = -kT \ln \eta_{ij} \quad (2.16)$$

and use the relation $G = -kT \ln Q$, we obtain

$$\left(\frac{\partial G}{\partial \mu_{ij}} \right)_{T, N_i} = \left(\frac{\partial \ln Q}{\partial \ln \eta_{ij}} \right)_{N_i} = \bar{N}_{ij}. \quad (2.17)$$

3. THE CONSTANT PRESSURE GRAND PARTITION FUNCTION

In order to escape the combinatorial problem presented by $\sum_{(N_A, N_B, \dots)}$ in equation (2.9) we consider an ensemble of assemblies in which the numbers N_i are not precisely fixed, but are determined implicitly by the absolute activities of the various components. The type of grand partition function most widely used is that which contains the volume as an extensive variable, namely

$$\Gamma(\lambda_A, \lambda_B, \dots; T, V) = \sum_{N_A} \sum_{N_B} \dots \lambda_A^{N_A} \lambda_B^{N_B} \dots \exp[-F(N_A, N_B, \dots; T, V)/kT]. \quad (3.1)$$

For given values of the absolute activities $\lambda_A, \lambda_B, \dots$ the value of Γ_V increases exponentially with V , tending to $\exp(PV/kT)$ where $P(\lambda_A, \lambda_B, \dots; T)$ is the

equilibrium pressure. The presence of V in (3.1) requires, however, the very condition which we sought to avoid in §2, namely $r_1 + r_2 + \dots + r_N = V$; we therefore consider tentatively the infinite sum

$$\Gamma(\lambda_A, \lambda_B, \dots; T, p) = \int_0^\infty \Gamma_V \exp(-pV/kT) dV, \quad (3.2)$$

where p is an arbitrary positive quantity having the dimensions of pressure. For values of p greater than P the right-hand side is clearly convergent, and is divergent if p is less than P . We shall now show that Γ may be evaluated explicitly in the range $p > P$.

First we note that

$$\Gamma(\lambda_A, \lambda_B, \dots; T, p) = \sum_{N_A} \sum_{N_B} \dots \lambda_A^{N_A} \lambda_B^{N_B} \dots Q(N_A, N_B, \dots; T, p) \quad (3.3)$$

which follows from the definition of Q . In this expression it is convenient to collect together terms corresponding to the same total number of particles, and write

$$\Gamma = \sum_{N=1}^{\infty} \Gamma_N(\lambda_A, \lambda_B, \dots; T, p),$$

$$\Gamma_N = \sum_{N_A+N_B+\dots=N} \dots \lambda_A^{N_A} \lambda_B^{N_B} \dots Q(N_A, N_B, \dots; T, p). \quad (3.4)$$

Now let us consider the nature of the terms which contribute to Γ_N . Since there is no restriction on the numbers N_A, N_B, \dots except that their sum is N , we may associate each term with a particular ordering of N molecules of arbitrary species on the circle. Referring to equation (2.9) we see that Γ_N may therefore be written in the simpler form

$$\Gamma_N(\lambda_A, \lambda_B, \dots; T, p) = \sum_a \sum_b \dots \sum_n \lambda_a \eta_{ab} \lambda_b \eta_{bc} \dots \lambda_n \eta_{na}, \quad \eta_{ij} = \eta_{ij}(T, p) \quad (3.5)$$

where each of the N suffixes a, b, \dots, n denotes a molecular species, and each summation is over all possible species. But the right-hand side of (3.5) may be expressed as the trace of the matrix \mathbf{M}^N , where

$$\mathbf{M} = \begin{bmatrix} \lambda_A \eta_{AA}, & \lambda_A \eta_{AB}, & \dots \\ \lambda_B \eta_{BA}, & \lambda_B \eta_{BB}, & \dots \\ \dots, & \dots, & \dots \end{bmatrix}; \quad (3.6)$$

and the trace of the N th power of a matrix equals the sum of the N th powers of its eigenvalues. Hence if $\theta_1, \theta_2, \dots$ are the eigenvalues of \mathbf{M} ,

$$\Gamma = \sum_{N=1}^{\infty} \Gamma_N = \sum_{N=1}^{\infty} (\theta_1^N + \theta_2^N + \dots). \quad (3.7)$$

Now we have already seen that if $p > P$, Γ is convergent; hence in this range all the eigenvalues of \mathbf{M} lie between -1 and $+1$ and the right-hand side of (3.7) may be summed to yield

$$\Gamma = \frac{\theta_1}{1-\theta_1} + \frac{\theta_2}{1-\theta_2} + \dots \quad (3.8)$$

But as p tends to P in the $\eta_{ij}(T, p)$, Γ tends to infinity; hence at least one of the eigenvalues of \mathbf{M} must tend to $+1$, which implies that in the limit

$$\Delta(\lambda_A, \lambda_B, \dots; T, P) \equiv \begin{bmatrix} \lambda_A \eta_{AA} - 1, & \lambda_A \eta_{AB}, & \dots \\ \lambda_B \eta_{BA}, & \lambda_B \eta_{BB} - 1, & \dots \\ \dots, & \dots, & \dots \end{bmatrix} = 0. \quad (3.9)$$

4. THE THERMODYNAMIC PROPERTIES

Equation (3.9) suffices to determine all the thermodynamic properties of the assembly. This may be seen as follows. Since in this equation the η_{ij} are all functions of T and P , P being the equilibrium pressure, we have a relation of the form

$$\Delta(\lambda_A, \lambda_B, \dots; T, P) = 0, \quad (4.1)$$

so that for all small changes consistent with equilibrium

$$\sum_i \frac{\partial \Delta}{\partial \lambda_i} d\lambda_i + \frac{\partial \Delta}{\partial T} dT + \frac{\partial \Delta}{\partial P} dP = 0. \quad (4.2)$$

Comparison with the Gibbs–Duhem–Margules equation

$$kT \sum_i N_i \frac{d\lambda_i}{\lambda_i} + SdT - VdP = 0 \quad (4.3)$$

shows that

$$N_i : S : V = \lambda_i \frac{\partial \Delta}{\partial \lambda_i} : kT \frac{\partial \Delta}{\partial T} : -kT \frac{\partial \Delta}{\partial P}, \quad (4.4)$$

so that the various concentrations and the entropy density are well-defined functions of the absolute activities, temperature and pressure.

It is also possible to draw immediate conclusions as to the average numbers of clockwise neighbour pairs of given types. Referring to equation (2.15), and dropping the bars, we write

$$\sum_i N_i \frac{d\lambda_i}{\lambda_i} + \sum_i \sum_j N_{ij} \frac{d\eta_{ij}}{\eta_{ij}} = 0. \quad (4.5)$$

But since Δ is a function of the λ_i and the η_{ij} , we may also write

$$\sum_i \frac{\partial \Delta}{\partial \lambda_i} d\lambda_i + \sum_i \sum_j \frac{\partial \Delta}{\partial \eta_{ij}} d\eta_{ij} = 0. \quad (4.6)$$

Comparing coefficients in (4.5) and (4.6) we deduce that

$$N_i : N_{ij} = \lambda_i \frac{\partial \Delta}{\partial \lambda_i} : \eta_{ij} \frac{\partial \Delta}{\partial \eta_{ij}} \quad (4.7)$$

whence

$$\begin{aligned} N_A : N_B : \dots : N_{AA} : N_{AB} : \dots \\ = \Delta_{AA} : \Delta_{BB} : \dots : \lambda_A \eta_{AA} \Delta_{AA} : \lambda_A \eta_{AB} \Delta_{AB} : \dots \end{aligned} \quad (4.8)$$

Finally, by Jacobi's theorem on the minors of the adjugate

$$\begin{vmatrix} \Delta_{ik} & \Delta_{il} \\ \Delta_{jk} & \Delta_{jl} \end{vmatrix} = \Delta \cdot \Delta_{ij, kl} = 0 \quad (4.9)$$

and so

$$\frac{N_{ik} N_{jl}}{N_{jk} N_{il}} = \frac{\eta_{ik} \eta_{jl}}{\eta_{jk} \eta_{il}}. \quad (4.10)$$

Readers familiar with the paper of Rushbrooke and Ursell will recognize a formal identity between equations (4.5) to (4.10) and the equations obtained by those authors. Indeed the present approach is closely similar to theirs, the physically important difference being that a term such as η_{AB} is an integral involving the intermolecular potential and the pressure, not a simple term $\exp(-\epsilon_{AB}/kT)$ where ϵ_{AB} is a fixed interaction energy between neighbours. It would therefore be a relatively simple matter to adapt their subsequent arguments and to show, as they did for the regular assembly, that no phase transition is possible in any multicomponent assembly with nearest neighbour interactions alone.

5. IDEAL AND NEARLY IDEAL SOLUTIONS

The condition for a solution to be ideal in all its components at a given temperature and pressure may be expressed concisely in the form

$$\sum_i \lambda_i / \lambda_{ii} = 1, \quad = \sum_i \lambda_i \eta_{ii}, \quad (5.1)$$

where λ_{ii} is the absolute activity of pure i , given by (2.7). Now Δ may be expanded in the form

$$\Delta = (-1)^n \left\{ 1 - \sum_i \lambda_i \eta_{ii} + \sum_{i < j} \sum \lambda_i \lambda_j \begin{vmatrix} \eta_{ii} & \eta_{ij} \\ \eta_{ji} & \eta_{jj} \end{vmatrix} - \sum_{i < j < k} \sum \lambda_i \lambda_j \lambda_k \begin{vmatrix} \eta_{ii} & \eta_{ij} & \eta_{ik} \\ \eta_{ji} & \eta_{jj} & \eta_{jk} \\ \eta_{ki} & \eta_{kj} & \eta_{kk} \end{vmatrix} + \dots \right\} \quad (5.2)$$

where n is the total number of components. For this expression to vanish identically subject to the condition (5.1), all the principal minors of $[\eta_{ij}]$, of order greater than unity, must also vanish. This implies that the matrix $[\eta_{ij}]$ is of rank unity, i.e. that the η_{ij} may be expressed in the form

$$\eta_{ij} = a_i b_j \quad (5.3)$$

where the a_i and the b_j are fixed numbers. But if (5.3) is fulfilled, it may be seen by direct expansion that

$$0 = (-1)^n \Delta = 1 - \sum_i \lambda_i \eta_{ii} \quad (5.4)$$

$$(-1)^{n-1} \Delta_{AA} = 1 - \sum_{i(\neq A)} \lambda_i \eta_{ii} = \lambda_A \eta_{AA} \quad (5.5)$$

$$(-1)^{n-1} \lambda_A \eta_{AB} \Delta_{AB} = \lambda_A \eta_{AB} \lambda_B \eta_{BA} = \lambda_A \eta_{AA} \lambda_B \eta_{BB} \quad (5.6)$$

whence

$$x_A = N_A / N = \Delta_{AA} / \sum_i \Delta_{ii} = \lambda_A \eta_{AA} \quad (5.7)$$

$$N_{AB} / N = \lambda_A \eta_{AB} \Delta_{AB} / \sum_i \Delta_{ii} = x_A x_B. \quad (5.8)$$

Equation (5.3) is therefore a necessary and sufficient condition for the solution to be ideal in all its components.

From equations (2.16) and (5.8) it is possible to obtain very simply the excess free energy of a nearly ideal solution of many components. For an ideal solution, by (5.3),

$$\eta_{ij} \eta_{ji} = \eta_{ii} \eta_{jj} \quad (5.9)$$

whence, in the notation of § 2,

$$\mu_{ij} + \mu_{ji} = \mu_{ii} + \mu_{jj}. \quad (5.10)$$

Further by (2.17)

$$(dG)_{N_{ij}, \mu_{ii}, T} = \sum_{i \neq j} \sum N_{ij} d\mu_{ij} = \sum_{i < j} \sum N x_i x_j d(\mu_{ij} + \mu_{ji}). \quad (5.11)$$

Hence, insofar as we can regard the non-ideal solution as formed from an ideal solution by slightly altering the off-diagonal terms μ_{ij} , its excess free energy will be, to the first order in these changes,

$$\Delta^* G = N \sum_{i < j} \sum x_i x_j (\mu_{ij} + \mu_{ji} - \mu_{ii} - \mu_{jj}). \quad (5.12)$$

Now by its definition μ_{ij} may be interpreted as the chemical potential at T , P of a pure species whose intermolecular potential is $\mu_{ij}(r)$. Hence if G_{ij} represents the molar Gibbs free energy of this species, also at T , P , we may write

$$\Delta^* G = \sum_{i < j} \sum x_i x_j (G_{ij} + G_{ji} - G_{ii} - G_{jj}). \quad (5.13)$$

It is important to note that the ideality of a solution at a particular temperature and pressure is no guarantee that at other temperatures the solution will be ideal; the excess free energy may be zero while its temperature or pressure derivative is finite. Differentiation of (5.13) with respect to temperature or pressure gives the excess entropy, heat and volume of mixing as

$$\Delta^*S = \sum_{i < j} x_i x_j (S_{ij} + S_{ji} - S_{ii} - S_{jj}) \quad (5.14)$$

$$\Delta^*H = \sum_{i < j} x_i x_j (H_{ij} + H_{ji} - H_{ii} - H_{jj}) \quad (5.15)$$

$$\Delta^*V = \sum_{i < j} x_i x_j (V_{ij} + V_{ji} - V_{ii} - V_{jj}) \quad (5.16)$$

where S_{ij} , H_{ij} , V_{ij} are the molar entropy, heat and volume of a pure species with intermolecular potential $u_{ij}(r)$. It follows that if we are able to infer, from the principle of corresponding states, the thermodynamic properties of such 'hybrid' species as functions of T and P , we shall be in a position to calculate the mixing properties of the solution from purely thermodynamic data on its components. The possibility of achieving this is a primary aim of the theory of solutions, and has been discussed by many authors [6, 7], the most recent study being that of Prigogine *et al.* [6]. We suggest that equations (5.13) to (5.16) may find useful application to nearly ideal solutions of real substances. It is already known, from the work of Prigogine and Lafleur, that the binary one-dimensional mixture exhibits some of the features of the cell model proposed for three-dimensional mixtures by Prigogine and Garikian, a model which successfully predicted some hitherto unexpected properties of certain simple mixtures. Whether these facts may be taken to justify the cell model is, however, a matter of opinion; the writer prefers the view that in the neighbourhood of ideality the small non-ideal terms in the free energy have an origin which is independent of the three-dimensional character of space. If this is indeed the case, one may with more confidence apply the foregoing equations to mixtures at high temperatures and low pressures, where any kind of cell model would clearly be quite unrealistic.

Finally, it should be stressed that the exact equations (3.9) and (4.4) cannot possibly apply to highly non-ideal, three-dimensional solutions. This is clear from the fact that in one dimension phase transitions are impossible, whereas they are a commonplace in three dimensions. It is suggested, therefore, that the only equations of this paper which have any bearing on real solutions are equations (5.13) to (5.16). It may be noted that these are at least consistent with those of the exact first-order theory of 'conformal' solutions [8].

On montre qu'un mélange à une seule dimension et à plusieurs composants, où les actions réciproques entre les voisins les plus proches sont $u_{ij}(r)$, obéit à l'équation d'état implicite

$$\Delta(\lambda_A, \lambda_B, \dots; T, P) \equiv |\lambda_i \eta_{ij} - \delta_{ij}| = 0$$

où λ_i est l'activité absolue de l'espèce i (divisée par le facteur cinétique), et

$$\eta_{ij}(T, P) = \int_0^\infty \exp[-\{\mu_{ij}(r) + Pr\}/kT] dr.$$

La concentration de l'espèce i est donc déterminée comme

$$-\lambda_i \frac{\partial \Delta}{\partial \lambda_i} \bigg/ kT \frac{\partial \Delta}{\partial P}.$$

Une solution à une seule dimension est idéale si, et seulement si, la matrice $[\eta_{ij}]$ est du rang de l'unité. L'énergie libre d'excès d'une solution presque idéale est

$$(\Delta^*G)_{T,P} = \sum_{i < j} x_i x_j (G_{ij} + G_{ji} - G_{ii} - G_{jj}),$$

où $G_{ij}(T, P)$ est l'énergie libre (de configuration) molaire de Gibbs d'une espèce 'hybride' ayant un potentiel d'action réciproque $u_{ij}(r)$.

Es wird gezeigt, dass ein eindimensionales Mehrkomponentengemisch mit Nächst-nachbar-Wechselwirkung $u_{ij}(r)$ der impliziten Zustandsgleichung

$$\Delta(\lambda_A, \lambda_B, \dots; T, P) = |\lambda_i \eta_{ij} - \delta_{ij}| = 0$$

folgt, wo λ_i die absolute Aktivität der Art i (durch einen kinetischen Faktor dividiert) ist, und

$$\eta_{ij}(T, P) = \int_0^\infty \exp[-\{\mu_{ij}(r) + Pr\}/kT] dr.$$

Die Konzentration der Art i wird folglich als

$$-\lambda_i \frac{\partial \Delta}{\partial \lambda_i} \bigg/ kT \frac{\partial \Delta}{\partial P}$$

bestimmt. Eine eindimensionale Lösung ist ideal, wenn, und nur wenn die Matrix $[\eta_{ij}]$ von der Ordnung Eins ist. Der Überschuss der freien Energie einer annähernd idealen Lösung wird als

$$(\Delta^*G)_{T,P} = \sum_{i < j} x_i x_j (G_{ij} + G_{ji} - G_{ii} - G_{jj})$$

bestimmt, wo $G_{ij}(T, P)$ die (Konfigurations-) molare freie Energie nach Gibbs einer 'hybriden' Art mit dem Wechselwirkungs-Potential $u_{ij}(r)$ ist.

REFERENCES

- [1] TAKAHASI, H., 1942, *Proc. phys.-math. Soc., Japan*, **24**, 60.
- [2] VAN HOVE, L., 1950, *Physica* **16**, 137.
- [3] PRIGOGINE, I., LAFLEUR, S., 1954, *Bull. Acad. Belg. Cl. Sci.*, (5) **40**, 484, 497.
- [4] KIKUCHI, R., 1955, *J. chem. Phys.*, **23**, 2327.
- [5] RUSHBROOKE, G. S., and URSELL, H. D., 1947, *Proc. Camb. phil. Soc.*, **44**, 263.
- [6] PRIGOGINE, I., BELLEMANS, A., and ENGLERT-CHVOLES, A., 1953, *J. chem. Phys.*, **24**, 518.
- [7] RICE, S. A., 1956, *J. chem. Phys.*, **24**, 357, 1283.
- [8] LONGUET-HIGGINS, H. C., 1951, *Proc. roy. Soc. A*, **205**, 247.
- [9] BROWN, W. B., 1958, *Mol. Phys.*, **1**, 68.

Thermodynamic properties of gas hydrates†

by J. C. PLATTEEUW and J. H. van der WAALS

Koninklijke/Shell-Laboratorium, Amsterdam
(N.V. De Bataafsche Petroleum Maatschappij)

(Received 6 September 1957)

A statistical mechanical description based on the Lennard-Jones and Devonshire model has been applied to the gas hydrates. The theory enables one to calculate dissociation pressures, compositions and heats of dissociation of several such gas hydrates. The agreement between the calculated values and the experimental data at present available supports the theory.

1. INTRODUCTION

Recent work on structure by Claussen [1], Pauling and Marsh [2] and von Stackelberg and Müller [3] has revealed that gas hydrates are three-dimensional inclusion compounds known as clathrates.

According to von Stackelberg and Müller [3], gas hydrates crystallize in one of two different frameworks, I and II, depending on the size of the imprisoned guest molecules. Each structure contains cavities of two different sizes.

A statistical mechanical treatment has already been given for the clathrates formed between quinol and non-polar gases [4]. As a more thorough test of this theory the present paper considers its extension to the case of the gas hydrates for which more experimental data are available.

2. EQUILIBRIUM RELATIONSHIPS

In a clathrate one is, thermodynamically speaking, dealing with a solution of a gas in a solid. The solid solvent itself is metastable relative to the normal modification of the cage-former. The stable form is denoted as the α -modification, the metastable clathrate lattice as the β -modification. The two components in the crystal are not joined by ordinary chemical bonds, but the interaction of the encaged M molecules with the surrounding network is similar to that found between adjacent molecules in a liquid. It is this interaction which stabilizes the complex.

The partition function of a clathrate containing one type of cavity was derived, using the following assumptions:

1. The dimensions of the cavities exclude multiple occupation by gas molecules.
2. The interaction of two M molecules in neighbouring cavities can be neglected.
3. The contribution to the partition function by the cage-forming molecules in the β -structure is not affected by the presence of the gas molecules.

† This work was presented by J. C. Platteeuw at the XVIth I.U.P.A.C. conference, Paris, July 1957.

Such a model corresponds to a three-dimensional generalization of localized adsorption without M-M interaction. Accordingly a Langmuir-type isotherm resulted for the chemical potential of the gas in the clathrate and an analogue of Raoult's law for that of the solid solvent (cf. equations (3.8) and (3.6) of [4]). The vapour pressures of argon-quinol clathrates of various compositions were indeed found to obey a Langmuir isotherm [5].

The previous treatment can easily be extended to the present case where one has two kinds of cavities. One then obtains for the vapour pressure of the gas in a hydrate

$$p_M = \frac{kT}{\Psi_1(T)} \frac{y_1}{1-y_1} = \frac{kT}{\Psi_2(T)} \frac{y_2}{1-y_2}. \quad (1)$$

In this expression y_i is the fraction of the cavities of type i occupied by a gas molecule and $\Psi_i(T)$ denotes the 'free volume' of the molecule in such a cavity,

$$\Psi_i(T) = \int_{\text{cell } i} \exp[-w_i(r)/kT] dV.$$

The function $w_i(r)$ represents the potential energy of the gas molecule in a cavity of type i when at a distance r from its centre and referred to the ideal gas.

For the chemical potential μ_W^H of water in the hydrate one obtains

$$\frac{\mu_W^H}{kT} = \frac{\mu_W^\beta}{kT} + \sum_i \frac{1}{m_i} \ln(1-y_i),$$

where μ_W^β is the chemical potential of water in its β -modification and m_i denotes the ratio of the number of water molecules to the number of cavities of the i th kind. For framework I for instance, the elementary unit of which contains 46 H₂O molecules arranged in such a way that two small and six larger cavities occur, $m_1=23$ and $m_2=23/3$.

Equilibrium between hydrate and ice requires

$$\mu_W^H = \mu_W^\alpha.$$

Hence, at this equilibrium, the degrees of occupation of the different cavities are interrelated according to

$$\frac{\Delta\mu}{kT} = - \sum_i \frac{1}{m_i} \ln(1-y_i), \quad (2)$$

where $\Delta\mu$ is the difference in chemical potential of the β - and α -modifications of ice. In the case of the quinol clathrates the sum in (2) contained one term only, and consequently such a clathrate when in equilibrium with α -quinol is expected to have a unique composition, independent of the nature of the enclosed gas. In a gas hydrate in equilibrium with ice this is no longer the case: (2) then merely expresses a relation between y_1 and y_2 , and the individual values of these quantities depend on the relative magnitudes of Ψ_1 and Ψ_2 through (1).

3. NUMERICAL CALCULATIONS

The actual calculations were restricted to gas hydrates of structure I and to (almost) spherical molecules M. (Hydrates of structure II are formed by relatively large organic molecules which cannot be represented by central force fields.)

According to von Stackelberg and Müller [3] the geometry of the cavities in structure I is as follows:

1. Smaller cavities (pentagonal dodecahedra)

The $z_1 = 20$ molecules are evenly distributed over the surface of a sphere with a radius

$$a_1 = 3.94_5 \text{ \AA}.$$

2. Larger cavities (tetrakaidecahedra)

8 H₂O molecules at a distance of 4.04 Å from the centre,

8 H₂O molecules at a distance of 4.42 Å from the centre,

4 H₂O molecules at a distance of 4.65 Å from the centre,

4 H₂O molecules at a distance of 4.24 Å from the centre.

Although these cavities are slightly oblate it is nevertheless assumed that the $z_2 = 24$ molecules are evenly distributed over the surface of a sphere with an average radius

$$a_2 = 4.30 \text{ \AA}.$$

As the force fields $w_1(r)$ and $w_2(r)$ may thus be expected to have approximately spherical symmetry, the functions $\Psi_1(T)$ and $\Psi_2(T)$ can be calculated by the method of Lennard-Jones and Devonshire in the same way as done for the quinol clathrates [4]. But before we do so a peculiar difficulty should be mentioned. In order to determine the three unknowns y_1 , y_2 and p_M from the three equations (1) and (2), it is necessary to know the difference in chemical potential between the metastable β -modification and ordinary ice.

Fortunately, the value of $\Delta\mu$ could be found from the composition of the bromine hydrate in equilibrium with ice at 273°K, which has been accurately determined by Miss Mulders [6], who found Br₂ · 8.47 H₂O. The bromine molecules are too large to be captured by the smaller cavities. Hence, $y_1 = 0$ and y_2 follows directly from the composition of the hydrate. The result is

$$\Delta\mu = 0.167 \text{ kcal/mole at } 273^\circ\text{K and } 0.055 \text{ atm,}$$

which is quite reasonable when compared with hydroquinone where

$$\Delta\mu = 0.13 \text{ kcal/mole at } 25^\circ\text{C [7].}$$

$\Delta\mu$ at higher pressures is given by

$$(\Delta\mu)_{273^\circ\text{K}, p} = 0.167 + (p - 0.055) \cdot 7 \times 10^{-5} \text{ kcal/mole,} \quad (3)$$

where p is in atm and the value 7×10^{-5} corresponds to the difference in molar volume between β - and α -ice, expressed in the appropriate dimension.

The application of the method of Lennard-Jones and Devonshire to the present problem is based on the assumption that the average contribution to the potential energy due to the interaction of an M molecule with any one of the z_i water molecules constituting the wall of the cage can be described by a Lennard-Jones potential,

$$\epsilon(R) = 4\epsilon^* \left\{ \left(\frac{\sigma^*}{R} \right)^{12} - \left(\frac{\sigma^*}{R} \right)^6 \right\},$$

where R is the distance between the M molecule and the particular water molecule considered. The energy parameter ϵ^* and distance parameter σ^* thus are characteristic for the interaction gas–water.

Once this assumption has been made the free volume functions can be calculated by numerical integration and one obtains $\Psi_i(T)$ as a function of the

two dimensionless variables $z_i\epsilon^*/kT$ and σ^*/a (cf. formula (4.12) of [4] with $\Psi(T) = h_A(T)/\Phi_A(T)$). Values of ϵ^* and σ^* were derived from those for the pure gas $M(\epsilon_M, \sigma_M)$ in the following manner.

For the distance parameter the 'hard sphere approximation' was used, $\sigma^* = \frac{1}{2}\sigma_M + 1.25$ (in Å), where 1.25 Å is the value of $\frac{1}{2}\sigma$ of an oxygen atom corresponding to its van der Waals radius of 1.40 Å reported by Pauling [8].

For the energy parameter the 'geometric mean relation' was used

$$\epsilon^* = (\epsilon_M \bar{\epsilon})^{1/2},$$

in which $\bar{\epsilon}$ is a parameter characteristic for the cage.

The observed dissociation pressure of argon hydrate at 273°K (corrected for gas imperfection) was chosen for the determination of this unknown parameter because the Lennard-Jones force-constants of argon, of all the gases considered, were believed to be the most reliable. The same applies for the dissociation pressure of its hydrate [9].

In the further calculations values of the force-constants of the noble gases were taken from Whalley and Schneider [10], those of CF₄, methane, ethane, ethylene, oxygen and nitrogen from Hirschfelder *et al.* [11]. The results are given in table 1. It is seen that the agreement between calculated and observed dissociation pressures for the hydrates of spherical molecules, where a range in sizes is covered from $\sigma_{\text{argon}} = 3.41$ Å to $\sigma_{\text{CF}_4} = 4.70$ Å, is very satisfactory.

Hydrate former	ϵ_M/k °K	σ_M in Å	Diss. pressure (atm)		Fraction of cavities occ.	
			calc.	obs.	y_1	y_2
Argon	119.5	3.408	95.5	95.5 [9]	0.825	0.841
Krypton	166.7	3.679	15.4	14.5 [12]	0.832	0.830
Xenon	225.3	4.069	1.0	1.15 [13]	0.813	0.835
Methane	142.7	3.810	19.0	26 [15]	0.818	0.836
CF ₄	152.5	4.70	1.6	≈ 1 [14]	0.282	0.894
Ethane	243	3.954	1.1	5.2 [15]	0.837	0.827
Ethylene	199.2	4.523	0.5	5.44 [16]	0.523	0.879
Oxygen	117.5	3.58	63		0.821	0.839
Nitrogen	95.05	3.698	90		0.810	0.845

Table 1. Dissociation pressures and degrees of occupation of gas hydrates at 273°K.

When applied to neon, the expressions mentioned above would indicate that no hydrate of this element exists. However, there are two effects which may still cause this compound to occur at a very high pressure.

1. According to (3) $\Delta\mu$ depends on pressure, $(\partial\Delta\mu/\partial p)_T = \Delta V$. The difference in molar volume, ΔV , of the two ice modifications undoubtedly decreases at higher pressures. By this effect $\Delta\mu$ increases less at increasing pressure than is found when using the assumption, made in the calculations, that ΔV is constant.

2. Multiple occupation by neon molecules of the larger cavities is possible. This phenomenon adds to the stabilization.

The present treatment gives a less satisfactory result for ethane hydrate, and is apparently invalid for ethylene hydrate. This is not surprising, because the theory requires isotropic molecules which can freely rotate in the cavities. Fairly

large oblong molecules like ethane, however, will not have a uniform orientational distribution in the oblate tetrakaidecahedral cavities. By this effect the partial molar entropy of the gas in the hydrate is decreased, and consequently, its vapour pressure increased. The ethylene molecule with its double bond, moreover, is certainly not isotropic.

Von Stackelberg [18] already predicted the dissociation pressures of a number of gas hydrates on the basis of Trouton's rule. By this method a systematic deviation in the ratio of observed to predicted pressure is found when going from argon ($p_{\text{obs.}}/p_{\text{calc.}}=1.4$ to CF_4 ($p_{\text{obs.}}/p_{\text{calc.}}=0.1$). This is due to the fact that the influence of molecular size is not properly taken into account.

Once the value of $\bar{\epsilon}$ is known, the energies of reaction of the gas molecules with the different cavities are predicted by the statistical theory. Hence the heats of formation of the hydrates mentioned in table 1 can be calculated. Methane and ethane hydrate are the only compounds for which the heats of reaction have been determined when the hydrates are formed from normal α -ice and gas [15]. On comparing these data (table 2) with the calculated heats of formation from β -ice and gas, we arrive at the conclusion that the difference in molar enthalpy between β - and α -ice must be very small.

Hydrate former	$nS_{\beta} + M(g) \rightarrow \text{hydrate}$ $-\Delta H_{273^{\circ}\text{K}} (\text{calc.})$	$nS_{\alpha} + M(g) \rightarrow \text{hydrate}$ $-\Delta H_{273^{\circ}\text{K}} (\text{obs.})$
CH_4	4.44 kcal	4.4 kcal
C_2H_6	6.17 kcal	6.3 kcal

Table 2. Heats of formation of methane and ethane hydrate.

Neglecting this difference, and using the calculated compositions for the hydrates, the heats of reaction accompanying their formation from liquid water and gas can be evaluated.

In table 3 the results are compared with the observed values available, expressed as heat evolved in kcal per mole gas.

Hydrate former	Calc.	Obs.
Argon	13.16	—
Krypton	14.39	14.0 ± 0.5 [17]
Methane	14.38	14.5 [15]
Xenon	16.28	16.7 ± 0.5 [17]
CF_4	17.88	—
Ethane	16.13	16.3 [15]
Oxygen	13.49	—
Nitrogen	13.34	—

Table 3. Heats of the reaction $n\text{H}_2\text{O}(l) + M(g) \rightarrow \text{hydrate}$.

The present theory is strongly supported by the fact that the use of one determined constant only is sufficient for the agreement of calculated dissociation pressures and heats of formation of several gas hydrates with the observed values.

The present work involved laborious numerical calculations to obtain the free volume functions required. These were performed on the digital computer 'Miracle' of this laboratory by Mr. J. Varwijk, to whom the authors' thanks are due.

Le modèle cellulaire de Lennard-Jones et Devonshire est appliqué aux hydrates de gaz. La théorie permet le calcul des pressions de dissociation, des compositions et des chaleurs de décomposition d'un nombre de ces hydrates. On trouve une concordance satisfaisante entre les valeurs théoriques et expérimentales.

Auf die Gashydrate wird eine statistisch-mechanische Beschreibung angewandt. Hierbei wird ein von Lennard-Jones und Devonshire vorgeschlagenes Modell zugrunde gelegt. Die Theorie gestattet die Berechnung von Zusammenstellung, Dissoziationsdrucken und -wärmen verschiedener Gashydrate. Die Uebereinstimmung zwischen den berechneten und den zur Zeit bekannten gemessenen Werten bestätigt die Theorie.

REFERENCES

- [1] CLAUSSEN, W. F., 1951, *J. chem. Phys.*, **19**, 1425.
- [2] PAULING, L., and MARSH, R. E., 1952, *Proc. nat. Acad. Sci., Wash.*, **38**, No.1, 112.
- [3] VON STACKELBERG, M., and MÜLLER, H. R., 1954, *Z. Electrochem.*, **58**, 25.
- [4] VAN DER WAALS, J. H., 1956, *Trans. Faraday Soc.*, **52**, 184.
- [5] PLATTEEUW, J. C., 1958, *Rec. Trav. chim. Pays-Bas* (to be published).
- [6] MULDER, E. M. J., 1937, *Thesis Delft*.
- [7] PLATTEEUW, J. C., KOK, D., and VAN DER WAALS, J. H., 1958, *Rec. Trav. chim. Pays-Bas* (to be published).
- [8] PAULING, L., 1945, *The Nature of the Chemical Bond* (Cornell University Press).
- [9] DIEPEN, G. A. M. (private communication).
- [10] WHALLEY, E., and SCHNEIDER, W. G., 1955, *J. chem. Phys.*, **23**, 1644.
- [11] HIRSCHFELDER, J. O., CURTISS, C. F., and BIRD, R. B., 1954, *Molecular Theory of Gases and Liquids* (New York: Wiley and Sons).
- [12] SCHROEDER, W., 1926, *Die Geschichte der Gashydrate* (Stuttgart: F. Enke), p. 86.
- [13] *Ibid.*, p. 87.
- [14] *Ibid.*, p. 59.
- [15] ROBERTS, O. L., BROWNSCOMBE, E. R., and HOWE, L. S., 1940, *Oil Gas J.*, Dec. 5, 37.
- [16] DIEPEN, G. A. M., 1947, *Thesis, Delft*.
- [17] VON STACKELBERG, M., 1949, *Naturwissenschaften*, **36**, 360.
- [18] VON STACKELBERG, M., 1954, *Z. Electrochem.*, **58**, 104.

RESEARCH NOTE

Dielectric properties of iodine in aromatic solvents at 9000 Mc/sec

by G. W. NEDERBRAGT and J. PELLE
Koninklijke/Shell-Laboratorium, Amsterdam
(N.V. De Bataafsche Petroleum Maatschappij)

(Received 31 May 1957)

Dielectric [1, 2] and spectroscopic [3, 4] data show that a strong interaction exists between iodine and aromatic molecules in solution. This interaction has been interpreted as a formation of a complex between I_2 and the aromatic molecule [5], and specific structures have been suggested for the complex. According to Fairbrother [1] polarization accompanies coordinate bond formation of an iodine molecule with a solvent molecule having electron donor character. Information about the relaxation of this polarization may be obtained from experiments in the microwave region.

At a radio-frequency ω the real part ϵ of the dielectric constant $\epsilon(1 - i \tan \delta)$ of a solution can be expected to lie between the static value ϵ_s and the value ϵ_∞ at a very high frequency according to [6]

$$\epsilon - \epsilon_\infty = (\epsilon_s - \epsilon_\infty) \sum \frac{G_i}{1 + \omega^2 \tau_i^2},$$

while

$$\epsilon \tan \delta = (\epsilon_s - \epsilon_\infty) \sum \frac{G_i \omega \tau_i}{1 + \omega^2 \tau_i^2},$$

where δ is the loss angle. The relaxation is characterized by a number of relaxation times τ_i with weight factors G_i .

The complex dielectric constants of solutions of iodine in benzene, *p*-xylene and 1,3,5-trimethylbenzene were determined by the authors at 8950 Mc/sec by means of the resonating TE_{01} cavity method [7].

	0.00 mol. per cent I_2		1.90 mol. per cent I_2	
	ϵ	$\tan \delta$	$\Delta \epsilon$	$\Delta \tan \delta$
Benzene	2.272	0.00046	0.0270	0.00065
<i>p</i> -xylene	2.262	0.00075	0.0261	0.00095
Mesitylene	2.282	0.00200	0.0290	0.00180

In the case of benzene and *p*-xylene the increase $\Delta \epsilon$ in the dielectric constant of the solvent by the addition of 1.90 mol. per cent of I_2 is about the same as found by Fairbrother at low frequency. If the density values of this author are used, molecular polarizations of $P = 39 \text{ cm}^3$ for I_2 in benzene and $P = 46 \text{ cm}^3$ for I_2 in *p*-xylene are found. As these figures lie very near the low frequency values (38.5 and 47 cm^3 , respectively) it is clear that the main decrease occurs at frequencies

higher than that used in the present experiment. For I_2 in mesitylene $P = 54 \text{ cm}^3$ is derived from ϵ at 8950 Mc/sec and $d_4^{25} = 0.8606$ and 0.8876 for solvent and solution respectively. The value of $\Delta \tan \delta$ is larger than with the other aromatic molecules and indicates that the difference between ϵ at 8950 Mc/sec and the static value is not negligible. At long wavelength outside the loss region ϵ will be larger by an amount $(\epsilon \tan \delta)^2 : (\Delta \epsilon - \Delta \epsilon_\infty)$ in the case of one relaxation time and otherwise more. This correction makes P nearly 56 cm^3 . The difference with $P = 31 \text{ cm}^3$ for I_2 in cyclohexane [1, 2] amounts to an apparent dipole moment of I_2 in mesitylene of $1.1D$.

In all three cases the relaxation is rapid. It can be characterized by an effective relaxation time as used by Fischer [8]. For ω well to the low frequency side of the loss region $\Delta(\epsilon \tan \delta) : (\Delta \epsilon - \Delta \epsilon_\infty) = \sum G_i \omega \tau_i = \omega \tau_{\text{eff}}$. From the measurements at 8950 Mc/sec together with a $\Delta \epsilon_\infty$ value calculated from $P = 31 \text{ cm}^3$ for I_2 without complex formation one derives $\omega \tau_{\text{eff}} = 0.2$ and $\tau_{\text{eff}} = 4 \times 10^{-12} \text{ sec}$ for the I_2 -mesitylene solution. This is a small value as compared to relaxation times of rigid dipole molecules. For chlorobenzene and bromobenzene [9] in benzene $\tau = 7.5$ and $10 \times 10^{-12} \text{ sec}$.

The main conclusion is that the short relaxation time of the I_2 -mesitylene solution is possible by movement of the I_2 molecule with respect to the mesitylene molecule. It is an indication probably of both a fairly free movement in the complex and a short lifetime of the complex, a conception which is consistent with its low energy of formation. This limits the significance of specific structure assignments.

Thanks are due to Mr. A. Kok for preparing the solutions and to Mr. J. J. de Jong for assistance with some of the measurements.

REFERENCES

- [1] FAIRBROTHER, F., 1948, *J. chem. Soc.*, 1051.
- [2] KORTÜM, G., 1952, *J. chim. Phys.*, **49**, C127.
- [3] BENESI, H. A., and HILDEBRAND, J. H., 1948, *J. Amer. chem. Soc.*, **70**, 2832; 1949, *Ibid.*, **71**, 2703.
- [4] ANDREWS, L. J., and KEEFER, R. M., 1952, *J. Amer. chem. Soc.*, **74**, 5200.
- [5] MULLIKEN, R. S., 1950, *J. Amer. chem. Soc.*, **72**, 600; 1955, *J. chem. Phys.*, **23**, 397.
- [6] BÖTTCHER, C. J. F., 1952, *Theory of electric polarization* (Amsterdam, Houston, London, New York: Elsevier Publishing Company), p. 367.
- [7] PENROSE, R. P., 1946, *Disc. Faraday Soc.*, 108.
- [8] FISCHER, E., 1949, *Z. Naturforsch.*, **4a**, 707.
- [9] WHIFFEN, D. H., and THOMPSON, H. W., 1946, *Disc. Faraday Soc.*, 114.

Wave functions for the methane molecule

by IAN M. MILLS

Department of Theoretical Chemistry, Cambridge University†

(Received 16 December 1957)

If the potential field due to the nuclei in the methane molecule is expanded in terms of a set of spherical harmonics about the carbon nucleus, only the terms involving s, f, and higher harmonic functions differ from zero in the equilibrium configuration. Wave functions have been calculated for the equilibrium configuration, first including only the spherically symmetric s term in the potential, and secondly including both the s and the f terms. In the first calculation the complete Hartree-Fock S.C.F. wave functions were determined; in the second calculation a variation method was used to determine the best form of the wave function involving f harmonics. The resulting wave functions and electron density functions are presented and discussed.

1. INTRODUCTION

It is well known that a useful approximation to the electron wave function in methane can be obtained by assuming that the charge distribution has spherical symmetry about the carbon atom. Longuet-Higgins and Brown [1] have derived significant results for the vibration frequencies without any further assumptions about the form of the electron wave function, and both Buckingham *et al.* [2] and Bernal [3] have actually calculated wave functions for such a model. Carter [4] has considered the method more generally, and calculated similar wave functions for silane. In the present work the results for methane have been extended, so as to obtain the best Hartree-Fock determinant wave function using this spherical model; also, in order to determine more precisely the value of the model, the leading non-spherical correction terms to the wave function have been calculated by expanding the functions of interest in terms of spherical harmonics about the carbon nucleus. The results of these two calculations are described in the first two sections below, and are briefly discussed in the fourth section; this work was carried out primarily for use in a perturbation calculation of vibration frequencies and infra-red intensities described in the succeeding paper, but the wave functions obtained may well be of value in other calculations also.

2. THE SPHERICAL APPROXIMATION

After separating the electronic and nuclear motions, the complete Hamiltonian for the ten electrons in methane may be written

$$H = \sum_{\mu=1}^{10} \left[-\frac{1}{2} \nabla_{\mu}^2 - \frac{Z}{r_{\mu}} - V(\mathbf{r}_{\mu}) \right] + \sum_{\mu > \nu} \frac{1}{r_{\mu\nu}} \quad (1)$$

(using atomic units; see for instance [6], p. 5). Here Z is the charge on the carbon nucleus, equal to 6 atomic units; \mathbf{r}_{μ} is the vector coordinate of the μ th

† Present address: The Department of Chemistry, The University, Reading, Berks.

electron measured from the carbon atom, and $r_{\mu\nu} = |\mathbf{r}_\mu - \mathbf{r}_\nu|$; finally $-V(\mathbf{r})$ is the potential of an electron at \mathbf{r} due to the four protons. We may expand $V(\mathbf{r})$ in a series of spherical harmonics about the carbon nucleus, as follows:

$$\begin{aligned}
 V(\mathbf{r}_\mu) &= \sum_{j=1}^4 \frac{1}{r_{\mu j}} = \sum_{j=1}^4 \sum_{k=0}^{\infty} \frac{r_{<}^k}{r_{>}^{k+1}} P_k(\cos \theta_{\mu j}) \\
 &= \sum_{j=1}^4 \left[\underbrace{\frac{1}{r_{>}}}_{\text{s term;}} + \underbrace{\frac{r_{<}}{r_{>}^2} \cos \theta_{\mu j}}_{\text{p term;}} + \underbrace{\frac{r_{<}^2}{r_{>}^3} \left(\frac{3}{2} \cos^2 \theta_{\mu j} - \frac{1}{2} \right)}_{\text{d term;}} \right. \\
 &\quad \left. + \underbrace{\frac{r_{<}^3}{r_{>}^4} \left(\frac{5}{2} \cos^3 \theta_{\mu j} - \frac{3}{2} \cos \theta_{\mu j} \right)}_{\text{f term;}} + \underbrace{\dots}_{\text{g and higher terms.}} \right]. \quad (2)
 \end{aligned}$$

Here \mathbf{r}_j is the vector coordinate of the j th proton, and $r_{>}$, $r_{<}$ are the greater and the lesser of $|\mathbf{r}_\mu|$ and $|\mathbf{r}_j|$. $\theta_{\mu j}$ is the angle between \mathbf{r}_μ and \mathbf{r}_j , and $P_k(z)$ is the normalized Legendre polynomial function of order k . The successive terms in this expansion have been labelled according to the type of surface harmonic function involved in their angular dependence.

In the equilibrium configuration, when the four protons are situated at the corners of a regular tetrahedron about the carbon nucleus, the terms involving p and d harmonics in the expansion (2) are zero. Thus if we ignore harmonics of symmetry f and higher, we obtain for the equilibrium configuration:

$$\begin{aligned}
 V(\mathbf{r}_\mu) &= \sum_{j=1}^4 \frac{1}{r_{>}} = \frac{4}{R_0}, \quad r_\mu < R_0 \\
 &= \frac{4}{r_\mu}, \quad r_\mu > R_0 \quad (3)
 \end{aligned}$$

where R_0 is the equilibrium CH distance. This is the approximation of a spherically symmetric equilibrium state, used in the present calculation; it actually corresponds to assuming that the protons are smeared out over a sphere of radius R_0 . Substituting (3) in (1), the Hamiltonian is formally similar to that for a 10-electron atom, and the lowest energy configuration will be the $(1s)^2(2s)^2(2p)^6 1S$ state corresponding to the Ne closed shell.

Using this approximation, and using the value $R_0 = 2$ atomic units, Buckingham *et al.* [2] derived the Hartree S.C.F. wave functions for methane, neglecting exchange. Bernal [3] recently repeated this calculation including exchange, but using analytical wave functions essentially similar to those used in atomic calculations; he was able to treat R_0 as a parameter to be varied so as to minimize the total energy, and in this way he found $R_0 = 1.975$ atomic units. In this work the complete Hartree-Fock wave functions, including exchange, were determined, since it was necessary to have the 'best' (i.e. lowest energy) Slater determinant wave function for use in the perturbation calculation described later. For convenience the value $R_0 = 2$ atomic units was used; the best observed value is 1.092 \AA [5], or 2.067 atomic units, and this difference is hardly significant compared to the approximations of the model. Longuet-Higgins and Brown [1] showed that for this model the proton sphere must include just $(6 + 3\sqrt{6}/8) = 6.92$ of the electrons in the equilibrium configuration; the wave functions derived here include 6.80 electrons within $R_0 = 2$, and 6.92 electrons within $R_0 = 2.02$. The wave functions of Buckingham *et al.* include 6.38 electrons within $R_0 = 2$.

The Hartree-Fock calculations were performed in exactly the manner described by Hartree [6]; the results are presented in tables 1 and 2 where the

Spherical approximation					f term
r	$P_{(1s)}$	$P_{(2s)}$	$P_{(2p)}$	$4\pi r^2 \rho^0(r)$	$q(r)$
0.02	+0.490	-0.092	+0.002	0.496	Zero
0.04	0.870	-0.164	0.006	1.568	Zero
0.06	1.159	-0.216	0.014	2.782	Zero
0.08	1.373	-0.254	0.023	3.902	Zero
0.10	1.527	-0.278	0.034	4.828	Zero
0.12	1.631	-0.292	0.046	5.504	Zero
0.14	1.695	-0.296	0.059	5.936	Zero
0.16	1.725	-0.292	0.074	6.156	Zero
0.18	1.730	-0.283	0.089	6.196	Zero
0.20	1.715	-0.268	0.104	6.090	Zero
0.22	1.683	-0.248	0.120	5.878	Zero
0.24	1.639	-0.224	0.136	5.586	Zero
0.26	1.586	-0.199	0.153	5.254	Zero
0.28	1.526	-0.171	0.169	4.892	0.001
0.30	1.461	-0.140	0.186	4.520	0.001
0.35	+1.290	-0.060	+0.227	3.647	0.002
0.40	1.119	+0.025	0.267	2.932	0.003
0.45	0.958	+0.110	0.305	2.418	0.006
0.50	0.812	+0.191	0.342	2.100	0.009
0.55	0.683	+0.267	0.376	1.928	0.014
0.60	0.570	+0.338	0.408	1.880	0.021
0.7	+0.388	+0.462	+0.466	2.044	0.038
0.8	0.264	+0.560	0.514	2.368	0.061
0.9	0.178	+0.635	0.555	2.732	0.090
1.0	0.120	+0.690	0.589	3.072	0.123
1.1	0.078	+0.728	0.616	3.362	0.163
1.2	0.048	+0.751	0.638	3.580	0.209
1.3	0.030	+0.764	0.654	3.740	0.262
1.4	0.018	+0.768	0.667	3.852	0.323
1.6	+0.008	+0.753	+0.678	3.902	0.446
1.8	0.003	0.717	0.674	3.746	0.577
2.0†	—	0.662	0.654	3.428	0.682
2.2	—	0.594	0.617	2.968	0.726
2.4	—	0.522	0.570	2.494	0.732
2.6	—	0.452	0.519	2.022	0.724
2.8	—	0.385	0.467	1.610	0.705
3.0	—	0.325	0.417	1.262	0.673
3.5	—	+0.206	+0.305	0.650	0.62
4.0	—	0.126	0.217	0.326	0.57
4.5	—	0.076	0.152	0.156	0.54
5.0	—	0.045	0.105	0.070	0.51
5.5	—	0.026	0.071	0.032	0.48
6.0	—	0.016	0.048	0.015	0.45

† Proton 'sphere' at $r = 2.0$ atomic units.

Table 1. Normalized radial wave functions for methane.

ϵ_{1s}	=	22.09	$F_0(1s\ 2s)$	=	0.738 ₅
ϵ_{2s}	=	1.787	$F_0(1s\ 2p)$	=	0.655 ₈
ϵ_{2p}	=	0.9022	$F_0(2s\ 2p)$	=	0.490 ₃
			$F_2(2p\ 2p)$	=	0.212 ₉
$I(1s)$	=	-19.870	$G_0(1s\ 2s)$	=	+0.040 ₈
$I(2s)$	=	-5.491 ₈	$G_1(1s\ 2p)$	=	+0.038 ₃
$I(2p)$	=	-4.853	$G_1(2s\ 2p)$	=	+0.304 ₀
$F_0(1s\ 1s)$	=	3.488 ₇			
$F_0(2s\ 2s)$	=	0.524 ₈			
$F_0(2p\ 2p)$	=	0.461 ₈			

Table 2. Energy parameters for methane in the spherical approximation. All in atomic units of energy. Hartree's notation, [6].

Total electronic energy of spherical model = -53.22.

radial wave functions $P(nl; r)$ and the important energy integrals are listed. The complete wave function Ψ is then a ten-electron determinant in the neon configuration involving the one-electron space functions:

$$\begin{aligned}\psi_{1s} &= \frac{1}{2\sqrt{\pi}} \frac{P(1s; r)}{r} \\ \psi_{2s} &= \frac{1}{2\sqrt{\pi}} \frac{P(2s; r)}{r} \\ \psi_{2p} &= \frac{\sqrt{3}}{2\sqrt{\pi}} \frac{P(2p; r)}{r} \cos \theta.\end{aligned}$$

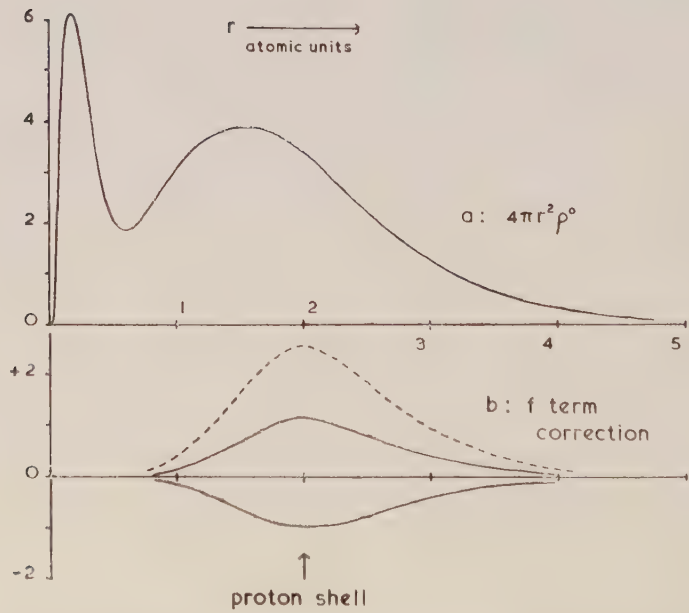


Figure 1. Radial density functions in electrons per atomic unit of length. The full lines in (b) show the correction to the density due to f harmonics, both in the direction of a proton (positive), and in the direction between three protons (negative),

The 1s function was calculated explicitly although it is very similar to that for the carbon atom; the 2s and 2p functions are, of course, considerably expanded from carbon atom functions, showing a greater concentration of the electrons in the region of the proton sphere (see the discussion in [2]). The total radial density function,

$$4\pi r^2 \rho = 2P_{1s}^2 + 2P_{2s}^2 + 6P_{2p}^2,$$

is shown in figure 1(a).

Calculated total energy of methane, $R_0=2$:			
(1) Spherical model :			
Electronic energy	-53.22		
Nuclear repulsion	+13.84	Total :	-39.38†
(2) Improved model :			
Electronic energy	-53.22-0.68		
Nuclear repulsion	+13.84	Total :	-40.06
Observed total energy of methane, equilibrium configuration :			
Sum of ionization potentials of C atom†	-38.04		
—and of four H atoms	-2.00		
Dissociation energy of CH ₄	+0.63		
Correction for zero point vibrations	+0.04	Total :	-40.71

Table 3. Total energy values in atomic units.

† Buckingham *et al.* who neglected exchange in calculating their wave functions, obtained a lower total energy by 1 atomic unit than that obtained here; this appears to be due to a considerable numerical error in their value for $I(1s)$. See also the note at the end of [4].

‡ Taken from *Tables of Atomic Energy Levels*, Circular 467 of National Bureau of Standards (1949).

The calculated total energy is shown in table 3, compared to the experimental total energy of C+4H and the known dissociation energy of methane; it is seen that the calculated total energy of the spherical model is about 3 per cent in error.

3. IMPROVED APPROXIMATION, INCLUDING f TERMS

The wave functions derived in the last section are based on a model which includes only the terms of spherical symmetry in the Hamiltonian, and it is very desirable to know how serious an error is involved in the neglect of f and higher terms in the expansion (2). Inclusion of the f term should correct for at least the major part of this error, since it is the first non-spherical term in the expansion which is not zero for reasons of symmetry; this term has been included by making a perturbation calculation on the wave functions derived for the spherical model. For the equilibrium configuration, the f term from (2) gives a perturbation potential function:

$$v(\mathbf{r}) = \frac{40\sqrt{\pi}}{3\sqrt{35}} \frac{r_{<}^3}{r_{>}^4} f_{xyz} \quad (4)$$

where

$$f_{xyz} = \frac{\sqrt{3}\sqrt{5}\sqrt{7}}{4\sqrt{\pi}} \sin^2 \theta \cos \theta \sin 2\phi$$

and where the four protons are assumed to lie in the directions of the maxima in the normalized surface harmonic f_{xyz} . The complete perturbation function will then be

$$- \sum_{\mu=1}^{10} v(\mathbf{r}_{\mu}).$$

A modified form of second-order perturbation theory was used for this calculation, as described by Pople and Schofield [7], and as used for the perturbation calculations described in the succeeding paper, where fuller details are given. This involves using a perturbed wave function of the form

$$\Psi = \Psi_0[1 + \sum_{\mu} q(\mathbf{r}_{\mu})] \quad (5)$$

where the function q is varied so as to minimize the energy for the perturbed system. A simple differential equation results for the function q .

Using the perturbation potential (4), q takes the form:

$$q(\mathbf{r}) = q(r) \cdot f_{xyz}. \quad (6)$$

The radial function $q(r)$ determined in this way is given in table 1. Unfortunately this correction function is too large to be regarded as a small perturbation, which is the assumption upon which it was derived; the correction to the radial density which results from the wave function (5) is shown by the dotted line of figure 1(b), where the correction is plotted along a maximum of the harmonic f_{xyz} . This improvement lowers the total energy by 0.28 atomic units.

A further improvement can be made by varying the amount of the correction function derived above to be mixed with the spherical wave function, and this is the basis of the final 'improved' function derived in this section. We assume a wave function

$$\Psi = \Psi_0[a + b \sum q(\mathbf{r})] \quad (7)$$

where $q(r)$ is the function derived above by the perturbation method, the radial part of which is given in table 1, but which we shall no longer regard as small compared to unity. We now vary a and b so as to minimize the energy, maintaining the normalization; this gives a simple secular equation from which we find:

$$a = 0.985, \quad b = 0.411 \quad (8)$$

with a lowering in the total energy of 0.68 atomic units from the energy of the spherical wave function Ψ_0 . It should be noted that the wave function (7) is normalized, whereas the wave function (5) is not normalized as it stands in so far as $q(\mathbf{r})$ cannot really be regarded as a small correction term. In table 3 the calculated energies using the spherical wave function Ψ_0 , and using the improved wave function given by (7) and (8), are compared with the observed energy for the methane molecule.

The electron density function corresponding to the improved wave function (7) is given by

$$\rho(\mathbf{r}) = a^2 \rho^0 + 2ab \rho^0 q(\mathbf{r}) + b^2 \rho^0 q(\mathbf{r})^2 \quad (9)$$

where $\rho^0(r)$ is the spherically symmetrical density function corresponding to Ψ_0 . Evidently the correction terms to the spherical part of the density, i.e. the last two terms in (9), represent an extra concentration of the electron density around each of the four protons, situated in the directions of the maxima of the surface harmonic f_{xyz} . In figure 1(b) this correction to the spherical part of the density

is plotted both along a maximum of the spherical harmonic f_{xyz} (i.e. through a proton), and along a minimum (i.e. through one of the 'holes' between three protons); the figure shows that the concentration of the electrons around the hydrogen atoms is sufficient to vary the electron density by a factor of 2 in going around the surface of the 'proton sphere'.

4. DISCUSSION

The wave functions derived for the spherical model of methane require little comment; they are very similar to those obtained by Buckingham *et al.*, except that they show the general contraction to be expected when the effects of electron exchange are included. The most notable result of this work is the considerable change in the total wave function which results from including the first non-spherical term in the expansion of the potential field. Thus the error in the calculated total energy is halved, and the electron density shows a considerable concentration around the four protons, when the non-spherical character of the wave function is allowed for. This non-spherical character may often be quite important in calculating observable quantities from an approximate wave function, and it seems that wave functions based on a spherical model for methane-type molecules should be used with caution.

Although the final wave function derived here is not in a very convenient form in terms of the ten-electron coordinates, it does integrate to give a convenient and simple form for the electron density function (9), which is the more useful function in physical applications. Moreover, most previous calculations for methane involve either implicit or explicit assumptions about the deviation from spherical symmetry in the wave function; the present work is an advance in that the contribution of f harmonics has been determined directly by a variational method. A wave function of this type must actually involve much higher harmonics if it is to represent adequately the cusp in the electron density which must truly occur at each of the protons, but the present work probably shows the major part of the non-spherical character in the electron density and is the most reliable wave function for the methane molecule at present available.

I am indebted to Professor H. C. Longuet-Higgins who suggested this problem, and also I am particularly indebted to Dr. J. A. Pople for many suggestions and discussions in the course of the work. It is a pleasure to acknowledge the help of Professor D. R. Hartree, F.R.S., in performing the Hartree-Fock calculations.

I wish to thank the Imperial Chemical Industries for a research fellowship during the tenure of which this work was carried out.

Lorsqu'on développe le champ de potentiel causé par les noyaux dans une molécule de méthane en fonction d'une série d'harmoniques supérieurs autour du noyau de carbone, seuls les termes contenant s , f et les harmoniques plus hauts ont une valeur qui diffère de zéro dans la configuration d'équilibre. On a calculé les fonctions d'onde pour la configuration d'équilibre, d'abord pour le cas où le potentiel ne contient que le terme s ayant une symétrie sphérique, et puis pour une autre fonction contenant les termes s et f . Dans le premier calcul on a déterminé les fonctions d'onde Hartree-Fock S.C.F. complètes; dans le deuxième calcul on a employé la méthode des variations pour déterminer la forme optimum de la fonction d'onde contenant les harmoniques f . On présente et discute les fonctions d'onde et de densité d'électrons obtenues.

Wenn man im Methanmolekül das von den Kernen hervorgerufene Potentialfeld nach Kugelfunktionen um den Kohlenstoffkern entwickelt, dann besitzen nur die Glieder mit s , f und höheren Kugelfunktionen einen von Null verschiedenen Wert in der Gleichgewichtskonfiguration. Wellenfunktionen für die Gleichgewichtskonfiguration wurden in zwei Näherungen berechnet, das eine Mal wurde ausschliesslich das kugelsymmetrische s -Glieder berücksichtigt, das andere Mal sowohl der s - als auch der f -Term. Bei der ersten Berechnung wurden die vollständigen Hartree-Fock-SCF-Wellenfunktionen bestimmt; bei der zweiten Berechnung wurde ein Variationsverfahren benutzt, um die beste Form der Wellenfunktion mit f -Termen zu ermitteln. Die erhaltenen Wellen- und Elektronendichtefunktionen werden mitgeteilt und erörtert.

REFERENCES

- [1] LONGUET-HIGGINS, H. C., and BROWN, D. A., 1955, *J. inorg. and nucl. Chem.*, **1**, 60.
- [2] BUCKINGHAM, R. A., MASSEY, H. S. W., and TIBBS, S. R., 1941, *Proc. roy. Soc. A*, **178**, 119.
- [3] BERNAL, M. J. M., 1953, *Proc. phys. Soc. Lond. A*, **66**, 514.
- [4] CARTER, C., 1956, *Proc. roy. Soc. A*, **235**, 321.
- [5] BOYD, D. R. J., and THOMPSON, H. W., 1953, *Proc. roy. Soc. A*, **216**, 143.
- [6] HARTREE, D. R., 1957, *The Calculation of Atomic Structures* (New York: John Wiley and Sons).
- [7] POPLE, J. A., and SCHOFIELD, P., 1957, *Phil. Mag.*, **2**, 591.

Vibrational intensities in methane

by IAN M. MILLS

Department of Theoretical Chemistry, Cambridge†

(Received 16 December 1957)

The absorption intensities of the two infra-red active vibrations in methane have been obtained from a perturbation calculation on the equilibrium wave functions derived in the preceding paper. The perturbation field is the change in the potential field due to the nuclei which results from moving the nuclei in the vibrational coordinate concerned, and a simplified form of second order perturbation theory, developed by Pople and Schofield, is used for the calculation. The main approximation involved is the neglect of f and higher harmonics in the spherical harmonic expansion of the nuclear field. The resulting dipole moment derivatives are approximately three times larger than the experimental values, but they show qualitative features and sign relationships which are significant.

The experimental intensity measurements are interpreted and discussed in relation to these results.

1. INTRODUCTION

In the past few years several workers have made accurate measurements of the absorption intensities of infra-red vibration bands, taking particular care to eliminate the experimental uncertainties, and often using a variety of isotopic species in order to resolve some of the sign ambiguities which arise in the interpretation; examples of such work are cited in references [1] to [5]. For the most part this work has been confined to diatomic or simple polyatomic molecules, and yet there have been few attempts to interpret the results obtained in wave mechanical terms, even in a qualitative manner. Moreover almost all such attempts [6-9] have involved to a greater or lesser degree assumptions which are equivalent to the 'bond moment hypothesis', in which the dipole moment is regarded as the sum of contributions from the individual bonds and changes in the dipole moment are analysed in terms of changes in these individual contributions. Experimentally this hypothesis has a very doubtful basis; it is known that 'bond moments' derived from infra-red intensities frequently show wide variations even for different vibrations of the same molecule [2], and they certainly do not have the same meaning as bond moments derived from measurements of the static dipole moment [6]. Theoretically it is found necessary to include the effects of orbital following and rehybridization in order to make sense of the model [6], and recently Coulson [10] has drawn attention to the existence of transverse components in the bond moment; it is evident that this model has lost the simplicity which was its redeeming feature. The quantum mechanical calculation of dipole moments is notoriously difficult, and must always involve approximations, but it seems that the division into bond moments is not a good basic approximation for calculating intensities: one should rather think in terms of wave functions extending over the whole molecule, as in calculating electronic spectra.

† Present address: The Department of Chemistry, The University, Reading, Berkshire.

The present work is an attempt to calculate the vibration intensities of the methane molecule by such a method. Methane was chosen because of its high symmetry, which makes possible the simplified calculation described below, and because it is a molecule for which the infra-red intensities [4, 5] and the normal coordinates are accurately known from experimental data (see Section 4 below). The calculation stands on its own and includes no adjustable parameters, and it does contain some drastic simplifications; although we can hardly hope to reproduce the experimental data to a high degree of accuracy by such a calculation, we can hope to gain some understanding of the problem and in particular some knowledge of the value (or otherwise) of our model.

2. GENERAL THEORY

The calculation of infra-red intensities involves determining the derivatives ($\partial \mathbf{p} / \partial Q$) of the molecular dipole moment \mathbf{p} with respect to the nuclear coordinates Q . To the Born–Oppenheimer approximation the dipole moment may be rigidly divided into two contributions: the nuclear moment \mathbf{p}_n which results from the bare nuclear charges, and the electron moment \mathbf{p}_e due to the distribution of electrons in the molecule. We may similarly write:

$$(\partial \mathbf{p} / \partial Q) = (\partial \mathbf{p}_n / \partial Q) + (\partial \mathbf{p}_e / \partial Q). \quad (1)$$

This corresponds to thinking of the change in the coordinate Q in two stages: first we move the bare nuclei, holding the electron wave function constant, and setting up a change in the dipole moment ($\partial \mathbf{p}_n / \partial Q$), and secondly we allow the electron wave function to ‘relax’ to its new minimum energy form, giving rise to a further change ($\partial \mathbf{p}_e / \partial Q$). The *energy* required to change the coordinate Q from equilibrium may be similarly divided:

$$\frac{\partial^2 E}{\partial Q^2} = \frac{\partial^2 n}{\partial Q^2} + \frac{\partial^2 e}{\partial Q^2} \quad (\text{equilibrium configuration}). \quad (2)$$

The first term in (2) will arise from nuclear–nuclear repulsions and nuclear–electron attractions; the second term represents the change in the kinetic and potential energy of the electrons as they relax, and must always be negative. The terms involving the first derivative of the energy must cancel, since we know that the total energy is at a minimum in equilibrium.

The change in the nuclear moment, ($\partial \mathbf{p}_n / \partial Q$), is readily determined when the form of the coordinate Q is known, but this term by itself is generally far too large (by a factor of the order of 10) to explain observed intensity measurements. The explanation is that the second term ($\partial \mathbf{p}_e / \partial Q$), giving the change in dipole moment due to the movement of the electrons, is always such as to nearly cancel the first term: in other words the electrons tend to follow the nuclei during the vibration. The question as to which term is the greater, which decides the sign of the overall change in dipole moment, depends on the particular vibration concerned; it is known from experimental data that the overall sign may be in either sense, even for different vibrations within the same molecule (see, for example, [2] on ethylene). However the total change in *energy* from equilibrium, equation (2), must always be positive if the molecule is stable.

One might hope to calculate the second term in (1), ($\partial \mathbf{p}_e / \partial Q$), by doing a perturbation calculation on the electron wave function in equilibrium, using the potential field set up by the movement of the nuclei as the perturbation. The

difficulty is that this requires a knowledge of both the ground and all the excited electronic state wave functions in the equilibrium configuration, and it is doubtful if there are any cases where we have adequate approximations to these functions. In the present work a modified form of second order perturbation theory was used, developed by Pople and Schofield [11], which requires a knowledge of only the ground electronic wave function in equilibrium, and which gives readily soluble equations in the highly symmetrical methane problem. If the unperturbed equilibrium wave function is written Ψ_0 , this being an antisymmetric function of the coordinates of all the N electrons, the perturbed wave function Ψ resulting from the perturbation field $v(\mathbf{r})$ is assumed to have the form

$$\Psi = \Psi_0 + \Psi_1 = \Psi_0 \left[1 + \sum_{\mu} u(\mathbf{r}_{\mu}) \right] \quad (3)$$

where $u(\mathbf{r})$ is a function of the same order as v , and the same function u is used for each of the electron coordinates in the sum in (3). If the function u is chosen to minimize the total energy, a simple differential equation for u is obtained [11]:

$$\text{div} [\rho_1^0 \text{grad } u] = 2\sigma \quad (4)$$

where,

$$\sigma(\mathbf{r}) = \rho_1^0(\mathbf{r}) \cdot v(\mathbf{r}) + \int \rho_2^0(\mathbf{r}\mathbf{r}') v(\mathbf{r}') d\mathbf{r}' \quad (5)$$

ρ_1^0 and ρ_2^0 being the electron density and the pair-electron density functions for the unperturbed wave function, defined by (6) and (7):

$$\rho_1^0(\mathbf{r}) = N \int \Psi_0^2 \cdot d\tau_2 \dots d\tau_N ds_1, \quad (6)$$

$$\rho_2^0(\mathbf{r}\mathbf{r}') = N(N-1) \int \Psi_0^2 \cdot d\tau_3 \dots d\tau_N ds_1 ds_2. \quad (7)$$

Here the integrations are over the spatial coordinates of all but one and all but two of the N electrons respectively, but over the spin coordinates of all the electrons.

When $u(\mathbf{r})$ has been found by solution of (4), with appropriate boundary conditions, the perturbation energy is given to the second order by:

$$\delta E = E_1 + E_2 \quad (8)$$

where

$$E_1 = \int \rho_1^0(\mathbf{r}) v(\mathbf{r}) d\mathbf{r} \quad (9)$$

and

$$E_2 = -\frac{1}{2} \int [\text{grad } u]^2 \rho_1^0 d\mathbf{r} = \int \sigma u d\mathbf{r}. \quad (10)$$

E_1 may involve both first and second order terms; E_2 is strictly second order, is always negative, and corresponds exactly to the relaxation energy represented by the second term of equation (2). The perturbed one-electron density function $\rho_1(\mathbf{r})$ is given by (6) with Ψ in place of Ψ_0 ; this gives:

$$\rho_1(\mathbf{r}) - \rho_1^0(\mathbf{r}) = 2\rho_1^0(\mathbf{r}) u(\mathbf{r}) + 2 \int \rho_2^0(\mathbf{r}\mathbf{r}') u(\mathbf{r}') d\mathbf{r}'. \quad (11)$$

Strictly the perturbed wave function should be renormalized before it is used to determine densities in this way, but since the perturbation is in any case assumed to be small to the first order, the effect of renormalizing on equation (11) is small to the second order and may be neglected.

This perturbation theory, in particular the derivation of equation (4), is dependent upon the assumption that Ψ_0 is the *exact* solution to the unperturbed problem. In practice only an approximate function Ψ_0 will be available, but this can be used

to find approximations for u , ρ_1 and E_2 ; it is important, however, that it should not be possible to improve the approximate solution Ψ_0 by a modification of the form (3). An antisymmetric determinant Ψ_0 made up of Hartree-Fock wave functions fulfils this requirement only if integrals of the type $\int \Psi_0 H_0 \Psi_1 d\tau$ are always exactly zero; when Ψ_0 is only an approximate eigenfunction of H_0 , this leads to the restriction that Ψ_1 , and hence the perturbation function $v(\mathbf{r})$, must be of a different symmetry from the unperturbed Hamiltonian H_0 .

3. APPLICATION TO METHANE

In the preceding paper [12] approximate wave functions were derived for the equilibrium configuration of the methane molecule. It was shown that the potential field due to the four protons in methane may be expanded in terms of spherical harmonics about the carbon atom (equation (2) of the preceding paper), and that if only the first three terms are retained, involving s, p and d harmonics, the expansion takes the form:

$$V(\mathbf{r}) = \sum_{j=1}^4 \left[\frac{1}{r_{>}} + \frac{r_{<}}{r_{>}^2} \cos \theta_j + \frac{r_{<}^2}{r_{>}^3} \left(\frac{3}{2} \cos^2 \theta_j - \frac{1}{2} \right) \right] \quad (12)$$

where \mathbf{r}_j is the vector coordinate of the j th proton, $r_{>}$ and $r_{<}$ are the greater and lesser of $|\mathbf{r}|$ and $|\mathbf{r}_j|$, and θ_j is the angle between \mathbf{r} and \mathbf{r}_j . In the equilibrium configuration this expression is spherically symmetrical, the p and d terms being zero, and using this approximation to the nuclear field the Hartree-Fock wave functions for the ground state were derived and listed in table 1 of the preceding paper.

Symmetry	Frequency (cm^{-1})	Intensity	
		A_i ($\text{cm}^{-1} \text{ sec}^{-1}$ at NTP)	$\Gamma_i = (A_i/\nu_i)$ (cm^2/mole)
$\nu_1 \quad a_1$	2915	(not observed)	(not observed)
$\nu_2 \quad e$	1534	$21.5 \times 10^{10} (a)$	$104 \pm 50\%$
$\nu_3 \quad f_2$	3019	$1075 \times 10^{10} (b)$ $900 \times 10^{10} (c)$ $970 \times 10^{10} (d)$	$2663 \pm 5\%$
$\nu_4 \quad f_2$	1306	$472 \times 10^{10} (b)$ $450 \times 10^{10} (c)$ $444 \times 10^{10} (f)$	$2703 \pm 5\%$

Table 1. Vibration frequencies and absorption intensities in methane.

(a) From an estimate by Burgess *et al.* [19].

(b) From Welsh and co-workers [4] and [5].

(c) From Thorndike [17].

(d) From Rollefson and Havens [18].

In the present work these wave functions were used as the basis for a perturbation calculation of the type described in the last section. The perturbing field was taken to be the change in $V(\mathbf{r})$, given by equation (12), which results from moving

the four protons in the manner of a vibrational symmetry coordinate; the perturbation energy to the second order should then give the electronic contribution to the force constant, $(\partial^2 e/\partial Q^2)$ in equation (2), and the perturbed electron density function may be integrated to give the change in electron dipole moment, $(\partial \mathbf{p}_e/\partial Q)$ in equation (1). The work of Longuet-Higgins and Brown [13], who considered the vibration frequencies of methane on a very simple spherical model entirely neglecting electron relaxation, suggests that equation (12) should be a useful approximation to the true nuclear field; this is the basic approximation of the present work.

Methane has four distinct vibration frequencies, appearing in three different symmetry classes as shown in table 1; the symmetry coordinates used, and the corresponding perturbation fields $\tau(\mathbf{r})$ obtained from equation (12), are given in the Appendix. The calculations are discussed below for each of the symmetry coordinates in turn.

S_1 : Breathing vibration.

Unfortunately our simplified perturbation theory cannot be applied to this coordinate, owing to the fact that $\tau(\mathbf{r})$ is a spherical function of the same symmetry as the unperturbed Hamiltonian (see the last paragraph of the preceding section). This is not true of any other coordinate in methane. Thus to obtain the breathing vibration frequency it would be necessary to repeat the Hartree-Fock calculations for a different value of R_0 . Carter [14] has done this by an approximate method, using the function of Buckingham *et al.* [15], with an approximate correction for the effects of exchange; he obtains a value for ν_1 about 10 per cent higher than the observed value.

S_2 : Twisting vibration.

Although this vibration is not infra-red active, the perturbation calculation was carried through in the hope of calculating a reasonable value for the twisting frequency ν_2 . The coordinates used, and the corresponding perturbation fields are given in equations (A.2) and (A.6). The correction function $u(\mathbf{r})$ takes the form

$$u(\mathbf{r}) = w_d(r) \cdot d_{(2z^2 - x^2 - y^2)} \quad (13)$$

for the coordinate S_{2a} , with a similar expression for S_{2b} , involving the surface harmonic d_{xy} . Equation (4) now simplifies to an equation for $w_d(r)$ in the single radial coordinate r , and the boundary conditions follow from the fact that Ψ must be univalued at $r=0$ and must tend to zero as $r \rightarrow \infty$. The equation was solved by numerical integration, and the function $w_d(r)$ is given in table 3.

The perturbation energy was calculated from equation (10), the two forms providing a check on the correctness of the solution for u ; this gave

$$(\partial^2 e/\partial S_2^2) = -0.078_0 \text{ atomic units.} \quad (14)$$

Contributions from E_1 , equation (9), are zero by symmetry. The term $(\partial^2 n/\partial S_2^2)$ arises only from nuclear-nuclear repulsion forces in this case, since there is no change in the nuclear-electron attraction energy for a pure bending coordinate in a spherically symmetrical electron distribution; we find

$$(\partial^2 n/\partial S_2^2) = \frac{3\sqrt{6}}{32 R_0^3} = +0.0287 \text{ atomic units,} \quad (15)$$

taking $R_0 = 2$ atomic units, as in the preceding paper. Hence for the total change in energy with respect to S_2 :

$$(\partial^2 E / \partial S_2^2) = +0.0287 - 0.078_0 = -0.049 \text{ atomic units.} \quad (16)$$

We thus obtain a negative vibration frequency, indicating that our model is unstable in this coordinate. Longuet-Higgins and Brown [13] used only the first term from (16) in their calculation, and this gives a frequency 1496 cm^{-1} , within 10 per cent of the experimental value†.

This result is disappointing, but in retrospect it is not difficult to understand. In fact it arises from the approximate character of the model, in which we have ignored terms of symmetry f and higher in the nuclear potential. In the preceding paper it was shown that inclusion of the f term makes a considerable difference to the equilibrium wave functions, giving rise to a concentration of the electron density around each of the protons and to a consequent lowering in the total energy of 0.6 atomic units. The effect of this on the force constant would be as follows: the positive term $(\partial^2 n / \partial S_2^2)$ would be considerably increased since there would be attractive forces between each proton and its 'pocket' of extra electrons, and these would always be such as to restore the equilibrium configurations; the negative term $(\partial^2 e / \partial S_2^2)$ should not be greatly altered, since it represents the relaxation energy gained by including d harmonics in the electron distribution, and the perturbation calculation by which this term was derived is not sensitive to the inclusion of f harmonics. In the *distorted* configuration the d harmonic terms in the density represent, to some extent, this concentration of electron density around the protons, and hence the electron relaxation energy is always large; but in the *equilibrium* configuration this concentration can only be represented by the inclusion of f harmonics. Thus the error in (16) may be largely attributed to the positive term being too small, because it contains no contribution from the nucleus-electron interactions.

The broad truth of this interpretation is verified by taking the improved wave function of section 2 in the preceding paper, which does include a term of symmetry f_{xyz} in the electron density, and using it to calculate the electron-nucleus interaction term which is lacking from equation (16): we find an extra contribution $+0.070$ atomic units in the term $(\partial^2 n / \partial S_2^2)$, so that (16) becomes

$$\begin{aligned} (\partial^2 E / \partial S_2^2) &= +0.0287 + 0.070 - 0.078 \\ &= +0.021 \text{ atomic units.} \end{aligned} \quad (17)$$

This gives a positive frequency of 1250 cm^{-1} , in reasonable agreement with experiment. However this is probably not significant since the two cancelling terms of (17) have here been calculated from two different equilibrium wave functions. One might finally observe that even when one calculates vibration frequencies from an equation of the form (2), they tend to appear as a small difference between two large quantities.

S_3 and S_4 : *Infra-red active vibrations.*

The threefold degenerate symmetry coordinates S_3 and S_4 are defined as a pure stretching and a pure bending coordinate according to equations (A.3) and

† Equation (15) is essentially the same as Longuet-Higgins and Brown's equation for the twisting frequency parameter, except that their expression includes the mass factor $3e^2/m$. The figure 1496 cm^{-1} given here differs from their figure of 1429 cm^{-1} owing to the different bond length used here (see the discussion in the preceding paper); this difference is of no significance.

(A.4) in the Appendix; the corresponding perturbation fields are given by equations (A.7) and (A.8). The true normal coordinates will be linear combinations of S_3 and S_4 , to be obtained by solving the appropriate secular equation; this will involve the three force constants

$$\left(\frac{\partial^2 E}{\partial S_3^2}\right), \left(\frac{\partial^2 E}{\partial S_3 \partial S_4}\right) \text{ and } \left(\frac{\partial^2 E}{\partial S_4^2}\right).$$

These may all be obtained, in principle, by perturbation calculations similar to that just described, and hence both the vibration frequencies and the normal coordinates may be determined.

In view of the above results for the twisting vibration there would seem to be little point in this calculation, for there is every reason to suppose that the results for these vibrations would show similar errors. However in calculating dipole moments, and hence infra-red intensities, the situation is not so bad, for the following reason. For both S_3 and S_4 the function u takes the form

$$u(\mathbf{r}) = w_p(r) \cdot \hat{p}_z + w_d(r) \cdot \hat{d}_{xy} \quad (18)$$

where w_p and w_d are radial functions; similarly the perturbed electron density has the form

$$\rho_1(\mathbf{r}) - \rho_1^0(\mathbf{r}) = \rho_p(r) \cdot \hat{p}_z + \rho_d(r) \cdot \hat{d}_{xy} \quad (19)$$

where ρ_p derives from w_p and ρ_d from w_d . Now when the electron density is expanded in terms of spherical harmonics, only the terms of p symmetry give rise to a dipole moment, hence it is only necessary to determine w_p in (18) and hence ρ_p in (19) in order to calculate $(\partial \mathbf{p}_e / \partial S_3)$. Moreover approximate calculations indicate that even if terms in f harmonics were included, using the improved wave functions of the preceding paper, the functions w_p and ρ_p would not be greatly changed; the main difference would be the appearance of higher harmonic terms in equations (18) and (19)—but these, of course, would give no dipole moment. Thus the simplified perturbation calculation, neglecting f and higher harmonics, may well give significant results for the dipole moment even though it does not give significant results for the energy.

The functions $w_p(r)$ have been calculated for the coordinates S_3 and S_4 , and they are listed in table 3. Equation (4) splits into separate equations for w_p and w_d in each case, and those for w_p were solved by numerical integration; the boundary conditions are again fixed by the limitations of continuity and of finite extension for the wave function. The corresponding density functions $\rho_p(r)$ were determined from equation (11), and are also given in table 3. Finally the dipole moment vectors $(\partial \mathbf{p}_e / \partial S_3)$ and $(\partial \mathbf{p}_e / \partial S_4)$ were obtained from the density functions by multiplying by \mathbf{r} and integrating, and the resulting contributions to the total dipole moment as a function of S_3 and S_4 are given in table 2. Also given in table 2 are the experimental dipole moment derivatives, and their relative signs, according to the interpretation of the infra-red intensity data discussed in the following section. The signs of the calculated dipole moment derivatives are illustrated in figure 1.

It will be seen from table 2 that the calculated dipole moment derivatives are about three times larger than the experimental values, but that they have the same relative magnitudes and relative signs. The absolute signs (which are not known

experimentally) are calculated to be such that for S_4 the effective bond moment μ_{CH} is in the direction C^+-H^- , and for S_3 the effective charge $\epsilon_{\text{CH}} = (\partial\mu_{\text{CH}}/\partial r)$ is in the opposite sense. Coulson [16] came to the same conclusion about the sense of

	Calculated			Observed (from table 4)
	Protons	Electrons	Total	
$(\partial p^z/\partial S_{3a})$	5.51	-2.48	+3.03	± 0.833
$(\partial p^z/\partial S_{4a})$	5.51	-6.89	-1.38	± 0.373

Table 2. Calculated and observed values of $(\partial p/\partial S_j)$ for the infra-red active vibrations of methane; (Debye/Å). The symmetry coordinates are defined in equations (A.3) and (A.4), and illustrated in figure 1.

r atomic units	S_2 $w_d(r)/\delta S_2$	S_3 $w_p(r)/\delta S_3$	S_4 $w_p(r)/\delta S_4$
0.0	—	—	—
0.1	0.000	-0.004	+0.003
0.2	0.000	-0.012	+0.008
0.3	0.000	-0.024	+0.016
0.4	0.001	-0.046	+0.032
0.5	0.003	-0.079	+0.057
0.6	0.005	-0.123	+0.091
0.7	0.009	-0.169	+0.130
0.8	0.013	-0.212	+0.169
0.9	0.018	-0.250	+0.206
1.0	0.023	-0.283	+0.243
1.2	0.035	-0.333	+0.313
1.4	0.047	-0.354	+0.381
1.6	0.061	-0.339	+0.444
1.8	0.073	-0.273	+0.500
2.0	0.082	-0.142	+0.543
2.2	0.087	+0.013	+0.569
2.4	0.087	+0.141	+0.583
2.6	0.085	+0.249	+0.589
2.8	0.082	+0.340	+0.589
3.0	0.078	+0.418	+0.583
3.5	0.065	+0.565	+0.555
4.0	0.051	+0.651	+0.508
4.5	0.035	+0.709	+0.461
5.0	0.021	+0.755	+0.411

Table 3. Calculated radial correction functions for the equilibrium wave function, due to each of the three non-symmetrical vibrational symmetry coordinates in methane.

the bond dipole in methane, but it is important to note that he was calculating the 'static bond moment' from the equilibrium wave functions, which may be very different from the effective bond moment required to explain a calculated value of the dipole moment derivative $(\partial \mathbf{p}/\partial S_4)$.

The difference of sign between μ and ϵ is significant, and may be understood in a qualitative way as follows. In figure 2(a) the radial density function $4\pi r^2 \rho_1^0$ is shown for the equilibrium configuration, and in figures 2(b) and 2(c) the relevant change in this density function in the Z direction is shown for unit displacement of the coordinates S_{3a} and S_{4a} . These are the terms $4\pi r^2 \rho_p$, from equation (19), of symmetry p_z , which give rise to a dipole moment in the distorted configuration. It is seen that for the stretching coordinate S_3 this increment in the density changes sign at the proton sphere, so that the resulting electron moment is the difference of two parts and is small relative to the nuclear contribution; for the bending coordinate the increment in the density has no such radial node and is correspondingly

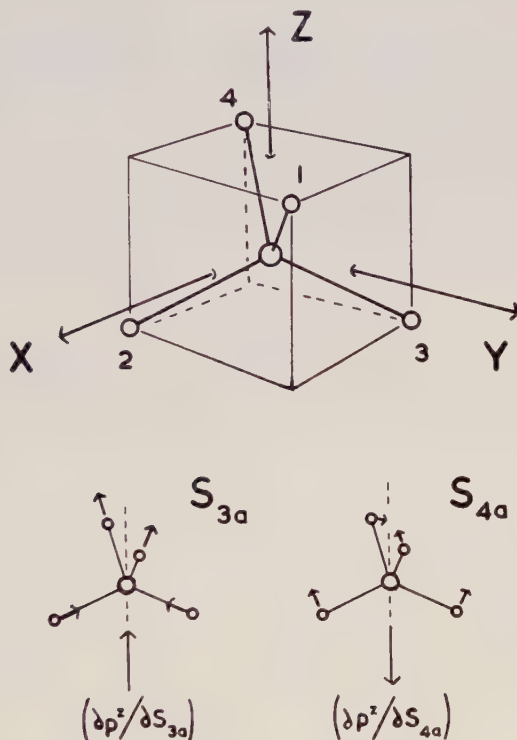


Figure 1. Coordinates in methane: r_i CH_i distance, and $\alpha_{ij} = \widehat{\text{H}_i\text{CH}_j}$. The two infra-red active symmetry coordinates, and the corresponding dipole moment derivatives, are also illustrated.

larger. This result follows from the fact that the p_z term in $v(\mathbf{r})$ shows a radial node for S_3 (equation A.7) but not for S_4 (equation A.8), for it is approximately true that changes in the electron density reflect changes in the potential field. The final result is that the term in the dipole moment due to electron relaxation is sufficiently large to reverse the proton moment in S_4 , but not in S_3 , leading to opposite signs for μ and ϵ .

Before discussing these results further, it is necessary to consider the interpretation of the infra-red intensity data upon which the experimental dipole-moment derivatives of table 2 are based. This is discussed in the following section.

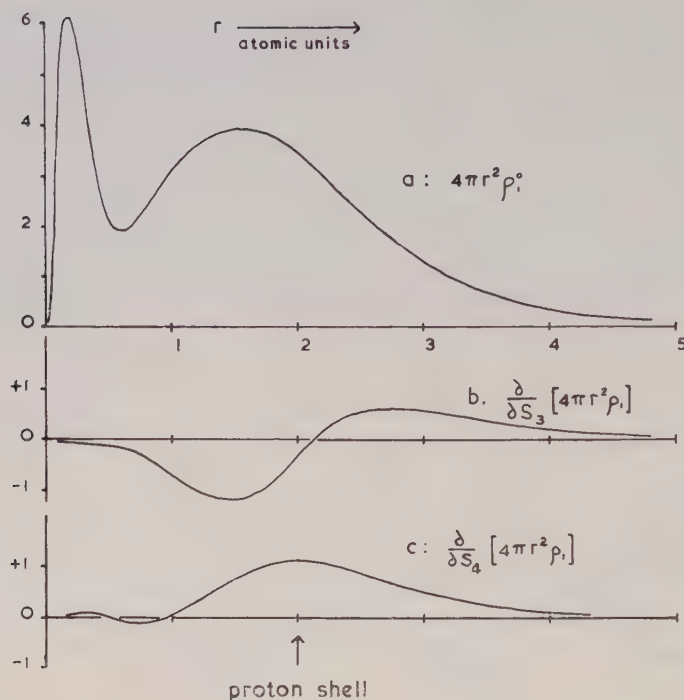


Figure 2. Radial density functions in electrons per atomic unit of length. (a) shows the equilibrium configuration; (b) and (c) show the p term from the derivatives with respect to the two infra-red active symmetry coordinates, plotted along a maximum of $\cos \theta$.

4. EXPERIMENTAL INTENSITY DATA

Undoubtedly the most reliable intensity measurements on the two infra-red active methane bands are those of Welsh and co-workers [4, 5], who used the Wilson-Wells technique with large excess pressures of argon, helium and nitrogen to ensure adequate pressure broadening. The measurements were extrapolated to zero pressure of the broadening gas to eliminate the effects of induced absorption, and this work is, in fact, a classic example of the use of the Wilson-Wells technique. Thorndike [17] and Rollefson and Havens [18] have also measured the intensities of these bands, the latter authors using a dispersion method. All the results are essentially in agreement and they are shown in table 1, both in Welsh's units and in units of $\Gamma_i = (A_i/\nu_i)$ (see [2]). The limits of error in table 1 are only intended to give a rough estimate of the reliability of the data. The twisting vibration ν_2 , which is symmetry forbidden in the infra-red, is made active by Coriolis interaction with ν_4 ; the intensity quoted in table 1 is an approximate estimate from the work of Burgess *et al.* [19].

Since the twisting vibration ν_2 is only made active by 'borrowing' intensity from ν_4 , the unperturbed intensity of ν_4 is obtained by adding the observed Γ values: $(\Gamma_2 + \Gamma_4)$ [2]. We thus obtain for the unperturbed intensities

$$\Gamma_3 = 2663 \text{ cm}^2/\text{mole}$$

$$\Gamma_4 = 2810 \text{ cm}^2/\text{mole}.$$

Taking the harmonic vibration frequencies (see below) to be

$$\omega_3 = 3156 \text{ cm}^{-1}, \quad \omega_4 = 1358 \text{ cm}^{-1}$$

and applying the relation [2]

$$\frac{\Gamma_i}{d_i} = \frac{1}{\omega_i} \frac{N\pi}{3c^2} \left(\frac{\partial \mathbf{p}}{\partial Q_i} \right)^2 \quad (20)$$

where d_i is the degeneracy of the coordinate Q_i , we find dipole moment derivatives

$$(\partial p^z / \partial Q_3) = \pm 1.410 \text{ Debye/\AA}(\text{amu})^{1/2}$$

$$(\partial p^z / \partial Q_4) = \pm 0.950 \text{ Debye/\AA}(\text{amu})^{1/2}.$$

To obtain derivatives with respect to the symmetry coordinates S_3 and S_4 the normal coordinate transformation must be known. Dennison's calculations [20] have been repeated for both CH_4 and all the deuterio-isotopes of methane, using the greatly improved frequency data now available [21]; the results are given in the Appendix and in table 5, where the calculated and observed vibration frequencies are given for all five molecules. For CH_4 and CD_4 the anharmonicity corrections were made, using the product rule, by the method described by Dennison [20]: it is assumed that the harmonic frequencies ω_i are related to the observed frequencies ν_i according to

$$\nu_i = \omega_i(1 - x_i) \quad (22)$$

and that for an isotopic species, indicated by an asterisk,

$$\omega/\omega_i^* = x_i/x_i^* \sim \nu_i/\nu_i^*. \quad (23)$$

These equations, with the product rule, serve to fix exactly the anharmonicity terms x_i for CH_4 and CD_4 , except in the F_2 class where the remaining degree of freedom was taken to be identical with Dennison's choice. The harmonic frequencies for CH_4 and CD_4 , thus determined, fix the general force field; the anharmonicities for the other molecules, given in table 5, are those which result from comparing the calculated ω 's with the observed ν 's.

Finally using the calculated normal coordinates for CH_4 given in the Appendix, we find the $(\partial \mathbf{p} / \partial S_j)$ values and effective bond moments given in table 4. The relations used are

$$\left. \begin{aligned} (\partial \mathbf{p} / \partial S_j) &= \sum_i (L^{-1})_{ij} (\partial \mathbf{p} / \partial Q_i) \\ Q_i &= \sum_j (L^{-1})_{ij} S_j \end{aligned} \right\} \quad (24)$$

where

and

$$\left. \begin{aligned} (\partial p^z / \partial S_3) &= + \frac{2}{\sqrt{3}} \epsilon_{\text{CH}} \\ (\partial p^z / \partial S_4) &= + \frac{2}{\sqrt{3}} (\mu_{\text{CH}} / R_0) \end{aligned} \right\} \quad (25)$$

In equations (25) μ_{CH} is taken to be positive in the sense C^-H^+ , and $\epsilon_{\text{CH}} = (\partial \mu_{\text{CH}} / \partial r)$.

	$(\partial \mathbf{p} / \partial S_3),$	ϵ_{CH}	$(\partial \mathbf{p} / \partial S_4),$	μ_{CH}/r_0
(++) choice	± 0.723	± 0.626	± 0.339	± 0.294
(+-) choice	± 0.833	± 0.721	∓ 0.373	∓ 0.323

Table 4. Dipole moment derivatives and bond moments from experimental data, in Debye/Angstrom.

The notation (++) or (+-) indicates the relative signs chosen for $(\partial \mathbf{p} / \partial Q_3)$ and $(\partial \mathbf{p} / \partial Q_4)$; for a particular choice the relative signs of $(\partial \mathbf{p} / \partial S_3)$ and $(\partial \mathbf{p} / \partial S_4)$ are fixed but the absolute signs are not fixed.

There is the usual choice to be made between the two possible sign combinations of the $(\partial \mathbf{p} / \partial Q_j)$ as they enter equation (24); this is indicated by the notation (++) and (+-) in table 4. This choice should strictly be made by

	CH ₄			CD ₄		
	ν	ω	x	ν	ω	x
1 a ₁	2915	3027	0.0368	2085	2141	0.026
2 e	1534	1567	0.0214	1092	1109	0.015
3 f ₂	3019	3156	0.0434	2259	2337	0.033
4 f ₂	1306	1358	0.0382	996	1026	0.029
	CH ₃ D			CD ₃ H		
	ν	ω	x	ν	ω	x
1 } a ₁	2945	3065	0.039	2142	2186	0.020
2 } a ₁	1300	1352	0.039	1003	1035	0.031
3 } a ₁	2200	2283	0.036	2993	3128	0.043
4 } e	3021	3156	0.043	2263	2337	0.032
5 } e	1471	1507	0.024	1036	1061	0.023
6 } e	1155	1197	0.035	1291	1324	0.025

	CH ₂ D ₂		
	ν	ω	x
1 } a ₁	2976	3098	0.040
2 } a ₁	2202	2232	0.014
3 } a ₁	1436	1474	0.026
4 } a ₂	1033	1058	0.024
5 } a ₂	1329	1357	0.020
6 } b ₁	3013	3156	0.045
7 } b ₁	1090	1126	0.032
8 } b ₂	2234	2337	0.044
9 } b ₂	1234	1277	0.034

Table 5. Calculated harmonic frequencies ω_i , observed frequencies ν_i , and anharmonicities x_i for the deuteromethanes; all in cm⁻¹.

comparing with intensity measurements on some isotopic species of the molecule; by applying the inverse of equation (24):

$$(\partial \mathbf{p} / \partial Q_i) = \sum_j L_{ji} (\partial \mathbf{p} / \partial S_j) \quad (26)$$

we can predict the vibrational intensities for any isotopic species using either choice of signs, and we should hope to find that only one sign combination gives self-consistency. Unfortunately there is only one measurement on an isotopic species of methane known to the author: this is a measurement of the intensity of the 2200 cm^{-1} vibration (CD stretching vibration) of CH_3D , made by Dr. W. T. King at the University of Washington (private communication.) He found an intensity:

$$\Gamma (\text{obs.}) = 182 \text{ cm}^2/\text{mole}, \quad 2200 \text{ cm}^{-1} \text{ region.}$$

Using the results of table 4 and the normal coordinates given in the Appendix we find either

$$(+ +) \text{ choice: } \Gamma = 519 \text{ cm}^2/\text{mole}$$

or

$$(+ -) \text{ choice: } \Gamma = 349 \text{ cm}^2/\text{mole.}$$

This leaves us with a startling discrepancy. The $(+ -)$ choice is obviously to be preferred, but even so the numbers differ by a factor of nearly 2; it is not conceivable that there could be such an error in the normal coordinates and one can only conclude that there is an error in the intensity data, probably in the measurement on CH_3D . This problem can only be solved by further intensity measurements on the deuteromethanes.

5. GENERAL DISCUSSION

Since the intensity measurements on CH_4 are undoubtedly more reliable than the one measurement on CH_3D , the latter should be regarded merely as a means of choosing between the two possible sign combinations. In so far as it is not inconsistent, the measurement on CH_3D definitely indicates that the $(+ -)$ choice is to be preferred, and accordingly the experimental data of table 2 are taken directly from the $(+ -)$ choice of table 4. We thus obtain opposite signs for $(\partial \mathbf{p} / \partial S_3)$ and $(\partial \mathbf{p} / \partial S_1)$, and as we have already seen this is in agreement with the results of the perturbation calculations. This may be regarded as further evidence for the correctness of the $(+ -)$ choice, since the only important change that results from selecting the $(+ +)$ choice is that the two derivatives must have the same sign, in contrast to the results of the calculation.

We may finally conclude that the infra-red intensities calculated in this work have qualitative significance, but are not quantitatively accurate. The errors appear to arise from the approximate nature of our model, in which we have neglected the higher harmonic terms in the nuclear field; it is probable that these errors could be largely removed by including f harmonics in all the calculations, but the labour involved would be considerable.

I am greatly indebted to both Professor H. C. Longuet-Higgins, who suggested this problem, and to Dr. J. A. Pople, who suggested the use of his modified perturbation theory and with whom I have had many invaluable discussions during the course of this work. I am also indebted to the Imperial Chemical Industries

for the award of a research fellowship during the tenure of which this work was carried out.

APPENDIX

The symmetry coordinates used for methane are defined below, where the internal coordinates used and the numbering of the atoms in relation to the cartesian axes are shown in figure 1.

$$S_1 = \frac{1}{2}(r_1 + r_2 + r_3 + r_4) \quad (\text{A.1})$$

$$\left. \begin{aligned} S_{2a} &= \frac{R_0}{2\sqrt{3}}(2\alpha_{12} + 2\alpha_{34} - \alpha_{13} - \alpha_{24} - \alpha_{32} - \alpha_{41}) \\ S_{2b} &= \frac{R_0}{2}(\alpha_{13} - \alpha_{32} + \alpha_{24} - \alpha_{41}) \end{aligned} \right\} \quad (\text{A.2})$$

$$S_{3a} = \frac{1}{2}(r_1 + r_4 - r_2 - r_3) \quad (\text{A.3})$$

$$S_{4a} = \frac{R_0}{\sqrt{2}}(\alpha_{23} - \alpha_{14}). \quad (\text{A.4})$$

The other components of the threefold degenerate coordinates S_3 and S_4 are obtained by permuting the subscripts 2, 3 and 4 on the internal coordinates. The perturbation fields $v(\mathbf{r})$ corresponding to these coordinates, derived from equation (12), are as follows:

$$\begin{aligned} \text{for } S_1: \quad v(\mathbf{r}) &= -\frac{2S_1}{R_0^2}, \quad r < R_0 \\ &= 0, \quad r > R_0 \end{aligned} \quad (\text{A.5})$$

$$\text{for } S_2: \quad v(\mathbf{r}) = -\frac{4\sqrt{(30\pi)} r_{<}^2}{15 r_{>}^3} d_{(2z^2 - x^2 - y^2)} \frac{S_{2a}}{R_0} \quad (\text{A.6})$$

with a similar expression for S_{2b} involving the harmonic d_{xy} .

$$\begin{aligned} \text{for } S_3: \quad v(\mathbf{r}) &= \frac{4\sqrt{\pi}}{3} \left[-\frac{2r}{R_0^2} p_z - \frac{3\sqrt{15}}{5} \frac{r^2}{R_0^3} d_{xy} \right] \frac{S_{3a}}{R_0}, \quad r < R_0 \\ &= \frac{4\sqrt{\pi}}{3} \left[\frac{R_0}{r^2} p_z + \frac{2\sqrt{15}}{5} \frac{R_0^2}{r^3} d_{xy} \right] \frac{S_{3a}}{R_0}, \quad r > R_0 \end{aligned} \quad (\text{A.7})$$

and for S_4 :

$$v(\mathbf{r}) = \frac{4\sqrt{\pi}}{3} \left[\frac{r_{<}^2}{r_{>}^3} p_z - \frac{\sqrt{15}}{5} \frac{r_{<}^2}{r_{>}^3} d_{xy} \right] \frac{S_{4a}}{R_0} \quad (\text{A.8})$$

where the expressions for the other components of S_3 and S_4 are obtained by permuting the subscripts x , y and z on the surface harmonic functions. In equations (A.5) to (A.8), p_z , d_{xy} and $d_{(2z^2 - x^2 - y^2)}$ denote the appropriate normalized surface harmonic functions, and $r_{>}$, $r_{<}$ denote the greater and lesser of $|\mathbf{r}|$ and R_0 .

The normal coordinate calculations were made by the F-G method of Wilson. The appropriate G matrix elements have all been published previously. The

harmonic frequencies for CH_4 and CD_4 , given in table 4, serve to fix the force field completely; we find for the five force constants, in dynes/Angstrom:

$$F_{11}=5.4388; \quad F_{22}=0.4860; \\ F_{33}=5.3704, \quad F_{34}=-0.1880, \quad F_{44}=0.4576.$$

Using these force constants the harmonic frequencies for all the deuterio-derivatives of methane, were calculated, and these are shown in table 4. The elements of the L^{-1} matrix which relates the symmetry coordinates S to the normal coordinates Q ($Q=L^{-1}S$) are shown below for the infra-red active class of CH_4 :

$$L^{-1}: \quad \begin{array}{cc} S_3 & S_4 \\ \begin{array}{c} Q_3 \\ Q_4 \end{array} \left[\begin{array}{cc} 0.9559 & -0.0211 \\ -0.0994 & 0.6474 \end{array} \right] & (\text{a.m.u.})^{\frac{1}{2}} \end{array}$$

For CH_3D the calculation was made using a different set of symmetry coordinates in terms of which the secular equation more nearly factorises; for the A symmetry class these are

$$S_1 = \frac{1}{\sqrt{3}}(r_1 + r_2 + r_3) \\ S_2 = \frac{R_0}{\sqrt{6}}(\alpha_{12} + \alpha_{23} + \alpha_{31} - \alpha_{14} - \alpha_{24} - \alpha_{34}) \\ S_3 = r_4$$

where the deuterium atom is assumed to be in the position 4. In terms of these coordinates the L matrix, used to calculate the predicted intensity of the C-D stretching vibration, is as follows:

$$L: \quad \begin{array}{ccc} Q_1 & Q_2 & Q_3 \\ \begin{array}{c} S_1 \\ S_2 \\ S_3 \end{array} \left[\begin{array}{ccc} 1.0078 & -0.0180 & +0.0601 \\ -0.0964 & 1.5382 & +0.2300 \\ -0.0927 & +0.0063 & 0.7557 \end{array} \right] & (\text{a.m.u.})^{-\frac{1}{2}} \end{array}$$

where the numbering of the normal coordinates corresponds to the numbering of the frequencies in table 5.

On a calculé les intensités d'absorption de deux vibrations du méthane, actives à l'infra-rouge, en faisant un calcul de perturbation avec les fonctions d'onde en état d'équilibre, dérivées dans l'article précédent. Le champ de perturbation est le changement du champ de potentiel causé par les noyaux, provenant du mouvement des noyaux dans la coordonnée correspondante de vibration; on a employé pour le calcul une forme simplifiée de la théorie des perturbations de deuxième ordre, développée par Pople et Schofield. La principale approximation consiste en l'omission de f et des harmoniques supérieurs dans le développement des harmoniques sphériques du champ nucléaire. Les valeurs des dérivées du moment dipolaire obtenues sont environ trois fois plus grandes que les valeurs expérimentales, mais elles possèdent des caractéristiques qualitatives et des relations de signe significatives.

En se basant sur ces résultats, on interprète et discute les mesures expérimentales d'intensité.

Es wurden Absorptionsintensitäten von zwei ultrarotaktiven Schwingungen im Methan berechnet, indem man eine Störungsrechnung mit den im vorangehenden Aufsatz abgeleiteten Wellenfunktionen durchführte. Das Störungsfeld ist die Änderung in dem

von den Kernen verursachten Potentialfeld, welche zustande kommt, wenn die Kerne sich in der entsprechenden Schwingungskordinate bewegen; eine von Pople und Schofield entwickelte vereinfachte Form der Störungstheorie zweiter Ordnung wird für die Berechnung benutzt. Die wichtigste Annäherung besteht in der Vernachlässigung von f und höheren Gliedern in der Entwicklung des Kernfeldes nach Kugelfunktionen. Die sich ergebenden Dipolmoment-Ableitungen sind annähernd dreimal so gross wie die Experimentalmerte, doch zeigen sie signifikante qualitative Merkmale und Zeichenabhängigkeiten.

In Bezug auf diese Ergebnisse werden die experimentellen Intensitätsmessungen gedeutet und erörtert.

REFERENCES

- [1] PENNER, S. S., and WEBER, D., 1951, *J. chem. Phys.*, **19**, 807, 817, 974.
- [2] GOLIKE, R. C., MILLS, I. M., PERSON, W., and CRAWFORD, B. L., 1956, *J. chem. Phys.*, **25**, 1266.
- [3] BENEDICT, W. S., HERMAN, R., MOORE, G. E., and SILVERMAN, S., 1957, *J. chem. Phys.*, **26**, 1671.
- [4] WELSH, H. L., PASHLER, P. E., and DUNN, A. F., 1951, *J. chem. Phys.*, **19**, 340.
- [5] WELSH, H. L., and SANDIFORD, P. J., 1952, *J. chem. Phys.*, **20**, 1646.
- [6] HORNIG, D. F., and McKEAN, D. C., 1955, *J. phys. Chem.*, **59**, 1133.
- [7] McKEAN, D. C., and SHATZ, P. F., 1956, *J. chem. Phys.*, **24**, 316.
- [8] COHAN, N. V., and COULSON, C. A., 1956, *Trans. Faraday Soc.*, **52**, 1163.
- [9] COULSON, C. A., and STEPHEN, M. J., 1957, *Trans. Faraday Soc.*, **53**, 272.
- [10] BURNELLE, L., and COULSON, C. A., 1957, *Trans. Faraday Soc.*, **53**, 402.
- [11] POPLER, J. A., and SCHOFIELD, P., 1957, *Phil. Mag.*, **2**, 591.
- [12] MILLS, I. M., 1958, *Mol. Phys.*, **1**, 99.
- [13] LONGUET-HIGGINS, H. C., and BROWN, D. A., 1955, *J. inorg. nucl. Chem.*, **1**, 60.
- [14] CARTER, C., 1956, *Proc. roy. Soc. A*, **235**, 321.
- [15] BUCKINGHAM, R. A., MASSEY, H. S. W., and TIBBS, S. R., 1941, *Proc. roy. Soc. A*, **178**, 119.
- [16] COULSON, C. A., 1942, *Trans. Faraday Soc.*, **38**, 433.
- [17] THORNDIKE, A. M., 1947, *J. chem. Phys.*, **15**, 868.
- [18] ROLLEFSON, R., and HAVENS, R., 1940, *Phys. Rev.*, **57**, 710.
- [19] BURGESS, J. S., BELL, E. E., and NIELSEN, H. H., 1953, *J. opt. Soc. Amer.*, **43**, 1058.
- [20] DENNISON, D. M., 1940, *Rev. mod. Phys.*, **12**, 175.
- [21] WILMSHURST, J. K., and BERNSTEIN, H. J., 1957, *Canad. J. Chem.*, **35**, 226.

The absorption spectra of aromatic carbonium ions in HF solution

by G. DALLINGA, E. L. MACKOR and A. A. VERRIJN STUART

Koninklijke/Shell-Laboratorium, Amsterdam
(N. V. De Bataafsche Petroleum Maatschappij)

(Received 4 December 1957)

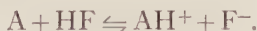
The absorption spectra between 2200 Å and 10 000 Å have been measured of the conjugate acids of a number of aromatic hydrocarbons dissolved in oxygen-free, anhydrous HF and HF-BF₃ mixtures, using a specially constructed cell. All spectra show very intense and characteristic absorption bands in the visible or near-ultra-violet region. In order to interpret these spectra, self-consistent field molecular orbital calculations have been made for the ground and excited states. The calculations, based on a π -electron model, were performed on an electronic digital computer.

It could be shown in a number of cases that the aromatic hydrocarbon (in the absence of oxygen) is present in the acid solution as one type of protonated species. In these cases good agreement is found between the experimental and calculated spectra. Conversely, the theoretical predictions allowed of the interpretation of other cases where the aromatic hydrocarbon, when dissolved in the acid, forms a mixture of different ions, corresponding to a more complicated spectrum.

Some of the solutions, if contacted with oxygen, display fundamental changes of spectrum. For perylene these are shown to be due to the monovalent positive ion of the hydrocarbon.

1. INTRODUCTION

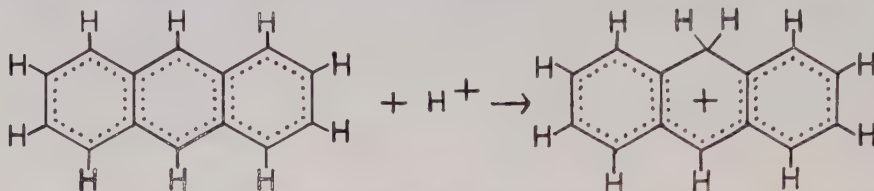
It has been established that aromatic hydrocarbons, when dissolved in HF, may react as bases:



The electronic absorption spectra of the carbonium ions (conjugate acids) AH⁺ derived from some substituted benzenes and unsubstituted polynuclear aromatic hydrocarbons have been measured by Reid [1]. The proton addition has also been studied by other techniques. In the first place the equilibrium constants of the reaction (basicity constants) have been measured for a large number of aromatic hydrocarbons [2, 3]. Secondly, the rates of H-D exchange in acid media have been determined [4, 5]. This exchange is believed to proceed via an activated complex resembling the AH⁺ ions.

In the present publication the results are reported of a systematic study of the electronic absorption spectra of aromatic carbonium ions of type AH⁺, varying in size from one to five rings.

In previous investigations proton addition has been assumed to lead to a structure as proposed by Gold and Tye [6] in their study of ions formed in strong acids. For anthracene the mechanism is illustrated by :



The discussion of such a system is attempted on the basis of a π -electron model. In the aromatic molecule an even number, say $2n$, of atomic orbitals (AO's) and the same number of π -electrons describe the system. In the ion two π -electrons are withdrawn to form a C-H bond on one of the aromatic carbon atoms; thus a methylenic group results, which is assumed not to participate in the conjugation. The effect of hyperconjugation [2, 7, 8] will not be taken into account. The ion, then, is represented by a system of $2n-1$ AO's and $2n-2$ π -electrons. The calculations [9] have been made according to the self-consistent field formalism developed by Roothaan [10] and simplified by Pople [11, 12].

2. EXPERIMENTAL

(In cooperation with Messrs. J. Gaaf and A. Kok)

2.1. Apparatus and measurements

The experiments were carried out in a variable thickness cell† with Linde synthetic white sapphire windows, the cell housing being made from a single block of nickel, and utilizing teflon gaskets and washers. The thicknesses of the windows being known, the sample thickness for each setting could be measured externally by means of a micrometer. It could be varied between 0.2 and 2.0 mm, the lower thickness allowing the measurement of fairly concentrated solutions. The cell will be described elsewhere.

Complete conversion of the molecule into the conjugate acid can practically always be obtained by lowering the temperature and/or addition of BF_3 [2, 3]. Reid's measurements [1] were made in $\text{HF} \cdot \text{BF}_3$ mixtures at temperatures of -20° to -80°C . In the present work all spectra were obtained at room temperature. In the case of weakly basic aromatic hydrocarbons a certain amount of BF_3 was added. Generally saturation of the solution sufficed, but in a few cases excess pressure had to be applied. A Cary model 14 spectrophotometer (thermostatted at 25°C) was used for recording the spectra.

The spectra are presented with reference to the solvent backgrounds. In our equipment anhydrous HF did not display any significant absorption from 1μ ($10\,000\text{\AA}$) down to 2500\AA , i.e. in the greater part of the region of interest. Dissolved BF_3 shows an intense absorption in the region below 2500\AA . In some cases NaF was added to the solutions. It does not contribute to the absorption at wavelengths exceeding 2500\AA .

2.2. Materials

Carefully purified samples of the aromatic hydrocarbons of different origin were used. Their ultra-violet spectra in *iso*-octane solutions were recorded and

† Designed by Messrs. J. H. A. Mekenkamp and F. Oltmans.

compared with the spectral data published by the American Petroleum Institute. Further details have been reported in earlier publications [2, 3, 4].

3. RESULTS

The spectra of the conjugate acids of aromatic hydrocarbons differ fundamentally from the spectra of the molecules from which they are derived. The broadness and general lack of structure, the intenseness, and the occurrence at long wavelengths of characteristic bands are well illustrated by figures 1 to 7, which summarize our results (see also Tables 1 and 2). Figures 1 to 5 also show the spectra calculated for the respective ions (upper parts of figures; position of bars = calculated wavelengths; height of bars = calculated oscillator strengths, the height of the box corresponding to a value 1.00).

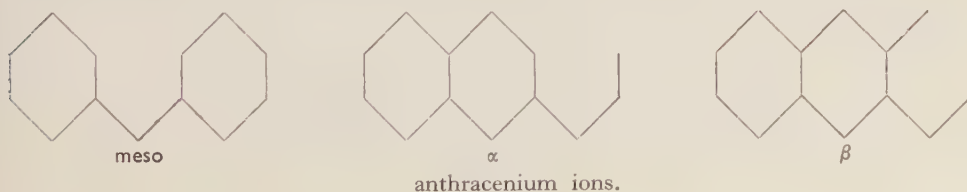
Since the proton addition is an equilibrium reaction Beer's law has been used to ascertain that complete conversion into the conjugate acids had been obtained in the concentration ranges applied. This could be achieved in almost all cases, sometimes by the addition of an amount of BF_3 . Of great importance was the exclusion of oxygen by evacuation of the filling system. If this was not done the spectra in some cases proved to be unstable. In the case of perylene the spectrum is changed drastically on contact of the solution with oxygen (cf. figure 7). Similar, though lesser changes were observed for pyrene and naphthacene. We believe that a good deal of the instabilities mentioned by Reid [1] must be due to the same cause. For the hydrocarbons of lowest basicity (biphenyl, naphthalene, phenanthrene) where high pressures of BF_3 were used, other irreproducible instabilities were observed.

The monoaromatic hydrocarbons of lower basicity are predominantly present, in HF-solutions, as molecules. In addition to the absorption shown by the aromatic molecule in non-acidic solution a band of relatively low intensity is observed at about 2900 Å. It is assigned to a 'charge transfer' complex of the molecule with HF. Similar observations have been made by Reid [1] for $\text{HF} + \text{BF}_3$ solutions. In sufficiently acidic solutions (addition of BF_3) the conjugate acids are more stable than these molecular complexes.

4. DISCUSSION

4.1. General remarks

As mentioned in the Introduction the observed spectra will be discussed on the basis of the type of conjugated system first suggested by Gold and Tye [6]. This approach seems justified in view of its success in the discussions of the basicity of the aromatic hydrocarbons [2], and their reactivities in acid media [4, 5] (hydrogen-deuterium exchange). The approach may be illustrated by the calculations made for the three carbonium ions derived from anthracene by the addition of a proton to a meso, an α and a β carbon atom, respectively. These ions all contain 13 aromatic carbon nuclei (13 AO's) and 12 π -electrons. Their conjugated parts may be represented as follows:



For the carbonium ion π -electron systems the self-consistent field method as formulated by Roothaan [10] and simplified by Pople [11, 12] was applied. The technical details of the calculations, which were performed on a Ferranti, Mark I* electronic digital computer, have been reported elsewhere [9]. The parameters used were adjusted to fit one case, viz. the spectrum of the naphthalene molecule.

For the anthracenium ions [5] the total π -electron energies have thus been found to be 11.95β , 11.65β and 11.39β , respectively (β being the resonance parameter, taken equal to 2.06 eV in the present calculations). The corresponding energy for the anthracene molecule [5] being 11.96β , one finds localization energies of 0.01β , 0.31β and 0.57β , respectively. The differences between these localization energies are so great that one may expect that only a very small percentage of the ions formed will be of the α or β type. The observed ratios of the rates of H-D exchange in acid solutions [5] support this expectation:

$$k_{\text{H-D}}(\text{meso}) : k_{\text{H-D}}(\alpha) : k_{\text{H-D}}(\beta) = 7250 : 5 : 1.$$

When, however, the proton affinities of non-equivalent aromatic carbon atoms are of the same order of magnitude one cannot predict, from the calculated localization energies, which ion, or ions, will be predominantly present. In these cases the calculated spectra provide essential information.

In this investigation use has been made of the influence of methyl and other alkyl substitutions on the aromatic hydrocarbons. It is known that such substitutions enhance the basicities of the molecules [3]. The enhancement of the proton affinity of a particular carbon atom in the molecule depends specifically on the position in which the substitution has been made. In 1,2-benzanthracene, for instance, the carbon atoms in the 9 and 10 positions have about equal proton affinities [5]. Depending on the position of methyl substitution the relative proton affinity of either carbon atom 9 or 10 may be enhanced by a factor of 10. The spectra of the conjugate acids of 10-methyl- and 3-methyl- 1,2-benzanthracene differ fundamentally owing to nearly exclusive proton addition in the 9 position in the former and the 10 position in the latter case [13, 14]. On the other hand, the small difference between the spectra of the conjugate acids of anthracene and 2-methylantracene (cf. figure 4) indicates that the meso positions are the most reactive in both cases.

The monoaromatic hydrocarbons, if completely converted into their conjugate acids, all show similar spectra (cf. figure 1 and Table 1).

Systematic differences in band positions are observed, which are of the order of 100–200 Å. There seems to exist a significant correlation with the well-known shifts of the ${}^1\text{L}_b$ band of benzene caused by methyl substitution.

From this and other examples it is concluded that the spectral 'alkyl shifts' are negligible as compared with the differences between the spectra of different ionic species. In the calculations, therefore, the effects of alkyl substitution have not been considered.

Interaction of singly excited configurations may be taken into account [12]. For the excitations of interest, relatively few of these configurations have to be considered [9]. In general, the lower frequency (longer wavelength) excitations are then lowered, but the main change is in the predicted intensities (oscillator strengths), which may become greater or smaller. Only in a few cases are these changes important. Striking examples are the calculations for the benzenium ion (considerable influence) and for the 9-phenanthrenium ion (small changes),

as may be seen in Table 3, where the significant predicted bands are collected, in both cases calculated from six excited configurations.

4.2. Catacondensed aromatic hydrocarbons

Benzene and Anthracene

As seen in figure 1 the spectrum of the benzenium ion is characterized by two bands (3700 Å and 2600 Å, approximately) and the indication of a third band (about 2000 Å). The anthracenium ion displays a single strong band (4080 Å) and a number of weak bands at shorter wavelengths. This is in complete agreement with the calculated spectra as shown in figures 1 and 4 respectively (cf. also Table 4,

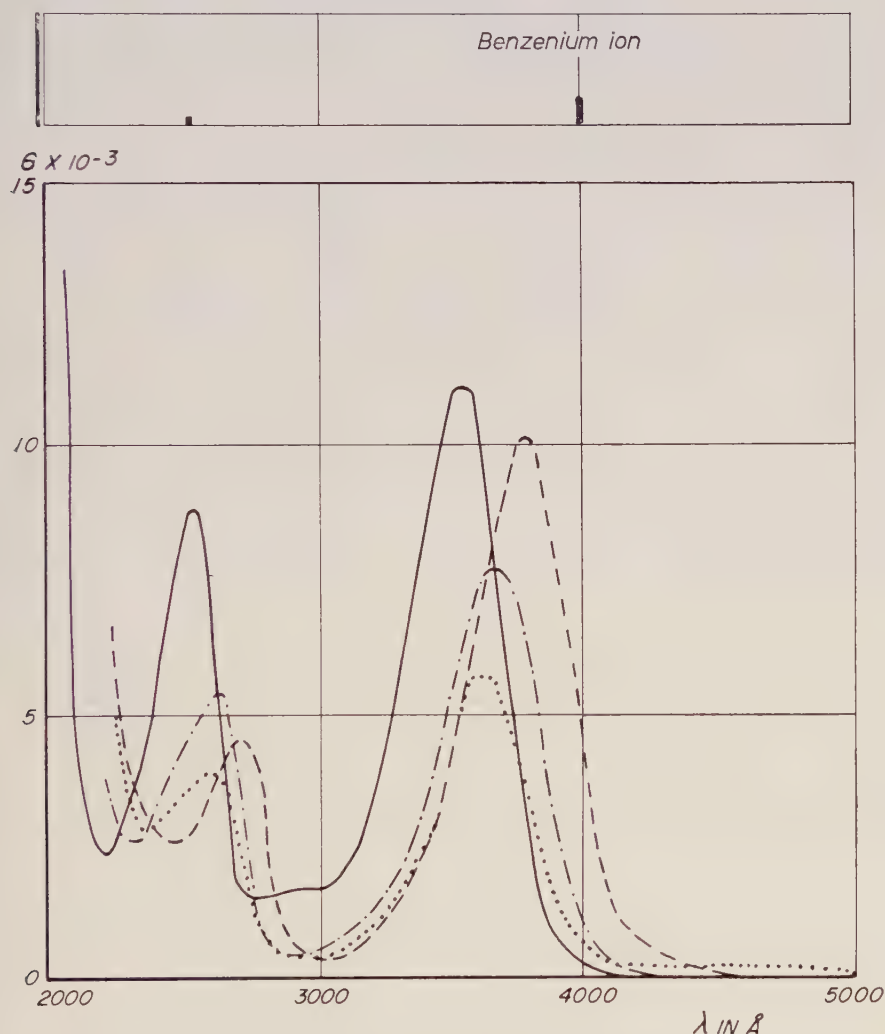


Figure 1. Monoaromatic hydrocarbons.

- Mesitylene in HF + BF₃
- · - · 1, 2, 3, 5-Tetramethylbenzene in HF + BF₃
- Pentamethylbenzene in HF
- Dimesityl in HF

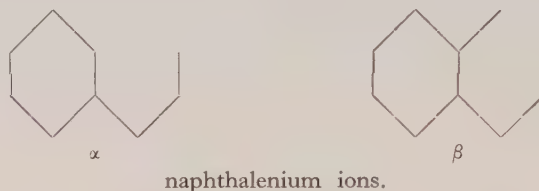
which contains the most significant bands calculated for a number of ionic species of interest).

Conjugate acid of :	Band A		Band B	
	λ	ϵ	λ	ϵ
Mesitylene	3550	11100	2560	8800
1, 2, 3, 5, tetramethylbenzene	3650	7500	2610	5350
Pentamethylbenzene	3770	9800	2720	4300
Dimesityl	3620	5800	2580	3900

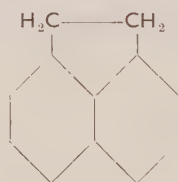
Table 1. Spectra of the conjugate acids of monoaromatic hydrocarbons.

Naphthalene

Two ions may be derived from naphthalene :



The spectra calculated for these two ions are entered in Table 4. The higher rate of H-D exchange [5] and the lower localization energy for the α position (leading to an estimated presence of 1 to 0.1 per cent of the β ion for unsubstituted naphthalene) suggest that the spectra of figure 2 and Table 2 should be interpreted as resulting from the α ion exclusively. For naphthalene and acenaphthene



such an assignment is acceptable (bands A, B and C (obs.) corresponding to the 4480 Å, 4050 Å and 2590 Å bands (calc.), respectively; assignment of band D is speculative).

The absence of band A in the spectra of the other naphthalenes is not understood. The fluorescence spectra of the conjugate acids of substituted naphthalenes are being studied at present, and may provide essential information. The very weak '5800 Å band' observed for acenaphthene and 3, 4-dimethylnaphthalene might be due to the presence of a small amount of the β ion (in acenaphthene, for instance, the intensity ratio of the observed 5850 Å and 3540 Å bands is 50 : 12 200; the corresponding calculated bands have oscillator strengths 0.15 (5840 Å ' β band') and 0.55 (4050 Å ' α band'), yielding an approximate ratio of one β ion to 70 α ions). Such an increased ratio may result from the alkyl substitution.

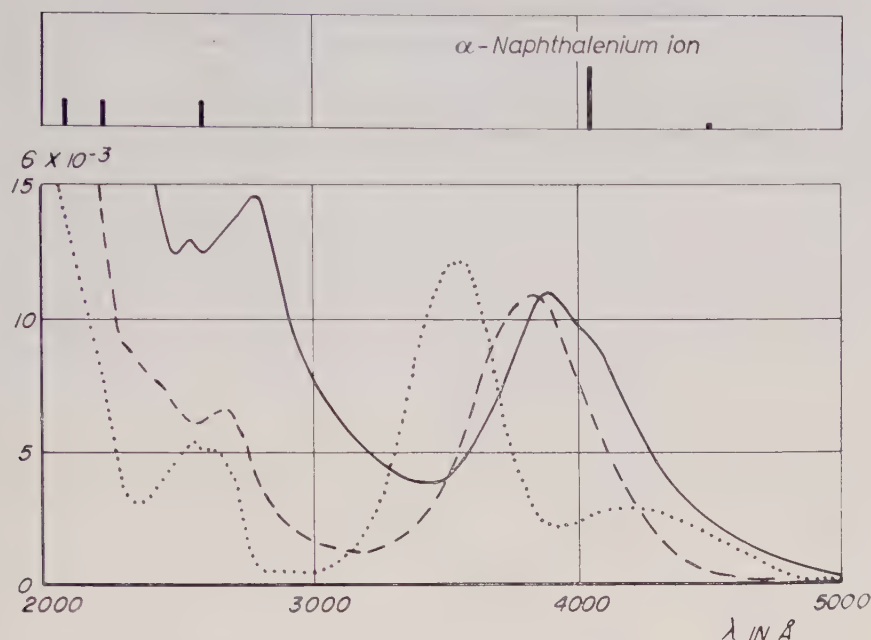


Figure 2. Naphthalenes.

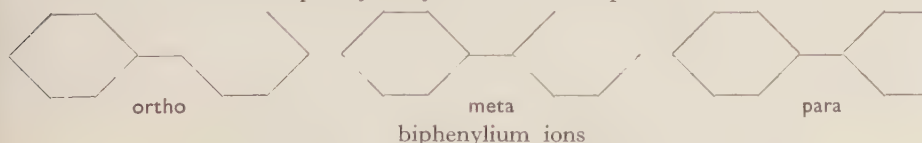
- Naphthalene in HF + BF₃ (3 atm).
 - - - 2, 3-dimethylnaphthalene in HF + BF₃.
 Acenaphthene in HF.

Conjugate acid of :	Band A		Band B		Band C		Band D	
	λ	ϵ	λ	ϵ	λ	ϵ	λ	ϵ
Naphthalene	4100	(shoulder)	3900	10900	2800	14800?	2540	13000?
1, 4-Dimethyl-naphthalene	—	—	3810	18700	2690	8900	2520	7600
2, 3-Dimethyl-naphthalene	—	—	3810	11200	2700	6600	2530	?
Acenaphthene	4200	2800	3540	12200	2640	~5000	2550	~5000

Table 2. Spectra of the conjugate acids of naphthalenes.

Biphenyl

Proton addition to biphenyl may occur in three positions :



The ortho and para positions show equal rates of H-D exchange [5] and the SCF localization energies are also nearly the same [5] (ortho: 0.59β ; meta: 0.88β ; para: 0.61β). There is reason to assume that the ortho/para ratio will exceed the

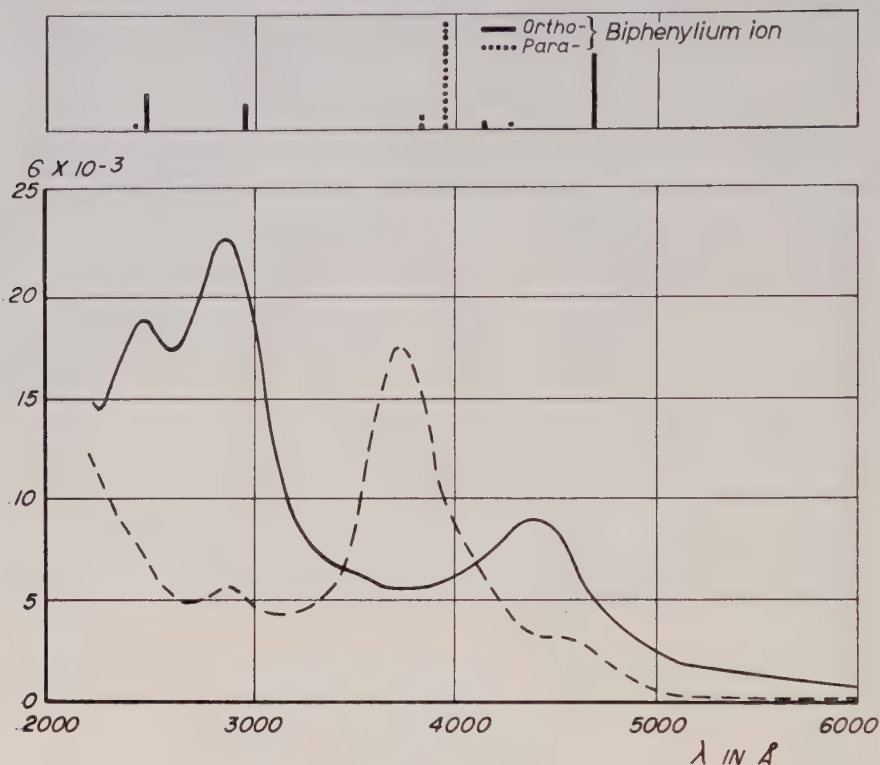


Figure 3. Biphentyls.

— Biphenyl in HF + BF₃ (3 atm).
 --- Fluorene in HF + BF₃.



No configuration interaction		Configuration interaction	
$\lambda(\text{\AA})$	f	$\lambda(\text{\AA})$	f
Benzenium ion			
3910	0.24	4000	0.21
2370	0.45	2540	0.06
2070	0.50	1990	0.99
9-Phenanthrenium ion			
5320	0.34	5610	0.29
4610	0.02	4620	0.03
3390	0.03	3440	0.02
2950	0.64	2940	0.70

Table 3. Result of the introduction of configuration interaction among six singly excited configurations for the benzenium and 9-phenanthrenium ions.

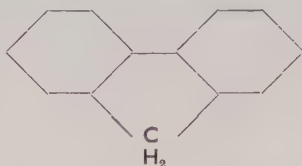
Benzenium ion (a)	4000 (0.21)	2540 (0.06)	1990 (0.99)			
Meso-anthracenium ion (a)	4200 (0.00)	4010 (0.14)	3980 (0.98)	2610 (0.22)		
α -Anthracenium ion (b)	5500 (0.39)	3890 (0.51)	2890 (0.30)	2380 (0.47)		
β -Anthracenium ion (b)	7190 (0.26)	3750 (0.49)	3050 (0.82)	2740 (0.42)		
α -Naphthalenium ion (a)	4480 (0.03)	4050 (0.55)	2590 (0.22)	2230 (0.19)	2140 (0.23)	
β -Naphthalenium ion (a)	5840 (0.15)	3450 (0.06)	3250 (0.03)	2520 (0.58)	2370 (1.19)	
Ortho-biphenylum ion (a)	4680 (0.69)	4130 (0.05)	2970 (0.23)	2490 (0.34)		
Meta-biphenylum ion (b)	6340 (0.05)	5720 (0.00)	2950 (0.56)	2790 (0.07)		
Para-biphenylum ion (a)	4280 (0.07)	3940 (0.97)	3800 (0.15)	2430 (0.01)		
1-Phenanthrenium ion (b)	4930 (0.54)	4150 (0.17)	3220 (0.20)	2740 (0.16)	2690 (0.11)	2490 (0.56)
2-Phenanthrenium ion (b)	5940 (0.19)	3770 (0.74)	3490 (0.08)	3020 (0.04)	3000 (0.77)	2450 (0.18)
3-Phenanthrenium ion (b)	4800 (0.14)	4520 (0.60)	3080 (0.17)	2920 (0.31)	2550 (0.24)	2480 (0.75)
4-Phenanthrenium ion (b)	5970 (0.19)	3990 (0.54)	3340 (0.01)	2940 (0.18)	2920 (0.42)	2520 (0.61)
9-Phenanthrenium ion (b)	5320 (0.34)	4610 (0.02)	3390 (0.03)	2950 (0.64)	2630 (0.62)	2360 (0.20)
Pyrenium ion (A) (b)	4240 (0.83)	4170 (0.09)	3460 (0.73)	2920 (0.07)	2470 (0.42)	2300 (0.00)
Pyrenium ion (B) (b)	6410 (0.13)	4560 (0.33)	3500 (0.09)	3160 (0.30)	2940 (0.62)	2650 (0.33)
3,4-Benzopyrenium ion (C) (b)	4420 (0.92)	3860 (0.13)	3820 (0.03)	3400 (0.74)	3170 (0.05)	2300 (0.06)
1,2-Benzopyrenium ion (D) (b)	4960 (0.64)	4020 (0.14)	3690 (0.89)	3600 (0.13)	2950 (0.00)	2830 (0.39)
1,2-Benzopyrenium ion (E) (b)	4660 (0.54)	3990 (0.34)	4390 (0.71)	3180 (0.09)	2860 (0.08)	2620 (0.02)
1,2-Benzopyrenium ion (F) (b)	6130 (0.19)	6020 (0.17)	4180 (0.14)	3490 (0.02)	3360 (0.10)	2890 (0.70)
Perylenium ion (G) (b)	4760 (0.88)	4090 (0.08)	3650 (0.76)	3600 (0.15)	2870 (0.05)	2810 (0.20)
Perylenium ion (H) (b)	5580 (0.55)	4150 (0.01)	3630 (0.81)	3550 (0.31)	2930 (0.48)	2740 (0.12)

(a) Configuration interaction taken into account.

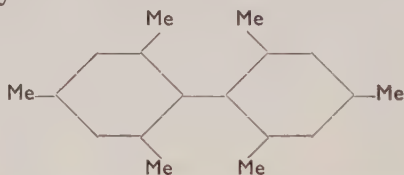
(b) Configuration interaction not taken into account.

Table 4. The spectra calculated for a number of carbonium ions (up to six most significant bands; structures see text; λ in Å; oscillator strengths between brackets). The S.C.F. energies of the ground states of the above ions and their parent molecules have been reported elsewhere [5], the corresponding bond orders and charge densities have not been published.

expected ratio of two. This is because of the steric interference between the H atoms on either side of the central bond, the strain of which is diminished when the methylenic group is formed in the ortho position. Such an enhanced relative proton affinity is encountered in all aromatic hydrocarbons where this structural configuration occurs (e.g. phenanthrene, 1,2-benzanthracene and perylene), and it is estimated to amount to about 0.1β for the localization energies (about 50 fold increase of relative basicity). This is borne out by the spectrum of the biphenyl conjugate acid, which is identified with the spectrum predicted for the ortho ion (cf. figure 3 and Table 4). The o, o'-substitution in fluorene



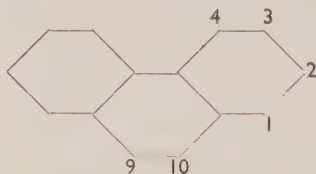
suffices to cause the formation of a predominant amount of para ions (cf. figure 3 and the predicted para ion spectrum in Table 4), but some ortho ions (about 10 per cent) are still present. The meta ion spectrum cannot be observed. The methyl substitution of dimesityl



causes the two rings to be oriented at nearly right angles, so that a spectrum resembling that of the benzenium ion results (cf. figure 1 and Tables 1 and 4).

Phenanthrene

Of the five different positions in this molecule the 1 and 9 positions have equal



Substance	Phenanthrene in HF + BF ₃ (a)	9-Methylphenanthrene in HF + BF ₃	Shriner/Geipel ion (b)
maximum	5100 Å (13000)	5100 Å (6300)	5490 Å (6000)
minimum	4700 Å	—	—
maximum	4100 Å (17000)	—	—
minimum	3700 Å	3900 Å	4260 Å
maximum		3200 Å (10250)	3325 Å (9200)
minimum		2970 Å	2950 Å
maximum		2590 Å (26900)	2680 Å (22000)
minimum		2320 Å	2430 Å

(a) According to Reid [1].

(b) According to Shriner and Geipel [15].

Table 5. The spectra of the conjugate acids of phenanthrene and 9-methylphenanthrene, and of the Shriner/Geipel ion.

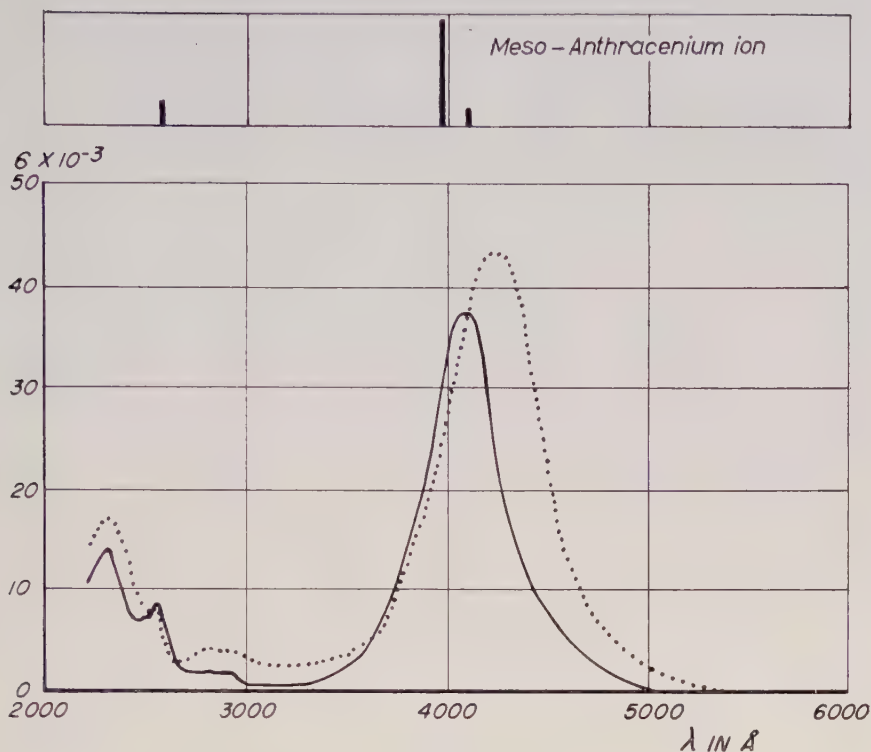
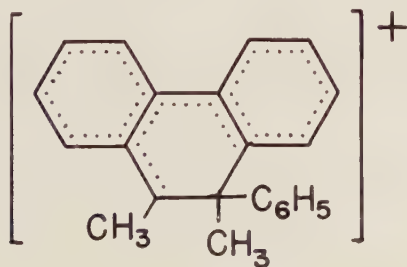


Figure 4. Anthracenes.

— Anthracene in HF.
 2-methylantracene in HF.

localization energies (0.45β). The 4 position (localization energy 0.54β) may have approximately the same proton affinity owing to the steric hindrance effect discussed above. From the predicted spectra (Table 4) it is not immediately clear how to interpret the conjugate acid spectrum of phenanthrene itself (figure 5 and Table 5). Methyl substitution in the 9 position, however, will enhance the proton affinity of the 10 position most. Thus the conjugate acid spectrum of 9-methylphenanthrene will represent the spectrum predicted for the 9 ion (the calculated 5320 Å, 2950 Å and 2630 Å bands corresponding to the observed 5100 Å, 3200 Å and 2590 Å bands). This assignment is supported by the spectrum of the ion:



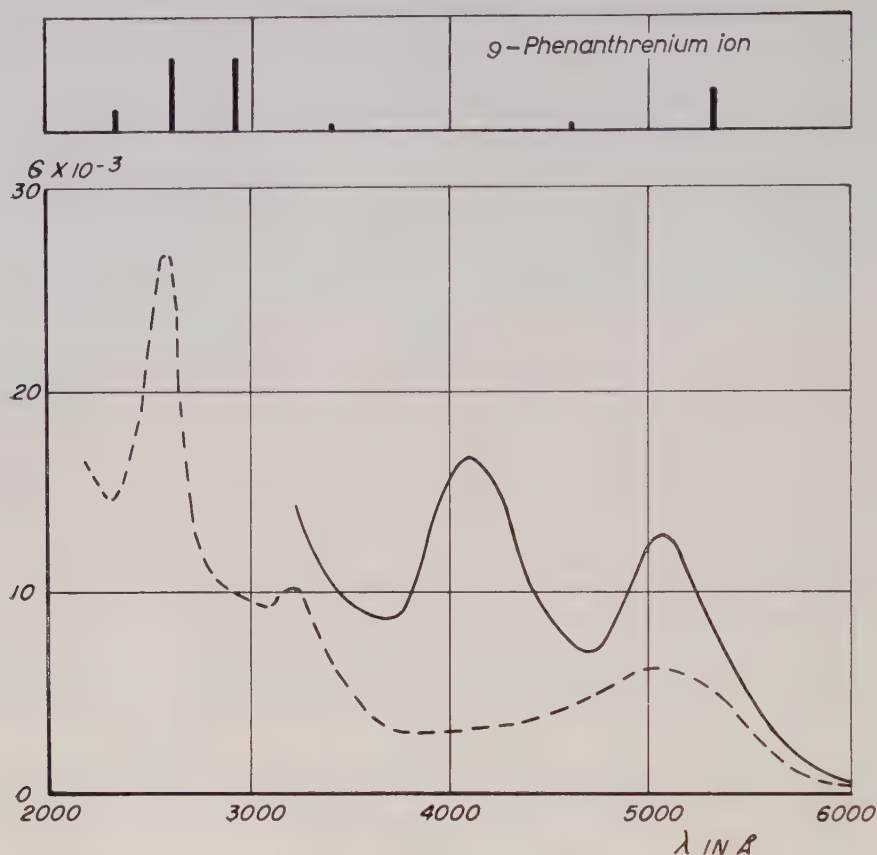


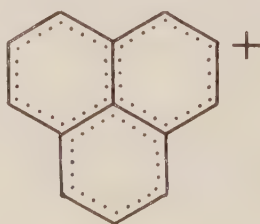
Figure 5. Phenanthrenes.

— Phenanthrene in $\text{HF} + \text{BF}_3$ (Reid [1]).
 --- 9-methylphenanthrene in $\text{HF} + \text{BF}_3$.

synthesized by Shriner and Geipel [15], which closely resembles the 9-methylphenanthrene conjugate acid spectrum (cf. Table 5), and contains the same π -electron system as the 9-phenanthrenium ion. The spectrum of the conjugate acid of phenanthrene is probably due to a mixture of ions, the 5200 Å peak corresponding to the 9 ion, and the 4100 Å band, which is absent in the conjugate acid spectra of the two phenanthrene derivatives, corresponding to the 4 ion (and, possibly, also the 1 ion).

4.3. Pericondensed aromatic hydrocarbons

Most of the ions derived from the pericondensed aromatic hydrocarbons have in common the perinaphthényl ion:



as part of their structures. For this ion, containing 13 AO's and 12 π -electrons, the following spectrum is calculated:

λ	4650	3850 ^d	2430	2420 ^d	2320	2190 ^d	2010 ^d	1990 ^d
f	(0.00)	(0.39)	(0.00)	(0.01)	(0.00)	(0.09)	(0.05)	(1.79)

[^d - doubly degenerate.]

Configuration interaction was taken into account; λ is given in Å, oscillator strengths are entered between brackets.

The spectrum of this ion has not been measured. In the conjugate acids considered this structure is substituted by vinyl, benzene and phenyl groups. These substitutions will remove the (symmetry) degeneracies, relax the symmetry selection rules forbidding certain transitions (also causing a more even distribution of intensities) and lead to the appearance of some weak bands at short wavelengths. The most important band of the perinaphthényl ion is the strong, doubly degenerate, 3850 Å band. It will be split up in the observed spectra of the pericondensed aromatic carbonium ions. These are indeed characterized by two intense bands in the 3500 Å and 4500–5000 Å region, respectively.

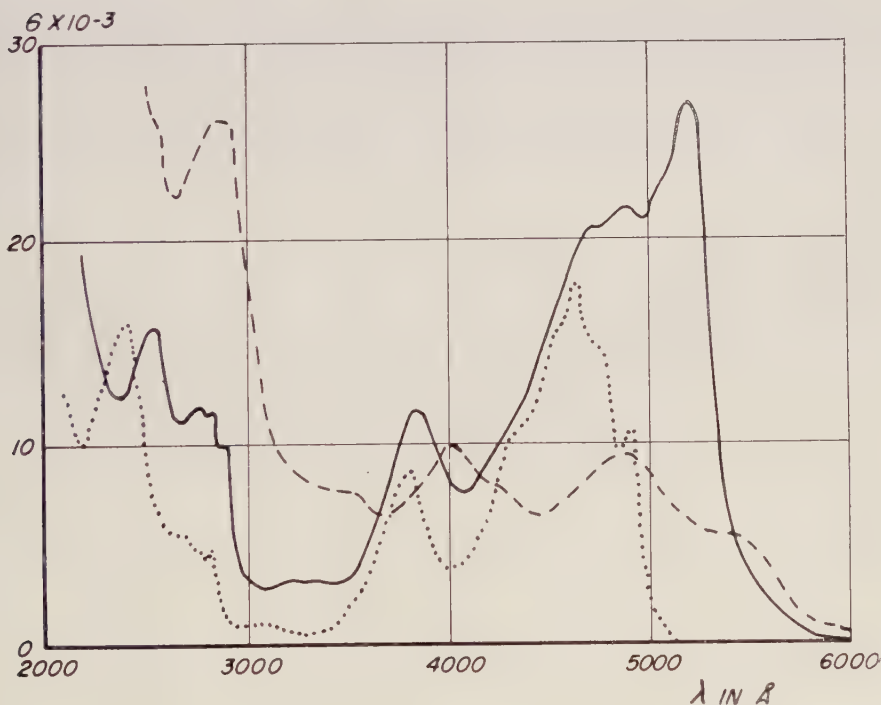
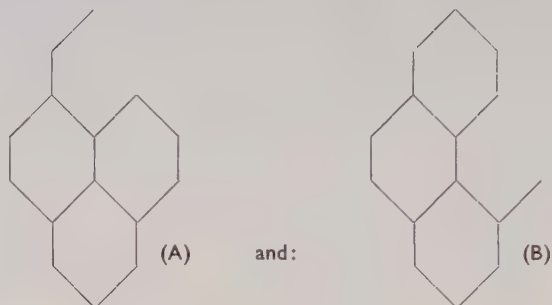


Figure 6. Pericondensed aromatic hydrocarbons.

- 3,4-benzopyrene in HF.
- Pyrene in HF.
- 1,2-benzopyrene in HF.

Pyrene

Pyrene may form three ions, the two most stable of which are represented by:



Structure (A) contains the perinaphthene ion residue (localization energy 0.15β); structure (B) (localization energy 0.37β) does not. This is reflected in the calculated spectra (see Table 4); ion (A) is characterized by two strong bands (4240 \AA and 3460 \AA , calculated), but the spectrum of ion (B) starts with a band of medium intensity at longer wavelength (6410 \AA , calculated). The pyrene conjugate acid spectrum (cf. figure 6) is assigned to structure (A). The absence of any absorption at wavelengths greater than 5200 \AA rules out the presence of (B) ions.

3,4-Benzopyrene

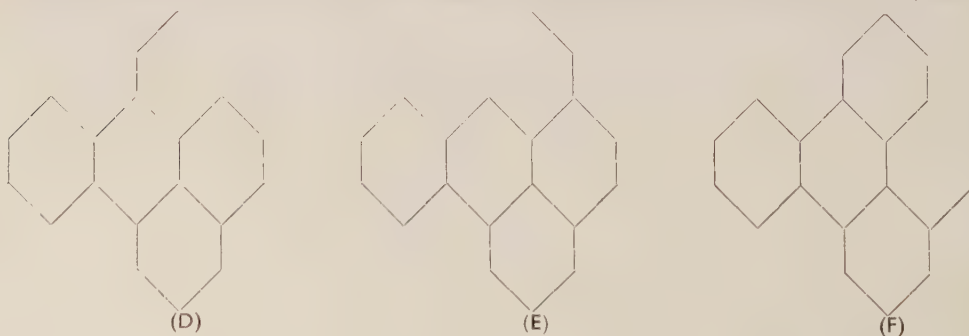
3,4-Benzopyrene may form twelve different ions. Ion (C), which contains



the perinaphthene ion structure, is by far the most stable. Its calculated spectrum (Table 4), which is again characterized by two strong bands (4420 \AA and 3400 \AA , calculated) agrees reasonably well with the observed spectrum (cf. figure 6).

1,2-Benzopyrene

1,2-Benzopyrene is not a clear-cut case. Three ions of comparable stabilities may be formed, (D) and (E) containing the perinaphthene ion structure, (F) not



containing this structure. Ion (D) has the lowest, ion (F) the highest localization energy. The not very characteristic spectrum (cf. figure 6) may be interpreted as being due to a mixture of (D) and (E), particularly in view of the enhanced proton affinity leading to (E) (steric hindrance). The absence of absorption at wavelengths over 5900 Å, however, excludes the presence of ion (F) (see calculated spectra, Table 4).

Perylene

Taking into account the steric hindrance effect, the ions (G) and (H) derived



from perylene (localization energies 0.03β and 0.13β , respectively) would be expected to occur in comparable quantities. The calculated spectra of the ions (Table 4) would lead to a spectrum for the mixture, predicted to be characterized by the following strong bands: 5580 Å, 4760 Å, 3650–3630 Å (doublet?). This is in agreement with the observed spectrum (cf. figure 7) if ion (H) is assumed to be somewhat more abundant.

4.4. Effects of oxygen

The effects of oxygen on the spectra of the carbonium ions resulting from proton addition seem to be most marked in the case of perylene. For naphthacene a lowering of the oxygen pressure resulted in a reversal of the changes. Apparently one is dealing with a structure-dependent equilibrium reaction. A speculation as to the structure of the reaction product may be made in connection with certain observations of Weissman, de Boer and Conradi [16], and Hoiijtink and Weijland [17].

Because of the even number of π -electrons in the 'protonated' ions these ions should be diamagnetic. MacLean and van der Waals [18] could not detect electron spin resonance (ESR) for perylene and anthracene dissolved in HF. In concentrated H_2SO_4 , however, Weissman, de Boer and Conradi [16] observed an ESR spectrum, which showed a remarkable resemblance to the ESR spectrum of the monovalent *negative* perylene ion (i.e. a perylene molecule *plus* one π -electron). Hoiijtink and Weijland [17] have pointed out that the electronic spectra of the H_2SO_4 solution of perylene, and of the negative ion [19, 20] are also very similar. According to these authors perylene must be present in concentrated H_2SO_4 as the monovalent *positive* ion (i.e. a perylene molecule *minus* one π -electron). The experimental data may be very well interpreted on the basis of the LCAO-MO model for these structures.

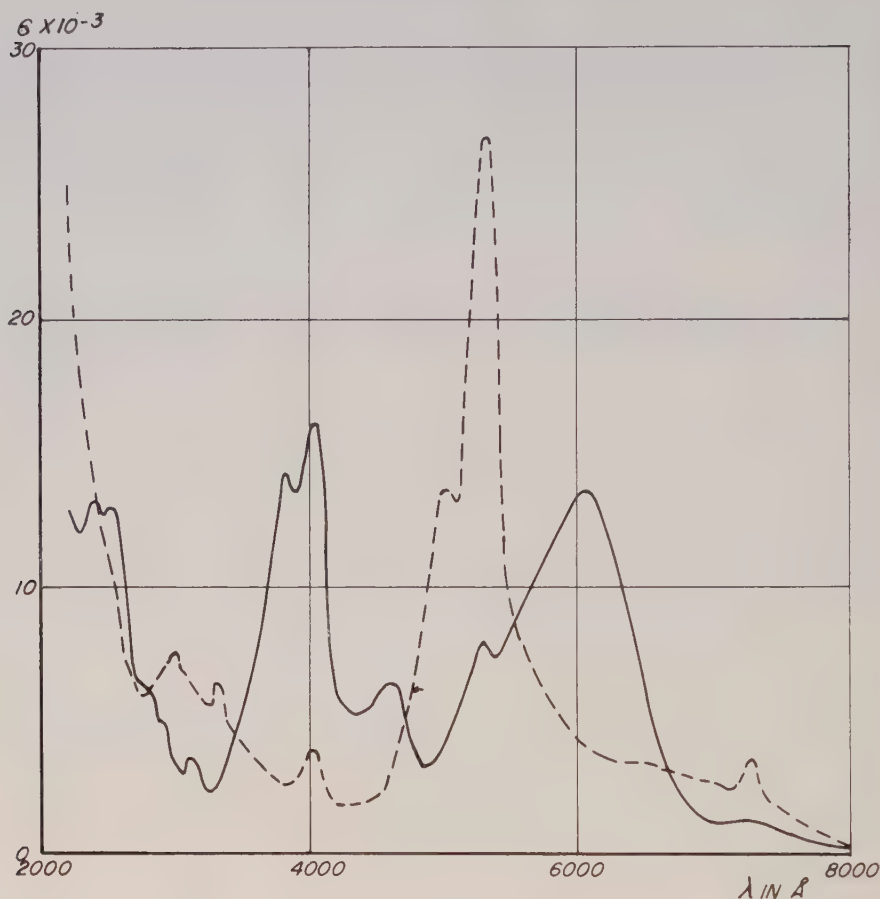
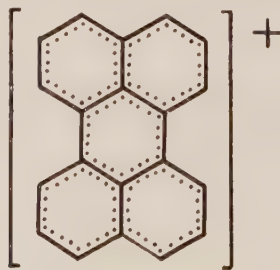


Figure 7. Perylene in HF.

— Oxygen excluded.
 ---- Contacted with oxygen.

The spectrum we have obtained for perylene dissolved in HF, and contacted with oxygen (cf. figure 7) is nearly identical with the spectrum of perylene dissolved in concentrated H_2SO_4 . We conclude that here also the monovalent positive ion:



—that is to say, a system described by 20 AO's and 19 π -electrons—has been formed by some kind of oxidation (H atom abstraction) from both positive ions of structures (G) and (H)—that is to say, systems described by 19 AO's and 18 π -electrons. The actual oxidation mechanism is being further investigated.

The cooperation of Dr. C. la Lau and Mr. J. Schout is gratefully acknowledged.

On a mesuré les spectres d'absorption entre 2200 et 10 000 Å des acides conjugués d'un nombre d'hydrocarbures aromatiques, dissous dans du HF et des mélanges HF-BF₃ anhydres en excluant l'oxygène. Une cuvette spécialement construite a été utilisée. Tous les spectres montrent des bandes d'absorption très intenses et caractéristiques dans la région visible et dans l'ultra-violet proche. Pour interpréter ces spectres on a fait des calculs par la méthode des orbitales moléculaires self-consistantes pour les états normal et excités. Ces calculs, basés sur un modèle ne tenant compte que des électrons π , ont été faits au moyen d'une machine à calculer électronique digitale.

On a pu montrer pour plusieurs cas que l'hydrocarbure aromatique (en l'absence d'oxygène) se trouve dans la solution acide sous la forme d'un seul type de complexe protoné. Dans ces cas on a trouvé un bon accord entre les spectres expérimentaux et calculés. Réciproquement, les prédictions théoriques ont permis d'interpréter d'autres cas, où l'hydrocarbure aromatique dissous dans l'acide produit un mélange de différents ions, donnant lieu à un spectre plus compliqué.

Quelques solutions, lorsqu'en contact avec l'oxygène, montrent des changements fondamentaux du spectre. Dans le cas du pérylène on a pu démontrer que ces changements sont dus à l'ion monovalent positif de l'hydrocarbure.

Die Absorptionsspektren der konjugierten Säuren einiger aromatischen Kohlenwasserstoffe wurden im Bereich zwischen 2200 und 10 000 Å gemessen. Hierzu wurden die Substanzen in HF bzw. in HF-BF₃-Gemischen unter Ausschluss von Sauerstoff und Feuchtigkeit gelöst. Die Messungen wurden in einer besonders konstruierten Küvette durchgeführt. Alle Spektren zeigen sehr starke und charakteristische Absorptionsbanden im Sichtbaren, sowie im nahen Ultraviolett. Um diese Spektren zu deuten, wurden self-consistent field MO-Berechnungen für die Grund-, sowie für die angeregten Zustände durchgeführt. Die auf einem π -Elektronmodell basierten Rechnungen wurden mittels einer elektronischen Rechenmaschine ausgeführt.

In zahlreichen Fällen konnte gezeigt werden, dass der aromatische Kohlenwasserstoff (bei Abwesenheit von Sauerstoff) in der sauren Lösung als ein einziger Proton-Additions-komplex auftritt. In diesen Fällen wird eine gute Übereinstimmung zwischen den experimentellen und den berechneten Spektren gefunden. Andererseits erlauben die theoretischen Schlussfolgerungen andere Fälle zu deuten, bei denen der aromatische Kohlenwasserstoff in saurer Lösung ein Gemisch verschiedener Ionen bildet, was zu einem komplizierteren Spektrum führt.

Bei Berührung mit Sauerstoff zeigen manche Lösungen grundlegende Änderungen im Spektrum. Im Falle des Perylens lassen sich dieselben auf das einwertige positive Ion des Kohlenwasserstoffs zurückführen.

REFERENCES

- [1] REID, C., 1954, *J. Amer. chem. Soc.*, **76**, 3264.
- [2] MACKOR, E. L., HOFSTRA, A., and VAN DER WAALS, J. H., 1958, *Trans. Faraday Soc.*, **54**, 66.
- [3] MACKOR, E. L., HOFSTRA, A., and VAN DER WAALS, J. H., 1958, *Trans. Faraday Soc.*, **54**, 186.
- [4] MACKOR, E. L., SMIT, P. J., and VAN DER WAALS, J. H., 1957, *Trans. Faraday Soc.*, **53**, 1309.
- [5] DALLINGA, G., VERRIJN STUART, A. A., SMIT, P. J., and MACKOR, E. L., 1957, *Z. Elektrochem.*, **61**, 1019.
- [6] GOLD, V., and TYE, F. L., 1952, *J. chem. Soc.*, 2173, 2181, 2184.
- [7] PICKETT, L. W., MULLER, N., and MULLIKEN, R. S., 1953, *J. chem. Phys.*, **21**, 1400.
- [8] MULLER, N., PICKETT, L. W., and MULLIKEN, R. S., 1954, *J. Amer. chem. Soc.*, **76**, 4770.
- [9] VERRIJN STUART, A. A., and KRUIZINGA, J. H. (to be published).
- [10] ROTHAAAN, C. C. J., 1951, *Rev. mod. Phys.*, **23**, 69.
- [11] POPLÉ, J. A., 1953, *Trans. Faraday Soc.*, **49**, 1375.
- [12] POPLÉ, J. A., 1955, *Proc. phys. Soc. Lond. A*, **68**, 81.
- [13] MACKOR, E. L., DALLINGA, G., HOFSTRA, A., and KRUIZINGA, J. H., 1956, *Rec. Trav. chim. Pays-Bas.*, **75**, 836.
- [14] VERRIJN STUART, A. A., and MACKOR, E. L., 1957, *J. chem. Phys.*, **27**, 826.

- [15] SHRINER, R. L., and GEIPEL, L., 1957, *J. Amer. chem. Soc.*, **79**, 227.
- [16] WEISSMAN, S. I., DE BOER, E., and CONRADI, J. J., 1957, *J. chem. Phys.*, **26**, 963.
- [17] HOIJTINK, G. J., and WEIJLAND, W. P., 1957, *Rec. Trav. chim. Pays-Bas.*, **76**, 836.
- [18] MACLEAN, C., and VAN DER WAALS, J. H., 1957, *J. chem. Phys.*, **27**, 827.
- [19] BALK, P., 1956, *Thesis*, Free University, Amsterdam.
- [20] BALK, P., DE BRUIJN, S., and HOIJTINK, G. J., 1957, *Rec. Trav. chim. Pays-Bas.*, **76**, 860.

Concentration quenching in fluorescent acene solutions

by A. DAMMERS-DE KLERK

Laboratory for General and Inorganic Chemistry, University of Amsterdam,
The Netherlands†

(Received 20 December 1957)

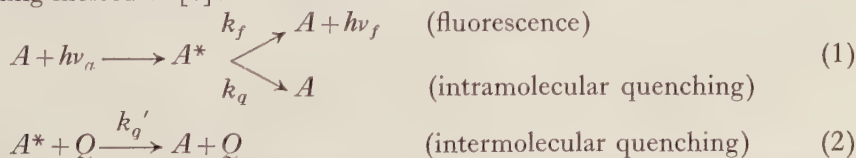
Measurements on the concentration dependence of the fluorescence intensity of dilute solutions of various acenes in *n*-hexane at 25°C show that the concentration quenching for benzene as a solute can be explained by simple collisional quenching. In solutions of naphthalene and anthracene the concentration quenching proceeds via an unstable excited complex resulting from the interaction of an excited and a non-excited molecule. The remarkable shape of the concentration curve of naphthalene is attributed to a contribution of the excited naphthalene complex to the total fluorescence intensity.

The average life-time τ of the fluorescent electronic state, as calculated from the measurements, amounts to about 2×10^{-6} sec for benzene and 5×10^{-7} sec for naphthalene.

1. INTRODUCTION

In the theory of Lewis and Kasha [1] on the photoluminescence of complex molecules the term fluorescence is applied exclusively to light emission accompanying electronic transitions from the lowest excited singlet state S_1 to the singlet ground state S_0 . According to these authors fluorescence quenching, as manifested in fluorescence quantum yields lower than unity, must be attributed to radiationless transitions from the S_1 state to the lowest triplet state T_0 (intersystem crossing). Apart from $T_0 \rightarrow S_1 \rightarrow S_0$ transitions giving rise to delayed fluorescence, which can be distinguished from direct $S_1 \rightarrow S_0$ fluorescence through a difference in decay time, the molecules in T_0 no longer contribute to the fluorescence intensity; they will return to S_0 either by radiationless processes (vibrational and thermal deactivation) or by emission of light (phosphorescence).

In principle, the singlet-triplet transitions involved in fluorescence quenching are forbidden because of the difference in electron spin momentum of the combining states [2]. However, the selection rule $\Delta S = 0$ may be violated as a result of interaction between the spin and orbital motion of the electrons [3]. Intramolecular fluorescence quenching will thus be observed if strong spin-orbit coupling constitutes an intrinsic feature of the excited molecules; intermolecular fluorescence quenching occurs when the spin-orbit coupling is effected or enhanced through interaction between excited molecules of the fluorescent substance and surrounding molecules [4]:



† Present address: Laboratory for Electrochemistry, University of Amsterdam, The Netherlands.

A is the acene molecule in the ground state, A^* the electronically excited acene molecule, Q the quenching molecule, h Planck's constant, ν_a the frequency of the incident light, ν_f the frequency of the fluorescence radiation, k_f the fluorescence rate constant, k_q the rate constant of intramolecular quenching, and k_q' the rate constant of intermolecular quenching.

Considerable attention has been paid to the mechanism of quenching in fluorescent solutions containing 'foreign' quenchers ('Fremdlöschung'; Bowen [4], Förster [6], Pringsheim [5].) Comparatively little is known, however, about a special case of intermolecular quenching in which molecules of the fluorescent substance itself act as quenchers (self-quenching):



The first type of self-quenching (interaction between excited molecules) leads to a fluorescence quantum yield, which is independent of the concentration of the fluorescent substance. The second type (interaction between excited and non-excited molecules) gives rise to a decreasing fluorescence quantum yield if the concentration of the fluorescent substance is increased (concentration quenching). In the present paper the shapes of the concentration quenching curves (fluorescence intensity versus concentration) of fluorescent acene solutions are analysed and conclusions are drawn with regard to the mechanism of the concentration quenching and the nature of the interaction between excited and non-excited molecules.

2. EXPERIMENTAL

In order to study the mechanism of the concentration quenching of dilute solutions of benzene, naphthalene and anthracene in *n*-hexane, fluorescence spectra of rather low intensity had to be measured. A schematic diagram of the spectroscopic and electronic parts of the apparatus used for this purpose is shown in figure 1, which may be considered self-explanatory. Some important details of the equipment have been discussed elsewhere [7, 8].

The light source Hg (a high-pressure mercury discharge tube) emits a line spectrum of high and constant intensity ranging from 2200 to 6000 Å. Monochromatic light is obtained with the aid of a suitable filter system F, which selects the frequency required for the excitation of the fluorescent electronic state in the acene solutions.

As in this arrangement only a small fraction of the fluorescence radiation emitted by the acene solution enters the Unicam monochromator U; the photoelectric current produced by the photomultiplier tube had to be amplified. The measured fluorescence intensity, as indicated by the galvanometer, was ascertained to be proportional to the absolute intensity produced by the fluorescent solution; the magnitude of the proportionality factor can be estimated from absolute intensity measurements [8]. The latter measurements are carried out by replacing the fluorescent solution by a light source of known intensity.

The band-width of the fluorescence radiation, leaving the Unicam monochromator, is of the order of 10 Å. Denoting the intensity of such a band by F^λ , the total fluorescence intensity F of the complete fluorescence spectrum can be obtained by integrating the quantity $F^\lambda d\lambda$ over the wavelength range of the spectrum.

As a matter of course, measurements on concentration quenching are easily affected by small amounts of foreign quenchers; high demands should thus be made upon the purity of the chemicals used. Especially paramagnetic substances [9] like oxygen, which greatly promote the spin-orbit coupling in the fluorescent molecules, may give rise to considerable fluorescence quenching, even when present in traces. The oxygen concentration in the solvent was therefore

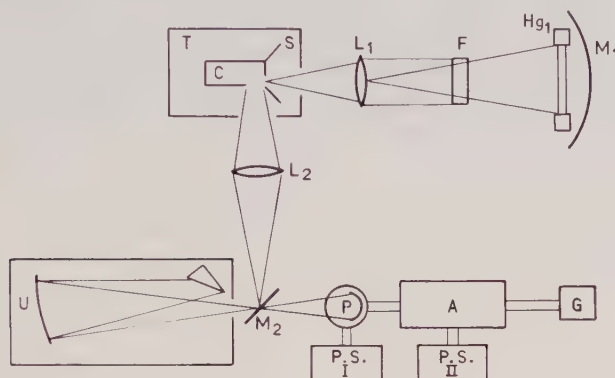


Figure 1. Apparatus for measuring low fluorescence intensities.

Hg.	Light source	T.	Thermostat
M.	Mirrors	U.	Unicum monochromator
F.	Filter system	P.	Photomultiplier
L.	Quartz lenses	A.	Amplifier
S.	Black screen	P.S.	Power supplies
C.	Quartz cuvette	G.	Galvanometer

reduced to about 10^{-6} mole/l; the fluorescent solutions were prepared in an essentially oxygen-free atmosphere of nitrogen. The apparatus used for the removal and determination of minute traces of oxygen—applicable to both gaseous and liquid samples—and the results obtained with this apparatus have been reported elsewhere [10].

3. CONCENTRATION QUENCHING OF BENZENE

Figure 2 shows the fluorescence intensity (in arbitrary units) of benzene at 2780 Å in *n*-hexane solution as a function of the concentration (linear concentration scale). Under the conditions prevailing in our experiments incomplete absorption of the incident light occurs at benzene concentrations lower than about 10^{-2} mole/l. The rising left-hand part of the concentration curve thus originates from increased light absorption as the benzene concentration becomes higher. However, if the incident light is absorbed almost completely, no further increase in fluorescence intensity is possible; the intermolecular quenching then causes the concentration curve to decline rapidly with increasing benzene concentration.

A quantitative interpretation of the curve in figure 2 can be obtained on the basis of a simple mechanism consisting of reaction (1) plus the quenching process



where k_q' is the rate constant of intermolecular quenching. From this scheme we derive

$$\frac{d(A^*)}{dt} = I_a - (k_f + k_q)(A^*) - k_q'(A^*)(A) = 0, \quad (4)$$

where the quantity I_a is proportional to the intensity of the absorbed light.

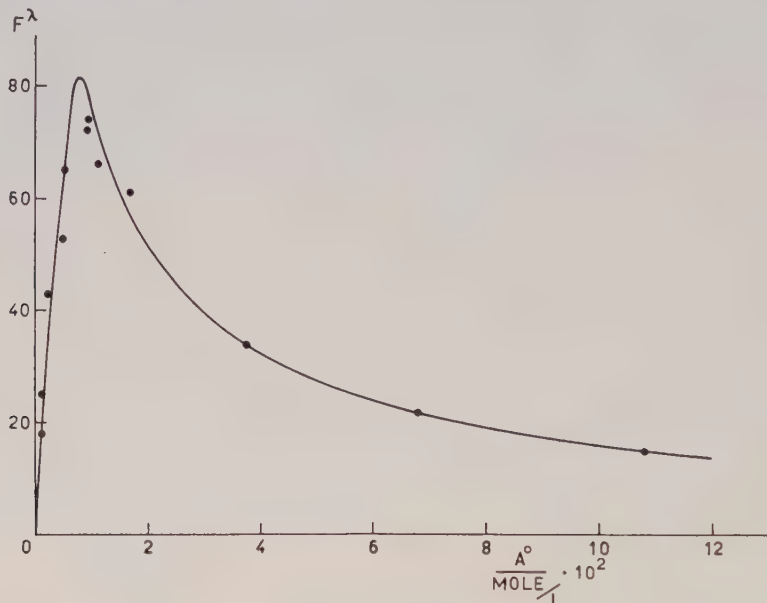


Figure 2. Concentration curve of benzene in *n*-hexane solution at 25°C (calculated curve and experimental points).

Introducing the total benzene concentration $(A^0) = (A) + (A^*)$ and the total (integrated) fluorescence intensity $F = k_f(A^*)$ we obtain

$$(A^0) = \frac{F}{k_f} - \frac{k_f + k_q}{k_q'} + \frac{I_a}{k_q'} \frac{k_f}{F} = \frac{F^\lambda}{k_f^\lambda} - \frac{k_f + k_q}{k_q'} + \frac{I_a}{k_q'} \frac{k_f^\lambda}{F^\lambda}, \quad (5)$$

where k_f^λ is the fluorescence rate constant at wavelength λ .

As explained above, it may be assumed that complete absorption takes place at concentrations at the right-hand side of the maximum in figure 2; the quantity I_a here becomes equal to the constant I_i which is proportional to the intensity of the incident light. From a curve based on equation (5)—using the method of least squares—we can calculate the constants k_f^λ , $(k_f + k_q)/k_q'$ and I_i/k_q' . In the left-hand part of the curve we may account for the decrease in I_a with decreasing concentration through the expression

$$I_a = I_i - I_c = I_i - I_i \exp[-k(A)] = I_i \left[1 - \exp \left\{ -k \left((A^0) - \frac{F^\lambda}{k_f^\lambda} \right) \right\} \right]; \quad (6)$$

I_c is the transmitted part of the incident light and the quantity k is proportional to the molar extinction: $k = \epsilon d / \log e$. We can estimate k from the molar extinction coefficient ϵ of the absorption band at 2600 Å and the length d of the path of the incident light in the fluorescent solution.

From our measurements at 2780 Å we derived:

$$k_f^\lambda = 2.03 \times 10^4 \text{ sec}^{-1}, \quad \frac{k_f + k_q}{k_q'} = 1.74 \times 10^{-2} \text{ mole/l}, \quad (7)$$

$$\frac{I_i}{k_q'} = 8.95 \times 10^{-5} (\text{mole/l})^2, \text{ and } k = 782 \text{ l/mole}.$$

In fact, the curve drawn in figure 2 which fits the observed points well has been calculated by solving simultaneously the equations (5) and (6) and using the values given in (7).

A more convenient representation of our results is obtained by introducing the fluorescence efficiency ϕ , which is the ratio of the number of fluorescence quanta emitted to the number of incident quanta absorbed.

From (5) it follows

$$\phi = \frac{k_f}{k_q'} \left/ \left\{ \frac{k_f + k_q}{k_q'} + (A^0) - \frac{F^\lambda}{k_f^\lambda} \right\} \right. \quad (8)$$

At infinite dilution both (A^0) and F^λ will vanish; the (maximal) quantum efficiency ϕ_0 then becomes

$$\phi_0 = \frac{k_f}{k_f + k_q} = \frac{1}{1 + k_q/k_f} \quad (9)$$

Combining the equations (8) and (9) we find the following expression for the relative quantum efficiency ϕ_r , i.e. the ratio of the quantum efficiency at concentration (A^0) to the quantum efficiency at infinite dilution.

$$\phi_r = \frac{\phi}{\phi_0} = \left[1 + \frac{k_q'}{k_f + k_q} \left\{ (A^0) - \frac{F^\lambda}{k_f^\lambda} \right\} \right]^{-1} = \frac{k_f + k_q}{I_a} \frac{F^\lambda}{k_f^\lambda} \quad (10)$$

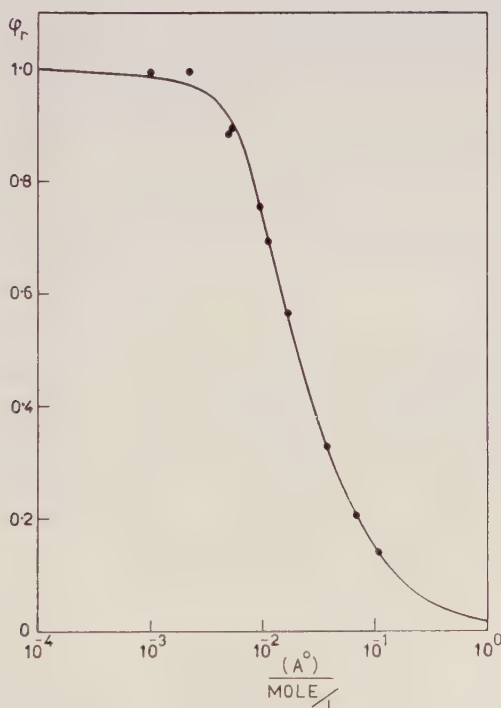


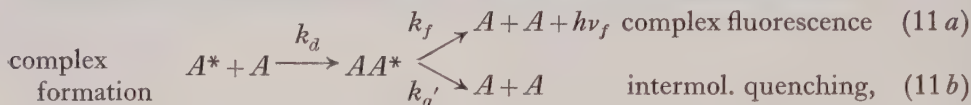
Figure 3. Relative quantum efficiency of benzene in *n*-hexane solution.

At each concentration A^0 the relative quantum efficiency can thus be calculated from the experimental value of F^λ , using only the values for the constants k_f^λ and $(k_f + k_q)/k_q'$; this is shown in figure 3 (logarithmic concentration scale). The

curve drawn in this graph has been calculated from the equations (5), (6) and (10) using the values of the constants (7).

4. CONCENTRATION QUENCHING OF NAPHTHALENE

In contrast to benzene, the fluorescence intensity of naphthalene solutions does not vanish at high concentrations. Ample measurements on oxygen-free naphthalene solutions in *n*-hexane showed that at concentrations higher than 10^{-2} mole/l the fluorescence quantum yield closely approaches a constant value, amounting to about 75 per cent of the quantum-yield at infinite dilution. This phenomenon may be explained with the aid of reaction (1) followed by



k_d is the rate constant of complex formation.

The interaction between A^* and A is thus assumed to lead to the formation of an excited complex AA^* , which does not exist in the ground state. Upon removal of the excitation energy—either by emission of a fluorescence quantum or by radiationless transitions—the complex is supposed to dissociate immediately into two normal naphthalene molecules. Furthermore, it is assumed that the frequency and the rate constant of the fluorescence originating from AA^* do not differ appreciably from the corresponding properties of the A^* fluorescence.

In the region of complete absorption of the incident light the above mechanism results in the following relation between the total naphthalene concentration $(A^0) = (A) + (A^*) + 2(AA^*)$ and the ratio F/F_∞ , i.e. the fluorescence intensity at concentration (A^0) to the constant intensity at high concentrations:

$$(A^0) = a(1-b) \left(\frac{F}{F_\infty} - 1 \right) + (2a-bc) + \frac{c}{F/F_\infty - 1}, \quad (12)$$

where

$$a = \frac{I_i}{k_f + k_q'}, \quad b = \frac{k_f + k_q}{k_q' - k_q}, \quad c = \frac{k_q' - k_q}{k_d}. \quad (13)$$

Comparing equation (12) with the experimental points in the declining part of the naphthalene fluorescence concentration curve, the following values are obtained:

$$a = 1.99 \times 10^{-4} \text{ mole/l}, \quad b = 3.12, \quad c = 1.92 \times 10^{-5} \text{ mole/l}. \quad (14)$$

Using these values the total relative quantum efficiency ϕ_r^t can be calculated from the expression

$$\phi_r^t = \frac{a}{a+1} \frac{F/F_\infty}{I_a/I_i}, \quad (15)$$

corrections for incomplete absorption being introduced in the same way as shown in the case of benzene. The separate contributions of the excited monomer A^* and the excited complex AA^* to the total relative quantum efficiency are given by the relations:

$$\phi_r^m = a \left(\frac{F/F_\infty}{I_a/I_i} - 1 \right) \quad \text{and} \quad \phi_r^c = a \left(1 - \frac{a}{a+1} \frac{F/F_\infty}{I_a/I_i} \right). \quad (16)$$

Curves for ϕ_r^t , ϕ_r^m and ϕ_r^c , calculated from (15) and (16) with the values of the

constants (14) are shown in figure 4 (logarithmic concentration scale), which also contains the experimental points.

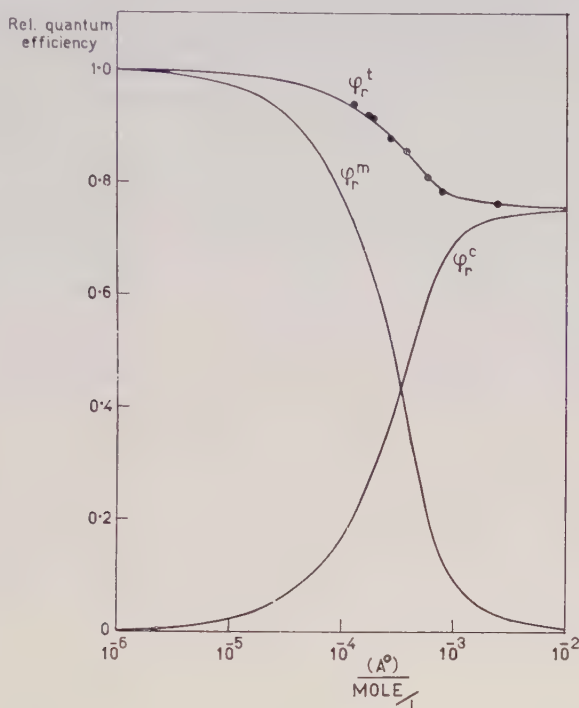
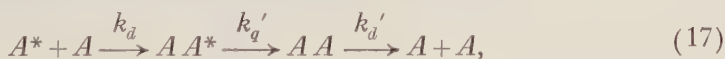


Figure 4. Relative quantum efficiency of naphthalene in *n*-hexane solution.

5. CONCENTRATION QUENCHING OF ANTHRACENE

As in the case of benzene, the concentration curve of anthracene approaches zero intensity at high concentrations. However, the concentration quenching in anthracene solutions cannot be explained by simple collisional quenching (reaction (2)) because of the well-known formation of stable non-excited dimers when irradiating anthracene with ultra-violet light [11, 12, 13]. This dianthracene is generated by deactivation of excited complexes resulting from the interaction between excited and non-excited anthracene molecules. Accordingly, the following mechanism was used in addition to reaction (1) for interpreting the intensity measurements on solutions of anthracene in *n*-hexane:



k_d' is the rate constant of the complex dissociation.

At sufficiently high concentrations — i.e. complete absorption — the relation between the total anthracene concentration $(A^0) = (A) + (A^*) + 2(AA) + 2(AA^*)$ and the fluorescence intensity F^λ leads to:

$$(A^0) = (1 - 2a) \frac{F^\lambda}{k_f^\lambda} + \left(2 \frac{a}{b} - c\right) + \frac{c k_f^\lambda}{b F^\lambda} \quad (18)$$

where

$$a = \frac{k_f + k_q}{k_q'} \frac{k_f + k_q}{k_d'}, \quad b = \frac{k_f + k_q}{I_i}, \quad c = \frac{k_f + k_q}{k_d}. \quad (19)$$

The expression for the relative quantum efficiency becomes

$$\phi_r = \frac{\phi}{\phi_0} = \frac{c}{(A^0) - [2(a/b) - c] - (1 - 2a) F^\lambda / k_f^\lambda} = \frac{k_f + k_q}{I_i} \frac{F^\lambda}{k_f^\lambda}. \quad (20)$$

An approximate value for k_f^λ can be derived from the life-time of the anthracene fluorescence as measured by Bowen [14] (viz. $\tau = 1.35 \times 10^{-8}$ sec) and the ratio of the fluorescence intensity F^λ at the wavelength under consideration (3980 Å) to the integrated fluorescence intensity F as observed in our experiments. Combining these data we find

$$k_f^\lambda = \frac{F^\lambda}{F} k_f \simeq \frac{F^\lambda}{F} \cdot \frac{1}{\tau} = \frac{1}{37} \frac{1}{1.35 \times 10^{-8}} = 2 \times 10^6 \text{ sec}^{-1}.$$

With the aid of this value, the constants a , b and c in (19) can now be calculated from the experimental points:

$$a = 5.93, \quad b = 1.79_5 \times 10^4 \text{ l/mole}, \quad c = 1.37_5 \times 10^{-4} \text{ mole/l.}$$

A graphical representation of ϕ_r as a function of (A^0) is shown in figure 5, where the above values of a , b , c and k_f^λ have been used. Corrections for incomplete absorption of the incident light were introduced in the usual way (see benzene).

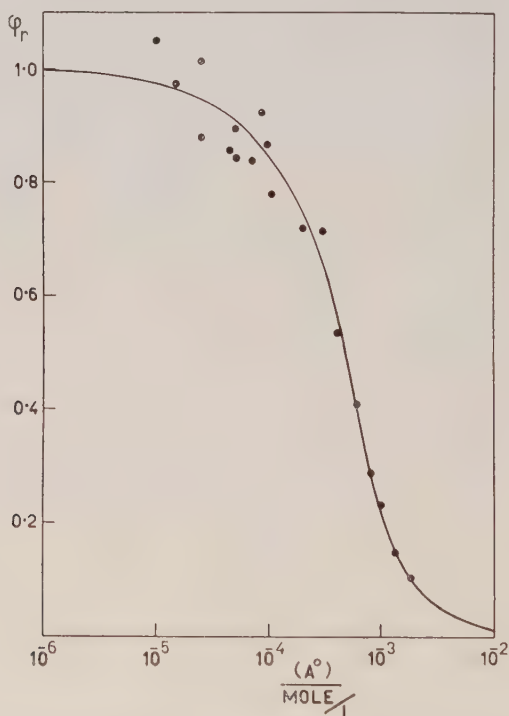


Figure 5. Relative quantum efficiency of anthracene in *n*-hexane solution.

6. CALCULATED RATE CONSTANTS

From the experiments outlined above, in combination with measurements on the ratio of F to F^λ (i.e. k_f to k_f^λ) and data on the fluorescence quantum yield at infinite dilution (Bowen [15]), we can calculate the values of the rate constants k_f , k_q , etc. The values thus obtained are collected in table 1,

With regard to the fluorescence life-time τ it may be remarked that the value for anthracene has been taken from Bowen [14]. The value for naphthalene as calculated from our experiments is about four times greater than the value given by Kasha [16] (viz. 1.02×10^{-6} sec). This discrepancy is not surprising because of the unreliability of life-time measurements.

	benzene	naphthalene	anthracene
k_f	$5.9 \times 10^5 \text{ sec}^{-1}$	$2.1 \times 10^6 \text{ sec}^{-1}$	$7.4 \times 10^7 \text{ sec}^{-1}$
k_{ii}	$4.7 \times 10^6 \text{ sec}^{-1}$	$3.4 \times 10^6 \text{ sec}^{-1}$	$8.7 \times 10^7 \text{ sec}^{-1}$
k_q	$3.1 \times 10^8 \text{ (l/mole. sec)}$	$5.2 \times 10^6 \text{ sec}^{-1}$	$4.4 \times 10^8 \text{ sec}^{-1}$
k_{il}	—	$9.3 \times 10^{10} \text{ (l/mole. sec)}$	$11.7 \times 10^{11} \text{ (l/mole. sec)}$
k_{il}	—	—	$2.9 \times 10^7 \text{ sec}^{-1}$
τ	$1.7 \times 10^{-6} \text{ sec}$	$4.7 \times 10^{-7} \text{ sec}$	$1.4 \times 10^{-8} \text{ sec}$

Table 1. Rate constants calculated from the concentration quenching.

Literature data on the τ value of benzene are not available. The value of the rate constant k_{il} for the formation of the excited complex AA^* is of the same order of magnitude as the bimolecular encounter rate constants calculated by La Mer *et al.* [17] on the basis of Smoluchowski's diffusion theory. This indicates that the formation of AA^* is not accompanied by a measurable energy of activation.

7. DISCUSSION

An interesting aspect of the present investigations is found in the properties of the excited complex AA^* in fluorescent acene solutions. In the case of benzene the concentration curve can be interpreted quantitatively by simple collisional quenching. This probably means that excited benzene dimers are very unstable from a 'chemical' point of view: the dissociation (accompanied by quenching) proceeds much faster than the emission of a fluorescence quantum by the complex (complex fluorescence). In fact, the low fluorescence quantum yield of benzene (maximal value 0.11) already indicates a high degree of spin-orbit coupling in the isolated molecule; it is therefore not surprising that already a very weak interaction between A^* and A results in considerable bimolecular quenching.

The concentration curve of naphthalene, which shows a remarkable residual fluorescence at relatively high concentrations, could be explained only by assuming the excited complex AA^* to fluoresce at the same wavelength as the excited monomer A^* . The interaction between A^* and A thus yields a complex of sufficient life-time to undergo complex fluorescence. On the other hand, the interaction is too weak to lead to complete quenching and the interaction energy is too small to affect the energy of the electronic states in the excited molecule. The latter phenomenon would give rise to a separate fluorescence band of the excited complex at longer wavelengths than the normal A^* fluorescence, as observed by Förster and Kasper [18] in solutions of pyrene.

Finally, the existence of excited complexes in anthracene solutions is evident from the formation of stable non-excited dimers via the process:



The absence of complex fluorescence may be attributed to strong intermolecular quenching in the complex AA^* .

The author most gratefully acknowledges the constructive criticism of Professor Dr. J. A. A. Ketelaar.

Des mesures de l'intensité de fluorescence de solutions diluées de plusieurs acènes en *n*-hexane à 25°C ont montré que dans le cas de benzène l'extinction en fonction de la concentration peut être expliquée en supposant qu'il s'agit d'une simple extinction par collision. Dans des solutions de naphthalène et d'anthracène cette extinction s'effectue via un complexe excité instable résultant de l'interaction d'une molécule excitée et une molécule non-excitée. La forme remarquable de la courbe de concentration du naphthalène est attribuée à la contribution de complexe excité de naphthalène à l'intensité de fluorescence totale.

A partir des résultats des mesures on a calculé que la durée moyenne τ de l'état électronique fluorescent est d'environ 2×10^{-6} pour le benzène et de 5×10^{-7} pour le naphthalène.

Die Fluoreszenzintensität verdünnter Lösungen verschiedener Azene in *n*-Hexan wird in Abhängigkeit von der Konzentration bei 25°C gemessen. Die Ergebnisse zeigen, dass die Konzentrationslöschung für Benzol durch eine einfache Stosslöschung erklärt werden kann. In Lösungen von Naphthalin und Anthrazen erfolgt die Konzentrationslöschung über einen instabilen angeregten Komplex, der aus einer angeregten und einer nicht-angeregten Molekel gebildet wird. Die merkwürdige Form der Konzentrationskurve des Naphthalins wird einem Beiträge des angeregten Naphthalinkomplexes zur Gesamtintensität der Fluoreszenz zugeschrieben.

Die durchschnittliche Lebensdauer τ des fluoreszierenden elektronischen Zustandes wird aus den Versuchsergebnissen zu 2×10^{-6} sek. für Benzol und 5×10^{-7} sek. für Naphthalin berechnet.

REFERENCES

- [1] KASHA, M., 1947, *Chem. Revs.*, **41**, 406.
- [2] KASHA, M., 1950, *Disc. Faraday Soc.*, **9**, 14.
- [3] MCCLURE, D. S., 1949, *J. chem. Phys.*, **17**, 905.
- [4] BOWEN, E. J., 1953, *Fluorescence of solutions* (London), p. 25.
- [5] PRINGSHEIM, P., 1949, *Fluorescence and Phosphorescence* (New York), p. 290.
- [6] FÖRSTER, TH., 1951, *Fluoreszenz Organischer Verbindungen* (Göttingen), p. 180.
- [7] DAMMERS-DE KLERK, A. and SPRUIT, F. J., 1956, *J. opt. Soc. Amer.*, **46**, 556.
- [8] DAMMERS-DE KLERK, A., 1956, *Thesis*, University of Amsterdam, the Netherlands.
- [9] YUSTER, P., and WEISSMANN, S. J., 1949, *J. chem. Phys.*, **17**, 1182.
- [10] DAMMERS-DE KLERK, A., and BOOT-MEURS, B., 1957, *Anal. Chim. Acta*, **16**, 296.
- [11] TAYLOR, H. A., and LEWIS, W. C. N., 1924, *J. Amer. chem. Soc.*, **46**, 1606.
CAPPER, N. S., and MARSH, J. K., 1925, *J. Amer. chem. Soc.*, **47**, 2849.
WEIGERT, P., 1927, *Naturwissenschaften*, **15**, 125.
- [12] SUZUKI, A., 1943, *Bull. chem. Soc., Japan*, **18**, 146; 1949, *Ibid.*, **22**, 172; 1950, *Ibid.*, **23**, 120.
- [13] COULSON, C. A., ORGEL, L. E., TAYLOR, W., and WEISS, J., 1955, *J. chem. Soc.*, 2961.
- [14] BOWEN, E. J., 1954, *Trans. Faraday Soc.*, **50**, 97.
- [15] BOWEN, E. J., and WILLIAMS, A. H., 1939, *Trans. Faraday Soc.*, **35**, 765.
- [16] KASHA, M., and NAUMANN, R. V., 1949, *J. chem. Phys.*, **17**, 516.
- [17] UMBERGER, J. Q., and LA MER, V. K., 1945, *J. Amer. chem. Soc.*, **67**, 1099.
WILLIAMSON, B., and LA MER, V. K., 1948, *J. Amer. chem. Soc.*, **70**, 717.
HODGES, K. C., and LA MER, V. K., 1948, *J. Amer. chem. Soc.*, **70**, 722.
ROWELL, J. C., and LA MER, V. K., 1951, *J. Amer. chem. Soc.*, **73**, 1630.
- [18] FÖRSTER, TH. and KASPER, K., 1954, *Z. phys. Chem. N.F.*, **1**, 275; 1955, *Z. Elektrochem.*, **59**, 976.

Electronic spectra of alternant hydrocarbon di-negative ions

by P. BALK, S. DE BRUIJN and G. J. HOIJTINK
Chemical Laboratory of the Free University, Amsterdam

(Received 4th December 1957)

The electronic spectra of the di-negative ions of anthracene, tetracene, perylene, terphenyl and quaterphenyl have been interpreted qualitatively, using the Hückel one-electron treatment and a correction for the correlation between the electrons which in the excited states move in broken shells. In this way the locations of the absorption bands in the visible and near ultra-violet could be satisfactorily predicted. The agreement between calculated and observed dipole strengths is not as good. On the average the calculated dipole strengths are twice to three times as high as the experimental values. For qualitative interpretations, however, the present treatment seems adequate.

1. INTRODUCTION

In a previous paper [1] the electronic spectra of various alternant hydrocarbon mononegative ions have been interpreted with the aid of a simple LCAOMO treatment including configuration interaction. The present paper deals with a similar treatment of the lower electron excitations in various alternant hydrocarbon di-negative ions.

2. THEORETICAL PART

In the ground state of an alternant hydrocarbon di-negative ion with $2n$ tervalent carbon atoms the n bonding π -orbitals and the lowest anti-bonding π -orbital are each occupied by two electrons. If these electrons are described by the one-electron wave functions

$$\phi_j(\nu) = \sum_{s=1}^{2n} c_{s,j} \varphi_s(\nu) \quad (1)$$

in which $\varphi_s(\nu)$ describes the electron ν in the $2p_z$ -orbital at the s th carbon atom, the configurations for the ground state and the singlet and triplet excited states may be described by the antisymmetrized products:

$${}^1\Psi_N = |\phi_1\bar{\phi}_1 \dots \phi_j\bar{\phi}_j \dots \phi_{n+1}\bar{\phi}_{n+1}| \quad (2)$$

$${}^3, {}^1\Psi_V = (1/\sqrt{2})\{|\phi_1\bar{\phi}_1 \dots \phi_j\bar{\phi}_k \dots \phi_{n-1}\bar{\phi}_{n+1}| \pm |\phi_1\bar{\phi}_1 \dots \phi_k\bar{\phi}_j \dots \phi_{n+1}\bar{\phi}_{n+1}|\} \quad (3)$$

where the $+$ and $-$ signs refer to the singlet and triplet state respectively.

As in the treatment of the electron excitations in alternant hydrocarbon mono-negative ions we assume that the addition of two electrons to the hydrocarbon molecule does not seriously alter the distribution of the residual electrons. Under this condition any pair of the $2n+2$ π -electrons in the alternant di-negative ion may be considered to move in the field of the $2n$ neutral carbon atoms [1, 2], so that the Hamiltonian becomes:

$$H(\mu, \nu) = \mathcal{H}(\mu) + \mathcal{H}(\nu) + e^2/r_{\mu\nu} \quad (4)$$

where $\mathcal{H}(\mu)$ and $\mathcal{H}(\nu)$ stand for the one-electron Hamiltonians of the electrons μ

and ν moving in the field of the $2n$ neutral carbon atoms and $e^2/r_{\mu\nu}$ involves the potential energy due to the repulsion between the electrons μ and ν .

In terms of Hückel MO's the energies of the singlet and triplet excited states relative to the ground state are:

$${}^1E_V = (x_j - x_k)\beta + \mathcal{J}_{j,k} + \mathcal{K}_{j,k} - \mathcal{J}_{j,j} \quad (5)$$

$${}^3E_V = (x_j - x_k)\beta + \mathcal{J}_{j,k} - \mathcal{K}_{j,k} - \mathcal{J}_{j,j} \quad (6)$$

where x_j and x_k stand for the roots of the Hückel secular equation, β denotes the resonance integral and

$$\mathcal{J}_{j,k} = \iint \phi_j(\mu)\phi_k(\mu) \frac{e^2}{r_{\mu\nu}} \phi_k(\nu)\phi_j(\nu) d\tau_\mu d\tau_\nu \quad (7)$$

$$\mathcal{K}_{j,k} = \iint \phi_j(\mu)\phi_k(\mu) \frac{e^2}{r_{\mu\nu}} \phi_j(\nu)\phi_k(\nu) d\tau_\mu d\tau_\nu. \quad (8)$$

The dipole moment and the dipole strength for the singlet singlet transition become:

$$\mathbf{M}_{N,1V} = e \int {}^1\Psi_N \mathbf{r} {}^1\Psi_V d\tau = e\sqrt{2} \int \phi_j(\nu) \mathbf{r} \phi_k(\nu) d\tau_\nu = \mathbf{m}_{j,k}\sqrt{2}, \quad (9)$$

$$D_{N,1V} = \mathbf{M}_{N,1V}^2 / e^2 = 2\mathbf{m}_{j,k}^2 / e^2. \quad (10)$$

If we restrict ourselves to the electron excitations which give rise to the absorption of light in the visible and the near ultra-violet, only the following excitations need be considered:

$$\left. \begin{matrix} n+1 \rightarrow k \\ n \rightarrow k \end{matrix} \right\} k \geq n+2. \quad (11)$$

In alternant hydrocarbon molecules the excitation $n \rightarrow k$ cannot be separated from the excitation $j \rightarrow n+1$, if $k = 2n+1-j$. The configurations due to these excitations have the same energy, so that first-order configuration interaction ought to be applied [3]. In the di-negative ion the excitations $j \rightarrow n+1$ cannot occur, as the $(n+1)$ th orbital is occupied by two electrons. Further configuration interaction has not been applied except in the case of the perylene di-negative ion. In the latter case configuration interaction is necessary, because of the fact that two of the four Hückel wave functions for the four-fold degenerate $(n+2)$ th π -electronic level have the same symmetry.

$n=5$ (a)	${}^1A_{1g} \rightarrow {}^1B_{3u}$ (b)	${}^1A_{1g} \rightarrow {}^1B_{2u}$ (b)	$\sigma_{\text{calc.}}$ (c)	$\sigma_{\text{obs.}}$ (c)	$D_{\text{calc.}}$	$D_{\text{obs.}}$ (d)	ρ (e)
$6 \rightarrow 7a$	x_1	y_1	18.1	16.3	6.40 } 1.54 } 3.32 }	2.11	0.27
$6 \rightarrow 8$			21.8	22			
$5 \rightarrow 7b$	x_2		26.9	29.9			

Table 1. [Anthracene] $^{--}$.

(a) n denotes the number of the highest bonding Hückel π -orbital in the molecule.

(b) Symmetry characters of the ground and excited states and directions of polarization x and y . In this and the other ions the x -axis has been taken as the longer axis.

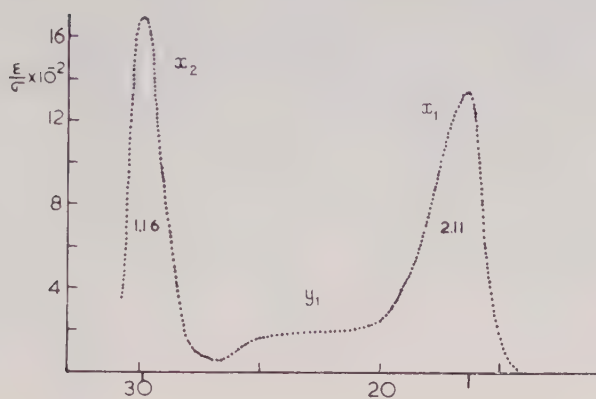
(c) Wave number in kilokaysers ($1 \text{ kK} = 1000 \text{ cm}^{-1}$).

(d) Dipole strengths calculated with the aid of the formula [1]:

$$D = 3.99 \times 10^{-4} \int (\epsilon/\sigma) d\sigma \quad (\text{in } \text{\AA}^2)$$

where ϵ is the molar extinction and σ stands for the wave number in kK.

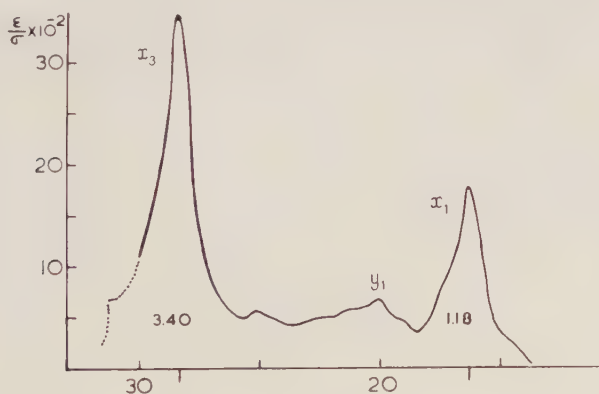
(e) $\rho = D_{\text{obs.}}/D_{\text{calc.}}$

Figure 1. Absorption spectrum of [anthracene]²⁻.

$n=9$	${}^1A_{1g} \rightarrow {}^1B_{3u}$	${}^1A_{1g} \rightarrow {}^1B_{2u}$	$\sigma_{\text{calc.}}$	$\sigma_{\text{obs.}}$	$D_{\text{calc.}}$	$D_{\text{obs.}}$	ρ
10 \rightarrow 11	x_1	y_1	15.3	16.2	10.17	1.18	0.12
10 \rightarrow 14			18.6	20.1	1.34		
10 \rightarrow 15	x_2^\dagger		29.1	25.1	0.04		
9 \rightarrow 12	x_3		25.5	28.3	4.32	3.40	0.79

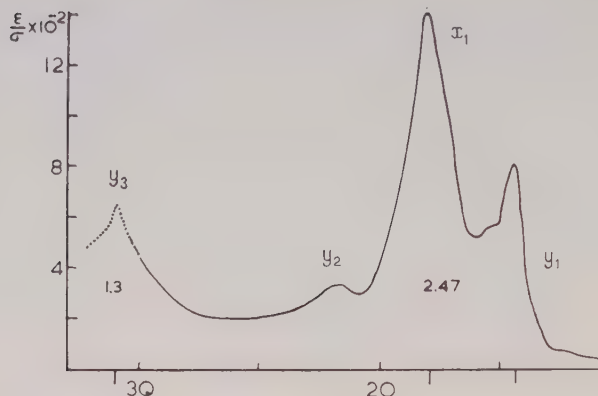
Table 2. [Tetracene]²⁻.

† The interaction between the configurations labelled x_2 and x_3 is negligible.

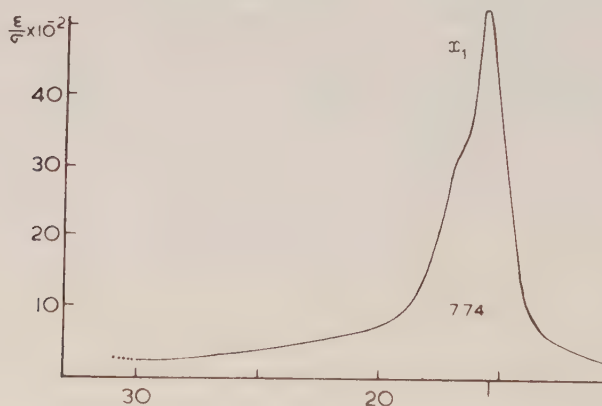
Figure 2. Absorption spectrum of [tetracene]²⁻.

$n=7$	${}^1A_{1g} \rightarrow {}^1B_{3u}$	${}^1A_{1g} \rightarrow {}^1B_{2u}$	$\sigma_{\text{calc.}}$	$\sigma_{\text{obs.}}$	$D_{\text{calc.}}$	$D_{\text{obs.}}$	ρ
8 \rightarrow 9a	x_1		17.9	17.9	6.99	2.47	0.23
8 \rightarrow 9b		y_1	14.0	14.4	0.08		
8 \rightarrow 9c		y_2	20.9	21.6	3.63		
7 \rightarrow 9d		y_3	30.4	30.9	2.58		

Table 3. [Perylene]²⁻.

Figure 3. Absorption spectrum of [perylene]⁻.

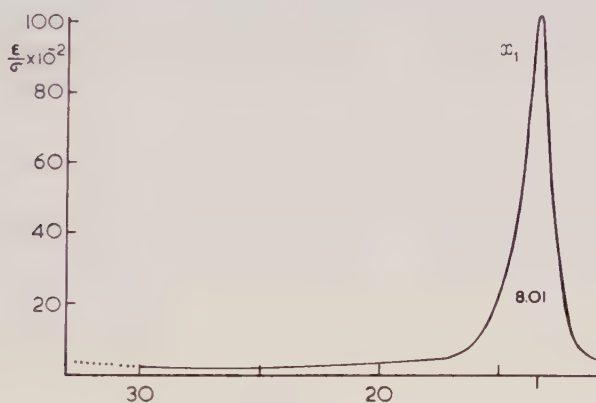
$n=6$	${}^1A_{1g} \rightarrow {}^1B_{3u}$	${}^1A_{1g} \rightarrow {}^1B_{2u}$	$\sigma_{\text{calc.}}$	$\sigma_{\text{obs.}}$	$D_{\text{calc.}}$	$D_{\text{obs.}}$	ρ
$7 \rightarrow 8a$	x_1	y_1	15.8	15.4	16.16	7.74	0.48
$7 \rightarrow 8b$					0.15		
$7 \rightarrow 10$	x_2				0.12		

Table 4. [Terphenyl]⁻.Figure 4. Absorption spectrum of [terphenyl]⁻.

In tables 1 to 5 the results of the calculations have been compared with the experimental data taken from an earlier paper [4]. The Coulomb and exchange integrals (7) and (8) have been calculated according to the procedure described by Pariser and Parr [5]. For the resonance parameter we have chosen the value $\beta = -20.5$ kilokayser ($= -20500 \text{ cm}^{-1}$). The same value has been used for the treatment of the electron excitations in the mono-negative ions [1]. It is worthwhile mentioning that the values of β obtained from the polarographic reduction of conjugated hydrocarbons and from theoretical calculations [2] are only slightly larger, viz. -21.4 and -21.1 kilokayser respectively. In

figures 1 to 5 the assignment of the absorption bands has been given. Since in these figures ϵ/σ has been plotted against σ the dipole strengths are directly proportional to the area of the 'absorption' bands.

$n=10$	${}^1A_{1g} \rightarrow {}^1B_{3u}$	${}^1A_{1g} \rightarrow {}^1B_{2u}$	$\sigma_{\text{calc.}}$	$\sigma_{\text{obs.}}$	$D_{\text{calc.}}$	$D_{\text{obs.}}$	ρ
11 \rightarrow 12	x_1	y_1	12.4	13.2	27.44	8.01	0.29
11 \rightarrow 13a					0.11		
11 \rightarrow 13b					0.02		
11 \rightarrow 15	x_2	y_2			0.19		
11 \rightarrow 17	x_3				0.01		

Table 5. [Quaterphenyl] $^{2-}$.Figure 5. Absorption of spectrum [quaterphenyl] $^{2-}$.

3. DISCUSSION

From the tables it appears that the present treatment gives a satisfactory prediction of the locations of the absorption bands. The agreement between calculated and observed dipole strengths is less satisfactory, though for a qualitative interpretation of the spectra the results are not discouraging. On the average the calculated dipole strengths are twice to three times as high as the experimental values. This discrepancy has also been found for alternant hydrocarbon molecules and the mono-negative ions. In the case of the perylene di-negative ion the interaction between the configurations due to the electron excitations $9 \rightarrow 9b$ and $8 \rightarrow 9c$ leads to a weak red and a stronger blue absorption band, whereas the experimental spectrum seems to show the reverse. A more extended configuration interaction may give better results. On the other hand it should be emphasized that more thorough calculations need not necessarily lead to better results. In contrast to the mono-negative ions the di-negative ions are strongly associated with the gegen-ions [4, 6] so that discrepancies between the present calculations and the experimental data may also arise from the fact that the electronic spectra are modified by interaction between the di-negative ions and the alkali ions. In general such a perturbation will have greater influence on the intensities than on the locations of the absorption bands.

Les spectres électroniques des ions di-négatifs de l'anthracène, du tétracène, du pérylène, du terphényle et du quaterphényle ont été interprétés qualitativement, en employant le traitement de Hückel avec une correction pour la corrélation entre les électrons qui se meuvent en couches incomplètes dans les états excités. En employant ce traitement, on a pu prédire d'une manière satisfaisante les positions des bandes d'absorption dans la région visible et l'ultra-violet proche. L'accord entre les forces d'oscillateur calculées et observées est moins bon. En moyenne, les forces d'oscillateur calculées sont 2-3 fois plus grandes que les valeurs expérimentales. Toutefois, le traitement décrit paraît suffire pour les interprétations qualitatives.

Die Elektronenspektren der zweifach negativen Ionen von Anthrazen, Tetrazen, Perylen, Terphenyl und Quaterphenyl wurden qualitativ gedeutet. Hierbei wurde die Hückel'sche Einelektronen-Behandlung zugrunde gelegt mit einer Korrektur für die Wechselbeziehung zwischen den Elektronen, die sich in den angeregten Zuständen in halbgefüllten Bahnen bewegen. Auf diese Weise konnte die Lage der Absorptionsbanden im sichtbaren Gebiet und im Ultravioletten befriedigend gedeutet werden. Die Uebereinstimmung zwischen den berechneten und den beobachteten Oszillatorstärken ist weniger gut. Im Durchschnitt sind die berechneten Oszillatorstärken zwei bis dreimal so gross wie die gefundenen Werte. Für eine qualitative Deutung scheint diese Behandlung jedoch genügend.

REFERENCES

- [1] BALK, P., DE BRUIJN, S., and HOIJTINK, G. J., 1957, *Rec. trav. chim.*, **76**, 908.
- [2] BALK, P., DE BRUIJN, S., and HOIJTINK, G. J., 1957, *Rec. trav. chim.*, **76**, 860.
- [3] DEWAR, M. J. S., and LONGUET-HIGGINS, H. C., 1954, *Proc. phys. Soc. Lond.*, A, **67**, 795.
- [4] BALK, P., HOIJTINK, G. J., and SCHREURS, J. W. H., 1957, *Rec. trav. chim.*, **76**, 813.
- [5] PARISER, R., and PARR, R. G., 1953, *J. chem. Phys.*, **21**, 466, 767 ; 1956, *J. chem. Phys.*, **24**, 250.
- [6] HOIJTINK, G. J., DE BOER, E., VAN DER MEIJ, P. H., and WEIJLAND, W. P., 1956, *Rec. trav. chim.*, **75**, 487.

Electron spin densities in alternant hydrocarbon mono-negative and mono-positive ions and in odd alternant hydrocarbon radicals

by G. J. HOIJTINK

Chemical Laboratory of the Free University, Amsterdam

(Received 16 December 1957)

A comparison is made between MO calculations of electron spin densities in alternant hydrocarbon mono-negative and mono-positive ions and in odd alternant hydrocarbon radicals. For the positive and negative ions the Hückel MO treatment leads to satisfactory results, whereas for radicals configuration interaction must be taken into account. In a preliminary communication McConnell and Chesnut (see ref [14]) also noticed the necessity of π - π interaction in the MO calculations of electron spin densities of hydrocarbon free radicals. In this way negative spin densities are found for those carbon atoms in the radical at which in the non-bonding MO the electron densities are zero. This difference between alternant ions and radicals is due to the fact that in the singly charged ions the odd electron ('positive hole') may approximately be considered to move in the electrostatic field of the neutral carbon atoms of the hydrocarbon molecule, whereas in odd alternant hydrocarbon radicals the odd electron forms an integral part of the neutral system.

1. INTRODUCTION

The electron spin resonance spectra of various hydrocarbon mono-negative and mono-positive ions [1] and of the hydrocarbon radicals triphenylmethyl [2] and perinaphthenyl [3] display a well-resolved hyperfine pattern, which is due to the interaction between the magnetic moments of the electrons and the protons. This hyperfine interaction requires a finite electron spin density at the protons of the odd electron system, which according to McConnell [4] and Weissman [5] arises from the interaction between the σ -electrons of the carbon-hydrogen bond and the π -electrons. As these authors have shown the electron spin density at the proton will be directly proportional to the electron spin density at the adjacent carbon atom. On the basis of this linear relationship De Boer [6] has interpreted the hyperfine structure in the electron spin resonance spectra of various hydrocarbon mono-negative and mono-positive ions using the Hückel MO treatment. This treatment, however, failed in the interpretation of the hyperfine structure in the electron spin resonance spectrum of the radical triphenylmethyl. On the other hand the valence bond treatment in its most simple form leads to a spin distribution which fits the experimental data satisfactorily [7]. As Brovetto and Ferroni [7] have shown the valence bond treatment gives high negative spin densities at those carbon atoms where in the Hückel non-bonding π -orbital the electron density is zero.

In the present paper this fundamental difference between alternant hydrocarbon mono-negative and mono-positive ions and alternant hydrocarbon radicals will be investigated. For that purpose more thorough MO calculations, allowing for interaction between the π -electrons, will be used.

2. ELECTRON SPIN DENSITIES IN ALTERNANT HYDROCARBON MONO-NEGATIVE AND MONO-POSITIVE IONS

Let us consider an alternant hydrocarbon molecule with $2n$ tervalent carbon atoms. The $2n$ π -electrons may be described by the orthonormal Hückel mo's:

$$\phi_j = \sum_{s=1}^{2n} c_{s,j} \varphi_s(\nu) \quad 1 \leq j \leq 2n \quad (1)$$

where $\varphi_s(\nu)$ describes the π -electron ν in the $2p_z$ -orbital at the s th carbon atom.

The anti-symmetrized product wave functions for the doublet ground and excited state configurations of the mono-negative ion now become [8]

$${}^2\Psi_N = |\phi_1 \bar{\phi}_1 \dots \phi_j \bar{\phi}_j \dots \phi_{n+1}| \quad (2)$$

$${}^2\Psi_A = |\phi_1 \bar{\phi}_1 \dots \phi_j \bar{\phi}_j \dots \phi_k| \quad k \geq n+2 \quad (3)$$

$${}^2\Psi_B = |\phi_1 \bar{\phi}_1 \dots \phi_j \bar{\phi}_{n+1} \dots \phi_{n+1}| \quad j \leq n \quad (4)$$

$${}^2\Psi_C = (1/\sqrt{2})\{|\phi_1 \bar{\phi}_1 \dots \phi_j \bar{\phi}_k \dots \phi_{n+1}| + |\phi_1 \bar{\phi}_1 \dots \phi_k \bar{\phi}_j \dots \phi_{n+1}|\} \quad (5)$$

$${}^2\Psi_D = (1/\sqrt{6})\{2|\phi_1 \bar{\phi}_1 \dots \phi_j \bar{\phi}_{n+1} \dots \phi_k| + |\phi_1 \bar{\phi}_1 \dots \phi_j \bar{\phi}_k \dots \phi_{n+1}| - |\phi_1 \bar{\phi}_1 \dots \phi_k \bar{\phi}_j \dots \phi_{n+1}|\} \quad (6)$$

If H stands for the complete Hamiltonian of the π -electronic system the matrix elements for the interaction between the ground state configuration N and the excited state configurations A, B, C and D, following Pople's procedure [9], become:

$$H_{N,A} = F_{n+1,k} \quad (7)$$

$$H_{N,B} = F_{j,n+1} + \langle j, n+1 | n+1, n+1 \rangle \quad (8)$$

$$H_{N,C} = F_{j,k} \sqrt{2} - \frac{1}{2} \sqrt{2} \langle j, n+1 | k, n+1 \rangle + \sqrt{2} \langle j, k | n+1, n+1 \rangle \quad (9)$$

$$H_{N,D} = (\sqrt{3}/\sqrt{2}) \langle j, n+1 | k, n+1 \rangle \quad (10)$$

where

$$\langle j, i | k, i \rangle = \iint \phi_j(\mu) \phi_i(\mu) \frac{e^2}{r_{\mu\nu}} \phi_k(\nu) \phi_i(\nu) d\tau_\nu d\tau_\mu \quad (11)$$

and

$$F_{j,k} = - \sum_{i=1}^n \langle j, i | k, i \rangle. \quad (12)$$

Now the ground state wave function after configuration interaction may be described by:

$$\Psi_N' = \eta \left\{ \Psi_N - \sum_{j,k} \lambda_A \cdot \Psi_A + \lambda_B \cdot \Psi_B + \lambda_C \cdot \Psi_C + \lambda_D \cdot \Psi_D \right\} \quad (13)$$

in which η denotes the normalization factor and

$$\lambda_A = \frac{H_{N,A}}{H_{A,A} - H_{N,N}}, \text{ etc.} \quad (14)$$

The electron spin densities at the various carbon atoms of the π -electronic system may now be derived from the integral

$$\int \Psi_N' S_z \Psi_N' d\tau, \quad (15)$$

where S_z stands for the sum of the spin operators of the individual π -electrons:

$$S_z = \sum_{\mu=1}^{2n+1} S_z(\mu).$$

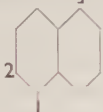

Neglecting terms in λ^2 and making use of (1), (13), (14) and (15) the electron spin density at the s th carbon atom becomes (in units of $\frac{1}{2}(\hbar/2\pi)$):

$$\rho_s = c_{s,n+1}^2 + 2 \sum_{j=1}^n \sum_{k=n+2}^{2n} \frac{F_{j,n+1} + \langle j, n+1 | n+1, n+1 \rangle}{H_{B,B} - H_{N,N}} c_{s,j} \cdot c_{s,n+1} - \frac{F_{n+1,k}}{H_{A,A} - H_{N,N}} c_{s,n+1} \cdot c_{s,k} + \frac{\langle j, n+1 | k, n+1 \rangle}{H_{D,D} - H_{N,N}} c_{s,j} \cdot c_{s,k} \quad (16)$$

From equation (16) the electron spin densities in the naphthalene and biphenyl mono-negative ions have been calculated. For that purpose the energies of the configurations relative to the ground state configuration N have been taken equal to the Hückel energies, so that

$$H_{D,D} - H_{N,N} = (x_j - x_k)\beta, \text{ etc.} \quad (17)$$

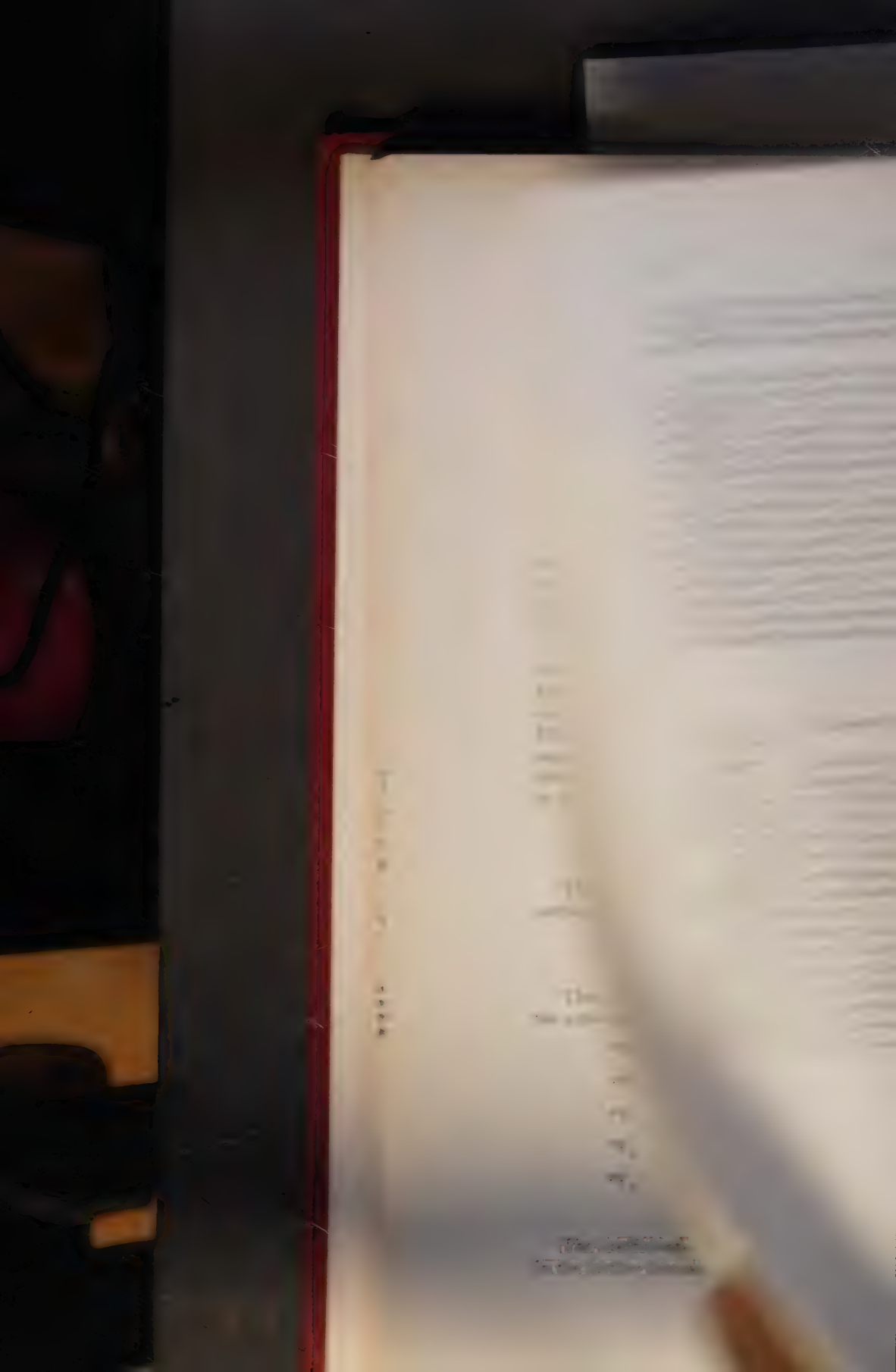
Here x_j and x_k stand for the roots of the Hückel secular equation corresponding to the j th and k th π -orbital and β denotes the resonance parameter, for which we have chosen $\beta = -2.6 \text{ eV}$ [10]. In this way the denominator in λ_D becomes lower than the exact value. In the cases of naphthalene and biphenyl, however, the difference is small in comparison with the absolute value of the denominator.

		ρ		
		$H.$	$H. + \text{C.I.}$	
[naphthalene] ⁻ 	1	0.181	0.221	$\rho_1/\rho_2 = 2.6 \text{ (H.)}$ $= 4.1 \text{ (H. + C.I.)}$
	2	0.069	0.054	
[biphenyl] ⁻ 	1	0.159	0.215	$\rho_1/\rho_3 = 1.8 \text{ (H.)}$ $= 3.5 \text{ (H. + C.I.)}$
	2	0.019	-0.018	
	3	0.089	0.062	
	4	0.123	0.115	

Electron spin densities in the naphthalene and biphenyl mono-negative ion.

The results of the calculations are listed in the table. Tuttle, Ward and Weissman [11] found that the experimental spectrum of the naphthalene mono-negative ion is matched in all details by a ratio in spin densities $\rho_1:\rho_2=2.8$.

The electron spin resonance spectrum of the biphenyl mono-negative ion unequivocally points to a ratio in spin densities $\rho_1/\rho_3=2.0$. Apparently the Hückel spin densities fit the experimental data more closely than the values obtained from the present treatment. This success of the Hückel treatment is not restricted to the negative ions of naphthalene and biphenyl. As De Boer has shown [6] this treatment gives a satisfactory interpretation of the electron spin resonance spectra of various alternant hydrocarbon mono-negative ions.



mouvant dans le champ électrostatique des atomes neutres de carbone dans la molécule d'hydrocarbure, tandis que dans les radicaux alternants impairs des hydrocarbures l'électron célibataire forme une partie intégrale du système neutre.

Die M.O.-Berechnungen der Elektronspindichten in alternierenden mono-negativen und mono-positiven Ionen der Kohlenwasserstoffe sowie in alternierenden Kohlenwasserstoffradikalen werden verglichen. Das Hückel'sche M.O.-Verfahren ergibt für das positive und das negative Ion befriedigende Resultate, wogegen für Radikale die konfigurationsnelle Wechselwirkung berücksichtigt werden muss. Nach einer vorläufigen Mitteilung beobachteten gleichfalls McConnell und Chesnut (vgl. Ref. [14]) die Notwendigkeit der π - π -Wechselwirkung in M.O.-Berechnungen der Elektronspindichten für freie Kohlenwasserstoffradikale. Auf diese Weise werden negative Spindichten für diejenigen Kohlenstoffatome des Radikals gefunden, an denen die Elektronendichten in den 'non-bonding orbitals' gleich Null sind. Dieser Unterschied zwischen den alternierenden Ionen und Radikalen wird dadurch bedingt, dass in Ionen mit einfacher Ladung das ungepaarte Elektron ('positives Loch') annähernd so betrachtet werden kann, als ob es sich im elektrostatischen Feld der neutralen Kohlenstoffatome des Kohlenwasserstoffmoleküls bewegt, wogegen in den alternierenden Kohlenwasserstoffradikalen das ungepaarte Elektron einen Integralteil des neutralen Systems bildet.

REFERENCES

- [1] WEISSMAN, S. I., TOWNSEND, J., PAUL, D. E., and PAKE, G. E., 1953, *J. chem. Phys.*, **21**, 2227.
- [2] JARRETT, H. S., and SLOAN, G. J., 1954, *J. chem. Phys.*, **22**, 1783.
- [3] SOGO, P. B., NAKAZAKI, M., and CALVIN, M., 1957, *J. chem. Phys.*, **26**, 1343.
- [4] MCCONNELL, H. M., 1956, *J. chem. Phys.*, **24**, 764.
- [5] WEISSMAN, S. I., 1956, *J. chem. Phys.*, **25**, 890.
- [6] DE BOER, E., 1956, *J. chem. Phys.*, **25**, 190.
DE BOER, E., 1957, *Thesis*, Free University, Amsterdam.
DE BOER, E., and WEISSMAN, S. I., in the press.
- [7] BROVETTO, P., and FERRONI, S., 1957, *Il Nuovo Cim.*, **5**, 142.
- [8] LONGUET-HIGGINS, H. C., and POPL, J. A., 1955, *Proc. phys. Soc. Lond.*, A, **68**, 591.
BALK, P., DE BRUYN, S., and HOIJTINK, G. J., 1957, *Rec. Trav. chim. Pays Bas.*, **76**, 907.
- [9] POPL, J. A., 1953, *Trans Faraday Soc.*, **49**, 1375.
- [10] BALK, P., BRUYN, DE S., and HOIJTINK, G. J., 1957, *Rec. Trav. chim. Pays Bas.*, **76**, 860.
- [11] TUTTLE, T. R., JR., WARD, R. L., and WEISSMAN, S. I., 1956, *J. chem. Phys.*, **25**, 189.
- [12] COULSON, C. A., and RUSHBROOKE, G. S., 1940, *Proc. Camb. phil. Soc.*, **36**, 193.
- [13] WEISSMAN, S. I., CONRADI, J. J., and DE BOER, E., 1957, *J. chem. Phys.*, **26**, 963.
- [14] MCCONNELL, H. M., and CHESNUT, D. B., 1957, *J. chem. Phys.*, **27**, 984.

A contribution to the theory of the exchange narrowing of spectral lines

by R. A. SACK

Department of Theoretical Chemistry, University of Cambridge
and

British Rayon Research Association, Manchester

(Received 8 January 1958)

The intensity distribution of a composite spectral line with exchange narrowing is calculated by integrating a matrix expression derived by Anderson [1]; the result, which is equally valid for classical and for quantum mechanical models, involves the inversion of a matrix with complex elements. The method is applied to symmetrical doublet and triplet lines and to lines of arbitrary multiplicity when all the transition probabilities are equal.

A quantum-mechanical theory of the narrowing of spectral lines by exchange or motion, which is of particular importance in nuclear magnetic resonance, has been derived by Anderson [1], by Kubo and Tomita [2] and by Kubo [3]. These authors calculate for several models the time-dependence of the auto-correlation function $\phi(\tau)$ for the mean dipole moment which determines the intensity distribution $I(\omega)$ of a spectral line according to

$$I(\omega) \sim \int_{-\infty}^{\infty} d\tau \exp(-i\omega\tau) \phi(\tau). \quad (1)$$

One important case considered is that of a composite line when the system can absorb radiation in any one of n different 'sites' in each of which it would show a sharp absorption line of frequency $\omega_j/2\pi$ ($j=1, 2, \dots, n$) in the absence of transitions between the sites; the Hamiltonians in the various sites, apart from the a.c. field, are assumed to commute with each other. (In the case of magnetic resonance this implies that the constant magnetic field in the different sites may vary in magnitude, but not in direction, and that the a.c. field must be normal to this.) If transitions of Markovian type from the j th to the k th site occur with a probability p_{jk} per unit time, Anderson [1] has shown that in the absence of saturation effects the auto-correlation function $\phi(\tau)$ becomes

$$\left. \begin{aligned} \phi(\tau) &= \mathbf{W} \cdot \exp[\tau(i\Omega + \Pi)] \cdot \mathbf{1}, & \tau > 0, \\ \phi(-\tau) &= \phi^*(\tau), \end{aligned} \right\} \quad (2)$$

where the n components of the vector \mathbf{W} are proportional to the occupation probabilities of the sites in equilibrium, $\mathbf{1}$ is a vector with all components equal to unity, Ω is a diagonal matrix with elements ω_j and Π is a matrix with elements

$$\left. \begin{aligned} \Pi_{jk} &= p_{jk}, \\ \Pi_{jj} &= - \sum_k p_{jk}, \end{aligned} \right\} \quad (j \neq k). \quad (3)$$

To solve (1) and (2) Anderson [1] suggests transforming the matrix $i\Omega + \Pi$ to diagonal form and finding its eigenvalues Λ_i ; $I(\omega)$ is then represented as

a sum of resonance distributions whose mean frequencies and widths are determined by the imaginary and real parts of the Λ_i respectively.

The purpose of this contribution is to point out that for $\phi(\tau)$ given by (2), equation (1) can be integrated without explicit diagonalization. Following Ledermann [4, 5] we obtain

$$\int_0^T \exp(-i\omega\tau)\phi(\tau) d\tau = \mathbf{W} \cdot [\exp\{\tau(\Pi + i\Omega - i\omega E_n)\}]_0^T \cdot (\Pi + i\Omega - i\omega E_n)^{-1} \cdot \mathbf{1} \quad (4)$$

where E_n is the unit matrix of order n . For $T \rightarrow \infty$ the integral converges only if the real parts of all the Λ_i are non-positive; the relevant convergence criteria have been derived by Ledermann [4] only for matrices with real elements and cannot be applied in the present case. Nevertheless, from physical arguments it is clear that the integral must converge, so that

$$I(\omega) \sim 2 \operatorname{Re} \mathbf{W} \cdot (i\omega E_n - i\Omega - \Pi)^{-1} \cdot \mathbf{1} \quad (5)$$

The calculation as to how the shape of a composite spectral line depends on the transition probabilities between the sites is thus reduced to the inversion of a matrix with complex elements, though in many cases the evaluation of the results may be facilitated by certain transformations applied to the vectors and the matrix. Anderson's results for the limiting cases of very slow and very rapid transitions in various models can be obtained as approximations for the series expansions of the inverted matrix (5).

Gutowsky, McCall and Slichter [6] have treated the problem of exchange narrowing for a classical model basing their calculations on the Bloch equations. They express the intensity distribution $I(\omega)$ for a doublet as the sum of two contributions which are determined as the unknowns in a set of two linear equations. If a phenomenologically introduced transverse relaxation time T_1 is taken to be infinite, their result is identical with that of Anderson [1] and Kubo [3]. A systematic generalization of the method of Gutowsky *et al.* [6] to an arbitrary number of lines leads to a result which is most conveniently expressed by equation (5).

The usefulness of formula (5) will be illustrated by three examples; in each case the reciprocal of the matrix is expressed as the matrix whose elements are the co-factors of the transposed original matrix, divided by its determinant Δ .

(a) Case of symmetric doublet

Here there is only one transition probability $p_{12} = p_{21} = p$; formula (5) leads to

$$\begin{aligned} I(\omega) &\sim 2 \operatorname{Re} \left\{ [1, 1] \begin{bmatrix} i(\omega - \omega_1) + p, & -p \\ -p, & i(\omega - \omega_2) + p \end{bmatrix}^{-1} \begin{bmatrix} 1 \\ 1 \end{bmatrix} \right\} \\ &= 2 \operatorname{Re} \left\{ \frac{[1, 1]}{\Delta} \begin{bmatrix} i(\omega - \omega_2) + p, & p \\ p, & i(\omega - \omega_1) + p \end{bmatrix} \begin{bmatrix} 1 \\ 1 \end{bmatrix} \right\} \\ &= 2 \operatorname{Re} \frac{4p + i(2\omega - \omega_1 - \omega_2)}{(\omega - \omega_1)(\omega - \omega_2) + ip(2\omega - \omega_1 - \omega_2)} \\ &= \frac{2p(\omega_1 - \omega_2)^2}{(\omega - \omega_1)^2(\omega - \omega_2)^2 + p^2(2\omega - \omega_1 - \omega_2)^2} \quad (6) \end{aligned}$$

This is the well-known formula derived by Gutowsky *et al.* [6], Anderson [1] and Kubo [3].

(b) Case of a symmetric triplet

For the sake of simplicity the frequencies will be stated as their differences from that of the central line; we then have $\omega_j = 0, \pm \delta$. The transition probabilities are

$$p_{01} = p_{0, -1}; \quad p_{10} = p_{-1, 0} = p'; \quad p_{1, -1} = p_{-1, 1} = p''. \quad (7)$$

If $p \neq p'$, the components of the vector \mathbf{W} will not be equal, but in the ratio $p:p':p$. Equation (5) now reads, apart from constant factors

$$I(\omega) \sim \text{Re} \left\{ [p, p', p] \begin{bmatrix} i(\omega - \delta) + p' + p'', & -p', & -p'' \\ -p, & i\omega + 2p, & -p \\ -p'', & -p', & i(\omega + \delta) + p' + p'' \end{bmatrix}^{-1} \begin{bmatrix} 1 \\ 1 \\ 1 \end{bmatrix} \right\}. \quad (8)$$

This expression can be evaluated as it stands, but it is useful first to transform the matrix by

$$T = T^{-1} = \begin{bmatrix} \sqrt{\frac{1}{2}} & 0 & \sqrt{\frac{1}{2}} \\ 0 & 1 & 0 \\ \sqrt{\frac{1}{2}} & 0 & -\sqrt{\frac{1}{2}} \end{bmatrix}. \quad (9)$$

We then obtain

$$\begin{aligned} I(\omega) &\sim \text{Re} \left\{ [\sqrt{2}p, p', 0] \begin{bmatrix} i\omega + p', & -\sqrt{2}p', & -i\delta \\ -\sqrt{2}p, & i\omega + 2p, & 0 \\ -i\delta, & 0, & i\omega + p' + 2p'' \end{bmatrix}^{-1} \begin{bmatrix} \sqrt{2} \\ 1 \\ 0 \end{bmatrix} \right\} \\ &= \text{Re} \frac{(i\omega + p' + 2p'')(2p + p')(i\omega + 2p + p') + p'\delta^2}{(i\omega + p' + 2p'')i\omega(i\omega + 2p + p') + \delta^2(i\omega + 2p)} \\ &= \text{Re} \left\{ \frac{2p + p'}{i\omega} + \frac{p'\delta^2 + i(2p + p')(i\omega + 2p)\delta^2/\omega}{2p\delta^2 - 2\omega^2(p + p' + p'') + i\omega[\delta^2 - \omega^2 + (2p + p')(2p'' + p')]} \right\}. \\ I(\omega) &\sim 2p\delta^2[\omega^2(2p'' + p') + p'\delta^2 + (2p + p')^2(2p'' + p')] \cdot D^{-1}, \end{aligned} \quad (10)$$

where

$$D = \omega^2(\delta^2 - \omega^2)^2 + 4p^2\delta^4 + 2\omega^2[p'(2p'' + p') - 2p(2p + p')]\delta^2 + \omega^2(2p + p')^2(2p'' + p')^2 + \omega^4[(2p + p')^2 + (2p'' + p')^2]. \quad (11)$$

The pair of equations simplifies considerably for several special cases. If $p' = 0$, the central line disappears, and the result becomes equivalent to (6). If $p = p'$, all three sites are equally populated, and we find

$$\begin{aligned} I(\omega) &\sim \frac{p(\delta^2 + 9p^2 + 18pp'' + \omega^2) + 2p''\omega^2}{\omega^2(\delta^2 - \omega^2)^2 + 4p^2\delta^4 + \omega^2\delta^2p(4p'' - 10p) + \omega^2p^2(3p + 6p'')^2 + \omega^4(10p^2 + 4pp'' + 4p''^2)}. \end{aligned} \quad (12)$$

The special solutions of (12) for $p'' = 0$ and $p'' = p$ have been discussed by Anderson [1] in the limit of very large and very small p ; the case $p'' = 2p$ has been treated in detail by Pople [7].

(c) Case of equal transition probabilities between any two sites

This model has been considered for the case of n equidistant lines by Anderson [1]; the equation (5) yields a formula valid for any arbitrary spacings. The calculation is rendered possible by the fact that all the diagonal minors

of a given order of the determinant of $(-\Pi)$ are equal; they are $m \times m$ determinants with diagonal elements $a = (n-1)p$ and off-diagonal elements $b = -p$; the value of such a determinant is (Aitken [8])

$$[a + (m-1)b](a-b)^{m-1} = (n-m)p(np)^{m-1}. \quad (13)$$

If the determinant Δ of $(i\omega E_n - i\Omega - \Pi)$ is expanded in terms of products of $(\omega - \omega_j)$, (13) yields:

$$\Delta = [a + (n-1)b](a-b)^{n-1} + i \sum_j (\omega - \omega_j)[a + (n-2)b](a-b)^{n-2} + i^2 \sum_{j,k} (\omega - \omega_j)(\omega - \omega_k)[a + (n-3)b](a-b)^{n-3} + \dots \quad (14)$$

$$= i \sum_j (\omega - \omega_j)n^{n-2}p^{n-1} + 2i^2 \sum_{j,k} (\omega - \omega_j)(\omega - \omega_k)n^{n-3}p^{n-2} + \dots \quad (15)$$

In the expression

$$I(\omega) \sim \text{Re}(N/\Delta) \quad (16)$$

the numerator N is given in view of (5) as the sum of all the signed minors of Δ , which in turn can be written (Aitken [8])

$$\left. \begin{aligned} N &= \partial\Delta/\partial a + \partial\Delta/\partial b \\ &= n(np)^{n-1} + i \sum_j (\omega - \omega_j)(n-1)(np)^{n-2} \\ &\quad + i^2 \sum_{j,k} (\omega - \omega_j)(\omega - \omega_k)(n-2)(np)^{n-3} + \dots \end{aligned} \right\}. \quad (17)$$

In both the numerator (17) and the denominator (15) of (16) the real and imaginary terms are separated and the real part of the quotient can be found without difficulty.

It should be pointed out that even for a continuous distribution of sites equation (5) is still formally valid; the inversion of a continuous matrix is then equivalent to the solution of a Fredholm integral equation (Whittaker and Watson [9]).

I wish to thank Dr. J. A. Pople for drawing my attention to this problem and for valuable discussions.

L'auteur a calculé la distribution de l'intensité d'une ligne spectrale composée en cas d'un rétrécissement d'échange en intégrant une expression en forme de matrice déduite par Anderson [1]; le résultat, qui tient également pour des modèles classiques et quantiques, comprend l'inversion d'une matrice à éléments complexes. La méthode est appliquée sur des lignes doublet et triplet symétriques et sur des lignes de multiplicité arbitraire, pour le cas ou toutes les probabilités de transition sont égales.

Die Intensitätsverteilung einer zusammengesetzten Spektrallinie mit Austausch-Verengung wird durch Integration eines Matrizenausdruckes berechnet, der von Anderson [1] abgeleitet worden ist. Das Ergebnis enthält die Inversion einer Matrix mit komplexen Elementen und ist ebenso für klassische wie für quantenmechanische Modelle gültig. Die Methode wird auf symmetrische Dublett- und Triplettlinien angewandt, sowie auf Linien willkürlicher Multiplizität, wenn alle Uebergangswahrscheinlichkeiten gleich gross sind.

REFERENCES

- [1] ANDERSON, P. W., 1954, *J. phys. Soc. Japan*, **9**, 316.
- [2] KUBO, R., and TOMITA, K., 1954, *J. phys. Soc. Japan*, **9**, 888.
- [3] KUBO, R., 1954, *J. phys. Soc. Japan*, **9**, 935.

- [4] LEDERMANN, W., 1950, *Proc. Camb. phil. Soc.*, **46**, 581.
- [5] LEDERMANN, W., 1951, *Proc. Camb. phil. Soc.*, **47**, 626.
- [6] GUTOWSKY, H. S., McCALL, D. W., and SLICHTER, C. P., 1953, *J. chem. Phys.*, **21**, 279.
- [7] POPLÉ, J. A., 1958, *Mol. Phys.*, **1**, 168.
- [8] AITKEN, A. C., 1939, *Determinants and Matrices* (Oliver and Boyd).
- [9] WHITTAKER, E. T., and WATSON, G. N., 1927, *A Course of Modern Analysis*, 4th edn. (Cambridge: University Press).

The effect of quadrupole relaxation on nuclear magnetic resonance multiplets

by J. A. POPLÉ

Department of Theoretical Chemistry, University of Cambridge

[Received 13 January 1958]

A theory of the broadening of multiplet components in magnetic resonance spectra of coupled nuclei due to electric quadrupole spin-lattice relaxation is presented. It is shown that the broadening of the components of the 1:1:1 triplet for nuclei of spin $\frac{1}{2}$ coupled to a nucleus of spin 1, is $\frac{3}{2}$ as great for the outer lines as for the central one, provided that the rate of quadrupole relaxation is not too large. This is in agreement with experimental observations on $^{14}\text{NH}_3$. A theory of the line shape of the partly collapsed multiplet at higher rates of quadrupole relaxation is also given.

1. INTRODUCTION

It is well known that nuclei with spin I greater than $\frac{1}{2}$ generally give broad signals in nuclear magnetic resonance spectra. This is because they possess electric quadrupole moments which interact with the fluctuating electric field gradients produced at the nucleus by other molecular degrees of freedom. Such interaction leads to rapid spin-lattice relaxation and consequently a broadening of signals. Nuclei with spin $I = \frac{1}{2}$ such as protons and ^{19}F , on the other hand, possess no quadrupole moments, so their spin-lattice relaxation times are longer and the signals correspondingly sharper.

If a nucleus of spin $\frac{1}{2}$ (or possibly a set of equivalent nuclei) is coupled to a nucleus of spin I ($> \frac{1}{2}$) by an interaction of the type $J\mathbf{I}_1 \cdot \mathbf{I}_2$, the spectra of both sorts of nucleus would consist of simple multiplets in the absence of quadrupole relaxation. The electric quadrupole relaxation mechanism will only operate on the nucleus of high spin and will affect the two multiplets in different ways. If the rate of relaxation is relatively slow, it will have the effect of broadening the individual components of both multiplets. However, if the rate becomes rapid enough, the multiplets will both coalesce into broad signals. Further increase then leads to further broadening of the spectrum of the high-spin nucleus, but that of the spin- $\frac{1}{2}$ nuclei will sharpen up to a single line, so that they are effectively decoupled. In qualitative terms, the disturbance of the high-spin nucleus is then so frequent that the transitions of the spin- $\frac{1}{2}$ nuclei cannot be associated with any particular state of the other. This explanation of the apparent lack of coupling of spin- $\frac{1}{2}$ nuclei with nuclei of high spin (such as chlorine) was put forward by Gutowsky *et al.* [1]. They gave a calculation based on a simplified model in which the second nucleus had spin $I = \frac{1}{2}$ but was subject to a fluctuating environment. Such a system shows a similar multiplet collapse.

This paper is primarily concerned with the effect of quadrupole relaxation on multiplets of this type, and applies particularly to spectra of protons coupled to ^{14}N . These sometimes show a single broad line and elsewhere a resolvable triplet structure (Roberts [2]). Recently Ogg and Ray [3] have recorded the proton and ^{14}N spectra of $^{14}\text{NH}_3$. These are discussed later in the paper.

In section 2 a theory is presented of the broadening of the individual lines by quadrupole relaxation which is not rapid enough to lead to complete multiplet collapse. This is followed in section 3 by an approximate theory of the shape of the spectrum of the spin- $\frac{1}{2}$ nuclei in the region of partial collapse.

2. QUADRUPOLE BROADENING OF MULTIPLET COMPONENTS

For simplicity, let us first consider a single nucleus of spin $\frac{1}{2}$ (which we shall suppose to be a proton) coupled to a nucleus of spin I . When these are placed in an external magnetic field the $2(2I+1)$ possible states can be classified by the spin components (n, m) in the direction of the field ($n = \pm \frac{1}{2}$, $m = -I, -I+1, \dots, +I$). The $(2I+1)$ transitions which give rise to the multiplet of the proton resonance spectrum are $(-\frac{1}{2}, m) \rightarrow (+\frac{1}{2}, m)$. Qualitatively these transitions can be said to arise from the resonance of the spin- $\frac{1}{2}$ nucleus in the presence of one of the $(2I+1)$ possible orientations of the other nucleus. The individual proton transitions will be broadened, therefore, if the lifetimes of the states of the second nucleus are short. Suppose that the high-spin nucleus in state m has a constant probability $(1/\tau_m)$ per unit time of undergoing a transition to another state. Then τ_m is the lifetime of state m and the line-shape function for this component is given by

$$g_m(\nu) = \frac{2\tau_m}{1 + 4\pi^2\tau_m^2(\nu - \nu_m)^2} \quad (2.1)$$

This is a normalized function proportional to the intensity at frequency ν when the natural frequency is ν_m . This expression is only valid if

- (i) other broadening mechanisms are negligible, and
- (ii) the broadening is small compared with the multiplet separation.

The problem reduces, then, to finding the lifetimes of the high-spin nucleus in its various states m . To do this we require the energy of interaction of the nuclear quadrupole moment with the fluctuating electric field gradient. Using the notation of Pound [4] this can be written in the form

$$F = \mathbf{Q} \cdot \nabla \mathbf{E} = \sum_{-2}^{+2} (-1)^p Q_p (\nabla E)_{-p}, \quad (2.2)$$

where \mathbf{Q} and $\nabla \mathbf{E}$ are dyadics representing the quadrupole moment and field gradient respectively. (Full definitions, which we shall not require, are given by Pound.) The matrix elements of F between different states of a nucleus of spin I are

$$\left. \begin{aligned} \langle m | F | m \rangle &= A[3m^2 - I(I+1)](\nabla E)_0 \\ \langle m | F | m \pm 1 \rangle &= \mp (6^{1/2}/2)A(2m \pm 1)[(I \pm m + 1)(I \mp m)]^{1/2}(\nabla E)_{\pm 1} \\ \langle m | F | m \pm 2 \rangle &= (6^{1/2}/2)A[(I \mp m)(I \mp m - 1)(I \pm m + 1)(I \pm m + 2)]^{1/2}(\nabla E)_{\pm 2} \end{aligned} \right\} \quad (2.3)$$

where

$$A = \frac{eQ}{2I(2I-1)}, \quad (2.4)$$

Q being the scalar nuclear quadrupole moment. All other matrix elements vanish, so a fluctuating electron field gradient can cause transitions in which $\Delta m = \pm 1$ or ± 2 . For simplicity we shall suppose that the environment of the nucleus is axially symmetric so that the components of the field gradient $(\nabla E)_q$

can be expressed in terms of the scalar

$$eq = -e \sum_j (3 \cos^2 \theta_j - 1) r_j^{-3}, \quad (2.5)$$

where θ_j is the angle between the direction of electron j and the symmetry axis. The components $(\nabla E)_q$ are then (Pound [4])

$$\left. \begin{aligned} (\nabla E)_0 &= \frac{1}{4} eq (3 \cos^2 \theta - 1), \\ (\nabla E)_{\pm 1} &= \pm \frac{1}{4} 6^{1/2} eq \sin \theta \cos \theta \exp(\pm i\phi), \\ (\nabla E)_{\pm 2} &= \pm \frac{1}{8} 6^{1/2} eq \sin^2 \theta \exp(\pm 2i\phi), \end{aligned} \right\} \quad (2.6)$$

where θ is the angle between the symmetry axis and the z -direction along which the nuclear spin is quantized.

To find the transition probabilities between the various states, we require the Fourier components of these quantities at the appropriate frequency. Following the method generally used in the theory of relaxation processes in liquids (Bloembergen *et al.* [5]), we suppose that there is a correlation time τ_c such that the autocorrelation or decay function for each component of the field gradient is $\exp(-t/\tau_c)$. τ_c is of the order of the time required for molecular reorientation. The transition probability $p_{i,j}$ between two states i and j due to the fluctuating Hamiltonian F is then

$$p_{i,j} = \hbar^{-2} |\langle i|F|j \rangle|^2 \frac{2\tau_c}{1 + 4\pi^2 \nu_{ij}^2 \tau_c^2} \quad (2.7)$$

where ν_{ij} is the frequency corresponding to the transition. Under the circumstances we are considering, the correlation time τ_c is short compared with the inverse frequency ν_{ij}^{-1} . Equation (2.7) may then be replaced by

$$p_{i,j} = 2\hbar^{-2} |\langle i|F|j \rangle|^2 \tau_c. \quad (2.8)$$

The mean square moduli of $(\nabla E)_p$ are all $\frac{1}{20} e^2 q^2$, so that $p_{i,j}$ can be evaluated using (2.3) and (2.8). For a nucleus with spin $I=1$, for example,

$$p_{-1,1} = p_{1,-1} = 2p_{0,\pm 1} = 2p_{\pm 1,0} = \frac{3}{20} e^4 \hbar^{-2} q^2 Q^2 \tau_c. \quad (2.9)$$

In general, the inverse lifetime of state m for a nucleus with spin I is given by

$$(1/\tau_m) = p_{m,m-2} + p_{m,m-1} + p_{m,m+1} + p_{m,m+2} = C(I, m) e^4 \hbar^{-2} q^2 Q^2 \tau_c \quad (2.10)$$

where $C(I, m)$ are numerical coefficients. The values of these for small I are (in order of increasing m):—

I	$C(I, m)$				
1	$\frac{9}{40}$	$\frac{6}{40}$	$\frac{9}{40}$		
$\frac{3}{2}$	$\frac{1}{10}$	$\frac{1}{10}$	$\frac{1}{10}$	$\frac{1}{10}$	
2	$\frac{10}{160}$	$\frac{13}{160}$	$\frac{10}{160}$	$\frac{13}{160}$	$\frac{10}{160}$
$\frac{5}{2}$	$\frac{45}{1000}$	$\frac{69}{1000}$	$\frac{54}{1000}$	$\frac{54}{1000}$	$\frac{69}{1000}$
				$\frac{45}{1000}$	

These quantities now give the ratios of the broadening components of a spin multiplet for a proton coupled to such a nucleus.

The broadening of the proton multiplet components can also be related to the spin-lattice relaxation time for the high-spin nucleus, and consequently to the broadening of the components of the high-spin spectrum.

The spin-lattice relaxation time is difficult to define if $I > 1$ so we shall only consider $I = 1$.

If n_- , n_0 and n_+ are the populations of the states with $I_z = -1, 0$ and $+1$ respectively, then

$$\left. \begin{aligned} \frac{dn_-}{dt} &= -(p_{-1,0} + p_{-1,1})n_- + p_{0,-1}n_0 + p_{1,-1}n_+, \\ \frac{dn_0}{dt} &= p_{-1,0}n_- - (p_{0,-1} + p_{0,+1})n_0 + p_{1,0}n_+, \\ \frac{dn_+}{dt} &= p_{-1,1}n_- + p_{0,1}n_0 - (p_{1,0} + p_{1,-1})n_+. \end{aligned} \right\} \quad (2.11)$$

The resultant magnetic moment in the z -direction is proportional to $(n_+ - n_-)$. Subtraction of the first and third of equations (2.11) (using equalities between the $p_{i,j}$ predicted by (2.8)) gives

$$\frac{d}{dt} (n_+ - n_-) = -\frac{1}{T_1} (n_+ - n_-) \quad (2.12)$$

where the spin-lattice relaxation time T_1 is given by†

$$1/T_1 = p_{0,1} + 2p_{-1,1} = \frac{3}{8} e^4 \hbar^{-2} q^2 Q^2 \tau_c. \quad (2.13)$$

Since the lifetime of the proton in each of its states will be relatively long, each component of the resonance multiplet of the spin-1 nucleus will be broadened independently by the same quadrupole mechanism. In fact, according to the Bloch treatment, the line shape under conditions where the relaxation times T_1 and T_2 are equal, is (Andrew [6])

$$g(\nu) = \frac{2T_1}{1 + 4\pi^2 T_1^2 (\nu - \nu_0)^2}. \quad (2.14)$$

This is similar to the line shape of the spin- $\frac{1}{2}$ multiplet components (equation (2.1)) but with τ_m replaced by T_1 . For protons coupled to nuclei of spin $I = 1$, for example, the theory predicts that the ratio of the broadening of the central component of the proton triplet to that of the outer components to that of any component of the high-spin multiplet will be 2:3:5.

The theory can be tested on ammonia $^{14}\text{NH}_3$, for which the proton and ^{14}N spectra have been measured by Ogg and Ray [7]. The fact that three equivalent protons are coupled to the ^{14}N nucleus rather than one does not affect the conclusions about broadening (which depend only on the probabilities of random transitions within the ^{14}N states). The proton spectrum shows the extra broadening of the outer components of the triplet very clearly and the experimental ratio (as measured by the heights) is close to the theoretical value 3:2 (Ogg

† This derivation of $1/T_1$ is not complete since pairs such as $p_{0,1}$ and $p_{1,0}$ are not quite equal by considerations of detailed balancing in thermal equilibrium. A more detailed argument along the lines used by Bloembergen *et al.* (5) for spin- $\frac{1}{2}$ nuclei, however, leads to the same result (2.13).

...

...

...

...

...

...

...

...

...

$\rho^2 = 2\pi^2$. Further $\delta = 2\pi f$ where f is the spin-rotating frequency. The shape of the absorption spectrum under these circumstances will depend on the dimensionless parameter

$$x = 2\pi\delta t = 2\pi f t P_Q^2 / \hbar^2 \quad (3.3)$$

is the spin-rotation relaxation time. If the frequency relative to the Larmor is the dimensionless quantity

$$y = 2\pi\delta\omega = \delta/\nu \quad (3.4)$$

is then proportional to

$$\frac{2\pi\delta\omega}{2\pi\nu} = \frac{P_Q^2}{\hbar^2} \frac{2\pi\delta t}{2\pi\nu} = \frac{2\pi\delta t}{2\pi\nu} \frac{P_Q^2}{\hbar^2} = \frac{2\pi\delta t}{2\pi\nu} \frac{P_Q^2}{\hbar^2} \quad (3.5)$$

of the frequency of ν for a series of values of x is shown in Figure 5. In these quadrupole relaxation (Figure 5) all the spectral features of lines broadened as discussed in section 2. As for the corresponding nuclear collapse, the nucleus in the outer peaks move apart as the x increases and eventually all three nucleus are a single signal.

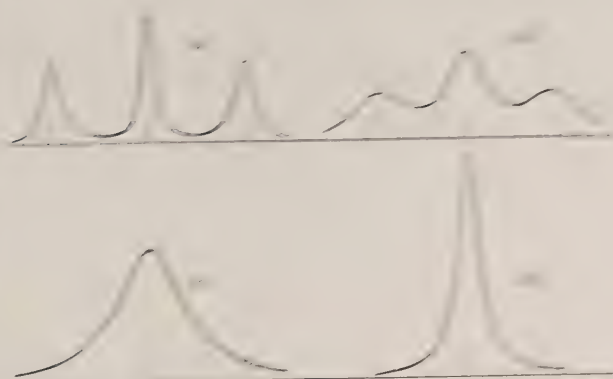


Figure 5. Theoretical intensities for the spectrum of nuclei of spin $\frac{1}{2}$ coupled to a nucleus of spin $\frac{3}{2}$ with quadrupole relaxation. The curves are calculated for various values of the parameter x in the absence of quadrupole relaxation.

Wenn man die Theorie der Quadrupolrelaxation in quadrupolen magnetischer Kernspin-Systeme anwendet, so muss man sich an die Relaxation, quadrupolare Spin-Relaxation und Quadrupolrelaxation des Systems anwenden. In der Tat ist die Quadrupolrelaxation des Systems ein quadrupolarer Kern, der in einem quadrupolaren Magnetfeld relaxiert. In diesem Fall ist die Quadrupolrelaxation des Systems ein quadrupolarer Kern, der in einem quadrupolaren Magnetfeld relaxiert. In diesem Fall ist die Quadrupolrelaxation des Systems ein quadrupolarer Kern, der in einem quadrupolaren Magnetfeld relaxiert.

Wenn man die Theorie der Quadrupolrelaxation in quadrupolen magnetischer Kernspin-Systeme anwendet, so muss man sich an die Relaxation, quadrupolare Spin-Relaxation und Quadrupolrelaxation des Systems anwenden. In der Tat ist die Quadrupolrelaxation des Systems ein quadrupolarer Kern, der in einem quadrupolaren Magnetfeld relaxiert. In diesem Fall ist die Quadrupolrelaxation des Systems ein quadrupolarer Kern, der in einem quadrupolaren Magnetfeld relaxiert.

hoch ist. Dies stimmt mit den experimentellen Beobachtungen an $^{14}\text{NH}_3$ überein. Eine Theorie der Liniengestalt des teilweise zusammengebrochenen Multipletts bei höheren Geschwindigkeiten der Quadrupolrelaxation wird ebenfalls angegeben.

REFERENCES

- [1] GUTOWSKY, H. S., MCCALL, D. W., and SLICHTER, C. P., 1953, *J. chem. Phys.*, **21**, 279.
- [2] ROBERTS, J. D., 1956, *J. Amer. chem. Soc.*, **78**, 4495.
- [3] OGG, R. A., and RAY, J. D., 1957, *J. chem. Phys.*, **26**, 1339, 1515.
- [4] POUND, R. V., 1950, *Phys. Rev.*, **79**, 685.
- [5] BLOEMBERGEN, N., PURCELL, E. M., and POUND, R. V., 1948, *Phys. Rev.*, **73**, 679.
- [6] ANDREW, E. R., 1955, *Nuclear Magnetic Resonance* (Cambridge: University Press).
- [7] OGG, R. A., and RAY, J. D., 1955, *Disc. Faraday Soc.*, **19**, 239.
- [8] SHOOLERY, J. N., 1955, *Disc. Faraday Soc.*, **19**, 215.
- [9] ANDERSON, P. W., 1954, *J. phys. Soc. Japan*, **9**, 316.
- [10] KUBO, R., 1954, *J. phys. Soc. Japan*, **9**, 935.
- [11] SACK, R. A., 1958, *Mol. Phys.*, **1**, 163.

Molecular orbital theory of aromatic ring currents

by J. A. POPLE

Department of Theoretical Chemistry, University of Cambridge

(Received 20 December 1957)

The London theory of the diamagnetic susceptibility of conjugated hydrocarbons is extended in a manner which leads to detailed information about the distribution of interatomic currents induced by a general magnetic field. The method is illustrated by a calculation of the currents flowing round the two closed rings of azulene in a uniform field. This suggests that the larger current flows in the five-membered ring.

1. INTRODUCTION

The large anisotropy of the diamagnetic susceptibilities of aromatic molecules has been interpreted satisfactorily in terms of interatomic electronic currents which flow round closed conjugated paths if the applied magnetic field is perpendicular to the molecular plane. The first quantitative theory of the magnitude of these currents was developed by Pauling [1] using a semi-classical model of an electrical network. Shortly afterwards, London [2] developed a quantum-mechanical method for determining molecular orbitals for the π -electrons of a conjugated hydrocarbon in the presence of a uniform magnetic field. This is an extension of the simple LCAO (linear combination of atomic orbital) method originally introduced by Hückel [3]. When applied to a number of polycyclic aromatic hydrocarbons, London's theory led to reasonably good agreement with the experimental data on relative magnetic susceptibilities and anisotropies.

More recently, it has been suggested that ring currents play a significant part in determining the proton magnetic resonance spectrum of aromatic molecules (Pople [4]). Using the simplest possible model of equal currents in each ring, Bernstein *et al.* [5] were able to interpret the chemical shifts between non-equivalent protons in some polycyclic hydrocarbons. Some anomalous solvent effects have been interpreted in a similar way by Bothnerby and Glick [6].

For a fuller understanding of the magnetic properties of aromatic molecules, it would be useful to know more about the distribution of magnetic polarization within the molecule. The original molecular orbital theory of London [2] only gave the total magnetic dipole moment due to ring currents when the molecule is placed in a uniform magnetic field. The present paper is primarily concerned with the extension of these calculations to the case of a non-uniform field and then, by the device of using a secondary test field, finding the distribution of magnetic moment between the rings of a polycyclic system. This can be interpreted as a measure of the current in each ring. Such a method avoids explicit reference to a current density operator.

2. GENERAL THEORY FOR CONJUGATED HYDROCARBONS

In the independent electron model it is assumed that the molecular orbitals ψ_i are eigenfunctions of a one-electron Hamiltonian. In the presence of a magnetic field with vector potential \mathbf{A} , this takes the form

$$\mathcal{H} = \frac{1}{2m} \left(\mathbf{p} + \frac{e}{c} \mathbf{A} \right)^2 + V, \quad (2.1)$$

where \mathbf{p} is the quantum mechanical momentum and V is an electrostatic potential energy which is assumed to take account of the repulsion of other mobile electrons in some averaged manner. We shall not need to specify it in detail.

For a *uniform* magnetic field \mathbf{H}_0 , \mathbf{A} may most conveniently be taken in the form

$$\mathbf{A} = -\frac{1}{2} \mathbf{r} \times \mathbf{H}_0, \quad (2.2)$$

where \mathbf{r} is the position vector of the electron referred to an arbitrary origin. However, the general theory is best developed without giving an explicit form for \mathbf{A} and can also apply to a non-uniform field.

In the absence of a magnetic field, the next step is usually to express the molecular orbitals as linear combinations of the $2p\pi$ carbon atomic orbitals ϕ_s . This is the LCAO approximation. When there is a magnetic field present, however, this is not satisfactory, for it is found that the best linear combinations will depend on the gauge transformation of the vector potential \mathbf{A} . London [2] overcame these difficulties by expressing the molecular orbitals ψ_i as linear combinations of modified atomic orbitals

$$\chi_s = \phi_s \exp \left\{ -\frac{2\pi ie}{hc} \mathbf{A}_s \cdot \mathbf{r} \right\}, \quad (2.3)$$

where \mathbf{A}_s is the vector potential at the centre of atom s . Thus

$$\psi_j = \sum_s c_{js} \chi_s, \quad (2.4)$$

where the coefficients c_{js} are to be determined by a variational procedure. The exponential factor in (2.3) eliminates gauge difficulties because

$$\left(\mathbf{p} + \frac{e\mathbf{A}}{c} \right)^2 \chi_s = \exp \left\{ -\frac{2\pi ie}{hc} \mathbf{A}_s \cdot \mathbf{r} \right\} \left[\mathbf{p} + \frac{e}{c} (\mathbf{A} - \mathbf{A}_s) \right]^2 \phi_s, \quad (2.5)$$

and $(\mathbf{A} - \mathbf{A}_s)$ is a local vector potential independent of choice of origin.

As is well known, the variational problem for the coefficients c_{js} leads to the secular equation

$$|\mathcal{H}_{st} - ES_{st}| = 0, \quad (2.6)$$

where

$$\left. \begin{aligned} \mathcal{H}_{st} &= \int \chi_s^* \mathcal{H} \chi_t d\tau, \\ S_{st} &= \int \chi_s^* \chi_t d\tau. \end{aligned} \right\} \quad (2.7)$$

In the simplest version of the theory, which we shall follow here, the overlap integral S_{st} is neglected if $s \neq t$.

Using (2.3) and (2.5), \mathcal{H}_{st} takes the form

$$\begin{aligned} \mathcal{H}_{st} &= \int \exp \left\{ \frac{2\pi ie}{hc} (\mathbf{A}_s - \mathbf{A}_t) \cdot \mathbf{r} \right\} \\ &\quad \times \phi_s^* \left\{ \frac{1}{2m} \left[\mathbf{p} + \frac{e}{c} (\mathbf{A} - \mathbf{A}_t) \right]^2 + V \right\} \phi_t d\tau. \end{aligned} \quad (2.8)$$

If $s=t$, the exponential factor is unity and the rest of the expression measures the basic energy of the atomic orbital, as modified by the local diamagnetic circulation represented by the term $(\mathbf{A} - \mathbf{A}_t)$. Since we are only interested in the *interatomic* currents we shall omit these terms and choose the zero of energy so that all diagonal terms \mathcal{H}_{ss} are zero.

The off-diagonal elements \mathcal{H}_{st} between atomic orbitals which are directly bounded are modified by the exponential factor in the integral (2.8). In London's analysis, this is replaced by its value at the mid point of the bond where

$$\mathbf{r} = \frac{1}{2} \{ \mathbf{R}_s + \mathbf{R}_t \} \quad (2.9)$$

\mathbf{R}_s and \mathbf{R}_t being the position vectors of the nuclei of atoms s and t . If the term $(\mathbf{A} - \mathbf{A}_t)$ is also omitted, we are left with

$$\mathcal{H}_{st} = \beta_{st} \exp \left\{ \frac{\pi i e}{\hbar c} (\mathbf{A}_s - \mathbf{A}_t) \cdot (\mathbf{R}_s + \mathbf{R}_t) \right\}, \quad (2.10)$$

where

$$\beta_{st} = \int \phi_s^* \left[\frac{1}{2m} \mathbf{p}^2 + V \right] \phi_t d\tau \quad (2.11)$$

is the corresponding matrix element in the non-magnetic theory, usually known as the resonance integral. To a first approximation, we may take β_{st} to have a common value β for all C-C bonds. Energies may then be measured in units of β and the secular equation written

$$| \mathcal{H}_{st} - x \beta \delta_{st} | = 0 \quad (2.12)$$

x being the dimensionless eigenvalue.

On expansion equation (2.12) leads to a polynomial in x , the coefficients all being expressible in terms of closed cyclic products of the type

$$\mathcal{H}_{ij} \mathcal{H}_{jk} \mathcal{H}_{kl} \dots \mathcal{H}_{pq} \mathcal{H}_{qi} | \beta^n, \quad (2.13)$$

where n is the number of factors. The simplest such product is just $\mathcal{H}_{ij} \mathcal{H}_{ji} | \beta^2$ which is real and independent of the magnetic field. If there are no closed cycles of bonds (as in linear polyenes for example), all solutions of (2.12) will be independent of the magnetic field, corresponding physically to the absence of ring currents. If closed cycles do exist, there will be complex expressions (2.13), all of which will be expressible as products of a number of irreducible products, corresponding to the number of rings. Thus in azulene there will be two independent cyclic products for the 5- and 7-membered rings separately and the product for the cyclic path round the perimeter will be the product of these.

Generalizing London's notation we shall write, for each irreducible circuit,

$$\mathcal{H}_{ij} \mathcal{H}_{jk} \dots \mathcal{H}_{qi} = \beta^n \exp(2\pi i f), \quad (2.14)$$

where

$$f = \frac{e}{2\hbar c} \sum' (\mathbf{A}_s - \mathbf{A}_t) \cdot (\mathbf{R}_s + \mathbf{R}_t) \quad (2.15)$$

the sum \sum' being over ordered pairs around the ring. This sum may be approximated by a closed line integral if we write

$$\mathbf{A}_s - \mathbf{A}_t = [(\mathbf{R}_s - \mathbf{R}_t) \cdot \nabla] \mathbf{A}. \quad (2.16)$$

Using Greek suffixes in a tensor notation, we then have

$$f = \frac{e}{\hbar c} \oint R_\beta (\nabla_\alpha A_\beta) dR_\alpha. \quad (2.17)$$

Transforming to a surface integral by Stokes' theorem

$$\begin{aligned}
 f &= \frac{e}{hc} \iint \epsilon_{\gamma\eta\alpha} \nabla_{\eta} [R_{\beta} (\nabla_{\alpha} A_{\beta})] dS_{\gamma}, \\
 &= \frac{e}{hc} \iint \epsilon_{\gamma\beta\alpha} (\nabla_{\alpha} A_{\beta}) dS_{\gamma}, \\
 &= - \frac{e}{hc} \iint \mathbf{H} \cdot d\mathbf{S},
 \end{aligned} \tag{2.18}$$

where \mathbf{H} ($= \text{curl } \mathbf{A}$) is the magnetic field. The quantity f is therefore proportional to the flux of the magnetic field through the ring. The sign in (2.18) is such that, if the circuit is traversed in the anticlockwise direction in the plane of the paper, f is equal to (e/hc) times the flux of \mathbf{H} *downwards* into the paper. For a uniform field \mathbf{H}_0 , the numerical value of f will be (eH_0S/hc) where S is the area enclosed by the ring.

From the Hermitean nature of the secular determinant, it is clear that only the real part of these cyclic products will appear. Thus, if the f -values corresponding to the irreducible circuits are f_1, f_2, \dots, f_n the secular equation when expanded will involve quantities such as $\cos 2\pi f_1$, $\cos 2\pi(f_1 + f_2)$ etc. If the applied magnetic field is treated as a small perturbation, the secular equation can be written

$$P(x) = 4\pi^2 \sum_{ij} Q_{ij}(x) f_i f_j, \tag{2.19}$$

where $P(x)$ is the unperturbed determinant and $Q_{ij}(x)$ is a set of polynomials such that $Q_{ij} = Q_{ji}$. The solutions, to order f^2 , can be written

$$x^{(p)} = x_0^{(p)} + 4\pi^2 \sum_{ij} x_{ij}^{(p)} f_i f_j, \tag{2.20}$$

where $x_0^{(p)}$ is the unperturbed eigenvalue and†

$$x_{ij}^{(p)} = Q_{ij}(x_0^{(p)}) / P'(x_0^{(p)}). \tag{2.21}$$

The total change in energy for any applied field \mathbf{H} can now be found by evaluating the f_i , finding the change of each energy level by (2.20) and then summing over occupied orbitals, including a factor of two for those containing two electrons.

We now turn to the problem of finding how the induced magnetic moment is distributed between the rings. This can be accomplished if we add to the primary field \mathbf{H} a secondary testing field \mathbf{H}' . This testing field may be thought of as that of a small magnetic dipole or some other non-uniform field. It is not necessary to specify it precisely. Since the total field is now $\mathbf{H} + \mathbf{H}'$, the quantities f_i have to be replaced by the sums $f_i + f'_i$, where f'_i is equal to $(-e/hc)$ times the flux of the testing field through the i th circuit. Equation (2.20) then takes the form

$$x^{(p)} = x_0^{(p)} + 4\pi^2 \sum_{ij} x_{ij}^{(p)} [f_i f_j + 2f'_i f_j + f'_i f'_j]. \tag{2.22}$$

The terms of the type $f'_i f_j$ give the energy (in units of β) due to the interaction of the testing field with the magnetic polarization due to the primary field. Since f'_i is proportional to the flux of the testing field through circuit i , we may say that the system, in the presence of the primary field only, behaves as if the i th circuit were

† We shall not consider cases where the unperturbed system has degenerate eigenvalues.

replaced by a magnetic shell with strength equal to $-\beta e/hc$ times the coefficient, of f_i' in (2.22). This may then be interpreted as the current in circuit i divided by c . In fact, this current is (anticlockwise)

$$\begin{aligned} J_i^{(p)} &= \frac{8\pi^2\beta e}{h} \sum_j x_{ij}^{(p)} f_j \\ &= -\frac{8\pi^2\beta e^2}{h^2 c} \sum_j x_{ij}^{(p)} \iint_{S_i} \cdot d\mathbf{S}. \end{aligned} \quad (2.23)$$

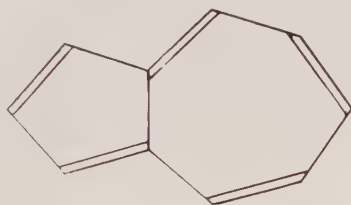
This applies to each orbital separately. For the total effective current in one circuit, this has to be summed over electrons. We therefore need to evaluate

$$\sum_p \lambda_p \sum_j x_{ij}^{(p)}, \quad (2.24)$$

where \sum_p is over occupied molecular orbitals ψ_p , and λ_p is the number of electrons in ψ_p (1 or 2).

3. RING CURRENTS IN AZULENE

We shall illustrate the theory of the last section by calculating the distribution of current induced in the azulene molecule



by a uniform magnetic field \mathbf{H}_0 perpendicular to the molecular plane. The non-dimensional secular equation takes the form

$$\begin{aligned} x^{10} - 11x^8 + 41x^6 - 61x^4 + 31x^2 - 2 \\ + 2 \cos(2\pi f_5) \{-x^5 + 4x^3 - 3x\} + 2 \cos(2\pi f_7) \{-x^3 + 2x\} - 2 \cos 2\pi(f_5 + f_7) = 0. \end{aligned} \quad (3.1)$$

Here f_5 and f_7 are the f -values for the 5- and 7-membered ring respectively. If these are small, (3.1) may be replaced by

$$\begin{aligned} x^{10} - 11x^8 + 41x^6 - 2x^5 - 61x^4 + 6x^3 + 31x^2 - 2x - 4 \\ = (2\pi f_5)^2 \{-x^5 + 4x^3 - 3x - 1\} + (2\pi f_7)^2 \{-x^3 + 2x - 1\} - 2(2\pi f_5)(2\pi f_7). \end{aligned} \quad (3.2)$$

This is now in the form of equation (2.19) and the quantities $x_{ij}^{(p)}$ can be deduced immediately.

p	$x_0^{(p)}$	$x_{55}^{(p)}$	$x_{57}^{(p)} = x_{75}^{(p)}$	$x_{77}^{(p)}$
1	2.31028	-0.02516	-0.00103	-0.00897
2	1.65157	+0.00610	+0.02735	+0.06021
3	1.35567	+0.02292	-0.07162	-0.05587
4	0.88698	+0.16012	+0.11286	-0.00859
5	0.47726	-0.19716	-0.09752	-0.01504

Reduced perturbation energies x_{ij} for occupied levels of azulene.

Expressions for the currents induced by a uniform field \mathbf{H}_0 follow :

$$\left. \begin{aligned} J_5 &= \frac{8\pi^2\beta e^2\mathbf{H}_0}{h^2c} \{0.06637S_5 + 0.05992S_7\}, \\ J_7 &= \frac{8\pi^2\beta e^2\mathbf{H}_0}{h^2c} \{0.05992S_5 + 0.05653S_7\}, \end{aligned} \right\} \quad (3.3)$$

where S_5 and S_7 are the areas of the five- and seven-membered rings respectively. The simplest assumption about the dimensions of the molecule is to suppose that the two ring are regular polygons with sides equal to a standard C-C bond length, taken as the corresponding distance in benzene. London's calculation on benzene gives

$$J_{\text{benzene}} = \frac{8\pi^2\beta e^2\mathbf{H}_0}{9h^2c} S_6, \quad (3.4)$$

so we may conveniently express the results (3.3) as a ratio to the corresponding benzene current in the same magnetic field. Since

$$S_5 : S_6 : S_7 = 5 \cot(\pi/5) : 6 \cot(\pi/6) : 7 \cot(\pi/7) \quad (3.5)$$

we obtain

$$\left. \begin{aligned} J_5/J_{\text{benzene}} &= 1.150, \\ J_7/J_{\text{benzene}} &= 1.069. \end{aligned} \right\} \quad (3.6)$$

These calculations indicate, therefore, that there is a slightly larger current in the five-membered ring, but the approximate equality suggests that most of the current flows directly around the perimeter. Because of its larger area, of course, the seven-membered ring will make the largest contribution to the total susceptibility.

On développe la théorie de London, relative à la susceptibilité magnétique des hydrocarbures conjugués, de manière à obtenir une information détaillée sur la distribution des courants interatomiques, induits par le champ magnétique général. On explique la méthode par le calcul des courants qui circulent dans les deux anneaux fermés de l'azulène dans un champ uniforme. Ceci mène à l'idée que le courant le plus fort passe dans le noyau de cinq éléments.

Die London'sche Theorie der diamagnetischen Suszeptibilität konjugierter Kohlenwasserstoffe wird erweitert, sodass man ausführliche Aussagen über die Verteilung der durch ein allgemeines magnetisches Feld induzierten interatomaren Ströme erhält.

Zur Erläuterung der Methode werden die Ströme berechnet, die in einem gleichförmigen Felde um die beiden geschlossenen Ringe des Azulens fließen. Die Ergebnisse legen den Schluss nahe, dass der grössere Strom im Fünfring fließt.

REFERENCES

- [1] PAULING, L., 1936, *J. chem. Phys.*, **4**, 673.
- [2] LONDON, F., 1937, *J. Phys. Radium*, **8**, 397.
- [3] HÜCKEL, W., 1931, *Z. Physik.*, **70**, 204, 279.
- [4] POPLÉ, J. A., 1956, *J. chem. Phys.*, **24**, 1111.
- [5] BERNSTEIN, H. J., SCHNEIDER, W. G., and POPLÉ, J. A., 1956, *Proc. roy. Soc. A*, **236**, 515.
- [6] BOTHNERBY, A. A., and GLICK, R. E., 1957, *J. chem. Phys.*, **26**, 1651.

A molecular orbital treatment of the vinyl chloride molecule

by M. SIMONETTA, G. FAVINI and S. CARRÀ

Physical Chemistry Department, University of Milan, Italy

(Received 30 December 1957)

A molecular orbital treatment of the vinyl chloride molecule by the SCF LCAO MO method was carried out. All the necessary integrals were calculated either theoretically or by an extension of the uniformly charged sphere approximation. At the end a Pariser and Parr treatment for the same molecule was performed and a tentative value for the β_{C-Cl} parameter is suggested.

1. INTRODUCTION

Vinyl chloride is a simple molecule particularly suitable for studying the application of the molecular orbital method with its most recent refinements to conjugated molecules including an heteroatom.

Goldstein [1] has recently carried out a semi-empirical treatment of vinyl chloride by the standard LCAO method as modified by Löwdin [2] to include overlap. In the present paper LCAO self-consistent field calculations of the π -electron energy levels, and ground state orbitals are performed, and from the results the ionization potential, bond lengths and frequency of the first $\pi-\pi$ transition are obtained and compared with experimental results. In the last paragraph a Pariser and Parr treatment of the same molecule is presented and we hope that the resulting empirical parameters will enable us to apply this simple method to the study of the electronic spectra of conjugated molecules containing a chlorine atom.

2. S.C.F. CALCULATIONS

The SCF method for a closed-shell ground state has been thoroughly described by Roothaan [3] and an application of its LCAO approximation to a conjugated system is found in the treatment of 1, 3-butadiene given by Parr and Mulliken [4].

The same general scheme in the calculations was followed here. The geometry of the molecule was assumed from electron diffraction data [5]: $C_a - C_b = 1.38 \text{ \AA}$; $C_b - Cl_c = 1.69 \text{ \AA}$; $\angle C_a \hat{C}_b Cl_c = 122^\circ$. The molecular orbitals are to be obtained by linear combination of three atomic orbitals, which we assumed to be Slater orbitals $2p_\pi$ for the carbon atoms and $3p_\pi$ for the chlorine atom, with $Z_0 = 3.18$

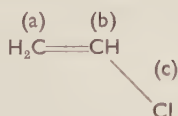


Figure 1.

and $Z_{c1} = 6.099$. In the molecule in the ground state four π -electrons will occupy the two lowest orbitals.

Numerical values of the necessary integrals over these atomic orbitals are given in Table 1. The symbolism for the integrals adopted here is the same as in the paper by Parr and Mulliken [4].

Integrals	Values	Integrals	Values
Overlap integrals:		Coulomb integrals:	
S_{ab}	0.266	$aa/aa = bb/bb$	16.930 (*)
S_{bc}	0.166	cc/cc	15.480 (*)
S_{ac}	0.022	aa/bb	8.903
Penetration integrals:		aa/cc	5.006
$a:bb = b:aa$	0.636	bb/cc	7.430
$a:cc$	0.028	Exchange integrals:	
$b:cc$	0.230	ab/ab	0.914
$c:aa$	0.338	ab/ac	0.056
$c:bb$	1.440	ab/bc	0.422
$a:bc$	0.055	bc/bc	0.326
$b:ac$	0.010	bc/ac	0.035
$c:ab$	0.236	ac/ac	0.005
$a:ab = b:ab$	3.231	Hybrid integrals:	
$a:ac$	0.261	$aa/ab = bb/ab$	3.436
$b:bc$	1.982	aa/bc	1.154
$c:ac$	0.317	aa/ac	0.241
$c:bc$	2.486	bb/bc	2.022
$a:aa = b:bb$	23.654 (*)	bb/ac	0.180
$c:cc$	28.506 (*)	cc/ab	1.654
Core integrals (b):		cc/bc	1.902
I_{aa}	-31.429	cc/ac	0.225
I_{bb}	-37.379		
I_{cc}	-39.074		
I_{ab}	-13.281		
I_{ac}	-1.241		
I_{bc}	-9.504		

Table 1. Integrals over atomic orbitals (a).

(a) Overlap integrals are dimensionless; all other integrals are in ev. Integrals marked with an asterisk (*) were evaluated theoretically.

(b) Owing to our approximations I_{pq} and I_{qp} are slightly different if $p \neq q$ and p and q indicate different atoms. The indicated I_{ac} and I_{bc} are the average values.

Not all of the integrals in Table 1 were available from the literature. Most of them were evaluated by us either theoretically or by an empirical method. Overlap integrals were taken from published tables [6]. Two-centre penetration integrals were calculated by an extension of the uniformly charged sphere method used by Pariser and Parr for the evaluation of electronic repulsion integrals [7]; their value is obtained as the sum of the contributions of the interaction of the electron in the π orbital with the nucleus and all the electrons present in the atom. As an example we give the details of the calculus of $a:bb$; the radius of

the spheres is 0.69 Å; the term for the interaction of the $2p_\pi$ electron of atom b with the nucleus and the two 1s electrons of atom a is given by:

$$2\left[\frac{e}{2} 4e \frac{1}{0.69\sqrt{5}}\right] = 37.317 \text{ ev};$$

the term for the interaction with the 2s electrons of atom a is:

$$-2\left[\frac{e}{2} e \frac{1}{0.69\sqrt{5}}\right] = -9.329 \text{ ev};$$

the terms for $2p_x$, $2p_y$ and $2p_z$ electrons of atom a are respectively:

$$-2\left[\left(\frac{e}{2}\right)^2 \left\{\frac{1}{1.146} + \frac{1}{1.970}\right\}\right] = -9.931 \text{ ev},$$

$$-4\left[\left(\frac{e}{2}\right)^2 \frac{1}{0.69\sqrt{6}}\right] = -8.518 \text{ ev},$$

$$-2\left[\left(\frac{e}{2}\right)^2 \left\{\frac{1}{1.38} + \frac{1}{0.69\sqrt{8}}\right\}\right] = -8.903 \text{ ev}.$$

The sum is: $a:bb = 37.317 - (9.329 + 9.931 + 9.518 + 8.903) = 0.636 \text{ ev}$ for the atom, or 9.538 for the positively charged ion. A complete discussion of the approximation involved in this simple method of evaluating the integrals will be given elsewhere; here we will compare in Table 2 a few of our results with the theoretical values obtained for the same integrals.

Integral	Our method	Theoretical (a)
a: bb	0.636	0.770 (b)
a: ab	3.231	2.105 (b)
aa/bb	8.903	9.096
ab/ab	0.914	0.998
aa/ab	3.436	3.426

Table 2. (Values in ev).

(a) See reference [9].

(b) These values were obtained using hydrogen-like orbitals.

Three-centre penetration integrals and penetration integrals involving two different orbitals were evaluated by the formula:

$$a:bc = \frac{1}{2}S_{bc}[a:bb + a:cc]. \quad (1)$$

Analogously hybrid and exchange integrals were calculated by the formula:

$$cc/ab = \frac{1}{2}S_{ab}[cc/aa + cc/bb]. \quad (2)$$

In Table 3 values of integrals for butadiene reported by Parr and Mulliken are compared with values for the same integrals, as calculated by us using equations (1) and (2). The agreement is excellent for exchange and hybrid integrals, but is less good for penetration integrals. However it is easily verified that these differences leave the matrix elements of secular determinants almost unchanged. Coulomb integrals were calculated by the uniformly charged sphere method. Core integrals were evaluated from the values of the other integrals and

the first ionization potential for a $2p_{\pi}$ electron in carbon ($W_{2p_C} = -11.54 \text{ eV}$) and the second ionization potential for a $3p_{\pi}$ electron in chlorine ($W_{3p_{Cl}} = -26.38 \text{ eV}$) [8].

A few integrals were obtained theoretically: aa/aa is taken from the literature [9]; the others [cc/cc , $c:c$, $a:a$] were evaluated by us according to the method of Goeppert-Mayer and Sklar [10]. Detailed calculations are reported in the Appendix. From the integral cc/cc the radius for the $3p_{\pi}$ orbital in the chlorine atom was obtained with the formula:

$$cc/cc = 15.480 = \frac{17}{10} \frac{14.395}{2R_{Cl}} \quad \text{and} \quad R_{Cl} = 0.7905 \text{ \AA}$$

and from aa/aa , $R_C = 0.723 \text{ \AA}$.

Integral	Parr and Mulliken	Present paper
exchange integrals:		
ab/ab	0.0252Z (a)	0.0235Z
bc/bc	0.0169Z (a)	0.0161Z
ac/ac	0.0004Z (a)	0.0003Z
ab/ac	0.0029Z (b)	0.0022Z
ab/bc	0.0147Z (b)	0.0151Z
bc/ac	0.0025Z (b)	0.0019Z
hybrid integrals:		
aa/ab	0.0834Z (b)	0.0842Z
bb/bc	0.0678Z (b)	0.0690Z
aa/bc	0.0384Z (b)	0.0397Z
aa/ac	0.0069Z (b)	0.0087Z
bb/ac	0.0107Z (b)	0.0070Z
penetration integrals:		
a: ab	0.0527Z (c)	0.0848Z
b: bc	0.0377Z (c)	0.0700Z
b: ac	0.0070Z (c)	0.0006Z
a: ac	0.0012Z (c)	0.0099Z
a: bc	0.0008Z (c)	0.0027Z

Table 3 (in atomic units).

(a) Theoretical values.

(b) Calculated by the formula: $pr/qs = S_{pr}S_{qs} [p'p'/q'q']$ where p' is a Slater $2p_{\pi}$ -carbon AO taken as located midway between atoms p and r ; q' is a Slater $2p_{\pi}$ -AO located midway between atoms q and s , and S_{pr} and S_{qs} are overlap integrals between the indicated AO.

(c) Calculated by the formula:

$$r: pq = S_{pq} [r: p'p']$$

where p' is a Slater $2p_{\pi}$ -AO located midway between atoms p and q .

As starting orbitals we used the orthonormal set of orbitals of Goldstein [1], recalculated by us to take account of a small difference in the values for the overlap integrals. The iterative method led us, after six trials, to the following molecular orbitals:

$$\psi_1 = 0.32204\phi_a + 0.51465\phi_b + 0.65035\phi_c$$

$$\psi_2 = 0.57212\phi_a + 0.37722\phi_b - 0.72416\phi_c$$

$$\psi_3 = 0.80351\phi_a - 0.83639\phi_b + 0.28557\phi_c$$

(where ϕ_i is the appropriate atomic orbital for atom i) and to the corresponding energy levels: $\epsilon_1 = -14.1337$ eV, $\epsilon_2 = -9.2891$ eV, $\epsilon_3 = 6.3651$ eV. The energy of the molecule in its different states is:

$$\begin{aligned} E_N &= 2\epsilon_1 + 2\epsilon_2 - J_{11} - J_{22} - 4J_{12} + 2K_{12} \\ E_{V_{13}} - E_N &= \epsilon_3 - \epsilon_2 - J_{23} + 2K_{23} \\ E_{T_{23}} - E_N &= \epsilon_3 - \epsilon_2 - J_{23} \end{aligned}$$

where $J_{ij} = \sum_{pqrs} c_{ip}c_{ir}(pr/qs)c_{jq}c_{js}$; $K_{ij} = \sum_{pqrs} c_{ip}c_{jr}(pr/qs)c_{jq}c_{is}$ and c_{ip} is the coefficient of the p th atomic orbital in the i th molecular orbital.

With our numerical values we have:

$$E_{T_{23}} - E_N = 5.8586 \text{ eV}, \quad E_{V_{13}} - E_N = 11.1842 \text{ eV}, \quad \bar{E}_{TV_{23}} - E_N = 8.5214 \text{ eV}.$$

The densities of π electrons, calculated from our orbitals by the method of Goldstein [1], are:

$$\begin{aligned} q_a &= 0.85821, & n_{ab} &= 0.40738, \\ q_b &= 0.81726, & n_{bc} &= 0.04005, \\ q_c &= 1.89658, & n_{ac} &= -0.01799. \end{aligned}$$

This gives a value of δ (the positive charge on the chlorine atom) equal to 0.10342, in good agreement with the value 0.06 obtained from the interpretation of microwave spectra [11]. Also the value obtained by us for the ionization potential of the vinyl chloride (-9.2841 eV) is in fairly close agreement with the experimental value given by Walsh [12] (-9.95 eV).

The agreement is not so satisfactory for the first π - π transition, as the experimental results of Walsh indicate that the transition occurs at about 6.7 eV. However it is known that the SCF method gives good results for the molecule in the ground state, but is not the best way of approach to the study of electronic spectra, where excited states are involved [4, 7].

From the calculated bond orders the length of the C-C bond can be predicted by a formula given by Coulson [13], and the same for the C-Cl bond according to Gordy's formula [14]†. The results are:

$$\begin{aligned} R_{C-C} &= 1.540 \frac{1.540 - 1.340}{1 + 0.8095(0.59262/0.40738)} = 1.448 \text{ \AA (exp. } 1.38 \text{ \AA)}, \\ R_{C-Cl} &= 1.73 \text{ \AA (exp. } 1.69 \text{ \AA)}. \end{aligned}$$

3. THE PARISER AND PARR METHOD

In the application of Pariser and Parr's method to our problem only three singlet configurations were included; namely V_0 , V_{13} and V_{23} . This implies that the results are sensitive to the choice of the starting orbitals. We tried two sets of initial orbitals: the orbitals obtained for the allyl ion by the standard LCAO treatment and those obtained for the vinyl chloride molecule by the same method using for the parameters values reported by Goldstein [1]. The necessary integrals were calculated in two different ways: adopting values obtained from Pariser and Parr's formulas or from our uniformly charged spheres approximation. Further, penetration integrals may be or may not be included (these integrals, when used, were always calculated by our method).

† The constants a and b in the formula are determined assuming $r = 1.761$ Å for the single bond C-Cl and $r = 1.555$ Å for the double bond $C=Cl^+$ [15].

The empirical parameter β_{C-C} was calculated from $\beta(r)$ formula given by Pariser and Parr: $\beta_{C-C} = -2.52$ eV; while the parameter β_{C-Cl} was taken as a variable, in order to reproduce the experimental ΔE . However the range in which β_{C-Cl} can be reasonably expected to fall should not be far from

$$\beta_{C-Cl} = \beta_{C-C} \frac{S_{C-Cl}}{S_{C-C}} = -1.57 \text{ eV.}$$

The results are summarized in figure 2. It can be seen that no reasonable value of β_{C-Cl} can reproduce the experimental ΔE (energy difference for the first $\pi-\pi$ transition) if we assume allyl ion orbitals as starting orbitals.

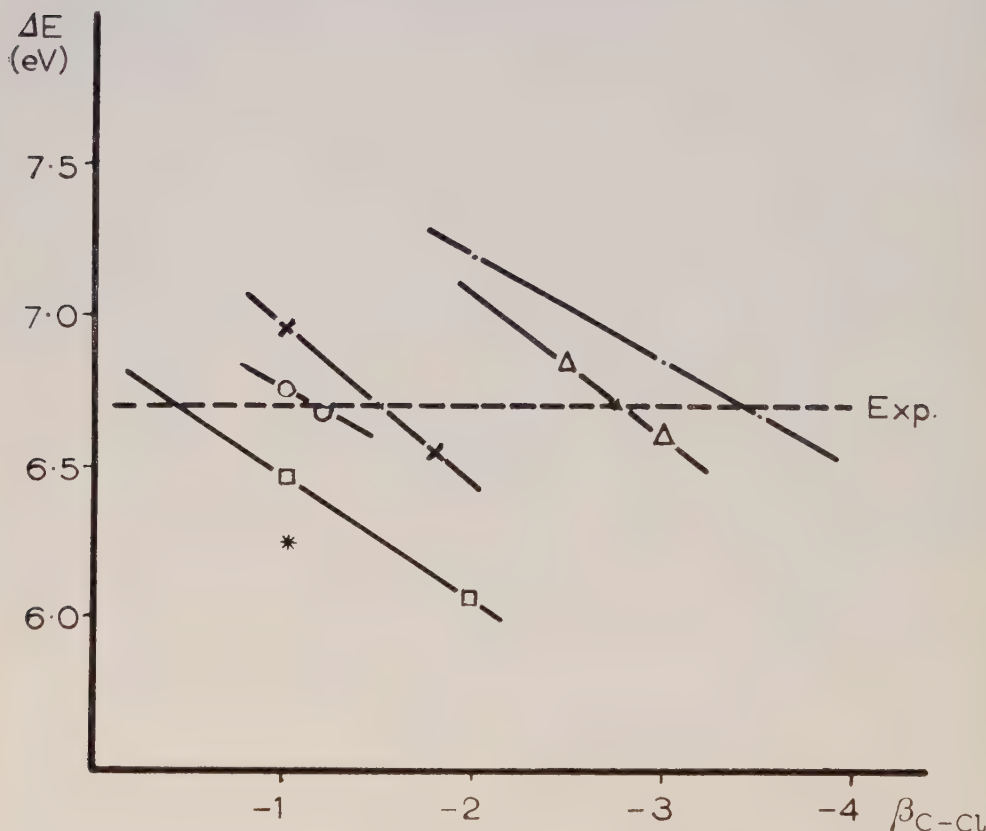


Figure 2.

- Allyl ion orbitals; P. and P. integrals, excluding penetration.
- △ Allyl ion orbitals; our integrals, including penetration.
- × Vinyl chloride orbitals; P. and P. integrals, including penetration.
- Vinyl chloride orbitals; P. and P. integrals, excluding penetration.
- Vinyl chloride orbitals; our integrals, including penetration.
- * Vinyl chloride orbitals; our integrals, excluding penetration.

A different situation is obtained with vinyl chloride orbitals: here we see that the use of Pariser and Parr values for the integrals, with or without inclusion of penetration integrals, leads to reasonable values for β_{C-Cl} . The most natural choice is perhaps $\beta_{C-Cl} = -1.5$ eV and the inclusion of the penetration integrals.

APPENDIX

The integral cc/cc for the chlorine atom is given by:

$$\text{cc/cc} = \left(\frac{2\alpha^7}{15\pi} \right)^2 \iint r_1^4 \exp(-2\alpha r_1) \sin^2 \vartheta_1 \cos^2 \phi_1 \\ \times \frac{2}{r_{12}} r_2^4 \exp(-2\alpha r_2) \sin^2 \vartheta_2 \cos^2 \phi_2 d\tau_1 d\tau_2,$$

where $\alpha = \frac{1}{3}Z$, $d\tau_i = r_i^2 \sin \vartheta_i dr_i d\vartheta_i d\phi_i$ and

$$\frac{1}{r_{12}} = \sum_{n=0} \sum_{m=n}^n (n-|m|)! [(n+|m|)!]^{-1} r_{<}^n r_{>}^{-n-1} P_n^{lm} \cos \vartheta_1 P_n^{lm} \cos \vartheta_2 \\ \times \exp[im(\phi_1 - \phi_2)]$$

where $r_{<}$ and $r_{>}$ are the lesser and the greater of r_1 and r_2 and the quantities P_n^{lm} are the associated Legendre functions. Therefore

$$\text{cc/cc} = 2 \left(\frac{2\alpha^7}{15\pi} \right)^2 \sum_{n=0} \sum_{m=n}^n (n-|m|)! [(n+|m|)!]^{-1} \int \cos^2 \phi_1 \cos^2 \phi_2 \\ \times \exp[im(\phi_1 - \phi_2)] d\phi_1 d\phi_2 \int \sin^3 \vartheta_1 \sin^3 \vartheta_2 P_n^{lm} \cos \vartheta_1 P_n^{lm} \cos \vartheta_2 d\vartheta_1 d\vartheta_2 \\ \times \int \exp(-2\alpha r_1) \exp(-2\alpha r_2) r_1^6 r_2^6 r_{<}^n r_{>}^{-n-1} dr_1 dr_2.$$

After evaluating the integrals the final result is:

$$\text{cc/cc} = 0.1966Z \text{ (in atomic units).}$$

As $Z = 6.099$ it follows $\text{cc/cc} = 15.4800 \text{ ev}$. The autopenetration integral $(c:cc)^{**}$ (two stars indicate double ionization) for the chlorine ion is given by:

$$(c:cc)^{**} = - \int H_c^{**}(1) c(1) c(1) d\tau_1.$$

As the K and L shell electrons are treated as if on the nucleus, the potential H_c^{**} on electron 1 due to the chlorine ion Cl^{2+} is:

$$H_c^{**} = - \frac{7e^2 2\alpha}{x_1} + e^2 \int \frac{\sigma(1)}{r_1} d\tau_1$$

where $x_1 = 2\alpha r_1$ and

$$\sigma = [2|\psi_{3s}|^2 + |\psi_{3p_x}|^2 + 2|\psi_{3p_y}|^2] = \frac{\alpha^3}{120\pi} x_1^4 e^{-x_1} \left[\frac{2}{3} + \cos^2 \vartheta + 2 \sin^2 \vartheta \sin^2 \phi \right]$$

and $c(1)c(1)$ is given by:

$$\frac{2\alpha^7}{15\pi} \left(\frac{x_1}{2\alpha} \right)^4 e^{-x_1} \sin \vartheta_1 \cos^2 \phi_1.$$

Numerical calculations give: $(c:cc)^{**} = 59.466 \text{ ev}$; therefore the autopenetration integral for the chlorine atom is:

$$c:cc = 59.466 - 2(15.480) = 28.506 \text{ ev}.$$

The autopenetration integral for the carbon ion was evaluated in the same way; the result is: $(a:aa)^* = 40.584 \text{ ev}$, from which

$$a:aa = 40.584 - 16.930 = 23.634 \text{ ev}.$$

Parr and Crawford [9] obtained for the same integral 25.343 ev, but using hydrogen-like wave functions instead of Slater's orbitals.

Les auteurs ont étudié la molécule du chlorure de vinyle par la méthode des orbitales moléculaires SCF LCAO MO. Toutes les intégrales nécessaires ont été calculées soit théoriquement soit par une extension de l'approximation de la sphère chargée uniformément. Finalement on a fait pour la même molécule un calcul selon Pariser et Parr. On propose une valeur tentative pour le paramètre β_{C-Cl} .

Die Vinylchlorid-Molekül wurde mit Hilfe der SCF-LCAO-MO-Methode berechnet. Alle erforderlichen Integrale wurden entweder theoretisch ausgerechnet oder durch Ausdehnung eines Näherungsverfahrens ermittelt, das von einer gleichmässig geladenen Kugel ausgeht. Schliesslich wurde für die gleiche Molekül eine Behandlung nach Pariser und Parr durchgeführt; ein Schätzwert für den β_{C-Cl} -Parameter wird vorgeschlagen.

REFERENCES

- [1] GOLDSTEIN, J. H., 1956, *J. chem. Phys.*, **24**, 507.
- [2] LÖWDIN, P. O., 1950, *J. chem. Phys.*, **18**, 365.
- [3] Roothaan, C. C. J., 1951, *Rev. mod. Phys.*, **23**, 69.
- [4] PARR, R. G., and MULLIKEN, R. S., 1950, *J. chem. Phys.*, **18**, 1338.
- [5] ALLEN, P. W., and SUTTON, L. E., 1950, *Acta cryst.*, **3**, 46.
- [6] MULLIKEN, R. S., RIEKE, C. A., ORLOFF, D., and ORLOFF, H., 1949, *J. chem. Phys.*, **17**, 1248.
- [7] PARISER, R., PARR, R. G., 1953, *J. chem. Phys.*, **21**, 466.
- [8] SKINNER, H. A., and PRITCHARD, H. O., 1953, *Trans. Faraday Soc.*, **49**, 1254.
MOORE, C. E., 1949, *Atomic Energy Levels*, Circ. 467 Nat. Bur. Stand. Washington.
- [9] PARR, R. G., and CRAWFORD, B. L., Jr., 1948, *J. Chem. Phys.*, **16**, 1049.
- [10] GOEPPERT-MAYER, M., and SKLAR, A. L., 1938, *J. chem. Phys.*, **6**, 645.
- [11] GOLDSTEIN, J. H., and BRAGG, J. K., 1950, *Phys. Rev.*, **78**, 347.
- [12] WALSH, A. D., 1945, *Trans. Faraday Soc.*, **41**, 35.
- [13] COULSON, C. A., 1939, *Proc. roy. Soc., A*, **169**, 413.
- [14] GORDY, W., 1947, *J. chem. Phys.*, **15**, 305.
- [15] PAULING, L., 1945, *The Nature of the Chemical Bond* (New York: Cornell University Press.)

Open shell calculations for the two- and three-electron ions†

by R. P. HURST, J. D. GRAY, G. H. BRIGMAN†
and F. A. MATSEN

Departments of Chemistry and Physics, University of Texas, Austin

[Received 30 December 1957]

Open shell calculations are made for all the three-electron atomic systems of the second period of the periodic table. These results are compared with corresponding two-electron and experimental energies.

It is noted that the improvement of open shell over closed shell calculations becomes less with increasing atomic number. In parallel trend the disparity of both from the experimental results increases with Z . An electron affinity of zero is found for the helium atom.

1. METHOD AND CALCULATIONS

In this paper are considered the results of open shell calculations with Slater-type orbitals for all possible three-electron atomic systems of the second period of the periodic table.

The open shell wave function permits some radial electron correlation, and hence, for a small number of electrons, at least, yields energies which are superior to those calculated more laboriously by the Hartree-Fock procedures [1, 2]. Atomic structure factors calculated from open shell wave functions show interesting differences from those calculated from closed shell wave functions [3]. The use of the open shell wave function for molecules should improve the calculation of molecular properties.

The calculations were made from the doublet state wave function developed by Brigman and Matsen [2] § for the lithium atom, namely

$$\Psi = \begin{pmatrix} abc \\ \alpha\beta\alpha \end{pmatrix}^{\uparrow} + \begin{pmatrix} bac \\ \alpha\beta\alpha \end{pmatrix} \quad (1)$$

† Supported by the Robert A. Welch Foundation of Houston and the Office of Ordnance Research, U.S. Army.

‡ Present address: Convair, Fort Worth, Texas.

§ These authors originally considered the two structures

$$\Psi = C_1\Phi_1 + C_2\Phi_2$$

where

$$\Phi_1 = \begin{pmatrix} abc \\ \alpha\beta\alpha \end{pmatrix} + \begin{pmatrix} bac \\ \alpha\beta\alpha \end{pmatrix}$$

and

$$\Phi_2 = \begin{pmatrix} acb \\ \alpha\beta\alpha \end{pmatrix} + \begin{pmatrix} cab \\ \alpha\beta\alpha \end{pmatrix}$$

but closer examination of the problem has shown that the second structure listed does not make a significant contribution to the energy.

$$\uparrow \begin{pmatrix} abc \\ \alpha\beta\alpha \end{pmatrix} \equiv \frac{1}{\sqrt{3!}} \begin{vmatrix} (a\alpha)_1 & (b\beta)_2 & (c\alpha)_1 \\ (a\alpha)_2 & (b\beta)_2 & (c\alpha)_2 \\ (a\alpha)_3 & (b\beta)_3 & (c\alpha)_3 \end{vmatrix}$$

where

$$\begin{aligned} a &\equiv \Psi_{1s}^*(\mathbf{a}) = (\mathbf{a}^3/\pi)^{1/2} \exp(-\mathbf{a}r) \\ b &\equiv \Psi_{1s}^*(\mathbf{b}) = (\mathbf{b}^3/\pi)^{1/2} \exp(-\mathbf{b}r) \\ c &\equiv \Psi_{2s}^*(\mathbf{c}) = (\mathbf{c}^5/3\pi)^{1/2} r \exp(-\mathbf{c}r). \end{aligned} \quad (2)$$

The optimum parameters were obtained through an iterative procedure developed as follows. Since the energy E depends upon a number of parameters X^1, X^2, \dots, X^n , we have

$$E = E(X^1, X^2, \dots, X^n) \quad (3)$$

subject to the requirement

$$\partial E / \partial X^i = 0 \quad (i = 1, 2, 3, \dots, n). \quad (4)$$

For a sufficiently small increment Δ this function may be approximated by the parabola

$$\begin{aligned} E(X^i) &= E(X_0^i) + \frac{E(X_1^i) - E(X_0^i)}{\Delta} (X^i - X_0^i) \\ &\quad + \frac{E(X_0^i) - 2E(X_1^i) + E(X_2^i)}{2\Delta^2} (X^i - X_0^i)(X^i - X_1^i) \end{aligned} \quad (5)$$

where

$$X_n^i - X_{n-1}^i = \Delta \quad (i = 1, 2, 3, \dots, n). \quad (6)$$

Finally since we require

$$\frac{\partial E(X^i)}{\partial X^i} = 0 \quad (4)$$

we obtain

$$X_*^i = \frac{X_0^i + X_1^i}{2} - \frac{\Delta[E(X_1^i) - E(X_0^i)]}{E(X_0^i) - 2E(X_1^i) + E(X_2^i)} \quad (i = 1, 2, 3, \dots, n). \quad (7)$$

In using this method a set of parameters $X_1^1, X_1^2, X_1^3, \dots, X_1^n$ is chosen and a calculation of the energy is made. Next, energy calculations are made using the parameters $X_0^1, X_1^2, \dots, X_1^n$ and $X_2^1, X_1^2, \dots, X_1^n$ where $X_0^1 - X_1^1 = -\Delta$ and $X_2^1 - X_1^1 = \Delta$. Then these results are substituted into equation (7) and an improved parameter X_*^1 is obtained. Using this improved result for X_1^1 the next parameter X_1^2 is improved and so forth until all the parameters have been improved. Finally, one begins again with the first parameter and continues this process, gradually reducing Δ until no changes in the parameters are obtained.

As the starting choice to begin the iteration, the 1s orbital exponents were taken from Shull and Löwdin's [1] open shell results for the helium-like ions and the 2s orbital exponents were chosen by the Slater rules. These results were extended, by the method they describe, to the rest of the elements of the second period of the table. The wave function in this case was

$$\Psi = [a(1)b(2) + a(2)b(1)] \quad (8)$$

where

$$a = (\mathbf{a}^3/\pi)^{1/2} \exp(-\mathbf{a}r), \quad b = (\mathbf{b}^3/\pi)^{1/2} \exp(-\mathbf{b}r). \quad (9)$$

2. RESULTS

In table 1 are given the results for the two-electron ions. The results up through C^{IV} , though previously obtained by Shull and Löwdin, are included for the sake of completeness. In table 2 are presented the results for the three-electron calculations. It has been found convenient to express the

	Open shell			Closed shell ($\alpha=1, \beta=0$)	
	α	β	Energy (a.u.)†	Energy (a.u.)†	Exp.energy[6] (a.u.)†
H^-	0.96169	0.57186	-0.51330	-0.4727	-0.52756
He	0.99903	0.29496	-2.8757	-2.8477	-2.9037
Li^+	0.99979	0.22625	-7.2487	-7.2227	-7.2801
Be^{2+}	0.99992	0.19093	-13.6230	-13.5977	-13.6568
B^{3+}	0.99996	0.16781	-21.9975	-21.9727	-22.0350
C^{4+}	0.99998	0.15151	-32.3723	-32.3477	-32.4159
N^{5+}	0.99999	0.13923	-44.7471	-44.7227	-44.8011
O^{6+}	0.99999	0.12955	-59.1220	-59.0977	-59.1913
F^{7+}	1.00000	0.12163	-75.4969	-75.4727	
Ne^{8+}	1.00000	0.11558	-93.8718	-93.8477	

Table 1. Results for the two-electron ions.

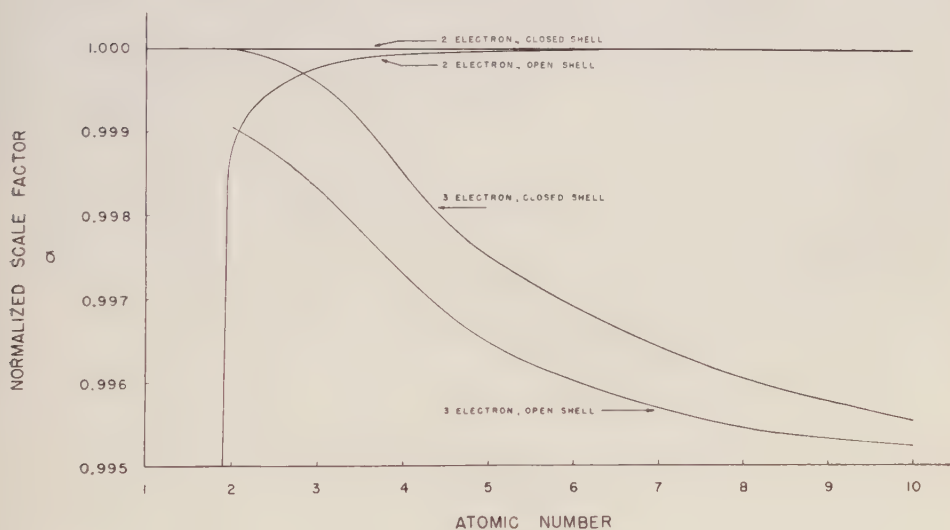
† Units $\mu_Z/\mu_H(27.190)$ ev.

Figure 1.

parameters α and β in terms of the *normalized scale factor* α and the *splitting parameter* β . These quantities are defined by the relations

$$\alpha = (Z - 5/16)\alpha(1 + \beta) \quad (10)$$

$$\beta = (Z - 5/16)\alpha(1 - \beta) \quad (11)$$

	Open shell			Closed shell ($\beta=0$)				
	α	β	c	Energy (a.u.)†	α	c	Energy (a.u.)†	Exp. energy[6] (a.u.)†
He ⁻	0.99905	0.29500	9.3750×10^{-7}	-2.8757	1.0000	0.0002749	-2.8477	
Li	0.99832	0.22930	0.63896	-7.4436	0.99960	0.63733	-7.4179	-7.4783
Be ⁻	0.99720	0.19441	1.0875	-14.2826	0.99848	1.0860	-14.2584	-14.3261
B ³⁺	0.99645	0.16900	1.5214	-23.3726	0.99752	1.5208	-23.3498	-23.4323
C ³⁺	0.99611	0.15242	1.9503	-34.7112	0.99694	1.9505	-34.6899	-34.7860
N ⁴⁺	0.99566	0.13864	2.3771	-48.2977	0.99642	2.3776	-48.2776	-48.3985
O ⁵⁺	0.99543	0.12745	2.8028	-64.1316	0.99604	2.8044	-64.1129	-64.2690
F ⁶⁺	0.99533	0.11801	3.2277	-82.2127	0.99577	3.2286	-82.1953	
Ne ⁷⁺	0.99521	0.11015	3.6508	-102.5411	0.99554	3.6541	-102.5249	

Table 2. Results for the three-electron ions.

† Units μ_Z/μ_H (27.190) ev.

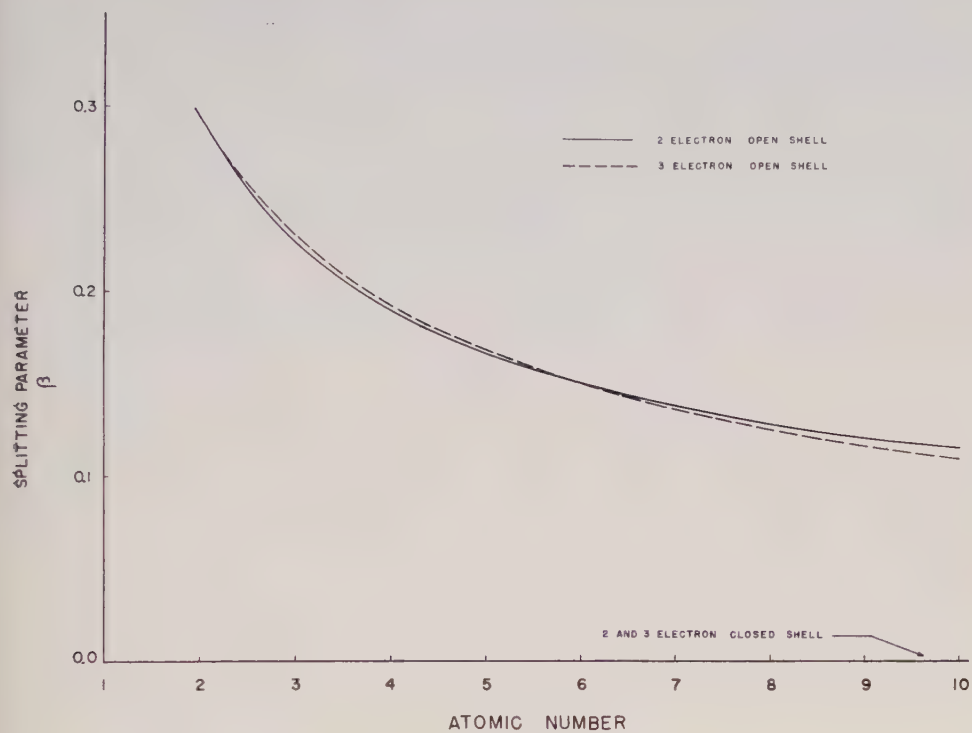


Figure 2.

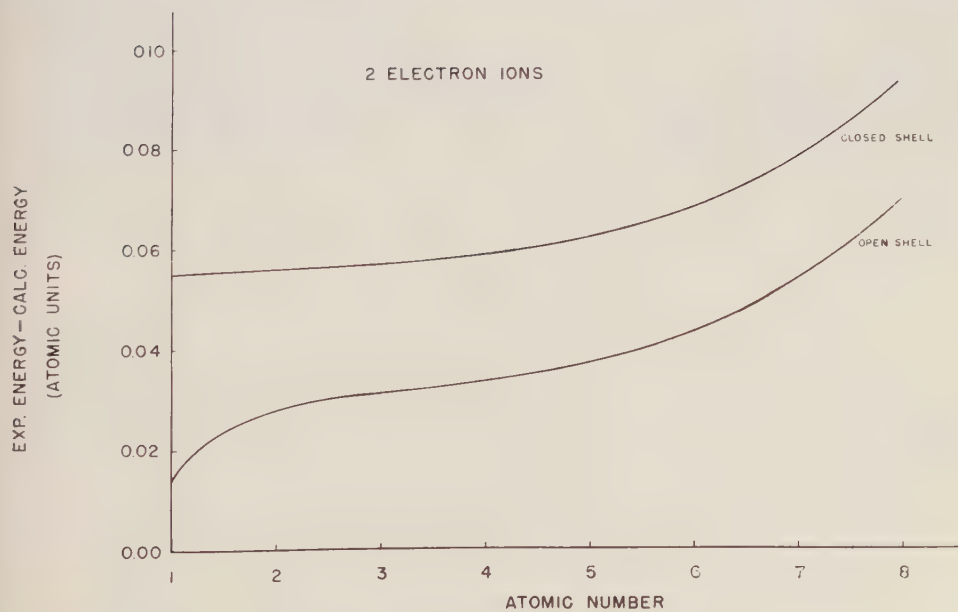


Figure 3.

α and β are plotted as shown in figures 1 and 2, and the differences between corresponding open and closed calculations and the experimental energies are given in figures 3 and 4.

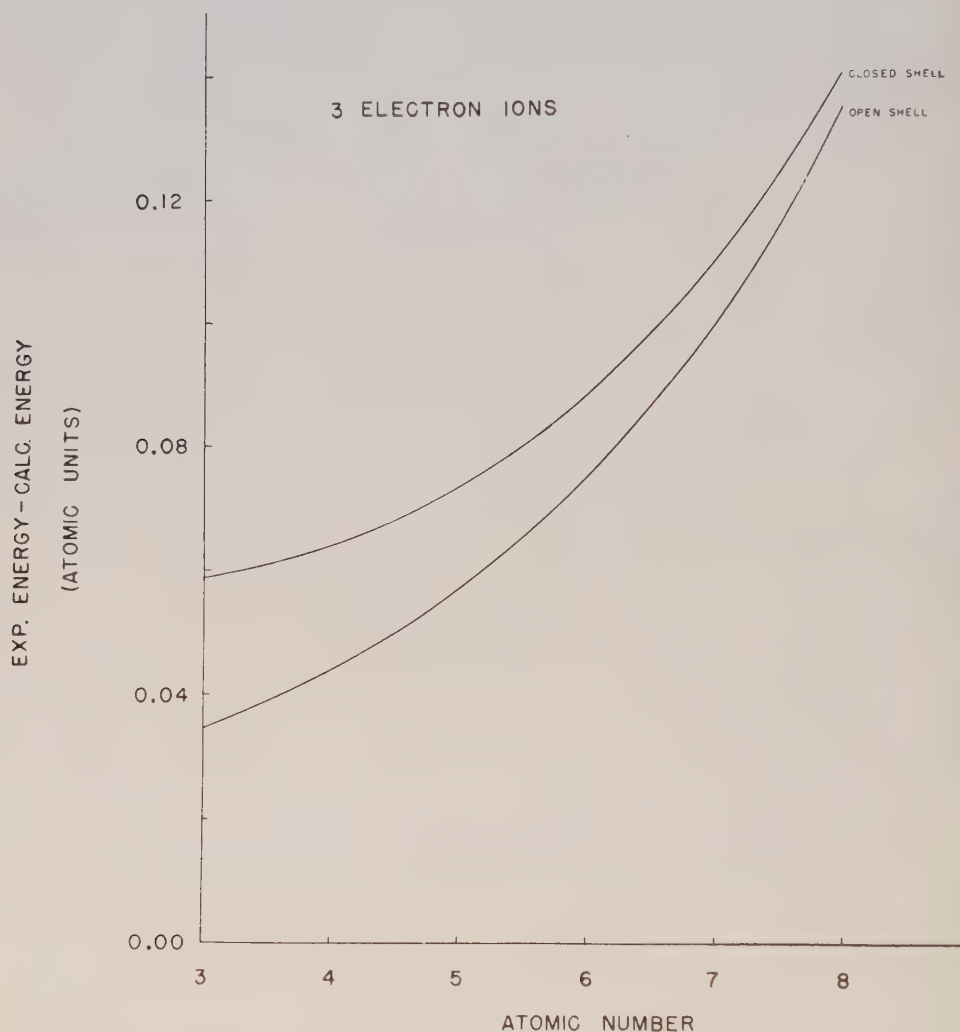


Figure 4.

3. DISCUSSION

Examination of tables 1 and 2 shows that the energy improvement of open shell calculations over the closed shell calculations becomes less with increasing atomic number. In parallel trend, in the two-electron case, the normalized scale factors α approach unity and the splitting parameters β approach zero the values for closed shells. The three-electron results are entirely analogous to those for two electrons except that α is close to unity for small Z and becomes slightly smaller with increasing Z .

It is of interest to note that the two- and three-electron results for helium are equal to the limit of error in the calculation, thus indicating an electron affinity

for this element of zero. This was true for both the open and closed configuration calculations. Glockler [4] has previously obtained the result -0.53 eV on the basis of an empirical relation. Bates [5] has more recently confirmed Glockler's value. Since the three-electron calculations for the other ions lie higher above the experimental results than corresponding two-electron calculations for the same atomic number, one might expect more accurate three-electron calculations to predict a slightly positive electron affinity for helium†. This, of course, is in qualitative as well as quantitative disagreement with Glockler and Bates' results.

The authors wish to express their appreciation to Mr. Robert D. Mitchell for his assistance with the electronic computer calculations presented in this paper.

NOTE. We understand (private communication) that Dr. E. A. Burke and Professor J. F. Mulligan have been working along very similar lines and have obtained results which are almost identical with ours. These authors have submitted their paper for publication in the *Journal of Chemical Physics*.

On fait des calculs basés sur la fonction d'onde d'une couche incomplète pour tous les systèmes atomiques à trois électrons de la seconde période de la table périodique, et on compare les résultats avec ceux des calculs semblables pour des systèmes à deux électrons et avec les énergies expérimentales.

L'on a constaté que l'avantage des calculs à base de couches incomplètes par rapport à ceux basés sur des couches complètes diminue à mesure que le numéro atomique augmente. D'une façon analogue l'écart entre les deux types de calcul d'une part et les résultats expérimentaux d'autre part augmente avec Z . Pour l'atome d'hélium on a trouvé une affinité électronique égale à zéro.

Open-shell-Berechnungen werden für alle Atomsysteme mit drei Elektronen in der zweiten Periode des Periodensystems durchgeführt. Die Ergebnisse werden mit den entsprechenden Berechnungen für zwei Elektronen, sowie mit gemessenen Energiewerten verglichen.

Es zeigt sich, dass die Verbesserung der *open-shell*-gegenüber den *closed-shell*-Berechnungen mit wachsender Ordnungszahl abnimmt. Gleichzeitig nimmt der Unterschied zwischen den experimentellen Ergebnissen und den Berechnungen nach beider Verfahren mit wachsender Ordnungszahl zu. Für des Heliumatom wird die Elektronenaffinität null gefunden.

REFERENCES

- [1] SHULL, H., and LÖWDIN, P.-O., 1956, *J. chem. Phys.*, **25**, 1035.
- [2] BRIGMAN, G. H., and MATSEN, F. A., 1957, *J. chem. Phys.*, **27**, 829.
- [3] HURST, R. P., MILLER, J., and MATSEN, F. A., 1958, *Acta cryst.* [to be published].
- [4] GLOCKLER, G., 1934, *Phys. Rev.*, **46**, 111.
- [5] BATES, D. R., 1947, *Proc. R. Irish Acad. A*, **51**, 151.
- [6] MOORE, C. E., 1949, *Atomic Energy Levels* [Washington: National Bureau of Standards], vol. 1.

† *Note added in proof.*—It is interesting in this connection that the existence of He⁻ has recently been reported.

WINDHAM, P. M., JOSEPH, P. J., and WEINMAN, J. A., 1958, *Phys. Rev.*, **109**, 1193.

RESEARCH NOTE

Paramagnetism in molecular compounds

by H. M. BUCK, J. H. LUPINSKI and L. J. OOSTERHOFF

Division of Theoretical Organic Chemistry, Leiden University

(Received 18 December 1957)

In the course of an investigation of molecular compounds derived from substituted polyphenylethylenes and substituted diphenyls it was found that many of these compounds show electron spin resonance (ESR). Similar phenomena have been reported by Kainer, Bijl and Rose-Innes [1] for complexes of *p*-phenylene diamine or N, N, N', N'-tetramethyl-*p*-phenylene diamine with benzoquinones.

In the table we have collected the results which have been obtained at room temperature except where otherwise stated.

The absorption intensity of the solid complexes was determined by comparison with diphenyl-picryl-hydrazyl (DPPH) and the spectroscopic splitting factor was found to be almost the same as that of DPPH. The ratio of absorption intensity of the compounds to that of DPPH suggested that the paramagnetism was much smaller than would be expected if they existed as free radicals. The results strongly support the idea that these compounds are to be considered as charge transfer complexes. A further investigation may even make it possible to distinguish between outer and inner complexes [6].

It is by no means clear whether the paramagnetism is to be ascribed to a triplet state. An elucidation of the structure of these and similar complexes will require a more quantitative study of the paramagnetism, in particular of its temperature dependence. This work and spectroscopic studies are in progress and will be reported in a later paper.

In connection with our work it is of interest to refer to papers by J. Weiss [7] who considered electron transfer processes as a first step in many oxidation reactions and to R. Wizinger [8] who by chemical considerations very clearly recognised molecular compounds of the type studied by us as charge transfer complexes.

We wish to thank Mr. G. Elsen for preparing some of the compounds.

REFERENCES

- [1] KAINER, H., BIJL, D., and ROSE-INNES, A. C., 1954, *Naturwissenschaften*, **41**, 303; 1956, *Nature*, **178**, 1462.
- [2] VAN ALPHEN, J., 1930, *Recueil*, **49**, 771.
- [3] NOELTING, E., and SOMMERHOFFS, E. O., 1906, *Ber. dtsch. chem. Ges.*, **39**, 76.
- [4] PFEIFFER, P., and WIZINGER, R., 1929, *Liebigs Ann. Chem.*, **461**, 132.
- [5] WIZINGER, R., and FONTAINE, I., 1927, *Ber. dtsch. chem. Ges.*, **60**, 1377.
- [6] REID, C., and MULLIKEN, R. S., 1954, *J. Amer. chem. Soc.*, **76**, 3869.
- [7] WEISS, J., 1942, *J. chem. Soc.*, 245; *Proc. roy. Soc. A*, **222**, 128.
- [8] WIZINGER, R., 1933, *Organische Farbstoffe*, 48-51.
- [9] KAINER, H., and ÜBERK, A., 1956, *Ber. dtsch. chem. Ges.*, **88**, 1147.

Table

Components	Examined in	Colour	ESR	Constitution
I. 4, 4'-dimethoxydiphenyl with :				
(a) nitric acid	solid	blue	+	1 : 2 [2]
	nitrobenzene (0°C)	blue	+	
(b) sulphuric acid	sulphuric acid	blue	—	
II. 4, 4'-dimethoxy-3, 3'-dibromodiphenyl with :				
(a) bromine (Br ₂)	solid	green	+	1 : 1
III. 4, 4'-diaminodiphenyl with :				
(a) bromine	solid	blue	+	1 : 2 2 : 1 ? 1 : 1 [3]
(b) iodine (I ₂)	solid	blue	+	
(c) tetranitromethane	solid	blue	+	
(d) 1, 3, 5-trinitrobenzene	solid	black	—	
IV. 4, 4'-bis-dimethylamino- diphenyl with :				
(a) bromine	solid	green	++	2 : 1 1 : 2
(b) iodine	solid	green	++	
(c) tetranitromethane	solid	green	++	
(d) 1, 3, 5-trinitrobenzene	solid	black	—	
V. α, α -bis-(4-methoxyphenyl)- ethylene with :				
(a) bromine	solid	violet	—	[4]
VI. α, α -bis-(4-dimethylamino- phenyl)-ethylene with :				
(a) bromine	solid	blue	—	1 : 2
VII. $\alpha, \alpha, \beta, \beta$ -tetrakis-(4- methoxyphenyl)-ethylene with :				
	solid	blue		[5]
	nitrobenzene	blue	+	
(a) bromine	nitromethane	blue	+	
	carbontetrachloride	brown		
VIII. $\alpha, \alpha, \beta, \beta$ -tetrakis-(4- dimethylaminophenyl)- ethylene with :				
(a) bromine	solid	blue	—	1 : 3
(b) iodine	solid	blue	—	1 : 3

Nuclear magnetic shielding of a hydrogen atom in an electric field

by T. W. MARSHALL and J. A. POPLE

Department of Theoretical Chemistry, Cambridge University

(Received 19 March 1958)

The nuclear magnetic screening constant of a hydrogen atom in a uniform electric field is calculated, neglecting any effect of electron spin. The screening is found to be reduced by the electric field for all directions of the applied magnetic field, the reduction being greatest if the two fields are perpendicular.

1. INTRODUCTION

It is well known that the nuclear magnetic screening effect of the electrons in a spherically symmetric atom (in an S-state) is easily calculated from the electron density [1]. This is because the effect of the applied magnetic field is to cause the whole electronic structure to rotate about the nucleus with the Larmor angular frequency $eH/2mc$. In a non-spherical environment, however, this free circulation is partly quenched and the magnitude of the screening is reduced by the addition of a 'paramagnetic' term which represents the effect of mixing of the ground and excited states by the magnetic field. This is usually more difficult to evaluate [2].

The purpose of this note is to present the results of a calculation of the nuclear magnetic screening in a hydrogen atom placed in an electric field, neglecting any effect of the spin of the electron. This represents perhaps the simplest situation in which the 'paramagnetic' effect has to be taken into account. The problem is exactly soluble, so the result is of some interest in comparing the relative importance of various terms. The analysis closely follows corresponding work on the magnetic susceptibility of a hydrogen atom in an electric field [3].

2. THEORY

If a hydrogen atom is placed in a uniform electric field E and a uniform magnetic field H , the complete Hamiltonian can be written

$$\mathcal{H} = \mathcal{H}_{00} + \mathcal{H}_{10} + \mathcal{H}_{01} + \mathcal{H}_{02}, \quad (2.1)$$

using a double suffix notation, the first suffix representing the order in E and the second the order in H . The separate parts are

$$\left. \begin{aligned} \mathcal{H}_{00} &= -(\hbar^2/2m)\nabla^2 - (e^2/r), \\ \mathcal{H}_{10} &= e\mathbf{E} \cdot \mathbf{r}, \\ \mathcal{H}_{01} &= (e/2mc)\mathbf{H} \cdot \mathbf{L}, \\ \mathcal{H}_{02} &= (e^2/8mc^2)[H^2r^2 - (\mathbf{H} \cdot \mathbf{r})^2], \end{aligned} \right\} \quad (2.2)$$

where L is the orbital angular momentum operator

$$\mathbf{L} = -i\hbar\mathbf{r} \times \nabla. \quad (2.3)$$

If the wave function is expanded in a similar manner

$$\psi = \psi_{00} + \psi_{10} + \psi_{01} + \psi_{20} + \dots, \quad (2.4)$$

the complete Schrödinger equation breaks up into separate equations in each order in E and H . These can be solved in turn and the parts of ψ determined [3]. The wave function ψ implies a certain distribution of current density which in turn sets up a secondary magnetic field $-\sigma H$ at the nucleus where σ is the screening constant. Our procedure, therefore, is to find this secondary magnetic field.

Since the hydrogen atom in an electric field is an axially symmetric system, we only have to consider the two cases of \mathbf{H} parallel or perpendicular to \mathbf{E} . These will give different shielding constants which we shall write σ_{\parallel} and σ_{\perp} . Since the shielding constant is really a second-order tensor, the value of σ for an intermediate direction making an angle θ with \mathbf{E} , will be

$$\sigma = \sigma_{\parallel} \cos^2 \theta + \sigma_{\perp} \sin^2 \theta. \quad (2.5)$$

We use polar coordinates with the direction of H as the polar axis. Then

$$\left. \begin{aligned} \mathcal{H}_{01} &= \frac{e\hbar H}{2mc i} \frac{\partial}{\partial \phi}, \\ \mathcal{H}_{02} &= \frac{e^2 H^2}{8mc^2} r^2 \sin^2 \theta, \\ \mathcal{H}_{10} &= eErP(\theta, \phi) = eEr \begin{cases} \cos \theta & (\text{parallel fields}), \\ \sin \theta \cos \phi & (\text{perpendicular fields}). \end{cases} \end{aligned} \right\} \quad (2.6)$$

The components of ψ required are (unnormalized)

$$\left. \begin{aligned} \psi_{00} &= \exp(-r'), & \psi_{01} &= 0, \\ \psi_{10} &= -\frac{1}{2}e^{-1}a^2E(r'^2 + 2r')\exp(-r')P(\theta, \phi), \\ \psi_{20} &= \frac{1}{48}e^{-2}a^4E^2\{(2r'^3 + 21r'^2) + (6r'^4 + 30r'^3 + 45r'^2)P^2(\theta, \phi)\}\exp(-r'), \\ \psi_{11} &= \begin{cases} 0 & (\text{parallel fields}), \\ \frac{ia^4EH}{24\hbar c}(2r'^3 + 11r'^2 + 22r')\exp(-r')\sin \theta \sin \phi & (\text{perpendicular fields}), \end{cases} \end{aligned} \right\} \quad (2.7)$$

where $r' = r/a$ and a is the Bohr radius ($= \hbar^2/me^2$).

The current density vector \mathbf{j} is given by

$$\left. \begin{aligned} \mathbf{j} &= -\frac{e^2}{2mcN}(\mathbf{H} \times \mathbf{r})\psi^*\psi - \frac{e\hbar}{2miN}\{\psi^*\nabla^2\psi - \psi\nabla^2\psi^*\}, \\ N &= \int \psi^*\psi d\tau. \end{aligned} \right\} \quad (2.8)$$

This in turn gives a magnetic field of

$$\mathbf{H}' = \int [\mathbf{r} \times \mathbf{j}/cr^3] d\tau \quad (2.9)$$

at the nucleus.

The secondary field can be written $\mathbf{H}_1' + \mathbf{H}_2'$ corresponding to the two parts of \mathbf{j} . The first part leads to the diamagnetic term in the general theory of Ramsey [2]

$$\sigma^d = \frac{e^2}{2mc^2} \int \frac{\rho \sin^2 \theta}{r} d\tau, \quad (2.10)$$

where ρ is the electron density in the absence of a magnetic field. (If ρ is spherically symmetric this reduces to the Lamb [1] atomic formula.) Now

$$\rho = \frac{\psi_{00}^2 + 2\psi_{00}\psi_{10} + 2\psi_{00}\psi_{20} + \psi_{10}^2 + \dots}{\int (\psi_{00}^2 + 2\psi_{00}\psi_{10} + \dots) d\tau}. \quad (2.11)$$

Carrying the expansion of σ^d in E as far as E^2 , we obtain

$$\left. \begin{aligned} \sigma_{\parallel}^d &= \frac{e^2}{3mc^2a} \left[1 - \frac{439}{40} \frac{a^4 E^2}{e^2} \right], \\ \sigma_{\perp}^d &= \frac{e^2}{3mc^2a} \left[1 - \frac{641}{80} \frac{a^4 E^2}{e^2} \right]. \end{aligned} \right\} \quad (2.12)$$

The paramagnetic contribution σ^p can be evaluated by considering the second term in the expression for \mathbf{j} (equation (2.8)). Noting that the component of $\mathbf{r} \times \nabla$ in the direction of \mathbf{H} is $\partial/\partial\phi$, we find that this part of the secondary magnetic field is (for the perpendicular case)

$$\left. \begin{aligned} H_2' &= -\frac{eh}{2mcNi} \int \left(\psi^* \frac{\partial\psi}{\partial\phi} - \psi \frac{\partial\psi^*}{\partial\phi} \right) \frac{1}{r^3} d\tau \\ &= \frac{2e\hbar}{mcNi} \int \psi_{11} \frac{\partial\psi_{10}}{\partial\phi} \frac{1}{r^3} d\tau, \end{aligned} \right\} \quad (2.13)$$

provided that only terms of order E^2 are considered. This gives

$$\sigma_{\perp}^p = -\frac{233}{144} \frac{a^3 E^2}{mc^2}. \quad (2.14)$$

Combining with (2.12), we obtain the final formulae

$$\left. \begin{aligned} \sigma_{\parallel} &= \frac{e^2}{3mc^2a} \left[1 - \frac{439}{40} \frac{a^4 E^2}{e^2} \right], \\ \sigma_{\perp} &= \frac{e^2}{3mc^2a} \left[1 - \frac{193}{15} \frac{a^4 E^2}{e^2} \right]. \end{aligned} \right\} \quad (2.15)$$

3. DISCUSSION

The above analysis shows that the magnetic screening of the nucleus by the electrons is reduced in all directions by the application of a uniform electric field, the reduction being greatest when the magnetic field is perpendicular to the electric field. This lowering of the screening constant is only partly due to the paramagnetic term, for the diamagnetic Lamb-type term is also reduced. This corresponds to the partial removal of electrons from the vicinity of the nucleus by the electric field and consequent reduction in the mean value of $1/r$.

It seems likely that the large reductions of the screening constants of protons when they form intermolecular hydrogen bonds are due to similar effects [4]. The hydrogen atom in a molecule is, of course, already in a strong electric field before forming a hydrogen bond, but the additional electrostatic field of the neighbouring molecule will lead to a reduction of screening. Intermolecular effects of this sort have also been discussed by Stephen [5].

On a calculé la constante d'écran magnétique nucléaire d'un atome d'hydrogène placé dans un champ électrique uniforme, en négligeant tout effet dû au spin électronique. On trouve que l'effet d'écran est réduit par le champ électrique, quelle que soit la direction du champ magnétique appliqué, et que la plus grande diminution a lieu quand les deux champs sont perpendiculaires.

Die kernmagnetische Abschirmungskonstante eines Wasserstoffatoms im homogenen elektrischen Feld wird unter Vernachlässigung des Elektronenspins berechnet. Es wird gezeigt, dass das elektrische Feld die Abschirmung für jede Richtung des Magnetfelds verkleinert; die Verringerung ist am stärksten, wenn die beiden Felder aufeinander senkrecht stehen.

REFERENCES

- [1] LAMB, W. E., 1941, *Phys. Rev.*, **60**, 817.
- [2] RAMSEY, N. F., 1950, *Phys. Rev.*, **77**, 567; **78**, 699.
- [3] BUCKINGHAM, A. D., and POPL, J. A., 1957, *Proc. Camb. phil. Soc.*, **53**, 262.
- [4] SCHNEIDER, W. G., BERNSTEIN, H. J., and POPL, J. A., 1958, *J. chem. Phys.*, **28**, 601.
- [5] STEPHEN, M. J., 1958, *Mol. Phys.*, **1**, 223.

On the nuclear magnetic shielding in the hydrogen molecule†

by H. F. HAMEKA

Department of Chemistry, Carnegie Institute of Technology, Pittsburgh,
Pennsylvania

(Received in final form 11 April 1958)

A simplified method is discussed for calculations of proton shielding in molecules by using wave functions which are constructed from gauge invariant atomic orbitals. The method is applied to the hydrogen molecule by means of a simple LCAO MO description. The computed total nuclear shielding constant is 3.2×10^{-5} .

1. INTRODUCTION

As a consequence of the increasing accuracy of nuclear magnetic resonance measurements, early investigators [1, 2, 3] drew attention to differences between the external magnetic field and the local fields at the positions of the various nuclei. These differences, which are due to the small magnetic fields caused by induced electronic currents, were calculated by Lamb [1] for all atoms with spherical symmetry, and it was first thought that all experimental results should be corrected by his method. For light nuclei the approximations used by Lamb are not very satisfactory, however, so that especially for the hydrogen molecule various attempts have been made to perform more accurate calculations of the proton shielding.

First-order perturbation treatments for the hydrogen molecule have been reported by Anderson [4], Newell [5] and Hylleraas and Skavlem [6], all of whom make use of more or less accurate wave functions. Ramsay [7, 8] has pointed out that not only a first-order perturbation term but also a second-order term should be included in these calculations. He derived a general expression for the proton shielding in the hydrogen molecule and showed that the term which results from the second-order perturbation is connected with the spin-rotational magnetic interaction constant, so that it may be determined empirically.

A different approach to the problem is the application of the variation principle, in which case the variational function ordinarily should contain a part which is proportional to the magnetic field H as well as a part which is proportional to the nuclear magnetic moment μ . This method has been applied by Das and Bersohn [9] and Hornig and Hirschfelder [10]. The most complete calculation of the proton shielding of the hydrogen molecule has been performed by Ishiguro and Koide [11], making use of a seven-term James-Coolidge-type function independent of H and μ and two additional James-Coolidge-type functions proportional to either H or μ_0 .

It should be observed that there is no difference in principle between the application of perturbation theory and the application of variational methods, because the terms which result from second-order perturbation theory in the first

† Research supported by a grant from the Alfred P. Sloan Foundation to Carnegie Institute of Technology.

case correspond to the terms which result from the parts of the wave function which are proportional to either H or μ in the second case. Usually the accuracy of such terms is none too good in either case.

A somewhat simplified calculation, making use of simple molecular orbital and Heitler-London wave functions has been performed by McGarvey [12].

In most of the calculations in the literature there appears to have been some confusion about the gauge invariance of the Schrödinger equation and the question of the choice of the origin for the vector potential. Especially in the considerations of McGarvey there are inconsistencies which may be mainly ascribed to this difficulty. It has been shown by Van Vleck [13] that for a calculation of diamagnetic susceptibilities, the analogue of equation (8) below is independent of the choice of origin; therefore Ramsay assumed that this would also be the case for a calculation of magnetic shielding. However, this is only true if all excited discrete states of the molecule as well as the continuum are included in the calculations. Because only a few excited states are taken into account in most actual calculations, the results become strongly dependent on the choice of origin, so that Ramsay's formulae are not very adequate for a performance of numerical calculations.

In a simple LACO MO treatment the difficulties may be resolved reasonably easily, and so we have performed the calculation for the hydrogen molecule with the aid of this description. It will be seen that certain terms enter the Hamiltonian which were not included in McGarvey's treatment. It is our opinion that for calculations on more complicated molecules the present procedure has some practical advantages with respect to previously reported procedures.

2. GENERAL CONSIDERATIONS

The vector potential for a homogeneous magnetic field \mathbf{H} and two magnetic dipoles μ^a and μ^b at positions A and B is

$$\mathbf{A} = \frac{1}{2} [\mathbf{H}\mathbf{r}] + \frac{[\mu^a \mathbf{r}_a]}{r_a^3} + \frac{[\mu^b \mathbf{r}_b]}{r_b^3} - \text{grad } \phi \quad (1)$$

where ϕ is an arbitrary continuous function of space; as is well known \mathbf{A} is not uniquely determined. The function ϕ may now be chosen in such a way as to determine the origin of \mathbf{A} :

$$\phi(\mathbf{q}) = \frac{1}{2} ([\mathbf{H}\mathbf{q}]\mathbf{r}) \quad (2)$$

$$\mathbf{A}(\mathbf{q}) = \frac{1}{2} [\mathbf{H}, \mathbf{r} - \mathbf{q}] + \frac{[\mu^a \mathbf{r}_a]}{r_a^3} + \frac{[\mu^b \mathbf{r}_b]}{r_b^3}. \quad (3)$$

The Schrödinger equation for an N particle system becomes then

$$\left[\sum_i \frac{1}{2m_i} \left(\mathbf{P}_i - \frac{e}{c} \mathbf{A}_i \right)^2 + V(\mathbf{r}_1, \mathbf{r}_2, \dots, \mathbf{r}_N) \right] \psi = E\psi. \quad (4)$$

Here each momentum \mathbf{P}_i must be corrected for the motion of the corresponding electron in the potential field \mathbf{A} ; the subscript i in \mathbf{A}_i indicates that in equation (3) the coordinates \mathbf{r}_i , \mathbf{r}_{ai} and \mathbf{r}_{bi} should be substituted instead of \mathbf{r} , \mathbf{r}_a and \mathbf{r}_b . Actually also different values \mathbf{q}_i may be employed for different electrons, but in our calculations there is not any need to do so.

Now if the eigenfunction ψ_k is a solution of the Schrödinger equation for a choice of origin \mathbf{q} , then according to the well-known properties of the gauge transformation, the corresponding eigenfunction ψ_k' for a choice of origin \mathbf{q}' is given by

$$\psi_k' = \psi_k \exp \sum_j [ie \{ \phi_j(\mathbf{q}') - \phi_j(\mathbf{q}) \} / \hbar c] \quad (5)$$

(cf. for instance Bohm [14]). Analogously, if $\bar{\psi}_k$ is an approximate solution for the energy value E_k and the choice of origin \mathbf{q} , the function

$$\bar{\psi}_k' = \bar{\psi}_k \exp \sum_j [ie \{ \phi_j(\mathbf{q}') - \phi_j(\mathbf{q}) \} / \hbar c] \quad (6)$$

will be an equivalent approximate solution for the case that \mathbf{q} is chosen as origin. That is to say, if it is known for which choice of origin a given function is an appropriate approximate solution of the Schrödinger equation, the corresponding function for another origin may be constructed by multiplication by the appropriate exponential function (phase factor).

For the hydrogen atom the well-known functions $\psi_{n,l,m}$ which are exact eigenfunctions in the absence of an electromagnetic field are approximate solutions in the presence of a magnetic field if the origin \mathbf{q} of the vector potential is taken as the atomic nucleus. Analogously, the well-known Slater functions, which are approximate solutions for more complex atoms are equivalent approximate solutions in the presence of a magnetic field if the origin of the vector potential is taken as the atomic nucleus. For any other choice of origin, for instance \mathbf{q} , which does not coincide with the position \mathbf{a} of the nucleus, the equivalent approximation becomes

$$\bar{\psi}'_{n,l,m} = \bar{\psi}_{n,l,m} \exp [ie \phi(\mathbf{q} - \mathbf{a}) / \hbar c]. \quad (7)$$

Consequently, for molecular calculations employing atomic orbitals, use must be made of the functions (7) if a general choice for the origin of the vector potential is made for the whole molecule.

As has been pointed out by Ramsay, the magnetic shielding constant σ_a for nucleus A is the coefficient of $(\boldsymbol{\mu} \cdot \mathbf{H})$ in the power series expansion of the energy of the ground state. Where there exists an anisotropy in magnetic shielding σ_{ai} may be defined analogously as the coefficient of $\mu_i^a H_i$. Hence

$$\sigma_{ai} = \left(\frac{\partial^2}{\partial \mu_i^a \partial H_i} \left[\mathcal{H}_{0,0} - \sum_{n=0} \frac{\mathcal{H}_{n,0} \mathcal{H}_{0,n}}{E_n - E_0} \right] \right)_{\boldsymbol{\mu} = \mathbf{H} = 0}. \quad (8)$$

Here $\mathcal{H}_{k,l}$ is

$$\mathcal{H}_{k,l} = \int \psi_k^* \mathcal{H} \psi_l d\tau. \quad (9)$$

It should be stressed that, although equation (8) resembles strongly a well known formula of second order perturbation theory, it has nothing to do with perturbation theory. In our case, namely, the unperturbed wave functions contain the magnetic field explicitly so that this case must be studied specifically. A more elaborate discussion of this situation has been offered in Appendix C. For the sake of mathematical simplicity the first term of equation (8) will be named the *first order perturbation term* and the second term will be named the *second order perturbation term*. No physical significance should be attached to this separation and indeed different separations have been applied by different authors, which renders a comparison of intermediate results somewhat difficult.

The exact eigenfunctions for the ground and excited states usually are not known, but it may be hoped that inserting approximate eigenfunctions into equation (8) also will yield a satisfactory result for σ . Actually this is at the present time the only approach which is available for complicated molecules. In order to obtain some idea as to whether or not satisfactory results might be obtained in this way it is only natural to perform a first calculation on the hydrogen molecule with the aid of a simple orbital description. The observation of Hylleraas and Skavlem [6] that the magnetic shielding does not seem to depend very strongly on the form of the wave function, is rather encouraging in this respect.

3. THE FIRST ORDER PERTURBATION TERM

If the positions of the two hydrogen nuclei are given by \mathbf{a} and \mathbf{b} , the wave function of the ground state of the hydrogen molecule will be taken as the simple LCAO MO form,

$$\psi_0 = \frac{\{s'_1(\mathbf{a}, \mathbf{q}) + s'_1(\mathbf{b}, \mathbf{q})\} \{s'_2(\mathbf{a}, \mathbf{q}) + s'_2(\mathbf{b}, \mathbf{q})\}}{2 + \langle s'(\mathbf{a}, \mathbf{q}) | s'(\mathbf{b}, \mathbf{q}) \rangle + \langle s'(\mathbf{b}, \mathbf{q}) | s'(\mathbf{a}, \mathbf{q}) \rangle} \quad (10)$$

where

$$s'_i(\mathbf{a}, \mathbf{q}) = s_{ai} \exp \left[\frac{1}{2} i e ([\mathbf{H}_1 \mathbf{q} - \mathbf{a}] r) / \hbar c \right] \\ s_{ai} = \pi^{-1/2} \exp(-r_{ai}). \quad (11)$$

Here, it will be noted, the atomic orbitals are written in a form which makes the wave function proper for any choice of the origin \mathbf{q} for the vector potential.

This wave function gives the following expansion for the matrix element producing the first order perturbation term of the shielding (cf. Appendix C)

$$\mathcal{H}_{0,0} = \{1 + \frac{1}{2} \langle s'(\mathbf{a}, \mathbf{q}) | s'(\mathbf{b}, \mathbf{q}) \rangle + \frac{1}{2} \langle s'(\mathbf{b}, \mathbf{q}) | s'(\mathbf{a}, \mathbf{q}) \rangle\}^{-1} \\ \times \{ \langle s'(\mathbf{a}, \mathbf{q}) | \mathcal{H}_q | s'(\mathbf{a}, \mathbf{q}) \rangle + \langle s'(\mathbf{b}, \mathbf{q}) | \mathcal{H}_q | s'(\mathbf{a}, \mathbf{q}) \rangle \\ + \langle s'(\mathbf{a}, \mathbf{q}) | \mathcal{H}_q | s'(\mathbf{b}, \mathbf{q}) \rangle + \langle s'(\mathbf{b}, \mathbf{q}) | \mathcal{H}_q | s'(\mathbf{b}, \mathbf{q}) \rangle \} \quad (12)$$

where the subscript in the \mathcal{H}_q indicates that in the Hamiltonian of equation (4) the origin of the vector potential should be taken as \mathbf{q} . Because each term in equation (12) is independent of the choice of origin for the vector potential, a special choice may be made in each term in such a way as to facilitate the calculations. Then

$$\mathcal{H}_{0,0} = \{1 + \frac{1}{2} \langle e^{i\alpha} s_a | s_b \rangle + \frac{1}{2} \langle e^{-i\alpha} s_b | s_a \rangle\}^{-1} \{ \langle s_a | \mathcal{H}_a | s_a \rangle \\ + \langle s_b | \mathcal{H}_b | s_b \rangle + \langle e^{i\alpha} s_a | \mathcal{H}_b | s_b \rangle + \langle e^{-i\alpha} s_b | \mathcal{H}_a | s_a \rangle \} \quad (13)$$

where

$$\alpha = \frac{1}{2} e ([\mathbf{H}, \mathbf{b} - \mathbf{a}] r) / \hbar c \quad (14)$$

or, if the z -axis is taken along the line AB and the distance between the two nuclei is R

$$\alpha = \frac{1}{2} e R (H_y x - H_x y) / \hbar c. \quad (15)$$

For a calculation of $\mathcal{H}_{0,0}$ the phase factors $e^{i\alpha}$ should thus be taken into account, but it will be seen that for our choice of the origins in \mathcal{H}_q most terms which depend on α may be neglected. For instance consider

$$\langle s'(\mathbf{b}, \mathbf{q}) | s'(\mathbf{a}, \mathbf{q}) \rangle = \sum_{n=0}^{\infty} \langle s_b | (i^n \alpha^n / n!) | s_a \rangle. \quad (16)$$

The first term is the well known overlap integral $\Delta_{1,1}$ of s_a and s_b , the second term is zero because of symmetry reasons and the other terms will not contribute to

$\mathcal{H}_{0,0}$ because they contain higher powers of H than one. From equation (4) it follows that the part of $\mathcal{H}_{0,0}$ which may contribute to the magnetic shielding becomes

$$\begin{aligned} \mathcal{H}_{0,0} = & (1 + \Delta_{1,1})^{-1} \{ \langle s_a | (\mathbf{A}_a)^2 | s_a \rangle + \langle s_b | (\mathbf{A}_b)^2 | s_b \rangle \\ & + \langle s_a | (\mathbf{A}_a)^2 + (\mathbf{A}_b)^2 | s_b \rangle + i \langle \alpha s_a | (\mathbf{A}_b)^2 - (\mathbf{A}_a)^2 | s_b \rangle \} \\ & - (ie/mc) \{ \langle \alpha s_a | (\mathbf{A}_b \mathbf{P}) | s_b \rangle - \langle \alpha s_b | (\mathbf{A}_a \mathbf{P}) | s_a \rangle \}. \end{aligned} \quad (17)$$

The fourth term contains parts which are proportional to either H^2 or μ^2 and does not contribute to the magnetic shielding. Therefore

$$\begin{aligned} \mathcal{H}_{0,0} = & \frac{e^2}{2mc^2(1 + \Delta_{1,1})} \left[\langle s_a | \left([\mathbf{H}\mathbf{r}_a] \frac{[\mu^a \mathbf{r}_a]}{r_a^3} \right) + \left([\mathbf{H}\mathbf{r}_a] \frac{[\mu^b \mathbf{r}_b]}{r_b^3} \right) | s_a \rangle \right. \\ & + \langle s_b | \left([\mathbf{H}\mathbf{r}_b] \frac{[\mu^a \mathbf{r}_a]}{r_a^3} \right) + \left([\mathbf{H}\mathbf{r}_b] \frac{[\mu^b \mathbf{r}_b]}{r_b^3} \right) | s_b \rangle \\ & + \langle s_a | \left([\mathbf{H}\mathbf{r}_a] \frac{[\mu^a \mathbf{r}_a]}{r_a^3} \right) + \left([\mathbf{H}\mathbf{r}_b] \frac{[\mu^b \mathbf{r}_b]}{r_b^3} \right) + \left([\mathbf{H}\mathbf{r}_b] \frac{[\mu^a \mathbf{r}_a]}{r_a^3} \right) \\ & + \left([\mathbf{H}\mathbf{r}_b] \frac{[\mu^b \mathbf{r}_b]}{r_b^3} \right) | s_b \rangle \left. \right] + \frac{ie}{mc(1 + \Delta_{1,1})} \left[\langle \alpha s_a | \frac{([\mu^a \mathbf{r}_a] \mathbf{P})}{r_a^3} | s_b \rangle \right. \\ & \left. - \langle \alpha s_b | \frac{([\mu^b \mathbf{r}_b] \mathbf{P})}{r_b^3} | s_a \rangle \right]. \end{aligned} \quad (18)$$

Or, finally, in terms of the integrals which have been defined and evaluated in Appendix A,

$$\begin{aligned} \mathcal{H}_{0,0} = & \{ e^2/2ma_0c^2(1 + \Delta_{1,1}) \} [(2I_1 + I_2 + 2I_3 - I_4 - I_5 - 2I_6 - I_7 + I_8) \\ & \times (H_x \mu_x^a + H_y \mu_y^a + H_x \mu_x^b + H_y \mu_y^b) + (2I_1 + 2I_7 + 4I_6)(H_z \mu_z^a \\ & + H_z \mu_z^b)] \end{aligned} \quad (19)$$

which becomes, after substitution of numerical values from Appendix A

$$\begin{aligned} \mathcal{H}_{0,0} = & [2.418(H_x \mu_x^a + H_x \mu_x^b + H_y \mu_y^a + H_y \mu_y^b) + 2.500(H_z \mu_z^a \\ & + H_z \mu_z^b)] \times 10^{-5}. \end{aligned} \quad (20)$$

4. THE SECOND ORDER PERTURBATION TERM

For a calculation of the second order perturbation term the matrix elements $\mathcal{H}_{n,0}$ must be determined. ($\mathcal{H}_{0,n}$ may then be calculated from the relation $\mathcal{H}_{n,0}^* = \mathcal{H}_{0,n}$.) Before this calculation is performed it is useful to determine which terms will be zero. The part of the operator \mathcal{H}_q which may introduce terms which depend either on H or on μ consists of terms which contain the coordinates of one electron only. Therefore excited states in which both electrons are in an excited orbital need not be considered because of the orthogonality of the orbitals. It should be observed here that those matrix elements which would be zero for a correct choice of wave functions (for instance of wave functions which result from a correct S.C.F. treatment) because of general quantum mechanical considerations, will be assumed to be equal to zero in our calculations, although for our special choice of wave functions they might be slightly different from zero as a consequence of the incorrect choice of wave functions. The non-zero matrix elements are therefore

$$\begin{aligned} \mathcal{H}_{n,0} = & \frac{1}{2(1 + \Delta_{0,0})^{3/2}(1 \pm \Delta_{n,n})^{1/2}} \int \{ \phi_n^*(\mathbf{a}, \mathbf{q}) \pm \phi_n^*(\mathbf{b}, \mathbf{q}) \} \left[\frac{1}{2m} (\mathbf{P} - \frac{e}{c} \mathbf{A}_q)^2 + V \right] \\ & \times \{ s(\mathbf{a}, \mathbf{q}) + s(\mathbf{b}, \mathbf{q}) \} d\tau. \end{aligned} \quad (21)$$

Taking into account the appropriate phase factors, one may express these integrals in terms of

$$\left. \begin{aligned} \mathcal{H}_{n,aa} &= (2m)^{-1} \langle \phi_{na} | (\mathbf{P} - (e/c)\mathbf{A}_a)^2 | s_a \rangle, \\ \mathcal{H}_{n,bb} &= (2m)^{-1} \langle \phi_{nb} | (\mathbf{P} - (e/c)\mathbf{A}_b)^2 | s_b \rangle, \\ \mathcal{H}_{n,ab} &= (2m)^{-1} \langle e^{i\alpha} \phi_{na} | (\mathbf{P} - (e/c)\mathbf{A}_b)^2 + 2mV | s_b \rangle, \\ \mathcal{H}_{n,ba} &= (2m)^{-1} \langle e^{-i\alpha} \phi_{nb} | (\mathbf{P} - (e/c)\mathbf{A}_a)^2 + 2mV | s_a \rangle. \end{aligned} \right\} \quad (22)$$

Because we need to determine the coefficient of $(\mu\mathbf{H})$ in the square of equation (21), we have to calculate the parts of equation (22) which are proportional either to H or to μ . In order to determine which part of equation (22) is proportional to H we may consider the operator

$$\Omega(H) = \frac{1}{2m} (\mathbf{P})^2 - \frac{e}{2mc} ([\mathbf{H}\mathbf{r}]\mathbf{P}) + V(\mathbf{r}). \quad (23)$$

Now it is found that

$$\left. \begin{aligned} \mathcal{H}_{n,aa} &= \mathcal{H}_{n,bb} = 0, \\ \mathcal{H}_{n,ab} &= (-iE_0 a_0^2) \langle \alpha \phi_{na} | s_b \rangle, \\ \mathcal{H}_{n,ba} &= (iE_0 a_0^2) \langle \alpha \phi_{nb} | s_a \rangle. \end{aligned} \right\} \quad (24)$$

If atomic orbitals up to and including $n=3$ are considered it is found that only contributions from $2p_x$, $2p_y$, $3p_x$ and $3p_y$ atomic orbitals are obtained in the case that the minus sign is considered in equation (21) and contributions from $3d_{xz}$ and $3d_{yz}$ for the plus sign.

In order to determine which part of equation (22) is proportional to μ we must consider the operator

$$\Omega(\mu) = -\frac{e}{mc} \left\{ \frac{([\mu^a \mathbf{r}_a]\mathbf{P})}{r_a^3} + \frac{([\mu^b \mathbf{r}_b]\mathbf{P})}{r_b^3} \right\}. \quad (25)$$

After substitution of this operator into equation (22) it is found that the part which is different from zero becomes

$$\left. \begin{aligned} \mathcal{H}_{n,aa} &= -\frac{\hbar e i}{m c a_0^3} \int \phi_{na} \left\{ \frac{\mu_y^b (z_b x_a - x_b z_a) - \mu_x^b (z_b y_a - y_b z_a)}{r_b^3 r_a} \right\} s_a d\tau, \\ \mathcal{H}_{n,bb} &= -\frac{\hbar e i}{m c a_0^3} \int \phi_{nb} \left\{ \frac{\mu_y^a (z_a x_b - x_a z_b) - \mu_x^a (z_a y_b - y_a z_b)}{r_a^3 r_b} \right\} s_b d\tau, \\ \mathcal{H}_{n,ab} &= -\frac{\hbar e i}{m c a_0^3} \int \phi_{na} \left\{ \frac{\mu_y^a (z_a x_b - x_a z_b) - \mu_x^a (z_a y_b - y_a z_b)}{r_a^3 r_b} \right\} s_b d\tau, \\ \mathcal{H}_{n,ba} &= -\frac{\hbar e i}{m c a_0^3} \int \phi_{nb} \left\{ \frac{\mu_y^b (z_b x_a - x_b z_a) - \mu_x^b (z_b y_a - y_b z_a)}{r_b^3 r_a} \right\} s_a d\tau. \end{aligned} \right\} \quad (26)$$

The contribution of the functions $2p_x$ and $2p_y$ is obtained by substitution of the appropriate one of them into equations (24) and (25) and formation of the double product of one of the results and the complex conjugate of the other:

$$\mathcal{H}''(2p_x) = \mathcal{H}''(2p_y) = -\frac{e^2 R E_0 J_1 (J_2 - J_3) \{H_x(\mu_x^a + \mu_x^b) + H_y(\mu_y^a + \mu_y^b)\}}{2mc^2 a_0 (E_2 - E_0) (1 + \Delta_{0,0}) (1 - \Delta_{2,2})}. \quad (27)$$

Similarly, one obtains

$$\mathcal{H}''(3p_x) + \mathcal{H}''(3p_y) = -\frac{e^2 R E_0 J_4 (J_5 - J_6) \{H_x(\mu_x^a + \mu_x^b) + H_y(\mu_y^a + \mu_y^b)\}}{2mc^2 a_0 (E_3 - E_0) (1 + \Delta_{0,0}) (1 - \Delta_{3,3})}. \quad (28)$$

The J 's and Δ 's are integrals defined and evaluated in Appendix B.

From the numerical results of Appendix B it may now easily be predicted that the contribution of the 3d functions will be negligible compared to that of the 3p functions. In the case of 3d functions, namely, only the plus sign in equation (22) will yield a result different from zero and an expression is obtained which is completely analogous to equation (28) and where all quantities are nearly of the same magnitude, except for the term $(1 - \Delta_{3,3})$ in the numerator, which should be replaced by $(1 + \Delta_{3,3})$. Because the overlap integral is close to unity this makes the contribution of the 3d functions almost twenty times smaller than the contribution of the 3p functions. Therefore it has not been taken into account.

Insertion of numerical values from Appendix B now yields

$$\begin{aligned}\mathcal{H}''(2p_x) + \mathcal{H}''(2p_y) &= 1.027\{H_x(\mu_x^a + \mu_x^b) + H_y(\mu_y^a + \mu_y^b)\} \times 10^{-5} \\ \mathcal{H}''(3p_x) + \mathcal{H}''(3p_y) &= 0.143\{H_x(\mu_x^a + \mu_x^b) + H_y(\mu_y^a + \mu_y^b)\} \times 10^{-5}\end{aligned}\quad (29)$$

where it has been assumed that the energy of the anti-bonding $2p_x$ and $3p_x$ orbitals are equal to E_0 , the errors which are introduced in this way being about 10 or 15 per cent (cf. Herzberg [15]).

5. DISCUSSION

Combination of equations (20) and (29) gives 2.445×10^{-5} for the first order perturbation term and 0.780×10^{-5} for the second order perturbation term, giving 3.225×10^{-5} for the total proton shielding constant. The most reliable values for the shielding constant are 2.774×10^{-5} following from Ishiguro and Koide's calculation [11] and 2.68×10^{-5} following from a combination of Anderson's treatment [4] and Ramsay's considerations [8].

It should be stressed that it is not our intention to suggest a better value for σ_H than has been reported previously, but just to suggest a simple method for calculating shielding constants which may easily be extended to more complicated systems and which does not involve too many computational difficulties. For instance, Ishiguro and Koide's calculations from James-Coolidge wave functions cannot be extended to more complicated molecules than hydrogen, whereas Ramsay's treatment requires a knowledge of the value of the rotational magnetic field at the position of the nucleus, which has been determined for a limited number of compounds only. Because of a rather inadequate choice of origin for the vector potential in Ramsay's formula, his paramagnetic part is expressed as a very slowly convergent series, which renders a direct calculation of this term rather difficult.

A remark should be made about the convergence of the series occurring in equation (8). Although the numerator in each term is practically equal to the ionization energy of the hydrogen molecule, it should be expected that the denominators will decrease rapidly with increasing n , namely in the same ratio as the overlap integrals between the functions $x.(1s)_n$ and the functions $(np_n)_n$. Although no general proof has been offered for the rapid convergence of this series our opinion is confirmed by the result of equation (29).

It is regrettable that our method is restricted to cases where the wave functions are constructed from atomic orbitals, but on the other hand it seems encouraging that with our crude description of the hydrogen molecule already an accuracy between 15 and 20 per cent. has been achieved. Our result might be improved by including more configurations in the wave functions; it seems that an inclusion of $2p\sigma$ orbitals in the description of the ground state will tend to lower the result.

It may be expected that similar calculations for more complicated molecules with the aid of Hartree-Fock wave functions will yield similarly accurate results. Investigations along these lines are in progress.

It is a pleasure to express my gratitude to Dr. R. G. Parr for his stimulating interest and many helpful suggestions and comments during the calculations and to the members of our quantum chemistry group, especially Dr. T. Arai and Mr. L. Snyder for many inspiring discussions.

APPENDIX A

The integrals which occur in the expression for the first order perturbation term are

$$\Delta_{11} = \int s_a s_b d\tau = e^{-R}(1 + R + \frac{1}{3}R^2) \quad (A1)$$

$$I_1 = \int s_a (x_a^2/r_a^3) s_a d\tau = \frac{1}{3} \quad (A2)$$

$$I_2 = \int s_a r_b^{-1} s_a d\tau = R^{-1}\{1 - e^{-2R}(1 + R)\} \quad (A3)$$

$$I_3 = \int s_a r_a^{-1} s_b d\tau = e^{-R}(1 + R) \quad (A4)$$

$$I_4 = \int s_a (x_b^2/r_b^3) s_a d\tau \quad (A5)$$

$$I_5 = \int s_b (Rz_a/r_a^3) s_b d\tau \quad (A6)$$

$$I_6 = \int s_a (x_a^2/r_a^3) s_b d\tau \quad (A7)$$

$$I_7 = \int s_a (Rz_a/r_a^3) s_b d\tau \quad (A8)$$

$$I_8 = \int s_a (R^2 x_a^2/r_a^3 r_b) s_b d\tau \quad (A9)$$

where the subscripts a and b of the $(1s)$ functions s and of the coordinates indicate that they should be taken with respect to the nuclei A and B ; the z -axis is taken along the line AB and R is the distance AB . All lengths are expressed in atomic units.

The integral I_4 may be written as

$$I_4 = \frac{1}{\pi} \int \frac{r^4 \sin^2 \theta \cos^2 \phi \sin \theta e^{-2r}}{(R^2 + r^2 - 2Rr \cos \theta)^{3/2}} dr d\theta d\phi. \quad (A10)$$

The integration over θ may be replaced by an integration over t if r is kept constant, where

$$t = (R^2 + r^2 - 2Rr \cos \theta)^{1/2}. \quad (A11)$$

Then, after integration over ϕ it is found that

$$I_4 = \frac{1}{4R^3} \int_0^\infty r e^{-2r} dr \int_{|R-r|}^{R+r} [-t^2 + 2(R^2 + r^2) - (R^2 - r^2)^2 t^{-2}] dt \quad (A12)$$

$$= (4/3R^3) \left\{ \int_0^R r^4 e^{-2r} dr + \int_R^\infty R^3 r e^{-2r} dr \right\} \quad (A13)$$

$$= \frac{1}{R^3} - R^{-2R} \left(\frac{1}{R^3} + \frac{2}{R^2} + \frac{2}{R} + 1 \right). \quad (A14)$$

Analogously, I_5 may be written as

$$I_5 = \pi^{-1} \int R \cos \theta e^{-2r} dr \sin \theta d\theta d\phi \quad (A15)$$

which may be reduced to

$$\begin{aligned} I_5 = (8R)^{-1} & \left[\int_0^R \{-(8R+4) + (8R^2+12R+6)r^{-1} - (4R^2+6R+3)r^{-2}\} e^{-2R+2r} dr \right. \\ & + \int_0^\infty \{(8R+4) + (\theta R^2+12R+6)r^{-1} + (4R^2+6R+3)r^{-2}\} e^{-2R-2r} dr \\ & \left. + \int_R^\infty \{(8R-4) + (-8R^2+12R-6)r^{-1} + (-4R^2+6R-3)r^{-2}\} e^{2R-2r} dr \right]. \end{aligned} \quad (A16)$$

The last two terms of each integral seem to present some difficulties if they are considered separately, but if they are all taken together the result is finite:

$$I_5 = \frac{1}{R} - e^{-2R} \left(\frac{1}{R} + 2 + 2R \right). \quad (A17)$$

The integrals I_6 and I_7 cannot be obtained in closed form. However,

$$I_6 = \pi^{-1} \int e^{-r} e^{-tr} r \sin^3 \theta \cos^2 \phi dr d\theta d\phi \quad (A18)$$

may be reduced to

$$\begin{aligned} I_6 = R^{-3} & \left[\int_0^\infty \{(2R+2)r + (4R^2+12R+12) + (2R^3+12R^2+30R+30)r^{-1} \right. \\ & + (2R^3+12R^2+30R+30)r^{-2}\} e^{-R-2r} dr + \int_0^R \{(2R+2)r - (4R^2 \\ & + 12R+12) + (2R^3+12R^2+30R+30)r^{-1} - (2R^3+12R^2+30R \\ & + 30)r^{-2}\} e^{-R} dr + \int_R^\infty \{(2R-2)r + (-4R^2+12R-12) + (2R^3-12R^2 \\ & + 30R-30)r^{-1} + (2R^3-12R^2+30R-30)\} e^{R-2r} dr \left. \right]. \end{aligned} \quad (A19)$$

This may be expressed in terms of the functions

$$-Ei(-x) = \int_x^\infty (e^{-t}/t) dt \quad (A20)$$

$$Q(R) = \int_0^R \frac{1 - e^{-2r}}{r} dr = \sum_{n=1}^{\infty} \frac{(-1)^{n+1} 2^n R^n}{n! n} \quad (A21)$$

so that I_6 becomes

$$\begin{aligned} I_6 = e^{-R} & (30R^{-3} + 30R^{-2} + 12R^{-1} + 2)Q(R) - \{(30R^{-3} - 30R^{-2} + 12R^{-1} \\ & - 2)e^R - (30R^{-3} + 30R^{-2} + 12R^{-1} + 2)e^{-R}\} Ei(-2R) - (60R^{-2} \\ & + 30R^{-1} + 7)e^{-R}. \end{aligned} \quad (A22)$$

Analogously I_7 is found to be

$$\begin{aligned} I_7 = e^{-R} & (6R^{-1} + 6 + 2R)Q(R) - \{(6R^{-1} - 6 + 2R)e^R \\ & - (6R^{-1} + 6 + 2R)e^{-R}\} Ei(-2R) - (12 + 6R)e^{-R} \end{aligned} \quad (A23)$$

and I_8 is

$$\begin{aligned} I_8 = R^{-1} & [(2R^2 + 6R + 6)e^{-R}Q(R) - \{(2R^2 - 6R + 6)e^R \\ & - (2R^2 + 6R + 6)e^{-R}\} Ei(-2R) - (6R^2 + 12R)e^{-R}]. \end{aligned} \quad (A24)$$

In the case of hydrogen $R=1.40$, so that

$$Q(1.40)=1.623\ 690\ 375. \quad (\text{A25})$$

The numerical values of the integrals are

$$\begin{aligned} I_1 &= 0.333\ 333\ 333 \\ I_2 &= 0.610\ 039\ 893 \\ I_3 &= 0.591\ 832\ 713 \\ I_4 &= 0.132\ 537\ 720 \\ I_5 &= 0.378\ 961\ 655 \\ I_6 &= 0.178\ 468\ 200 \\ I_7 = I_8 &= 0.228\ 724\ 196 \\ \Delta_{1,1} &= 0.752\ 947\ 3 \end{aligned} \quad (\text{A26})$$

APPENDIX B

The integrals in terms of which the second order perturbation term is expressed are

$$J_1 = (4\pi\sqrt{2})^{-1} \int e^{-ra} x^2 e^{-rb/2} d\tau \quad (\text{B1})$$

$$J_2 = (4\pi\sqrt{2})^{-1} \int e^{-ra/2} (x^2/r_a^3 r_b) e^{-rb} d\tau \quad (\text{B2})$$

$$J_3 = (4\pi\sqrt{2})^{-1} \int e^{-rb/2} (x^2/r_a^3 r_b) e^{-rb} d\tau \quad (\text{B3})$$

$$J_4 = (\sqrt{2}/81\pi) \int e^{-ra} (6-r_b) x^2 e^{-rb/3} d\tau \quad (\text{B4})$$

$$J_5 = (\sqrt{2}/81\pi) \int e^{-ra/3} (6-r_a) (x^2/r_a^3 r_b) e^{-rb} d\tau \quad (\text{B5})$$

$$J_6 = (\sqrt{2}/81\pi) \int e^{-rb/3} (6-r_a) (x^2/r_a^3 r_b) e^{-rb} d\tau \quad (\text{B6})$$

$$\Delta_{2,2} = (32\pi)^{-1} \int x^2 e^{-ra/2} e^{-rb/2} d\tau \quad (\text{B7})$$

$$\Delta_{3,3} = (2/3^8\pi) \int (6-r_a)(6-r_b) x^2 e^{-ra/3} e^{-rb/3} d\tau. \quad (\text{B8})$$

The integrals J_1 , J_4 , $\Delta_{2,2}$ and $\Delta_{3,3}$ are tabulated in various places, they may easily be calculated by means of elliptical coordinates.

The calculation of J_3 and J_4 may be carried out according to the methods which have been discussed in Appendix A. One finds

$$\begin{aligned} J_2 = (2R^2\sqrt{2})^{-1} [& \{6e^{-R/2} - 2(R^2 + 3R + 3)e^{-R}\} \\ & + \frac{1}{2}(R^2 + 3R + 3)e^{-R} S(R) - \frac{1}{2}\{(R^2 - 3R + 3)e^R \\ & - (R^2 + 3R + 3)e^{-R}\} Ei(-\frac{3}{2}R) + \frac{1}{3}\{(8R + 8)e^{-R} \\ & - (4R + 8)e^{-R/2}\}] \end{aligned} \quad (\text{B9})$$

where

$$S(R) = \sum_{n=1}^{\infty} \frac{1 + (-1)^{n+1} 3^n R^n}{2^n \cdot n \cdot n!}. \quad (\text{B10})$$

Furthermore

$$J_3 = (27R^3\sqrt{2})^{-1} [4 - (4 + 6R)e^{-3R/2} + 9R^2e^{-3R/2} + (27/2)Ei(-\frac{3}{2}R)] \quad (B11)$$

$$\begin{aligned} J_5 = (2\sqrt{2}/81R^2) [& \{36e^{-R/3} - (12R^2 + 36R + 36)e^{-R}\} \\ & + (3R^2 + 9R + 9)e^{-R}T(R) - \{(3R^2 - 9R + 9)e^R \\ & - (3R^2 + 9R + 9)e^{-R}\}Ei(-\frac{4}{3}R) - 1/16\{(189R + 279)e^{-R/3} \\ & - (12R^2 + 279R + 279)e^{-R}\}] \end{aligned} \quad (B12)$$

where

$$T(R) = \sum_{n=1}^{\infty} \frac{2^n}{3^n} \frac{1 + (-1)^{n+1} 2^n R^n}{n! n} \quad (B13)$$

and

$$\begin{aligned} J_6 = (4\sqrt{2}/243R^3) [& \frac{81}{32} - (\frac{81}{32} + \frac{63}{16}R - \frac{3}{4}R^2)e^{-4R/3} + 6R^2e^{-4R/3} \\ & + 9R^3Ei(-\frac{4}{3}R)] \end{aligned} \quad (B14)$$

so that

$$\begin{aligned} J_1 &= 0.677\,573\,197 \\ J_2 &= 0.053\,717\,711 \\ J_3 &= 0.029\,721\,271 \\ J_4 &= 0.256\,475\,909 \\ J_5 &= 0.030\,312\,435 \\ J_6 &= 0.015\,938\,612 \\ \Delta_{2,2} &= 0.952\,880\,97 \\ \Delta_{3,3} &= 0.924\,285\,66 \end{aligned} \quad (B15)$$

APPENDIX C

Although the expression equation (8) is a well known formula of perturbation theory the conditions under which it has been used for this work are slightly different from the usual case, and also the matrix elements are defined in a slightly unusual way. Therefore it may be of interest to give the derivation of equation (8) in the present circumstances, although the procedure is completely analogous to perturbation theory.

Let us consider a system, which in the absence of a magnetic field has the Hamiltonian $\mathcal{H}^{(0)}$ and the eigenfunctions $\psi_k^{(0)}$:

$$\mathcal{H}^{(0)}\psi_k^{(0)} = E_k^{(0)}\psi_k^{(0)}. \quad (C1)$$

For the sake of simplicity it will be assumed that there is no degeneracy.

In the presence of a magnetic field the Hamiltonian, eigenfunctions and eigenvalues will be

$$\begin{aligned} \mathcal{H} &= \mathcal{H}^{(0)} + H\mathcal{H}_q^{(1)} + \mu\mathcal{H}^{(2)} + \mu H\mathcal{H}_q^{(3)} \\ E_k &= E_k^{(0)} + HE_k^{(1)} + \mu E_k^{(2)} + \mu HE_k^{(3)} + \dots \\ \tilde{\psi}_k &= \tilde{\psi}_k^{(0)} + H\tilde{\psi}_k^{(1)} + \mu\tilde{\psi}_k^{(2)} + \mu H\tilde{\psi}_k^{(3)} + \dots \end{aligned} \quad (C2)$$

where the subscript q in the Hamiltonian means that \mathbf{q} is the origin of the vector potential and $\tilde{\psi}_k^{(0)}$ is the wave function $\psi_k^{(0)}$ multiplied by the appropriate phase factor (see § 2), so that $\tilde{\psi}_k^{(i)}$ depends on \mathbf{q} and H . The functions $\tilde{\psi}_k^{(1)}\tilde{\psi}_k^{(2)}$ and

$\tilde{\psi}_k^{(3)}$ will be developed in terms of the wave functions $\tilde{\psi}_k^{(0)}$ which form a complete set:

$$\begin{aligned}\tilde{\psi}_k^{(1)} &= \sum_m a_{km} \tilde{\psi}_m^{(0)} \\ \tilde{\psi}_k^{(2)} &= \sum_n b_{kn} \tilde{\psi}_n^{(0)} \\ \tilde{\psi}_k^{(3)} &= \sum_r c_{kr} \tilde{\psi}_r^{(0)}.\end{aligned}\quad (C3)$$

Before performing the derivation of equation (8) it will be observed that

$$\langle \tilde{\psi}_i^{(0)} | \tilde{\psi}_j^{(0)} \rangle = \delta_{ij}. \quad (C4)$$

The matrix elements $\langle \tilde{\psi}_i^{(0)} | \mathcal{H}^{(\alpha)} | \tilde{\psi}_j^{(0)} \rangle$ are functions of the magnetic field H . They may be expressed as a power series of H :

$$\langle \tilde{\psi}_i^{(0)} | \mathcal{H}^{(\alpha)} | \tilde{\psi}_j^{(0)} \rangle = \sum_{n=0}^{\infty} \langle \tilde{\psi}_i^{(0)} | \mathcal{H}^{(\alpha)} | \tilde{\psi}_j^{(0)} \rangle_n H^n. \quad (C5)$$

The Schrödinger equation of the perturbed system is

$$\begin{aligned} & [\{ \mathcal{H}^{(0)} + H \mathcal{H}_q^{(0)} + \mu \mathcal{H}^{(2)} + \mu H \mathcal{H}^{(3)} \} - \{ E_k^{(0)} + H E_k^{(1)} + \mu E_k^{(2)} + \mu H E_k^{(3)} + \dots \}] \\ & \times [\tilde{\psi}_k^{(0)} + H \sum_m a_{km} \tilde{\psi}_m^{(0)} + \mu \sum_n b_{kn} \tilde{\psi}_n^{(0)} + \mu H \sum_r c_{kr} \tilde{\psi}_r^{(0)} + \dots] = 0. \end{aligned} \quad (C6)$$

If this expression is multiplied by $\tilde{\psi}_l^{(0)*}$ and integrated it should be identically zero, so that the coefficients of H and μ are zero. This yields for the ground state

$$\begin{aligned} & \langle \tilde{\psi}_l^{(0)} | \mathcal{H}^{(0)} | \tilde{\psi}_0^{(0)} \rangle_1 - \langle \tilde{\psi}_l^{(0)} | E_0^{(0)} | \tilde{\psi}_0^{(0)} \rangle_1 + \langle \tilde{\psi}_l^{(0)} | \mathcal{H}_q^{(1)} | \tilde{\psi}_0^{(0)} \rangle_0 \\ & - \langle \tilde{\psi}_l^{(0)} | E_0^{(1)} | \tilde{\psi}_0^{(0)} \rangle_0 + \sum_m a_{0m} \langle \tilde{\psi}_l^{(0)} | \mathcal{H}^{(0)} | \tilde{\psi}_m^{(0)} \rangle_0 - \sum_m a_{0m} \langle \tilde{\psi}_l^{(0)} | E_0^{(0)} | \tilde{\psi}_m^{(0)} \rangle_0 = 0 \end{aligned} \quad (C7)$$

and

$$\begin{aligned} & \langle \tilde{\psi}_l^{(0)} | \mathcal{H}^{(2)} | \tilde{\psi}_0^{(0)} \rangle_0 - \langle \tilde{\psi}_l^{(0)} | E_0^{(2)} | \tilde{\psi}_0^{(0)} \rangle_0 + \sum_n b_{0n} \langle \tilde{\psi}_l^{(0)} | \mathcal{H}^{(0)} | \tilde{\psi}_n^{(0)} \rangle_0 \\ & - \sum_n b_{0n} \langle \tilde{\psi}_l^{(0)} | E_0^{(0)} | \tilde{\psi}_n^{(0)} \rangle_0 = 0. \end{aligned} \quad (C8)$$

It may then be found that

$$a_{0l} = \frac{\langle \tilde{\psi}_l^{(0)} | \mathcal{H}^{(0)} | \tilde{\psi}_0^{(0)} \rangle_1 + \langle \tilde{\psi}_l^{(0)} | \mathcal{H}_q^{(1)} | \tilde{\psi}_0^{(0)} \rangle_0}{E_0^{(0)} - E_l^{(0)}} \quad (C9)$$

$$b_{0l} = \frac{\langle \tilde{\psi}_l^{(0)} | \mathcal{H}^{(2)} | \tilde{\psi}_0^{(0)} \rangle_0}{E_0^{(0)} - E_l^{(0)}}. \quad (C10)$$

If equation (C6) is multiplied by $\tilde{\psi}_0^{(0)*}$ and an integration is performed, the coefficient of μH becomes

$$\begin{aligned} & \sum_r c_{0r} \langle \tilde{\psi}_0^{(0)} | \mathcal{H}^{(0)} | \tilde{\psi}_r^{(0)} \rangle_0 - \sum_r c_{0r} \langle \tilde{\psi}_0^{(0)} | E_0^{(0)} | \tilde{\psi}_r^{(0)} \rangle_0 + \sum_n b_{0n} \langle \tilde{\psi}_0^{(0)} | \mathcal{H}_q^{(1)} | \tilde{\psi}_n^{(0)} \rangle_0 \\ & - \sum_n b_{0n} \langle \tilde{\psi}_0^{(0)} | E_0^{(1)} | \tilde{\psi}_n^{(0)} \rangle_0 + \sum_m a_{0m} \langle \tilde{\psi}_0^{(0)} | \mathcal{H}^{(2)} | \tilde{\psi}_m^{(0)} \rangle_0 - \sum_m a_{0m} \langle \tilde{\psi}_0^{(0)} | E_0^{(2)} | \tilde{\psi}_m^{(0)} \rangle_0 \\ & + \sum_n b_{0n} \langle \tilde{\psi}_0^{(0)} | \mathcal{H}^{(0)} | \tilde{\psi}_n^{(0)} \rangle_1 - \sum_n b_{0n} \langle \tilde{\psi}_0^{(0)} | E_0^{(0)} | \tilde{\psi}_n^{(0)} \rangle_1 + \langle \tilde{\psi}_0^{(0)} | \mathcal{H}_q^{(3)} | \tilde{\psi}_0^{(0)} \rangle_0 \\ & - \langle \tilde{\psi}_0^{(0)} | E_0^{(3)} | \tilde{\psi}_0^{(0)} \rangle_0 + \langle \tilde{\psi}_0^{(0)} | \mathcal{H}^{(2)} | \tilde{\psi}_0^{(0)} \rangle_1 - \langle \tilde{\psi}_0^{(0)} | E_0^{(2)} | \tilde{\psi}_0^{(0)} \rangle_1 = 0. \end{aligned} \quad (C11)$$

This yields

$$\begin{aligned} E_0^{(3)} &= \langle \tilde{\psi}_0^{(0)} | \mathcal{H}_q^{(3)} | \tilde{\psi}_0^{(0)} \rangle_0 + \langle \tilde{\psi}_0^{(0)} | \mathcal{H}^{(2)} | \tilde{\psi}_0^{(0)} \rangle_1 + \sum_n b_{0n} \{ \langle \tilde{\psi}_0^{(0)} | \mathcal{H}_q^{(1)} | \tilde{\psi}_n^{(0)} \rangle_0 \\ & + \langle \tilde{\psi}_0^{(0)} | \mathcal{H}^{(0)} | \tilde{\psi}_n^{(0)} \rangle_1 \} + \sum_m a_{0m} \langle \tilde{\psi}_0^{(0)} | \mathcal{H}^{(2)} | \tilde{\psi}_m^{(0)} \rangle_0 \end{aligned} \quad (C12)$$

or, after substitution of (C9) and (C10)

$$\begin{aligned}
E_0^{(3)} = & \langle \tilde{\psi}_0^{(0)} | \mathcal{H}_a^{(3)} | \tilde{\psi}_0^{(0)} \rangle_0 + \langle \tilde{\psi}_0^{(0)} | \mathcal{H}^{(2)} | \tilde{\psi}_0^{(0)} \rangle_1 \\
& + \sum_l \frac{\langle \tilde{\psi}_0^{(0)} | \mathcal{H}^{(2)} | \tilde{\psi}_l^{(0)} \rangle \{ \langle \tilde{\psi}_l^{(0)} | \mathcal{H}^{(0)} | \tilde{\psi}_0^{(0)} \rangle_1 + \langle \tilde{\psi}_l^{(0)} | \mathcal{H}_a^{(1)} | \tilde{\psi}_0^{(0)} \rangle_0 \}}{E_0^{(0)} - E_l^{(0)}} \\
& + \sum_l \frac{\langle \tilde{\psi}_l^{(0)} | \mathcal{H}^{(2)} | \tilde{\psi}_0^{(0)} \rangle_0 \{ \langle \tilde{\psi}_0^{(0)} | \mathcal{H}_a^{(1)} | \tilde{\psi}_l^{(0)} \rangle_0 + \langle \tilde{\psi}_0^{(0)} | \mathcal{H}^{(0)} | \tilde{\psi}_l^{(0)} \rangle_1 \}}{E_0^{(0)} - E_l^{(0)}}
\end{aligned} \quad (C13)$$

which is equivalent to equation (8).

On étudie une méthode simplifiée pour le calcul de l'effet d'écran des protons dans les molécules en utilisant des fonctions d'onde construites à partir d'orbitales atomiques gauge-invariantes. On applique la méthode à la molécule d'hydrogène au moyen d'une représentation LCAO MO. La constante d'écran nucléaire totale calculée est $3,2 \times 10^{-5}$.

Eine vereinfachte Methode zur Berechnung der Protonenabschirmung in Molekülen wird beschrieben, bei der aus eichinvarianten Atomfunktionen aufgebaute Wellenfunktionen benutzt werden. Die Methode wird auf das Wasserstoffmolekül unter Benutzung einer einfachen LCAO MO Beschreibung angewandt. Die Kernabschirmungskonstante wird zu insgesamt $3,2 \times 10^{-5}$ berechnet.

REFERENCES

- [1] LAMB, W. E., 1941, *Phys. Rev.*, **60**, 817.
- [2] DICKINSON, W. C., 1950, *Phys. Rev.*, **80**, 563.
- [3] KNIGHT, W. D., 1949, *Phys. Rev.*, **76**, 1259.
- [4] ANDERSON, H. L., 1949, *Phys. Rev.*, **76**, 1460.
- [5] NEWELL, G. F., 1950, *Phys. Rev.*, **80**, 476.
- [6] HYLLEAAS, E., SKAVLEM, S., 1950, *Phys. Rev.*, **79**, 117.
- [7] RAMSAY, N. F., 1950, *Phys. Rev.*, **77**, 567.
- [8] RAMSAY, N. F., 1950, *Phys. Rev.*, **78**, 699.
- [9] DAS, T. P., and BERSOHN, R., 1956, *Phys. Rev.*, **104**, 849.
- [10] HORNIG, J. F., and HIRSCHFELDER, J. O., 1955, *J. chem. Phys.*, **23**, 474.
- [11] ISHIGURO, E., and KOIDE, S., 1954, *Phys. Rev.*, **94**, 350.
- [12] MCGARVEY, B. R., 1957, *J. chem. Phys.*, **27**, 68.
- [13] VAN VLECK, J. H., 1932, *The Theory of Electric and Magnetic Susceptibilities* (Oxford: University Press).
- [14] BOHM, D., 1955, *Quantum Theory* (New York: Prentice-Hall), p. 358.
- [15] HERZBERG, G., 1955, *Spectra of Diatomic Molecules* (New York: D. van Nostrand Company), p. 340.
- [16] RAMSAY, N. F., 1951, *Phys. Rev.*, **83**, 540.
- [17] LONDON, F., 1937, *J. Phys. Radium*, **8**, 397.

Nuclear spin coupling by electron orbital polarization

by J. A. POPLE

Department of Theoretical Chemistry, University of Cambridge

(Received 15 April 1958)

A theory is presented of the coupling of nuclear spins in a molecule by the induction of electronic orbital currents. An approximate expression for the contribution of this effect to the total coupling constant is derived in terms of the anisotropy of the magnetic screening of the nuclei involved. The theory is applied to some coupling constants involving fluorine nuclei, for which the electron orbital contribution is found to be an appreciable but not dominant part. It can have either sign, but is usually positive.

1. INTRODUCTION

The development of high resolution nuclear magnetic resonance (NMR) spectroscopy has led to a considerable amount of information on the coupling of nuclear spins in molecules. In fluid phases, where the direct dipole interaction of nuclear magnetic moments averages out, the resonance spectra show fine structure which can be interpreted in terms of an empirical Hamiltonian proportional to the scalar product of the nuclear spin vectors. This coupling occurs through the electronic structure, either by virtue of currents induced by the nuclear magnetic moments or by polarization of the electron spins.

The first satisfactory quantitative theory of the effect in the hydrogen molecule was given by Ramsey and Purcell [1] who showed that the polarization of electron spins by the Fermi or 'contact' term in the Hamiltonian was most important. In a later paper, Ramsey [2] gave a complete theory of both the spin and orbital contributions to the interaction, which confirmed the dominant role of the spin part in H_2 . The general method, however, involves integrals over many-electron wave functions for which explicit forms have to be taken in applications to complex molecules. McConnell [3] developed the analysis further, using molecular orbital theory, each molecular orbital being expressed as a linear combination of atomic orbitals (LCAO). This enabled the total effect to be broken down into localized parts. McConnell's work confirmed that nuclear spin coupling via electron orbital motion was negligible for proton-proton interactions, but suggested that significant contributions of this type might occur for other atoms.

The aim of this paper is to develop an approximate relation between the orbital contribution to spin-coupling constants and certain features of the theory of nuclear magnetic screening in an external field (which determines the 'chemical shift' in NMR). It is found that orbital contributions may be large if the screening constant for either of the two nuclei is highly *anisotropic*. The quantitative relationship then permits estimates of the spin-coupling term to be made from measurements or calculations of this anisotropy, together with the geometrical details of the molecule.

In developing the theory of nuclear spin coupling, it is useful to think of one nucleus as a magnetic probe investigating the magnetic polarization (here orbital currents) produced by the other. We shall proceed, therefore, by first considering the distribution of current induced by a single nucleus (§ 2) and follow this with the approximate calculation of the coupling constant in § 3. In the final section, the theory is applied to some interactions involving fluorine nuclei.

2. ELECTRONIC ORBITAL CURRENTS INDUCED BY A NUCLEAR MAGNETIC MOMENT

The motion of electrons in any magnetic field is determined by the Hamiltonian

$$\mathcal{H} = \sum_j \frac{1}{2m} \left(\mathbf{p}_j + \frac{e}{c} \mathbf{A}_j \right)^2 + V \quad (2.1)$$

where \mathbf{p}_j is the momentum of electron j and \mathbf{A}_j the corresponding value of the vector potential. V is the electrostatic potential energy. If the vector potential \mathbf{A} is just that of a single nucleus with a magnetic moment $\gamma \hbar \mathbf{I}$ (γ being the magnetogyric ratio and \mathbf{I} the nuclear spin vector), so that

$$\mathbf{A} = \gamma \hbar r^{-3} (\mathbf{I} \times \mathbf{r}), \quad (2.2)$$

the current could be found from the expectation value of the current density operator using the Hamiltonian (2.1). However, it is possible to get a rough idea of the distribution of current and its effect on spin-coupling without solving this quantum-mechanical problem in detail. This is because there is a connection between the theory of currents induced by a nuclear moment and the theory of the magnetic screening of a nucleus in an external uniform field. In particular, we shall find that the *total* magnetic moment of the current induced by the nucleus can be related to the theory of the screening constant. Suppose we seek the energy of the system in the field of both the nuclear moment (potential \mathbf{A}') and a uniform field (potential \mathbf{A}'') so that

$$\mathbf{A} = \mathbf{A}' + \mathbf{A}''. \quad (2.3)$$

If this vector potential is treated as a perturbation and the energy expansion carried to second order, the cross term between \mathbf{A}' and \mathbf{A}'' will give the interaction energy of the currents induced by the dipole with the external field, and therefore the corresponding dipole moment.

But this same cross term is also equal to the interaction energy between the nuclear magnetic dipole and the currents induced by the external field. This is exactly what is measured in a nuclear resonance experiment on the electronic screening constant (if there are no complications due to spin-coupling). In fact, if the uniform field is H_i (using Greek letters for tensor suffixes), the field at the nucleus will be reduced to

$$H_\alpha - \sigma_{\alpha\beta} H_\beta \quad (2.4)$$

where $\sigma_{\alpha\beta}$ is the dimensionless screening tensor such that $-\sigma_{\alpha\beta} H_\beta$ is the magnetic field at the nucleus due to the induced currents. Thus the orbital magnetic moment induced by a nuclear moment $\gamma \hbar \mathbf{I}_\alpha$ must be

$$-\gamma \hbar \sigma_{\alpha\beta} I_\beta. \quad (2.5)$$

This, of course, is the total magnetic moment of all the electronic currents and does not specify their distribution within the molecule. The most convenient way of doing this is to divide the total into individual atomic contributions. This is only an approximate procedure, likely to be realistic if the principal circulations occur within atoms, rather than from one atom to another. (The

ring currents of aromatic hydrocarbons, for example, could not be well represented in this way.) In most cases, the greater part of the total moment will be due to electronic currents in the atom possessing the magnetic nucleus. This might not be true for hydrogen, where the number of atomic electrons is low, but the currents induced by hydrogen nuclei are small in any case. For other nuclei, however, we may approximate the local moment by the total moment (2.5).

The magnetic moments of circulations on other atoms can be found approximately if it is assumed that an atomic magnetic susceptibility can be defined for each. Thus, if there is an atom with susceptibility χ_i at the point \mathbf{R}_i , the induced moment will be

$$\boldsymbol{\mu}_i = \gamma \hbar \{3(\mathbf{I} \cdot \mathbf{R}_i)\mathbf{R}_i - R_i^2 \mathbf{I}\} R_i^{-5} \chi_i. \quad (2.6)$$

It should be noted that χ_i is usually negative (diamagnetism).

3. NUCLEAR SPIN-COUPLING CONSTANTS

Consider now a molecule with two nuclei possessing magnetic moments $\gamma \hbar \mathbf{I}$ and $\gamma' \hbar \mathbf{I}'$, the position vector of the second relative to the first being \mathbf{R} . Then the coupling energy via electron orbital polarization is equal to twice the interaction of the moment of the second nucleus with the currents induced by the first (the interaction of the first with the currents induced by the second being the same by a reciprocal theorem). These currents can be divided into

- (a) currents on the atom with $\gamma \hbar \mathbf{I}$ as nucleus,
- (b) currents on the atom with $\gamma' \hbar \mathbf{I}'$ as nucleus,
- (c) currents on all other atoms.

We have already seen that currents of type (a) have a moment $-\gamma \hbar \sigma_{\alpha\beta} \mathbf{I}_\beta$ which is conveniently located at the nucleus. The corresponding magnetic field at the second nucleus is $\gamma \hbar \epsilon_{\alpha\beta} \sigma_{\beta\gamma} \mathbf{I}_\gamma$, $\epsilon_{\alpha\beta}$ being the dipole interaction tensor

$$\epsilon_{\alpha\beta} = \{R^2 \delta_{\alpha\beta} - 3R_\alpha R_\beta\} R^{-5}. \quad (3.1)$$

The secondary field due to currents of type (b) can be expressed in terms of the screening constant of the second nucleus $\sigma_{\beta\gamma}'$. Since the unscreened field is $-\gamma \hbar \epsilon_{\beta\gamma} \mathbf{I}_\gamma$, the contribution of screening is $\gamma \hbar \epsilon_{\alpha\beta} \sigma_{\beta\gamma}' \mathbf{I}_\gamma$.

The effect of currents on other atoms can also be estimated by a dipole approximation using (2.6). Let \mathbf{R}_i and \mathbf{R}_i' be the position vectors of any third nucleus relative to the two under investigation. If $\epsilon_{i\alpha\beta}$ and $\epsilon_{i\alpha\beta}'$ are the tensors corresponding to (3.1) but with \mathbf{R} replaced by \mathbf{R}_i or \mathbf{R}_i' , the moment induced in atom i is $-\gamma \hbar \epsilon_{i\alpha\beta} \mathbf{I}_\beta \chi_i$ and the field at the nucleus $\gamma \hbar \mathbf{I}'$ is $\gamma \hbar \chi_i \epsilon_{i\alpha\beta} \epsilon_{i\beta\gamma}' \mathbf{I}_\gamma$.

Adding these three contributions and multiplying by the required factor of two, we get the interaction energy of the two nuclei via electron orbital motion in the form $T_{\alpha\gamma} \mathbf{I}_\alpha \mathbf{I}_\gamma'$ where

$$T_{\alpha\gamma} = -2\gamma\gamma' \hbar^2 [\epsilon_{\alpha\beta} (\sigma_{\beta\gamma} + \sigma_{\beta\gamma}') + \sum_i^* \epsilon_{i\alpha\beta} \epsilon_{i\beta\gamma}' \chi_i]. \quad (3.2)$$

Here \sum_i^* is a sum over all other atoms.

When averaged over all directions of the molecular axes relative to the spins \mathbf{I} and \mathbf{I}' , $T_{\alpha\gamma} \mathbf{I}_\alpha \mathbf{I}_\gamma'$ takes the form $\hbar J^{(\text{orb})} \mathbf{I} \cdot \mathbf{I}'$ where the constant $J^{(\text{orb})}$ is the orbital contribution to the spin-coupling constant (measured in cycles/sec) and has the value

$$J^{(\text{orb})} = \frac{2}{3} \hbar^{-1} T_{\alpha\alpha} = -\frac{2}{3} \hbar^{-1} \gamma\gamma' \hbar^2 [\epsilon_{\alpha\beta} (\sigma_{\alpha\beta} + \sigma_{\alpha\beta}') + \sum_i^* \epsilon_{i\alpha\beta} \epsilon_{i\alpha\beta}' \chi_i]. \quad (3.3)$$

The quantity

$$\epsilon_{\alpha\beta}\sigma_{\alpha\beta} = R^{-5}\{R^2\sigma_{\alpha\alpha} - 3R_{\alpha}R_{\beta}\sigma_{\alpha\beta}\} \quad (3.4)$$

will only be non-zero if the tensor $\sigma_{\alpha\beta}$ is anisotropic. This is clear on qualitative grounds, for if it were isotropic, the corresponding nucleus would merely behave as if it had a reduced but *constant* moment $\gamma\hbar\mathbf{I}(1-\sigma)$ and the interaction would average to zero on rotation as with the permanent moment only.

The part of (3.2) involving the screening tensors can be simplified if we suppose that the environment of each nucleus is *axially symmetric*. There will then be only two principal values σ_{\parallel} and σ_{\perp} and we may write

$$\Delta\sigma = \sigma_{\parallel} - \sigma_{\perp} \quad (3.5)$$

for the anisotropy. On evaluation of the contracted product in the final term the full expression for $J^{(\text{orb})}$ takes the form

$$\begin{aligned} J^{(\text{orb})} = & -\frac{2}{3}\hbar^{-1}\gamma\gamma'\hbar^2\{R^{-3}[\Delta\sigma(1-3\cos^2\theta) + \Delta\sigma'(1-3\cos^2\theta')] \\ & - 3\sum_i^* \chi_i R_i^{-3} R_i'^{-3} (1-3\cos^2\theta_i)\} \end{aligned} \quad (3.6)$$

where θ and θ' are the respective angles between the symmetry axes of the screening tensors and the line joining the two magnetic nuclei. θ_i is the angle subtended at atom i by these two nuclei.

4. APPLICATIONS

The various quantities appearing in the expression (3.6) for the orbital coupling constant can all be found approximately either by calculation or empirically from other data. The theory can then be used as a simple method of estimating the magnitude of the orbital contribution in molecules.

Let us first consider the final term representing interaction via a third atom. For atoms such as carbon or nitrogen χ_i may be taken to be roughly -10^{-29} (from Pascal constants). For two protons ($\gamma=\gamma'=2.68 \times 10^4$) at distances of 10^{-8} cm on opposite sides of such an atom ($\theta_i=180^\circ$) we obtain a calculated contribution to $J^{(\text{orb})}$ of $+4.8$ c/s. These are extreme conditions and the magnitude will usually be smaller. It is reasonable to suppose, therefore, that the coupling via currents induced on a third atom will always be negligible.

The remaining part of the expression (3.7) depends on the screening anisotropies $\Delta\sigma$. Since the screening constants for protons spread over a smaller range than other nuclei, the orbital contributions to proton-proton coupling constants will be smaller than those involving other nuclei.

We shall apply the theory to some molecular groups involving fluorine nuclei on which there have been some theoretical [4] and experimental [5] studies of the screening anisotropy. The theory of Saika and Slichter [4] indicated that the screening of the ^{19}F nucleus was greater along the bond direction so that $\Delta\sigma$ is positive. Their calculations gave $\Delta\sigma = 3 \times 10^{-3}(1-i)$ where i is a measure of ionic character (varying from zero in F_2 to unity in a free F^- ion). For H-F or C-F bonds an intermediate value should be chosen and we shall take $\Delta\sigma = 10^{-3}$. (An indirect experimental determination for 1, 3, 5 trifluorobenzene gives

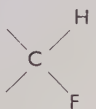
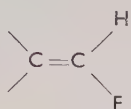
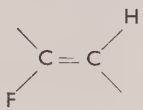
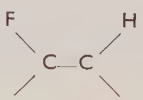
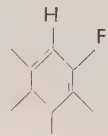
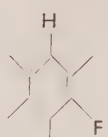
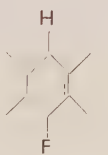
Compound	$J_{\text{HF}}^{(\text{orb})}$ (calc) (c/s)	J_{HF} (obs) (c/s)	Ref.
HF	+ 150	615	[6]
	+ 13.3	44 to 81	[7]
	+ 12.9	72 to 81	[8]
	+ 3.6	12 to 40	[8]
	0	1 to 8	[8]
	0	6 to 10†	[9]
	+ 1.0	6 to 8†	[9]
	+ 1.1	2†	[9]

Table 1. Calculated orbital contributions and observed total spin coupling constants between protons and ^{19}F nuclei.

† In some compounds *ortho* and *meta* constants were established to have the same sign. In others *ortho* and *para* constants have opposite signs.

$\Delta\sigma = 7.5 \times 10^{-4}$ [5].) If the screening anisotropy for hydrogen is neglected, the theory then gives

$$\left. \begin{aligned} J_{\text{HF}}^{(\text{orb})} &= 75.2R^{-3}(3\cos^2\theta - 1)10^{-24} \text{ c/s} \\ J_{\text{FF}}^{(\text{orb})} &= 70.8R^{-3}[(3\cos^2\theta - 1) + (3\cos^2\theta' - 1)]10^{-24} \text{ c/s} \end{aligned} \right\} \quad (4.1)$$

for the contributions to proton-fluorine and fluorine-fluorine constants respectively.

These formulae have been applied to nuclei in some simple molecular groups[†]; the results are given in tables 1 and 2 together with the observed total coupling

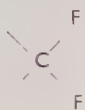
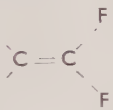
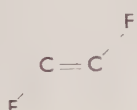
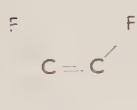
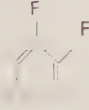
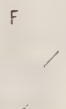

Compound	$J_{\text{FF}}^{(\text{orb})}$ (calc) (c/s)	$J_{\text{FF}}^{(\text{obs})}$ (c/s)	Ref.
	+ 13.3	158	[10]
	+ 13.8	27 to 87	[8]
	+ 5.2	115 to 124	[8]
	- 1.8	33 to 58	[8]
	- 1.7	20	[9]
	+ 1.6	2 to 4	[9]
	+ 1.7	12 to 15	[9]

Table 2. Calculated orbital contributions and observed total spin constants between ^{19}F nuclei.

[†] In these calculations F-H and C-H distances were taken as 1 Å, C-F and C=C as 1.35 Å and C \cdots C (aromatic) as 1.4 Å. Valence angles of $109\frac{1}{2}^\circ$ and 120° were assumed for tetrahedral and trigonal carbon atoms respectively.

constants. These calculations suggest that the orbital contribution is no longer a negligible part of the total but that it is still less important than the remaining contribution due to spin polarization. It is interesting to note that the equations (4.1) can lead to contributions of either sign but for most of the groups considered it is predicted to be positive. The signs of the observed values are not generally known, although different signs have been established for some meta and para H-F constants in substituted benzenes [9]. In fluorinated ethylenes, the theory leads to a larger coupling for nuclei in the *trans* configuration than for the *cis* as is found experimentally, but the calculated magnitudes are so small that this cannot be the principal cause of the difference.

On présente une théorie du couplage des spins nucléaires dans une molécule par induction de courants électroniques orbitaux. On a écrit une expression approchée, en fonction de l'anisotropie de l'effet d'écran des noyaux intéressés, de la contribution de cet effet à la constante de couplage totale. La théorie est appliquée à quelques constantes de couplage faisant intervenir des noyaux de fluor, pour lesquels la contribution électronique orbitale est appréciable mais non primordiale. Son signe est variable, mais généralement positif.

Eine Theorie der Koppelung der Kernspins in einem Molekül durch in den Elektronenbahnen induzierte Ströme wird entwickelt. Der Beitrag dieses Effekts zur Gesamtkopplungskonstanten wird angenähert durch die Anisotropie der kernmagnetischen Abschirmung bestimmt. Die Theorie wird auf einige Fluorkerne betreffende Kopplungskonstante angewandt, für welche der Beitrag der Elektronenbahnen zwar einen beträchtlichen, aber keinen überragenden Anteil liefert; dieser Beitrag kann beiderlei Vorzeichen haben, ist aber meistens positiv.

REFERENCES

- [1] RAMSEY, N. F., and PURCELL, E. M., 1952, *Phys. Rev.*, **85**, 143.
- [2] RAMSEY, N. F., 1953, *Phys. Rev.*, **91**, 303.
- [3] MCCONNELL, H. M., 1956, *J. chem. Phys.*, **24**, 460.
- [4] SAIKA, A., and SLICHTER, C. P., 1954, *J. chem. Phys.*, **22**, 26.
- [5] GUTOWSKY, H. S., and WOESSNER, D. E., 1956, *Phys. Rev.*, **104**, 843.
- [6] SOLOMON, I., and BLOEMBERGEN, N., 1956, *J. chem. Phys.*, **25**, 261.
- [7] MEYER, L. H., and GUTOWSKY, H. S., 1953, *J. phys. Chem.*, **57**, 481.
- [8] MCCONNELL, H. M., REILLY, C. A., and MCLEAN, A. D., 1956, *J. chem. Phys.*, **24**, 479.
- [9] GUTOWSKY, H. S., HOLM, C. H., SAIKA, A., and WILLIAMS, G. A., 1957, *J. Amer. chem. Soc.*, **79**, 4596.
- [10] DRYSDALE, J. J., and PHILLIPS, W. D., 1957, *J. Amer. chem. Soc.*, **79**, 319.

The effect of molecular interaction on magnetic shielding constants

by M. J. STEPHEN

Department of Theoretical Chemistry, University of Cambridge

(Received 2 December 1957)

The effect of molecular interactions on magnetic shielding constants in gases and liquids is considered using simple statistical mechanics and treating the molecules as points. For gases at ordinary pressures the effects are small. For liquids and solutions two effects may be important. (i) Magnetic moments induced in neighbouring molecules give rise to a magnetic field at the nucleus of the molecule considered. (ii) The electron distribution in the molecule may be distorted by the electric field due to neighbouring molecules and a change in the intramolecular shielding constant will then take place. The magnitude of these effects is estimated and their relative importance in different molecules is discussed.

1. INTRODUCTION

Most measurements of high resolution nuclear magnetic resonance spectra are made on liquid samples. It is important, in order to obtain the correct intramolecular shielding constant, to make allowance for effects such as volume susceptibility, sample shape and detailed solvent interactions on the resonance line position.

The influence of volume susceptibility and sample shape has been considered by Dickinson [1]. Bothner-By and Glick [2] have shown that detailed solvent or solute interactions are important for molecules having a large diamagnetic anisotropy, e.g. aromatic molecules. This they suggest is due to the magnetic moments induced in neighbouring molecules giving rise to a magnetic field at the nucleus of the molecule considered. Schneider *et al.* [3], in a study of magnetic shielding constants in vapours and liquids, have shown that where strong hydrogen bonds are formed in the liquid there is a large difference in shielding between the liquid and the gas after the correction considered by Dickinson [1] has been applied. Schneider *et al.* [3] have suggested that this is due to a modification of the intramolecular shielding constant by the strong electric field of the hydrogen bond.

In this paper the effect of molecular interactions on magnetic shielding constants in gases and liquids is considered using simple statistical mechanics and treating the molecules as points. For gases at ordinary pressures the effects are small but for liquids and solutions there will, in general, be an appreciable correction due to solvent interaction. Only in the case of isotropic solute and solvent molecules would Dickinson's classical correction be adequate.

2. THEORY

Consider a macroscopic specimen volume V_m (the molar volume) containing N (Avogadro's number) molecules all in their ground electronic state which is taken to be a totally symmetric singlet state. The whole specimen is in a uniform

magnetic field which has the value \mathbf{H}_0 at large distances from the specimen. The magnetic field which acts upon a molecule will be called the effective field. The discrepancy between the effective field which acts upon a molecule and the macroscopic magnetic field in the same neighbourhood is clearly due only to the contribution to the effective field of matter in the close neighbourhood of the molecule. Hence a sphere of radius R large compared with the dimensions of the molecule under discussion is drawn around this molecule. The difference between the macroscopic magnetic field \mathbf{H} acting on the molecule in the sphere and the field \mathbf{H}_0 at large distances from the sample is due to the matter contained within the sphere and the rest of the sample. It is easily shown (Dickinson [1]) that

$$\mathbf{H} = \mathbf{H}_0 \{1 - (N_1 - 4\pi/3)\kappa\} = \mathbf{H}_0 (1 - \alpha\kappa) \quad (1)$$

where κ is the volume susceptibility and N_1 is a shape factor. $N_1 = 2\pi$ for an infinite cylinder and $4\pi/3$ for a sphere. The magnetic field acting on the molecule due to neighbouring molecules must be considered microscopically and it is denoted by \mathbf{G} . Thus the total effective field acting on a molecule is $\mathbf{H} + \mathbf{G}$.

In order to obtain the magnetic shielding constant for a magnetic nucleus $\mu^{(i)}$ in molecule i the term in $\mu^{(i)}\mathbf{H}_0$ in the energy of molecule i is required. The energy of the i th molecule expanded in powers of the effective magnetic field (for a configuration τ of the specimen) in a tensor notation is

$$\begin{aligned} u(\tau\mathbf{FH}) = u(\tau) &- \mu_\alpha^{(i)}(H_\alpha + G_\alpha^{(i)}) + \sigma_{\alpha\beta}^{(i)}(H_\alpha + G_\alpha^{(i)})\mu_\beta^{(i)} \\ &- \frac{1}{2}\chi_{\alpha\beta}^{(i)}(H_\alpha + G_\alpha^{(i)})(H_\beta + G_\beta^{(i)}) - \zeta_{\alpha\beta\gamma}^{(i)}(H_\alpha + G_\alpha^{(i)})\mu_\beta^{(i)}F_\gamma^{(i)} \\ &- \phi_{\alpha\beta\gamma\delta}^{(i)}(H_\alpha + G_\alpha^{(i)})\mu_\beta^{(i)}F_\gamma^{(i)}F_\delta^{(i)} \dots \end{aligned} \quad (2)$$

$\sigma_{\alpha\beta}$ is the intramolecular shielding tensor, $\chi_{\alpha\beta}$ the diamagnetic susceptibility and $\zeta_{\alpha\beta\gamma}$ and $\phi_{\alpha\beta\gamma\delta}$ describe the effect of an electric field \mathbf{F} on the intramolecular shielding constant of the molecule. $\mathbf{G}^{(i)}$ and $\mathbf{F}^{(i)}$ are the magnetic and electric fields respectively due to all the other molecules at the molecule i .

The magnetic dipole moment $\mathbf{m}^{(i)}$ of molecule i is obtained from (2) by differentiation with respect to H_0 . Thus if \mathbf{e} is a unit vector in the direction of \mathbf{H}_0

$$\begin{aligned} m_\alpha^{(i)}e_\alpha = \{ &\mu_\alpha^{(i)} - \sigma_{\alpha\beta}^{(i)}\mu_\beta^{(i)} + \chi_{\alpha\beta}^{(i)}(H_\beta + G_\beta^{(i)}) + \zeta_{\alpha\beta\gamma}^{(i)}\mu_\beta^{(i)}F_\gamma^{(i)} \\ &+ \phi_{\alpha\beta\gamma\delta}^{(i)}\mu_\beta^{(i)}F_\gamma^{(i)}F_\delta^{(i)} \} \left\{ (1 - \alpha\kappa)e_\alpha + \frac{\partial G_\alpha^{(i)}}{\partial H_0} \right\}. \end{aligned} \quad (3)$$

The shielding constant for molecule i in the medium, denoted by $\Sigma^{(i)}$ to distinguish it from the intramolecular shielding constant $\sigma^{(i)}$, is given by (this is equivalent to the definition of Meyer *et al.* [4]):

$$1 - \Sigma^{(i)} = \overline{\left\langle \frac{\partial}{\partial \mu^{(i)}} m_\alpha^{(i)} e_\alpha \right\rangle} \quad (4)$$

where the bar implies an average over all directions of \mathbf{e} for $H_0 = \mu^{(i)} = 0$ and the angular brackets an average over all configurations τ with a Boltzmann type weighting factor appropriate to a molecule in zero external magnetic field.

The field $\mathbf{G}^{(i)}$ is supposed due only to point magnetic dipoles in neighbouring molecules. Thus

$$G_\alpha^{(i)} = - \sum_{j \neq i} \epsilon_{\alpha\beta}^{(ij)} m_\beta^{(j)} \quad (5)$$

where

$$\epsilon_{\alpha\beta}^{(ij)} = r_{ij}^{-5} (r_{ij}^2 \delta_{\alpha\beta} - 3r_{ij\alpha} r_{ij\beta}).$$

From (3) and (5)

$$\begin{aligned}\frac{\partial G_{\alpha}^{(i)}}{\partial H_0} &= - \sum_{j \neq i} \epsilon_{\alpha\beta}^{(ij)} \chi_{\beta\epsilon}^{(j)} e_{\epsilon} + O(\chi^2) \\ \frac{\partial G_{\alpha}^{(i)}}{\partial \mu^{(i)}} &= O(\chi^2).\end{aligned}\quad (6)$$

Substituting (6) and (3) in (4) and averaging over all directions of \mathbf{e} it is found (retaining only first order terms)

$$\Sigma^{(i)} = \alpha\kappa + \sigma^{(i)} + \frac{1}{3} \left\langle \sum_{j \neq i} \epsilon_{\alpha\beta}^{(ij)} \chi_{\alpha\beta}^{(j)} \right\rangle - \frac{1}{3} \zeta_{\alpha\alpha\gamma}^{(i)} \langle F_{\gamma}^{(i)} \rangle - \frac{1}{3} \phi_{\alpha\alpha\gamma\delta}^{(i)} \langle F_{\gamma}^{(i)} F_{\delta}^{(i)} \rangle \quad (7)$$

where $\sigma = \frac{1}{3} \sigma_{\alpha\alpha}$.

3. THE IMPERFECT GAS

For an imperfect gas the shielding constant is expanded in inverse powers of the molar volume V_m :

$$\Sigma^{(i)} = \Sigma_0^{(i)} + \Sigma_1^{(i)}/V_m + \dots \quad (8)$$

Σ_0 is the shielding constant for an isolated molecule in the medium and Σ_1 gives the influence of the interaction of the molecules in pairs. From (7) and (8)

$$\begin{aligned}\Sigma_0^{(i)} &= \alpha\kappa + \sigma^{(i)} \\ \Sigma_1^{(i)} &= \lim_{V_m \rightarrow \infty} (\Sigma^{(i)} - \Sigma_0^{(i)}) V_m.\end{aligned}\quad (9)$$

The terms involving the electric field \mathbf{F} in (7) are only important in liquids (see later) and so for gases these terms will be neglected. Two molecule types are now considered.

3.1. Spherical and tetrahedral molecules

For these molecules $\chi_{\alpha\beta} = \chi \delta_{\alpha\beta}$ and from (7)

$$\Sigma^{(i)} = \alpha\kappa + \sigma^{(i)} + O(\chi^2).$$

and so after correction for the bulk susceptibility (which will be small in gases) this reduces to the value for an isolated molecule.

3.2. Anisotropic molecules

For these molecules from (7) and (9)

$$\Sigma_1^{(i)} = \frac{1}{3} \lim_{V_m \rightarrow \infty} \left\langle \sum_{j \neq i} \epsilon_{\alpha\beta}^{(ij)} \chi_{\alpha\beta}^{(j)} \right\rangle V_m. \quad (10)$$

If the molecules are axially symmetric and there are two independent components of the susceptibility tensor χ^{\parallel} (along axis) and χ^{\perp} then (10) reduces to

$$\Sigma_1^{(i)} = \Delta\chi \lim_{V_m \rightarrow \infty} \left\langle \sum_{j \neq i} r_{ij}^{-3} \left(\frac{1}{3} - \cos^2 \theta_j \right) \right\rangle V_m \quad (11)$$

where $\Delta\chi = \chi^{\parallel} - \chi^{\perp}$ and θ_j is the angle between the axis of molecule j and the line joining nucleus $\mu^{(i)}$ and molecule j . Equation (11) has been evaluated for two types of axially symmetric molecule.

3.2.1. Molecules with permanent electric dipoles

The interaction energy between two molecules is taken to be of the Stockmayer [5] type, that is

$$u_{12} = 4\epsilon \left\{ \left(\frac{r_0}{r} \right)^{12} - \left(\frac{r_0}{r} \right)^6 \right\} + \frac{\mu_0^2}{r^3} (2 \cos \theta_1 \cos \theta_2 + \sin \theta_1 \sin \theta_2 \cos \phi)$$

where μ_0 is the permanent electric dipole moment of the molecule. After averaging in (11) it is found that

$$\Sigma_1^{(i)} = N\Delta\chi \left\{ -\left(\frac{\pi\tau^2}{1080}\right) H_9(y) + O(\tau^4) \right\}$$

where $\tau = \mu_0^2/\epsilon r_0^3$ and $y = 2(\epsilon/kT)^{1/2}$. The functions $H_n(y)$ have been tabulated by Buckingham and Pople [6].

For methyl fluoride at room temperature $\tau = 3.0$, $y = 1.6$ and $r_0 = 3.5 \text{ \AA}$ (Buckingham [7]) and thus $\Sigma_1^{(i)} = -0.63 N\Delta\chi$. This will only be an important correction at high pressures. Then taking $\Delta\chi = 10^{-29} \text{ e.m.u.}$, at atmospheric pressure $\Sigma_1^{(i)}/V_m = 1.5 \times 10^{-10}$.

3.2.2. Molecules with permanent electric quadrupoles

The interaction potential is assumed to comprise a Lennard-Jones 6:12 central force potential together with the electrostatic interaction energy of two quadrupoles that is (Buckingham [7])

$$u_{12} = 4\epsilon \left\{ \left(\frac{r_0}{r}\right)^{12} - \left(\frac{r_0}{r}\right)^6 \right\} + \frac{3\Theta^2}{4r^5} \{ 1 - 5 \cos^2 \theta_1 - 5 \cos^2 \theta_2 + 17 \cos^2 \theta_1 \cos^2 \theta_2 \\ + 16 \sin \theta_1 \sin \theta_2 \cos \theta_1 \cos \theta_2 \cos \phi + 2 \sin^2 \theta_1 \sin^2 \theta_2 \cos^2 \phi \}$$

where Θ is the permanent electric quadrupole moment. After averaging in (11) it is found that

$$\Sigma_1^{(i)} = N\Delta\chi \left\{ -\left(\frac{\pi\lambda^2}{252}\right) H_{13}(y) + O(\lambda^4) \right\}$$

where $\lambda = \Theta^2/\epsilon r_0^5$ and $y = 2(\epsilon/kT)^{1/2}$.

For carbon dioxide (the values would be similar for acetylene) at room temperature $\Theta = 3.5 \times 10^{-26} \text{ e.s.u.}$, $\epsilon/k = 182.4^\circ\text{K}$ and $r_0 = 3.94 \text{ \AA}$ (Buckingham [7]) and thus $\Sigma_1^{(i)} = -0.054 N\Delta\chi$. This will again only be important at high pressures.

4. LIQUIDS

As shown above, shielding constants measured in gases at ordinary pressures will lead to correct values for the intramolecular shielding constant. In order to isolate the shielding effect of interaction in the liquid after the bulk susceptibility correction has been applied $\Delta\Sigma^{(i)}$ is defined by $\Delta\Sigma^{(i)} = \Sigma^{(i)} - \alpha\kappa - \sigma^{(i)}$. Two types of molecule are now considered.

4.1. Isotropic molecules

For these molecules $\chi_{\alpha\beta} = \chi\delta_{\alpha\beta}$; $\zeta_{\alpha\beta\gamma} = 0$; $\phi_{1111} = \phi_{2222} = \phi_{3333} = \phi_a$; $\phi_{1122} = \phi_{1133}$ etc. = ϕ_b . From (7)

$$\Delta\Sigma^{(i)} = -(\phi_a + 2\phi_b)\langle F^2 \rangle. \quad (12)$$

Measurements on methane in liquid and vapour phase lead to identical shielding constants after correction for the bulk susceptibility has been made (Schneider *et al.* [3]). It is concluded that (12) is negligible. For the hydrogen atom (Marshall and Pople [8])

$$\phi_a = \frac{439}{120} \frac{a_0^3}{mc^2} = 6.6 \times 10^{-19} \text{ e.s.u.}, \\ \phi_b = \frac{193}{45} \frac{a_0^3}{mc^2} = 7.7 \times 10^{-19} \text{ e.s.u.}$$

and an upper bound to $\langle F^2 \rangle$ may be calculated in liquid methane. If the uncertainty in the results of Schneider *et al.* [3] is taken to be 0.10×10^{-6} or 4 c/s (which includes an uncertainty in the bulk susceptibility correction) and for ϕ_a and ϕ_b the exact values for the hydrogen atom are used then $\langle F^2 \rangle \leq 5 \times 10^{10}$ e.s.u. This compares well with the value of 10^{11} e.s.u. estimated by Buckingham and Stephen [9] from the latent heat of vaporization. $\langle F^2 \rangle$ would be expected to be less than 5×10^{10} e.s.u. for methane as ϕ_a and ϕ_b for methane would be larger than for the hydrogen atom.

4.2. Anisotropic molecules

For axially symmetric molecules with the 3 axis along the molecular axis the non-zero components of the tensors required in (7) are

$$\begin{aligned} \chi_{33} &= \chi^{\parallel}; & \zeta_{333} &= \zeta^{\parallel} \\ \chi_{11} &= \chi_{22} = \chi^{\perp}; & \zeta_{113} &= \zeta_{223} = \zeta^{\perp} \\ \phi_{1111} &= \phi_{2222}; & \phi_{3333}; & \phi_{1122} = \phi_{2211}; & \phi_{1133} &= \phi_{2233}; & \phi_{3311} &= \phi_{3322}. \end{aligned}$$

From (7)

$$\Delta\Sigma^{(i)} = \Delta\chi^{(i)} \left\langle \sum_{j \neq i} r_{ij}^{-3} \left(\frac{1}{3} - \cos^2 \theta_j \right) \right\rangle - \zeta^{(i)} \langle F_3^{(i)} \rangle - \{ 2\phi_1^{(i)} \langle F_1^{(i)2} \rangle + \phi_3^{(i)} \langle F_3^{(i)2} \rangle \} \quad (13)$$

where

$$\begin{aligned} \Delta\chi &= \chi^{\parallel} - \chi^{\perp}; & \zeta &= \zeta^{\parallel} + 2\zeta^{\perp}; \\ \phi_1 &= \phi_{1111} + \phi_{1122} + \phi_{3311}; & \phi_3 &= 2\phi_{1133} + \phi_{3333}. \end{aligned}$$

The various terms in (13) will be discussed separately.

The first term will be most important for molecules with a large anisotropy in magnetic susceptibility and intermolecular force. For benzene $\Delta\chi = -9 \times 10^{-29}$ e.m.u. (Krishnan *et al.* [10]) and a calculation from the density of liquid benzene gives $r_{ij} \geq 3$ Å. From the crystal structure taking nearest neighbours into account

$$\left\langle \sum_{j=i} \left(\frac{1}{3} - \cos^2 \theta_j \right) \right\rangle = -0.14$$

and thus

$$\Delta\chi \left\langle \sum_{j \neq i} r_{ij}^{-3} \left(\frac{1}{3} - \cos^2 \theta_j \right) \right\rangle = +0.47 \times 10^{-6}.$$

This calculation for point molecules does not take into account the fact that the protons in a benzene molecule will in general be closer to neighbouring molecules than 3 Å and thus actually a larger value would be obtained.

For molecules with small anisotropy in susceptibility the first term in (13) will not be the most important, as may be seen as follows. The maximum value of $|\frac{1}{3} - \cos^2 \theta_j|$ is $\frac{2}{3}$ and taking the average distance of approach as 2 Å we obtain

$$\Delta\chi \left\langle \sum_{j \neq i} r_{ij}^{-3} \left(\frac{1}{3} - \cos^2 \theta_j \right) \right\rangle = -10^{23} \Delta\chi.$$

If $\Delta\chi = -1 \times 10^{-29}$ e.m.u. this term will at most give a shift of 1×10^{-6} and in general would be expected to be smaller. Measurement of shielding constants of molecules in gas and liquid phase gives shifts due to interactions in the liquid which are much larger than this, especially for liquids where strong hydrogen bonds are formed, e.g. for water $\Delta\Sigma = -4.5 \times 10^{-6}$ (Schneider *et al.* [3]). This is where the last two terms in (13) will be most important. Schneider *et al.* [3] have already pointed out that where the electron cloud of a molecule is distorted by an electric

field a change in shielding will take place. They have only considered terms of the type ϕF^2 whereas in molecules without centres of symmetry the term ζF would be most important if the expansion in powers of F is valid.

Some limits may be put on the value of F . For polar liquids (where there are no strong hydrogen bonds) $\langle F_3 \rangle$ may be estimated from Onsager's model. Thus

$$\langle F_3 \rangle = \frac{2(\epsilon - 1)(n^2 - 1)\mu_0}{3(2\epsilon + n^2)\alpha} \quad (14)$$

where ϵ and n are the dielectric constant and refractive index respectively, μ_0 the permanent electric dipole moment and α the electric polarizability. For hydrogen chloride $\epsilon = 4.60$, $n = 1.257$, $\mu_0 = 1.03D$ and $\alpha = 2.64 \times 10^{-24} \text{ cm}^3$ (International Critical Tables) and then from (14) $\langle F_3 \rangle = 0.5 \times 10^5 \text{ e.s.u.}$ The field due to a bare proton at a distance of 2 \AA is $1.2 \times 10^6 \text{ e.s.u.}$ This would be the value of $\langle F \rangle$ more appropriate to a liquid where strong hydrogen bonds are formed.

The calculation for the hydrogen atom shows $\phi \simeq 10^{-18} \text{ e.s.u.}$ and as $\sigma \simeq 10^{-6} \text{ e.s.u.}$ it would be expected that $\zeta \simeq 10^{-12}$. Thus in strongly hydrogen bonded liquids $\langle F \rangle \simeq 10^6 \text{ e.s.u.}$, $\phi \langle F^2 \rangle \simeq 10^{-6}$ and $\zeta \langle F \rangle \simeq 10^{-6}$ and both terms are important. For polar molecules not forming strong hydrogen bonds $\langle F \rangle \simeq 10^5 \text{ e.s.u.}$ and the terms $\zeta \langle F \rangle$ will be more important. The signs of ζ and ϕ are difficult to decide except by an appeal to experiment. In all the hydrogen bonded liquids considered by Schneider *et al.* [3] the protons are less shielded in the liquid than in the gas. Thus it is concluded that the signs of ζ and ϕ are positive.

Bothner-By and Naar-Colin [11] have suggested that an induced anisotropy in the susceptibility of neighbouring molecules may be important. This is discussed in the Appendix and shown to be usually negligible.

Further information about the above terms can be obtained from measurements on solutions (see below).

5. SOLUTIONS

Consider a sample containing βN molecules of type a and $(1 - \beta)N$ molecules of type b . For simplicity both types of molecule are assumed to be axially symmetric. From (13) and (7) the shielding constants for molecules a and b may be written

$$\Sigma^{(a)} = \alpha \{ \beta \kappa_a + (1 - \beta) \kappa_b \} + \sigma^{(a)} + \beta L_{aa} + (1 - \beta) L_{ab} \quad (15)$$

$$\Sigma^{(b)} = \alpha \{ \beta \kappa_a + (1 - \beta) \kappa_b \} + \sigma^{(b)} + \beta L_{ba} + (1 - \beta) L_{bb}, \quad (16)$$

where

$$L_{aa} = \Delta \chi^{(a)} \langle r_{aa'}^{-3} (\frac{1}{3} - \cos^2 \theta_{a'}) \rangle - \zeta^{(a)} \langle F_3^{(a)}(a') \rangle$$

$$L_{ab} = \Delta \chi^{(b)} \langle r_{ab}^{-3} (\frac{1}{3} - \cos^2 \theta_b) \rangle - \zeta^{(a)} \langle F_3^{(a)}(b) \rangle$$

$$L_{ba} = \Delta \chi^{(a)} \langle r_{ba}^{-3} (\frac{1}{3} - \cos^2 \theta_a) \rangle - \zeta^{(b)} \langle F_3^{(b)}(a) \rangle$$

$$L_{bb} = \Delta \chi^{(b)} \langle r_{bb'}^{-3} (\frac{1}{3} - \cos^2 \theta_{b'}) \rangle - \zeta^{(b)} \langle F_3^{(b)}(b') \rangle.$$

$F_3^{(a)}(b)$ etc. is the electric field at molecule a due to molecules of type b and these fields are taken to be additive and proportional to the concentration. The last term in (13) has been omitted and strongly hydrogen-bonded liquids will not be considered.

Equations (15) and (16) show that if the L are concentration independent then the shielding constant for a molecule will vary linearly with concentration. This

condition will be fulfilled where molecules a and b have a similar shape and electronic structure. Where molecules a and b are very dissimilar the behaviour with concentration will be more complex as the L will in general show some concentration dependence. These two situations are illustrated by results of Bothner-By and Glick [2]. For mixtures of methylene chloride and methylene bromide the shielding constants were found to vary linearly with concentration. For solutions of benzene in aliphatic solvents the behaviour is more complex.

The difference in the shielding constants for molecules a and b is from (15) and (16)

$$\Sigma^{(a)} - \Sigma^{(b)} = \sigma^{(a)} - \sigma^{(b)} + \beta(L_{aa} - L_{ba}) + (1 - \beta)(L_{ab} - L_{bb}). \quad (17)$$

This will be concentration-dependent in general except where $L_{aa} = L_{ba}$ and $L_{ab} = L_{bb}$, which would be the case for molecules of similar shape and electronic structure. Bothner-By and Glick [2] have found that $\Sigma^{(a)} - \Sigma^{(b)}$ is concentration-independent for mixtures of methylene chloride and methylene bromide. These two molecules would seem to fulfil the above condition. Equation (17) shows that where $\Sigma^{(a)} - \Sigma^{(b)}$ is concentration-independent it would be reasonable to take $\Sigma^{(a)} - \Sigma^{(b)} = \sigma^{(a)} - \sigma^{(b)}$ the difference in the intramolecular shielding constants (unless rather fortuitously $L_{aa} - L_{ba} = L_{ab} - L_{bb}$).

Bothner-By and Glick have made a number of measurements of the dependence of the shielding constant on sample susceptibility. Let $\Sigma^{(a)}(0)$ be the shielding constant of molecule a measured in the pure liquid and $\Sigma^{(a)}(\infty)$ the shielding constant of molecule a extrapolated to infinite dilution in solvent b . From (15)

$$\Sigma^{(a)}(0) - \Sigma^{(a)}(\infty) = \alpha\Delta\kappa + L_{aa} - L_{ab} \quad (18)$$

where $\Delta\kappa = \kappa_a - \kappa_b$. Thus only in the case of an isotropic solute and solvent where $L_{aa} = L_{ab} = 0$ would $(\Sigma^{(a)}(0) - \Sigma^{(a)}(\infty))/\Delta\kappa$ equal α , ($= 2\pi/3$ for an infinite cylinder).

Molecule	Solvent	$10^6\Delta\kappa$	$10^6(\Sigma^{(a)}(0) - \Sigma^{(a)}(\infty))$	10^6L_{aa}
Benzene	CCl_4	0.075	0.84	0.68
Toluene	CCl_4	0.064	0.73	0.60
Chlorobenzene	CCl_4	0.004	0.75	0.74
Benzonitrile	CCl_4	0.034	0.66	0.65
Methyl chloride	CCl_4	0.120	0.36	0.11
Methyl bromide	CCl_4	-0.038	-0.10	-0.02
Methyl iodide	CCl_4	-0.227	-0.60	-0.13

If the solvent is isotropic $L_{ab} = 0$ (15) shows that measurement of shielding constants in isotropic solvents, e.g., CCl_4 , and extrapolation to infinite dilution, after the bulk susceptibility correction, should give the correct intramolecular shielding constants as measured in the gas phase. This has only been tested in the case of methane (§ 4). Unfortunately none of the results of Schneider *et al.* [3] (measurements on gases and liquids) and Bothner-By and Glick [2] (measurements on solutions in CCl_4) overlap.

From (18) for an isotropic solvent ($L_{ab} = 0$)

$$\Sigma^{(a)}(0) - \Sigma^{(a)}(\infty) = \alpha\Delta\kappa + L_{aa}$$

and from the results of Bothner-By and Glick L_{aa} may be calculated. The results are given in the table.

For the aromatic compounds the main contribution to L_{aa} will arise out of the large anisotropy in the diamagnetic susceptibility. In particular for benzene where $\zeta = 0$ and $L_{aa} = \Delta\chi^{(a)} \langle r_{aa'}^{-3} (\frac{1}{3} - \cos^2 \theta_{a'}) \rangle$ the magnitude and sign agree with the estimate made in § 4. For the methyl halides the discussion in § 4 indicates that both terms in L_{aa} would be small and roughly of equal magnitude.

6. DISCUSSION

It is shown that measurements of shielding constants in gases (except at very high pressures) or in solution in an isotropic solvent will lead, after extrapolation to infinite dilution and correction for bulk susceptibility, to the correct intramolecular shielding constant.

In liquids or anisotropic solvents there will in general be two important types of correction:

(i) The magnetic moments induced in neighbouring molecules give rise to a magnetic field at the nucleus of the molecule under consideration.

(ii) If the electron distribution in a molecule is distorted by a strong electric field a modification of the intramolecular shielding constant takes place.

The present calculations show that effects of type (i) are most important in aromatic molecules and account for the shielding constants observed in aromatic liquids. This type of interaction in aromatic liquids gives a contribution to the shielding constant of the order of 0.70×10^{-6} (see table). Effects of type (ii) are most important for strongly polar molecules and molecules which form strong hydrogen bonds. The contribution to the shielding constant from hydrogen bonding is generally larger than that due to effects of type (i) in aromatic liquids and of opposite sign, e.g. for water $\Delta\Sigma = -4.5 \times 10^{-6}$. In some molecules both effects would be expected to be important. Acetylene is an interesting case where the effect of interaction in the pure liquid gives $\Delta\Sigma = -1.3 \times 10^{-6}$ or 52 c/s (Schneider *et al.* [3]). If the intramolecular shielding constant is divided into contributions from bonds a large part of this shielding is due to the π electrons (Stephen [12]). π electrons are easily polarizable and thus it is expected that effect (ii) would be important. The anisotropy in the magnetic susceptibility of the π electrons is also large (Tillieu [13]) and effect (i) would also be expected to be important.

From the results of measurements on solutions the magnitudes of the above effects may be obtained. These results are especially of interest where either the solute or solvent is isotropic in which case interesting information about the intermolecular forces between either solvent or solute or two solute molecules may be obtained.

APPENDIX

The effect of an induced anisotropy in the magnetic susceptibility of a molecule may be allowed for by expanding the susceptibility in powers of the electric field \mathbf{F} acting on the molecule. Thus only considering terms linear in \mathbf{H} the magnetic dipole moment of molecule j is

$$m_{\beta}^{(j)} = \chi_{\beta\gamma}^{(j)} H_{\gamma} + 2\xi_{\alpha\beta\gamma}^{(j)} F_{\alpha}^{(j)} H_{\gamma} + \eta_{\alpha\delta\beta\gamma}^{(j)} F_{\alpha}^{(j)} F_{\delta}^{(j)} H_{\gamma} \quad (19)$$

where $\chi_{\beta\gamma}$ is the ordinary diamagnetic susceptibility and $\xi_{\alpha\beta\gamma}$ and $\eta_{\alpha\delta\beta\gamma}$ are the

tensors defined by Buckingham and Pople [14] in connection with the Cotton-Mouton effect and give the influence of an electric field on the diamagnetic susceptibility.

From (19) it is seen that in order to include an induced anisotropy in the magnetic susceptibility $\chi_{\alpha\beta}^{(j)}$ in (7) must be replaced by

$$\chi_{\alpha\beta}^{(j)} + 2\xi_{\gamma\alpha\beta}^{(j)} F_{\gamma}^{(j)} + \eta_{\gamma\delta\alpha\beta}^{(j)} F_{\gamma}^{(j)} F_{\delta}^{(j)}. \quad (20)$$

For spherical molecules $\xi^{(j)}=0$ and there are two independent components of $\eta^{(j)}$ which, following Buckingham and Pople are called η^{\parallel} and η^{\perp} . Substituting (20) in (7) it is found that a term

$$2(\eta^{\parallel} - \eta^{\perp}) \left\langle \sum_{j \neq i} r_{ij}^{-3} (F_1^{(j)2} - F_3^{(j)2}) \right\rangle \quad (21)$$

must be included in (12). This term depending on both the anisotropy in η and F^2 will normally be negligible as an approximate calculation shows. For the hydrogen atom (Buckingham and Pople [14])

$$\eta^{\parallel} = -\frac{159}{16} \frac{a_0^6}{mc^2} = -2.66 \times 10^{-43} \text{ e.s.u.},$$

$$\eta^{\perp} = -\frac{797}{48} \frac{a_0^6}{mc^2} = -4.45 \times 10^{-43} \text{ e.s.u.}$$

Assuming $\langle F_1^{(j)2} - F_3^{(j)2} \rangle \simeq 10^{11} \text{ e.s.u.}$ (which is probably too large for non-polar substances) and $r_{ij} = 3 \text{ \AA}$ then (21) has a value of 1.3×10^{-9} . $\xi=0$ for all molecules with centres of symmetry and similar considerations would be expected to hold. When the molecules are less symmetrical and $\xi \neq 0$ the induced anisotropy is larger but in this case the shielding in the liquid is dominated by modification of the intramolecular shielding constant by the electric field.

On étudie l'effet des interactions moléculaires sur les constantes d'écran magnétiques dans les gaz et les liquides, en utilisant une mécanique statistique simple, et en considérant les molécules comme ponctuelles. Pour les gaz, et aux pressions ordinaires, les effets sont faibles. Pour les liquides et les solutions, deux effets peuvent être importants. (1) Des moments magnétiques induits dans les molécules voisines donnent lieu à un champ magnétique au noyau de la molécule considérée. (2) La distribution électronique de la molécule peut être déformée par le champ électrique dû aux molécules voisines et il y aura alors un chargement de la constante d'écran intramoléculaire. On donne une estimation de l'ordre de grandeur de ces effets et on compare leur importance pour différentes molécules.

Der Einfluss der molekularen Wechselwirkungen auf die magnetischen Abschirmungskonstanten in Gasen und Flüssigkeiten wird mittels einfacher statistisch-mechanischer Methoden berechnet, wobei die Moleküle als Massenpunkte behandelt werden. Für Gase sind die Effekte bei gewöhnlichen Drucken klein. In Flüssigkeiten und Lösungen können zwei Effekte bedeutsam werden. (1) Die in den benachbarten Molekülen induzierten magnetischen Momente können am Kern des betrachteten Moleküls ein magnetisches Feld hervorrufen. (2) Die Elektronenverteilung im Molekül kann durch das von den andern Molekülen herrührende Feld verzerrt werden, wodurch die innermolekulare Abschirmungskonstante verändert wird. Der Betrag dieser Effekte wird abgeschätzt und ihre relative Bedeutung bei verschiedenen Molekülen erörtert.

REFERENCES

- [1] DICKINSON, W., 1951, *Phys. Rev.*, **81**, 717.
- [2] BOTHNER-BY, A. A., and GLICK, R., 1957, *J. chem. Phys.*, **26**, 1647, 1651.
- [3] SCHNEIDER, W. G., BERNSTEIN, H. J., and POPLÉ, J. A., 1957, *J. chem. Phys.* (to be published).
- [4] MEYER, L. H., SAIKA, A., and GUTOWSKY, H. S., 1953, *J. Amer. chem. Soc.*, **75**, 4567.
- [5] STOCKMAYER, W. H., 1941, *J. chem. Phys.*, **9**, 398.
- [6] BUCKINGHAM, A. D., and POPLÉ, J. A., 1956, *Trans. Faraday Soc.*, **51**, 1173.
- [7] BUCKINGHAM, A. D., 1956, *Trans. Faraday Soc.*, **52**, 747.
- [8] MARSHALL, T. W., and POPLÉ, J. A., 1957, *Mol. Phys.*, **1**, 199.
- [9] BUCKINGHAM, A. D., and STEPHEN, M. J., 1957, *Trans. Faraday Soc.*, **53**, 884.
- [10] KRISHNAN, K. S., GUHA, B. C., and BANERJEE, S., 1933, *Phil. Trans.*, **231**, 235.
- [11] BOTHNER-BY, A. A., and NAAR-COLIN, C., 1957, *J. chem. Phys.* (to be published).
- [12] STEPHEN, M. J., 1957, *Proc. roy. Soc. A*, **243**, 264.
- [13] TILLIEU, J., 1957, *Ann. Phys., Paris*, **2**, 472.
- [14] BUCKINGHAM, A. D., and POPLÉ, J. A., 1956, *Proc. phys. Soc., Lond. B*, **69**, 1133.

Hyperconjugation in the electron resonance spectra of free radicals

by A. D. McLACHLAN

Department of Theoretical Chemistry, Cambridge University

(Received 7 May 1958)

The electron resonance hyperfine splitting a_H produced by protons of a methyl group attached to one of the aromatic carbon atoms of a π -electron radical is calculated by the valence bond theory, treating the exchange interaction between the odd electron and the methyl group as a perturbation. The formula $a_H = Q\rho$ which relates a_H for a ring proton with the spin density ρ on the aromatic carbon atom also holds for methyl protons. Q is predicted to be positive with a theoretical value of about 28 gauss in the ethyl radical. Experimental data for several radicals indicate that Q is about 25 gauss. It is suggested that the CH_3 and CH_2 protons appear to be equivalent in the spectrum of the ethyl radical because Q has the same magnitude for both. The spectra of some Wurster's blue ions are interpreted on the assumption that hyperconjugation takes place between methyl groups and the nitrogen atoms.

1. INTRODUCTION

Measurements on the electron resonance spectra of certain organic free radicals containing methyl groups often reveal a hyperfine structure due to interaction between the unpaired electron and the protons of the methyl group. Examples of this phenomenon are the ethyl radical [1], the methyl-substituted semiquinone ions [2] the dimethylmethyl radical [3], Wurster's blue ions [4] and the radical $(\text{CH}_3)_2\text{COH}$ [5] which is produced when isopropanol is mixed with hydrogen peroxide and irradiated with ultra-violet light in a rigid glass. In this paper we shall attempt to interpret the magnitudes of these effects.

There are two main ways [6] in which a proton may interact with an unpaired electron. The first is by direct dipole-dipole forces between the magnetic moments of the two particles. The second is through the so-called Fermi term in the Hamiltonian, which depends on the density of unpaired electron spin at the magnetic nucleus. Of these two effects the first is averaged out to zero if the molecule is rotating rapidly, as it does in a liquid, though even in a glass the molecular rotation is usually sufficiently rapid for the dipole-dipole interactions to be averaged out. The Fermi interaction, however, is not affected by molecular rotation. It will occur if the wave function of the unpaired electron has a finite amplitude at the nucleus of any proton in the molecule, in particular if the unpaired electron finds its way into the 1s orbital surrounding the proton. (The 2s orbital of a given hydrogen atom is of too high energy to contribute appreciably to the wave function.) Measurements on the atomic spectrum of hydrogen show that if δ is the spin density in the 1s orbital then the hyperfine splitting in gauss due to the Fermi interaction is $502 \times \delta$.

2. ELECTRONIC STRUCTURE OF THE RADICALS

The radicals we shall consider all have one common structural feature, namely that a methyl group is attached to a trigonal planar carbon (or nitrogen) atom

which in one of the conventional structures carries the unpaired electron in a $2p\pi$ atomic orbital. In describing the electronic structure of such a radical one may adopt either the molecular orbital or the valence bond theory. Bersohn [7] has applied the molecular orbital theory to the semiquinones, and has calculated the spin densities on the methyl protons by taking into account the delocalization of the unpaired electron on to the methyl group. This amounts to invoking charge transfer between the methyl group and the trivalent carbon atom, an effect which is often referred to as hyperconjugation. In valence bond theory, however, hyperconjugation may also be understood to mean the introduction of unconventional pairing schemes, in which the odd electron of the trivalent atom is paired with an electron of the methyl group, without any accompanying transfer of charge. This effect is physically distinct from charge transfer and it is, therefore, important to know how far it may be expected to contribute to the observed hyperfine splittings.

There is another important difference between the two theories. As has been pointed out by McConnell [8] the molecular orbital theory without configurational interaction leads to unpaired spin densities which are all of the same sign. This is because the theory takes no account of correlation between electrons of opposite spin. It is found experimentally, however, that spin densities are sometimes of opposite signs on different atoms, as would be expected from a wave function of the valence bond type. For these two reasons it seems worth while re-investigating the problem by the valence bond method.

3. CALCULATION OF THE WAVE FUNCTION

Figure 1 depicts the atomic orbitals of a radical in which the odd electron occupies the $2p_z$ orbital of a trigonal carbon atom with three coplanar sp^2 bonds, one of which joins it to a methyl group. This model can represent either a saturated system such as the ethyl radical, or one of the canonical structures for a conjugated molecule such as Wurster's blue. Disregarding all the atomic orbitals except those labelled in the diagram we may designate by ψ_0 the 'normal' structure, in which t_1 is paired with h_1 , t_2 with h_2 , t_3 with h_3 , and t_4 with c_1 , the electron in orbital p being unpaired. Symbolically we may write

$$\psi_0 = (t_1 h_1)(t_2 h_2)(t_3 h_3)(t_4 c_1)p. \quad (3.1)$$

This wave function would be a good approximation if there were no exchange between the orbital p and any of the other orbitals, and if the only exchange integrals of importance in the methyl group were those belonging to the four main bonds. In reality, however, the orbital p will have appreciable exchange integrals with the orbitals t_1 , t_2 , t_3 and c_1 , and this will have the effect of mixing ψ_0 with structures such as

$$\psi_c = (t_1 h_1)(t_2 h_2)(t_3 h_3)(c_1 p)t_4 \quad (3.2)$$

$$\psi_1 = (t_1 p)(t_2 h_2)(t_3 h_3)(t_4 c_1)h_1 \quad (3.3)$$

$$\psi_2 = (t_1 h_1)(t_2 p)(t_3 h_3)(t_4 c_1)h_2 \quad (3.4)$$

$$\psi_3 = (t_1 h_1)(t_2 h_2)(t_3 p)(t_4 c_1)h_3 \quad (3.5)$$

in which the unpaired spin is on t_4 , h_1 , h_2 or h_3 . We shall neglect the exchange integrals between the hydrogen atoms and p , as these orbitals are widely separated and we also ignore the exchange integral between p and t_4 , as the product of p and t_1 is probably small everywhere. The five wave functions ψ_0 , ψ_1 , ψ_2 , ψ_3 and ψ_c

may be represented by diagrams as in figure 2 and will be the only functions requiring consideration if we consistently neglect exchange integrals between orbitals of the methyl group which are not paired in ψ_0 .

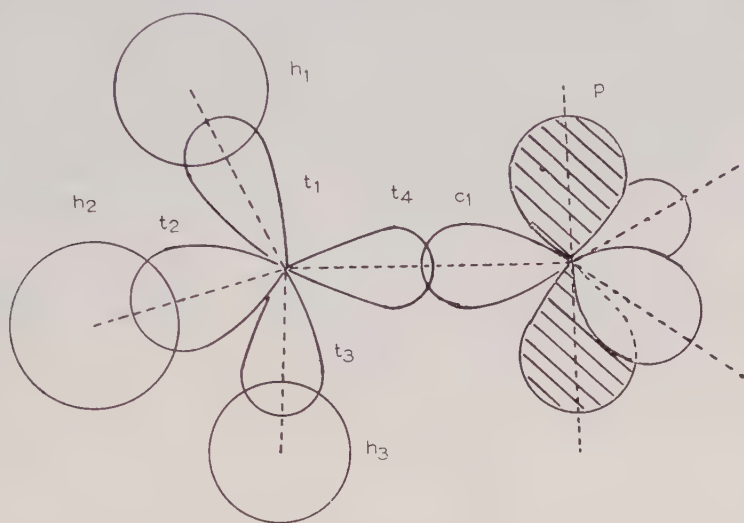


Figure 1. Orbitals for the valence bond calculation.

We describe the system by a perturbed wave function to which ψ_0 is the zeroth approximation, regarding the exchange integrals $J(t_1p)$ and $J(c_1p)$ as perturbations. In order to do this it is first necessary to determine the correct zeroth-order eigenfunctions of the unperturbed Hamiltonian H ; these will be orthogonal combinations of ψ_0 , ψ_1 , ψ_2 , ψ_3 and ψ_c . The matrix $[H_{ij} - WS_{ij}]$ in this system of functions is

$$\begin{Bmatrix} -W & -\frac{1}{2}W & -\frac{1}{2}W & -\frac{1}{2}W & -\frac{1}{2}W \\ -\frac{1}{2}W & -\frac{3}{2}J(t_1h_1) - W & -\frac{1}{4}W & -\frac{1}{4}W & -\frac{1}{4}W \\ -\frac{1}{2}W & -\frac{1}{4}W & -\frac{3}{2}J(t_2h_2) - W & -\frac{1}{4}W & -\frac{1}{4}W \\ -\frac{1}{2}W & -\frac{1}{4}W & -\frac{1}{4}W & -\frac{3}{2}J(t_3h_3) - W & -\frac{1}{4}W \\ -\frac{1}{2}W & -\frac{1}{4}W & -\frac{1}{4}W & -\frac{1}{4}W & -\frac{3}{2}J(t_4c_1) - W \end{Bmatrix} \quad (3.6)$$

where W is measured from H_{00} and $J(ab)$ represents the exchange integral

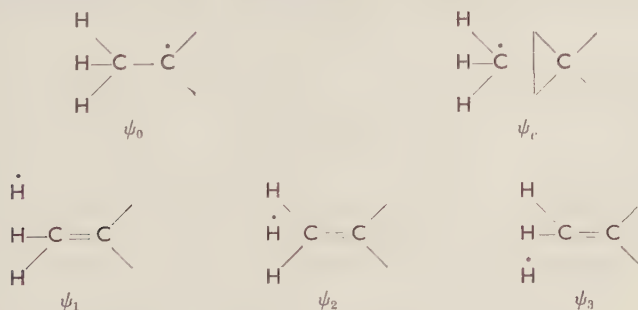


Figure 2. Diagrams of the basic structures.

between the atomic orbitals a and b . Diagonalization of this matrix leads to the following zeroth-order wave functions and energy levels

$$\left. \begin{aligned} \Phi_0 &= \psi_0, & W &= 0, \\ \Phi_1 &= \frac{1}{\sqrt{3}}(\psi_0 - 2\psi_c), & W &= -2J(t_1c_1), \\ \Phi_2 &= \psi_0 - \frac{2}{3}(\psi_1 + \psi_2 + \psi_3), & W &= -2J(th), \\ \Phi_3 &= \frac{1}{\sqrt{3}}(\psi_1 + \omega\psi_2 + \omega^2\psi_3), & W &= -\frac{3}{2}J(th), \\ \Phi_4 &= \frac{1}{\sqrt{3}}(\psi_1 + \omega^2\psi_2 + \omega\psi_3), & W &= -\frac{3}{2}J(th), \end{aligned} \right\} \quad (3.7)$$

$$\omega = \exp(2\pi i/3).$$

The perturbed wave function for the ground state is now written in the form

$$\Phi_0 + \lambda_1\Phi_1 + \lambda_2\Phi_2 + \lambda_3\Phi_3 + \lambda_4\Phi_4. \quad (3.8)$$

The matrix elements of the perturbation between Φ_0 and the other wave functions are found by standard methods [9] to be

$$\left. \begin{aligned} V_{01} &= -\frac{1}{2}\sqrt{3}J(c_1p), \\ V_{02} &= -\frac{1}{2}[J(t_1p) + J(t_2p) + J(t_3p)], \\ V_{03} &= -\frac{1}{4}\sqrt{3}[J(t_1p) + \omega J(t_2p) + \omega^2 J(t_3p)], \\ V_{04} &= -\frac{1}{4}\sqrt{3}[J(t_1p) + \omega^2 J(t_2p) + \omega J(t_3p)]. \end{aligned} \right\} \quad (3.9)$$

The perturbed wave function therefore takes the form

$$\psi = \psi_0 + \frac{J(c_1p)}{2J(c_1t_4)}[\psi_c - \frac{1}{2}\psi_0] + \sum_{r=1,2,3} \frac{J(t_r p)}{2J(t_r h)}[\psi_r - \frac{1}{2}\psi_0]. \quad (3.10)$$

4. CALCULATION OF THE SPIN DENSITY

According to McConnell [10] the operator ρ_x representing the spin density in the atomic orbital χ may be defined by the equation

$$\rho_x \sum_{\mu} S_{\mu z} = \sum_{\mu} \Delta\chi(\mu) S_{\mu z} \quad (4.1)$$

where $\Delta\chi(\mu)$ is zero unless electron μ is in orbital χ , that is to say, the matrix elements of $\Delta\chi(\mu)$ between orbitals χ' and χ'' are

$$\langle \chi'(\mu) | \Delta\chi(\mu) | \chi''(\mu) \rangle = \delta\chi' \chi \delta\chi\chi'' \quad (4.2)$$

The expectation value of (4.1) for the function ψ given by (3.10) leads to spin densities [11]

$$\pm \frac{J(t_1p)}{2J(t_1h_1)} \quad (4.3)$$

in the orbitals h_1 and t_1 of the CH_1 bond. Similarly the spin densities in the orbitals t_4 and c_1 of the C-C bond are found to be

$$\pm \frac{J(c_1p)}{2J(c_1t_4)} \quad (4.4)$$

The total spin density in each bond is zero and the spin polarization of both types of bond depends only on the exchange integrals between the orbital p and the two orbitals involved in the bond.

It is not difficult to show that the *total* spin density in the four bonds around the methyl carbon atom is zero to the first order even if the unperturbed wave

function contains unconventional structures in which orbitals such as t_1 and h_2 are paired. The presence of unpaired spin density in the methyl group may be regarded as due to the presence in the perturbed wave function of terms involving excited triplet states of the methyl group.

So far it has been assumed that the odd electron in the orbital p always has spin α . If, however, the part of the molecule containing the trivalent carbon atom resonates between various structures with different spins in the orbital p it can be shown that in the valence bond theory the spin polarization induced in the methyl group is proportional to the unperturbed spin density in p . This implies that the hyperfine splitting constant a_H for a methyl proton is related to the spin density ρ on the trivalent atom by a formula

$$a_H = Q\rho \quad (4.5)$$

of the same type as for a proton directly attached to this atom [12]. According to the valence bond theory, therefore, the hyperfine structure due to methyl protons arises in the same way as that due to protons directly attached to the unsaturated system; exchange coupling between non-bonded atomic orbitals modifies the conventional pairing scheme for the electrons in the bonds and allows the unpaired spin to move on to a proton.

It has been found experimentally [13] that the value of Q for protons attached directly to the unsaturated atom is about -28 gauss, though for the benzene negative ion a smaller value of -22.5 gauss is found. We shall now obtain a theoretical estimate of Q for a methyl proton and compare it with the available experimental data.

Since the methyl group rotates rapidly about the C-C bond the three protons are equivalent and produce a hyperfine splitting proportional to the average value of $J(t_1p)$. This is $\frac{1}{2}(J_0 + J_1)$ where J_0 and J_1 are the respective values of this exchange integral when the CH_3 bond is perpendicular or parallel to the nodal plane of p . J_1 will be very small and may be neglected; hence the spin density on each proton becomes

$$\rho_H = \frac{J_0}{4J(t_1h_1)}\rho_p \quad (4.6)$$

where ρ_p is the spin density in orbital p . The spin density in t_4 has already been found, and is

$$\rho_C = \frac{J(c_1p)}{2J(c_1t_1)}\rho_p \quad (4.7)$$

In the valence bond theory without overlap the binding energy of a bond AB is $Q(ab) + J(ab)$, where $Q(ab)$ is the Coulomb integral, and $J(ab)$ the exchange integral. The contributions of Q and J to the binding energy are about 15 per cent and 85 per cent respectively ([9], p. 247). We can therefore take the exchange integrals to be 85 per cent of the measured dissociation energies of the C-H and C-C bonds. The dissociation energy of the C-H bond in the reaction $CH_4 \rightarrow CH_3 + H$ is 4.42 ± 0.04 eV, and that of the C-C bond in $C_2H_6 \rightarrow 2CH_3$ is 3.6 ± 0.04 eV [16], so that $J(t_1h_1) = -3.75$ eV and $J(c_1t_4) = -3.0$ eV. J_0 is the sum of integrals involving p and the s and p orbitals on the methyl carbon atom. The most important term is $\frac{2}{3}J(pp')$. $J(pp')$ can be found empirically in ethylene with a C=C distance of 1.34 \AA , but the C-CH₃ bond length is considerably greater, being 1.46 \AA in methyl acetylenes, and 1.54 \AA in mesitylene and hexamethylbenzene [17]. A theoretical estimate by Altmann [14] is that

$J(pp') = -1.24$ ev for a C-C distance of 1.54 \AA in ethylene, giving $J_0 = -0.827$ ev. He also gives a purely theoretical value of $+0.968$ ev for the electrostatic integral $J(c_1p)$. (Alternatively one may deduce a value of 1.17 ev from measurements on the atomic spectrum of carbon [12].)

Substitution of these values leads to spin densities

$$\rho_H = 0.055, \quad \rho_C = -0.16, \quad (4.8)$$

where ρ_p has been set equal to unity. Since $a_H = 502$ gauss when $\rho_H = 1$ we deduce that the value of Q in (4.5) is

$$Q = 28 \text{ gauss.} \quad (4.9)$$

Q is positive for methyl protons, negative for ring protons, and the magnitude is almost the same for both. Molecular orbital theory also predicts a positive sign.

Experimental estimates of Q are quite close to this. Symons [5] found that the radical $(\text{CH}_3)_2\text{COH}$ gives seven equidistant lines with $a_H = 20$ gauss, indicating $Q = 20$ for each methyl proton. Bersohn [7] investigated some methyl-substituted semiquinone ions by molecular orbital theory, and calculated electron densities on the ring carbon atoms. Comparison of his calculated electron densities with the measured values of a_H in the different quinones enables one to obtain estimates of Q for the various molecules and positions of substitution; these values lie in the neighbourhood of 25 gauss.

Another radical of considerable interest is the ethyl radical studied by Gordy [1]. The conventional structure for this radical is



with chemically non-equivalent hydrogen atoms. Gordy found, however, that the electron resonance spectrum is characteristic of a set of five equivalent protons with $a_H = 26$ gauss. This might be taken to indicate that the radical has a labile structure in which the hydrogen atoms can exchange through a bridged configuration, but the experiments were carried out at a very low temperature (77°K), and theoretical considerations [15] favour the conventional structure for the radical. The calculations of the present paper suggest, however, that the two kinds of proton in the radical appear as equivalent not because they exchange places but because the values of Q are much the same (about ± 26 gauss) for both types.

5. WURSTER'S BLUE IONS

In the preceding sections we have discussed radicals in which the methyl group is attached to a carbon atom; the mechanism we have described should, however, come into play if the atom attached to the methyl group is a nitrogen atom bearing an unpaired spin. The Wurster's blue ions



where R is CH_3 or H , are radicals of this type. The main features of their electron resonance spectra can be interpreted on the assumption that the NH and NCH_3 protons are effectively equivalent and produce large splittings, and that the finer details are due to the four CH protons in the ring. (The nitrogen atoms contribute no structure as ^{14}N has a quadrupole moment which links its spin orientation to the molecular rotation.)







Ion	Observed spectrum [4]	Assignment
	13 triplets separated by 7.4 gauss. Separation of triplet lines 2.1 gauss.	13 lines from the 12 N protons are each split into quintets by the 4 ring protons. Quintets look like triplets.
	27 lines separated by 2.8 gauss.	9 lines 8.4 gauss apart from the 8 N protons split into overlapping quintets with a separation of 2.8 gauss by the ring protons.
	7 groups separated by 8.5 gauss.	No structure from D because of its quadrupole moment. N protons give 7 lines 8.5 gauss apart. These are split into quintets by the ring protons.
	9 groups separated by 9.5 gauss.	9 lines from N protons split into quintets by the ring protons.
	24 lines about 2 gauss apart.	7 lines 8 gauss apart from the N protons, split into quintets with $a_H = 2$ gauss by the ring protons.
	15 lines about 2 gauss apart.	4 N protons give 5 lines separated by 8.5 gauss split into quintets 2 gauss apart, making about 17 strong lines.

Table 1. Hyperfine structure of Wurster's blue ions.

In Table 1 we interpret the spectra obtained by Weissmann [4] on these assumptions. The methyl and NH protons ($Q=25$) produce a splitting of about 8 gauss; that due to the ring protons ($Q=-28$) is about 2 gauss. The spin densities on the two nitrogen atoms and the four ring carbon atoms are, therefore, by (4.5)

$$\rho_N = 0.32, \quad \rho_C = 0.071. \quad (5.1)$$

A simple molecular orbital calculation, with Coulomb integrals equal and resonance integrals equal gives

$$\rho_N = 0.33, \quad \rho_C = 0.068. \quad (5.2)$$

An alternative calculation, with $\alpha_N = \alpha_C + \beta_{CC}$ and $\beta_{CN} = \beta_{CC}$ leads to

$$\rho_N = 0.22, \quad \rho_C = 0.078. \quad (5.3)$$

It therefore appears that not only the qualitative features of the spectra, but also the hyperfine splittings produced by various sorts of proton, agree well with the theory.

6. CONCLUSIONS

It would clearly be unwise to attach too much significance to the numerical agreement between our calculations and hyperfine splittings in the compounds

we have studied, in view of the crude approximations in the valence bond theory. Nevertheless our results suggest that spin polarization of the bonds in a methyl group may be at least as important as electron delocalization in accounting for the hyperfine splittings due to methyl groups.

I wish to acknowledge gratefully an award by the D.S.I.R., and to thank Professor H. C. Longuet-Higgins for his help and discussions.

On calcule le dédoublement hyperfin de résonance électronique a_H , dû aux protons d'un groupe méthyle attaché à un des atomes de carbone aromatiques d'un radical à électrons π , par la méthode des fonctions de liaison, en considérant l'interaction d'échange entre l'électron célibataire et le groupe méthyle comme une perturbation. La formule $a_H = Q\rho$, qui relie la valeur a_H pour un proton du cycle à la densité de spin ρ sur l'atome de carbone aromatique, est valable aussi pour les protons du groupe méthyle. On prévoit une constante Q positive avec une valeur théorique d'environ 28 gauss dans le radical éthyle. Les résultats expérimentaux indiquent que Q vaut sensiblement 25 gauss. Les protons appartenant à un CH_3 ou à CH_2 semblent être équivalents dans le spectre du radical éthyle, puisque Q est du même ordre de grandeur dans les deux cas. Les spectres de quelques ions du type bleu de Wurster sont interprétés en supposant qu'il y a hyperconjugaison entre les groupes méthyles et les atomes d'azote.

Die durch die Protonen einer an ein aromatisches Kohlenstoffatom gebundenen Methylgruppe hervorgerufene Hyperfein-Aufspaltung a_H bei der Elektronenresonanz in Radikalen mit π -Elektronen wird nach der Theorie der Spinvalenzen berechnet, wobei die Austauschwechselwirkung zwischen dem ungepaarten Elektron und der Methylgruppe als Störung behandelt wird. Die Formel $a_H = Q\rho$, die das a_H für ein Ringproton mit der Spinbesetzung ρ am betreffenden aromatischen Kohlenstoffatom verbindet, gilt auch für die Methylprotonen. Der Rechnung nach ist Q stets positiv und beträgt beim Äthylradikal ungefähr 28 Gauss; nach experimentellen Messungen ist Q etwa 25 Gauss. Die scheinbare Äquivalenz der Protonen in den CH_3 und CH_2 Gruppen kann dadurch erklärt werden, dass Q in beiden Fällen gleich gross ist. Die Spektren einiger Ionen von Wursters Blau werden unter der Annahme gedeutet, dass zwischen den Methylgruppen und Stickstoffatomen Hyperkonjugierung stattfindet.

REFERENCES

- [1] GORDY, W., and McCORMICK, C. G., 1956, *J. Amer. chem. Soc.* **78**, 3244.
- [2] VENKATARAMAN, B., and FRAENKEL, G. K., 1955, *J. chem. Phys.*, **23**, 588.
- [3] JARRETT, H. S., and SLOAN, G. J., 1954, *J. chem. Phys.*, **22**, 1783.
- [4] WEISSMANN, 1954, *J. chem. Phys.*, **22**, 1135.
- [5] GIBSON, J. F., INGRAM, D. J. E., SYMONS, M. C. R., and TOWNSEND, M. G., 1957, *Trans. Faraday Soc.*, **53**, 914.
- [6] ABRAGAM, A., and PRYCE, M. H. L., 1951, *Proc. roy. Soc. A*, **205**, 135.
- [7] BERSOHN, R., 1956, *J. chem. Phys.*, **24**, 1066.
- [8] McCONNELL, H. M., and CHESNUT, D. B., 1958, *J. chem. Phys.*, **28**, 107.
- [9] EYRING, H., WALTER, J., and KIMBALL, G. E., 1944, *Quantum Chemistry* (New York: John Wiley and Sons), p. 232.
- [10] McCONNELL, H. M., 1957, *J. mol. Spectroscopy*, **1**, 11.
- [11] McCONNELL, H. M., and DEARMAN, H. H., 1958, *J. chem. Phys.*, **28**, 51.
- [12] McCONNELL, H. M., 1956, *J. chem. Phys.*, **24**, 764.
- [13] McCONNELL, H. M., 1957, *Ann. Rev. phys. Chem.*, **8**, 105.
- [14] ALTMANN, S. L., 1951, *Proc. roy. Soc. A*, **210**, 327, 343.
- [15] LONGUET-HIGGINS, H. C., 1958, *Special Publication Chem. Soc.* **9**, 5.
- [16] COTTRELL, T. L., 1954, *The Strengths of Chemical Bonds* (London: Butterworths), pp. 181, 201.
- [17] PAULING, L., and BROCKWAY, L. O., 1937, *J. Amer. chem. Soc.*, **59**, 1223.

Structures of electron-transfer and related molecular complexes in the solid state

by O. HASSEL

Department of Chemistry, Oslo University

(Received 14 May 1958)

Some results obtained during the last years from x-ray investigations of solid addition compounds thought to be formed by electron transfer between molecules containing closed shell atoms are discussed. It is hoped that the results which apply directly to solids only might contribute to the understanding of the bonds formed also in the complexes which have been proved to be present also in liquid mixtures.

The forces between molecules containing closed shell atoms only which result in the formation of more or less stable molecular addition complexes are of fundamental interest both to chemists and physicists. Much attention has recently been devoted to the complexes believed to be formed by electron transfer from one molecule to another. Among the electron donor molecules those containing oxygen, nitrogen and other atoms known to possess lone electron pairs play an important part and also aromatic hydrocarbons. Of the electron acceptors the most interesting class comprises the pure halogens and molecules containing two different halogen atoms.

Many interesting results regarding the stability of addition compounds in liquid mixtures have been derived from spectroscopic measurements, but significant results have also been obtained using other physical methods. It is evident, however, that conclusions regarding the atomic arrangement in addition complexes cannot confidently be drawn from results obtained with the help of what we should like to call 'indirect methods'. It would therefore certainly be useful to apply also the more direct x-ray interferometric methods if we wish to establish with greater certainty some of the principles governing the architecture of addition complexes of the above-mentioned type.

Unfortunately, the possibilities are still rather restricted as far as liquid systems are concerned. In any case it appears rather probable that fundamental results may be obtained from x-ray crystallographic work, results which might be expected to have some significance also for complexes persisting in liquid systems.

In order to gather such material systematic x-ray work was started a few years ago in this laboratory. It is evident that experimental difficulties had to be expected because many of the most interesting solid compounds to be investigated are unstable, highly sensitive to moisture or have low melting points. The structure determinations so far carried out, although limited in number and in some cases not fully completed, will, we hope, be of sufficient significance to be of aid for the theoretical interpretations of the nature of the bonds holding the molecules together. In some cases, e.g. certain relatively stable complexes between amines and halogens, it appears most unlikely that the results obtained

for the solid state will not be directly applicable to liquid systems. The weak complexes between benzene and halogens, however, may have a different shape in the crystal and in the liquid. In the latter cases the interaction is probably less localized than in the former.

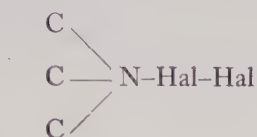
We are now going to give a survey of the chief results so far obtained from our x-ray work on the structure of solid addition compounds. It is our hope that some of the suggestions regarding the structure of addition complexes which do not conform with established facts regarding interatomic distances and have very weak experimental foundations will be quoted with greater caution in the future in textbooks and monographs.

We start with the addition compounds formed by ethers and thioethers with halogens (Br_2 and I_2). Here it was found that the oxygen (sulphur) atom and the two halogen atoms are situated on a straight line. The fact that the link between the donor and a halogen atom is stronger in the case of an iodine atom than in the case of bromine or chlorine is clearly brought out by the finding that in compounds formed with iodine monochloride it is the iodine and not the chlorine atom which is directly linked to the donor atom, and also by the observed donor-halogen distances. The experimental result that two ether oxygen atoms belonging to different dioxan molecules can be linked together in a linear arrangement O-Hal-Hal-O was rather unexpected at first. Such arrangements are of course less likely to be found if the two halogen atoms are not of the same kind.

Crystal structure work has been continued on addition compounds containing amines and halogens. The 1:1 compound between pyridine and iodine monochloride was reinvestigated by Hagbarth Wang. More accurate intensity data was obtained by integrating densitometer measurements on the Weissenberg photographs. The x-ray work was carried out at room temperature, at -50°C and -180°C . The results previously obtained [1] were substantially confirmed. The whole complex is planar. The N-I and I-Cl distances derived from the new material (see table 1) agree closely with the values obtained earlier. Difficulties met with when trying to grow single crystals of the corresponding compound between pyridine and iodine have so far prevented us from investigating its crystal structure. In the case of the quinoline-iodine compound, however, good crystals are easily obtained and a crystal structure investigation has recently been started.

Turning now to aliphatic amine-halogen compounds the structure of a 1:2 compound between hexamethylene-tetramine and bromine should be mentioned [2]. Both N-Br-Br groups were found to be *linear*, one N-Br and the three C-N bonds forming a nearly regular tetrahedral group. The similarity of the N-Hal-Hal groups in this compound and in the pyridine- ICl compound might, we thought, be due to the fact that both amines in question are very weak bases. We therefore wished to investigate also halogen addition compounds of some of the amines having larger dissociation constants. After having cleared up some unexpected difficulties which we met with when trying to prepare single crystals of addition compounds between dimethylamine and halogens (see below) we turned to halogen addition compounds of trimethylamine. The crystal structure of the I_2 addition compound has now been determined by Knut O. Strømme, that of the ICl addition compound by H. Hope. As we had expected, the two substances are not isomorphous. The addition complexes are, however,

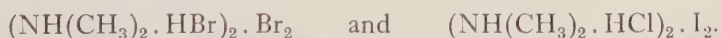
closely similar and turned out to have structures of a type which might have been expected from the results mentioned above for the hexamethylenetetramine-bromine compound. Here again the



grouping is tetrahedral in shape and the N-Hal-Hal arrangement linear. The N-I distance is (within the experimental error) identical in both cases and equal to the distance found in the pyridine-ICl compound. From table 1 it may also be seen that the lengthening of the halogen-halogen bond due to the establishment of the N-halogen bond is very nearly the same in the trimethylamine compounds and in the pyridine-ICl compound.

Our findings make it clear that the idea first expressed by Hantsch [3] that the solid addition compounds between amines and halogens contain positive ions (e.g. bromotrimethylammonium or iodopyridinium ions) and negative halogen ions can no longer be accepted.

Another assumption put forward by earlier observers and according to which the direct reaction products obtained from amines and halogens may without risk be recrystallized from non-aqueous solvents will also have to be corrected. We have as a matter of fact found that single crystals obtained in this way at room temperature or higher temperatures may contain more hydrogen than the direct addition compound. Recrystallizing the products obtained from dimethylamine and bromine or dimethylamine and ICl we obtained single crystals which are isomorphous. The crystal structure analyses carried out by Knut O. Strømme show, however, that these crystals are not those of simple addition compounds. They contain nearly linear chains of four halogen atoms, in the first case consisting of four bromine atoms, in the latter case of two chlorine and two iodine atoms in the sequence Cl-I-I-Cl. The distance between the two atoms in the middle of the chain is not much greater than in the free molecules of bromine or iodine, being 2.42 and 2.74 Å. The distance between one of the outer halogen atoms and the nearer of the two atoms in the middle of the chain is considerably larger, amounting to 3.03 Å for Br-Br and to 3.11 Å for Cl-I. This finding makes it appear very probable that both compounds are halogen addition compounds not of the dimethylamine itself but rather of its hydrobromide with bromine or its hydrochloride with iodine. The compositions would then be



The same crystals were subsequently obtained from the dimethylamine hydrobromide on addition of bromine and from the hydrochloride by adding iodine. The distance from the nitrogen atom to the 'outer' halogen atom of the chain is 3.04 in the case of chlorine, 3.14 in the case of bromine. This indicates the presence of a hydrogen bond between the nitrogen atom and the halogen atom. The angle N-Hal-Hal is not far from 90° (94.2° in the HCl-I₂ compound, 95.5° in the HBr-Br₂ compound). The Hal-Hal-Hal angle was found equal to 173° in both cases. The 'outer' halogen atoms appear to retain a considerable part of their ionic character in these compounds.

As regards the structure of charge transfer complexes, several models have been suggested for the complexes between aromatic hydrocarbons and halogens. It would indeed be of great interest to determine experimentally their precise atomic arrangement in order to decide whether for example a localized interaction between one halogen atom and the π electron cloud above an individual C-C bond can be traced or not. The benzene-iodine interaction for example might of course be studied in a crystalline 1:1 compound between the two components. Unfortunately, it appears very difficult to grow crystals corresponding to such a compound. Choosing bromine instead of iodine, however, we have succeeded in determining the crystal structure of the 1:1 compound. In this investigation which was carried out well below the melting point of the compound (-14°C) at temperatures between -40° and -50°C , Knut O. Strømme was able to obtain Weissenberg photographs rotating the crystal about the crystallographic a and c axes of the (monoclinic) crystals. The space group cannot be unambiguously determined on the basis of x-ray extinction criteria alone. Assuming the most symmetrical group ($C2/m$) to be the correct one, Fourier maps were worked out using the intensities of the zero layer line reflections. From these maps the positions not only of the heavy (bromine) atoms but also of the carbon atoms could be derived. The conclusion could be drawn that the bromine atoms are symmetrically situated on the common chief axis of two neighbouring benzene rings. The crystal is built up of chains consisting of alternating benzene and bromine molecules. The Br-Br distance is very little different from that found in the free molecule. The distance from each bromine atom to the centre of the nearest benzene ring is 3.36 \AA . The most striking feature of this structure is of course the fact that each bromine atom is symmetrically situated with respect to all C-C bonds of one particular benzene ring. This of course is quite different from the situation in the solid benzene-silver perchlorate compound where a localized interaction between one silver ion and the electron cloud associated with particular C-C bonds is obvious. The weakness of the bond in the bromine compound is indicated by the steep fall in x-ray intensities for increasing reflection angles. The arrangement of the molecules in the solid compound does not, however, exclude the possibility that the arrangement may be different in the 1:1 complex in liquid mixtures.

Finally we should like to mention that the crystal structures of some addition compounds between ethers and molecules containing active hydrogen atoms are also being studied. In the case of the compound diethylether-dichlorobromoethane it was found that a bond exists between the oxygen atom of the ether and the carbon atom of the methane derivative, the O-H-C separation being 3.1 \AA . More recently the structure of the 1:1 compound of 1,4 dioxan and sulphuric acid is being studied by Chr. Rømming. It may already be stated with confidence that this structure is built up of chains containing alternating H_2SO_4 and dioxane molecules, both hydrogen atoms of a sulphuric acid molecule taking part in hydrogen bonds to oxygen atoms of adjacent dioxan molecules. The O-H-O bonds appear to be of normal length.

The data presented in table 1, although in some cases still capable of further refinement, are thought to allow some conclusions to be drawn in addition to those mentioned in a previous communication [4]. The surprisingly short distance from tertiary nitrogen to directly bonded halogen atoms (found especially for iodine, but also in the case of bromine) indicates the presence of

a bond not essentially weaker than ordinary covalent bonds. The lengthening of the adjacent halogen-halogen bond (relative to the bond length in free halogen molecules) on the other hand may be taken as an indication of the weakening of this bond due to the change in electronic structure of at least one of the two halogen atoms. Considering the fact that both halogen atoms in the crystalline addition compounds between 1·4 dioxane and bromine (or iodine) are linked to oxygen atoms may, we think, indicate that the second halogen atom in the simple 1:1 compound (evidently present in liquid mixtures) is not essentially altered by the bond formation between the oxygen and the first halogen atom. We think it probable, therefore, that the halogen atom directly linked to the donor atom has acquired a ten-electron system, whereas the second halogen atom retains its original octet of electrons. If this is so, one would expect to find an arrangement of the five electron pairs in the first halogen atom resembling those assumed to occur in atoms of non-transition elements with five electron pairs. In such cases, according to current ideas one would expect a linear atomic arrangement corresponding to that observed in the ions ICl_2^- and I_3^- —with hybrid orbitals in the ten-electron atom of the sp^3d_{2s} type. The arrangement: donor atom—Hal—Hal in all the addition complexes which have so far been studied in crystals has been found to be *linear*. We take this as an indication of a marked analogy between these complexes and the trihalide ions just mentioned. If this is so, the function of halogen ions when forming trihalide ions with halogen molecules may be regarded as analogous to that of oxygen, nitrogen and other atoms containing lone electron pairs when forming addition compounds with halogen molecules.

Compound	Space group	<i>n</i>	<i>a</i>	<i>b</i>	<i>c</i>	β	Distance observed
Pyridine . ICl	P2 ₁ /c	4	4·25	12·29	14·07	(°) 94·4	N—I = 2·30 I—Cl = 2·54
(CH ₃) ₃ N . I ₂	Pnma	4	8·29	8·34	11·37	—	N—I = 2·27 I—I = 2·84
(CH ₃) ₃ N . ICl	Pbca	8	11·52	11·08	10·77	—	N—I = 2·30 I—Cl = 2·53 I—I = 2·74
2(NH(CH ₃) ₂ . HCl) . I ₂	C2	4	20·43	5·88	5·45	94·3	I—Cl = 3·11
2(NH(CH ₃) ₂ . HBr) . Br ₂	C2	4	20·00	6·01	5·38	94·6	Br ² —Br ³ = 2·42 Br ¹ —Br ² = 3·03
2(N(CH ₃) ₃ . HBr) . Br ₂	Pc	4	5·75	12·45	11·44	107·7	Br ² —Br ³ = 2·4 Br ¹ —Br ² = 3·0
Benzene . Br ₂	C2/m	2	7·75	8·83	5·94	99·3	Br—Br = 2·28 Br—C = 3·70
(C ₂ H ₅) ₂ O . CHCl ₂ Br	Pna2 ₁	4	9·49	14·12	7·16	—	O—H—C = 3·1
Dioxan . H ₂ SO ₄	P2 ₁ /c	4	13·22	7·74	7·71	92·5	—

Table 1.

Since a considerable amount of evidence regarding the structure of crystalline addition compounds has now been gathered we think it possible to draw some conclusions regarding the probable structure of some of the complexes in liquid mixtures. For example we feel convinced that the complexes containing amine

and halogen molecules will be built up in exactly the same way as that observed in the crystals, at least in the melts or when dissolved in non-polar or moderately polar solvents. It also appears very probable, we think, that the halogen complexes of ethers will exhibit the linear O-Hal-Hal arrangements observed in crystals, and that, these lines form angles of approximately 110° with the carbon-oxygen bonds. The arrangement suggested by Mulliken [5] in which both halogen atoms are directly linked to the ether oxygen atom would lead to very small Hal-O-Hal angles which are indeed very improbable. In the case of halogen complexes formed by ketones the situation is probably rather similar with the exception that the direction of the O-Hal-Hal line is likely to lie in the plane containing the three nearest carbon atoms. Unfortunately, the crystal structures of addition compounds formed e.g. by acetone and halogens are still unknown. In the case of the solid 1:1 compounds we believe that chains may be formed, each keto oxygen atom being linked to *two* independent halogen atoms. If this is so an angle of approximately 110° is to be expected between the two linear O-Hal-Hal-O arrangements meeting in the keto oxygen atom. The structure of the crystalline 1:1 compound between acetone and bromine is now being investigated in our laboratory and we hope to be able to give a report on the result before long.

Table 1 contains a condensed summary of crystal structure results not previously reported and also some newer data relating to structures reported in previous publications (compare [4]).

We wish to express our sincere gratitude towards The Rockefeller Foundation for financial aid that has made the x-ray investigations possible.

On discute quelques résultats obtenus ces dernières années à partir de recherches, au moyen des rayons x, sur des composés d'addition solides que l'on croit être formés par transfert d'électrons entre molécules contenant des atomes à couches électroniques complètes. On espère que les résultats, qui s'appliquent directement aux solides seuls, pourront contribuer aussi à la compréhension des liaisons formées dans les complexes que l'on sait être présents dans les mélanges liquides.

Es werden einige Ergebnisse besprochen, die in den letzten Jahren durch Röntgenstrahlenuntersuchungen an festen Molekülverbindungen erhalten wurden, die vermutlich durch Elektronentransfer zwischen Molekülen gebildet werden, die Atome mit abgeschlossenen Schalen enthalten. Es ist zu erwarten, dass die Ergebnisse, die sich unmittelbar nur auf Festkörper beziehen, auch über die Bindungen in den Molekülkomplexen Aufschluss geben könnten, die auch in flüssigen Gemischen nachweislich vorhanden sind.

REFERENCES

- [1] HASSEL, O., and RØMMING, CHR., 1956, *Acta Chem. Scand.*, **10**, 696.
- [2] EIA, G., and HASSEL, O., 1956, *Acta Chem. Scand.*, **10**, 139.
- [3] HANTSCH, A., 1905, *Ber.* **38**, 2161.
- [4] HASSEL, O., 1957, *Proc. chem. Soc.*, p. 250.
- [5] MULLIKEN, R. S., 1950, *J. amer. chem. Soc.*, **72**, 600.

Proton magnetic resonance of aromatic carbonium ions

I. Structure of the conjugate acid

by C. MACLEAN, J. H. VAN DER WAALS and E. L. MACKOR

Koninklijke/Shell-Laboratorium, Amsterdam
(N.V. De Bataafsche Petroleum Maatschappij)

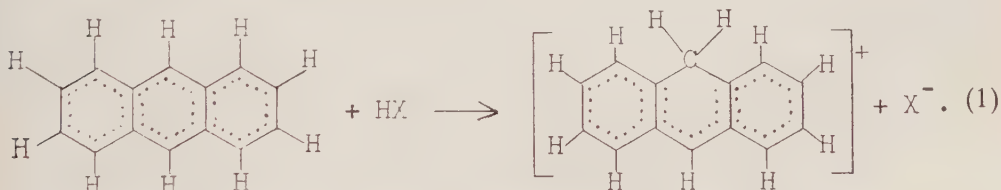
(Received 14 May 1958)

N.M.R. spectra of aromatic carbonium ions obtained by dissolving highly basic aromatic hydrocarbons in $\text{CF}_3\text{COOH} + \text{H}_2\text{O}$. BF_3 or $\text{HF} + \text{BF}_3$ were measured. The resonance of the protons in the CH_2 group in the carbonium ion was detected. It was concluded that this configuration, formed by the addition of the proton to the most reactive carbon atom in the hydrocarbon, has an 'aliphatic' character.

In most instances the N.M.R. spectra of the carbonium ions are blurred by exchange reactions. The character of these reactions is discussed.

INTRODUCTION

In previous papers [1] the formation of carbonium ions (conjugate acids) resulting from proton addition to aromatic hydrocarbons in acid solutions has been discussed. It was assumed that the proton is bonded to one particular aromatic carbon atom in each case. In this well-defined model, originally proposed by Gold and Tye [2], the two electrons required to bind the proton are withdrawn from the π -electron system. Thus an 'aliphatic' CH_2 group results†. For anthracene, for instance, the most reactive meso position is involved:



Although the model was found to be completely adequate no direct proof could be given for the existence of the suggested structure. The main purpose of the present paper is to report experiments which provide this proof unambiguously.

Since the problem is to detect the presence of an aliphatic CH_2 group among aromatic CH groups proton magnetic resonance seems to be a useful technique. It is clear that the kinetics connected with reaction (1) are an important aspect in the experiments, because a rapid chemical exchange causes broadening of the

† The proton may be added to an aromatic carbon atom carrying an alkyl substituent R;

one then has to detect an 'aliphatic' $\begin{array}{c} \text{H} \\ | \\ \text{C} \\ | \\ \text{R} \end{array}$ group.

'aliphatic' proton line, or even fusion of the latter with the line due to the acid solvent protons [3]. For this reason, measurements have been made on a number of aromatic hydrocarbons covering a considerable range of basicities (proton affinities). Also, experiments have been conducted in solvents differing in acidity.

The discussion given in the following sections is mainly concerned with the structural problem. Other features, such as the kinetics of the equilibrium reaction, specific solvent effects, and the analysis of the proton resonances not connected with the 'aliphatic' CH_2 group will be touched upon only briefly.

EXPERIMENTAL

The proton magnetic resonance spectra were recorded at room temperature using a Varian high resolution spectrometer operating at 40 Mc/s (Model V 4300); use was made of the spinning-sample method. The well-known side-band technique [4] was applied in order to measure the separations of the resonance peaks. An internal standard was obtained by adding a small amount of benzene to the samples. In this paper relevant spectral peaks will be presented with reference to the benzene line. Thus, if a particular resonance peak appears at a higher field than the benzene peak, the shift in cycles per second (c/s) will be given the plus sign.

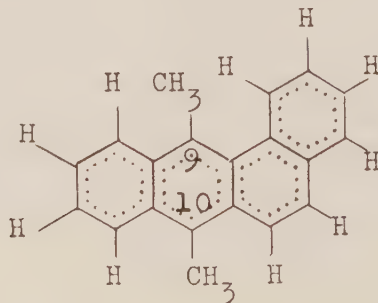
The hydrocarbons were dissolved in concentrations of 1-4 mole per cent in acid mixtures of $\text{CF}_3\text{COOH} + \text{H}_2\text{O} \cdot \text{BF}_3$ (or the deuterated mixture $\text{CF}_3\text{COOD} + \text{D}_2\text{O} \cdot \text{BF}_3$) containing 5-30 mole per cent $\text{H}_2\text{O} \cdot \text{BF}_3$ (or $\text{D}_2\text{O} \cdot \text{BF}_3$). About 0.5 mole per cent benzene was added; it is such a weak base that it is always present as the molecule and provides a clear 'marker' signal. The solutions were sealed in Pyrex sample tubes (outer diameter 5 mm).

The solutions of the hydrocarbons in $\text{HF} + \text{BF}_3$ were made by saturation of the mixture of hydrocarbon and freshly distilled anhydrous HF with BF_3 . Solutions up to 4 mole per cent were prepared in this manner. Again about 0.5 mole per cent of benzene was added. These solutions were transferred to a sample tube made of Teflon (outer diameter 4 mm).

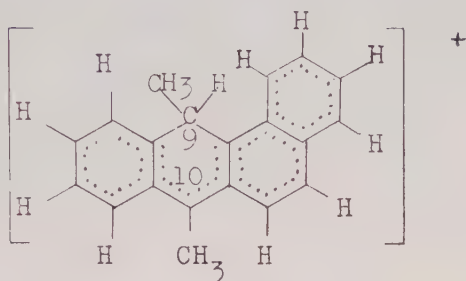
MEASUREMENTS AND DISCUSSION

Proof of the presence of the hypothetical structure

An aromatic hydrocarbon of high basicity in a solvent of high acidity offers the best chances that a carbonium ion of the structure in question will have a sufficient lifetime. As an example of such a hydrocarbon, 9,10-dimethyl-1,2-benzanthracene



was chosen. Its conjugate acid shows an ultra-violet absorption spectrum closely resembling that of 10-methyl-1,2-benzanthracene dissolved in an acid. This indicates that proton addition in the 9 position must be expected almost exclusively [5]:

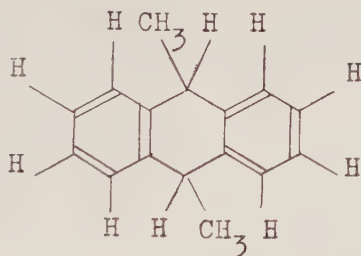


The choice of 9,10-dimethyl-1,2-benzanthracene provides some additional advantages, which will manifest themselves in the subsequent discussion.

Figure 1 shows the N.M.R. spectrum of 9,10-dimethyl-1,2-benzanthracene in three different solvents,

- carbon tetrachloride (figure 1 (a)),
- $\text{CF}_3\text{COOH} + \text{H}_2\text{O} \cdot \text{BF}_3$ (figure 1 (b)),
- $\text{CF}_3\text{COOD} + \text{D}_2\text{O} \cdot \text{BF}_3$ (figure 1 (c)).

In addition the N.M.R. spectrum of 9,10-dihydro-9,10-dimethyl anthracene (*trans*):



dissolved in carbon tetrachloride is shown (figure 1 (d)). The positions of the relevant resonance peaks in these spectra are given in table 1. These four spectra prove the presence of an 'aliphatic' configuration



in the conjugate acid beyond doubt.

In the molecular spectrum (figure 1 (a)) no proton resonance is found between the complicated spectrum of the aromatic protons from -70 to -18 c/s on the one hand and the peaks (158 and 171 c/s) connected with the methyl groups on the other. The acid solution, however, shows a resonance at 69 c/s (figure 1 (b)). Not only its mere presence, but also its well-resolved quadruplet structure proves its origin to be the added proton. The fine structure can only result from the four different spin states of the nearby methyl group. In the

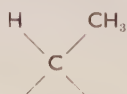
molecule the methyl groups in the 9 and 10 positions are not equivalent, since there are two methyl peaks at 158 c/s and 171 c/s. In the carbonium ion the non-equivalence is much more marked; the peaks are now at 142 c/s and 220 c/s. The methyl peak at highest field is split into a doublet, and must, therefore, be assigned to the methyl group in the 9 position, as a result of the spin $\frac{1}{2}$ of the proton added to carbon atom 9. The splittings of both the quadruplet and the doublet amount to about 7 c/s.

Substance	Fig. no.	Solvent	Methyl proton peaks (c/s)	'Aliphatic' proton peaks (c/s)
9, 10-dimethyl-1, 2-benzanthracene	1 (a)	CCl_4	158 171	—
	1 (b)	$\text{CF}_3\text{COOH} + \text{H}_2\text{O} \cdot \text{BF}_3$ (27 mole per cent)	142 216 223	CHR : 69 —
	1 (c)	$\text{CF}_3\text{COOD} + \text{D}_2\text{O} \cdot \text{BF}_3$ (24 mole per cent)	144 225	—
9, 10-dihydro-9, 10-dimethylantracene (<i>trans</i>)	1 (d)	CCl_4	225 233	CHR : 130 —
Anthrone	1 (e)	$\text{CF}_3\text{COOH} + \text{H}_2\text{O} \cdot \text{BF}_3$ (24 mole per cent)	—	CH_2 : 93

Table 1. Positions with respect to benzene peak of 'aliphatic' proton peaks of 9, 10-dimethyl-1, 2-benzanthracene (molecule, ion), 9, 10-dihydro-9, 10-dimethylantracene (molecule) and anthrone (ion).

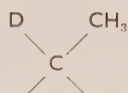
The ratios of the integrated intensities in figure 1 (b) of the aromatic proton peaks (-70 to -18 c/s), the quadruplet (69 c/s) and the peaks of the methyl groups (142 and 220 c/s) correspond well with the expected ratios of 10:1:3:3.

A final piece of evidence is obtained if one compares the carbonium ion spectrum (figure 1 (b)) with the spectrum of the molecule 9, 10-dihydro-9, 10-dimethylantracene (figure 1 (d)). The configuration



in the latter case causes a quadruplet and a doublet very similar in position and splitting to the corresponding peaks in the carbonium ion spectrum.

When a completely deuterated acid is used as the solvent for 9, 10-dimethyl-1, 2-benzanthracene the N.M.R. spectrum of figure 1 (c) is obtained. The differences between figures 1 (b) and 1 (c) result from the presence of the configuration



in the latter case. The shoulders on the wings of the 220 c/s methyl peak must be due to the small concentration of protons in the deuterated acid. The effect of the magnetic moment of the deuteron (nuclear spin 1) on this peak was not

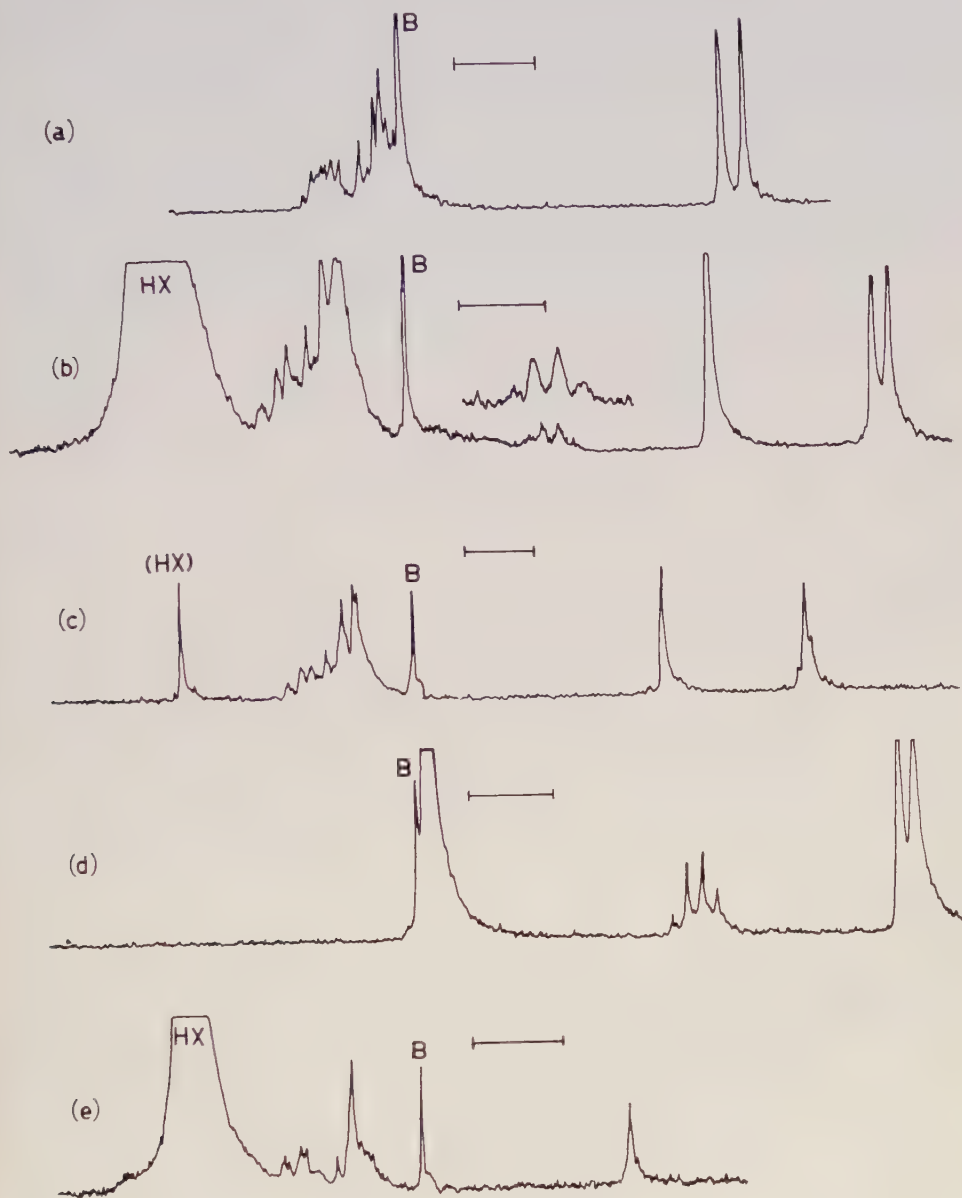


Figure 1. Proton magnetic resonance spectra at 40 Mc/s of:

- (a) 9, 10-dimethyl-1, 2-benzanthracene in CCl_4 .
- (b) *Idem* in $\text{CF}_3\text{COOH} + 22$ mole per cent $\text{H}_2\text{O} \cdot \text{BF}_3$. The quadruplet has been enlarged for clarity.
- (c) *Idem* in $\text{CF}_3\text{COOD} + 24$ mole per cent $\text{D}_2\text{O} \cdot \text{BF}_3$ (isotopic purity ~ 96 per cent).
- (d) 9, 10-dihydro-9, 10-dimethylantracene in CCl_4 .
- (e) Anthrone in $\text{CF}_3\text{COOH} + 24$ mole per cent $\text{H}_2\text{O} \cdot \text{BF}_3$.

The scale (40 c/s) is indicated in the spectra. Internal standard: benzene (B). The magnetic field increases from left to right. For peak separations see table 1.

observed. One would expect a triplet with an overall separation of 2 c/s, but this is smaller than the half-width of the exchange-broadened line†. The positions of the methyl peaks, assigned to the methyl group in the 9 position, at 220 c/s in the conjugate acid of dimethylbenzanthracene correspond satisfactorily with the position of the peak in cyclohexane (231 c/s) or the methyl peaks in 9, 10-dihydro-9, 10-dimethylantracene (228 c/s). The resonance peak of the methyl group in the 10 position in the conjugate acid of dimethylbenzanthracene is shifted to lower fields (142 c/s). This must be a chemical shift. Molecular orbital calculations show that a considerable fraction of the net positive charge of the ion is concentrated on carbon atom 10, and one must assume that the shielding of the protons in the methyl group near this positive charge is lowered. No such effect is noticed for the methyl group in the 9 position, which forms part of an electrically neutral 'aliphatic' configuration.

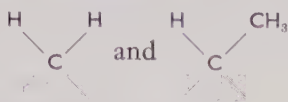
The N.M.R. spectra of the conjugate acids of a number of other aromatic hydrocarbons were also determined. In table 2 the positions of the resonance peaks of the protons in the 'aliphatic' configurations with respect to the benzene

Substance	Solvent	Methyl proton peaks (c/s)	'Aliphatic' proton peaks (c/s)
Pentamethylbenzene	CCl ₄	202	—
	CF ₃ COOH + H ₂ O . BF ₃ (30 mole per cent)	196, 199, 204	not observed
	HF + BF ₃	180, 187, 198	CH ₂ : 102
Hexamethylbenzene	HF + BF ₃	193	CHR : 131
Hexaethylbenzene	CCl ₄	CH ₂ : 193 CH ₃ : 246	—
	HF + BF ₃	CH ₂ : 185 CH ₃ : 254	CHR : 120
9, 10-dimethylantracene	CCl ₄	166	—
	CF ₃ COOH + H ₂ O . BF ₃ (17 mole per cent)	148 223 231	CHR : 102
Pyrene	HF + BF ₃	—	CH ₂ : 122
3, 4-benzopyrene	CF ₃ COOH + H ₂ O . BF ₃ (19 mole per cent)	—	CH ₂ : 160

Table 2. Positions with respect to benzene peak of 'aliphatic' proton resonance peaks of various aromatic hydrocarbons and their conjugate acid ions. Spectra of pentamethyl-benzene: see figures 2 and 3.

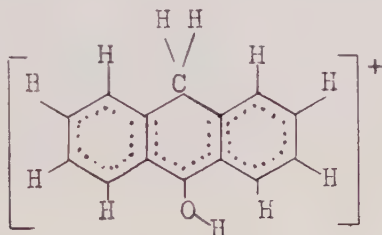
† Exchange reactions similar to the ones that cause blurring of the spectra may lead to rapid hydrogen-deuterium exchange in the compound under the experimental circumstances. It was found, however, that this exchange is so slow that no change in N.M.R. spectrum of figure 1 (c) was observed within the first hour after preparation of the solution. This apparent contradiction will be further discussed in a subsequent publication. (Cf. also the experiments of Varshavskii, Lozhkina and Shatenshtein [7].)

peak can be found. It will be seen that for these conjugate acids the resonance peaks corresponding with the configurations



have been detected at similar separations.

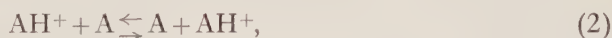
In general oxygen-containing aromatic hydrocarbons are much more basic than the corresponding parent compounds. An interesting example is provided by anthrone, which, if dissolved in an acid solvent ($\text{CF}_3\text{COOH} + \text{H}_2\text{O} \cdot \text{BF}_3$ in our experiment) forms a carbonium ion of the following structure:



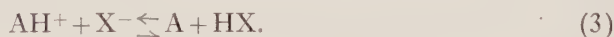
This may be considered as the OH substituted conjugate acid of anthracene. Its N.M.R. spectrum (figure 1(e)), as expected, shows considerable detail. The sharp aliphatic proton resonance peak is observed at 93 c/s.

Exchange phenomena

The N.M.R. spectra of the conjugate acid ions formed by aromatic hydrocarbons in acid solution are blurred in many cases owing to exchange. The reactions primarily responsible for this blurring are the proton transfers:



or

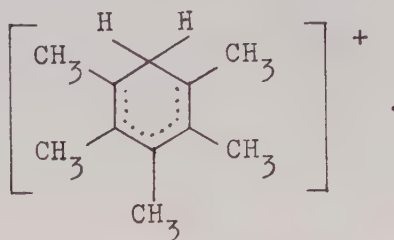


Which of the two reactions predominates depends entirely on the conditions of the experiment. For a strong base in a strong acid reaction (3) has been found to be endothermic [6], and in our opinion, reaction (2) will then predominate. If this assumption is correct the rate of exchange will decrease if the acidity of the solvent is increased or if a more basic hydrocarbon is chosen. In the extreme case of 9,10-dimethyl-1,2-benzanthracene the exchange reaction is slow relative to 7 c/s as can be concluded from the multiplets of the CHCH_3 configuration, which are well resolved here (figure 1(b)).

The effect of the acid strength of the solvent was investigated. The N.M.R. spectra of pentamethylbenzene dissolved in $\text{HF} + \text{BF}_3$ and in a series of CF_3COOH solutions containing increasing amounts of $\text{H}_2\text{O} \cdot \text{BF}_3$ were studied. Let us first consider the spectrum of pentamethylbenzene in the solvent of highest acidity, $\text{HF} + \text{BF}_3$, recorded in figure 2. On the high field wing of the strong HF proton resonance peak the benzene marker is distinguished†. At 102 c/s one observes

† Although HF is a very suitable solvent for studies of this nature in many respects, its disadvantage is that aromatic proton resonances cannot be measured very well because of the overlapping by the broad acid-proton peak.

a blurred CH_2 proton peak, and at 180 c/s, 187 c/s and 198 c/s three peaks occur, which are connected with the methyl groups. They appear in an intensity ratio of 1:2:2. The most significant features of this spectrum can be interpreted in terms of the carbonium ion:



The resonance of the aliphatic protons falls in the expected region. The splitting of the methyl peaks is due to different chemical shifts, which can be understood as resulting from different charge concentrations on the aromatic carbon atoms. Molecular orbital calculations predict the net positive charge to be mainly concentrated on the *ortho* and *para* carbon atoms. We tentatively assign the 180 c/s, 187 c/s and 198 c/s peaks to the *para*, *ortho* and *meta* methyl groups, respectively. From the figure, however, it is seen that some weaker satellites are also present in the group of the methyl peaks. These are not explained by the above interpretation. The more detailed structure may be due to the presence of carbonium ions in which the proton is added to one of the methyl-substituted carbon atoms.

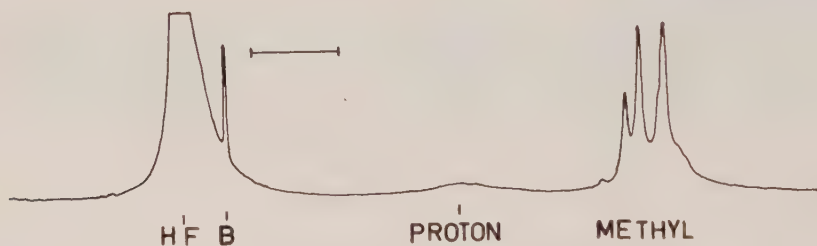


Figure 2. Proton magnetic resonance spectrum of pentamethyl benzenium ion. Solvent: $\text{HF} + \text{BF}_3$. The scale (40 c/s) is indicated. Field increasing from left to right. The solvent peak appears at the lower field side. Internal standard: benzene (B).

In the solutions of pentamethylbenzene in $\text{CF}_3\text{COOH} + \text{H}_2\text{O} \cdot \text{BF}_3$ the CH_2 signal of the ion and the CH signal of the molecule were both absent. Because of proton exchange those signals must have fused with the signal of the acid protons; from the separation between the CH_2 and acid proton signals (about 250 c/s) it follows that the rate of exchange is at least 1000 sec^{-1} . When no $\text{H}_2\text{O} \cdot \text{BF}_3$ is added to the solvent the signal due to the aromatic CH configuration in the molecule is still observed.

The CH_3 signal, on the contrary, remains well defined. Figure 3 shows the resonance due to the methyl groups of pentamethylbenzene in CF_3COOH solutions which contain 0, 12, 20 and 30 mole per cent of $\text{H}_2\text{O} \cdot \text{BF}_3$, respectively. The ratio of pentamethylbenzene occurring in the basic state A and in the conjugate acid AH^+ in each of the solutions was estimated from its ultra-violet

absorption spectrum; the ratios are given in the legend of figure 3. At the highest acidity, where $[A]/[AH^+] \leq 0.1$ a triplet is observed which is nearly identical with the triplet observed in $HF + BF_3$ (figure 3(d)). The fraction present as A increases from the right to the left in figure 3. Each of the three signals due to the *ortho*, *meta* and *para* methyl protons, respectively, is the weighted average of the corresponding signals in the molecule A and ion AH^+ . Since in the molecule the three signals of the three non-equivalent groups of methyl hydrogen practically coincide, the triplet gradually fuses into a single line if progressively weaker acids are used.

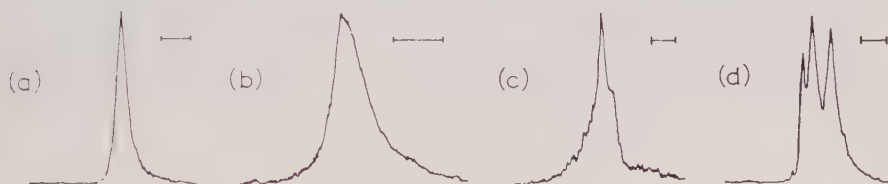


Figure 3. The methyl resonances of pentamethyl benzene in different solvents. The scale (8 c/s) is indicated in the spectra.

- (a) In CF_3COOH . $[A]/[AH^+] > 100$.
- (b) In $CF_3COOH + 12$ mole per cent $H_2O \cdot BF_3$. $[A]/[AH^+] \approx 10$.
- (c) In $CF_3COOH + 20$ mole per cent $H_2O \cdot BF_3$. $[A]/[AH^+] \approx 3$.
- (d) In $CF_3COOH + 30$ mole per cent $H_2O \cdot BF_3$. $[A]/[AH^+] \leq 0.1$.

In the solutions of pentamethylbenzene in $CF_3COOH + H_2O \cdot BF_3$ side reactions occur: in the course of a few hours the methyl resonances change markedly. There are indications that transalkylation has taken place.

We gratefully acknowledge the stimulating interest shown by Dr. A. A. Verrijn Stuart and the skilful experimental assistance of Mr. J. Gaaf.

On a mesuré des spectres 'RMN' d'ions carbonium aromatiques obtenus en dissolvant des hydrocarbures aromatiques fortement basiques dans $CF_3COOH + H_2O \cdot BF_3$ ou $HF + BF_3$. L'étude a révélé la résonance du groupe CH_2 dans l'ion carbonium. Les spectres mènent à la conclusion que cette configuration, résultant de l'addition du proton à l'atome le plus réactif de carbone dans l'hydrocarbure, a un caractère 'aliphatique'.

Dans la plupart des cas les spectres 'RMN' des ions carbonium sont confondus par suite de réactions d'échange. Le caractère de ces réactions est discuté.

Die NMR-Spektren aromatischer Karboniumionen aus Lösungen von stark basischen Aromaten in $CF_3COOH + H_2O \cdot BF_3$ oder $HF + BF_3$ wurden aufgenommen. Dabei wurde die Resonanz der CH_2 -Gruppe im Karboniumion nachgewiesen. Diese Struktur entsteht durch Anlagerung des Protons an das reaktivste Kohlenstoffatom des Kohlenwasserstoffs, und die Spektren führen zur Schlussfolgerung, dass diese Konfiguration einen 'aliphatischen' Charakter hat.

In den meisten Fällen werden die NMR-Spektren der Karboniumionen infolge von Austauschreaktionen flacher und breiter. Der Charakter dieser Reaktionen wird besprochen.

REFERENCES

- [1] DALLINGA, G., MACKOR, E. L., and VERRIJN STUART, A. A., 1958, *Mol. Phys.*, **1**, 123; and references quoted therein.
- [2] GOLD, V., and TYE, F. L., 1952, *J. chem. Soc.*, 2172.
- [3] GUTOWSKY, H. S., and SAIKA, A., 1953, *J. chem. Phys.*, **21**, 1688.
- [4] ARNOLD, J. T., and PACKARD, M. G., 1951, *J. chem. Phys.*, **19**, 1608.
- [5] VERRIJN STUART, A. A., and MACKOR, E. L., 1957, *J. chem. Phys.*, **27**, 826.
- [6] MACKOR, E. L., HOFSTRA, A., and VAN DER WAALS, J. H., 1958, *Trans. Faraday Soc.*, **54**, 186.
- [7] VARSHAVSKIĬ, YA. M., LOZHKINA, M. G., and SHATENSHTĖIN, A. I., 1957, *J. phys. Chem., U.S.S.R.*, **31**, 1377.

and $\phi(\mathbf{r}_2, \mathbf{v}_2)$ are Maxwellian velocity distributions appropriate to the local hydrodynamic velocities and temperatures at the points \mathbf{r}_1 and \mathbf{r}_2 . That this pair distribution function leads to finite fluxes in the presence of gradients is essentially due to the discontinuity in the intermolecular potential, which allows the transfer of finite amounts of energy and momentum in the infinitesimal time of a molecular collision. It is fairly obvious—and this is confirmed by our calculation—that every discontinuity in the intermolecular potential function gives rise to impulsive interactions, whose contribution makes itself evident even in the zeroth approximation; we therefore adopt equation (2.1) as the starting point for our calculation of the viscosity and thermal conductivity of the dense square well fluid.

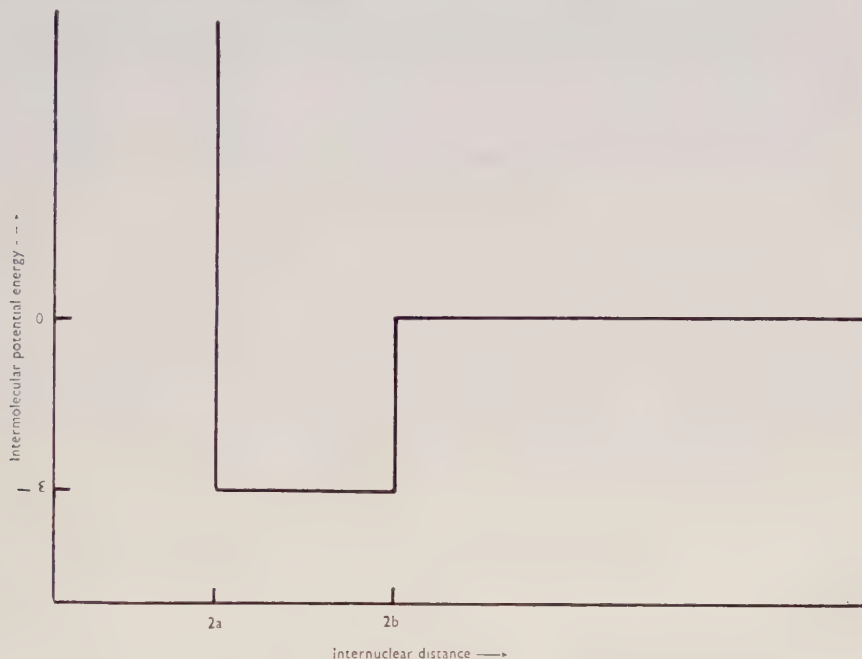


Figure 1. The square well potential.

The same authors were able to obtain the coefficient of self-diffusion, D , by making the additional assumption [1] that the velocity auto-correlation function decays exponentially with time:

$$\begin{aligned}\langle \mathbf{v}(0) \cdot \mathbf{v}(t) \rangle &\equiv \langle v^2 \rangle_{t=0} + t \left(\frac{d}{dt} \right)_{t=0} \langle \mathbf{v}(0) \cdot \mathbf{v}(t) \rangle + \dots \\ &= \langle v^2 \rangle \exp(-\zeta t).\end{aligned}\quad (2.2)$$

It was shown that under this assumption the coefficient of self-diffusion is given by

$$D \equiv \frac{\langle r^2 \rangle}{6t} = \frac{1}{3} \int_0^\infty \langle \mathbf{v}(0) \cdot \mathbf{v}(t) \rangle dt = \frac{\langle v^2 \rangle}{3\zeta} \quad (2.3)$$

(r is the displacement of a single molecule in a time t); the friction constant ζ is determined by the second term in the series expansion (2.2) of $\langle \mathbf{v}(0) \cdot \mathbf{v}(t) \rangle$, and may accordingly be written

$$\zeta = - \frac{1}{\langle v^2 \rangle} \lim_{\Delta t \rightarrow 0} \left\{ \frac{\langle \mathbf{v} \cdot \Delta \mathbf{v} \rangle}{\Delta t} \right\} \quad (2.4)$$

where $\Delta \mathbf{v}$ is the vector increment in velocity of a molecule, in a positive time interval Δt . This expression for ζ , and of course the value of $\langle v^2 \rangle$, may be calculated using the assumed form (2.1) for the distribution function; the earlier remarks with regard to this assumption again apply. We shall thus determine D , for the dense square well fluid, from (2.3) by making use of the two assumptions (2.1) and (2.2).

3. METHOD OF CALCULATION

The calculations of the thermal conductivity λ , the shear viscosity η , the bulk viscosity κ , and the coefficient of self-diffusion D proceed along very much the same lines as those described in earlier papers of this series. The important new feature of the square well potential compared with the rigid sphere potential is that in the former it is possible to distinguish four different types of bimolecular collision, namely:

(i) When two molecules collide at a distance equal to the repulsive diameter $2a$, they will exchange energy and momentum in exactly the same manner as two rigid spheres. Both kinetic energy and momentum are conserved, so that there is merely a reversal of the component of relative velocity along the line of centres.

(ii) When two molecules, initially moving apart, reach the outer edge of the attractive well with a relative kinetic energy less than ϵ , the relative velocity of separation is reversed; kinetic energy and momentum are again conserved.

(iii) When the molecules are, as in (ii), initially moving apart, but reach a distance $2b$ with relative kinetic energy greater than ϵ , they will escape from one another's attraction. Momentum is, of course, conserved, but an amount ϵ of their relative kinetic energy will instantaneously be converted into potential energy.

(iv) When two spheres approach one another from a distance greater than the attractive diameter, they will suffer an increase in their velocity of approach on collision, an amount of potential energy ϵ being converted into relative kinetic energy.

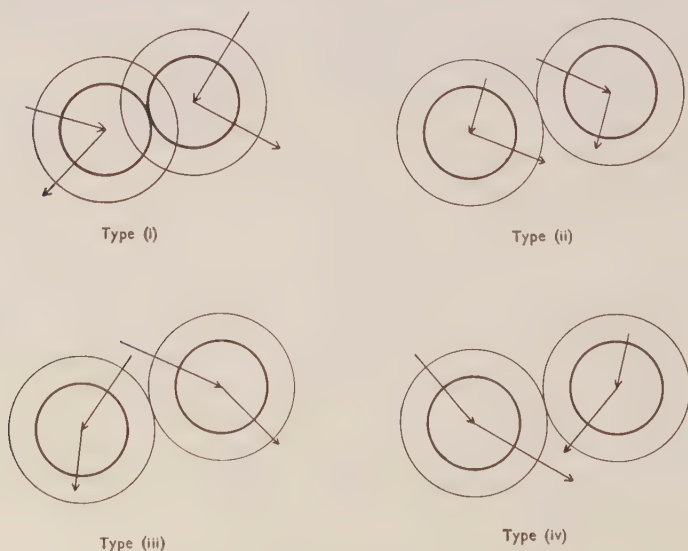


Figure 2. The four types of collision.

These four possibilities are shown diagrammatically in figure 2. In carrying out the calculations below it is found that in every case there is a contribution to the transport coefficient from each of the four types of collision; the contributions of type (iv) are negative, however, as is understandable physically.

In order to obtain the thermal conductivity we shall evaluate the heat flux when the assembly is subjected to a temperature gradient; similarly the shear and bulk viscosities are obtained by calculating the flows of momentum in the assembly when it is subjected to certain gradients of the hydrodynamic velocity. To obtain the desired fluxes, and also the friction constant ζ in (2.4), we follow a procedure explained in more detail in an earlier paper [2]. We begin by writing a general expression for the contribution of molecular collisions to these quantities. Consider a small but finite volume ΔV in the assembly, and a short time interval Δt . We define a function Δ_{12} to have the value unity if spheres, initially at $\mathbf{r}_1, \mathbf{v}_1$ and $\mathbf{r}_2, \mathbf{v}_2$, will collide with each other in ΔV during Δt , and otherwise zero—in the case of the square well model the collision may be any one of the four types described above. Then the heat flux, the momentum flux, and the friction constant may each be expressed in the general form

$$J = \lim_{\Delta t \rightarrow 0} \frac{1}{\Delta V \Delta t} \cdot \frac{1}{2} \int \dots \int f_2 \Delta_{12} j_{12} d\mathbf{r}_1 d\mathbf{r}_2 d\mathbf{v}_1 d\mathbf{v}_2, \quad (3.1)$$

where f_2 is the non-equilibrium pair distribution function and j_{12} is the contribution to J resulting from the collision of spheres at $\mathbf{r}_1, \mathbf{v}_1$ and $\mathbf{r}_2, \mathbf{v}_2$.

If, within the short time interval Δt , spheres at $\mathbf{r}_1, \mathbf{v}_1$ and $\mathbf{r}_2, \mathbf{v}_2$ are to collide with each other in one of the four possible ways, restrictions are implied on the speed of approach, u , and on the separation, $|\mathbf{r}_2 - \mathbf{r}_1|$, of the two spheres. These restrictions, for each type of collision, are given in Table 1. In this table w

Type of collision	Allowed range of speed of approach, u	Allowed range of intermolecular separation, $ \mathbf{r}_2 - \mathbf{r}_1 $	Relevant values of equilibrium pair density, $n_2^0(\mathbf{r}_1, \mathbf{r}_2)$ (cm^{-6})
(i)	$0 < u < \infty$	$2a < \mathbf{r}_2 - \mathbf{r}_1 < 2a + u\Delta t$	α
(ii)	$-w < u < 0$	$2b > \mathbf{r}_2 - \mathbf{r}_1 > 2b + u\Delta t$	β
(iii)	$u < -w < 0$	$2b > \mathbf{r}_2 - \mathbf{r}_1 > 2b + u\Delta t$	β
(iv)	$0 < u < \infty$	$2b < \mathbf{r}_2 - \mathbf{r}_1 < 2b + u\Delta t$	β'

Table 1.

represents the critical relative velocity for escape, and has the value $2\sqrt{(\epsilon/m)}$, where m is the mass of each molecule. The statistical approximations are introduced by assuming, for the pair distribution function f_2 , the simple form (2.1). On examining the restrictions on $|\mathbf{r}_2 - \mathbf{r}_1|$ just mentioned, we see that there are three ranges of this separation for which the value of the equilibrium pair density n_2^0 is relevant; these values, denoted α , β , and β' , are written in Table 1 next to the separation $|\mathbf{r}_2 - \mathbf{r}_1|$ for which they are appropriate.

The square well model is introduced explicitly in evaluating the contributions, j_{12} , to the fluxes and the friction constant ζ . Expressions for j_{12} appropriate to each type of collision, obtained by simple dynamical calculations, are given in

Table 2 for each case. In these expressions **l** is the unit vector along the line of centres (1→2) at collision, **i** is the unit vector in the *i*-direction, $u = (\mathbf{v}_1 - \mathbf{v}_2) \cdot \mathbf{l}$, and $v = (\mathbf{v}_1 + \mathbf{v}_2) \cdot \mathbf{l}$.

Type of collision	Contributions, j_{12} , to the quantities J :		
	J =energy flux	J =flux of i -momentum in the j -direction	$J = \zeta = \frac{-1}{\langle v^2 \rangle} \lim_{\Delta t \rightarrow 0} \left\{ \frac{\langle \mathbf{v} \cdot \Delta \mathbf{v} \rangle}{\Delta t} \right\}$
(i)	$ma\mathbf{v}u\mathbf{l}$	$2amu(\mathbf{l} \cdot \mathbf{i})(\mathbf{l} \cdot \mathbf{j})$	$\frac{-1}{\langle v^2 \rangle} (v-u)u$
(ii)	$mb\mathbf{v}u\mathbf{l}$	$2bmu(\mathbf{l} \cdot \mathbf{i})(\mathbf{l} \cdot \mathbf{j})$	$\frac{-1}{\langle v^2 \rangle} (v-u)u$
(iii)	$mbv \left[\frac{u}{2} - \frac{1}{2} \sqrt{(u^2 - v^2)} \right] \mathbf{l}$	$2bm \left[\frac{u}{2} - \frac{1}{2} \sqrt{(u^2 - v^2)} \right] (\mathbf{l} \cdot \mathbf{i})(\mathbf{l} \cdot \mathbf{j})$	$\frac{-1}{\langle v^2 \rangle} (v-u) \left[\frac{u}{2} - \frac{1}{2} \sqrt{(u^2 - v^2)} \right]$
(iv)	$mbv \left[\frac{u}{2} - \frac{1}{2} \sqrt{(u^2 + v^2)} \right] \mathbf{l}$	$2bm \left[\frac{u}{2} - \frac{1}{2} \sqrt{(u^2 + v^2)} \right] (\mathbf{l} \cdot \mathbf{i})(\mathbf{l} \cdot \mathbf{j})$	$\frac{-1}{\langle v^2 \rangle} (v-u) \left[\frac{u}{2} - \frac{1}{2} \sqrt{(u^2 + v^2)} \right]$

Table 2.

To obtain the thermal conductivity, we use (3.1) to evaluate the flux of heat when there is a small temperature gradient in the assembly. The substitutions for f_2 , j_{12} and Δ_{12} , and the method of evaluating the integrals are described in an appendix. Dividing the total heat flow, so calculated, by $-\text{grad } T$, we obtain the thermal conductivity

$$\lambda = \frac{32k}{3} \sqrt{\left(\frac{\pi kT}{m}\right)} \left\{ \alpha a^4 + \beta b^4 \Xi\left(\frac{\epsilon}{kT}\right) \right\}, \tag{3.2}$$

where

$$\Xi\left(\frac{\epsilon}{kT}\right) = 1 - \left(\frac{\epsilon}{2kT}\right) \exp\left(\frac{-\epsilon}{kT}\right) + \left(\frac{\epsilon}{2kT}\right) \exp\left(\frac{-\epsilon}{2kT}\right) K_1\left(\frac{\epsilon}{2kT}\right), \tag{3.3}$$

in which $K_1(\epsilon/2kT)$ is the modified Bessel function of the second kind [5]. The

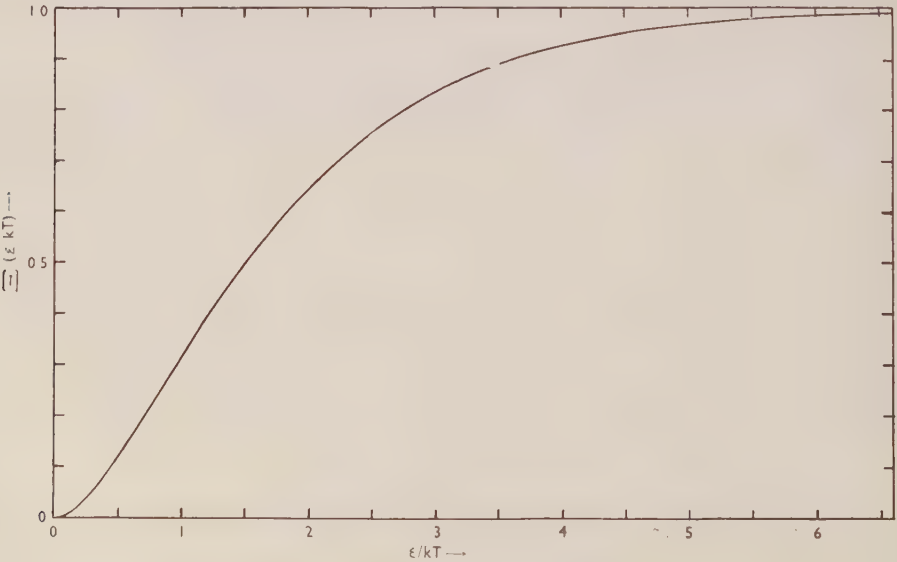


Figure 3. The function $\Xi(\epsilon/kT)$.

behaviour of the function is shown in figure 3. In writing (3.2), and other results, use is made of the fact that

$$\beta'/\beta = \exp\{-\epsilon/kT\}. \quad (3.4)$$

Values of the shear and bulk viscosities are obtained in a similar way. For the former we consider the fluid subjected to a y -gradient of the x -component of the hydrodynamic velocity, and then calculate the flux of x -momentum in the y -direction; the ratio of this flux to the gradient gives the shear viscosity as

$$\eta = \frac{64}{15} \sqrt{(\pi mkT)} \left\{ \alpha a^4 + \beta b^4 \Xi \left(\frac{\epsilon}{kT} \right) \right\}. \quad (3.5)$$

To obtain the bulk viscosity we consider the fluid subjected to a uniform contraction, and calculate the flux of x -momentum in the x -direction. In this case we get two terms in the flow. The first is independent of the rate of strain, and represents the collisional contribution to the hydrostatic pressure, namely

$$P - nkT = \frac{16\pi kT}{3} \left\{ \alpha a^3 - \beta b^3 \left[1 - \exp \left(\frac{-\epsilon}{kT} \right) \right] \right\}, \quad (3.6)$$

where n is the number density of the fluid. The other term in the momentum flux is proportional to the rate of strain, and when divided by it gives the bulk viscosity

$$\kappa = \frac{64}{9} \sqrt{(\pi mkT)} \left\{ \alpha a^4 + \beta b^4 \Xi \left(\frac{\epsilon}{kT} \right) \right\}. \quad (3.7)$$

To obtain the friction constant ζ , and hence the coefficient of self-diffusion D , we need consider only the equilibrium state of the fluid. Using the Maxwellian single-particle velocity distribution prescribed by the assumption (2.1), we obtain the familiar result

$$\langle v^2 \rangle = 3kT/m. \quad (3.8)$$

It is then straightforward to calculate ζ , from (3.1), and hence D , from (2.3) and (3.8). The result is

$$D = \frac{3n}{32} \sqrt{\frac{kT}{\pi m}} \left\{ \alpha a^2 + \beta b^2 \Xi \left(\frac{\epsilon}{kT} \right) \right\}^{-1}. \quad (3.9)$$

4. DISCUSSION

The shortcomings of the statistical assumption (2.1) have been discussed previously [1, 2, 3]. One such shortcoming is the neglect of correlations between the velocities of neighbouring molecules, the so-called molecular chaos approximation. As a particular case, important in the square well fluid, consider two successive collisions of a pair of molecules. The first will introduce a particular correlation between the velocities of the two molecules; if the approximation is to be a good one the 'memory' of this correlation must be largely destroyed before the second collision of the two molecules—this must be done by collisions with other, 'third-body' molecules. It is evident that this will be the case if each molecule has several others in its immediate neighbourhood. The 'machine experiments' of Alder and Wainwright [6] are relevant in this regard. These authors used fast electronic computers to study the detailed dynamics of assemblies of particles. Their results show that for square well molecules (with $b/a = 1.8$ and $T = 1.66 \epsilon/k$) there is an average of eight other molecules within the attractive diameter of each molecule even at the relatively low density of one fifth of the close packed density (liquid argon is nearly twice this dense). This suggests that the

molecular chaos approximation is not unreasonable in dense fluids of square well molecules.

We have obtained the transport coefficients in terms of the parameters a , b and ϵ describing the potential well, and of the two particular values α and β of the equilibrium pair density in configuration space, n_2^0 . There is one equation, (3.5), relating α and β , but this leaves us still with one unknown function of temperature and density in our values of the transport coefficients. Because of this the results cannot be compared directly with experimental transport coefficients.

This gloomy situation is, however, relieved by a striking feature of the calculated transport coefficients λ (3.2), η (3.5), and κ (3.7): α , β and the well parameters a , b and ϵ occur only in the factor $\{\alpha a^4 + \beta b^4 \Xi(\epsilon/kT)\}$, which is common to all three coefficients. This is due to the fact (see Table 2) that for each of the fluxes involved the same functions of the speed of approach, u , appear in the integrands of (3.1); the depth of the potential well, $\epsilon = mw^2/4$, appears explicitly only in these functions. Because of this common factor, we obtain the particularly simple ratios

$$\lambda/\eta = 5k/2m, \quad \kappa/\eta = 5/3. \quad (4.1)$$

These are exactly the ratios previously obtained for non-attracting rigid spheres [1, 3]; it is now evident that these ratios will also be predicted for fluids in which the intermolecular potential is more complicated, as long as the potential is entirely a step-function of the intermolecular distance and is not such as to render the molecular chaos approximation unreasonable. It is therefore of some interest to compare these ratios with those of experimentally determined transport coefficients.

In Table 3 the calculated value of λ/η is compared with the experimental value for several liquids to which the square well model might be expected to apply fairly well. The temperatures considered were dictated by the availability of

Liquid	Temp. (°K)	$10^{-6}(\lambda/\eta)_{\text{exptl.}}$ (erg g ⁻¹ deg ⁻¹)	$10^{-6}(\lambda/\eta)_{\text{theor.}}$ (erg g ⁻¹ deg ⁻¹)	References
Argon	84.2	4.5	5.2	[7, 8]
	87.3	4.8	5.2	
Helium I	2.5	51.0	52.0	[9, 10] [11]
	4.0	94.0	52.0	
Nitrogen	69.2	6.6	7.4	[12, 8]
	77.3	8.8	7.4	
Oxygen	74.0	5.5	6.5	[13, 14]
	83.6	7.0	6.5	
	90.2	8.0	6.5	
Hydrogen	16.7	61.0	103.0	[15, 14]
	20.4	95.0	103.0	
Deuterium	20.2	31.0	51.6	[16, 14]
	23.2	43.2	51.6	

Table 3.

experimental data. Two conclusions emerge from this comparison. The first is that for these simple liquids the theory gives the correct order of magnitude of the ratio λ/η . The other is that the predicted lack of dependence on temperature of this ratio is incorrect. The viscosity of real liquids varies much more rapidly with temperature than does their thermal conductivity—that our theory predicts the same temperature dependence for λ and η must be reckoned as a shortcoming.

The approximations implicit in the ratios (4.1) should be recalled. No account has been taken of the convective contributions to the thermal conductivity and the shear viscosity, or of the effect on the collisional contributions of higher approximations to the pair distribution function. It is interesting, in this regard, to compare the present theory to Enskog's theory for dense fluids of rigid spheres [17, 18, 1]; in the latter theory, in the first approximation, the predominant term, in both the thermal conductivity and the shear viscosity, is that corresponding to the zeroth approximation used in this paper, while the additional terms may be seen (reference [18], pp. 645–649, 527) to affect the ratio λ/η only slightly. To the bulk viscosity, however, there is no convective contribution, and our approximation to the collisional contribution corresponds exactly to that appearing in the first approximation of the Enskog theory for rigid spheres. For this reason the present calculation of the bulk viscosity might be regarded as more reliable than those of the thermal conductivity and the shear viscosity. On the basis of these considerations we would expect the predicted ratio $\kappa/\eta = 5/3$ of (4.1) to be an upper limit, though κ and η should be of the same order of magnitude.

This last expectation is not, apparently, borne out by experimental data on liquid argon or, for that matter, liquid oxygen, nitrogen and hydrogen. For liquid argon at 85°K measurements of sound absorption [19] are consistent with the entire effect being due to shear viscosity and thermal conduction [20], there being no detectable contribution from bulk viscosity. This disagreement may, of course, be due either to the inadequacy of the square well model or to some intrinsic defect in our theory of this model.

In order to make an absolute calculation of the shear viscosity by our theory, we need not only the inner and outer radii, a and b , and the depth ϵ , of the square well, but also the corresponding values α and β of the pair density. The parameters a , b and ϵ have been derived [21] for argon from the viscosity of the dilute gas. In order to calculate α and β we use the fact that the equilibrium pressure (3.6) and the coefficient of self-diffusion (3.9) both involve these parameters, but in different combinations. Fortunately the coefficient of self-diffusion of liquid argon at 84°K has recently been measured [22], and the equation of state is also known in this region [23, 24]. Combination of these data leads to

$$\alpha = 2.3 \times 10^{45} \text{ cm}^{-6},$$

$$\beta = 4.1 \times 10^{44} \text{ cm}^{-6};$$

inserting these values into (3.5) we obtain the shear viscosity as 2.0 millipoise, the experimental value [8] being 2.8 millipoise. This agreement is very satisfactory, especially since in calculating the shear viscosity we have taken into account only the collisional contribution.

In conclusion a word should be said about the relative accuracy of our theoretical expressions for the various transport coefficients. One would have expected the most accurate of these to be equation (3.7) for the bulk viscosity and

equation (3.9) for the coefficient of self-diffusion; the bulk viscosity is entirely collisional in origin and the mechanism of self-diffusion entirely convective, as assumed in our theory. The shear viscosity and the thermal conductivity, on the other hand contain convective terms of which our simple theory does not take account. It is not clear at present why our expression for the bulk viscosity fails when applied to liquid argon.

ACKNOWLEDGEMENTS

We were stimulated by discussions with Professor T. A. Litovitz and Professor W. H. Stockmayer.

One of us (J. P. V.) acknowledges gratefully a Scholarship awarded by the National Research Council of Canada.

APPENDIX

EVALUATION OF THE INTEGRALS

Each of the four types of collision makes a contribution to the fluxes (3.1); these contributions are calculated separately. As an example we here treat in detail the contribution to the heat flux, under a small temperature gradient, arising from collisions of type (iii). We have mentioned that, if Δ_{12} is not to vanish, restrictions are implied on $|\mathbf{r}_2 - \mathbf{r}_1|$ and on u ; we shall see that these restrictions allow us to replace the integrals of (3.1) by simpler ones.

Consider first the restriction

$$2b > |\mathbf{r}_2 - \mathbf{r}_1| > 2b + u\Delta t. \quad (\text{A } 1)$$

Since Δt is infinitesimal, we know that $|\mathbf{r}_2 - \mathbf{r}_1| \approx 2b$ and it has been pointed out that only the single value β of the equilibrium pair density n_2^0 is relevant. We can thus write the assumed form (2.1) of the pair distribution function f_2 , taking the temperature to be T at the point of contact, as

$$\begin{aligned} \beta \times & \left[\frac{m}{2\pi k(T - b\mathbf{l} \cdot \text{grad } T)} \right]^{3/2} \exp \left\{ \frac{-m\mathbf{v}_1^2}{2k(T - b\mathbf{l} \cdot \text{grad } T)} \right\} \\ & \times \left[\frac{m}{2\pi k(T + b\mathbf{l} \cdot \text{grad } T)} \right]^{3/2} \exp \left\{ \frac{-m\mathbf{v}_2^2}{2k(T + b\mathbf{l} \cdot \text{grad } T)} \right\}. \end{aligned} \quad (\text{A } 2)$$

This is expanded in powers of $\text{grad } T$ and becomes, discarding terms after the first power,

$$\beta \left[\frac{m}{2\pi kT} \right]^3 \exp \left\{ \frac{-m(\mathbf{v}_1^2 + \mathbf{v}_2^2)}{2kT} \right\} \left[1 + \frac{mb\mathbf{l} \cdot \text{grad } T}{2kT^2} (\mathbf{v}_2^2 - \mathbf{v}_1^2) \right]. \quad (\text{A } 3)$$

Also the volume element available to \mathbf{r}_2 , for a given \mathbf{r}_1 , is given by

$$d\mathbf{r}_2 = -4b^2 u \Delta t \, d\mathbf{l} \quad (\text{A } 4)$$

where $d\mathbf{l}$ is the element of solid angle at \mathbf{l} . The contribution to (3.1) may now be written with these expressions for f_2 and $d\mathbf{r}_2$, and with the tabulated value of j_{12} ; $d\mathbf{r}_1$ is integrated immediately over the volume ΔV . If we insert the remaining restriction, $u < -w$, we can replace Δ_{12} by its value unity, when the contribution to the heat flux becomes

$$\begin{aligned} & \int \int \dots \int_{u < -w} \frac{\beta m^3}{(2\pi kT)^3} \exp \left\{ \frac{-m(\mathbf{v}_1^2 + \mathbf{v}_2^2)}{2kT} \right\} \left[1 + \frac{mb\mathbf{l} \cdot \text{grad } T}{2kT^2} (\mathbf{v}_2^2 - \mathbf{v}_1^2) \right] \\ & \times \left[mbv \left(\frac{u}{2} - \frac{\sqrt{(u^2 - w^2)}}{2} \right) \right] 2b^2 u \, d\mathbf{l} \, d\mathbf{v}_1 \, d\mathbf{v}_2. \end{aligned} \quad (\text{A } 5)$$

The term which is independent of $\text{grad } T$ may be discarded, since on integrating over all directions \mathbf{l} it will clearly vanish†. The expression is then integrated over components of \mathbf{v}_1 and \mathbf{v}_2 perpendicular to \mathbf{l} ; the result, after transforming from the variables $\mathbf{v}_1 \cdot \mathbf{l}$ and $\mathbf{v}_2 \cdot \mathbf{l}$ to u and v , is

$$\frac{\beta m^3 b^4}{8\pi k^2 T^3} \int (\mathbf{l} \cdot \text{grad } T) \mathbf{l} d\mathbf{l} \int_{-\infty}^{\infty} v^2 \exp \left\{ \frac{-mv^2}{2kT} \right\} dv \int_{-\infty}^{\infty} u^2 [u - \sqrt{(u^2 - w^2)}] \\ \times \exp \left\{ \frac{-mu^2}{2kT} \right\} du. \quad (\text{A } 6)$$

The only difficult integration is of the second term in the u -integral. This is done with the transformation $x = \sqrt{(u^2 - w^2)}$, using the fact (see reference [5], example 40, p. 384)

$$2 \int_0^{\infty} x^2 \sqrt{(x^2 + \theta)} \exp(-x^2) dx = -\frac{\theta}{2} \exp\left(\frac{\theta}{2}\right) K_1\left(\frac{\theta}{2}\right). \quad (\text{A } 7)$$

The contribution is thus found to be

$$\frac{-32k}{3} \sqrt{\frac{\pi kT}{m}} (\beta b^4) \left\{ \frac{1}{2} \exp\left(\frac{-\epsilon}{kT}\right) + \frac{\epsilon}{2kT} \exp\left(\frac{-\epsilon}{kT}\right) \right. \\ \left. + \frac{\epsilon}{4kT} \exp\left(\frac{-\epsilon}{2kT}\right) K_1\left(\frac{\epsilon}{2kT}\right) \right\} \text{grad } T. \quad (\text{A } 8)$$

Adding the four contributions gives the total heat flux $J = -\lambda \text{grad } T$.

On expose une théorie cinétique simplifiée de l'interaction pour des molécules sphériques dont l'interaction est décrite par un potentiel du type 'puits carré'. Les hypothèses statistiques de cette théorie correspondent de près à celles de la théorie des fluides denses de sphères rigides de Longuet-Higgins et Pople. La conductibilité thermique λ et les coefficients de viscosité η et κ doivent être dans le rapport:

$$\lambda : \eta : \kappa = \frac{k}{2} : \frac{m}{5} : \frac{m}{3}$$

où k est la constante de Boltzmann et m la masse de la molécule. Il faudrait, pour pouvoir calculer la valeur absolue de l'un de ces coefficients, être renseigné de façon indépendante sur la distribution d'équilibre des paires de molécules. Cela est possible à partir de la constante d'auto-diffusion D , dont la valeur est aussi fournie par la théorie. Pour l'argon, la valeur mesurée de D conduit à une valeur théorique de η en bon accord avec l'expérience; cependant, pour ce liquide, on observe un rapport κ/η bien plus petit que celui prévu.

Es wird eine vereinfachte kinetische Theorie für kugelförmige Moleküle, deren Wechselwirkung durch ein Kastenpotential dargestellt ist entwickelt. Die statistischen Annahmen entsprechen genau denen, die Longuet-Higgins und Pople in ihrer Theorie der Flüssigkeiten aus starren Kugeln gemacht haben. Für die Wärmeleitfähigkeit λ , Scherviskosität η und Volumviskosität κ ergibt sich das Verhältnis

$$\lambda : \eta : \kappa = \frac{k}{2} : \frac{m}{5} : \frac{m}{3}$$

wobei k die Boltzmannsche Konstante und m die Molekülmasse bedeuten. Zur Berechnung der Absolutwerte dieser Koeffizienten muss ein bestimmter Wert der Paarverteilung Gleichgewicht bekannt sein. Dieser kann mittels der Selbstdiffusionskonstanten D berechnet werden, deren Betrag sich ebenfalls aus der Theorie ergibt. Für Argon führt der gemessene Wert von D zu einem theoretischen Wert von η , der mit dem experimentellen gut übereinstimmt; doch ist bei dieser Flüssigkeit das gemessene Verhältnis $\kappa : \eta$ wesentlich kleiner als das berechnete.

† In calculating the bulk viscosity, however, the corresponding term does not vanish, owing to the form of j_{12} in that case. This results in a term in the momentum flux representing the collisional contribution to the pressure.

REFERENCES

- [1] LONGUET-HIGGINS, H. C., and POPL, J. A., 1956, *J. chem. Phys.*, **25**, 884.
- [2] LONGUET-HIGGINS, H. C., POPL, J. A., and VALLEAU, J. P., 1958, *Symposium on Statistical Mechanics* (New York: Interscience Publishers Inc.), in the press.
- [3] LONGUET-HIGGINS, H. C., and VALLEAU, J. P., 1956, *Disc. Faraday Soc.*, **22**, 47.
- [4] VALLEAU, J. P., 1958, *Mol. Phys.*, **1**, 63.
- [5] WHITTAKER, E. T., and WATSON, G. N., 1952, *A Course of Modern Analysis* (Cambridge: University Press), Chap. 17.
- [6] ALDER, B. J., and WAINWRIGHT, T., 1956, private communication.
- [7] UHLIR, A., Jr., 1952, *J. chem. Phys.*, **20**, 463.
- [8] RUDENKO, N. S., and SCHUBNIKOV, L. W., 1934, *Phys. Z. Sowjet.*, **6**, 470.
- [9] BOWERS, R., 1952, *Proc. phys. Soc. Lond.*, **A**, **65**, 511.
- [10] BOWERS, R., and MENDELSSOHN, K., 1950, *Proc. roy. Soc. A*, **204**, 364.
- [11] DE TROYER, A., VAN IITERBEEK, A., and VAN DEN BERG, G. J., 1951, *Physica*, **17**, 50.
- [12] POWERS, R. W., MATTOX, R. W., and JOHNSTON, H. L., 1954, *J. Amer. chem. Soc.*, **76**, 5968.
- [13] ZIEBLAND, H., and BURTON, J. T. A., 1955, *Brit. J. appl. Phys.*, **6**, 416.
- [14] VAN IITERBEEK, A., and VAN PAEMEL, O., 1941, *Physica*, **8**, 133.
- [15] POWERS, R. W., MATTOX, R. W., and JOHNSTON, H. L., 1954, *J. Amer. chem. Soc.*, **76**, 5972.
- [16] POWERS, R. W., MATTOX, R. W., and JOHNSTON, H. L., 1954, *J. Amer. chem. Soc.*, **76**, 5974.
- [17] CHAPMAN, S., and COWLING, T. G., 1939, *The Mathematical Theory of Non-Uniform Gases* (Cambridge: University Press), Chap. 11.
- [18] HIRSCHFELDER, J. O., CURTISS, C. F., and BIRD, R. B., 1954, *Molecular Theory of Gases and Liquids* (New York: John Wiley), Chap. 9.
- [19] GALT, J. K., 1948, *J. chem. Phys.*, **16**, 505.
- [20] MARKHAM, J. J., BEYER, R. T., and LINDSAY, R. B., 1951, *Rev. mod. Phys.*, **23**, 395.
- [21] HOLLERAN, E. M., and HULBURT, H. M., 1951, *J. chem. Phys.*, **19**, 232.
- [22] CORBETT, J. W., and WANG, J. H., 1956, *J. chem. Phys.*, **25**, 422.
- [23] BALY, E. C. C., and DONNAN, F. G., 1902, *J. chem. Soc., Lond.*, **81**, 907.
- [24] RICE, O. K., 1946, *J. chem. Phys.*, **14**, 324.

A normal coordinate treatment of the plane symmetrical XY_4 molecule†

by C. W. F. T. PISTORIUS
554 Glyn Street, Hatfield, Pretoria, South Africa

(Received 18 March 1958)

The secular equations for the various irreducible representations of the plane XY_4 molecule (symmetry point group D_{4h}) are deduced by means of Wilson's **F-G** matrix method, using the most general harmonic force field. The equations for the case of the svff are also given.

1. INTRODUCTION

Although the plane symmetrical XY_4 type of molecule has been treated on the basis of the svff (Wilson [1], Kohlrausch [2]), no rigorous investigation on the basis of the most general harmonic force field (MGHFF) has, to the author's knowledge, as yet been made.

Even more strangely, no plane XY_4 type molecules or ions have as yet been studied experimentally with regard to their vibrational frequencies, although quite a number of such ions are known, such as ICl_4^- , and all XY_4 ions of Pd^{2+} , Pt^{2+} , Cu^{2+} , Ag^{2+} and Au^{3+} , and it should be comparatively simple to find the Raman-active fundamental frequencies of these substances.

The most convenient method for obtaining the normal frequencies of a molecule is the one utilizing the 'symmetry coordinates' (Wilson [3, 4]). These symmetry coordinates must be such that they transform in accordance with the characters of the vibration types concerned and at the same time be normalized and mutually orthogonal. In this group-theoretical method the elements of a matrix **F** related to the potential energy, and the elements of a matrix **G** related to the kinetic energy, are obtained. From these matrices the secular equations giving the vibrational frequencies in terms of the force constants are deduced.

2. SYMMETRY AND SELECTION RULES

The plane XY_4 molecule belongs to the symmetry point group D_{4h} . As such, it can be deduced from the relevant character table that such a structure will give rise to one non-degenerate type A_{1g} vibration (ν_1), one non-degenerate type A_{2u} vibration (ν_2), one non-degenerate type B_{1g} vibration (ν_3), one non-degenerate type B_{1u} vibration (ν_4), one non-degenerate type B_{2g} vibration (ν_5) and two doubly degenerate type E_u vibrations (ν_6 , ν_7). The type A_{2g} and type B_{1u} vibrations are out-of-plane deformation vibrations, while all the others are in-plane vibrations. ν_1 , ν_5 and ν_6 are associated with essentially valency vibrations, and ν_3 and ν_7 with mainly deformation vibrations.

† Based on part of a dissertation to be submitted in partial fulfilment of the requirements of the Ph.D. degree at the University of South Africa, Pretoria, South Africa.

A glance at the relevant selection rules (Herzberg [5]) will verify that the type A_{2u} and type E_u vibrations are infra-red active, and that the types A_{1g} , B_{1g} and B_{2g} vibrations are Raman active, while the type B_{1u} vibration is inactive both in the infra-red and in the Raman effect. ν_1 is polarized, ν_3 is partially polarized and ν_5 is depolarized in the Raman effect. Because this molecule possesses a centre of symmetry, the rule of mutual exclusion holds. The forms of the normal vibrations are shown in figure 1.

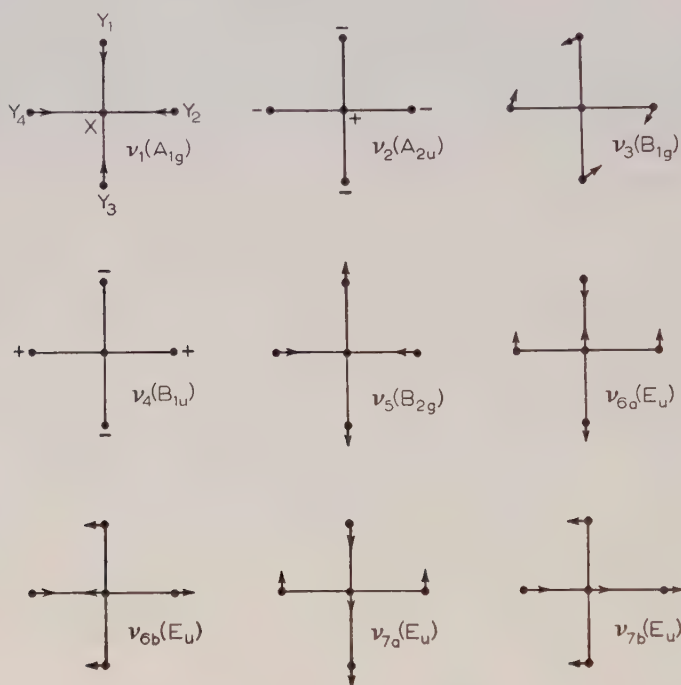


Figure 1. Normal vibrations of the plane XY_4 molecule. — indicates a motion downwards into the plane, and + a motion upwards out of the plane.

3. COORDINATES

The chemical bonds are along the four equivalent $Y-X$ distances. Since there are seven in-plane vibrational degrees of freedom, we need seven in-plane internal coordinates to describe the motion. We choose Δd_1 , Δd_2 , Δd_3 , Δd_4 and $d\Delta\alpha_{12}$, $d\Delta\alpha_{23}$, $d\Delta\alpha_{34}$, $d\Delta\alpha_{41}$, where Δd_i is the change in the length of the i th $Y-X$ bond, and $\Delta\alpha_{ij}$ is the change of the angle between the i th and j th $Y-X$ bonds. The angles are multiplied by the equilibrium bond length d in order to keep the dimensions of the force constants referring to angle bending the same as those of the bond stretching force constants. The atoms Y are numbered consecutively. It is seen that one redundant coordinate is needed, and that a suitable redundancy is the sum of the changes of the interbond angles.

We also require two out-of-plane internal coordinates, as there are two out-of-plane vibrational degrees of freedom. A suitable choice is $d\Delta\gamma_{13}$ and $d\Delta\gamma_{24}$, where $\Delta\gamma_{i,i+2}$ is the out-of-plane angle between d_i and d_{i+2} .

A suitable set of symmetry coordinates is:

Redundant coordinate,

$$R_1 = \frac{1}{2}d(\Delta\alpha_{12} + \Delta\alpha_{23} + \Delta\alpha_{34} + \Delta\alpha_{41}) \equiv 0.$$

For the type A_{1g} vibration,

$$R_1 = \frac{1}{2}(\Delta d_1 + \Delta d_2 + \Delta d_3 + \Delta d_4).$$

For the type A_{2u} vibration,

$$R_1 = d(\Delta\gamma_{13} + \Delta\gamma_{24})/\sqrt{2}.$$

For the type B_{1g} vibration,

$$R_1 = \frac{1}{2}d(\Delta\alpha_{12} - \Delta\alpha_{23} + \Delta\alpha_{34} - \Delta\alpha_{41}).$$

For the type B_{1u} vibration,

$$R_1 = d(\Delta\gamma_{24} - \Delta\gamma_{13})/\sqrt{2}.$$

For the type B_{2g} vibration,

$$R_1 = \frac{1}{2}(\Delta d_1 - \Delta d_2 + \Delta d_3 - \Delta d_4).$$

For the type E_u vibrations,

$$R_{1a} = (\Delta d_1 - \Delta d_3)/\sqrt{2},$$

$$R_{1b} = (\Delta d_2 - \Delta d_4)/\sqrt{2},$$

$$R_{2a} = \frac{1}{2}d(\Delta\alpha_{12} - \Delta\alpha_{23} - \Delta\alpha_{34} + \Delta\alpha_{41}),$$

$$R_{2b} = \frac{1}{2}d(\Delta\alpha_{12} + \Delta\alpha_{23} - \Delta\alpha_{34} - \Delta\alpha_{41}).$$

It can be seen that these symmetry coordinates are all normalized and mutually orthogonal, and that they transform according to the character table (Wilson [6]) of the symmetry point group D_{4h} .

4 POTENTIAL ENERGY

The most general harmonic potential function in terms of the internal coordinates is given by the expression

$$\begin{aligned} 2V = & f_d[(\Delta d_1)^2 + (\Delta d_2)^2 + (\Delta d_3)^2 + (\Delta d_4)^2] \\ & + 2f_{dd}[(\Delta d_1 + \Delta d_3)(\Delta d_2 + \Delta d_4)] \\ & + 2f'_{dd}[(\Delta d_1)(\Delta d_3) + (\Delta d_2)(\Delta d_4)] \\ & + 2df_{d\alpha}[(\Delta\alpha_{12})(\Delta d_1 + \Delta d_2) + (\Delta\alpha_{23})(\Delta d_2 + \Delta d_3) \\ & \quad + (\Delta\alpha_{34})(\Delta d_3 + \Delta d_4) + (\Delta\alpha_{41})(\Delta d_4 + \Delta d_1)] \\ & + 2df'_{d\alpha}[(\Delta\alpha_{12})(\Delta d_3 + \Delta d_4) + (\Delta\alpha_{23})(\Delta d_4 + \Delta d_1) \\ & \quad + (\Delta\alpha_{34})(\Delta d_1 + \Delta d_2) + (\Delta\alpha_{41})(\Delta d_2 + \Delta d_3)] \\ & + d^2f_{\alpha}[(\Delta\alpha_{12})^2 + (\Delta\alpha_{23})^2 + (\Delta\alpha_{34})^2 + (\Delta\alpha_{41})^2] \\ & + 2d^2f_{\alpha\alpha}[(\Delta\alpha_{12} + \Delta\alpha_{34})(\Delta\alpha_{23} + \Delta\alpha_{41})] \\ & + 2d^2f'_{\alpha\alpha}[(\Delta\alpha_{12})(\Delta\alpha_{34}) + (\Delta\alpha_{23})(\Delta\alpha_{41})] \\ & + d^2f_{\gamma}[(\Delta\gamma_{13})^2 + (\Delta\gamma_{24})^2] \\ & + 2d^2f_{\gamma\gamma}[(\Delta\gamma_{13})(\Delta\gamma_{24})] \\ & + 2df_{d\gamma}[(\Delta\gamma_{13})(\Delta d_1 + \Delta d_3) + (\Delta\gamma_{24})(\Delta d_2 + \Delta d_4)] \\ & + 2df'_{d\gamma}[(\Delta\gamma_{13})(\Delta d_2 + \Delta d_4) + (\Delta\gamma_{24})(\Delta d_1 + \Delta d_3)] \\ & + 2d^2f_{\gamma\gamma}[(\Delta\gamma_{13} + \Delta\gamma_{24})(\Delta\alpha_{12} + \Delta\alpha_{23} + \Delta\alpha_{34} + \Delta\alpha_{41})]. \end{aligned}$$

The force constants used are f_d (representing the force between X and Y atoms); f_{dd} (representing the interaction between stretching and stretching

when the two stretching bonds are adjacent); $f_{dd'}$ (representing the same interaction when the two bonds concerned are opposite each other); $f_{d\alpha}$ (representing the interaction between bond stretching and interbond angle bending when the stretching bond is one of the two bonds forming the bending angle); $f_{d\alpha'}$ (representing the same interaction when the stretching bond is not one of the two bonds forming the bending angle concerned); f_{α} (representing the force associated with interbond angle bending); $f_{\alpha\alpha}$ (representing the interaction between interbond angle bending and interbond angle bending when the two bending angles concerned are adjacent); $f_{\alpha\alpha'}$ (representing the same interaction when the two angles concerned are opposite each other); f_{γ} (representing the force associated with out-of-plane bending); $f_{\gamma\gamma}$ (representing the interaction between two simultaneous out-of-plane bendings); $f_{d\gamma}$ (representing the interaction between bond stretching and out-of-plane bending when the same bond is taking part in both motions); $f_{d\gamma'}$ (representing the same interaction when no bond is participating in both motions) and $f_{\alpha\gamma}$ (representing the interaction between interbond angle bending and out-of-plane bending).

By means of the proper matrix multiplications it is now seen that the **F**-matrix elements for the various irreducible representations are given by:

For the type A_{1g} vibration,

$$F_{11} = f_d + 2f_{dd} + f_{dd'}.$$

For the type A_{2u} vibrations,

$$F_{11} = f_{\gamma} + f_{\gamma\gamma}.$$

For the type B_{1g} vibration,

$$F_{11} = f_{\alpha} - 2f_{\alpha\alpha} + f_{\alpha\alpha'}.$$

For the type B_{1u} vibration,

$$F_{11} = f_{\gamma} - f_{\gamma\gamma}.$$

For the type B_{2g} vibration,

$$F_{11} = f_d - 2f_{dd} + f_{dd'}.$$

For the type E_u vibrations,

$$\begin{aligned} F_{11} &= f_d - f_{dd'}, \\ F_{12} &= F_{21} = \sqrt{2}(f_{d\alpha} - f_{d\alpha'}), \\ F_{22} &= f_{\alpha} - f_{\alpha\alpha'}. \end{aligned}$$

5. KINETIC ENERGY

Using standard principles (Wilson [3, 4]), the **G**-matrix elements are found to be:

For the type A_{1g} vibration,

$$G_{11} = \mu_y.$$

For the type A_{2u} vibration,

$$G_{11} = 2\mu_y + 8\mu_x.$$

For the type B_{1g} vibration,

$$G_{11} = 4\mu_y.$$

For the type B_{1u} vibration,

$$G_{11} = 2\mu_y.$$

For the type B_{2g} vibration,

$$G_{11} = \mu_y.$$

For the type E_u vibrations,

$$\begin{aligned} G_{11} &= \mu_y + 2\mu_x, \\ G_{12} &= G_{21} = -2\sqrt{(2)}\mu_x, \\ G_{22} &= 2\mu_y + 4\mu_x. \end{aligned}$$

Here μ_y is the reciprocal mass of a Y atom and μ_x is the reciprocal mass of the centre atom.

6. SECULAR EQUATIONS

The secular equations, giving the fundamental frequencies in terms of the force constants, can now be written down for the various symmetry species. We find:

For the type A_{1g} vibration,

$$\lambda_1 = (2\pi c\nu_1)^2 = F_{11}G_{11} = (f_d + 2f_{dd} + f_{dd'}) \cdot \mu_y.$$

For the type A_{2u} vibration,

$$\lambda_2 = (2\pi c\nu_2)^2 = F_{11}G_{11} = 2(f_\gamma + f_{\gamma\gamma})(\mu_y + 4\mu_x).$$

For the type B_{1g} vibration,

$$\lambda_3 = (2\pi c\nu_3)^2 = F_{11}G_{11} = 4(f_\alpha - 2f_{\alpha\alpha} + f_{\alpha\alpha'}) \cdot \mu_y.$$

For the type B_{1u} vibration,

$$\lambda_4 = (2\pi c\nu_4)^2 = F_{11}G_{11} = 2(f_\gamma - f_{\gamma\gamma}) \cdot \mu_y.$$

For the type B_{2g} vibration,

$$\lambda_5 = (2\pi c\nu_5)^2 = F_{11}G_{11} = (f_d - 2f_{dd} + f_{dd'}) \cdot \mu_y.$$

For the type E_u vibrations,

$$(-\lambda)^2 + (-\lambda)(F_{11}G_{11} + F_{22}G_{22} + 2F_{12}G_{12}) + |F| \cdot |G| = 0$$

where the roots are $\lambda_6 = (2\pi c\nu_6)^2$ and $\lambda_7 = (2\pi c\nu_7)^2$. This can be written as

$$\lambda_6 + \lambda_7 = [(f_d - f_{dd'}) + 2(f_\alpha - f_{\alpha\alpha'})](\mu_y + 2\mu_x) - 8\mu_x(f_{d\alpha} - f_{d\alpha'})$$

and

$$\lambda_6\lambda_7 = [(f_d - f_{dd'})(f_\alpha - f_{\alpha\alpha'}) - 2(f_{d\alpha} - f_{d\alpha'})^2][2\mu_y(\mu_y + 4\mu_x)].$$

7. CONCLUSIONS

It is worth noting that, as expected, the three vibrational degrees of freedom that are added because of the presence of a central atom, viz. A_{2u} and one of the degenerate E_u vibrations, are the only cases where μ_x appears in the \mathbf{G} -matrix elements. This is equivalent to the statement that the other vibrations would still possess the same forms if no centre atom were present.

It must also be noted that data for a second isotopic species are necessary if it is desired to evaluate all the force constants.

In practice, when no isotopic data are available, it would probably be best to neglect $(f_{d\alpha} - f_{d\alpha'})$ if μ_y is larger than $3\mu_x$. If this is not the case, it would be advisable to neglect $f_{dd'}$ instead.

In the ideal case we are able to evaluate $f_d, f_{dd}, f_{dd'}, (f_{d\alpha} - f_{d\alpha'}), (f_\alpha - f_{\alpha\alpha'}), (f_{\alpha\gamma} - f_{\alpha\gamma'}), f_\gamma$ and $f_{\gamma\gamma'}$. For this the type E_u fundamental frequencies of a second isotopic species are necessary. Note that only one datum is added in such a case, as the other will be merely a consequence of the Redlich-Teller product rule.

In the case of the SVFF all the force constants are zero except f_d , f_α and f_γ . In that case the equations would reduce to:

$$\begin{aligned} A_{1g}: \quad \lambda_1 &= f_d \cdot \mu_y, \\ A_{2u}: \quad \lambda_2 &= 2f_\gamma(\mu_y + 4\mu_x), \\ B_{1g}: \quad \lambda_3 &= 4f_\alpha \cdot \mu_y, \\ B_{1u}: \quad \lambda_4 &= 2f_\gamma \cdot \mu_y, \\ B_{2g}: \quad \lambda_5 &= f_d \cdot \mu_y, \\ E_u: \quad \lambda_6 + \lambda_7 &= (f_d + 2f_\alpha)(\mu_y + 2\mu_x), \\ &\quad \lambda_6\lambda_7 = 2f_\alpha \cdot f_d \cdot \mu_y(\mu_y + 4\mu_x). \end{aligned}$$

An artificial degeneracy is consequently introduced between ν_1 and ν_5 . However, it is immediately removed if a more general force field is assumed.

The author wishes to thank Professor P. V. Pistorius, of the University of Pretoria, Pretoria, South Africa, for his continued interest.

On obtient les équations séculaires relatives aux différentes représentations irréductibles de la molécule plane XY_4 (groupe D_{4h} de symétrie) au moyen de la méthode des matrices FG due à Wilson, et en utilisant le champ de force harmonique le plus général. Les équations pour le cas du champ de forces simples de valence sont aussi données.

Die Säkulargleichungen für die verschiedenen Darstellungen für ein ebenes Molekül XY_4 mit der Punktsymmetriegruppe D_{4h} werden mittels der Wilsonschen Methode der F- und G-Matrizen abgeleitet, wobei das allgemeinste harmonische Potential benutzt wird. Die Gleichungen für den Fall reiner Valenzkräfte werden ebenfalls angegeben.

REFERENCES

- [1] WILSON, E. B. Jr., 1935, *J. chem. Phys.*, **3**, 59.
- [2] KOHLRAUSCH, K. W. F., 1938, *Der Smekal-Raman-Effekt*, Ergänzungsband 1931-37 (Berlin: Springer-Verlag).
- [3] WILSON, E. B. Jr., 1939, *J. chem. Phys.*, **7**, 1041.
- [4] WILSON, E. B. Jr., 1941, *J. chem. Phys.*, **9**, 76.
- [5] HERZBERG, G., 1945, *Infra-red and Raman Spectra of Polyatomic Molecules* (New York: Van Nostrand Company, Inc.).
- [6] WILSON, E. B. Jr., DECIUS, J. C., and CROSS, P. C., 1945, *Molecular Vibrations* (New York: McGraw-Hill Book Company, Inc. Table X-7, p. 328).

RESEARCH NOTES

Rotatory dispersion in hydrated cobaltous salts

by M. J. STEPHEN

Department of Theoretical Chemistry, Cambridge University

(Received 6 May 1958)

Some observations have been made on the dispersion of the Faraday rotation in solutions of cobaltous salts [1, 2]. In view of our greatly increased knowledge of the optical and magnetic properties of transition-metal ions it is interesting to see whether the dispersion of the Faraday rotation can be predicted.

Kramers [3] showed that the rotation θ of the plane of polarization per unit length (taking the static magnetic field H in the z -direction parallel to the direction of the propagation of the light) is given by

$$\theta = \frac{4\pi v^2 N i}{h c \bar{n} S} \sum_{f,g} \frac{[(X)_{fg}(Y)_{fg}]}{v^2 - v_{fg}^2} \exp\left(\frac{-h\nu_f}{kT}\right) \quad (1)$$

where N is the number of atoms in unit volume, \bar{n} the average refractive index and S the partition function. X and Y are the components of the total electronic dipole moment along the x - and y -axes respectively and the square brackets indicate a vector product. The summation f is over all occupied states each being weighted with the appropriate Boltzmann factor and the summation g is over all excited states†.

We can put (1) in a more convenient form for calculation as follows. Consider one term

$$(X)_{fg}(Y)_{gf} - (Y)_{fg}(X)_{gf} \quad (2)$$

Using the commutation relation

$$[L_z, X] = i\hbar Y$$

equation (2) becomes after expansion

$$\frac{-i}{\hbar} \sum_h \{ (X)_{fg}(L_z)_{gh}(X)_{hf} - (X)_{fg}(X)_{gh}(L_z)_{hf} + \text{complex conjugate} \}. \quad (3)$$

In the case of crystal fields weak compared with the term splitting we may simplify equation (3) by only considering diagonal elements of L_z . This approximation will be rigorous in the case of atoms showing Russell-Saunders coupling and in the weak field limit where L is a good quantum number. It will also be a good approximation if there is only one important optical transition.

From equations (1) and (3) we obtain

$$\theta = \frac{8\pi v^2 N}{\hbar^2 c \bar{n} S} \sum_{f,g} \frac{|(X)_{fg}|^2}{v^2 - v_{fg}^2} \{ (L_z)_{gg} - (L_z)_{ff} \} \exp\left(\frac{-h\nu_f}{kT}\right). \quad (4)$$

† In Kramers' formula a factor 4π has been omitted as can be seen by comparison of his equations (32) and (34).

As we are considering optical transitions which are formally forbidden as electric dipole transitions and are probably induced by the Stark effect in the fluctuating crystalline electric fields, the effect of the static magnetic field on the intensities will be small and will be neglected.

Following Rosenfeld [4] we separate equation (4) into paramagnetic and diamagnetic parts. Let

$$\nu_{gf} = \nu_{gf}^{(0)} + H\nu_{gf}^{(1)}$$

and

$$\frac{1}{\nu^2 - \nu_{gf}^2} = \frac{1}{\nu^2 - \nu_{gf}^{(0)2}} \left\{ 1 + \frac{2H\nu_{gf}^{(0)}\nu_{gf}^{(1)}}{\nu^2 - \nu_{gf}^{(0)2}} \right\}. \quad (5)$$

Substituting (5) in (4) we obtain the paramagnetic rotation defined by

$$\theta_p = \frac{8\pi\nu^2 N}{h^2 c \bar{n} S} \sum_{f,g} \frac{|(X)_{fg}|^2}{\nu^2 - \nu_{gf}^{(0)2}} \{ (L_z)_{gg} - (L_z)_{ff} \} \exp\left(\frac{-h\nu_f}{kT}\right) \quad (6)$$

and the diamagnetic part

$$\theta_d = \frac{16\pi\nu^2 NH}{h^2 c \bar{n} S} \sum_{f,g} \frac{|(X)_{fg}|^2}{\nu^2 - \nu_{gf}^{(0)2}} \frac{\nu_{gf}^{(0)}\nu_{gf}^{(1)}}{\nu^2 - \nu_{gf}^{(0)2}} \{ (L_z)_{gg} - (L_z)_{ff} \} \exp\left(\frac{-h\nu_f}{kT}\right). \quad (7)$$

We may draw some interesting conclusions from equations (6) and (7).

(a) The factor $(L_z)_{gg} - (L_z)_{ff}$ shows that the two states must differ in the component of angular momentum along the direction of propagation of the radiation. Physically this may be interpreted as the change in angular momentum being transferred to the radiation, the plane of polarization thus being rotated.

(b) If the ground state of the ion is orbitally non-degenerate the paramagnetic term will vanish unless the somewhat different frequencies of the different multiplet components of the important absorption lines are taken into account. Thus for ions in S-states the paramagnetic rotation will be very small.

(c) If the ion has an orbitally degenerate ground state the paramagnetic effect will be large and temperature-dependent and depends essentially on the difference in population in a magnetic field of the sub-levels of the ground state. In particular if the ground state is a Kramers doublet the variation with temperature and magnetic field will be given by $\tanh \mu\beta H/kT$ where $\pm \mu\beta H$ are the Zeeman energies of the two components of the doublet.

(d) The diamagnetic effect, by equation (7), depends on the Zeeman splitting of the levels in a magnetic field and will normally be small and temperature-independent. However, very near a transition frequency of the ion it will be the dominant term owing to the stronger resonance denominator.

Abragam and Pryce [5] have discussed the energy levels and optical spectrum of hydrated cobaltous salts; from their data together with the oscillator strengths measured by Jørgensen [6] the Faraday rotation in the neighbourhood of the transitions at 19400 cm^{-1} and 21550 cm^{-1} has been calculated. The crystal field parameters of Abragam and Pryce were slightly modified to obtain better agreement with the energy levels predicted by the optical spectrum. The values taken were $G = 23800 \text{ cm}^{-1}$ and $E_p = 10300 \text{ cm}^{-1}$, with the tetragonal field and spin-orbit coupling as in Abragam and Pryce.

These figures show that the crystal field energy is not small compared with the term splitting. We are considering here the lowest optical transition (except for a very weak transition at about 15000 cm^{-1}) and we would expect much

higher states not to mix to an appreciable extent with the ground state and excited state considered; thus equations (6) and (7) will be applicable.

Even in the case of a very strong crystal field the approximation made in obtaining equation (4) should be applicable but for a different reason. If in equation (3) we denote the ground state and excited state in the d^n manifold by f and g respectively then for strong crystal fields matrix elements of the type $(L_z)_{fh}$ and $(L_z)_{gh}$ where h is some intermediate state within the d^n manifold will be large. However, in this case matrix elements of the type $(X)_{fh}$ or $(X)_{gh}$ are

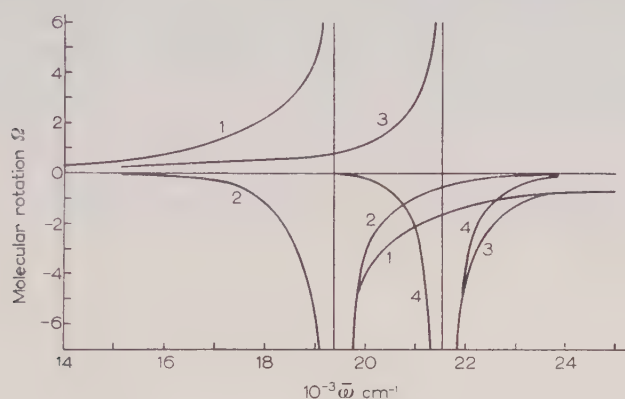


Figure 1. Paramagnetic and diamagnetic parts of the molecular rotation $\Omega \left(\frac{\text{min cm}^2}{\text{gauss mol}} \right)$ in CoSO_4 solution.

- (a) $\bar{\omega} = 19\,400 \text{ cm}^{-1}$. 1. paramagnetic. 2. diamagnetic.
 (b) $\bar{\omega} = 21\,550 \text{ cm}^{-1}$. 3. paramagnetic. 4. diamagnetic.

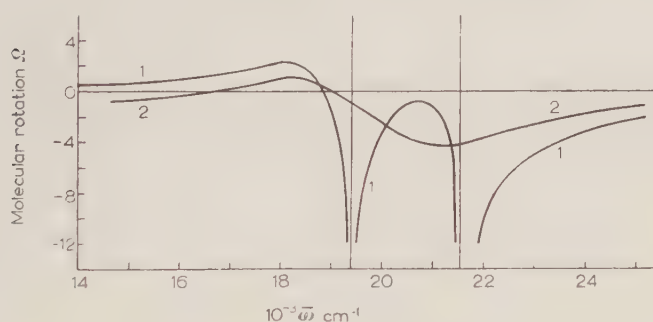


Figure 2. Molecular rotation $\Omega \left(\frac{\text{min cm}^2}{\text{gauss mol}} \right)$ in CoSO_4 solution.

1. Calculated. 2. observed.

formally zero, the corresponding transitions having no electric dipole moment; their appearance is probably due to the Stark effect produced by the fluctuating crystalline electric field; these elements are thus small. If the intermediate state h arises out of some other electron configuration such as $d^{n-1}p$, matrix elements of the type $(X)_{fh}$ or $(X)_{gh}$ will be large but those of type $(L_z)_{fh}$ or $(L_z)_{gh}$ will now be zero.

In figure 1 the separate contributions to the rotation and in figure 2 the total calculated rotation is compared with the experimental results of Miescher [1] on cobalt sulphate solution. The calculated dispersion curve agrees well with the measured curve on either side of the transitions where the paramagnetic part is the most important. Very close to the absorption lines, which have been taken to be infinitely sharp, the agreement is not so good. Here the rotation depends on the difference between two large quantities (the diamagnetic term being predominant) and in this region damping effects would be important and would smooth out the calculated curve. In making the comparison with experiment the effect of the anion has been neglected. This can be important as is shown by comparison of the results of Miescher [1] on cobalt sulphate and chloride solutions and can have the effect of raising or lowering the observed dispersion curve but should not affect the general shape.

The author would like to thank Dr. L. E. Orgel, who suggested this problem, for much useful discussion.

REFERENCES

- [1] MIESCHER, E., 1930, *Helv. phys. Acta*, **3**, 93.
- [2] ROBERTS, R. W., 1930, *Phil. Mag.*, **9**, 361.
- [3] KRAMERS, H. A., 1930, *Proc. Acad. Sci. Amst.*, **33**, 959.
- [4] ROSENFELD, L., 1929, *Z. Phys.*, **57**, 835.
- [5] ABRAGAM, A., and PRYCE, M. H. L., 1951, *Proc. roy. Soc. A*, **206**, 173.
- [6] JØRGENSEN, C. K., 1954, *Acta chem. scand.*, **8**, 1495.

Evaluation of coulomb repulsion integrals from spectroscopic data

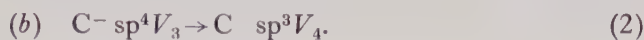
by R. D. BROWN

Chemistry Department, University of Melbourne, Carlton, N.3,
Victoria, Australia

[Received 25 March 1958]

It has been demonstrated that, when theoretical values are used for the coulomb repulsion integrals which arise in molecular orbital calculations, errors occur in predictions of molecular spectroscopic intervals but that these errors may be reduced by using values for such coulomb integrals obtained from spectroscopic data. It seems that the theoretical values for the integrals are unsatisfactory because Slater functions do not adequately describe electron distributions in atoms and ions. Pariser [1] considered that it was better to

evaluate $(2p/2p)$, the coulomb repulsion between two $2p\pi$ electrons, for example, by considering the processes



For the first process

$$\Delta E_a = I_c = -W(2p)$$

while for the second

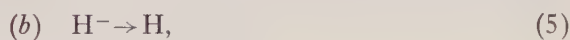
$$\Delta E_a = A_c = -W(2p) - (2p/2p).$$

Hence

$$(2p/2p) = \Delta E_a - \Delta E_b = I_c - A_c, \quad (3)$$

where I_c and A_c are the ionization potential and electron affinity of carbon in its V_4 valence state.

It is instructive to consider the simplest case, of evaluating $(1s/1s)$ from consideration of the processes



so that

$$(1s/1s) = I_H - A_H = \Delta E_a - \Delta E_b. \quad (6)$$

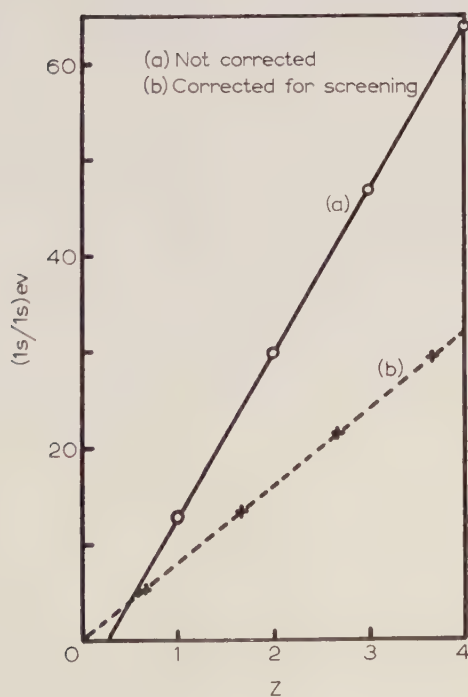


Figure 1.

If equation (6) is applied to the isoelectronic series of one-electron systems and the resulting $(1s/1s)$ values plotted against the nuclear charge, the graph shown in figure 1 is obtained. The values of the integral are given accurately by the equation

$$(1s/1s) = 16.99(Z - 0.244) \text{ ev.} \quad (7)$$

It is not surprising to find the integral to vary linearly with Z because when evaluated theoretically using hydrogenic functions it becomes $17.00Z \text{ ev}$; but the unsatisfactory feature of equation (7) is that the integral vanishes for positive Z whereas to be physically applicable the repulsion should tend to zero as Z tends to zero. The difficulty associated with (7) may be resolved by more careful consideration of (6). When deriving (6) it was assumed that ΔE_b may be dissected into a nuclear attraction portion I_H and an electron repulsion portion $(1s/1s)$ and that I_H is identical with ΔE_a . However in the process (4) the electron is removed from an orbital such that the effective nuclear charge is unity whereas in (5) the orbital from which the electron is removed corresponds to an effective nuclear charge of less than unity because of the screening arising from the presence of the other $1s$ electron. According to Slater's [2] rules the effective nuclear charge is reduced by 0.3 owing to the screening by the other electron so that when using (6) we should use a corrected value of I_H . It is easy to correct I_H for a change in Z because for hydrogenic systems

$$I = 13.6Z^2. \quad (8)$$

Since I is sensitive to the value of Z Slater's approximate rules may not be adequate for obtaining the appropriate Z . We have therefore used (8) and the experimental ionization energies of H^- and He , namely 0.747 ev [3]† and 24.585 ev [4]† to find the value of the screening constant such that when (6) is used we find $(1s/1s) = \alpha Z$. The value found is 0.33_0 , remarkably close to Slater's value.

When the experimental values of I for the isoelectronic series corresponding to (4) are corrected for this screening and then used in (6) to obtain $(1s/1s)$ the result is

$$(1s/1s) = 8.00Z \text{ ev} \quad (9)$$

and comparison of (9) and (7) emphasizes the importance of this screening correction in the evaluation of coulomb repulsion integrals from spectroscopic data. Corresponding corrections must be applied when (3) is used to evaluate $(2p/2p)$. Results of calculations for integrals involving these higher orbitals and incorporating the screening correction will be reported elsewhere.

REFERENCES

- [1] PARISER, R., 1953, *J. chem. Phys.*, **21**, 568.
- [2] SLATER, J. C., 1930, *Phys. Rev.*, **36**, 57.
- [3] HENRICH, L. R., 1944, *Astrophys. J.*, **99**, 59.
- [4] MOORE, C. E., *Atomic Energy Levels*, Vol. I (N.B.S. Circular 467).

† The conversion factor $1 \text{ cm}^{-1} = 1.23978 \times 10^{-4} \text{ ev}$ (Dumond and Cohen, *Rev. mod. Phys.* 1953, **25**, 691) has been used for obtaining values in ev.

Application of Brønsted's principle of congruence to n-alkane mixtures

by J. HIJMANS

Koninklijke/Shell-Laboratorium, Amsterdam
(N.V. De Bataafsche Petroleum Maatschappij)

(Received 13 May 1958)

As an explanation of the thermodynamic behaviour of normal-alkane mixtures, Brønsted and Koefoed [1] in 1946 introduced the so-called *principle of congruence*. According to these authors the thermodynamic properties of a mixture of n-alkanes are determined by an average chain-length,

$$n = \sum_i n_i x_i; \quad (1)$$

n_i being the number of carbon atoms in a molecule of the i th species, and x_i the mole fraction of that species in the mixture. Mixtures with the same average chain-length are said to be congruent. Thus for instance if n is integral, all mixtures with average chain-length n are congruent with the pure substance $C_n H_{2n+2}$.

The principle of congruence is supported in the first place by the results of Brønsted and Koefoed's own vapour pressure [1] and solubility[2] experiments. But also the heats of mixing, which were determined in 1950 by van der Waals and Hermans [3], are in excellent agreement with Brønsted's principle. Recently Desmijter and van der Waals [4] published values of the volume contraction on mixing for a number of n-alkane mixtures. They found a fairly good agreement between their excess volumes, on the one hand, and the corresponding "excess volumes", derived with Brønsted's principle from the molar volumes of pure alkanes, on the other hand.

In view of this result we have investigated whether the excess volumes, measured by Desmijter and van der Waals in different mixtures, are also *mutually consistent*, from the standpoint of the principle of congruence. Therefore, we have plotted in figure 1 the excess volume for the mixture pentane-hexadecane as a function of the average chain-length, $n = 5x_5 + 16x_{16}$ (upper curve). The excess volume of a mixture of two n-alkanes having chain-lengths n_1 and n_2 should be represented by the difference in height between this curve and the straight line:

$$v^{id} = \frac{n_2 - n}{n_2 - n_1} v(n_1) + \frac{n - n_1}{n_2 - n_1} v(n_2) \quad (2)$$

where $v(n_1)$ (or $v(n_2)$ respectively) is the excess volume of a pentane-hexadecane mixture with an average chain-length of n_1 (or n_2). In order to compare a mixture of two alkanes $C_{n_1}H_{2n_1+2}$ and $C_{n_2}H_{2n_2+2}$ with a pentane-hexadecane mixture of the same average chain-length we have added the linear expression (2) to the excess volumes which have been measured in the C_{n_1}/C_{n_2} -mixture. The points which

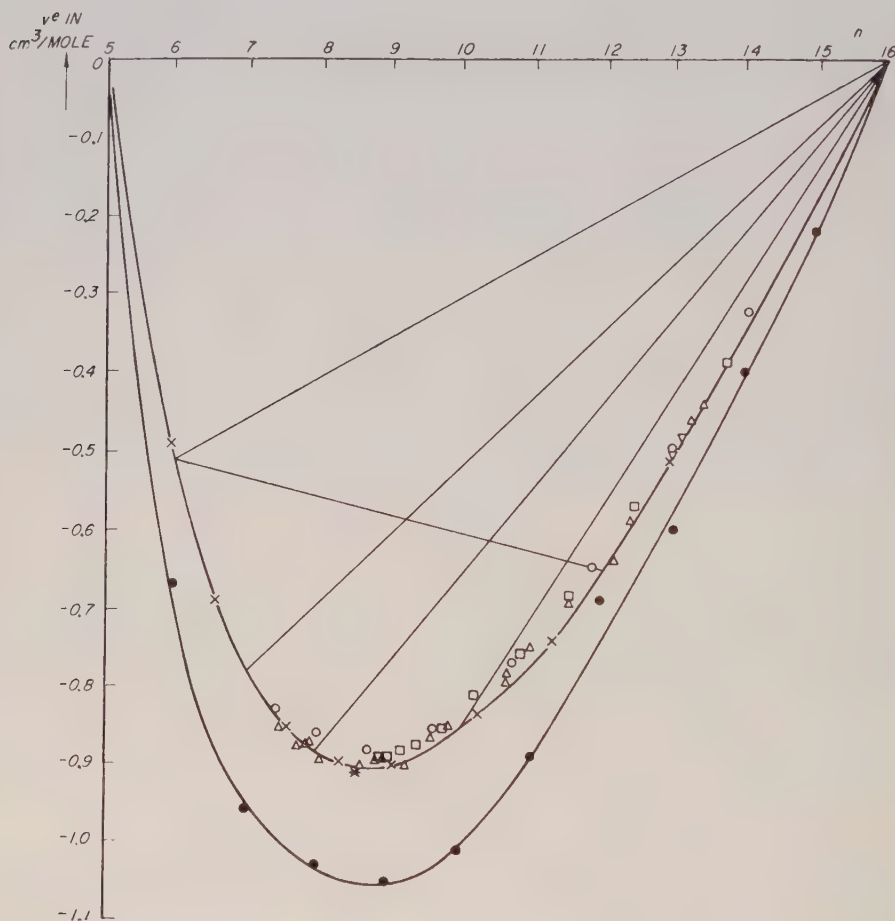


Figure 1. Excess volume for binary alkane mixtures and for pure alkanes plotted as a function of the average chain-length.

- | | | | |
|---|------------------------------------|---|---|
| × | Mixture $C_5 H_{12}-C_{16} H_{34}$ | ▽ | Mixture $C_{10} H_{22}-C_{16} H_{34}$ |
| ○ | Mixture $C_6 H_{14}-C_{16} H_{34}$ | ✱ | Mixture $C_6 H_{14}-C_{12} H_{26}$ |
| △ | Mixture $C_7 H_{16}-C_{16} H_{34}$ | ● | Calculated from data of pure substances |
| □ | Mixture $C_8 H_{18}-C_{16} H_{34}$ | | $C_6 H_{14} \dots C_{15} H_{32}$ |

are obtained in this way for five different mixtures agree to within the experimental accuracy with each other and with the C_5/C_{16} curve. In fact the mutual agreement between different mixtures is better than the agreement between mixtures and pure substances (the dots in figure 1). As has been remarked by Desmijter

et al., it may be relevant in this connection that the data for the pure substances refer to liquids which were saturated with air, whereas the measurements on the mixtures were carried out under air-free conditions.

In figure 2 the same procedure has been applied to the excess heat function according to van der Waals and Hermans. Here, too, there is a good mutual agreement between the different mixtures.

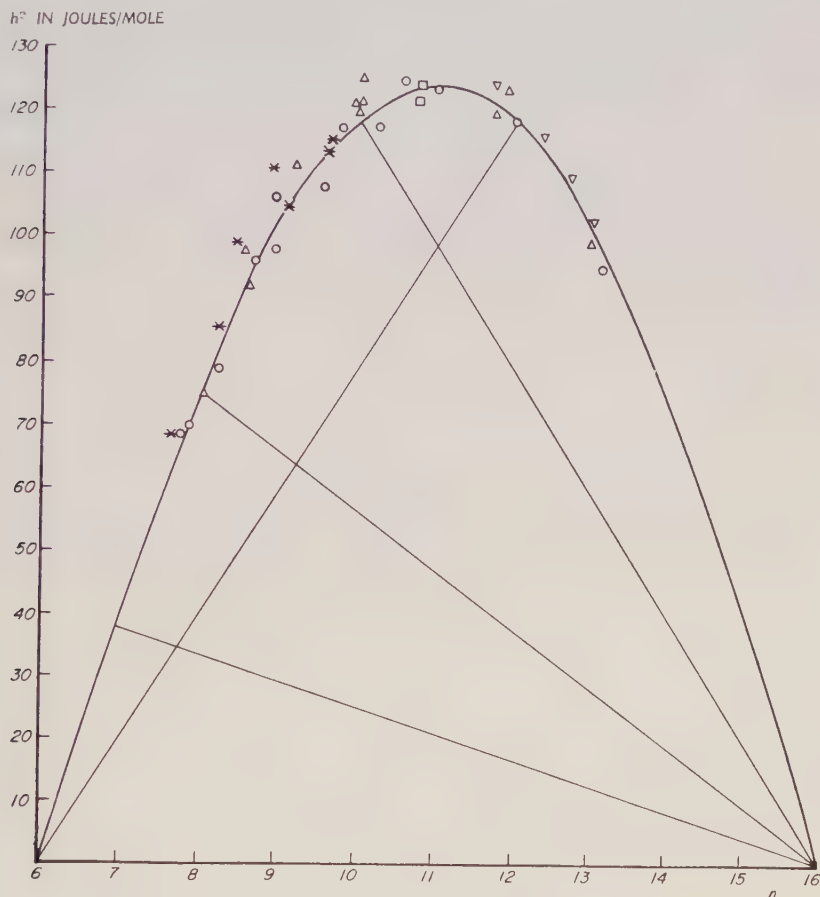


Figure 2. Enthalpy of mixing for binary alkane mixtures plotted as a function of the average chain-length.

- Mixture C₆ H₁₄-C₁₆ H₃₄
- △ Mixture C₇ H₁₆-C₁₆ H₃₄
- Mixture C₈ H₁₈-C₁₆ H₃₄
- ▽ Mixture C₁₀ H₂₂-C₁₆ H₃₄
- ✱ Mixture C₆ H₁₄-C₁₂ H₂₆

The mutual consistency of the experimental data thus provides additional support for the principle of congruence. On the other hand this consistency may also be considered as an indication of the reliability of the experimental results.

REFERENCES

- [1] BRØNSTED, J. N., and KOEFOED, J., 1946, *Kgl. Danske Videnskab. Selskab., Mat.-fys. Medd.*, **22**, No. 17, 1.
- [2] KOEFOED, J., 1953, *Disc. Faraday Soc.*, **15**, 207.
- [3] VAN DER WAALS, J. H., and HERMANS, J. J., 1950, *Rec. Trav. Chim. Pays Bas.*, **69**, 971; 1951, **70**, 101.
- [4] DESMIJTER, A., and VAN DER WAALS, J. H., 1958, *Rec. Trav. Chim. Pays Bas.*, **77**, 53.

Ring currents and proton magnetic resonance in aromatic molecules

by R. McWEENY

Departments of Mathematics, Physics and Chemistry
University College of North Staffordshire

(Received 19 June, 1958)

The molecular orbital theory is adapted to the calculation of magnetic shielding constants in aromatic molecules. The usual LCAO perturbation theory is generalized to take account of the imaginary perturbation due to an external magnetic field. The induced field at a point is then calculated by inserting a test dipole, adopting approximations due to London, and using the perturbation theory to evaluate a coupling energy. The results differ somewhat from those obtained in a rather different manner by Pople.

1. INTRODUCTION

It is well known that the diamagnetic anisotropy of an aromatic hydrocarbon may be attributed to induced currents in its π -electron system, and that these currents may be regarded as flowing round the various rings. This picture, first proposed by Pauling [7], was formulated in quantum mechanical terms by London [4] and has since been used extensively (see, for instance, McWeeny [6]; Mayot *et al.* [5]; Bergman *et al.* [1]). Calculated diamagnetic anisotropies are usually in quite good agreement with experiment.

Recently, interest in this field has been revived. The induced ring currents are equivalent to magnetic shells and the field at an attached proton (peripheral hydrogen atom) consequently differs from the applied field H owing to the resultant secondary field H' : this effect is revealed by shifts in the magnetic resonance peaks of the various protons. The problem of finding the secondary field differs somewhat from that of finding the total induced moment (and hence susceptibility) and the treatments given so far (Bernstein *et al.* [2], Pople [8]) are somewhat less satisfactory. The general pattern of the shifts within a given molecule is nicely interpreted, even on the Pauling model; but the 'absolute' shifts are not accounted for, large anomalies occurring on going from one molecule to another. It is probable that these anomalies are due partly to the experimental techniques employed; for example, the use of pure liquids instead of dilute solutions with a common solvent. Nevertheless, even the better of the two theories (Pople [8]), besides being difficult to apply to large molecules, contains undesirable semiclassical features which (as will be seen presently) lead to gross under-estimates of H' . In this paper we shall give a direct method of calculation of the field at any point, also based on the London theory, which is easily applied even to large molecules.

2. FORMULATION: THE LONDON THEORY

In the presence of a magnetic field \mathbf{H} , which may be assumed normal to the plane of the molecule, the MO's of the π electrons are built out of AO's $\phi_1, \phi_2 \dots \phi_m$ related to those in the absence of the field by

$$\phi_i = \phi_i^{(0)} \exp \left\{ -2\pi i \left(\frac{e}{hc} \right) \mathbf{A}_i \cdot \mathbf{r} \right\}. \quad (2.1)$$

Here $\phi_i^{(0)}$ has roughly the form of an atomic 2p orbital (although we shall assume the set is orthonormal) and \mathbf{A}_i is the value of the magnetic vector potential at the i th nucleus. For a uniform field, along the normal, $\mathbf{H} = H\mathbf{n}$, $\mathbf{A} = -\frac{1}{2}\mathbf{r} \times \mathbf{H}$ and at the i th nucleus $\mathbf{A}_i = -\frac{1}{2}\mathbf{R}_i \times \mathbf{H}$. With London's approximations, the secular problem for the MO's differs from that without the field merely by field-dependent phase factors in the resonance integrals:

$$\beta_{ij} = \beta_{ij}^{(0)} \exp \left\{ \pi i \left(\frac{e}{hc} \right) (\mathbf{A}_i - \mathbf{A}_j) \cdot (\mathbf{R}_i + \mathbf{R}_j) \right\} \quad (2.2)$$

or, using simple geometry,

$$\beta_{ij} = \beta_{ij}^{(0)} \exp \left\{ 2\pi i \left(\frac{e}{hc} \right) S_{ij} H \right\} \quad (2.3)$$

where S_{ij} is the signed area of the triangle formed by the origin (at which $A=0$) and the bond $i \rightarrow j$, counted positive if $i \rightarrow j$ is right handed about the normal \mathbf{n} . For hydrocarbons the common coulomb integral, α , may be taken as an energy zero; and it is assumed that $\beta_{ij}^{(0)} = \beta$ or 0, according as $i \rightarrow j$ is a real bond or not.

It is well known that the expanded secular equation reduces to the form

$$p(x) = q_1(x) \cos 2\pi f_1 + q_2(x) \cos 2\pi f_2 + \dots$$

where $p(x)$, $q_1(x)$, \dots are polynomials in x ($= (E - \alpha)/\beta$) and $f_i = (e/hc)S_i H$, where S_i is the area of a closed circuit containing one or more rings. If f_i and S_i are used for *irreducible* circuits (single rings), the cosine terms will include $\cos 2\pi(f_1 + f_2)$, $\cos 2\pi(f_1 + f_2 + f_3)$, etc. and expansion up to terms in H^2 then gives

$$P(x) = 4\pi^2 \sum_{i,j} Q_{ij}(x) f_i f_j. \quad (2.4)$$

As was first observed by London, the solutions to this order are related to those with $H=0$ by

$$x^{(p)} = x_0^{(p)} + 4\pi^2 \sum_{i,j} x_{ij}^{(p)} f_i f_j, \quad x_{ij}^{(p)} = Q_{ij}(x_0^{(p)})/P'(x_0^{(p)}). \quad (2.5)$$

Since $E^{(p)} = \alpha + x^{(p)}\beta$ the total perturbation energy may be written

$$E_{\text{mag}} = \sum_i -\frac{1}{2} M_i \mathbf{S}_i \cdot \mathbf{H} \quad (2.6)$$

where, with n_p as the occupation number of the p th orbital,

$$M_i = -8\pi^2\beta \left(\frac{e}{hc} \right)^2 \sum_p^{\text{occ}} n_p \sum_j x_{ij}^{(p)} (\mathbf{S}_j \cdot \mathbf{H}). \quad (2.7)$$

Now the potential energy of an induced dipole, with $\mathbf{M} = \chi\mathbf{H}$, is $-\frac{1}{2}\mathbf{M} \cdot \mathbf{H}$; and for a uniform shell of strength M and vector area \mathbf{S} it is $-\frac{1}{2}M\mathbf{S} \cdot \mathbf{H}$. The magnetic energy (2.6) is thus identical with that of a set of magnetic shells, one for each ring in the molecule, with strengths given by (2.7). The sum in this expression invariably turns out negative, β is negative, and the induced moment is thus

negative: this corresponds to diamagnetism, the moment opposing the field, and the magnetic shell for each ring may be formally associated with an induced current $j_i = M_i c$ (circulating clockwise about the applied field).

This resolution of the total induced moment into terms associated with the various rings (which is a simplified form of that given by Pople [8]) is essentially formal: it will be accurate in giving the secondary field at large distances, where only the *total* moment matters, but not necessarily satisfactory near the molecule. The induced currents are not of course *line* currents and the induced shells cannot be strictly uniform. The further step of representing each shell by a point dipole at the centre of the ring introduces additional approximations which are clearly rather poor. And it is questionable whether calculations based upon (2.7), which become rather elaborate with more than two rings, represent a significant and worthwhile advance on those which use the naïve Pauling model.

It is however still possible to employ a London-type energy calculation, again avoiding explicit use of the current density operator, by introducing a *point dipole* as a test body and evaluating the coupling energy between it and the induced current distribution in the molecule. If a dipole of moment $\mathbf{m} = m\mathbf{n}$ is introduced at any point in the molecular plane, this point being chosen as origin, the vector potential at point \mathbf{r} will be

$$\mathbf{A} = -\frac{1}{2} H \mathbf{r} \times \mathbf{n} - m \frac{\mathbf{r} \times \mathbf{n}}{r^3}. \quad (2.8)$$

It is then easily seen that (2.3) is replaced by

$$\beta_{ij} = \beta_{ij}^{(0)} \exp \left\{ 2\pi i \left(\frac{e}{hc} \right) S_{ij} \left(H + \frac{m}{R_i^3} + \frac{m}{R_j^3} \right) \right\}. \quad (2.9)$$

If the total perturbation energy can be evaluated, the term linear in m will represent the required coupling energy and, by definition, may be identified with $-H'm$. It is not easy, however, to evaluate the perturbation energy by direct expansion of the secular determinant. Instead, we shall develop a perturbation method along the lines of Coulson and Longuet-Higgins [3]—but without the restriction to *real* perturbations.

3. THE POLARIZABILITY METHOD

Using the abbreviation $\beta_{ij} = \beta_{ij}^{(0)} \exp i\theta_{ij}$, the perturbation is represented by the matrix Δ with elements

$$\Delta_{ij} = \beta_{ij}^{(0)} (i\theta_{ij} - \frac{1}{2}\theta_{ij}^2 + \dots). \quad (3.1)$$

If the zero-field MO's are $\psi_J = \sum_i \phi_i^{(0)} c_{iJ}$, the first and second-order energy changes are given by

$$\delta E_J^{(1)} = \Delta_{JJ} = \sum_{i,j} c_{iJ}^* \Delta_{ij} c_{jJ} \quad (3.2)$$

$$\delta E_J^{(2)} = \sum_{K(\neq J)} \frac{\Delta_{JK} \Delta_{KJ}}{E_J - E_K} = \sum_{K(\neq J)} \sum_{i,j} \frac{c_{iJ}^* \Delta_{ij} c_{jK} c_{K}^* \Delta_{kl} c_{lJ}}{E_J - E_K} \quad (3.3)$$

which together include all terms up to the second degree in the θ 's. The total first-order change, found by summing over all doubly occupied MO's is clearly

$$\delta E^{(1)} = \sum_{i,j} \Delta_{ij} P_{ji} \quad (3.4)$$

where \mathbf{P} , with elements

$$P_{ij} = 2 \sum_{J \text{ occ}} c_{iJ} c_{jJ}^*, \quad (3.5)$$

is the bonding matrix. The second order change arises from perturbation of the wave function and may be related to the change in the bonding matrix (and hence to the 'polarizabilities'). Clearly

$$\delta E^{(2)} = \sum_{r,s} \sum_{t,u} \Delta_{rs} \pi_{rs,tu} \Delta_{tu} \quad (3.6)$$

where

$$\pi_{rs,tu} = 2 \sum_J^{\text{occ}} \sum_{K(\neq J)} \frac{c_{rJ}^* c_{sK} c_{tK}^* c_{uJ}}{E_J - E_K}. \quad (3.7)$$

On the other hand, the first order change in the MO ψ_J is given by

$$\delta c_{rJ} = \sum_{K(\neq J)} \sum_{t,u} \frac{c_{rK} (c_{tK}^* \Delta_{tu} c_{uJ})}{E_J - E_K} \quad (3.8)$$

and from (3.5) and (3.7) it readily follows that

$$\delta P_{rs} = \sum_{u,t} (\pi_{sr,tu} + \pi_{tu,rs}) \Delta_{tu}. \quad (3.9)$$

The expression (3.6) can now be written alternatively,

$$\delta E^{(2)} = \frac{1}{2} \sum_{r,s} \Delta_{rs} \delta P_{sr}. \quad (3.10)$$

These results may be reduced by writing $\Delta_{rs} = X_{rs} + iY_{rs}$ and using Hermitian symmetry. From (3.9) we obtain

$$P_{sr} = \sum_{(tu)} \pi_{rs,(tu)} X_{tu} + \sum_{(tu)} \bar{\pi}_{rs,(tu)} (iY_{tu}) \quad (3.11)$$

where

$$\left. \begin{aligned} \pi_{rs,(tu)} &= \pi_{rs,tu} + \pi_{rs,ut} + \pi_{tu,rs} + \pi_{ut,rs} \\ \bar{\pi}_{rs,(tu)} &= \pi_{rs,tu} - \pi_{rs,ut} + \pi_{tu,rs} - \pi_{ut,rs} \end{aligned} \right\}. \quad (3.12)$$

These quantities are, respectively, the polarizabilities of bond $s \rightarrow r$ for real and for pure imaginary perturbations: the order of the suffixes is important and makes it necessary to associate a direction with each bond; and in the summation $\sum_{(tu)}$ each bond appears only once (suffixes in the agreed order).

Similarly from (3.10) and (3.11), it follows that

$$\begin{aligned} \delta E^{(2)} &= \sum_{(rs)} \sum_{(tu)} X_{rs} X_{tu} \mathcal{R}(\pi_{rs,(tu)}) + \sum_{(rs)} \sum_{(tu)} X_{rs} (iY_{tu}) i\mathcal{I}(\bar{\pi}_{rs,(tu)}) \\ &\quad + \sum_{(rs)} \sum_{(tu)} (iY_{rs}) X_{tu} i\mathcal{I}(\pi_{rs,(tu)}) + \sum_{(rs)} \sum_{(tu)} (iY_{rs}) (iY_{tu}) \mathcal{R}(\bar{\pi}_{rs,(tu)}). \end{aligned}$$

Now in the absence of magnetic fields (i.e. in the *unperturbed* system) the wave function can always be written in real form; and the results are simplest if this form is assumed. In this case

$$\delta E^{(2)} = \sum_{(rs)} \sum_{(tu)} X_{rs} X_{tu} \pi_{(rs)(tu)} - \sum_{(rs)} \sum_{(tu)} Y_{rs} Y_{tu} \bar{\pi}_{(rs)(tu)} \quad (3.13)$$

$$\mathcal{R}(\delta P_{rs}) = \sum_{(tu)} \pi_{(rs)(tu)} X_{tu}, \quad \mathcal{I}(\delta P_{rs}) = \sum_{(tu)} \bar{\pi}_{(rs)(tu)} Y_{tu} \quad (3.14)$$

where, adopting a more symmetrical definition,

$$\left. \begin{aligned} \pi_{(rs)(tu)} &= (\pi_{rs,tu} + \pi_{rs,ut} + \pi_{sr,ut} + \pi_{sr,tu}) \\ \bar{\pi}_{(rs)(tu)} &= (\pi_{rs,tu} - \pi_{rs,ut} + \pi_{sr,ut} - \pi_{sr,tu}) \end{aligned} \right\}. \quad (3.15)$$

The first quantity is the mutual polarizability of bonds rs and tu , as defined by Coulson and Longuet-Higgins, while the second is the supplementary term required in dealing with complex perturbations. It should be noted that $\bar{\pi}_{(rs)(tu)}$

is antisymmetric in both pairs, rs and tu , and that this is consistent with the Hermitian character of the perturbation which it describes: the agreed order of the pairs defining each bond (e.g. $r < s$) is therefore immaterial.

The evaluation of the quantities $\pi_{rs,tu}$, which determine both the real and imaginary polarizabilities, is simplified (cf. Coulson and Longuet-Higgins [3]) by noting that the summation over K , in (3.7), may be confined to the unoccupied MO's; and, in the case of alternant hydrocarbons, by the well-known pairing property of the MO's. The result then becomes (remembering $E_j = \alpha + x_j\beta$)

$$\beta\pi_{rs,tu} = 2 \sum_{J,K}^{\text{occ}} \frac{c_{rJ}c_{sK}c_{tK}c_{uJ}}{x_J - x_K} (-1)^{v_s + v_t} \quad (3.16)$$

where $v_i = 1$ or 2 according as atom i is in the 'starred set' or the 'unstarred set'. In this case we also have $\pi_{sr,ut} = \pi_{rs,tu}$ and (3.15) reduces accordingly.

4. DETERMINATION OF THE FIELD

It is convenient to measure areas in terms of S , that of a benzene ring (taken positive), and distances in terms of the length, a , of a C-C bond. If $S_{ij} = s_{ij}S$ and $R_i = r_i a$ the quantity θ_{ij} in (3.1) is then, from (2.9),

$$\theta_{ij} = 2\pi \left(\frac{e}{hc} \right) S s_{ij} \left\{ H + \left(\frac{m}{a^3} \right) k_{ij} \right\} \quad (4.1)$$

where $k_{ij} = \left(\frac{1}{r_i^3} + \frac{1}{r_j^3} \right)$

This perturbation is dealt with by putting $X_{ij} = \beta(-\frac{1}{2}\theta_{ij}^2)$ and $Y_{ij} = \beta\theta_{ij}$. Since \mathbf{P} is a symmetric matrix the imaginary term does not appear in $\delta E^{(1)}$, which becomes

$$E_{\text{mag}}^{(1)} = -\beta \left(\frac{2\pi e}{hc} \right)^2 S^2 \sum_{(ij)} P_{ij} s_{ij}^2 \left(H^2 + \frac{2Hm}{a^3} k_{ij} + \dots \right). \quad (4.2)$$

The second-order term becomes

$$E_{\text{mag}}^{(2)} = -\beta \left(\frac{2\pi e}{hc} \right)^2 S^2 \sum_{(ij)} \sum_{(kl)} \beta \bar{\pi}_{(ij)(kl)} s_{ij} s_{kl} \left\{ H^2 + \frac{2Hm}{a^3} \left(\frac{k_{ij} + k_{kl}}{2} \right) + \dots \right\}. \quad (4.3)$$

The total magnetic energy therefore differs from that with the dipole absent by a coupling term

$$\delta E_{\text{mag}} = -mH' = -2\beta \left(\frac{2\pi e}{hc} \right)^2 \frac{S^2 Hm}{a^3} (\sigma_1 + \sigma_2) \quad (4.4)$$

where

$$\sigma_1 = \sum_{(ij)} P_{ij} s_{ij}^2 k_{ij}, \quad \sigma_2 = \sum_{(ij)} \sum_{(kl)} \beta \bar{\pi}_{(ij)(kl)} s_{ij} s_{kl} \left(\frac{k_{ij} + k_{kl}}{2} \right). \quad (4.5)$$

These sums are dimensionless quantities which depend on the geometry of the molecule.

Example: Benzene. In the benzene molecule $P_{ij} = 2/3$ for each real bond: the 'imaginary' self-polarizability of each bond is $\beta \bar{\pi}_{(ij)(ij)} = -5/9$, and for all other pairs of bonds $\beta \bar{\pi}_{(ij)(kl)} = 1/9$, provided $i \rightarrow j$ and $k \rightarrow l$ point the same way round the ring. Consider a dipole at a point r bond lengths from the centre of the ring on a line through one vertex. Let $s_{12} (= s_{61}) = s_1$, $s_{23} (= s_{56}) = s_2$, $s_{34} (= s_{45}) = s_3$, and $k_{12} (= k_{61}) = k_1$ etc. Then it follows easily that

$$(\sigma_1 + \sigma_2) = \frac{4}{9} [s_1^2 k_1 + s_2^2 k_2 + s_3^2 k_3 + s_1 s_2 (k_1 + k_2) + s_2 s_3 (k_2 + k_3) + s_1 s_3 (k_1 + k_3)].$$

To obtain an expression valid at large distances (where it should lead to a dipole field) we expand everything in terms of r : this gives finally

$$(\sigma_1 + \sigma_2) = -\frac{1}{9r^3} \left[1 + \frac{9}{8} \frac{1}{r^2} + \frac{843}{128} \frac{1}{r^4} - \dots \right].$$

The secondary field at the dipole is thus

$$H' = 2\beta \left(\frac{2\pi e}{hc} \right)^2 \frac{S^2 H}{a^3} \left(-\frac{1}{9} \right) \left(\frac{\mu}{r^3} \right) \quad (4.6)$$

where $\mu \rightarrow 1$ for r large, showing that the induced moment may be regarded as a point dipole at large distances but that a correction factor

$$\mu = 1 + \frac{9}{8} \frac{1}{r^3} + \frac{843}{128} \frac{1}{r^4} - \dots \quad (4.7)$$

must in general be added. Since β is negative the field outside the ring augments the primary field: but inside the ring the field changes sign, becoming

$$2\beta \left(\frac{2\pi e}{hc} \right)^2 \frac{S^2 H}{a^3} \left(\frac{2}{9} \right)$$

at the centre. The field is compared with that predicted on the simple theory in figure 1. The infinity at points on the ring itself would of course arise if a classical

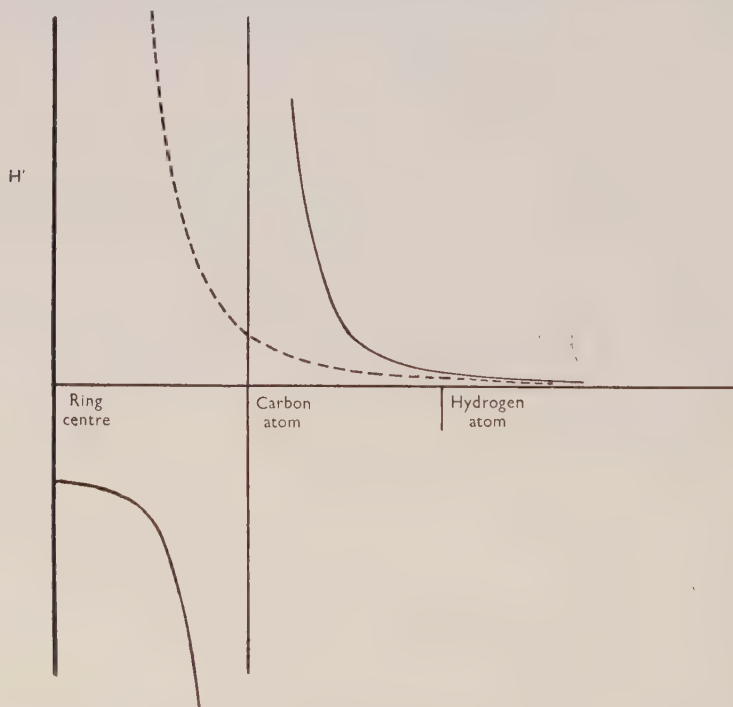
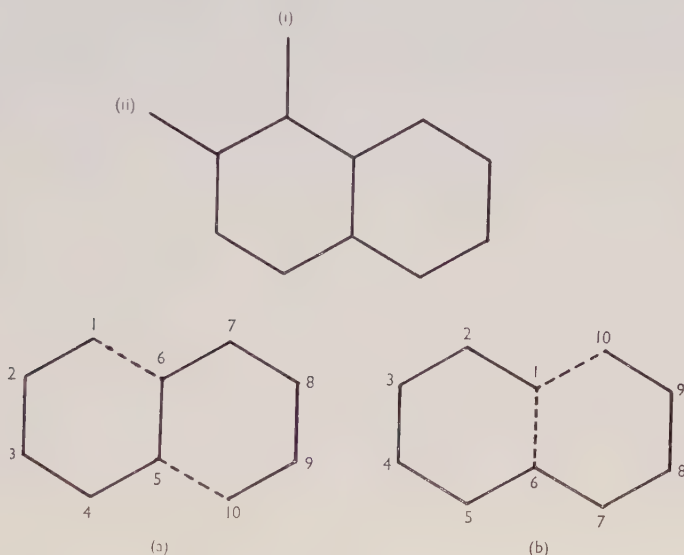


Figure 1. Field due to induced current in a benzene ring. The broken line represents the point dipole approximations.

line-current flowed round the ring, although the precise behaviour in this region cannot be reliably estimated with the approximation (2.2). On the other hand, the point dipole approximation (1st term of (4.7)) is very poor even one bond length away from the ring: inclusion of the higher terms in (4.7) raises the estimated field by 80 per cent.

The evaluation of the sums (4.5) would evidently be excessively tedious in the case of a polycyclic molecule, besides requiring knowledge of a very large number of hitherto untabulated polarizabilities. It will now be shown that by a suitable unitary transformation the original problem may be reduced to one in which only *one bond* of each ring is perturbed. This means, for example, that the 136 terms in σ_z for phenanthrene may be reduced to 6.



It will be sufficient to consider the naphthalene molecule, figure 2. Let the atoms be numbered along any chain which is continuous and open (i.e. without loops): two such chains are shown. The rings of the actual molecule are then completed by two further links, one in each ring. Let $\omega_{ij} = \exp(i\theta_{ij})$ where θ_{ij} is defined in (4.1): then the matrix of the perturbed Hamiltonian in the original AO basis is, with the numbering system (a),

$$h = \begin{bmatrix} \alpha & \beta\omega_{12} & & & & \beta\omega_{16} & & & & & \\ \beta\omega_{12}^* & \alpha & \beta\omega_{23} & & & & & & & & \\ & \beta\omega_{23}^* & \alpha & \beta\omega_{34} & & & & & & & \\ & & \beta\omega_{34}^* & \alpha & \beta\omega_{45} & & & & & & \\ & & & \beta\omega_{45}^* & \alpha & \beta\omega_{56} & & & & & \\ \beta\omega_{61} & & & & \beta\omega_{56}^* & \alpha & \beta\omega_{67} & & & \beta\omega_{5,10} & \\ & & & & & \beta\omega_{67}^* & \alpha & \beta\omega_{78} & & & \\ & & & & & & \beta\omega_{78}^* & \alpha & \beta\omega_{89} & & \\ & & & & & & & \beta\omega_{89}^* & \alpha & \beta\omega_{9,10} & \\ & & & & & & & & \beta\omega_{9,10}^* & \alpha & \\ & & & & \beta\omega_{10,5} & & & & & & \end{bmatrix}. \quad (5.1)$$

$$(\bar{\phi}_1 \bar{\phi}_2 \dots \bar{\phi}_m) = (\phi_1 \phi_2 \dots \phi_m) \mathbf{U} \quad (5.2)$$

where \mathbf{U} is the diagonal matrix

$$\mathbf{U} = \text{diag. } (1, \omega_{12}^*, \omega_{12}^* \omega_{23}^*, \omega_{12}^* \omega_{23}^* \omega_{34}^*, \dots)$$

with general element

$$U_{ii} = \omega_{12}^* \omega_{23}^* \dots \omega_{i-1, i}^* \quad (5.3)$$

then the matrix of the Hamiltonian referred to the new orbitals will be $\bar{\mathbf{h}} = \mathbf{U}^\dagger \mathbf{h} \mathbf{U}$. Remembering that $\omega_{ji} = \omega_{ij}^*$ and $|\omega_{ij}| = 1$, \mathbf{h} is seen to have the form (5.1) with all the near-diagonal ω 's replaced by 1's and

$$\begin{aligned} \omega_{61} &\rightarrow \bar{\omega}_{61} = U_{66}^\dagger \omega_{61} U_{11} = \omega_{12} \omega_{23} \omega_{34} \omega_{45} \omega_{56} \omega_{6,1} = \exp [i\theta_{(1)}], \text{ say,} \\ \omega_{10,5} &\rightarrow \bar{\omega}_{10,5} = U_{10,10}^\dagger \omega_{10,5} U_{55} = (\omega_{12} \omega_{23} \dots \omega_{9,10}) \omega_{10,5} (\omega_{12}^* \omega_{23}^* \dots \omega_{45}^*) \\ &= \omega_{56} \omega_{67} \omega_{78} \omega_{89} \omega_{9,10} \omega_{10,5} = \exp [i\theta_{(2)}], \text{ say.} \end{aligned}$$

The only field-perturbed links are then those which complete circuits in the molecule and in each case θ_{ij} is replaced by $\theta_{(\mu)} = \sum_{i \rightarrow j} \theta_{ij}$ where \sum denotes an

ordered sum along the circuit which $i \rightarrow j$ completes. This result is quite general and continues to hold when the circuits which are completed enclose more than one ring. In case (b) (figure 2), for instance, bond $6 \rightarrow 1$ completes a one-ring circuit but bond $10 \rightarrow 1$ completes a two-ring circuit: in each case the 'circuit' comprises all or part of the original open chain and the *one* connecting link. The result is also valid if the original chain contains branches: side chains with free ends have ω 's which may be transformed away without any effect on the elements which ultimately remain. This last result shows at once that the perturbations to be applied depend on the presence of *closed circuits* and that without such circuits the field has no effect: moreover, side chains affect the results only through their effect on the bond orders and polarizabilities of the unperturbed system (though such effects may evidently be considerable, cf. McWeeny [6], 1951 b).

Let $P_{(\mu)}$ be the order of the bond which completes the μ th circuit and $\bar{\pi}_{(\mu)(\nu)}$ the mutual polarizability of two such bonds, each taken in the direction in which the circuit is described. Let $\mathcal{S}_{(\mu)} = \sum_{i \rightarrow j} s_{ij}$ and $\mathcal{K}_{(\mu)} = \sum_{i \rightarrow j} s_{ij} k_{ij}$ be ordered sums along the μ th circuit. It follows immediately that the secondary field at the dipole is still given by (4.4) but that (4.5) is replaced by

$$\left. \begin{aligned} \sigma_1 &= \sum_{(\mu)} P_{(\mu)} \mathcal{S}_{(\mu)} \mathcal{K}_{(\mu)} \\ \sigma_2 &= \sum_{(\mu)} \sum_{(\nu)} \beta \bar{\pi}_{(\mu)(\nu)}^{\frac{1}{2}} [\mathcal{S}_{(\mu)} \mathcal{K}_{(\nu)} + \mathcal{K}_{(\mu)} \mathcal{S}_{(\nu)}]. \end{aligned} \right\} \quad (5.4)$$

Examples

(1) Benzene. For one ring the calculation becomes trivial. Numbering the atoms along the positive direction, the circuit is completed by bond $6 \rightarrow 1$; $\mathcal{S}_{(1)} = 1$ and $\mathcal{K}_{(1)} = (s_{12} k_{12} + s_{23} k_{23} + \dots + s_{61} k_{61})$. Thus $\sigma_1 = \frac{2}{3} \mathcal{K}_{(1)}$ and $\sigma_2 = -\frac{5}{9} \mathcal{K}_{(1)}$. The secondary field at the dipole may be written

$$H' = 2\beta \left(\frac{2\pi e}{hc} \right)^2 \frac{S^2 H}{a^3} \left(-\frac{1}{9} \right) (-\mathcal{K}_{(1)}). \quad (5.5)$$

It is easily verified that the factor $-\mathcal{K}_{(1)}$ reduces to (μ/r^3) (cf. (4.7)) for a distant point on the line through two opposite vertices: it may be called the 'distance factor' and depends only upon the geometry of the molecule. The factor which here takes the value $-1/9$ will be called the 'current density factor' since it

measures the moment of the induced magnetic shell or, in the Pauling model, the ring current.

(2) Naphthalene. It is useful to illustrate the two alternative calculations, based upon chains (a) and (b) of figure 2.

(a) Denoting bonds $6 \rightarrow 1$ and $10 \rightarrow 5$ by 1 and 2, $\mathcal{S}_{(1)} = 1$ (right-handed about the upward normal) while $\mathcal{S}_{(2)} = -1$. $\mathcal{K}_{(1)}$ is just the sum occurring in the benzene case, while $\mathcal{K}_{(2)}$ is a similar sum taken in the reverse direction. If $K(\mathbf{r}_\mu)$ is the positively taken sum for a field-point whose position vector relative to the μ th ring-centre is \mathbf{r}_μ , then $\mathcal{K}_{(1)} = K(\mathbf{r}_1)$ and $\mathcal{K}_{(2)} = -K(\mathbf{r}_2)$. The bond orders and self-polarizabilities are $P_{(1)} = P_{(2)} = 0.5547$, $\beta\bar{\pi}_{(1)(1)} = \beta\bar{\pi}_{(2)(2)} = -0.4660$; and the mutual polarizability is $\beta\bar{\pi}_{(1)(2)} = -0.0327$. Inserting these values in (5.4) we obtain

$$\begin{aligned}\sigma_1 &= 0.5547[K(\mathbf{r}_1) + K(\mathbf{r}_2)], \\ \sigma_2 &= -0.4333[K(\mathbf{r}_1) + K(\mathbf{r}_2)].\end{aligned}$$

This gives finally

$$H' = 2\beta \left(\frac{2\pi e}{\hbar c} \right)^2 \frac{S^2 H}{a^3} [(-0.1214)(-K(\mathbf{r}_1)) + (-0.1214)(-K(\mathbf{r}_2))] \quad (5.6)$$

showing that each ring contributes additively to the field, with a benzene-like distance factor but with an enhanced current density factor. At large distances $-K(\mathbf{r}) \rightarrow 1/r^3$ and each ring behaves like an induced dipole, the current round the boundary being 1.093 times the benzene value (a result in accord with the previously calculated susceptibility, $\chi/\chi_B = 2.186$).

(b) Bonds $6 \rightarrow 1$ and $10 \rightarrow 1$ (1 and 2, say) both complete positive circuits with $\mathcal{S}_{(1)} = 1$, $\mathcal{S}_{(2)} = 2$. Clearly $\mathcal{K}_{(1)} = K(\mathbf{r}_1)$ and $\mathcal{K}_{(2)} = K(\mathbf{r}_1) + K(\mathbf{r}_2)$ (the central bond being counted twice but with opposite signs). Inserting the relevant bond orders etc. we find the quite different results

$$\begin{aligned}\sigma_1 &= 1.6277K(\mathbf{r}_1) + 1.1094K(\mathbf{r}_2), \\ \sigma_2 &= -1.5063K(\mathbf{r}_1) - 0.9880K(\mathbf{r}_2).\end{aligned}$$

This again leads, of course, to (5.6): but the result shows that relationships must exist among the polarizabilities, for although the choice of chain is arbitrary $\sigma_1 + \sigma_2$ must be invariant. Comparison of various possible ways of completing the two rings shows, for instance, that $\bar{\pi}_{(12)(45)} = \bar{\pi}_{(12)(67)} = \bar{\pi}_{(12)(9,10)}$ etc. The number of distinct polarizabilities is therefore very much smaller for imaginary perturbations than for real.

6. CONCLUSION

Since the sums $\mathcal{S}_{(\mu)}$ and $\mathcal{K}_{(\mu)}$, which appear in (5.4), can always be written in the form $\pm \sum_{(\mu)} s_i$, $\pm \sum_{(\mu)} K(\mathbf{r}_i)$, where the summations run over all the single rings included within circuit μ (contributions from internal boundaries cancelling—cf. Stokes theorem) and s_i is the area of a single ring[†], it follows that the secondary field can always be easily expressed in the form (cf. 5.6)

$$H' = 2\beta \left(\frac{2\pi e}{\hbar c} \right)^2 \frac{S^2 H}{a^3} \left\{ \sum_i J_i [-K(\mathbf{r}_i)] \right\} \quad (6.1)$$

[†] In units of that of a benzene ring i.e. $S_i = s_i S$.

in which each ring in the molecule makes its own contribution. This should be compared with the approximation used by Bernstein *et al.* [2], which is equivalent to putting $J_1 = J_2 = \dots = J_{\text{benz}}$ and $-K(\mathbf{r}) = 1/r^3$. The latter approximation is evidently severe (figure 1—for a peripheral proton in benzene the necessary factor is $\mu = 1.794$): the former probably breaks down in large molecules and certainly in those where there is some degree of 'bond fixation'. Some illustrative results are collected in Table 1. Clearly most of the absolute error is masked on introducing the ratios; but the corrections introduced by the more complete theory are still significant. It would be particularly interesting to revise the results of Bernstein *et al.* who considered a range of molecules in which there are considerable disparities among the ring currents (J_1, J_2, \dots) in order to see whether the absolute shifts are better accounted for.

	H' (BSP)	H'	H'/H'_{benz}
Benzene proton	1.0	1.794	1.0
Naphthalene proton (i)	1.432	2.286	1.392
Naphthalene proton (ii)	1.16	2.165	1.207

Table 1.

(BSP: Bernstein *et al.* [2].)

Finally, it is worth noting that the quantum mechanical treatment lends considerable support to the semiclassical picture in which line-localized currents flow round the hexagons, provided the actual currents are calculated by the present method (or that of Pople, [8])†. For if the currents measured by J_1, J_2, \dots are assumed to flow round circular paths, each of radius ar_0 such that $\pi(ar_0)^2 = S$, the field is given by (6.1) with

$$-K(r) = \frac{1}{r^3} \left[1 + \frac{9}{8} \left(\frac{r_0}{r} \right) + \frac{225}{192} \left(\frac{r_0}{r} \right)^4 + \dots \right]. \quad (6.2)$$

This result, for the field due to a uniform circular shell of unit moment, removes nearly half of the error of the point dipole approximation for a benzene proton and agrees closely with the quantum mechanical result at greater distances‡.

It is also noteworthy that the quantum mechanical results may be duplicated by approximating the field contribution from one bond by the Biot-Savart expression for the field due to a unit line current and withdrawing from the integrand a factor $1/r^3$, giving it a 'mean value' for bond i - j of

$$\left(\frac{1}{r_i^3} + \frac{1}{r_j^3} \right).$$

Since an approximation of this kind is inherent in (2.2) it is not profitable to pursue the comparison further. For most purposes it should be completely satisfactory to use (6.1) with $-K(\mathbf{r}) = \mu/r^3$, where μ is given by (4.7).

† Reference to 2.7 shows that, in the present notation, $J_i = \sum_p^{\text{occ}} n_p \sum_j x_{ij}(p) s_j$. It should be noted, however, that this expression is invalid if degenerate (unperturbed) levels occur.

‡ A referee has drawn my attention to a paper by Waugh and Fessenden (*J. Amer. chem. Soc.*, 1957, **79**, 846) in which the classical (Pauling) model is used but the point dipole is replaced by a uniform shell.

On adapte la théorie des orbitales moléculaires au calcul des constantes d'écran magnétiques de molécules aromatiques. La théorie usuelle des perturbations dans le procédé LCAO est généralisée pour tenir compte d'une perturbation imaginaire due à un champ magnétique externe. La théorie est une variante de celle de London, mais diffère légèrement du développement fait par Pople de cette même théorie.

Die MO-Theorie wird auf die Berechnung der magnetischen Abschirmkonstanten in aromatischen Molekeln angewandt. Die übliche LCAO-Störungstheorie wird verallgemeinert, so dass auch die imaginäre Störung durch ein äusseres Magnetfeld berücksichtigt wird. Die Theorie ist eine Variante der von London gegebenen, weicht jedoch etwas von Pople's Erweiterung der letzteren ab.

REFERENCES

- [1] BERGMANN, E. D., HOARAU, J., PACAULT, A., PULLMAN, A., and PULLMAN, B., 1952, *J. Chim. phys.*, **49**, 474.
- [2] BERNSTEIN, A. J., SCHNEIDER, W. G., and POPLE, J. A., 1956, *Proc. roy. Soc. A*, **236**, 515.
- [3] COULSON, C. A., and LONGUET-HIGGINS, H. C., 1947, *Proc. roy. Soc. A*, **191**, 39.
- [4] LONDON, F., 1937, *J. Phys. Radium*, **8**, 397.
- [5] MAYOT, M., BERTHIER, G., and PULLMAN, B., 1951, *J. Phys. Radium*, **12**, 652.
- [6] McWEENY, R., 1951 a, *Proc. phys. Soc. Lond. A*, **64**, 261; 1951 b, *Ibid.*, **64**, 921; 1952, *Ibid.*, **65**, 839.
- [7] PAULING, L., 1936, *J. chem. Phys.* **4**, 673.
- [8] POPLE, J. A., 1958, *Mol. Phys.* **1**, 175

Nuclear magnetic resonance spectra of compounds of the B-subgroup metals

by L. E. ORGEL

Department of Theoretical Chemistry,
University Chemical Laboratory, Cambridge

(Received 3 June 1958)

The paramagnetic contributions to the susceptibilities of compounds of B-subgroup ions and the chemical shifts observed in their nuclear magnetic resonance spectra are shown to depend on interconfigurational mixing brought about by environments of less than cubic symmetry. Order of magnitude calculations are made for Pb^{2+} compounds and agree reasonably well with experiment.

In a recent paper it was shown that both the temperature-independent paramagnetic contributions to the susceptibilities and the chemical shifts of the nuclear magnetic resonance spectra of cobaltic complexes are due to the presence of low-lying paramagnetic states of the d^6 configuration which are mixed with the diamagnetic ground state by a magnetic field [1]. In this paper we shall discuss in a similar fashion the problem of the susceptibilities and the chemical shifts of ions which have filled shells in the free state but are subject to extensive interconfigurational mixing in environments of low symmetry. We shall be particularly interested in the Pb^{2+} ion, for experimental evidence on a number of lead compounds has recently been published. The general discussion, however, applies equally to Ga^+ , In^+ , Tl^+ , Ge^{2+} , Sn^{2+} , As^{3+} , Sb^{3+} , Bi^{3+} , etc. We shall also make some general comments on the effect of interconfigurational mixing on the nuclear magnetic resonance spectra of ions with filled d^{10} shells, particularly Cu^+ , Ag^+ , Au^+ , Hg^{2+} , and Tl^{3+} .

We consider first an ion with the configuration $d^{10}s^2$. Insofar as we neglect configuration interaction, the second-order paramagnetic contributions to the susceptibility and the chemical screening constant are automatically zero, for the 1S ground state has no non-vanishing matrix elements of the angular momentum operators with excited states. We have shown elsewhere that extensive stereochemical evidence makes it certain that in environments which lack a centre of symmetry the $d^{10}s^2$, 1S ground state is mixed extensively with states of the $d^{10}sp$ and $d^{10}p^2$ configurations and furthermore that the abnormal stereochemistry of Pb^{2+} , Sb^{3+} , Bi^{3+} , etc., ions in many of their compounds is a result of the stabilization energy resulting from s - p mixing in non-centrosymmetric environments [2, 3].

If we suppose that the two unshared electrons of the metal ion occupy the orbital

$$\phi = \alpha\psi_s + (1 - \alpha^2)^{1/2}\psi_{p_z} \quad (1)$$

and further that the main contributions to the temperature-independent paramagnetism come from this unshared electron pair, we may write this

contribution to the susceptibility as

$$\chi_T = \frac{2}{3} N \left(\frac{e\hbar}{2mc} \right)^2 \frac{4(1-\alpha^2)}{E} \quad (2)$$

where E is the energy of the first excited singlet state of the central ion above the ground state, that is, the energy of the singlet-singlet transition corresponding to the excitation of an electron from the ϕ orbital to the p_x and p_y orbitals. Extensive experimental evidence shows that E varies from 5 to 7 eV in Pb^{2+} compounds [3], so that the paramagnetic contribution to the susceptibility can take any value up to about 8×10^{-6} , if it is assumed that in highly unsymmetrical environments $\alpha = 1/\sqrt{2}$, that is, s-p mixing is complete.

There is an extensive experimental literature on the bulk susceptibility of Pb^{2+} compounds [4], but its interpretation is made difficult partly by discrepancies between the values given by different workers and partly by uncertainties in the contributions of the anions to the total susceptibility. (This is much more serious for Pb^{2+} than for Co^{3+} compounds, since the predicted paramagnetic contribution is an order of magnitude smaller for the former.) There is one example, however, which is not subject to these uncertainties, namely PbO , the susceptibility of which has been measured both in its tetragonal (red) and orthorhombic (yellow) forms [5]. The mole susceptibilities are 47.1×10^{-6} and 44×10^{-6} for the red and yellow forms respectively. We shall see that the difference of 3.1×10^{-6} , corresponding to a change in the p contribution to the inert pair of a little less than 40% (i.e. to a change in α^2 of about 0.20) is in quite reasonable agreement with the nuclear magnetic resonance data. The paramagnetic contribution to the susceptibility should be very markedly anisotropic.

Following the treatment given in the previous paper [1] the expression for the paramagnetic contribution to the chemical shielding is

$$\sigma = - \frac{e^2}{3m^2c^2} \left(\frac{1}{r^3} \right) \frac{4(1-\alpha^2)}{E}. \quad (3)$$

Qualitatively the shielding should clearly increase with the electrical asymmetry of the environment of the metal ion for this determines the extent of s-p mixing and hence the magnitude of $(1-\alpha^2)$.

Nuclear magnetic resonance data for a number of lead compounds have recently been published [6]. A very qualitative interpretation of the large

Compound	σ	σ^*
Pb	0	-1.47
PbO (yellow)	0.74	-0.73
PbO (red)	1.12	-0.35
PbCl_2	1.23	-0.24
$\text{Pb}(\text{C}_2\text{O}_4)_2$	1.23	-0.24
PbZrO_3	1.25	-0.24
$\text{Pb}(\text{NO}_3)_2$	1.46	-0.01
PbSO_4	1.47	0
$\text{Pb}(\text{acetate})_2$ (solution)	1.26	-0.21
$\text{Pb}(\text{NO}_3)_2$ (solution)	1.41	-0.06
PbSO_4 (solution)	1.41	-0.06

Table 1. Chemical shifts of Pb^{2+} compounds, σ relative to Pb (metal), and σ^* relative to PbSO_4 .

chemical shifts which were observed was given, which is in essential agreement with our theory. In column 2 of Table 1 we reproduce the chemical shift data on Pb^{2+} compounds relative to metallic lead and in column 3 the shifts (paramagnetic) relative to PbSO_4 .

A survey of these chemical shifts in the light of known crystal structures reveals just such a correlation as is to be expected if the paramagnetic term is due to the mixing by asymmetric environments of 6p orbitals with the 6s orbital. PbSO_4 and $\text{Pb}(\text{NO}_3)_2$ are isomorphous with the corresponding Ca^{2+} and Ba^{2+} salts [7], and the metal ion is in a rather symmetrical environment. The fact that they have the lowest paramagnetic contribution to the shielding is thus readily understood. In PbZrO_3 the Pb^{2+} ion has three close oxide neighbours on one side at 2.53–2.58 Å [8], in PbO (red) there are four near neighbours in a plane at 2.31 Å [7], while in PbO (yellow) there are three near neighbours but it is not certain whether the Pb–O distance is 2.15 Å or 2.19 Å [9]. In these structures which display the characteristic non-centrosymmetric coordination of Pb^{2+} by oxide ions the paramagnetic contribution to the screening increases with the asymmetry of the environment.

The crystal structures of the oxalate and acetate of lead are not known. PbCl_2 has a markedly asymmetric environment [10] in accord with the fairly large paramagnetic shift, but in the absence of comparable data on other halide structures no more quantitative discussion is possible.

We can deduce from the solution data that the hydrated Pb^{2+} ion is in an essentially symmetrical environment while in the acetate complex the Pb^{2+} ion has a markedly asymmetric environment. Similar considerations apply to the acetate complex of the Tl^+ ion [11].

The quantitative calculations of the shifts is not possible in the absence of detailed, independent evidence on the extent of s–p mixing. However, order of magnitude calculations are encouraging. $(1/r^3) = 16a_0^{-3}$ for the neutral lead atom in the configuration $6s^26p^2$, and if allowance is made for the charge on the Pb^{2+} ion this must be increased at least to $20a_0^{-3}$ and perhaps to a much greater value [12]. If we accept this value and make the same assumptions as in the estimation of bulk susceptibilities we predict chemical shifts of up to 0.4° . The total range of observed shifts is 0.73° which, considering the approximations involved, particularly the uncertainty in $(1/r^3)$, agrees reasonably well with the calculated range. If this interpretation is correct the difference of 0.38° between the chemical shielding in red and yellow PbO corresponds to a difference of about 0.25 in α^2 . This is to be compared with a value of 0.20 deduced from magnetic susceptibility measurements.

In the absence of detailed knowledge of the parameters involved we have neglected in this discussion: (i) spin–orbit interaction; (ii) covalent bonding, and the consequent reduction of the matrix elements of L ; (iii) mixing of the 6s with 6d and higher orbitals.

All of these could cause appreciable changes in the calculated magnetic properties, and it is for this reason that we do not believe that the numerical results of this treatment are to be taken as more than guides to the magnitudes of the effects discussed. We have not given as complete a treatment as we did for the Co^{3+} compounds but rather indicated a plausible model and shown that the effects calculated from it agree with experiment to within a factor of 2,

IONS WITH THE d^{10} CONFIGURATION

We have suggested elsewhere [2] that d s mixing is the cause of the centrosymmetric distortions from cubic symmetry which occur in the environments of d^{10} ions having low-lying d^9 excited states. If this is so we should again expect marked paramagnetic contributions both to the susceptibility and to the chemical screening constant. The expressions for the paramagnetic terms in the susceptibility and the chemical screening constant have just the forms of those for compounds in which s - p mixing is important, but the numerical constant is three times as large.

GENERAL OBSERVATIONS

The susceptibilities and the chemical screening constants provide important information about the electric asymmetry of the environment of ions with d^{10} and $d^{10}s^2$ ground states which is complementary to that obtained in nuclear quadrupole resonance experiments. Although accurate predictions of the chemical shifts cannot be made on account of our ignorance of the extent of s - p or s - d mixing, empirical information on the chemical shifts together with optical absorption spectra should enable the variation of s - p or s - d mixing with the nature of the ligand to be determined accurately for complexes in solution. It is also possible that the actual extent of mixing could be determined, although only approximately, and the assumption, for example, s - p mixing is essentially complete in PbO (yellow) tested.

On montre que la contribution paramagnétique à la susceptibilité des composés d'ions du sous-groupe B, et les déplacements chimiques observés dans leurs spectres de résonance magnétique nucléaire dépendent de combinaisons interconfigurationnelles qui sont dues à des environnements dont la symétrie est inférieure à la symétrie cubique. On a fait des calculs d'ordres de grandeur pour des composés de l'ion Pb^{2+} : ils sont en accord raisonnable avec l'expérience.

Für Verbindungen von Ionen der B-Untergruppe wird gezeigt, dass die paramagnetischen Beiträge zu den Suszeptibilitäten ebenso wie die *chemical shifts*, die in den kernmagnetischen Resonanzspektren beobachtet werden, durch eine interkonfigurationelle Mischung bedingt werden. Diese wird durch die Umgebung verursacht, wenn deren Symmetriegrad kleiner als kubisch ist. Für Verbindungen des Pb^{2+} werden die Größenordnungen abgeschätzt; diese sind in brauchbarer Übereinstimmung mit der Erfahrung.

REFERENCES

- [1] GRIFFITH, J. S., and ORGEL, L. E., 1957, *Trans. Faraday Soc.*, 1958.
- [2] ORGEL, L. E., *J. chem. Soc.* (in press).
- [3] JØRGENSEN, C. K., 1957, *Thesis*, Copenhagen.
- [4] GRILLOT, E., 1946, *J. Chim. phys.*, **43**, 169.
- [5] MATHER, R. N., and NEVGI, M. B., 1936, *Z. Phys.*, **100**, 615.
- [6] PIETTE, L. H., and WEAVER, H. E., 1958, *J. chem. Phys.*, **28**, 735.
- [7] LANDOLT-BÖRNSTEIN, 1955, *Zahlenwerte*, 6th edn., vol. 1, Pt. 4.
- [8] JONA, F., SHIRANE, G., MAGGI, F., and PEPINSKY, R., 1957, *Phys. Rev.*, **105**, 849.
- [9] BYSTRÖM, A. A., 1948, *Arkiv f. Kemi*, **25A**, No. 13.
- [10] See BYSTRÖM, A. A., 1947, *Arkiv f. Kemi*, **24A**, No. 33, and references therein.
- [11] GUTOWSKY, H. S., and MCGARVEY, B. R., 1953, *Phys. Rev.*, **91**, 81.
- [12] BARNES, R. G., and SMITH, W. V., 1954, *Phys. Rev.*, **93**, 95.

Long range spin-spin interactions in high resolution nuclear magnetic resonance and the concept of hyperconjugation

by R. A. HOFFMAN

Department of Physics, University of Uppsala, Uppsala, Sweden

(Received 25 July 1958)

Indirect spin-spin couplings between methyl groups attached to unsaturated organic molecules and protons directly bonded to unsaturated carbon atoms have been observed in several molecules. An attempt is made to account in a qualitative way for the observed spin-spin couplings by ascribing them largely to hyperconjugation between methyl group orbitals and π -electron orbitals. The connection of these observations with electron spin resonance spectra is mentioned.

1. INTRODUCTION

The study of multiplet spectra arising from indirect spin-spin couplings [1] is of considerable interest in the study of molecular structure. Long range couplings between nuclei which are not directly bonded to one another, are especially interesting, since these are dominated by a (nuclear spin)-(electron spin)-(electron spin)-(nuclear spin) mechanism [2, 3].

This paper is an initial report on the study of very long range couplings between nuclei separated from one another by four or more bond lengths. The splittings observed are due to coupling between methyl group protons and protons on attached unsaturated organic molecules.

The magnitudes of these coupling constants $J_{NN'}$ range from the value 1.25 c/s in *trans*-crotonaldehyde to values well below the best resolution of the instrument (≤ 0.3 c/s).

2. EXPERIMENTAL PROCEDURE

The spectra were obtained with a Varian model 4300 spectrometer operating at 40 Mc/s and equipped with a 12 in. V4012A-HR magnet from the same company and a field stabilizer. In order to obtain the ultimate resolution it was necessary to reshim the magnet every day before the runs, most of which were done during nights and weekends. The room temperature ($\sim 28^\circ\text{C}$) and the temperature of the cooling water had to be monitored very carefully. Because the magnet cooling water was supplied by a heat exchanger it was possible to keep the temperature of the cooling water very close to room temperature. This is thought to improve the stability of the system.

The separation of lines was measured by the modulation side-band technique [4] with a modulation frequency of 25 c/s, which was calibrated against the power line.

The shifts relative to benzene (table 3) were obtained from samples containing mixtures of the standard (20 to 50 mole per cent) and the compound investigated. In dilute solutions of the mixtures in carbon tetrachloride all these shifts increase, but the features mentioned in the discussion below are still observed.

3. RESULTS

Partly resolved spectra have been obtained for isoprene, crotonaldehyde, mesitylene and 2, 5-dimethylthiophene. The number and separation of lines for the methyl spectra are given in table 1.

Compound	Number of lines methyl band	Splittings c/s
$\text{CH}_2=\text{C}(\text{CH}_3)\cdot\text{CH}=\text{CH}_2$	3	$1\cdot10 \pm 0\cdot05$
$\text{CH}_3\cdot\text{CH}=\text{CH}\cdot\text{CHO}$	2×2	$\begin{cases} 6\cdot55 \pm 0\cdot20^\dagger \\ 1\cdot25 \pm 0\cdot10 \end{cases}$
1,3,5- $(\text{CH}_3)_3\text{C}_6\text{H}_3$	4	$0\cdot62 \pm 0\cdot06$
2,5- $(\text{CH}_3)_2\text{C}_4\text{H}_2\text{S}$	3	$0\cdot45 \pm 0\cdot10$

Table 1.

† Coupling between the methyl protons and the proton attached to the *adjacent* carbon atom (given for comparison).

The methyl spectrum of 2, 5-dimethylthiophene consists of three equidistant lines, with large overlapping and some distortion due to too high sweep rate. The sweep could not be made slow enough to obtain true slow passage conditions. The methyl spectrum of mesitylene consists of four equally separated peaks, the intensities of which agree fairly well with the binomial coefficients 1:3:3:1. A possible interpretation is that the coupling between each methyl proton and each aromatic proton is the same. Thus one would expect the spectrum of the aromatic protons to consist of 10 lines with a binomial intensity distribution. Although only a few of these lines have been seen, the equal separation between these, and the gaussian shape of the resonance envelope support this interpretation.

One has to be cautious, however, in evaluating the coupling constants from this spectrum, since a correct treatment can only be made using the wave functions corresponding to the symmetry of the molecule†. The spectrum is shown in figure 1.

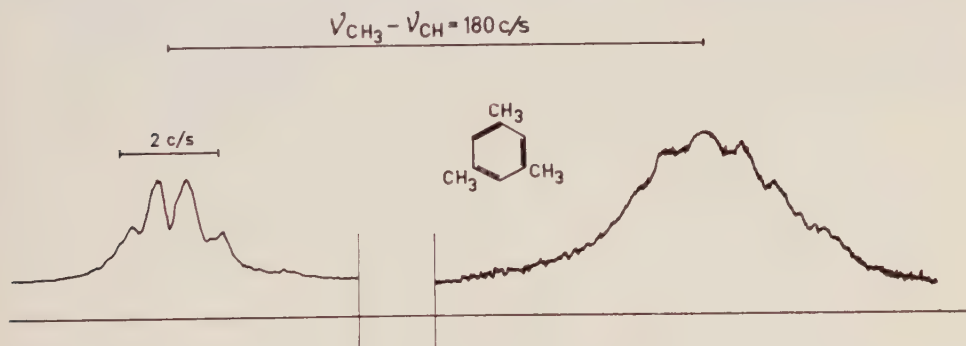


Figure 1. Spectrum from mesitylene (1,3,5-trimethylbenzene). The d.c. field decreases from the left to the right. Slight reductions in sweep rate and r.f. field, and an increase in gain by a factor of ten were made for the latter (aromatic proton) part of the spectrum.

† This important addition is due to a remark by J. A. Pople at the Oxford Discussion of the "Radio Frequency Spectroscopy Group", 21-22 April 1958.

The spectra of the compounds listed in table 2 could not be resolved. Although several of the compounds listed show an apparent line width equal to or exceeding that of mesitylene, the spectra expected for most of them are considerably more complicated. As can be seen from the table, the methyl lines of ortho- and para-xylene are very narrow, their widths being hardly distinguishable from the apparent line widths of, e.g. benzene.

Compound	Number of lines methyl group	Approximate† line widths c/s
$\text{CH}_3 \cdot \text{C}_6\text{H}_5$?	1.5
$o\text{-(CH}_3)_2 \cdot \text{C}_6\text{H}_4$?	1.0
$m\text{-(CH}_3)_2 \cdot \text{C}_6\text{H}_4$	several	2.0
$p\text{-(CH}_3)_2 \cdot \text{C}_6\text{H}_4$?	1.0
$o\text{-CH}_3 \cdot \text{C}_6\text{H}_4\text{Cl}$?	1.5
$m\text{-CH}_3 \cdot \text{C}_6\text{H}_4\text{Cl}$	several	2.0
$m\text{-CH}_3 \cdot \text{C}_6\text{H}_4\text{Br}$?	2.0
$o\text{-CH}_3 \cdot \text{C}_6\text{H}_4\text{NO}_2$?	1.5
$m\text{-CH}_3 \cdot \text{C}_6\text{H}_4\text{NO}_2$?	2.5
$p\text{-CH}_3 \cdot \text{C}_6\text{H}_4\text{CHO}$	6	2.0

Table 2.

† Of methyl group bands.

Evidence for some broadening mechanism is, however, given by the fact that no wiggles appear on the recorder trace after passing through the lines under exactly the same conditions that will give wiggles after passage through the lines of pure benzene or hydroxyl protons in impure ethanol.

4. DISCUSSION

The spectra show several interesting features. (1) In the series of methyl-substituted benzenes the splittings are largest in *m*-xylene and mesitylene. The spectra of these compounds also have the largest shifts of the ring protons (table 3). This order might be expected, since a methyl group tends to increase

Compound	Internal shifts† p.p.m.	Relative shifts‡ of ring protons p.p.m.
$\text{CH}_3 \cdot \text{C}_6\text{H}_5$	4.91 ± 0.05	0.10 ± 0.02
$o\text{-(CH}_3)_2 \cdot \text{C}_6\text{H}_4$	4.93 ± 0.05	0.14 ± 0.02
$m\text{-(CH}_3)_2 \cdot \text{C}_6\text{H}_4$	4.73 ± 0.05	0.30 ± 0.04
$p\text{-(CH}_3)_2 \cdot \text{C}_6\text{H}_4$	4.78 ± 0.05	0.20 ± 0.02
$1,3,5\text{-(CH}_3)_3 \cdot \text{C}_6\text{H}_3$	4.48 ± 0.05	0.46 ± 0.02

Table 3.

† Methyl proton band to ring proton band.

‡ Benzene standard.

the electron density in the ortho and para positions. Further, in *m*-xylene the band from the ring protons is quite broad (half-width $\simeq 6$ c/s). This is to be contrasted with toluene where the corresponding band width is less than 3 c/s the one from *o*-xylene being narrower by another factor of two or so.

The methyl bands all occur at the same field except in *o*-xylene where it is shifted 0.1 p.p.m. towards higher field. (2) The coupling between the methyl group and the nearest methylene in isoprene is definitely larger than any other very long range coupling in that molecule. (3) In crotonaldehyde the methyl doublet is split in a subdoublet with a separation between the lines as large as 1.25 c/s due to coupling between the methyl protons and the proton in α -position to the aldehyde-group, whereas the aldehyde proton gives merely a doublet showing no additional coupling to the proton in β -position.

It is thought that these phenomena indicate the following interpretation. The main contribution to very long range couplings is due to hyperconjugation between the π -electron orbitals of the unsaturated molecule and the π -orbital of the methyl group [5].

McConnell [3] has computed the π -electron contribution to nuclear spin-spin couplings of aromatic protons and found that this contribution should not exceed 2 c/s. This kind of coupling, however, involves a number of (electron spin)-(electron-spin) links. Some of these interactions might act as bottlenecks for the transmission of spin polarization.

Since hyperconjugation involves delocalization of the electrons forming the C-H bond, the polarizability of the hydrogen orbitals due to π -electrons and vice versa should be enhanced in spite of less delocalization of electrons in the C-C bond as compared to first-order conjugation. Mulliken *et al.* [6] have constructed group orbitals for the H_3 group in methyl. The orbitals of the type

$$\psi(H_a) + \psi(H_b) - 2\psi(H_c)$$

have approximately the same symmetry as a $\psi(2p\pi)$ carbon orbital and thus can interact strongly with π -electrons of the attached system.

Experimental support of this view can also be obtained from electron spin resonance measurements on methyl-substituted semiquinones, 1,4-naphtho-semiquinone and dimesitylmethyl [7-9].

The spectra of these compounds reveal hyperfine splittings due to the methyl protons of the same order of magnitude (and usually slightly larger) as those due to the ring protons.

Even larger splittings have been observed in 'frozen in' aliphatic free radicals such as the one obtained from isopropanol, the hyperfine splittings of which have been explained by the use of hyperconjugating structures [10].

Since McConnell [3] used the hyperfine splitting due to aromatic protons as measured in electron spin resonance experiments to get an estimate of the σ - π -electron interaction and thus to the π -electron contribution to the nuclear spin-spin couplings, it might seem plausible that the spin-spin coupling between a hyperconjugating methyl group and an aromatic proton should be of the same order of magnitude as the coupling between aromatic protons.

However, the effective Hamiltonian for the (π -electron)-(proton spin) coupling mixes the singlet ground state molecular wave function with excited states [11]. Hyperconjugation has the effect of raising the energy of the ground state orbitals and lowering the energy of the lowest lying excited state [12]. This effect should enhance the π -electron contribution to all indirect nuclear spin-spin couplings. No attempt has been made to estimate the expected couplings.

Since a computation of the hyperfine structure of electron spin resonances in methyl-substituted semiquinones has recently been carried out [13], it is felt that a continued study of long range couplings of methyl groups attached to unsaturated organic compounds is also of some theoretical interest. There is an additional interest in the study of methyl-substituted aromatic molecules, since some of these have proved to be strongly carcinogenic [14].

A complete evaluation of the chemical shifts and spin-spin coupling constants of crotonaldehyde and some other compounds will be published later. Further investigations including other substances are going on.

The author wishes to express his gratitude to Professor Kai Siegbahn for his interest and much helpful advice, to Dr. D. J. E. Ingram for valuable discussions, to T. Vänngård and S. Gronowitz for interesting discussions and to the latter for providing suitable samples. This research has been sponsored by the State Council of Technical Research (of Sweden).

On a observé, dans plusieurs molécules, des couplages spin-spin indirects des groupes méthyles attachés à des molécules organiques non-saturées avec les protons liés directement aux atomes de carbone non saturés. On essaye d'expliquer de façon qualitative les couplages spin-spin observés en les attribuant en grande partie à l'interaction par hyperconjugaison entre les orbitales des groupes méthyles et les orbitales des électrons π . La relation entre ces observations et les spectres de résonance de spin électronique est mentionnée.

In einigen ungesättigten organischen Molekeln wurden indirekte Spin-Spin-Kopplungen zwischen Methylgruppen und Protonen, die direkt an ungesättigte Kohlenstoffatome gebunden sind, beobachtet. Es wird versucht, die gemessenen Spin-Spin-Kopplungen qualitativ zu deuten. Dabei werden sie überwiegend einer Hyperkonjugation zwischen den Elektronenbahnen der Methylgruppen und denen der π -Elektronen zugeschrieben. Auf den Zusammenhang dieser Beobachtungen mit den Elektronenspin-Resonanzspektren wird hingewiesen.

REFERENCES

- [1] For general reviews see: LÖSCHE, A., 1957, *Kerninduktion* (Berlin), pp. 362-403.
PAKE, G. E., 1956, in *Solid State Physics* 2, edited by Seitz, F., and Turnbull, D., p. 54. ABRAGAM, A., 1957, *Nuovo Cim. Suppl.*, **6**, 1015.
- [2] MCCONNELL, H. M., 1956, *J. chem. Phys.*, **24**, 460.
- [3] MCCONNELL, H. M., 1957, *J. Mole. Spectroscopy*, **1**, 11.
- [4] ANDERSON, W. A., 1956, *Phys. Rev.*, **102**, 151.
- [5] For a general review of Hyperconjugation see for example: BAKER, J. W., 1952, *Hyperconjugation* (Oxford). CRAWFORD, V. A., 1949, *Quart. Rev.*, **3**, 226. COULSON C. A., 1952, *Valence* (Oxford) p. 307ff.
- [6] MULLIKEN, R. S., RIEKE, C. A., BROWN, W. G., 1941, *J. Amer. chem. Soc.*, **63**, 45.
- [7] JARRETT, H. S., and SLOAN, G. J., 1954, *J. chem. Phys.*, **22**, 1783.
- [8] VENKATARAMAN, B., and FRAENKEL, G. K., 1955, *J. chem. Phys.*, **23**, 588 and 1955, *J. Amer. chem. Soc.*, **77**, 2707.
- [9] WERTZ, J. E., and VIVO, J. L., 1956, *J. chem. Phys.*, **24**, 479.
- [10] GIBSON, J. F., INGRAM, D. J. E., and SYMONS, M. C. R., 1957, *Trans. Faraday Soc.*, **53**, 914.
- [11] RAMSEY, N. F., 1953, *Phys. Rev.* **91**, 303.
- [12] See references [5] p. 30 resp. p. 237 and also PULLMAN, B., and A., 1952, *Les Théories électroniques de la chimie organique* (Paris: Masson & Cie), pp. 513-519.
- [13] BERSOHN, R., 1956, *J. chem. Phys.*, **24**, 1066.
- [14] PULLMAN, A., 1945, *C. R. Acad. Sci., Paris*, **221**, 140.

High resolution hydrogen resonance spectra of trisubstituted benzenes

by R. E. RICHARDS and T. SCHAEFER

Lincoln College, Oxford

(Received 10 June 1958)

High resolution hydrogen resonance spectra are given for a number of asymmetrically trisubstituted derivatives of benzene. In some cases the spectra can be analysed as AB_2 , ABB' or ABX cases. The ABB' case, in which the B nuclei have identical chemical shifts but are unequally coupled to A, is discussed and illustrated. The spin-spin coupling constants between protons (a) ortho to one another lie in the range 7 to 9 c/s, (b) meta to one another occur near 2.5 c/s and (c) para to one another are less than 1 c/s.

1. INTRODUCTION

The detailed analysis of the high resolution nuclear magnetic resonance spectrum of an organic compound may be very difficult if there are several groups of chemically shifted nuclei with spin-spin coupling constants between them which are comparable with the chemical shifts [1]. It may often be found, however, that some compounds give spectra which approximate more or less closely to simpler cases, and then values of the chemical shifts and coupling constants might be obtained without carrying out a detailed analysis for the fully complicated case.

Measurements are described below on a number of trisubstituted derivatives of benzene in which the protons of the aromatic ring constitute cases AB_2 , ABX , or ABC , in which A, B, and C refer to nuclei with closely similar chemical shifts and X refers to a nucleus with a very large chemical shift. The detailed analysis of the ABC spectrum is difficult, and so the possibility is explored of approximating the spectra to one of the simpler cases.

The variation in the values of the chemical shifts and spin-spin coupling constants as the substituents are changed is of value for the correlation of these quantities with molecular structure.

2. EXPERIMENTAL

3-nitro-*o*-xylene and 3-chloro-2-toluidine were measured as pure liquids. 3-methyl salicylic acid was measured in solution in ether, and 3-nitro-salicylic acid, 2,5-dichloro-nitrobenzene and 2,4-dinitro-chlorobenzene were measured in solution in acetone. The compounds were all obtained commercially.

The high resolution measurements were made with a spectrometer built in this laboratory [2]. A permanent magnet is used, with a field equivalent to a nuclear resonance frequency of 29.9200 Mc/s for protons. Samples were sealed into glass tubes of inside diameter about 4 mm and a resolving power of 1-2 parts in 10^8 is normally attainable. The separation of the lines was obtained by the conventional method of applying an audio-frequency modulation to the magnetic field [3].

3. RESULTS

The proton spectra for the six compounds are shown in figures 1-6. The frequencies of the lines in c/s relative to one of them are given under the peaks. The numbers below the peaks refer to the numbering of the lines in the analyses described in the discussion.

4. DISCUSSION

The energy levels for the three spin $\frac{1}{2}$ cases have been described previously [1, 4]. The results of the analyses of the spectra will therefore be summarized in tabular form.

4.1. 3-nitrosalicylic acid

The spectrum in figure 1 shows two groups of lines, apart from the single intense line at low field due to the protons of the carboxyl and hydroxyl groups. The two groups of lines are well separated and this indicates that the coupling constants are considerably smaller than the chemical shift.

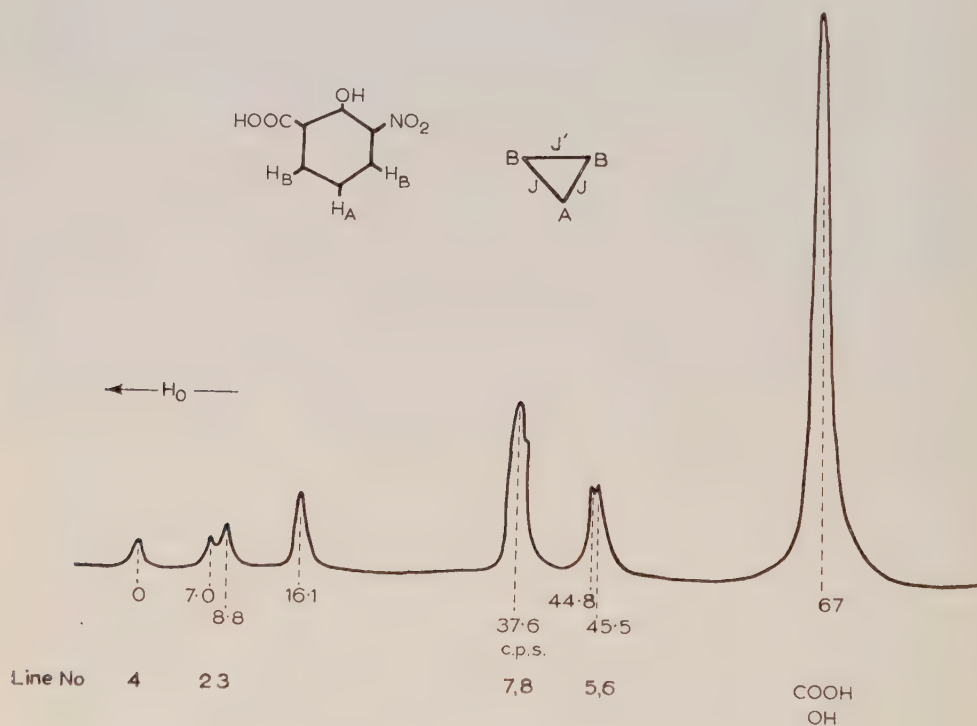


Figure 1. Hydrogen resonance of 3-nitrosalicylic acid.

From the appearance of this spectrum it is clear that it approximates closely to the case AB₂: the two protons meta to one another experience a field $H_0(1-\sigma_B)$ which is greater than the field $H_0(1-\sigma_A)$ at proton A in figure 1. There is a plane of symmetry through A. If the coupling constants are described as in figure 1 and if $\sigma_A > \sigma_B$, the energies and theoretical intensities of the nine possible transitions obtained are given in Table 1. The factor, η , is $\gamma/2\pi$, where γ is the magnetogyric ratio of the nucleus.

Transition and origin	Energy	Relative intensity
1. A	$\frac{1}{2}\eta H_0(2-\sigma_A-\sigma_B)+\frac{3}{4}J-C$	$[\sqrt{(2)}\sin\theta+\cos\theta]^2$
2. A	$\eta H_0(1-\sigma_B)-C-B$	$[\sqrt{(2)}\sin(\phi-\theta)+\cos\phi\cos\theta]^2$
3. A	$\eta H_0(1-\sigma_A)$	1
4. A	$\frac{1}{2}\eta H_0(2-\sigma_A-\sigma_B)-\frac{3}{4}J-B$	$[\cos\phi-\sqrt{(2)}\sin\phi]^2$
5. B	$\eta H_0(1-\sigma_B)-C+B$	$[\sqrt{(2)}\cos(\phi+\theta)-\sin\phi\cos\theta]^2$
6. B	$\frac{1}{2}\eta H_0(2-\sigma_A-\sigma_B)+\frac{3}{4}J+C$	$[\sqrt{(2)}\cos\theta-\sin\theta]^2$
7. B	$\eta H_0(1-\sigma_B)+C-B$	$[\sqrt{(2)}\cos(\phi-\theta)+\cos\phi\sin\theta]^2$
8. B	$\frac{1}{2}\eta H_0(2-\sigma_A-\sigma_B)-\frac{3}{4}J+B$	$[\sqrt{(2)}\cos\phi+\sin\phi]^2$
9. comb.	$\eta H_0(1-\sigma_B)+C+B$	$[\sqrt{(2)}\sin(\theta-\phi)-\sin\theta\sin\phi]^2$

Table 1. Energies and intensities for AB₂ ($\sigma_A > \sigma_B$).

In Table 1 the positive quantities B, and C and the angles θ and ϕ are defined by the equations

$$\left. \begin{aligned} B \cos 2\phi &= \frac{1}{2}\eta H_0(\sigma_A - \sigma_B) + \frac{1}{4}J \\ B \sin 2\phi &= J/\sqrt{2} \\ C \cos 2\theta &= \frac{1}{2}\eta H_0(\sigma_A - \sigma_B) - \frac{1}{4}J \\ C \sin 2\theta &= J/\sqrt{2} \end{aligned} \right\} \quad (4.1)$$

Line number	Energy (c/s)		Relative intensities	
	Calculated	Observed	Calculated	Observed
1.	15.6	16.1	1.56	1.9
2.	6.7	7.0	0.84	0.9
3.	8.7	8.8	1	1.1
4.	-0.2	0	0.61	0.7
5.	44.7	44.8	1.37	2.1
6.	46.0	45.5	1.39	
7.	37.1	37.6	2.53	
8.	37.8	37.6	2.37	
9.	85.1	—	0.007	—

Table 2. Observed and calculated spectrum for 3-nitrosalicylic acid.
Observed intensities are estimated from heights of lines.

Transition 9 is a combination line corresponding to the simultaneous change of the z -component of spin of all three nuclei. It is forbidden in the limit of zero coupling constant or zero chemical shift and is always weak and very rarely appears. The appearance of the spectrum depends completely on the ratio $J/\eta H_0(\sigma_A - \sigma_B)$. Because of the symmetry, J' does not affect the spectrum and we cannot obtain its value.

It may be noted from Table 1, as an aid in the practical analysis, that line 3 gives the position of pure chemical shift of proton A unmodified by spin coupling. The corresponding position for the B nuclei is the mean of transitions 5 and 7.

If the lines are assigned as shown in figure 1 we may obtain the following parameters:

$$J = 8.0 \text{ c/s}, \quad \eta H_0(\sigma_A - \sigma_B) = 32.2 \text{ c/s}.$$

Using these values, the calculated and observed energies and intensities are compared in Table 2. Observed intensities are calculated from the heights of the lines, as it is not practicable to estimate the areas of such overlapping lines. Lines 5, 6 and 7, 8 are wider than the others, and so the observed intensities would be greater than 2.1 if areas were measured. The combination line was not observed, presumably because of its very low intensity.

The similar shielding of the B protons is in agreement with other work [5] in which it appears that carboxyl and nitro groups produce similar effects on chemical shifts in aromatic compounds. For example, the proton resonance spectra of benzoic acid and of nitrobenzene are very much alike.

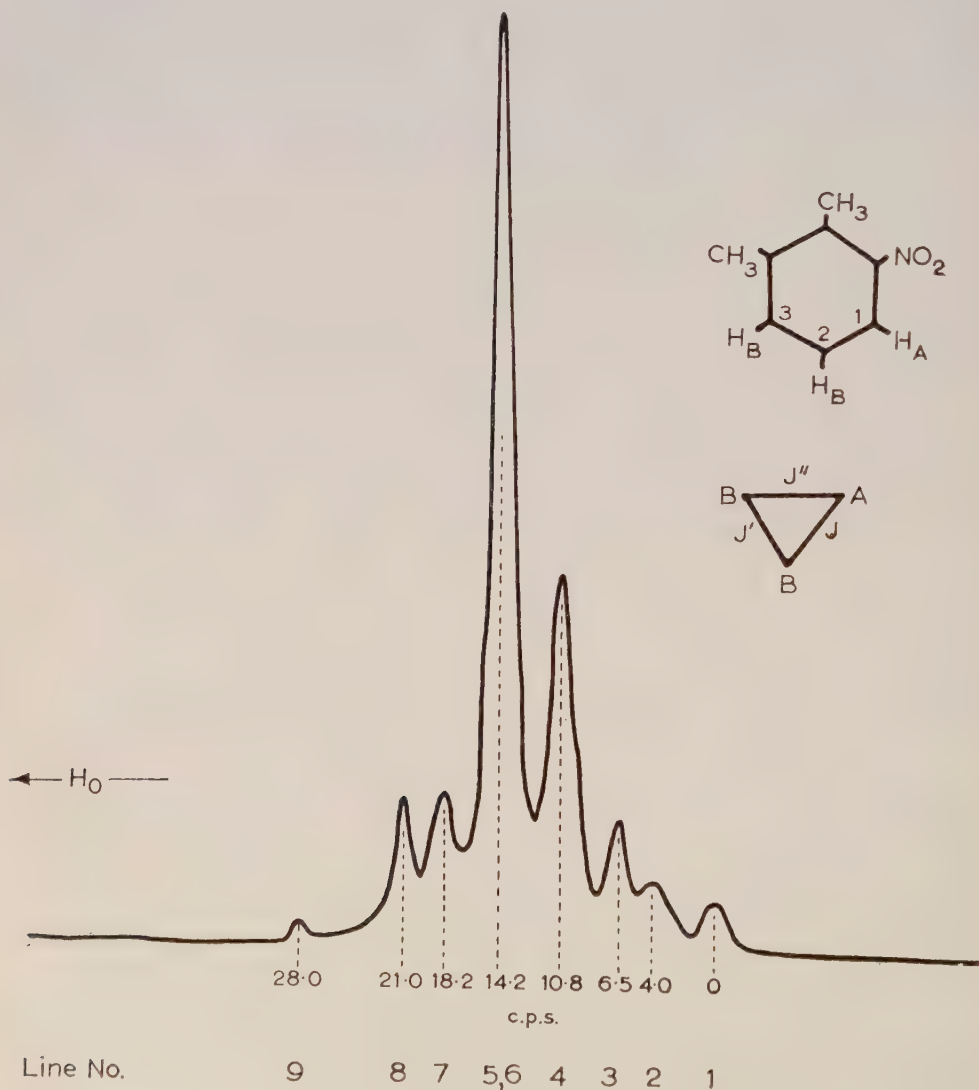


Figure 2. Hydrogen resonance of 3-nitro-o-xylene.

4.2. 3-nitro-*o*-xylene

The ring hydrogen spectrum of 3-nitro-*o*-xylene (figure 2) is more complex. The methyl groups are shifted to high field by 5 parts per million. It is clearly an AB₂ spectrum but the chemical shift is closer in value to the coupling constants J . An ABC or ABX spectrum would have 12 lines arranged differently.

It is improbable that protons 1 and 3 should both be shielded equally and more than proton 2, so we shall consider the case that proton 1, ortho to the nitro group, is the least shielded and the chemical shifts of protons 2 and 3 are nearly equal. Although there is no plane of symmetry, we assume that the B protons are magnetically equivalent and therefore wave functions can be written for them which are eigenfunctions of the covering operations of the group D_{σh}, just as for the usual AB₂ case. The wave function for the three protons, however, has no symmetry about the plane through A. On the assumption that the basic functions for the usual AB₂ case are valid we can calculate the energies and transitions which are given in Table 3. The coupling constants are defined in figure 2.

Transition and origin	Energy	Relative intensity
1. A	$\frac{1}{2}\eta H_0(2-\sigma_A-\sigma_B)+\frac{3}{8}(J+J'')+D_+$	$[\sqrt{(2)\sin\phi_+-\cos\phi_+}]^2$
2. A	$\eta H_0(1-\sigma_B)+D_++D_-$	$[\sqrt{(2)\sin(\phi_+-\phi_-)+\cos\phi_+\cos\phi_-}]^2$
3. A	$\eta H_0(1-\sigma_A)$	1
4. A	$\frac{1}{2}\eta H_0(2-\sigma_A-\sigma_B)-\frac{3}{8}(J+J'')+D_-$	$[\sqrt{(2)\sin\phi_-+\cos\phi_-}]^2$
5. B	$\eta H_0(1-\sigma_B)+D_+-D_-$	$[\sqrt{(2)\cos(\phi_+-\phi_-)+\cos\phi_+\sin\phi_-}]^2$
6. B	$\frac{1}{2}\eta H_0(2-\sigma_A-\sigma_B)+\frac{3}{8}(J+J'')-D_+$	$[\sqrt{(2)\cos\phi_++\sin\phi_+}]^2$
7. B	$\eta H_0(1-\sigma_B)-D_++D_-$	$[\sqrt{(2)\cos(\phi_+-\phi_-)-\sin\phi_+\cos\phi_-}]^2$
8. B	$\frac{1}{2}\eta H_0(2-\sigma_A-\sigma_B)-\frac{3}{8}(J+J'')-D_-$	$[\sqrt{(2)\cos\phi_--\sin\phi_-}]^2$
9. comb.	$\frac{1}{2}\eta H_0(1-\sigma_B)-D_+-D_-$	$[\sqrt{(2)\sin(\phi_+-\phi_-)+\sin\phi_+\sin\phi_-}]^2$

Table 3. Energies and intensities for ABB' ($\sigma_B > \sigma_A$).

In Table 3 the positive quantities D_+ and D_- and angles ϕ_+ , ϕ_- are defined by the equations

$$\left. \begin{aligned} D_- \cos 2\phi_+ &= \frac{1}{2}\eta H_0(\sigma_B - \sigma_A) + \frac{1}{8}(J + J'') \\ D_+ \sin 2\phi_+ &= \frac{1}{2\sqrt{2}}(J + J'') \\ D_- \cos 2\phi_- &= \frac{1}{2}\eta H_0(\sigma_B - \sigma_A) - \frac{1}{8}(J + J'') \\ D_- \sin 2\phi_- &= \frac{1}{2\sqrt{2}}(J + J'') \end{aligned} \right\} \quad (4.2)$$

Notice that J , the coupling constant between the two B protons does not affect the energies, just as in the exact AB₂ case. If we now proceed with the analysis on the basis of the assignment of lines given in figure 2, we obtain

$$J + J'' = 11.7 \text{ c/s}, \quad \eta H_0(\sigma_B - \sigma_A) = 8.7 \text{ c/s}.$$

In Table 4 the calculated energies and intensities are compared with the observed ones.

Line number	Energy c/s		Relative intensities	
	Calculated	Observed	Calculated	Observed
1.	0	0	0.27	0.3
2.	3.7	4.0	0.38	0.4
3.	7.1	6.5	1	0.8
4.	10.8	10.8	2.34	2.4
5.	13.8	14.2	3.31	6.1
6.	14.2	14.2	2.69	
7.	17.8	18.2	1.23	1.0
8.	21.0	21.0	0.64	1.0
9.	28.0	28.0	0.01	0.1

Table 4. Observed and calculated spectrum for 3-nitro-o-xylene.
Observed intensities are estimated from heights of lines.

It is known that in many aromatic compounds the ortho coupling constant lies between 8 and 9 c/s, while the meta coupling constant takes on values from 1 to 3 c/s [6]. Clearly, 11.7 c/s is a reasonable value for the sum of these if the signs of the proton coupling constants are taken as positive [7].

An analysis of this spectrum was also carried out on the assumption that proton 2 was A, and protons 1 and 3 were B. The agreement obtained with the experimental spectrum was less satisfactory than the one described above.

4.3. 3-chloro-2-toluidine

The ring proton spectrum shown in figure 3 has eight well-resolved lines and is therefore not an ABC or ABX spectrum. The general appearance is that

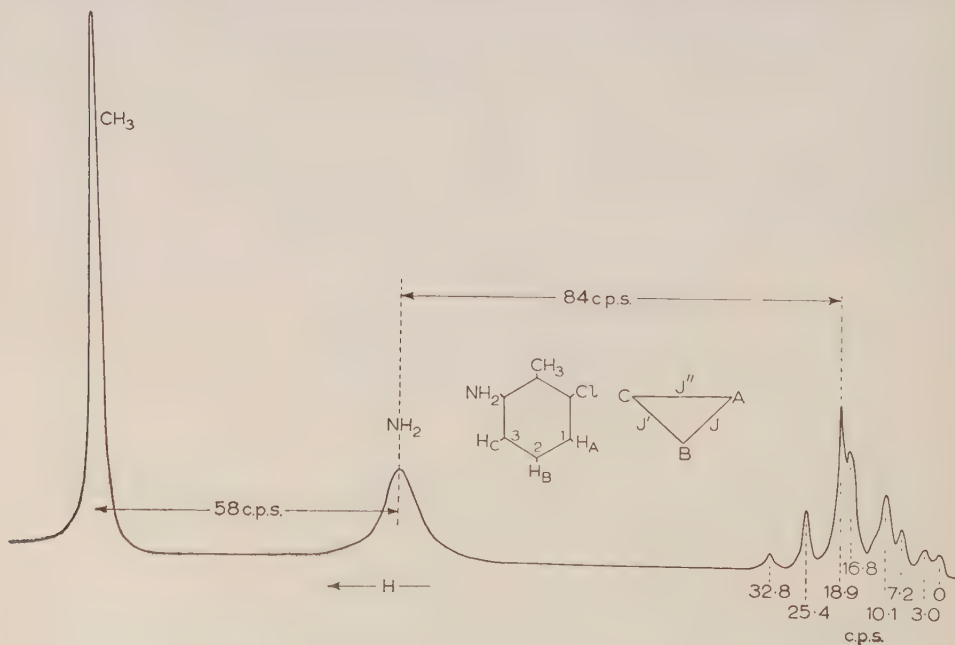


Figure 3. Hydrogen resonance of 3-chloro-2-toluidine.

of an AB_2 spectrum but on this assumption it is impossible to obtain consistent values for the parameters and the discrepancy is many times larger than experimental error.

On the assumption that protons 2 and 3 are B we obtain $J+J''=11.1$ c/s from Table 3. This is reasonable but again the values for D_+ and D_- are not in conformity. We conclude that we are dealing with a case ABC which is very nearly AB_2 . The unresolved line on the high field side of the band at 10.1 c/s is compatible with this conclusion. The value of 11.1 c/s for $J+J''$ indicates that protons 2 and 3 experience very nearly the same field H_B .

4.4. 2,5-dichloronitrobenzene

The proton spectrum shown in figure 4 clearly shows its independence of the ortho proton coupling constant, which is much larger than any splittings present in the two groups of lines. We are dealing with the situation where protons 2 and 3, both ortho to chlorine, experience a field H_B smaller than H_A at proton 1 ortho to the nitro group.

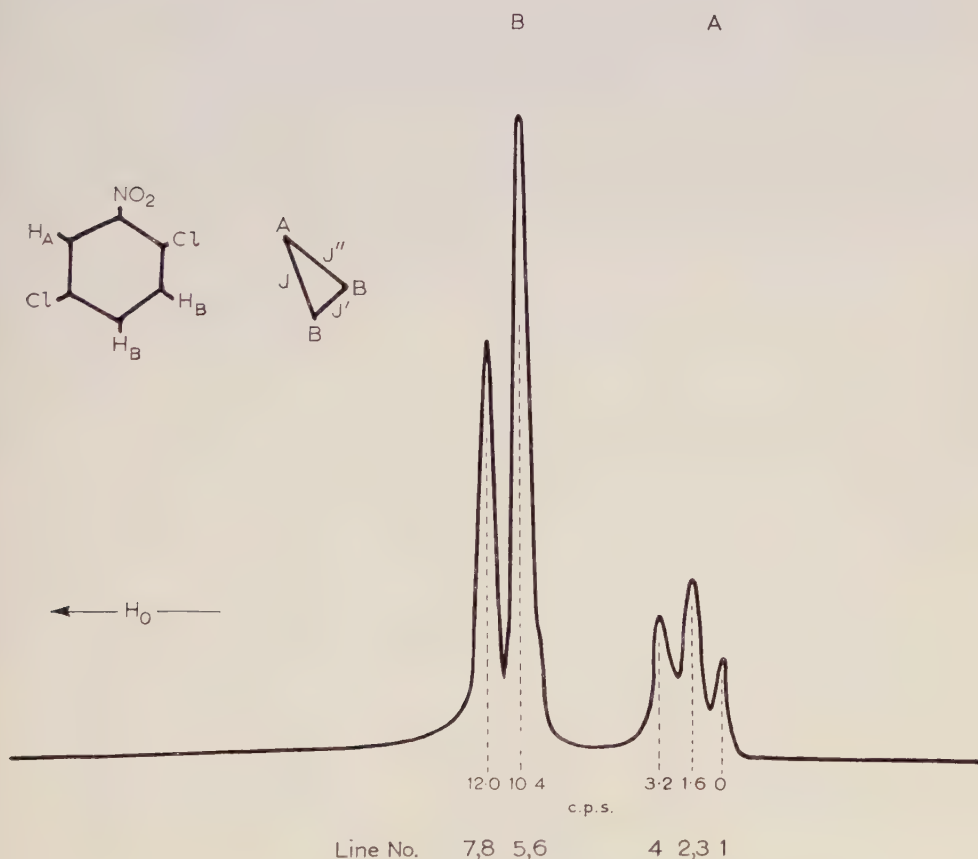


Figure 4. Hydrogen resonance of 2-5-dichloro-nitrobenzene.

Proton 1 is meta and para to protons 2 and 3 and the spectrum is a good illustration of case ABB' ; the splittings do not represent any single coupling

constant. By the use of Table 3 and the assignments given in figure 4 we derive

$$J + J'' = 3.2 \text{ c/s}, \quad \eta H_0(\sigma_B - \sigma_A) = 9.8 \text{ c/s}.$$

The splitting of the two lines in the B spectrum is in fact the *average* of J and J'' and since the para proton coupling constant is always small and often nearly zero, the splitting of 1.6 c/s is about half the meta proton coupling constant.

Line number	Energy c/s		Relative intensity	
	Calculated	Observed	Calculated	Observed
1.	0	0	0.73	0.82
2.	1.7	1.6	0.90	1.88
3.	1.5	1.6	1.00	
4.	3.2	3.2	1.37	1.47
5.	10.5	10.4	2.37	7.6
6.	10.4	10.4	2.34	
7.	12.1	12.0	1.74	4.6
8.	12.0	12.0	1.52	

Table 5. Observed and calculated spectrum for 2, 5-dichloronitrobenzene. Observed intensities calculated from heights of lines.

The observed and calculated energies and intensities are compared in Table 5. The agreement with experiment is good except for the intensity of the line at 10.4 c/s. The combination line, 9, was not observed.

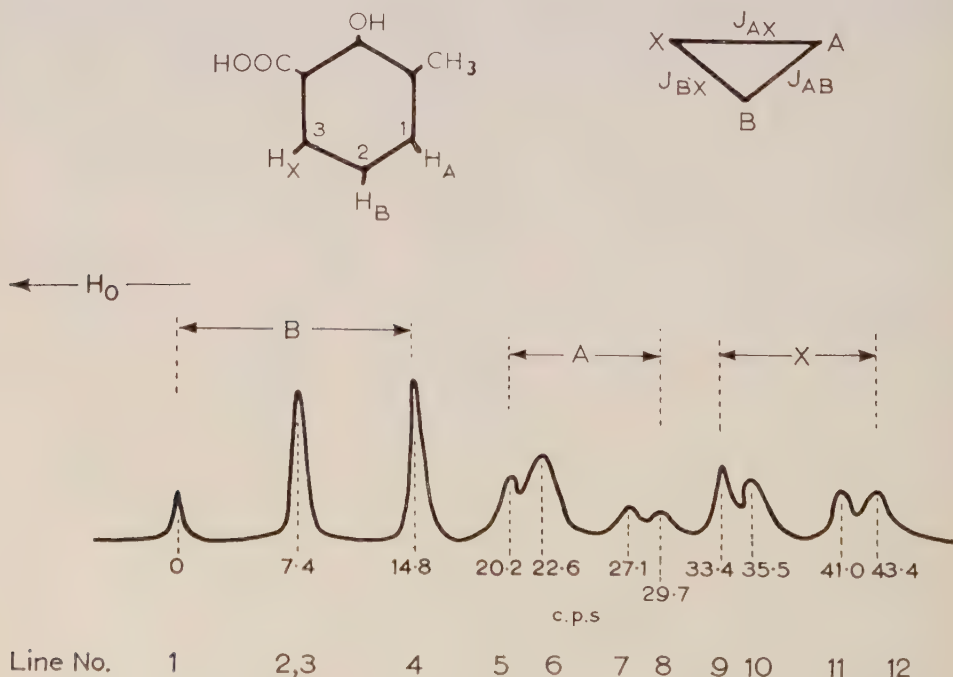


Figure 5. Hydrogen resonance of 3-methyl-salicylic acid.

4.5. 3-methyl-salicylic acid

The ring proton spectrum shown in figure 5 has three groups of lines. The three lines at high field are from proton 2 and on the assumption that proton 3, ortho to the carboxyl group, is least shielded, the lines have their origin as indicated in figure 5.

Although we are clearly dealing with a case ABC it can be seen that the AB lines form a composite group, with the intensities peaked as the lines approach $\frac{1}{2}\eta H_0(2-\sigma_A-\sigma_B)$. An ABX analysis may therefore be feasible even though the X lines are not far removed from the A and B lines. The energies and intensities for an ABX group are given in Table 6.

Transition and origin	Energy	Relative intensity
1. B	$\frac{1}{2}\eta H_0(2-\sigma_A-\sigma_B)-\frac{1}{4}(2J_{AB}+J_{AX}+J_{BX})-A_-$	$(\cos \gamma_- - \sin \gamma_-)^2$
2. B	$\frac{1}{2}\eta H_0(2-\sigma_A-\sigma_B)-\frac{1}{4}(2J_{AB}-J_{AX}-J_{BX})-A_+$	$(\cos \gamma_+ - \sin \gamma_+)^2$
3. B	$\frac{1}{2}\eta H_0(2-\sigma_A-\sigma_B)+\frac{1}{4}(2J_{AB}-J_{AX}-J_{BX})-A_-$	$(\cos \gamma_- + \sin \gamma_-)^2$
4. B	$\frac{1}{2}\eta H_0(2-\sigma_A-\sigma_B)+\frac{1}{4}(2J_{AB}+J_{AX}+J_{BX})-A_+$	$(\cos \gamma_+ + \sin \gamma_+)^2$
5. A	$\frac{1}{2}\eta H_0(2-\sigma_A-\sigma_B)-\frac{1}{4}(2J_{AB}+J_{AX}+J_{BX})+A_-$	$(\cos \gamma_- + \sin \gamma_-)^2$
6. A	$\frac{1}{2}\eta H_0(2-\sigma_A-\sigma_B)-\frac{1}{4}(2J_{AB}-J_{AX}-J_{BX})+A_+$	$(\cos \gamma_+ + \sin \gamma_+)^2$
7. A	$\frac{1}{2}\eta H_0(2-\sigma_A-\sigma_B)+\frac{1}{4}(2J_{AB}-J_{AX}-J_{BX})+A_-$	$(\cos \gamma_- - \sin \gamma_-)^2$
8. A	$\frac{1}{2}\eta H_0(2-\sigma_A-\sigma_B)+\frac{1}{4}(2J_{AB}+J_{AX}+J_{BX})+A_+$	$(\cos \gamma_+ - \sin \gamma_+)^2$
9. X	$\eta H_0(1-\sigma_X)-\frac{1}{2}(J_{AX}+J_{BX})$	1
10. X	$\eta H_0(1-\sigma_X)+A_+-A_-$	$\cos^2(\gamma_+-\gamma_-)$
11. X	$\eta H_0(1-\sigma_X)-A_++A_-$	$\cos^2(\gamma_+-\gamma_-)$
12. X	$\eta H_0(1-\sigma_X)+\frac{1}{2}(J_{AX}+J_{BX})$	1
13. comb.	$\eta H_0(1+\sigma_X)$	0
14. comb.	$\eta H_0(1-\sigma_X)-A_+-A_-$	$\sin^2(\gamma_+-\gamma_-)$
15. comb.	$\eta H_0(1-\sigma_X)+A_++A_-$	$\sin^2(\gamma_+-\gamma_-)$

Table 6. Energies and intensities for ABX.

The positive quantities A_- and A_+ and angles γ_+ , γ_- in Table 6 are defined by

$$\left. \begin{aligned} A_+ \cos 2\gamma_+ &= \frac{1}{2}\eta H_0(\sigma_B - \sigma_A) + \frac{1}{4}(J_{AX} - J_{BX}) \\ A_+ \sin 2\gamma_+ &= \frac{1}{2}J_{AB} \\ A_- \cos 2\gamma_- &= \frac{1}{2}\eta H_0(\sigma_B - \sigma_A) - \frac{1}{4}(J_{AX} - J_{BX}) \\ A_- \sin 2\gamma_- &= \frac{1}{2}J_{AB} \end{aligned} \right\} \quad (4.5)$$

By taking appropriate differences between the energies in Table 6 one may arrive at values for all the experimental parameters. For instance, A_- is equal to half the separation between lines 2 and 6 or between lines 4 and 8, and J_{AB} is equal to the separation between lines 1 and 3 or between lines 5 and 7.

The transitions are assigned as in figure 5 and the values found for the parameters are as follows:

$$\begin{aligned} J_{AB} &= 7.2 \text{ c/s,} \\ J_{BX} &= 7.7 \text{ c/s,} \\ J_{AX} &= 2.3 \text{ c/s,} \\ \eta H_0(\sigma_B - \sigma_A) &= 15.9 \text{ c/s,} \\ \eta H_0(\sigma_A - \sigma_X) &= 15.2 \text{ c/s.} \end{aligned}$$

In Table 7 the observed energies and intensities are compared with the ones calculated from these values.

Line Number	Energy c/s		Relative intensity	
	Calculated	Observed	Calculated	Observed
1.	0	0	0.64	0.7
2.	7.5	7.4	0.53	2.1
3.	7.1	7.4	1.36	
4.	14.6	14.8	1.47	
5.	19.9	20.2	1.36	1.0
6.	22.5	22.6	1.47	1.3
7.	27.0	27.1	0.64	0.5
8.	29.6	29.7	0.53	0.5
9.	33.4	33.4	1	1.1
10.	35.9	35.5	0.99	0.9
11.	40.9	41.0	0.99	0.7
12.	43.4	43.4	1	0.7

Table 7. Observed and calculated spectrum of 3-methylsalicylic acid.
Observed intensities calculated from heights of lines.

The agreement in Table 7 is remarkably good, considering the approximations involved. A calculation based on second-order perturbation theory gives substantially the same results for the parameters but the discrepancy between calculated and observed intensities is larger.

4.6. 2,4-dinitrochlorobenzene

The proton spectrum in figure 6 does not show three clearly defined groups of lines neither is it an AB_2 spectrum. It corresponds to the general ABC case which

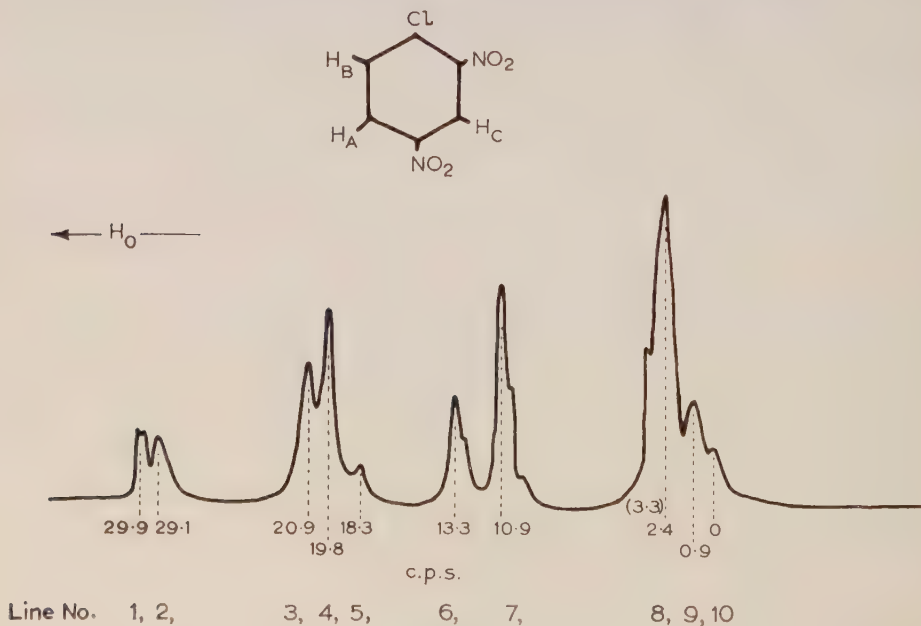


Figure 6. Hydrogen resonance of 2-4-dinitro-chlorobenzene.

calls for the diagonalization of 3×3 matrices. However, if we assume proton 1, ortho to chlorine, to be shielded more than proton 2, ortho to one nitro group, which is in turn more shielded than proton 3, ortho to two nitro groups, we may still extract some information from the spectrum.

Lines 3, 4, 5 arise from overlapping A and B lines while lines 8, 9, 10 are due to C. The separation between lines 6 and 7, 3 and 5, and 8 and 10 will correspond roughly to the meta coupling constant between protons 2 and 3. This spacing is about 2.5 c/s. The separation between lines 1 and 2 (0.8 c/s) and lines 9 and 10 (0.9 c/s) is approximately equal to the para coupling constant between protons 3 and 1. The ortho coupling constant between protons 1 and 2 will be approximated by the separation of the centre of the bands formed by lines (1, 2), (3, 4, 5) and (6, 7). This is about 9 c/s. The chemical shifts between the three protons are approximately equal to 10 c/s.

5. GENERAL

From these measurements it is clear that spectra which are strictly of a complicated type, can sometimes be analysed in simpler terms without very serious loss of accuracy in the chemical shifts and spin-spin coupling constants.

In the case of 2,5-dichloronitrobenzene, the spectrum may be described as ABB' , in which the B protons have identical chemical shifts, but the coupling constants between A and B and A and B' are different. In these circumstances it appears that the B spectrum shows two strong lines, the separation of which is approximately equal to the *average* of J_{AB} and $J_{AB'}$. This may also be the case for fluorobenzene [8] in which the hydrogen resonance consists of a doublet of separation 6.8 c/s.

There is no indication that in these compounds any of the spin-spin coupling constants are negative. The results of these measurements confirm earlier measurements [6] that the coupling constants do not vary greatly with the substituent in aromatic compounds. The compounds described above give values for the ortho H-H coupling constant of 9, 7.7, 7.1, and 8.0 c/s compared with values of 8.1 to 9.2 c/s in *p*-disubstituted benzenes [6]. Meta coupling constants found are 2.5 and 2.3 c/s and a para constant of 0.9 c/s. The values $J_p + J_m = 3.2$ and $J_o + J_m = 11.1$ and 11.7 are also consistent with these results.

We are grateful to the Royal Dutch/Shell Group for a post-graduate scholarship to one of us (T. S.). We also thank the Royal Society, the Department of Scientific and Industrial Research, Shell Petroleum Company, and the Hydrocarbon Research Group of the Institute of Petroleum and the Coal Board for grants in aid of apparatus.

On donne les spectres de résonance protonique à haute résolution d'un certain nombre de dérivés trisubstitués asymétriques du benzène. Dans certains cas on peut analyser les spectres comme étant du type AB_2 , ABB' ou ABX . Le cas ABB' , dans lequel les noyaux B ont des déplacements chimiques identiques, mais n'ont pas le même couplage avec A, est discuté et un exemple est donné. Les constantes de couplage spin-spin (*a*) sont comprises dans l'intervalle 7 c/s à 9 c/s pour des protons en position ortho; (*b*) valent environ 2.5 c/s pour des protons en meta; (*c*) sont inférieures à 1 c/s pour des protons en para.

Für eine Reihe asymmetrisch dreifach substituierter Benzolderivate werden die Wasserstoff-Resonanzspektren hoher Auflösung mitgeteilt. In manchen Fällen lassen sich diese Spektren als AB₂-, ABB'-bzw. ABX-Typen analysieren. Der ABB'-Typ, bei dem die B-Kerne den gleichen *chemical shift* aufweisen, aber in verschiedener Weise an A gekoppelt sind, wird besprochen und erläutert. Die Spin-Spin-Kopplungs-konstanten zwischen Protonen (*a*) in ortho-Stellung zueinander liegen im Bereich von 7 bis 9 Hz, (*b*) bei meta-Stellung in der Nähe von 2,5 Hz und (*c*) bei para-Stellung unterhalb von 1 Hz.

REFERENCES

- [1] GUTOWSKY, H. S., McCALL, D. W., and SLICHTER, C. P., 1951, *Phys. Rev.*, **84**, 589.
McCONNELL, H. M., McLEAN, A. D., and REILLY, C. A., 1952, *J. chem. Phys.*, **23**, 1152.
BERNSTEIN, H. J., POPL, J. A., and SCHNEIDER, W. G., 1957, *Canad. J. Chem.*, **35**, 65.
- [2] LEANE, J., RICHARDS, R. E., and SHAEFER, J. (to be published).
- [3] ARNOLD, J. T., and PACKARD, M. E., 1951, *J. chem. Phys.*, **19**, 1608.
- [4] BANNERJEE, M. K., DAS, T. P., and SAHA, A. K., 1954, *Proc. roy. Soc. A*, **226**, 490.
- [5] Unpublished work in this laboratory.
- [6] RICHARDS, R. E., and SHAEFER, T., 1958, *Trans. Faraday Soc.*, **54**, 1280.
- [7] McCONNELL, H. M., 1956, *J. chem. Phys.*, **24**, 460.
- [8] GUTOWSKY, H. S., MEYER, L. H., and McCALL, D. W., 1955, *J. chem. Phys.*, **23**, 982.

The pressure-induced rotational absorption spectrum of hydrogen : II

by J. P. COLPA† and J. A. A. KETELAAR

Laboratory for General and Inorganic Chemistry of the University of Amsterdam, The Netherlands

(Received 14 May 1958)

A formula is derived for the integrated intensity of pressure-induced rotational transitions in pure gases and gas mixtures at moderate pressures. This formula is applied to the pressure induced rotational spectrum of hydrogen, described in a previous article. A good agreement between the observed and the calculated intensities can be obtained if it is assumed that the induction of the transition moments is mainly caused by the quadrupole field of the hydrogen molecule. In an analogous way, the intensity of the induced simultaneous vibrational-rotational transition in mixtures of carbon monoxide and hydrogen is calculated.

1. A GENERAL FORMALISM FOR THE INTEGRATED INTENSITY OF PRESSURE-INDUCED TRANSITIONS IN GASES OF MODERATE PRESSURES

For a general discussion of the theory of pressure-induced infra-red absorption spectra we refer to the publications of Van Kranendonk [1, 2]. In the present article we will give a simple derivation of the formula for the intensity of pressure-induced bands at moderate gas densities, by a generalization of the intensity formula for infra-red active transitions. At moderate densities from 1–100 Am only binary interactions are of importance, as was the case under the conditions of our experiments described in our previous article [3].

The integrated specific absorption A (shortly called intensity) is defined by

$$A = \int \alpha(\nu) d\nu \quad (1)$$

in which ν is the wave number and α is the absorption coefficient as defined by Lambert's law. For infra-red active transitions, the intensity associated with a transition from a d_i -fold degenerate level i to a d_f -fold degenerate level f is

$$A_{i \rightarrow f} = \frac{8\pi^3 \nu_{if}}{3hc} n \left\{ \frac{F_i}{d_i} - \frac{F_f}{d_f} \right\} \sum_{rs} |\mu_{ir/s}|^2 \quad (2)$$

(see Herzberg [4]). In this formula r and s number the degenerate sublevels of the lower state i and the upper state f . The summation is extended over all possible combinations of upper and lower sublevels; $|\mu_{ir/s}|$ is the matrix element of the electric dipole moment; n is the total number of molecules per cm^3 ; ν_{if} is the wave number at which the transition is observed; F_i and F_f give the fraction of the molecules present in state i respectively state f . The other symbols have their usual meaning. For normal infra-red work F_i/d_i is used instead of $\{F_i/d_i - F_f/d_f\}$ in (2).

† Present address: Koninklijke/Shell-Laboratorium, Amsterdam.

However, if the upper level has a non-negligible population the term $F_i/d_i - F_f/d_f$ must be included in order to correct for the induced emission [5]. For pure rotational spectra this refinement is always necessary. Suppose the matrix elements in (2) are zero for the unperturbed molecules in a gas of low density, and magnetic dipole radiation and electric quadrupole radiation may be neglected.

At higher densities dipole moments may be induced by intermolecular forces. At moderate pressures we only need to consider binary interactions. The induced moment depends on the distance R between the centres of two interacting molecules, on the vibrational normal coordinates r_1 and r_2 and on the orientations δ_1, ϕ_1 and δ_2, ϕ_2 relative to the intermolecular axis (figure 1)

$$\mu = f(R, r_1 \delta_1 \phi_1, r_2 \delta_2 \phi_2).$$

For the calculation of the matrix elements we assume that the total nuclear wave function of the pair of molecules before and after the absorption is the product of the unperturbed rotational and vibrational wave functions of the molecules 1 and 2. This approximation may be justified by the fact that the experimentally observed frequencies are nearly independent of pressure, and coincide almost exactly with the frequencies of the isolated molecules. We define a matrix element ($\mu(R)$) by the following equation:

$$(\mu^{i r f s}(R)) = \int \phi_v^*(r_1)_i \phi_v^*(r_2)_i \phi_{\text{rot}}^*(\delta_1 \phi_1)_i \phi_{\text{rot}}^*(\delta_2 \phi_2)_i \mu(R, r_1, r_2, \delta_1 \phi_1, \delta_2 \phi_2) \\ \times \phi_v(r_1)_f \phi_v(r_2)_f \phi_{\text{rot}}(\delta_1 \phi_1)_f \phi_{\text{rot}}(\delta_2 \phi_2)_f d\tau_1 d\tau_2. \quad (3)$$

The subscripts v and rot refer to vibrational and rotational wave functions. This matrix element (3) is still a function of R .

The contribution (dA) of the pairs with intermolecular distance R to the intensity may be calculated substituting $|\mu^{ij}(R)|$ as given by (3) for $|\mu^{i r f s}|$ in (2), in which for n has to be taken the number of pairs per cm^3 with intermolecular distance between R and $R + dR$.

Statistical mechanics gives for this density of pairs [19]

$$\frac{1}{2} n_1^2 \cdot 4\pi R^2 \exp[-E(R)/kT] dR. \quad (4a)$$

The density of pairs consisting of molecules of two different types is

$$n_1 n_2 4\pi R^2 \exp[-E(R)/kT] dR, \quad (4b)$$

in which n_1 and n_2 are the densities (number of molecules per cm^3) of the gases 1 and 2. $\exp[-E(R)/kT]$ is the approximation for the radial distribution function for binary interactions, in which $E(R)$ is defined so that for $R \rightarrow \infty$ $E \rightarrow 0$. Substituting (4a) for n in (2) and (3) for $|\mu|$ in (2) we find for the contribution of the pairs with intermolecular distance R to the absorption intensity

$$dA = \frac{8\pi^3 \nu}{3hc} \frac{n_1^2}{2} \left(\frac{F_i}{d_i} - \frac{F_f}{d_f} \right) \sum_{rs} |\mu(R)^{i r f s}|^2 \exp[-E(R)/kT] 4\pi R^2 dR. \quad (5)$$

Integrating (5) we find for the intensity caused by self-induction

$$A_0 = \frac{8\pi^3 \nu}{3hc} \frac{n_1^2}{2} \sum_B \left(\frac{F_i}{d_i} - \frac{F_f}{d_f} \right) \int 4\pi R^2 \exp[-E(R)/kT] \sum_{rs} |\mu(R)^{i r f s}|^2 dR. \quad (6a)$$

If a transition in species 1 is also induced by a foreign gas 2 we find for the part of the intensity caused by foreign induction

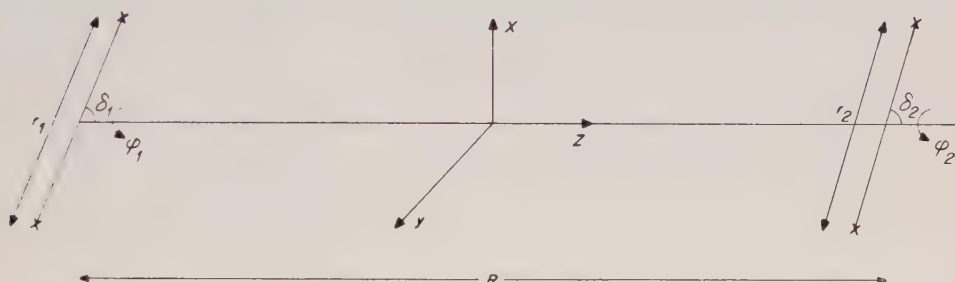
$$A_m = \frac{8\pi^3 \nu}{3hc} n_1 n_2 \sum_B \left(\frac{F_i}{d_i} - \frac{F_f}{d_f} \right) \int 4\pi R^2 \exp[-E(R)/kT] \sum_{rs} |\mu(R)^{i r f s}|^2 dR. \quad (6b)$$

\sum_B means that for a calculation of the total intensity a summation must be made over all transitions occurring in the absorption band. In (6a) and (6b) F_i/d_i and F_f/d_f for a pair are equal to the products of the analogous quantities of the individual molecules in the pair; they specify the probability that the two interacting molecules each have a certain energy level.

2. A FORMALISM FOR THE INTENSITY OF PRESSURE-INDUCED ROTATIONAL SPECTRA OF MOLECULES WITH $D_{\infty h}$ SYMMETRY. SELECTION RULES

2.1. A series expansion for the induced dipole moment

The coordinate system we use is given in figure 1. In our calculations we also use the coordinates $\frac{1}{2}\sqrt{2}(x+iy)$; $\frac{1}{2}\sqrt{2}(x-iy)$ and z ; they will be denoted by $+$, $-$ and 0 .



The components of the induced moment may be expanded as a function of the vibrational coordinates

$$\mu^\kappa(R, r_1, r_2, \delta_1\phi_1, \delta_2\phi_2) = \mu_0^\kappa(R, r_1=r_e, r_2=r_e, \delta_1\phi_1, \delta_2\phi_2) + (r_1-r_e) \frac{\partial \mu^\kappa}{\partial r_1} + (r_2-r_e) \frac{\partial \mu^\kappa}{\partial r_2}, \quad (7)$$

(r_e =equilibrium distance) κ indicates the component $+$, $-$ or 0 . The first term in (7) has to be used for the description of the pure rotational spectrum, the second and the third term give rise to matrix elements for induced vibrational transitions [1] and need not be considered for the pure rotational spectra. We expand the angular dependence of the first term of (7) as a series of products of spherical harmonics

$$\mu_0^\kappa(R\delta_1\phi_1\delta_2\phi_2) = 2\pi \sum_{\substack{\lambda_1\mu_1 \\ \lambda_2\mu_2}} D^\kappa(\lambda_1\mu_1\lambda_2\mu_2) Y_1(\lambda_1\mu_1) Y_2(\lambda_2\mu_2). \quad (8)$$

The coefficients D^κ are functions of the intermolecular distance R . $Y_j(\lambda_j\mu_j)$ is a spherical harmonic, normalized to unity, $j=1, 2$;

$$Y(\lambda\mu) = \theta_{\lambda,|\mu|}(\delta) \frac{1}{\sqrt{(2\pi)}} \exp(i\mu\phi),$$

in which $\theta_{\lambda,|\mu|}(\delta)$ is a normalized associated Legendre polynomial (for a list of these functions see Pauling and Wilson [6]).

2.2. A series expansion for the intensity of induced rotational transitions

For rotational transitions, the matrix element (3) has the form

$$\int \phi_{\text{rot}}^* (\delta_1 \phi_1)_i \phi_{\text{rot}}^* (\delta_2 \phi_2)_f \mu(R, \delta_1 \phi_1, \delta_2 \phi_2)_f \phi_{\text{rot}} (\delta_1 \phi_1)_f \phi_{\text{rot}} (\delta_2 \phi_2)_f d\tau_1 d\tau_2. \quad (9)$$

We assume that the functions ϕ_{rot} are the unperturbed rotational wave functions, so that for ϕ_{rot} may be substituted a spherical harmonic $Y(J, m)$ in which J and m are the rotational and the magnetic quantum number.

We describe the initial state of the interacting pair by the quantum numbers $J_1 m_1 J_2 m_2$ and the final state by $J_1' m_1' J_2' m_2'$. When μ is given by (8) the matrix element (9) for a transition $J_1 m_1 J_2 m_2 \rightarrow J_1' m_1' J_2' m_2'$ (abbreviated by $i \rightarrow f$) is

$$|\mu_{i \rightarrow f}^{\kappa}(R)| = 2\pi \sum_{\substack{\lambda_1 \mu_1 \\ \lambda_2 \mu_2}} |D^{\kappa}(\lambda_1 \mu_1 \lambda_2 \mu_2)| |\langle J_1 m_1 | \lambda_1 \mu_1 J_1' m_1' \rangle| |\langle J_2 m_2 | \lambda_2 \mu_2 J_2' m_2' \rangle|. \quad (10)$$

The symbol $\langle Jm | \lambda \mu J'm' \rangle$ is used for $\int Y^*(Jm) Y(\lambda \mu) Y(J'm') d\tau$.

For the total intensity of a transition $J_1 J_2 \rightarrow J_1' J_2'$ (10) must be squared and then a summation must be carried out over the degenerate states $m_1 m_1' m_2 m_2'$. In

$$\sum_{\substack{m_1 m_1' \\ m_2 m_2'}} |\mu_{i \rightarrow f}^{\kappa}(R)|^2$$

two types of terms occur.

1. Quadratic terms:

$$4\pi^2 |D^{\kappa}(\lambda_1 \mu_1 \lambda_2 \mu_2)|^2 \sum_{m_1 m_1'} |\langle J_1 m_1 | \lambda_1 \mu_1 J_1' m_1' \rangle|^2 \sum_{m_2 m_2'} |\langle J_2 m_2 | \lambda_2 \mu_2 J_2' m_2' \rangle|^2. \quad (11)$$

2. Cross terms:

$$\begin{aligned} & 4\pi^2 \{D^{\kappa}(\lambda_1 \mu_1 \lambda_2 \mu_2)\} \{D^{\kappa}(\lambda_1' \mu_1' \lambda_2' \mu_2')\}^* \\ & \times \sum_{m_1 m_1'} \langle J_1 m_1 | \lambda_1 \mu_1 J_1' m_1' \rangle \langle J_1 m_1 | \lambda_1' \mu_1' J_1' m_1' \rangle^* \\ & \times \sum_{m_2 m_2'} \langle J_2 m_2 | \lambda_2 \mu_2 J_2' m_2' \rangle \langle J_2 m_2 | \lambda_2' \mu_2' J_2' m_2' \rangle^*. \end{aligned} \quad (12)$$

Matrix elements like $\langle Jm | \lambda \mu J'm' \rangle$ have been extensively studied by Racah [7]. We shall use the following properties of these elements. A summation

$$\sum_{m m'} \langle Jm | \lambda \mu J'm' \rangle \langle Jm | \lambda' \mu' J'm' \rangle^* \quad (13)$$

is zero, unless $\mu = \mu'$ and $\lambda = \lambda'$. If $\lambda = \lambda'$ and $\mu = \mu'$ the value of the summation is independent of μ . We use the following abbreviation

$$\sum_{m m'} |\langle Jm | \lambda \mu J'm' \rangle|^2 = \frac{1}{2\pi} S_{\lambda}(J, J'). \quad (14)$$

As a consequence of these properties the cross terms (12) vanish. Using the definition (14) we get

$$\sum_{\substack{m_1 m_1' \\ m_2 m_2'}} |\mu_{i \rightarrow f}^{\kappa}(R)|^2 = \sum_{\substack{\lambda_1 \mu_1 \\ \lambda_2 \mu_2}} |D^{\kappa}(\lambda_1 \mu_1 \lambda_2 \mu_2)|^2 S_{\lambda_1}(J_1, J_1') S_{\lambda_2}(J_2, J_2') \quad (15)$$

in which the coefficients D^{κ} are functions of R . Substituting (15) in (6a) we find

$$\begin{aligned} A_0 = & \frac{8\pi^3 \nu}{3hc} \frac{n_1^2}{2} \sum_B \left\{ \frac{F(J_1)}{2J_1+1} \frac{F(J_2)}{2J_2+1} - \frac{F(J_1')}{2J_1'+1} \frac{F(J_2')}{2J_2'+1} \right\} \\ & \times \int 4\pi R^2 \left\{ \sum_{\substack{\lambda_1 \mu_1 \\ \lambda_2 \mu_2 \\ \kappa}} |D^{\kappa}(\lambda_1 \mu_1 \lambda_2 \mu_2)|^2 S_{\lambda_1}(J_1, J_1') S_{\lambda_2}(J_2, J_2') \right\} \exp[-E(R)/kT] dR. \end{aligned} \quad (16a)$$

For foreign induced absorption a completely analogous formula may be derived starting from (6*b*).

$$A_m = \frac{8\pi^3\nu}{3hc} n_1 n_2 \sum_B \left\{ \frac{F(J_1)}{(2J_1+1)(2J_2+1)} - \frac{F(J_1')}{(2J_1'+1)(2J_2'+1)} \right\} \\ \times \int 4\pi R^2 \left\{ \sum_{\substack{\lambda_1 \mu_1 \\ \lambda_2 \mu_2 \\ K}} |D^K(\lambda_1 \mu_1 \lambda_2 \mu_2)|^2 S_{\lambda_1}(J_1, J_1') S_{\lambda_2}(J_2, J_2') \right\} \exp(-E(R)/kT) dR. \quad (16b)$$

The application of formulae (16*a*) and (16*b*) is not restricted to infra-red spectra; they apply also to rotational transitions that may be expected in the microwave region. Probably the microwave absorption in pure CO₂, observed by Birnbaum and Maryott [8], is of this kind.

2.3. Selection rules for pressure-induced rotational transitions

The coefficients $S_\lambda(J, J')$

For a discussion of the selection rules we consider the expression (15) for the square of the matrix element. We make first a remark about the possible values of λ_1 and λ_2 . For a pair of H₂ molecules (or any other pair of molecules both having $D_{\infty h}$ symmetry) the dipole moment must be left unchanged when δ is converted to $\pi - \delta$ and ϕ to $\phi + \pi$. This means that in the series expansion (8) the values for λ_1 and λ_2 must be even or zero. For pairs with two similar molecules an angle-independent term $D^K(0000)$ in (8) must be zero. For pairs with two different molecules this term may occur, but even then one need not consider this term, for it does not occur in the description of rotational transitions. The first important coefficients are $D^K(2\mu, 00)$ and $D^K(00, 2\mu)$. The selection rules are determined by the values for $\Delta J = J' - J$ for which $S_\lambda(J, J') \neq 0$. Applying recursion formulae and orthogonality relations for Legendre Polynomials we obtained the following results:

$$\left. \begin{aligned} S_0(J, J') &= 0 \text{ unless } J = J', \quad S_0(J, J) = \frac{1}{2}(2J+1). \\ S_2(J, J') &= 0 \text{ unless } \Delta J = \pm 2 \text{ or } \Delta J = 0, J = J' \neq 0. \end{aligned} \right\} \quad (17)$$

$$\left. \begin{aligned} S_2(J, J+2) &= 2\pi \sum_{m m'} |\langle Jm | 2\mu J+2, m' \rangle|^2 = \frac{3}{4} \frac{(J+1)(J+2)}{2J+3}. \\ S_2(J, J-2) &= 2\pi \sum_{m m'} |\langle Jm | 2\mu J-2, m' \rangle|^2 = \frac{3}{4} \frac{J(J-1)}{2J-1}. \\ S_2(J, J) &= 2\pi \sum_{m m'} |\langle Jm | 2\mu Jm' \rangle|^2 = \frac{1}{2} \frac{J(J+1)(2J+1)}{(2J-1)(2J+3)}. \end{aligned} \right\} \quad (18)$$

In general $S_\lambda(J, J') \neq 0$ for λ is even, if $|J' - J| = 0, 2, 4, \dots, \lambda$. As in our calculations λ_1 and λ_2 are 0 or 2, we shall not consider formulae for $S_\lambda(J, J')$ etc. in detail†.

The terms with $D^K(2\mu, 00)$ resp. $D^K(00, 2\mu)$ give the selection rules $\Delta J_1 = 2$, $\Delta J_2 = 0$ and $\Delta J_1 = 0$, $\Delta J_2 = 2$ respectively. If indices 1 and 2 both refer to H₂, these two rules give rise to equivalent transitions; but if index 2 refers to N₂, $\Delta J_1 = 2$, $\Delta J_2 = 0$ describes induced H₂ transitions and $\Delta J_2 = 0$, $\Delta J_2 = 2$ describes induced N₂ rotational transitions.

We also meet in our calculations coefficients $D^K(2\mu_1 2\mu_2)$. They contribute to the intensity when $\Delta J_1 = 2$; $\Delta J_2 = 0$ and $\Delta J_1 = 0$, $\Delta J_2 = 2$, but also when $\Delta J_1 = 2$, $\Delta J_2 = 2$. These transitions, in which both molecules of a pair make a

† cf. § 3.2, Table 1.

transition absorbing only one quantum, are the simultaneous transitions or double transitions. For a further discussion of the selection rules for induced rotational transitions we refer to Galatry and Vodar [17], and for induced simultaneous vibrational transitions to Hooze and Ketelaar [18].

3. CALCULATION OF THE INTENSITY OF THE PRESSURE-REDUCED ROTATIONAL ABSORPTION SPECTRUM OF HYDROGEN

3.1. *The nature of the inducing forces*

In order to evaluate the coefficients $D^{\kappa}(\lambda_1\mu_1\lambda_2\mu_2)$ we will discuss the forces that contribute to the induction of the dipoles.

1. Dipole moments may be induced by the electric fields of each of the molecules of a pair.

2. Induction may be caused by overlap forces.

For the calculation of the intensity of the induced vibrational spectrum of hydrogen both kinds of forces appeared to be important as was shown by Van Kranendonk [1]. We shall show that for the induced rotational spectrum to a good approximation the intensity may be calculated on the basis of the assumption that the electric fields cause the induction and that overlap forces may be neglected.

(a) The electric field of a $D_{\infty h}$ molecule may be described as a quadrupole field. When such a molecule is close to another molecule, the field of the first one induces a dipole in the second one. Direction and magnitude of the induced moment depend on orientation and intermolecular distance. Classically we get the following picture:

A rotating H_2 molecule induces, e.g. in a helium or argon atom, a vibrating dipole field. The frequency of the induced moment is twice the rotational frequency of the H_2 molecule. The factor 2 comes in because of the $D_{\infty h}$ symmetry of the quadrupole field and is the classical analogue of the selection rule $\Delta J = 2$. Although the induced moment is located in the noble gas atom, it depends on the rotational coordinates of the H_2 molecule and gives rise to absorption at a hydrogen rotational frequency. In induced absorption, the two molecules behave as one complex in their interaction with the electromagnetic radiation field. One can easily see that the induced intensity caused by this effect depends on the quadrupole moment of H_2 and on the polarizability of the foreign gas molecule, or for self-induced absorption on the polarizability of a hydrogen molecule.

(b) In our example (a) the foreign molecule itself had no inducing field, but when we take, e.g. N_2 or HCl as a foreign molecule, we have a second effect that contributes to the induction. The quadrupole field of a rotating N_2 or the dipole field of a rotating HCl molecule induces a vibrating dipole in a H_2 molecule. When we assume the polarizability of hydrogen to be isotropic, this induced moment can explain an induction of N_2 rotational transitions or an enhancement of the intensity of the rotational spectrum of HCl. When we consider the fields of the N_2 or HCl molecule to be vibrating, we can see that the vibrational spectrum of N_2 may be induced, or the intensity of a HCl vibrational band may be enhanced.

However, when we take into account the anisotropy of the polarizability of H_2 , we see that the moment induced by N_2 or HCl in H_2 also depends on the

rotational coordinates of the H_2 molecule and gives a contribution to the intensity of transitions characteristic for hydrogen. Pure rotational transitions of hydrogen may be induced and also simultaneous transitions in which take part a H_2 rotational transition and a N_2 or HCl vibrational or rotational transition (see also § 4). In these cases the moment is induced by the foreign molecule in hydrogen, contrary to the effect under (a).

Usually the effect mentioned under (a) gives a much larger contribution to pure rotational absorption bands than the effect (b). We gave the description for the foreign-induced absorption. Of course both effects are present for the self-induced absorption. From the above-mentioned model it is clear that the induced moment for self-induced absorption is to a first approximation proportional to the polarizability of H_2 and for foreign-induced absorption to the polarizability of the foreign molecule. The intensity must be roughly proportional to the square of the polarizability. This is only true if overlap forces may be neglected. In the induced vibrational spectrum of H_2 , the Q -branch ($\Delta n = 1$, $\Delta J = 0$) is mainly due to overlap forces, whereas the S -branch ($\Delta n = 1$, $\Delta J = 2$) is caused by quadrupole fields (see Van Kranendonk [1]). Because of the very small polarizability of He we see that the S -branch in the vibrational spectrum induced by He has a very low intensity, whereas the Q -branch induced by He, and due to overlap forces, is as strong as the self-induced Q -branch (see Welsh [9]). In the case of the induced rotational spectrum we see that He has very little effect in inducing transitions [3, 10]. This is in accordance with the assumption that only electric field effects are of importance. In the formulae derived in the next sections, we neglected the contribution of overlap forces.

3.2. Formulae for the intensity of induced rotational transitions, neglecting the anisotropy of the polarizability

Molecule 1 (figure 1) has a quadrupole moment Q_1 . The components of the quadrupole field of molecule 1 at the position of molecule 2 are:

$$\left. \begin{aligned} F_{1,x} &= -\frac{3Q_1}{R^4} \cos \delta_1 \sin \delta_1 \cos \phi_1, \\ F_{1,y} &= -\frac{3Q_1}{R^4} \cos \delta_1 \sin \delta_1 \sin \phi_1, \\ F_{1,z} &= +\frac{3Q_1}{R^4} \frac{1}{2} (3 \cos^2 \delta_1 - 1). \end{aligned} \right\} \quad (19)$$

Instead of F_x, F_y, F_z we use $F^\pm = \frac{1}{2} \sqrt{2} (F_x \pm iF_y)$ and $F^0 = F_z$. This leads to:

$$\left. \begin{aligned} F_1^+ &= -\frac{3}{2} \sqrt{2} \frac{Q_1}{R^4} \cos \delta_1 \sin \delta_1 \exp(+i\phi_1) = -\sqrt{(2\pi)} \frac{\sqrt{30}}{5} \frac{Q_1}{R^4} Y_1(2, +1), \\ F_1^- &= -\frac{3}{2} \sqrt{2} \frac{Q_1}{R^4} \cos \delta_1 \sin \delta_1 \exp(-i\phi_1) = -\sqrt{(2\pi)} \frac{\sqrt{30}}{5} \frac{Q_1}{R^4} Y_1(2, -1), \\ F_1^0 &= +\frac{3Q_1}{R^4} \frac{1}{2} (3 \cos^2 \delta_1 - 1) = +\sqrt{2\pi} \frac{\sqrt{90}}{5} \frac{Q_1}{R^4} Y_1(2, 0). \end{aligned} \right\} \quad (20)$$

In (20) we expressed the angular dependence in spherical harmonics. When

molecule 2 has a quadrupole moment Q_2 , the components of the field of this molecule at the position of molecule 1 are

$$\left. \begin{aligned} F_2^+ &= \sqrt{(2\pi)} \frac{\sqrt{30}}{5} \frac{Q_2}{R^4} Y_2(2, 1), \\ F_2^- &= \sqrt{(2\pi)} \frac{\sqrt{30}}{5} \frac{Q_2}{R^4} Y_2(2, -1), \\ F_2^0 &= -\sqrt{(2\pi)} \frac{\sqrt{90}}{5} \frac{Q_2}{R^4} Y_2(2, 0). \end{aligned} \right\} \quad (21)$$

For the calculation of the induced moments, the polarizability tensor has been brought into a suitable form (see Appendix). An electric field \mathbf{F} induces in a cylindrically symmetrical molecule a dipole; the components of its moment μ are:

$$\left. \begin{aligned} \mu^+ &= F^+ \left\{ \sqrt{(2\pi)} \sqrt{2} Y(0, 0) \alpha - \Delta \sqrt{(2\pi)} \frac{\sqrt{10}}{15} Y(2, 0) \right\} \\ &\quad + F^- \left\{ \Delta \sqrt{(2\pi)} \frac{2\sqrt{15}}{15} Y(2, +2) \right\} + F^0 \left\{ \Delta \sqrt{(2\pi)} \frac{\sqrt{30}}{15} Y(2, +1) \right\} \\ \mu^- &= F^+ \left\{ \Delta \sqrt{(2\pi)} \frac{2\sqrt{15}}{15} Y(2, -2) \right\} + F^- \left\{ \sqrt{(2\pi)} \sqrt{2} Y(0, 0) \alpha \right. \\ &\quad \left. - \Delta \sqrt{(2\pi)} \frac{\sqrt{10}}{15} Y(2, 0) \right\} + F^0 \left\{ \Delta \sqrt{(2\pi)} \frac{\sqrt{30}}{15} Y(2, -1) \right\} \\ \mu^0 &= F^+ \left\{ \Delta \sqrt{(2\pi)} \frac{\sqrt{30}}{15} Y(2, -1) \right\} + F^- \left\{ \Delta \sqrt{(2\pi)} \frac{\sqrt{30}}{15} Y(2, -1) \right\} \\ &\quad + F^0 \left\{ \sqrt{(2\pi)} \sqrt{2} Y(0, 0) \alpha + \Delta \sqrt{(2\pi)} \frac{2\sqrt{10}}{15} Y(2, 0) \right\} \end{aligned} \right\} \quad (22)$$

α is the average polarizability, $(\alpha_{\parallel} + 2\alpha_{\perp})/3$ and $\Delta = \alpha_{\parallel} - \alpha_{\perp}$ is the anisotropy of the polarizability. The angular dependence is expressed in normalized spherical harmonics. The α in the diagonal elements of (22) formally has the factor $\sqrt{(2\pi)} \sqrt{2} Y(0, 0) = 1$ in order to express all elements in spherical harmonics.

The total induced moment μ is the vector sum of the moments μ_1 and μ_2 induced in the molecules 1 and 2.

$$\mu = \mu_1 + \mu_2 = \bar{\alpha}_1 \mathbf{F}_2 + \bar{\alpha}_2 \mathbf{F}_1, \quad (23)$$

in which $\bar{\alpha}$ represents the polarizability tensor as given by (22) and \mathbf{F}_1 and \mathbf{F}_2 are the electric fields whose components are expressed by (20) and (21). After making the necessary substitutions and collecting the terms with the same product of spherical harmonics we obtain the coefficients $D^{\kappa}(\lambda_1 \mu_1 \lambda_2 \mu_2)$ as defined by (8). These coefficients are collected in Table 1.

The first six coefficients, viz. those proportional to α_1 and α_2 we call the isotropic coefficients; the other ones are called anisotropic coefficients.

As a first approximation we consider the polarizability to be isotropic. The correction for the anisotropy can be calculated separately by evaluating the contribution of the anisotropic terms after substituting these terms in (16a) or (16b).

According to the discussion of the selection rules (§2.3) we expect in the approximation in which only the isotropic coefficients are used, the selection rules $\Delta J_1 = 2$, $\Delta J_2 = 0$ and $\Delta J_1 = 0$, $\Delta J_2 = 2$. For self-induced absorption we have $Q_1 = Q_2$ and $\alpha_1 = \alpha_2$ so that $D^{\kappa}(2 \mu \ 0 \ 0) = D^{\kappa}(0 \ 0 \ 2 \ \mu)$.

$$\begin{aligned}
 D^{\pm}(2 \pm 1 0 0) &= -\frac{Q_1 \alpha_2}{R^4} \frac{2\sqrt{15}}{5} & D^{\pm}(0 0 2 \pm 1) &= \frac{Q_2 \alpha_1}{R^4} \frac{2\sqrt{15}}{5} \\
 D^0(2 0 0 0) &= \frac{Q_1 \alpha_2}{R^4} \frac{6\sqrt{5}}{5} & D^0(0 0 2 0) &= -\frac{Q_2 \alpha_1}{R^4} \frac{6\sqrt{5}}{5} \\
 D^{\pm}(2 \mp 1 2 \pm 2) &= -\frac{Q_1 \Delta_2}{R^4} \frac{2\sqrt{2}}{5} & D^{\pm}(2 \pm 2 2 \mp 1) &= \frac{Q_2 \Delta_1}{R^4} \frac{2\sqrt{2}}{5} \\
 D^{\pm}(2 \pm 1 2 0) &= \frac{2\sqrt{3}}{15R^4} \{Q_1 \Delta_2 - 3Q_2 \Delta_1\} \\
 D^{\pm}(2 0 2 \pm 1) &= \frac{2\sqrt{3}}{15R^4} \{3Q_1 \Delta_2 - Q_2 \Delta_1\} \\
 D^0(2 - 1 2 + 1) &= D^0(2 + 1 2 - 1) = -\frac{2}{5R^4} \{Q_1 \Delta_2 - Q_2 \Delta_1\} \\
 D^0(2 0 2 0) &= \frac{4}{5R^4} \{Q_1 \Delta_2 - Q_2 \Delta_2\}.
 \end{aligned}$$

Table 1.

For the calculation of the intensity of an induced transition with $\Delta J=2$, we only calculate the intensity for $\Delta J_1=2$, $\Delta J_2=0$ and multiply afterwards the intensity so obtained by a factor 2. Doing this we only need the three coefficients $D^{\pm}(2 \mu 0 0)$ of Table 1 for substitution in (16 a). Further we substitute $J_1'=J_1+2$; $J_2'=J_2$; $S_2(J_1, J_2+2)$ and $S_0(J_2, J_2)$ as given by (18) and (17). The summation \sum_B becomes \sum_{J_2} ; and $\sum_{J_2} F(J_2)=1$. We finally obtain for the intensity of a transition $\Delta J=2$ in this approximation:

$$\begin{aligned}
 A_0 &= \frac{48\pi^4\nu}{hc} n_{H_2}^2 \left\{ \frac{F(J)}{2J+1} - \frac{F(J+2)}{2J+5} \right\} \frac{(J+1)(J+2)}{2J+3} Q_{H_2}^2 \alpha_{H_2}^2 \\
 &\quad \times \int_0^{\infty} \frac{\exp[-E(R)/kT]}{R^6} dR. \quad (24)
 \end{aligned}$$

For the intensity caused by foreign-induction we obtain an analogous result. We denote the H_2 molecule by index 1; the foreign molecule by 2. If molecule 2 is for example a N_2 molecule, the transitions $\Delta J_1=0$, $\Delta J_2=2$ are rotational transitions corresponding to the N_2 rotational frequencies in the microwave region. We can omit therefore these transitions for the calculation of the intensity in the infra-red region, and as a consequence we also omit the coefficients $D^{\pm}(0 0 2 \mu)$. In (16 b) we make the same substitutions as was done in (16 a). This leads to the result:

$$\begin{aligned}
 A_m &= \frac{48\pi^4\nu}{hc} n_{H_2} n_2 \left\{ \frac{F(J)}{2J+1} - \frac{F(J+2)}{2J+5} \right\} \frac{(J+1)(J+2)}{2J+3} Q_{H_2}^2 \alpha_2^2 \\
 &\quad \times \int \frac{\exp[-E(R)/kT]}{R^6} dR. \quad (25)
 \end{aligned}$$

As in the derivation of (25) the anisotropy of the polarizability and the quadrupole field of molecule 2 have been neglected, it is immediately clear that (25) may also be applied to the foreign induction by noble gases.

The integral $\int \exp[-E(R)/kT] R^{-6} dR$ has been evaluated numerically. For $E(R)$ we used a Lennard-Jones potential

$$E(R) = 4\epsilon \left\{ \left(\frac{d}{R} \right)^{12} - \left(\frac{d}{R} \right)^6 \right\}.$$

For the calculation of the integral in (25) we made the usual approximation $\epsilon_{1,2} = \sqrt{(\epsilon_1 \epsilon_2)}$ and $d_{1,2} = \frac{1}{2}(d_1 + d_2)$. Numerical values for ϵ and d have been taken from Hirschfelder *et al.* [11]. (It appeared that for pure hydrogen and hydrogen mixtures the integral, neglecting the relatively small temperature dependence, may be approximated roughly by $\frac{1}{3}d^{-5}$. For our calculations we used the exact values.) The values for α and Δ have been taken from the tables in Landolt-Börnstein [12]. For the quadrupole moment of H_2 we used the theoretical value of James and Coolidge, $Q = 0.6 \times 10^{-26}$ e.s.u. [13].

For a comparison of the calculated and the experimental values [3], we calculated the sum of the intensities of the transitions $J = 1 \rightarrow J = 3$; $J = 2 \rightarrow J = 4$; $J = 3 \rightarrow J = 5$. In order to obtain the integrated quadratic absorption coefficient used in our experimental work [3] we substituted for n_{H_2} and n_2 the value for a density of 1 Amagat, viz. 2.69×10^{19} . The values for $F(J)$ are to be found in Table 2 of our first article [3]. In Table 2 the intensities obtained from (24) and (25) are collected and compared with the experimental values.

	H_2-H_2	H_2-He	H_2-N_2	H_2-A	H_2-CO	
$-60^\circ C$	$\Gamma_{theor.}$ $\Gamma_{exp.}$ $\Gamma_{theor.}/\Gamma_{exp.}$	1.34 1.64 0.82	— — —	3.22 4.0 0.80	3.5 4.6 0.76	— — —
$+25^\circ C$	$\Gamma_{theor.}$ $\Gamma_{exp.}$ $\Gamma_{theor.}/\Gamma_{exp.}$	1.49 1.88 0.80	0.17 ~ 0.2 ~ 0.85	3.5 4.5 0.78	3.75 5.1 0.74	4.0 5.5 0.73
$+80^\circ C$	$\Gamma_{theor.}$ $\Gamma_{exp.}$ $\Gamma_{theor.}/\Gamma_{exp.}$	1.57 2.05 0.77	— — —	3.6 4.7 0.77	3.9 5.3 0.74	— — —

Table 2. Integrated quadratic absorption coefficients in $10^{-3} \text{ cm}^{-2} \text{ Am}^{-2}$.

3.3. Correction on the intensity calculation for the anisotropy of the polarizability

The calculations made above may be refined for H_2-H_2 , H_2-N_2 and H_2-CO considering the anisotropy of the polarizability and the electrostatic fields of the N_2 and CO molecules. The correction can be made by substituting the coefficients $D^\kappa(2\mu_1 2\mu_2)$ of Table 1 in (16a) and (16b).

For the self-induced spectrum we have $Q_1 = Q_2$; $\Delta_1 = \Delta_2$; $\alpha_1 = \alpha_2$. Calculating the correction for transitions $\Delta J_1 = 2$, $\Delta J_2 = 0$ and $\Delta J_1 = 0$, $\Delta J_2 = 2$ we find by the methods outlined above that for self-induced absorption the intensity as given by (24) must be multiplied by a correction factor

$$\left\{ 1 + \frac{16}{45} \left(\frac{\Delta_1}{\alpha_1} \right)^2 \sum_{J'} F(J_1) \frac{1}{2} \frac{J_1(J_1+1)}{(2J_1+3)(2J_1-1)} \right\}.$$

With the values $F(J)$ for hydrogen [3] this factor becomes $\{1 + 0.057(\Delta/\alpha)\}$. In the spectral region in which we measured the induced spectrum we must expect the following simultaneous rotational transitions

$$\left. \begin{array}{l} J_1 = 1, J_2 = 1 \rightarrow J_1 = 3, J_2 = 3 \text{ at } 1173 \text{ cm}^{-1} \\ J_1 = 1, J_2 = 0 \rightarrow J_1 = 3, J_2 = 2 \\ J_1 = 0, J_2 = 1 \rightarrow J_1 = 2, J_2 = 3 \\ J_1 = 0, J_2 = 0 \rightarrow J_1 = 2, J_2 = 2 \text{ at } 708 \text{ cm}^{-1} \end{array} \right\} \text{ at } 940 \text{ cm}^{-1}$$

For a good comparison between the experimental intensity in the region of 400 cm^{-1} to 1300 cm^{-1} and the calculated intensity we must include in our calculations the contribution of these simultaneous transitions. All elements necessary for a calculation of the intensity of these transitions are mentioned in the previous sections. The results are summarized in Table 3. Comparing

Frequency	708 cm^{-1}	940 cm^{-1}	1173 cm^{-1}
Intensity -60°C	0.0005	0.0041	0.0068
25°C	—	0.0027	0.0055
80°C	—	0.0022	0.0050

Table 3. Calculated intensities of some simultaneous rotational transitions in $10^{-3}\text{ cm}^{-2}\text{ Am}^{-2}$.

Table 3 with Table 2, we see that these simultaneous transitions are very weak; consequently we could not observe them separately besides the stronger broad bands at 814 cm^{-1} and 1034 cm^{-1} [3]. We expect, however, that at lower temperatures at which the intensity of the bands at 814 cm^{-1} and 1034 cm^{-1} vanishes, the bands due to the simultaneous transitions are observable.

The correction of the foreign induced intensity for anisotropy is somewhat more complicated, since $\Delta_1 \neq \Delta_2$ and $Q_1 \neq Q_2$. The CO molecule besides a quadrupole moment has a small dipole moment. For mixtures of CO and H_2 we extended the intensity calculations, including in the series expansion (8) also terms describing the influence of the dipole moment of CO. However, it appeared that the influence of the weak dipole field of CO is considerably less than that of the relatively strong quadrupole field; in the vibrational ground state the CO molecule behaves as a quadrupole molecule. We need not discuss the calculations in detail; the corrected values for the intensities are summarized in Table 4. In the calculated intensities for $\text{H}_2\text{-N}_2$ and $\text{H}_2\text{-CO}$ mixtures we included also the contribution of the simultaneous transitions $\Delta J = 2$ falling in the region of our spectrum. For the quadrupole moments see Hirschfelder *et al.* [11] and Feeny *et al.* [14].

		$\text{H}_2\text{-H}_2$	$\text{H}_2\text{-N}_2$	$\text{H}_2\text{-CO}$
-60°C	$\Gamma_{\text{calc.}}$	1.35	3.35	—
	$\Gamma_{\text{exp.}}$	1.62	4.0	—
	$\Gamma_{\text{calc.}}/\Gamma_{\text{exp.}}$	0.83	0.84	—
$\pm 25^\circ\text{C}$	$\Gamma_{\text{calc.}}$	1.51	3.64	4.16
	$\Gamma_{\text{exp.}}$	1.88	4.5	5.5
	$\Gamma_{\text{calc.}}/\Gamma_{\text{exp.}}$	0.81	0.81	0.76
$+80^\circ\text{C}$	$\Gamma_{\text{calc.}}$	1.62	3.74	—
	$\Gamma_{\text{exp.}}$	2.05	4.7	—
	$\Gamma_{\text{calc.}}/\Gamma_{\text{exp.}}$	0.79	0.80	—

Table 4. Integrated specific absorption coefficients in $10^{-3}\text{ cm}^{-2}\text{ Am}^{-2}$.

§ 4. THE INTENSITY OF THE SIMULTANEOUS VIBRATIONAL-ROTATIONAL TRANSITION IN MIXTURES OF CO AND H₂

In our previous article [3] we described a band at 2730 cm⁻¹ observed in mixtures of CO and H₂ and interpreted it as due to a simultaneous transition in which the CO vibrational transition and the $J=1 \rightarrow J=3$ rotational transition take part. We will discuss here the intensity of this band.

In a pair consisting of a H₂ molecule (index 1) and a CO molecule (index 2) the induced moment may be caused by the following effects:

1. The dipole field of CO induces a dipole in H₂.
2. The quadrupole field of CO induces a dipole in H₂.
3. The quadrupole field of H₂ induces a dipole in CO.
4. Overlap forces induce a dipole.

There is a large amount of similarity in the physical properties of the iso-electronic molecules CO and N₂. One of the most important differences is that only the CO molecule has a dipole field. In mixtures of N₂ and H₂ we could not observe the simultaneous vibrational-rotational transition analogous to that in CO-H₂ mixtures. Therefore we assume that the dipole field of CO plays an important role in the induction (effect 1). The dipole moment is small ($\sim 0.1 D$), but as we have here a vibrational transition in the CO molecule, we are not interested in the moment itself but in the derivative with respect to the internuclear distance $(\partial\mu/\partial r)_{r=r_0}$; for CO this quantity is very large (3.14×10^{-10} e.s.u. [15]). We make the assumption that the simultaneous transition is mainly due to the vibrating dipole field of the CO molecule. This field induces in a H₂ molecule a dipole that depends on the rotational coordinates of the H₂ molecules because of the anisotropy of the polarizability of H₂.

Using the definition of F^\pm and F^0 as given in § 2.2 we find for the components of the dipole field of molecule 2 (CO) at the position of molecule 1 (H₂)

$$\left. \begin{aligned} F_2^\pm &= -\sqrt{(2\pi)^{\frac{1}{3}}} \sqrt{6} \frac{\mu_2}{R^3} Y_2(1, \pm 1) \\ F_2^0 &= +\sqrt{(2\pi)^{\frac{2}{3}}} \sqrt{6} \frac{\mu_2}{R^3} Y_2(1, 0). \end{aligned} \right\} \quad (26)$$

In (26) we have expressed again the angular dependence in spherical harmonics; μ_2 is the dipole moment of CO; it is a function of the internuclear distance r_2 in CO.

The components of the induced moment μ are obtained by substituting (26) in the tensor expression (22). We can omit in (22) the angle-independent terms α , because they are of no use in the description of transitions in which the rotational quantum number of molecule 1 changes. After substitution we see that the relevant terms of μ^\pm and μ^0 may be expressed in a series expansion of the following type:

$$\mu^\kappa(R, r_2, \delta_1 \phi_1, \delta_2 \phi_2) = 2\pi \frac{\mu_2(r_2)}{R^3} \Delta_1 \sum_{\mu_1, \mu_2} G^\kappa(2\mu_1 1\mu_2) Y_1(2, \mu_1) Y_2(1, \mu_2). \quad (27)$$

The coefficients G^κ are easily obtained from (22) and (26). In the calculation we only need the sum of their squares; we found

$$\sum_{\substack{\mu_1 \mu_2 \\ \kappa}} |G(2\mu_1 1\mu_2)|^2 = \frac{16}{9}. \quad (28)$$

The square of the matrix element for a transition

$$J_1, m_1, J_2, m_2, n_2 = 0 \rightarrow J_1' m_1' J_2' m_2', n_2 = 1$$

after summation over $m_1 m_1' m_2 m_2'$ is given by

$$\sum_{\substack{m_1 m_1' \\ m_2 m_2'}} |\mu_{i \rightarrow f}^\kappa|^2 = \frac{\Delta_1^2}{R^6} |\mu_2|^2 \sum_{\mu_1 \mu_2} |G^\kappa(2\mu_1 1\mu_2)|^2 S_2(J_1, J_1') S_1(J_2, J_2'). \quad (29)$$

(As mentioned in § 2.2 the cross terms vanish on summation.) In (29) we have

$$|\mu_2| = \int \phi_v(n_2=0) \mu_2 \phi_v(n_2=1) d\tau;$$

this is the matrix element describing the vibrational transition in CO:

$$S_1(J_2, J_2') = 2\pi \sum_{m_2 m_2'} |\langle J_2 m_2 | 1\mu_2 | J_2' m_2' \rangle|^2.$$

Applying the recursion formula for Legendre polynomials one easily proves that $S_1(J_2, J_2') \neq 0$ only when $\Delta J_2 = \pm 1$. A calculation gives

$$S_1(J_2, J_2+1) = \frac{1}{2}(J_2+1); \quad S_1(J_2, J_2-1) = \frac{1}{2}J_2; \quad (30)$$

$S_2(J_1, J_1')$ is discussed in § 2.2.

Substituting (18), (28) and (30) in (29) and the result in (6*b*) we find the intensity for the transitions $\Delta n_2 = 1$, $\Delta J_2 = \pm 1$, $\Delta J_1 = +2$; F_f in (6*b*) equals zero, all the CO molecules are in the vibrational groundstate;

$$\frac{F_i}{d_i} = \frac{F(J_1)}{(2J_1+1)} \cdot \frac{F(J_2)}{(2J_2+1)}.$$

For the calculation of the total intensity of the simultaneous transition we have to carry out a summation of the above mentioned intensity for $\Delta J_2 = 1$ and $\Delta J_2 = -1$ for all values of J_2 . The result is

$$A = \frac{8\pi^3 \nu}{3hc} n_{H_2} n_{CO} \frac{F(J_1)}{2J_1+1} \Delta_1^2 |\mu_2|^2 \frac{2}{3} \frac{(J_1+1)(J_1+2)}{(2J_1+3)} 4\pi \int \frac{\exp[-E(R)/kT]}{R^6} dR. \quad (31)$$

We can give this expression a simpler form. The intensity of the infra-red active vibrational band of CO is

$$A_2 = \frac{8\pi^3 \nu_2}{3hc} n_2 |\mu_2|^2. \quad (32)$$

Substituting (32) in (31) we find for the simultaneous vibrational-rotational transition an intensity

$$A = A_2 \frac{\nu}{\nu_2} n_1 \Delta_1^2 \frac{F(J_1)}{2J_1+1} \frac{8\pi}{3} \frac{(J_1+1)(J_1+2)}{(2J_1+3)} \int \frac{\exp[-E(R)/kT]}{R^4} dR. \quad (33)$$

We see that the intensity of the simultaneous transitions is proportional to the intensity of the infra-red active transition of CO. A_2 has been measured by Penner and Weber [15] and is found to be $258 \text{ cm}^{-2} \text{ Am}^{-1}$. After the necessary calculations we find for the integrated quadratic absorption coefficient

$$\Gamma_m = 1.2 \times 10^{-5} \text{ cm}^{-2} \text{ Am}^{-2}.$$

The experimental value was $1.5 \times 10^{-5} \text{ cm}^{-2} \text{ Am}^{-2}$ [3, 10], so that our approximate theory gives a very reasonable account of the intensity of this induced band. An expression for the intensity of simultaneous vibrational transitions [10] will be published elsewhere [20].

The authors wish to express their thanks to Dr. J. van Kranendonk for helpful discussions.

This work is part of the research programme of the Stichting voor Fundamenteel Onderzoek der Materie (Foundation for Fundamental Research on Matter, F.O.M.) and was made possible by financial support from the Nederlandse Organisatie voor Zuiver-Wetenschappelijk Onderzoek (Netherlands Organization for Pure Research, Z.W.O.).

APPENDIX

The polarizability tensor

We indicate the polarizability of a cylindrically symmetrical molecule in the direction of the molecular axis by α_{\parallel} and in the direction perpendicular to the axis by α_{\perp} ; we define the anisotropy Δ by $\alpha_{\parallel} - \alpha_{\perp}$. The components of the dipole moment \mathbf{P} induced by an electric field \mathbf{F} may be calculated according to the method outlined, e.g. by Stuart [16]. Using the coordinate directions of figure 1, the result is

$$\begin{aligned} P_x &= F_x \{\alpha_{\perp} + \Delta \sin^2 \delta \cos^2 \phi\} + F_y \{\Delta \sin^2 \delta \cos \phi \sin \phi\} + F_z \{\Delta \sin \delta \cos \delta \cos \phi\}, \\ P_y &= F_x \{\Delta \sin^2 \delta \sin \phi \cos \phi\} + F_y \{\alpha_{\perp} + \Delta \sin^2 \delta \sin^2 \phi\} + F_z \{\Delta \sin \delta \cos \delta \sin \phi\}, \\ P_z &= F_x \{\Delta \sin \delta \cos \delta \cos \phi\} + F_y \{\Delta \sin \delta \cos \delta \sin \phi\} + F_z \{\alpha_{\parallel} + \Delta \cos^2 \delta\}. \end{aligned}$$

We preferably use a system with complex coordinates

$$\begin{aligned} F^{\pm} &= \frac{1}{2} \sqrt{2} (F_x \pm i F_y) & F^0 &= F_z \\ P^{\pm} &= \frac{1}{2} \sqrt{2} (P_x \pm i P_y) & P^0 &= P_z. \end{aligned}$$

Using these coordinates we find

$$\begin{aligned} P^+ &= F^+ \{\alpha_{\perp} + \frac{1}{2} \Delta \sin^2 \delta\} + F^- \{\frac{1}{2} \Delta \sin^2 \delta \exp(+2i\phi)\} + F^0 \{\sqrt{\frac{1}{2}} \Delta \sin \delta \cos \delta \\ &\quad \times \exp(+i\phi)\}, \\ P^- &= F^+ \{\frac{1}{2} \Delta \sin^2 \delta \exp(-2i\phi)\} + F^- \{\alpha_{\perp} + \frac{1}{2} \Delta \sin^2 \delta\} + F^0 \{\sqrt{\frac{1}{2}} \Delta \sin \delta \cos \delta \\ &\quad \times \exp(-i\phi)\}, \\ P^0 &= F^+ \{\sqrt{\frac{1}{2}} \Delta \sin \delta \cos \delta \exp(-i\phi)\} + F^- \{\sqrt{\frac{1}{2}} \Delta \sin \delta \cos \delta \exp(i\phi)\} \\ &\quad + F^0 \{\alpha_{\parallel} + \Delta \cos^2 \delta\}. \end{aligned}$$

We now introduce the average polarizability $\alpha = \frac{1}{3}(2\alpha_{\perp} + \alpha_{\parallel}) = \alpha_{\perp} + \frac{1}{3}\Delta$ and express the elements of the polarizability tensor in α , Δ and normalized spherical harmonics $Y(\lambda, \mu)$ (for a table of these functions we refer to Pauling and Wilson [6]). The final result is:

$$\left. \begin{aligned} P^+ &= F^+ \left\{ \alpha - \Delta \sqrt{2\pi} \frac{\sqrt{10}}{15} Y(2, 0) \right\} + F^- \left\{ \Delta \sqrt{2\pi} \frac{2\sqrt{15}}{15} Y(2, +2) \right\} \\ &\quad + F^0 \left\{ \Delta \sqrt{2\pi} \frac{\sqrt{30}}{15} Y(2, +1) \right\}, \\ P^- &= F^+ \left\{ \Delta \sqrt{2\pi} \frac{2\sqrt{15}}{15} Y(2, +2) \right\} + F^- \left\{ \alpha - \Delta \sqrt{2\pi} \frac{\sqrt{10}}{15} Y(2, 0) \right\} \\ &\quad + F^0 \left\{ \Delta \sqrt{2\pi} \frac{\sqrt{30}}{15} Y(2, -1) \right\}, \\ P^0 &= F^+ \left\{ \Delta \sqrt{2\pi} \frac{\sqrt{30}}{15} Y(2, -1) \right\} + F^- \left\{ \Delta \sqrt{2\pi} \frac{\sqrt{30}}{15} Y(2, +1) \right\} \\ &\quad + F^0 \left\{ \alpha + \Delta \sqrt{2\pi} \frac{2\sqrt{10}}{15} Y(2, 0) \right\}. \end{aligned} \right\} \quad (34)$$

In our calculations we used $\alpha \sqrt{(2\pi)} \sqrt{2} Y(0, 0)$ instead of α , in order to get more symmetrical formulae. With the expression (34) the polarizability tensor may

be simply separated into the isotropic or spherical part of the polarizability and the completely anisotropic part.

On a dérivé une formule donnant l'intensité intégrée des transitions de rotation induites par pression dans les gaz purs et les mélanges gazeux à des pressions modérées. Cette formule a été appliquée au spectre de rotation induit par pression de l'hydrogène, décrite dans une publication antérieure. On obtient un bon accord entre les intensités mesurées et calculées en supposant que l'induction des moments de transition est dû principalement au champ quadrupolaire de la molécule d'hydrogène.

L'intensité d'une transition de combinaison entre la transition de vibration du monoxyde de carbone et une transition de rotation de l'hydrogène se calcule d'une manière analogue.

Für die integrale Intensität von druckinduzierten Rotationsübergängen in reinen Gasen, sowie in Gasgemischen wird eine Formel abgeleitet. Sie wird auf das druckinduzierte Rotationsspektrum von Wasserstoff angewandt, das in einer früheren Arbeit beschrieben ist. Eine gute Uebereinstimmung zwischen den beobachteten und den berechneten Intensitäten lässt sich erreichen wenn man annimmt, dass die Induktion der Uebergangsmomente im wesentlichen durch das Quadrupolfeld der Wasserstoffmolekel verursacht wird.

In analoger Weise wird die Intensität des induzierten simultanen Rotations-Schwingungsübergangs für Mischungen von Kohlenmonoxyd und Wasserstoff berechnet.

REFERENCES

- [1] VAN KRANENDONK, J., 1952, *Thesis*, Amsterdam, VAN KRANENDONK, J., and BIRD, R. B., 1951, *Physica*, **17**, 953.
- [2] VAN KRANENDONK, J., 1957, *Physica*, **23**, 825, 1958, *Ibid.*, **24**, 347.
- [3] COLPA, J. P., and KETELAAR, J. A. A., 1958, *Mol. Phys.*, **1**, 14.
- [4] HERZBERG, J., 1950, *Spectra of Diatomic Molecules* (New York: Van Nostrand).
- [5] WILSON, E. B., DECIUS, J. C., and CROSS, P. C., 1955, *Molecular Vibrations* (New York: McGraw-Hill).
- [6] PAULING, L., and WILSON, E. B., 1935, *Introduction to Quantum Mechanics* (New York: McGraw-Hill).
- [7] RACA, G., 1942, *Phys. Rev.*, **61**, 186; **62**, 438 and 1943, **63**, 367.
- [8] BIRNBAUM, G., MARYOTT, A. A., and WACHER, P. F., 1954, *J. chem. Phys.*, **22**, 1782.
- [9] CRAWFORD, M. F., WELSH, H. L., McDONALD, J. C. F., and LOCKE, J. L., 1950, *Phys. Rev.*, **80**, 469.
- [10] COLPA, J. P., 1957, *Thesis*, Amsterdam.
- [11] HIRSCHFELDER, J. O., CURTISS, C. F., and BIRD, R. B., 1954, *Molecular Theory of Gases and Liquids* (New York: Wiley).
- [12] LANDOLT-BÖRNSTEIN, 1951, *Zahlenwerte und Funktionen III* (Berlin).
- [13] JAMES, H. M., and COOLIDGE, A. S., 1938, *Astrophys. J.*, **87**, 438.
- [14] FEENY, H., MADIGOSKY, W., and WINDERS, B., 1957, *J. chem. Phys.*, **27**, 898.
- [15] PENNER, S. S., and WEBER, D., 1951, *J. chem. Phys.*, **19**, 807.
- [16] STUART, H. A., 1952, *Die Struktur des freien Moleküls* (Berlin: Springer Verlag).
- [17] GALATRY, L., and VODAR, B., 1956, *C.R. Acad. Sci., Paris*, **242**, 1871.
- [18] HOOGE, F. N., and KETELAAR, J. A. A., 1957, *Physica*, **23**, 423.
- [19] FOWLER, R. H., and GUGGENHEIM, E. A., 1939, *Statistical Thermodynamics* (Cambridge: University Press).
- [20] COLPA, J. P., and KETELAAR, J. A. A., *Physica* (to be published).

The probabilities of triplet-singlet transitions in aromatic hydrocarbons and ketones†

by H. F. HAMEKA‡ and L. J. OOSTERHOFF

Leiden University, Department of Theoretical Organic Chemistry

(Received 18 May 1958)

Calculations have been performed on the probabilities of triplet-singlet transitions in benzene and acetone in connection with the decay times of the phosphorescence. The transition probability was determined from the extent to which excited singlet states are mixed with the triplet state. The assumption that in benzene the phosphorescent state has $^3B_{2u}$ properties—so that the $^1B_{1u}$ singlet state is mixed with it—yields the best agreement with the experimental data. In the case of acetone the phosphorescence was considered as a triplet-singlet transition in which only the electrons of the CO group are involved. In both cases the agreement with experiment is as satisfactory as in other calculations on transition probabilities, the figures for the decay times being 190 and 7 seconds for benzene and 7.8 and 0.6 milliseconds for acetone. The ratio of the calculated decay times is in good agreement with the experimental result (2.4×10^4 and 1.2×10^4).

1. INTRODUCTION

Many organic compounds in solid or highly viscous solution show a strong afterglow after excitation by ultra-violet light [29]. In the last two decades extensive and systematic investigations of this phenomenon (phosphorescence) have been reported [12, 13]. Spectra as well as decay times of the afterglow were studied. Usually the light emitted has a lower frequency than corresponds to the first absorption band. The decay times vary considerably [17]: for ketones they are of the order of magnitude of milliseconds, for aromatic hydrocarbons values of about 10 seconds are found.

A qualitative explanation of these phosphorescence phenomena was suggested by Jablonski [8, 9]. According to his scheme a molecule is raised by light absorption from the ground state G to an excited state E from where a transition to the phosphorescent state P takes place (figure 1). The return of the molecule from P to G is assumed to be nearly forbidden, corresponding to the long lifetime of the phosphorescent state.

To this scheme Lewis and Kasha [12, 13] added the assumption that the metastable P-level is a triplet state, whereas G and E are singlet states. A strong experimental argument in favour of this assumption is the measured increase in magnetic susceptibility of the molecule on excitation, which has been reported by Lewis and Calvin [14] and Lewis *et al.* [15] and by Evans [2] for fluorescein, 1-hydroxy-2-naphthoic acid and triphenylene. The experiments of Evans show quite clearly that the increase in magnetic susceptibility is caused by the presence

† This paper is mainly based on a portion of a doctoral thesis which was submitted by the first author to the University of Leiden in 1956. A survey of this work was reported at the "Colloque International sur le Calcul des Fonctions d'Onde Moleculaires", Paris, 1957.

‡ Present address: Chemistry Department, Carnegie Institute of Technology, Pittsburgh, Pa.

of molecules in the phosphorescent state. The idea of a triplet-singlet transition is also supported by the results of Weissman and Lipkin [28], who by a wide-angle interference study of the phosphorescence of fluorescein, showed that the process involves an electric dipole transition.

On the other hand the theory does not look wholly consistent. If the $P \rightarrow G$ transition is singlet-triplet forbidden the same applies to the $E \rightarrow P$ transition even in case this is a radiationless transition and it is difficult to see how this would not impede a sufficient population of molecules in the phosphorescent state. An estimate of this population and the required $E \rightarrow P$ transition probability even gives a very high value (see e.g. Pringsheim [31], pp. 257 and 437). This argument has recently been stressed by Porter [23, 24] in connection with his high intensity flash studies. As an alternative explanation Porter suggested a $g \rightarrow g$ mechanism for the phosphorescence whereas in the Jablonski scheme the other two transitions would have $g \rightarrow u$ or $u \rightarrow g$ character. The phosphorescence would then be due to a quadrupole or magnetic dipole radiation. This suggestion has been discussed elsewhere [6] but it may be mentioned here that this mechanism is in contradiction with the results of Weissman and Lipkin [28] already referred to.

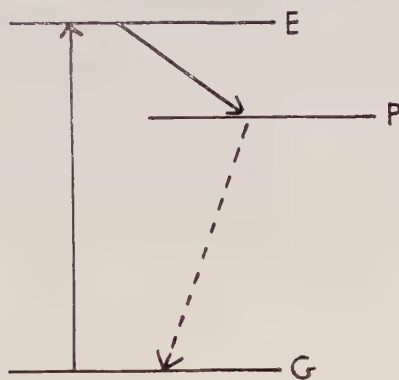


Figure 1.

It is also noteworthy that one has failed to detect a phosphorescent triplet state by paramagnetic resonance experiments in spite of several attempts that have been made in various laboratories.

A better understanding of the mechanism of the phosphorescence might be obtained from a calculation of the probability of the triplet-singlet transition.

McClure [17], who has measured the decay times of some organic compounds, first tried to interpret his results by assuming that the spin-orbit energy is the sum of the spin-orbit energies of the atoms. This simple description of the triplet-singlet emission did not yield satisfactory results, however, especially in the case of the aromatic hydrocarbons, where the values of the decay times thus obtained were much smaller than the corresponding experimental values. More recently McClure [18] has indicated in which way the decay time depends on the spin-orbit energy for the benzene molecule. This author showed that all one-centre and two-centre integrals do not contribute to this energy and in this way the long lifetime of aromatic molecules in the phosphorescent state may be understood. A calculation of the spin-orbit energy itself which is necessary to determine the decay time, was not performed.

Mizushima and Koide [20] have tried to calculate the average time the benzene molecule will stay in one of the higher triplet states, assuming that the transition to the ground state takes place via an intermediate state. From this they made an estimate of the decay time of the phosphorescence. It is our contention however, that their approach of the problem is not wholly adequate.

We have chosen benzene and acetone as examples for our calculations because they are representatives of the two most important classes of organic compounds for which the decay time of the phosphorescence has been measured (the aromatic hydrocarbons and the ketones).

2. THE PERTURBATION OF TRIPLET AND SINGLET STATES IN THE BENZENE MOLECULE

For a quantum mechanical description of the benzene molecule use will be made of ideas which were first expressed by Hückel [7] and which later were extended by Goepfert-Mayer and Sklar [5] who took the Pauli principle properly into account and included the repulsions between electrons in the calculation of energy levels. It is assumed that only π -electrons are involved in the spectral transitions under consideration. The wave functions of the π -electrons are written as combinations of antisymmetrized products of one-electron wave functions. Each of the one electron wave functions is represented as a linear combination of atomic orbitals and can be written as

$$\phi_k = N^{-1} \sum_{j=0}^5 a_j \exp(-2\pi i k j / 6); \quad (1)$$

a_j is a p_z orbital at carbon atom j , N the normalization constant.

As has been pointed out by Hückel and Goepfert-Mayer and Sklar, in the ground state of the benzene molecule two of the six electrons are in the state $k=0$, whereas the remaining four occupy the states ± 1 . The lowest excited states of the molecule are obtained by assuming one of the electrons of a ± 1 state to pass into a ± 2 state. According to the Pauli principle the ground state of the molecule must be a singlet state whereas the four excited states may have singlet as well as triplet properties. With the aid of the auxiliary functions

$$\left. \begin{aligned} S(12) &= \frac{1}{\sqrt{2}} (\alpha_1 \beta_2 - \beta_1 \alpha_2) \\ T_x(12) &= \frac{1}{\sqrt{2}} (\beta_1 \beta_2 - \alpha_1 \alpha_2); \quad T_y(12) = \frac{i}{\sqrt{2}} (\beta_1 \beta_2 + \alpha_1 \alpha_2); \\ T_z(12) &= \frac{1}{\sqrt{2}} (\alpha_1 \beta_2 + \beta_1 \alpha_2) \\ {}^1\chi &= S(12) S(34) S(56) \\ {}^3\chi &= S(12) S(34) \{C_x T_x(56) + C_y T_y(56) + C_z T_z(56)\}, \end{aligned} \right\} \quad (2)$$

the antisymmetrized wave functions of the π -electrons may now be written as

$$\left. \begin{aligned} \psi_0 &= (6!)^{-1/2} \sum_P \delta_P P \phi_0(1) \phi_0(2) \phi_1(3) \phi_1(4) \phi_{-1}(5) \phi_{-1}(6) {}^1\chi \\ {}^k\psi_1 &= (6!)^{-1/2} \sum_P \delta_P P \phi_0(1) \phi_0(2) \phi_1(3) \phi_1(4) \phi_{-1}(5) \phi_2(6) {}^k\chi \\ {}^k\psi_2 &= (6!)^{-1/2} \sum_P \delta_P P \phi_0(1) \phi_0(2) \phi_{-1}(3) \phi_{-1}(4) \phi_1(5) \phi_{-2}(6) {}^k\chi \\ {}^k\psi_3 &= (6!)^{-1/2} \sum_P \delta_P P \phi_0(1) \phi_0(2) \phi_1(3) \phi_1(4) \phi_{-1}(5) \phi_{-2}(6) {}^k\chi \\ {}^k\psi_4 &= (6!)^{-1/2} \sum_P \delta_P P \phi_0(1) \phi_0(2) \phi_{-1}(3) \phi_{-1}(4) \phi_1(5) \phi_2(6) {}^k\chi. \end{aligned} \right\} \quad (3)$$

From symmetry considerations it may be derived that the wave functions corresponding to the molecular energy levels are (cf. [5])

$$\left. \begin{array}{ll} {}^1A_{1g} & \psi({}^1A_{1g}) = \psi_0 \\ {}^k B_{1u} & \psi({}^k B_{1u}) = 2^{-1/2}({}^k \psi_1 + {}^k \psi_2) \\ {}^k B_{2u} & \psi({}^k B_{2u}) = 2^{-1/2}({}^k \psi_1 - {}^k \psi_2) \\ {}^k E_{1u} & \begin{cases} \psi_1({}^k E_{1u}) = {}^k \psi_3 \\ \psi_2({}^k E_{1u}) = {}^k \psi_4 \end{cases} \end{array} \right\} \quad (4)$$

where use has been made of the notation of Mulliken and Placzek [22].

The singlet levels have all been identified with the energy levels obtained from the absorption spectrum, but there is still some doubt with regard to the symmetry properties of the phosphorescent state (cf. [1, 5, 25, 26]). If the phosphorescent state is assumed to be a triplet it may have either B_{1u} or B_{2u} symmetry, so that for a calculation of the probability to the ground state both possibilities will have to be considered.

The spectral transitions of a molecule are determined by the positions of the energy levels on which the frequency of the emitted or absorbed light depends and the probability of the transition which is closely connected to the intensity. The probability of a spectral emission transition may be represented by

$$W_{m,n} = C \nu_{m,n}^3 \left| \sum_i \langle \psi_m | e_i \mathbf{r}_i | \psi_n \rangle \right|^2; \quad (5)$$

$\nu_{m,n}$ is the frequency of the light emitted and ψ_m and ψ_n the wave functions of the two states. The integration has to be performed over space and spin coordinates. From this formula it can be concluded that the probability of a triplet-singlet transition is zero to a first approximation, since the triplet and singlet spin functions are orthogonal. It is possible to obtain a finite transition probability, however, by correcting the wave functions by means of perturbation theory for the spin-orbital interaction, i.e. by investigating to what extent singlet functions are added to triplet functions and conversely in consequence of the spin perturbation. The addition of a small fraction of a singlet to a triplet function will give a finite probability for the transition from the triplet state to the ground state.

The mixing of the triplet and singlet functions will be determined by the spin-orbit energy if the spin-spin interaction, which is much smaller, is not taken into account. Then the perturbation energy operator may be represented by [11]

$$H^{(1)} = \sum_i (\mathbf{A}_i \mathbf{S}_i), \quad (6)$$

where

$$\mathbf{A}_i = \frac{e}{mc} \left\{ \mathbf{H}_i + \frac{1}{2mc} [\mathbf{F}_i \mathbf{p}_i] \right\} + \frac{e^2}{m^2 c^2} \sum_j \frac{[\mathbf{p}_j - \frac{1}{2} \mathbf{p}_i, \mathbf{r}_{ij}]}{r_{ij}^3}. \quad (7)$$

\mathbf{H}_i and \mathbf{F}_i are here the magnetic and electric field of the molecular skeleton at the position of the electron i respectively. In the last term the part containing the p_j represents the magnetic field due to the electrons other than i , whereas the part containing p_i is due to the electron i moving in the electric field of the other electrons, thus being the counterpart of the second term. In our case \mathbf{H}_i is equal to zero, so that $H^{(1)}$ is homogeneous and of the first degree in the momenta and is composed of terms each of which depends on the space coordinates of two electrons at the most.

For a calculation of the probabilities of triplet-singlet transition the perturbation of a triplet function caused by the operator $H^{(1)}$ will be investigated. If the

solutions of the unperturbed problem $H^{(0)}\psi^{(0)} = E^{(0)}\psi^{(0)}$ are denoted by a superscript 0, then

$$^3\psi_j = ^3\psi_j^{(0)} + ^3\psi_j^{(1)}. \quad (8)$$

The last term of (8) is given by

$$^3\psi_j^{(1)} = - \sum_k \frac{H_{kj}^{(1)}}{E_k^{(0)} - E_j^{(0)}} \psi_k^{(0)}, \quad (9)$$

$$H_{kj}^{(1)} = \langle ^1\psi_k^{(0)} | H^{(1)} | ^3\psi_j^{(0)} \rangle. \quad (10)$$

McClure [16] has shown that the matrix elements of $H^{(1)}$ will only have values different from zero for combinations of the states B_{1u} and B_{2u} .

By using the following property of the operator $H^{(1)}$ which is Hermitian and purely imaginary

$$\langle f | H^{(1)} | g \rangle = - \langle f^* | H^{(1)} | g^* \rangle, \quad (11)$$

it is found that

$$H^{(1)}(^1B_{1u}, ^3B_{2u}) = \langle ^1\psi_1 | H^{(1)} | ^3\psi_1 \rangle + \langle ^1\psi_1^* | H^{(1)} | ^3\psi_1 \rangle \quad (12)$$

$$H^{(1)}(^1B_{2u}, ^3B_{1u}) = \langle ^1\psi_1 | H^{(1)} | ^3\psi_1 \rangle - \langle ^1\psi_1^* | H^{(1)} | ^3\psi_1 \rangle. \quad (13)$$

3. THE SPIN-ORBIT PERTURBATION IN BENZENE EXPRESSED IN INTERATOMIC INTEGRALS

The probability of the triplet-singlet transition in benzene depends on the matrix elements $H^{(1)}(^1B_{1u}, ^3B_{2u})$ or $H^{(1)}(^1B_{2u}, ^3B_{1u})$. According to (12) and (13) their determination requires the calculation of the integrals

$$\left. \begin{aligned} \langle ^1\psi_1 | H^{(1)} | ^3\psi_1 \rangle &= \langle ^1\psi_1 | K_5 S_5^z + K_6 S_6^z + L(5, 6) + N(1, 2, 3, 4; 5, 6) | ^3\psi_1 \rangle \\ \langle ^1\psi_1^* | H^{(1)} | ^3\psi_1 \rangle &= \langle ^1\psi_1^* | K_5 S_5^z + K_6 S_6^z + L(5, 6) + N(1, 2, 3, 4; 5, 6) | ^3\psi_1 \rangle \end{aligned} \right\} \quad (14)$$

where

$$\left. \begin{aligned} K_i &= \frac{e}{2m^2c^2} [\mathbf{F}_i \mathbf{p}_i]_z, \\ L(5, 6) &= \frac{4\pi}{h} (\Lambda_{56} S_5^z + \Lambda_{65} S_6^z), \\ N(1, 2, 3, 4; 5, 6) &= \frac{4\pi}{h} \sum_{j=1}^4 (\Lambda_{5j} S_5^z + \Lambda_{6j} S_6^z + \Lambda_{j5} S_j^z + \Lambda_{j6} S_j^z) \end{aligned} \right\} \quad (15)$$

and

$$\Lambda_{12} = -\Omega_{12} - 2\Omega_{21}, \quad (16)$$

$$\Omega_{12} = \frac{e^2 h}{8\pi m^2 c^2} \frac{[\mathbf{r}_1 - \mathbf{r}_2, \mathbf{p}_1]_z}{r_{12}^3}. \quad (17)$$

In these formulae only the terms arising from $A_i^z S_i^z$ appear, because for all other terms the integrand will be antisymmetric in z and therefore will yield zero on integration. Corresponding to the three parts into which the operator $H^{(1)}$ has been split the integrals in (14) will be denoted by $\overline{K}_1, \overline{L}_1, \overline{N}_1$, and $\overline{K}_2, \overline{L}_2, \overline{N}_2$.

After integration over the spin variables and over those space coordinates that do not occur in the operator it is found that

$$\overline{K}_1 = \frac{\hbar}{4\pi} \{ \langle \phi_{-1} | K | \phi_{-1} \rangle - \langle \phi_2 | K | \phi_2 \rangle \} \quad (18)$$

$$\overline{L}_1 = \langle \phi_{-1}(1) \phi_2(2) | \Omega_{12} | \phi_{-1}(1) \phi_2(2) \rangle + \langle \phi_2(1) \phi_{-1}(2) | \Omega_{12} | \phi_{-1}(1) \phi_2(2) \rangle \\ - \langle \phi_{-1}(1) \phi_2(2) | \Omega_{12} | \phi_2(1) \phi_{-1}(2) \rangle - \langle \phi_2(1) \phi_{-1}(2) | \Omega_{12} | \phi_2(1) \phi_{-1}(2) \rangle \quad (19)$$

$$\overline{N}_1 = 2 \langle \phi_0(1) \phi_{-1}(2) | \Lambda_{21} | \phi_0(1) \phi_{-1}(2) \rangle - 2 \langle \phi_0(1) \phi_2(2) | \Lambda_{21} | \phi_0(1) \phi_2(2) \rangle \\ + 2 \langle \phi_1(1) \phi_{-1}(2) | \Lambda_{21} | \phi_1(1) \phi_{-1}(2) \rangle - 2 \langle \phi_1(1) \phi_2(2) | \Lambda_{21} | \phi_1(1) \phi_2(2) \rangle \\ - \langle \phi_{-1}(1) \phi_0(2) | \Lambda_{12} + \Lambda_{21} | \phi_0(1) \phi_{-1}(2) \rangle + \langle \phi_2(1) \phi_0(2) | \Lambda_{12} + \Lambda_{21} | \phi_0(1) \phi_2(2) \rangle \\ - \langle \phi_{-1}(1) \phi_1(2) | \Lambda_{12} + \Lambda_{21} | \phi_1(1) \phi_{-1}(2) \rangle + \langle \phi_2(1) \phi_1(2) | \Lambda_{12} + \Lambda_{21} | \phi_1(1) \phi_2(2) \rangle \quad (20)$$

$$\overline{K}_2 = 0 \\ \overline{L}_2 + \overline{N}_2 = 8 \langle \phi_{-2}(1) \phi_{-1}(2) | \Omega_{12} | \phi_1(1) \phi_2(2) \rangle + 4 \langle \phi_{-1}(1) \phi_{-2}(2) | \Omega_{12} | \phi_2(1) \phi_1(2) \rangle. \quad (21)$$

These results have been obtained in a similar manner to those for the case of four electrons, which has been discussed in Appendix A.

Substituting for ϕ_k the molecular orbital expression (1) one may now express \overline{K}_1 , \overline{L}_1 , \overline{N}_1 and $\overline{L}_2 + \overline{N}_2$ in interatomic integrals. By using the results of Appendix B, it is found that

$$\overline{K}_1 = - \frac{eh^2\sqrt{3}}{8\pi^2m^2c^2} \int a(1) \left(F_x \frac{\partial}{\partial y_1} - F_y \frac{\partial}{\partial x_1} \right) b(1) d\tau_1 \quad (22)$$

and

$$\overline{L}_1 = -4 \langle b, c | \Pi | a, c \rangle - 4 \langle b, d | \Pi | a, d \rangle, \quad (23)$$

$$\overline{N}_1 = 28 \langle c, a | \Pi | b, a \rangle + 28 \langle d, a | \Pi | c, a \rangle + 8 \langle b, c | \Pi | a, b \rangle \\ + 20 \langle b, d | \Pi | a, c \rangle + 4 \langle b, e | \Pi | a, d \rangle, \quad (24)$$

$$\overline{L}_2 + \overline{N}_2 = -8 \langle b, c | \Pi | a, b \rangle + 8 \langle b, d | \Pi | a, c \rangle - 4 \langle b, c | \Pi | a, d \rangle \quad (25)$$

where a, b, c, \dots denote the atomic p_z orbitals belonging to atom a, b, c, \dots and for example

$$\langle b, c | \Pi | a, b \rangle = \frac{e^2 h^2 q \sqrt{3}}{192 \pi^2 m^2 c^2 a_0^3} \frac{q^{10}}{1024 \pi^2} \\ \times \int \tau_1^2 \tau_2^2 \exp \left\{ - \frac{q}{2} (r_{1b} + r_{1a} + r_{2c} + r_{2b}) \right\} \left\{ \frac{x_1 - x_2}{r_{12}^3} \frac{y_1 - a_y}{r_{1a}} \right. \\ \left. - \frac{y_1 - y_2}{r_{12}^3} \frac{x_1 - a_x}{r_{1a}} \right\} d\tau_1 d\tau_2 \quad (26)$$

As before r_1 and r_2 are the coordinates of the electrons, r_{12} is the distance between them, r_{1a} and r_{1b} are the distances between electron 1 and the nuclei a and b respectively, r_{2b} and r_{2c} are the distances between electron 2 and the respective nuclei b or c and a denotes the coordinates of nucleus a . All lengths are expressed in terms of atomic units; q is the effective nuclear charge.

4. NUMERICAL CALCULATIONS AND RESULTS

From the result obtained in §3 it will appear that all integrals in \overline{L}_1 , \overline{N}_1 and $\overline{L}_2 + \overline{N}_2$ which have to be calculated may be written as

$$J = \langle f(1)g(2) | \Pi(1, 2) | f^1(1)g^1(2) \rangle, \quad (27)$$

where f and f^1 as well as g and g^1 are a set of two p_z functions belonging either to the same or two adjacent carbon nuclei. Although these integrals may be calculated

exactly it seemed sufficient for our purpose to use an appropriate approximation. Since the integrals represent interactions between charge clouds which are rather far apart a reasonable approximation of the integrals J is given by

$$J = \Pi(\bar{1}, \bar{2}) \langle f | f^1 \rangle \langle g | g^1 \rangle, \quad (28)$$

where $\bar{1}$ and $\bar{2}$ in the interaction operator Π denote the positions in which the two pairs of functions f, f^1 and g, g^1 overlap mostly.

With the aid of this approximation it is found that

$$\bar{L}_1 = -0.391 C \quad (29)$$

$$\bar{N}_1 = (2.737 + 2.100 S) C \quad (30)$$

$$\bar{L}_2 + \bar{N}_2 = -0.510 C \quad (31)$$

$$C = \frac{qe^2 h^2 S \sqrt{3}}{192 \pi^2 m^2 c^2 a_0^3}.$$

S , the overlap integral of p_z functions of two adjacent carbon nuclei is taken as 0.262. For q , the effective nuclear charge the value given by Zener [30], has been taken.

For a calculation of \bar{K}_1 some simplifying assumptions with respect to the electric field have to be made. If F is the electric field resulting from point charges e at the positions of the six carbon atoms, then

$$\bar{K}_1 = -2.342 C. \quad (32)$$

The question may arise as to whether or not a calculation where not only the six π -electrons but also the other valence electrons are explicitly considered will yield a very different result from what has been obtained. Then a similar calculation should be performed with antisymmetrized wave functions for 30 electrons. The only extra terms which will occur in the matrix element represent the energy of the two triplet electrons with respect to both the magnetic and electric field of the electrons forming the σ -bond. It may be shown that the energy with respect to the magnetic field is zero (cf. [6]). Therefore the formulae (22), (23), (24) and (25) also hold in this case if F represents the electric field of point charges $+4e$ at the carbon nuclei, of point charges e at the hydrogen nuclei and of the valence electrons forming the C-C and C-H bonds. With the aid of (28) \bar{K}_1 has been estimated in this case, it was found that

$$\bar{K}_1 = -2.143 C. \quad (33)$$

Although this result does not differ much from (32) it will yield a considerably different value for the spin-orbit coupling. Because (33) has been obtained according to the more correct procedure it will be used for our further considerations; the values resulting from the use of (32) will be given in parentheses in order to show to which extent rather small deviations in the electric field strength will affect our results.

By using the expressions (29), (30), (31), (32) and (33) and the values of S and q already given the matrix elements $H^{(1)}(^1B_{1u}, ^3B_{2u})$ and $H^{(1)}(^1B_{2u}, ^3B_{1u})$ may be calculated. It is found that $C = 7.073 \times 10^{-7}$ erg. This yields

$$\begin{aligned} H^{(1)}(^1B_{1u}, ^3B_{2u}) &= 4.60 \times 10^{-17} \text{ erg } (3.18 \times 10^{-17} \text{ erg}) \\ &= 2.87 \times 10^{-5} \text{ ev } (1.99 \times 10^{-5} \text{ ev}), \end{aligned}$$

$$\begin{aligned} H^{(1)}(^1B_{2u}, ^3B_{1u}) &= 6.50 \times 10^{-17} \text{ erg } (5.08 \times 10^{-17} \text{ erg}) \\ &= 4.05 \times 10^{-5} \text{ ev } (3.17 \times 10^{-5} \text{ ev}). \end{aligned}$$

With these values the probabilities of the transitions from the states $^3B_{2u}$ and $^3B_{1u}$ to the ground state can be calculated according to the formula (Mulliken [21])

$$f(^3B_{2u}, ^1A_{1g}) = \left\{ \frac{H^{(1)}(^1B_{1u}, ^3B_{2u})}{E(^1B_{1u}) - E(^3B_{2u})} \right\}^2 \frac{E(^3B_{2u}) - E(^1A_{1g})}{E(^1B_{1u}) - E(^1A_{1g})} f(^1B_{1u}, ^1A_{1g}), \quad (34)$$

in which f represents the oscillator strength of the corresponding absorption transition. The energy differences given by Roothaan and Mulliken [25] are $E(^1B_{1u}) - E(^3B_{2u}) = 2.4 \text{ eV}$ and $E(^3B_{2u}) - E(^1A_{1g}) = 3.8 \text{ eV}$, and according to Kleven and Platt [10] $f(^1B_{1u}, ^1A_{1g}) = 0.1$. After substituting these values in (34) it appears that

$$f(^3B_{2u}, ^1A_{1g}) = 8.8 \times 10^{-12} (4.2 \times 10^{-12}). \quad (35)$$

The decay time of this transition is connected with the oscillator strength in the following way (cf. [21])

$$\tau = \frac{mc}{8\pi e^2} \cdot \frac{1}{f(^3B_{2u}, ^1A_{1g})} \cdot \frac{1}{\{E(^3B_{2u}) - E(^1A_{1g})\}^2}. \quad (36)$$

This yields $\tau = 190$ seconds (400 seconds). The value of τ obtained experimentally is 7 seconds.

If it had been assumed that the triplet state had B_{1u} symmetry properties, the calculated decay time would have been greater by a factor of about five. From an equation analogous to (34) it may easily be found that

$$f(^3B_{1u}, ^1A_{1g}) = 2.1 \times 10^{-12} (1.3 \times 10^{-12}), \quad (37)$$

since $f(^1B_{2u}, ^1A_{1g}) = 0.002$ and $E(^3B_{2u}) - E(^3B_{1u}) = 1.1 \text{ eV}$. In this case the decay time = 800 sec (1300 sec).

It will be noticed that in our calculations molecular vibrations have not been taken into account. For many purposes the influence of vibrations on electronic transitions may in first approximation be neglected, but in our case this procedure may be unwarranted. In the first place it should be investigated whether the one-centre and two-centre integrals would obtain non-zero values when vibrations are considered. Moreover our procedure is somewhat inconsistent because the oscillator strengths of the $^1B_{1u} \rightarrow ^1A_{1g}$ and $^1B_{2u} \rightarrow ^1A_{1g}$ transitions would be zero if the coupling with vibrations had been neglected completely. It is our intention to investigate these problems more closely. For a preliminary discussion see [6].

5. SPIN-ORBIT PERTURBATION OF SINGLET AND TRIPLET STATES IN ALIPHATIC KETONES†

McClure [17] reported a phosphorescent transition of acetone at $26\,000 \text{ cm}^{-1}$, with a decay time of 0.6 milliseconds. For other aliphatic ketones similar transitions were found in the same spectral region and also having decay times of the order of milliseconds. It is reasonable therefore to attribute this phosphorescence to the C=O bond.

Our calculations are based on wave functions similar to those introduced by McMurtry [19]. It is assumed that three trigonally hybridized σ -functions are involved in the bonding of the carbon atom of the C=O group to the two neighbouring carbon atoms and the O atom (see figure 2). These functions, composed

† Recently similar calculations on formaldehyde were performed by the late Dr. Jerome W. Sidman, who obtained practically identical results. We are indebted to Dr. Sidman for having sent us these calculations before publishing them in the *J. chem. Phys.*

in the usual way of 2s and 2p Slater orbitals at the carbon atom denoted by s_c , and x_c, y_c, z_c , respectively, are

$$\left. \begin{aligned} t_1 &= 3^{-1/2} s_c - 6^{-1/2} x_c - 2^{-1/2} y_c \\ t_2 &= 3^{-1/2} s_c - 6^{-1/2} x_c + 2^{-1/2} y_c \\ t_3 &= 3^{-1/2} s_c + (3/2)^{-1/2} x_c \end{aligned} \right\} \quad (38)$$

Similarly the hybridized σ -functions of the oxygen atom are

$$\left. \begin{aligned} u_1 &= y_0 \\ u_2 &= c s_0 + (1 - c^2)^{1/2} x_0 \\ u_3 &= (1 - c^2)^{1/2} s_0 - c x_0 \end{aligned} \right\} \quad (39)$$

where s_0, x_0 and y_0 now denote Slater functions at the oxygen atom. The C-O σ -bond may then be represented by $(t_3 u_3)^2$, where

$$(t_3 u_3) \sim (t_3 + u_3) \quad (40)$$

and the C-O π -bond by $(z_c z_0)^2$ if

$$(z_c z_0) \sim (z_c + z_0). \quad (41)$$

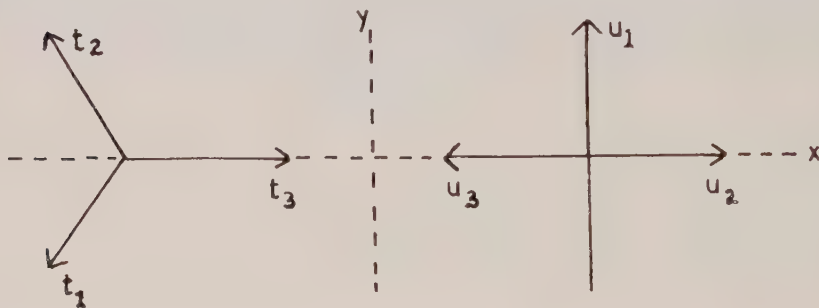


Figure 2.

Indicating only that part of the wave function of interest for the present discussion we may write the ground state as

$$G \dots (t_3 u_3)^2 (z_c z_0)^2 u_2^2 u_1^2. \quad (42)$$

The functions t_1 and t_2 participate in the σ -bonds with neighbouring carbon atoms.

According to McMurtry the lowest excited states of the molecule are obtained by assuming one of the lone pair electrons of the oxygen atom to pass from the u_1 orbital into an antibonding $(t_3 u_3)$ or $(z_c z_0)$ orbital

$$\overline{(t_3 u_3)} \sim (t_3 - u_3), \quad \overline{(z_c z_0)} \sim (z_c - z_0). \quad (43)$$

In this way the following states arise

$$^3, ^1A \dots (t_3 u_3)^2 (z_c z_0)^2 u_2^2 u_1 \overline{(t_3 u_3)} \quad (44)$$

$$^3, ^1B \dots (t_3 u_3)^2 (z_c z_0)^2 u_2^2 u_1 \overline{(z_c z_0)}. \quad (45)$$

The $^1G \rightarrow ^1B$ transition, which in this approximation is forbidden, is identified with the long wavelength absorption at $34\,000\text{ cm}^{-1}$ with oscillator strength $f=0.0004$, whereas the absorption at $51\,000\text{ cm}^{-1}$ and $f=0.032$ is ascribed to the $^1G \rightarrow ^1A$ transition on account of the theoretically calculated f value.

McClure [17] observed that methyl substitution at the α -carbon atom gives rise to variation of the f -value of the absorption at $51\,000\text{ cm}^{-1}$ similar to the variation of the phosphorescence. From this he concluded that the 1A -state is the principal perturbing singlet state responsible for the finite triplet-singlet transition probability.

If we assume that the phosphorescent level is 3B the mixing with 1A depends on the matrix element

$$M = \langle ^1A | H^{(1)} | ^3B \rangle, \quad (46)$$

where $H^{(1)}$ is given by (6). Indicating the electric field of the molecule in the ground state, when the oxygen atom has been depleted of one lone pair electron in the orbital u_1 , by F , the matrix element can be written as

$$M = -\frac{eh}{8\pi m^2 c^2} \langle (\overline{z_c z_0}) | F_y p_z | (t_3 u_3) \rangle \quad (47)$$

plus terms accounting for the detailed spin-orbit interaction of the electrons, which presumably are of minor importance. Equation (47) may be approximated by

$$M = -\frac{eh}{16\pi m^2 c^2} [\langle z_c | F_y p_z | t_3 \rangle + \langle z_0 | F_y p_z | u_3 \rangle]. \quad (48)$$

6. NUMERICAL CALCULATIONS AND RESULTS

For a calculation of (48) use will be made of atomic Slater functions

$$\left. \begin{aligned} z_c &= (q_c^5/32\pi)^{1/2} \exp(-\tfrac{1}{2}q_c r_c), \\ z_0 &= (q_0^5/32\pi)^{1/2} \exp(-\tfrac{1}{2}q_0 r_0), \end{aligned} \right\} \quad (49)$$

and similar expressions for the other atomic wave functions, where the origin is taken at the nucleus of the atom. The constants $q_c = 3.18$ and $q_0 = 4.55$ have been introduced by Zener [30] and Slater [27] to adapt these functions to energy calculations.

To calculate (48) it will be assumed that F is the electric field of a point charge $q'_c e$ in the first integral and the electric field of a point charge $q'_0 e$ in the second integral. The constants q'_c and q'_0 will be determined from the values of the potential energy of a π -electron with respect to a carbon nucleus surrounded by four valence electrons and with respect to an oxygen nucleus surrounded by five valence electrons. It will be supposed that these energies are equal to $q'_c q_c e^2/4a_0$ and $q'_0 q_0 e^2/4a_0$, respectively. It will thus be assumed that the electric field F which will be used for a calculation of M is equal to the electric field from which the potential energies may be evaluated. The constants q'_c and q'_0 are found to be $q'_c = 1.01$ and $q'_0 = 3.19$. Then M may be derived from

$$M = \frac{ie^2 h^2 \sqrt{2}}{1024 \pi^3 a_0^3 m^2 c^2 \sqrt{3}} \left[q'_c q_c^5 \int \frac{z_c^2 \exp(-q_c r_c)}{r_c^3} d\tau - q'_0 q_0^5 \int \frac{z_0^2 \exp(-q_0 r_0)}{r_0^3} d\tau \right], \quad (50)$$

which yields

$$|M| = \frac{e^2 h^2 (q'_0 q_0^3 - q'_c q_c^3) \sqrt{2}}{768 \pi^2 m^2 c^2 a_0^3 \sqrt{3}}. \quad (51)$$

After substituting the values for the constants it is found that $M = 132\text{ cm}^{-1}$. The oscillator strength of the transition from the 3B state to the ground state is then given by:

$$f(^3B, G) = \frac{|M|^2}{[E(^1A) - E(^3B)]^2} \cdot \frac{E(^3B) - E(G)}{E(^1A) - E(G)} f(^1A, G). \quad (52)$$

This yields $f(^3B, G) = 2.85 \times 10^{-7}$. According to (36) $\tau = 7.8$ milliseconds, while the experimental value is 0.6 millisecond. The calculated decay time would have been shortened if the addition of the 3A state to the ground state had also been taken into account. Since this contribution was difficult to estimate and is probably much smaller than the one calculated it has not been further investigated.

7. DISCUSSION AND GENERAL REMARKS

The results obtained for benzene (and other aromatic hydrocarbons) and for ketones are in themselves no convincing support for the idea of the phosphorescence being a triplet-singlet transition. On the other hand the discrepancies between the theory and experiment can be amply accounted for by the approximations in the models as well as in the calculations. In the case of benzene, for instance, one value for the decay time was 400 seconds, but a more detailed consideration of the electric field reduced this value to 190 seconds. On the other hand an experimental value is 7 seconds, but a corrected value of 35 seconds has also been reported [4]. These figures show that a discrepancy between calculated and experimental decay times is no argument against the assumption that phosphorescence corresponds to a triplet-singlet emission.

An important feature of the results is that the ratios of the decay times of the phosphorescence of aromatic hydrocarbons and of ketones which has the order of magnitude of 10^4 agrees with the results of our calculations. If the triplet properties of the phosphorescent state were established unambiguously, it might conversely be concluded that the detailed correlations between electronic motions do not effect the spin-orbit energy substantially.

The observed photomagnetism of the phosphorescent molecule [2] is doubtless a strong argument in favour of the triplet-singlet model. On the other hand there remain a number of difficult aspects which require an explanation before the triplet-singlet suggestion can be fully accepted. The fact that no paramagnetic absorption of the molecule in its phosphorescent state has ever been measured in spite of several attempts may be due to a broadening of the resonance line but a quantitative explanation is still lacking. The very high efficiency of the transition from an excited singlet to the phosphorescent triplet state is also difficult to understand [23]. It is still uncertain whether the theoretically expected and experimentally observed symmetry properties of the phosphorescent triplet state agree, cf. [26, 1, 5, 25]. It is very probable that a study of the influence of the coupling between electronic and vibrational motions will contribute to the solution of these problems. At the end of section 4 the effect of vibrations has been touched upon but we hope to give the results of a further study in a later paper.

Note added in proof.—We have learned that Hutchison (private communication) recently succeeded in observing electron spin resonance of the phosphorescent state of naphthalene, and thus showed that it is a triplet state.

APPENDIX A

As an illustration of the reduction of the matrix element of the spin-orbit interaction operator with respect to a triplet and a singlet state, a system of four electrons will be considered. The orbital part of the wave functions of state A is

$$u_A = a_1 a_2 b_3 c_4.$$

If it is a singlet state u_A has to be combined with the spin function

$$^1\chi = \frac{1}{2}(\alpha_1\beta_2 - \beta_1\alpha_2)(\alpha_3\beta_4 - \beta_3\alpha_4) \quad (53)$$

and in case of a triplet state with a linear combination of the spin functions

$$\left. \begin{aligned} ^3\chi_x &= \frac{1}{2}(\alpha_1\beta_2 - \beta_1\alpha_2)(\beta_1\beta_2 - \alpha_1\alpha_2) \\ ^3\chi_y &= \frac{1}{2}i(\alpha_1\beta_2 - \beta_1\alpha_2)(\beta_1\beta_2 + \alpha_1\alpha_2) \\ ^3\chi_z &= \frac{1}{2}(\alpha_1\beta_2 - \beta_1\alpha_2)(\alpha_1\beta_2 + \beta_1\alpha_2). \end{aligned} \right\} \quad (54)$$

The complete wave function is then

$$^kA \dots (4!)^{-1/2} \sum_p \delta_p P a_1 a_2 b_3 c_4 {}^k\chi. \quad (55)$$

The spin-orbit operator can be written as

$$H^{(1)} = \sum_i \sum_{\alpha=x,y,z} (L_i^\alpha + \sum_j \Lambda_{ij}^\alpha) S_i^\alpha, \quad (56)$$

where L_i depends on the coordinates of electron i and Λ_{ij} depends on the coordinates of the electrons i and j . The matrix element then becomes

$$\langle {}^1A | H^{(1)} | {}^3A \rangle = \sum_{(ij)} \sum_p \delta_p \langle P a_1 a_2 b_3 c_4 | L_i + \Lambda_{ij} | a_1 a_2 b_3 c_4 \rangle \langle P {}^1\chi | S_i | {}^3\chi \rangle. \quad (57)$$

The x , y or z components are not explicitly indicated as no mixing of these components occurs and the results for the different components are completely similar. With regard to the operators L_i only the permutation (1 2 3 4) needs to be considered whereas with the operators Λ_{ij} it is sufficient to take into account (1 2 3 4), (1 2 4 3), (1 4 3 2), (4 2 3 1), (1 3 2 4), (3 2 1 4). The corresponding integrals over the spin variables can easily be evaluated by an extension of, for example, Pauling's island method. The result is

$$\begin{aligned} \langle {}^1A | H^{(1)} | {}^3A \rangle &= \langle b | L | b \rangle - \langle c | L | c \rangle \\ &+ \langle b_1 c_2 | \Lambda_{12} - \Lambda_{21} | b_1 c_2 \rangle + \langle c_1 b_2 | \Lambda_{12} - \Lambda_{21} | b_1 c_2 \rangle \\ &+ 2 \langle a_1 b_2 | \Lambda_{21} | a_1 b_2 \rangle - 2 \langle a_1 c_2 | \Lambda_{21} | a_1 c_2 \rangle \\ &+ \langle c_1 a_2 | \Lambda_{12} + \Lambda_{21} | a_1 c_2 \rangle - \langle b_1 a_2 | \Lambda_{12} + \Lambda_{21} | a_1 b_2 \rangle. \end{aligned} \quad (58)$$

In a similar way one finds with $u_B = a_1 a_2 b_3 d_4$

$$\begin{aligned} \langle {}^1A | H^{(1)} | {}^3B \rangle &= - \langle c | L | d \rangle + \langle b_1 c_2 | \Lambda_{12} - \Lambda_{21} | b_1 d_2 \rangle + \langle c_1 b_2 | \Lambda_{12} - \Lambda_{21} | b_1 d_2 \rangle \\ &- 2 \langle a_1 c_2 | \Lambda_{21} | a_1 d_2 \rangle + \langle c_1 a_2 | \Lambda_{12} + \Lambda_{21} | a_1 d_2 \rangle, \end{aligned} \quad (59)$$

whereas

$$\langle {}^3A | H^{(1)} | {}^1B \rangle = \langle {}^1A | H^{(1)} | {}^3B \rangle - 2 \langle c_1 b_2 | \Lambda_{12} - \Lambda_{21} | b_1 d_2 \rangle. \quad (60)$$

APPENDIX B

Integrals of the type

$$J = \int \phi_j^*(1) \phi_k^*(2) \Omega_{12} \phi_l(1) \phi_m(2) d\tau_1 d\tau_2 = \langle j, k | \Omega | l, m \rangle$$

can be reduced when use is made of the symmetry properties of the ϕ_k and of the Hermitian character and the symmetry of Ω .

$$\Omega_{12} = \frac{e^2 \hbar}{8\pi m^2 c^2} \frac{[\mathbf{r}_1 - \mathbf{r}_2, \mathbf{p}_1]_z}{r_{12}^3} \quad \text{and} \quad \phi_k = \sigma^{-1/2} \sum_{n=0}^5 \lambda^{-kn} a_n, \quad (61)$$

where $\lambda = \exp(2\pi i/\sigma)$ and a_n is the p_z -function belonging to atom n . If D is a rotation about the sixfold axis over $2\pi/\sigma$ and S a reflection with respect to the plane

through the atoms 0 and 3 and the sixfold axis

$$\begin{aligned} D\phi_k &= \lambda^k \phi_k & D\Omega &= \Omega \\ S\phi_k &= \phi_{-k} = \phi_k^* & S\Omega &= -\Omega = \Omega^*. \end{aligned} \quad (62)$$

Moreover Ω_{12} is Hermitian and purely imaginary with respect to 1 and symmetric with respect to 2. Therefore eight equivalent expressions can be written for J :

$$\begin{aligned} \langle j, k | \Omega | l, m \rangle &= \langle j, -m | \Omega | l, -k \rangle = -\langle -l, k | \Omega | -j, m \rangle \\ &= -\langle -l, -m | \Omega | -j, -k \rangle = -\langle -j, -k | \Omega | -l, -m \rangle \\ &= -\langle -j, m | \Omega | -l, k \rangle = \langle l, -k | \Omega | j, -m \rangle = \langle l, m | \Omega | j, k \rangle. \end{aligned} \quad (63)$$

As the integrand has to be invariant under rotation $j+k-l-m=0, \pm 6, \dots$ substitution of the formula for ϕ into J leads to

$$\begin{aligned} \langle j, k | \Omega | l, m \rangle &= \frac{1}{36} \sum_{r,s,t,u} \lambda^{jr+ks-lt-mu} \langle a_r a_s | \Omega | a_t a_u \rangle \\ &= \frac{1}{6} \sum_{\rho, \sigma, \tau} \lambda^{j\rho+k\sigma-l\tau} \langle a_\rho a_\sigma | \Omega | a_\tau a_0 \rangle, \end{aligned} \quad (64)$$

where the substitutions $r=\rho+u$, $s=\sigma+u$, $t=\tau+u$ are used. J can be written as $\frac{1}{8} \times$ the sum of the eight expressions (63) which gives the result

$$\begin{aligned} J &= \frac{1}{8} i \sum_{\rho, \sigma, \tau} \sin \frac{1}{6} \pi (j+l)(\rho-\tau) \cos \frac{1}{6} \pi (k+m) \sigma \cos \frac{1}{6} \pi (j-l)(\rho+\sigma-\tau) \\ &\quad \times \langle a_\rho a_\sigma | \Omega | a_\tau a_0 \rangle. \end{aligned} \quad (65)$$

For the integrals $\langle a_\rho a_\sigma | \Omega | a_\tau a_0 \rangle = \langle \rho, \sigma | \tau, 0 \rangle$ the following relations hold:

$$\begin{aligned} \langle \rho, \sigma | \tau, 0 \rangle &= \langle \rho-\sigma, -\sigma | \tau-\sigma, 0 \rangle = \langle -\tau, -\sigma | -\rho, 0 \rangle = \langle \sigma-\tau, \sigma | \sigma-\rho, 0 \rangle \\ &= -\langle \tau, \sigma | \rho, 0 \rangle = -\langle \tau-\sigma, -\sigma | \rho-\sigma, 0 \rangle = -\langle -\rho, -\sigma | -\tau, 0 \rangle \\ &= -\langle \sigma-\rho, \sigma | \sigma-\tau, 0 \rangle. \end{aligned} \quad (66)$$

All of these integrals occur in the expression for J with the same coefficient. These coefficients are zero for $\rho=\tau$. If overlap of p_z -functions belonging to non-adjacent carbon atoms is neglected it is only necessary to consider $\sigma=0$, $\sigma=\pm 1$, $\rho=\tau\pm 1$. Integrals with $\tau=0$ are zero since the integrand is antisymmetric with respect to a plane through two adjacent carbon atoms and perpendicular to the plane of the benzene ring. Inspection of the coefficients of the remaining integrals leads to the formula

$$\begin{aligned} \langle \phi_j \phi_k | \Omega | \phi_l \phi_m \rangle &= \frac{2}{3} i \sin \frac{1}{8} \pi (j+l) \{ \cos \frac{1}{2} \pi (j-l) \langle 2, 0 | 1, 0 \rangle \\ &\quad + \cos \frac{1}{6} \pi (j-l) \cos \pi (j-l) \langle 3, 0 | 2, 0 \rangle \\ &\quad + 2 \cos \frac{1}{6} \pi (k+m) \cos \frac{1}{3} \pi (j-l) \langle 2, 1 | 1, 0 \rangle \\ &\quad + 2 \cos \frac{1}{6} \pi (k+m) \cos \frac{2}{3} \pi (j-l) \langle 3, 1 | 2, 0 \rangle \\ &\quad + \cos \frac{1}{6} \pi (k+m) \cos \pi (j-l) \langle 4, 1 | 3, 0 \rangle \}. \end{aligned} \quad (67)$$

On a fait des calculs des probabilités de transitions triplet-singlet dans le benzène et l'acétone en rapport avec la constante de décroissance de la phosphorescence. La probabilité de transition a été déterminée à partir du degré auquel les états singlet excités sont mélangés aux états triplet. En supposant que dans le benzène l'état phosphorescent ait des propriétés ${}^3B_{2u}$ —de telle sorte que l'état singlet ${}^1B_{1u}$ y est mélangé—on obtient le meilleur accord avec les données expérimentales. Dans le cas d'acétone la phosphorescence a été considérée comme une transition triplet-singlet ne se rapportant qu'aux électrons du groupe CO.

La correspondance entre la théorie et l'expérience est égale à celle obtenue dans d'autres calculs de probabilités de transitions. Les valeurs de la constante de décroissance trouvées sont de 190 et 7 secondes pour le benzène et de 7,8 et 0,6 millisecondes pour l'acétone. Le rapport des constantes de décroissance calculées est en bon accord avec le résultat expérimental ($2,4 \times 10^4$ et $1,2 \times 10^4$).

Die Wahrscheinlichkeiten für Triplett-Singulett-Uebergänge in Benzol und Azeton wurden zusammen mit den Abklingzeiten der Phosphoreszenz berechnet. Die Uebergangswahrscheinlichkeit wurde aus dem Ausmass bestimmt, in dem die angeregten Zustände mit dem Triplettzustand gemischt sind.

Die Annahme, dass der phosphoreszierende Zustand in Benzol $^3B_{2u}$ -Eigenschaften besitze—so dass der $^1B_{1u}$ -Singulettzustand damit gemischt ist—führt zur besten Uebereinstimmung mit den experimentellen Daten. Im Falle des Azetons wurde die Phosphoreszenz als ein Triplett-Singulett-Uebergang aufgefasst, an dem sich nur die Elektronen der CO-Gruppe beteiligen. Die Uebereinstimmung zwischen Theorie und Experiment ist ebenso befriedigend wie in anderen Berechnungen der Uebergangswahrscheinlichkeiten. Man findet nämlich Abklingzeiten von 190 bzw. 7 sec für Benzol und 7,8 bzw. 0,6 millisee für Azeton. Das Verhältnis der berechneten Abklingzeiten ist mit dem Versuchswert in guter Uebereinstimmung ($2,4 \times 10^4$ und $1,2 \times 10^4$).

REFERENCES

- [1] CRAIG, D. P., 1950, *J. chem. Phys.*, **18**, 236.
- [2] EVANS, D. F., 1955, *Nature, Lond.*, **176**, 777.
- [3] FÖRSTER, TH., 1949, *Naturwissenschaften*, **36**, 240.
- [4] GILMORE, E. H., GIBSON, G. E., and McCLURE, D. S., 1952, *J. chem. Phys.*, **20**, 829.
- [5] GOEPPERT-MAYER, M., and SKLAR, A. L., 1938, *J. chem. Phys.*, **6**, 645.
- [6] HAMEKA, H. F., 1956, *Thesis*, Leiden.
- [7] HÜCKEL, E., 1931, *Z. Phys.*, **70**, 204.
- [8] JABLONSKI, A., 1933, *Nature, Lond.*, **131**, 839.
- [9] JABLONSKI, A., 1935, *Z. Phys.*, **94**, 38.
- [10] KLEVEN, H. B., and PLATT, J. R., 1949, *J. chem. Phys.*, **17**, 470.
- [11] KRAMERS, H. A., 1933, *Die Grundlagen der Quantummechanik*.
- [12] LEWIS, G. N., and KASHA, M. J., 1944, *J. Amer. chem. Soc.*, **66**, 2100.
- [13] LEWIS, G. N., and KASHA, M. J., 1945, *J. Amer. chem. Soc.*, **67**, 994.
- [14] LEWIS, G. N., and CALVIN, M., 1945, *J. Amer. chem. Soc.*, **67**, 1232.
- [15] LEWIS, G. N., CALVIN, M., and KASHA, M. J., 1949, *J. chem. Phys.*, **17**, 804.
- [16] McCLURE, D. S., 1949, *J. chem. Phys.*, **17**, 665.
- [17] McCLURE, D. S., 1949, *J. chem. Phys.*, **17**, 905.
- [18] McCLURE, D. S., 1952, *J. chem. Phys.*, **20**, 682.
- [19] McMURRY, H. L., 1941, *J. chem. Phys.*, **9**, 231.
- [20] MIZUSHIMA, M., and KOIDE, S., 1952, *J. chem. Phys.*, **20**, 765.
- [21] MULLIKEN, R. S., 1939, *J. chem. Phys.*, **7**, 14.
- [22] MULLIKEN, R. S., and PLACZEK, B., 1933, *Phys. Rev.*, **43**, 279.
- [23] PORTER, G., and WINDSOR, W., 1954, *Disc. Faraday Soc.*, **17**, 178.
- [24] PORTER, G., 1954, *Disc. Faraday Soc.*, **17**, 228, 229.
- [25] ROTHMAN, C. C. J., and MULLIKEN, R. S., 1948, *J. chem. Phys.*, **16**, 118.
- [26] SHULL, H., 1949, *J. chem. Phys.*, **17**, 295.
- [27] SLATER, J. C., 1930, *Phys. Rev.*, **36**, 57.
- [28] WEISSMAN, S. I., and LIPKIN, D., 1942, *J. Amer. chem. Phys.*, **64**, 1916.
- [29] WIEDEMANN, E., 1888, *Ann. Phys.*, **34**, 446.
- [30] ZENER, C., 1930, *Phys. Rev.*, **36**, 51.
- [31] PRINGSHEIM, P., 1949, *Fluorescence and Phosphorescence* (London).

Theory of the Renner effect in the NH_2 radical

by J. A. POPLE and H. C. LONGUET-HIGGINS

Department of Theoretical Chemistry, Cambridge University

(Received 31 July 1958)

The observations of Dressler and Ramsay on the vibronic absorption spectrum of the NH_2 radical are interpreted quantitatively in terms of the Renner effect. The use of a perturbation method leads to frequency predictions which are in good accord with experiment and confirm the view of these authors that the absorption band is associated with transitions between the components of an electronic Π state which are widely separated by electronic-vibrational interaction.

1. INTRODUCTION

Dressler and Ramsay [1] have recently investigated the lowest electronic transition of the NH_2 radical and its deuterated isotope in absorption, and find that the spectra have an unusual type of vibrational structure. Their measurements strongly suggest that the radical is linear in the upper state, but that in this state the vibronic energy depends markedly on the total angular momentum about the molecular axis. They have interpreted this as a case of the 'Renner effect', that is, a strong coupling between the electronic and vibrational motions leading to a breakdown of a Born-Oppenheimer (fixed-nucleus) approximation. Renner [2] showed that an electronic Π state of a linear molecule splits into two real components when the molecule is bent; one of these is symmetric and the other antisymmetric about the plane of the deformed molecule. The electronic energies of the two states (evaluated in fixed nuclear configurations) diverge from one another as the angle of bending increases, and may behave in any one of the three ways illustrated in figure 1 where the abscissa denotes the extent of deformation. Renner considered only the case depicted in figure 1 (a), where

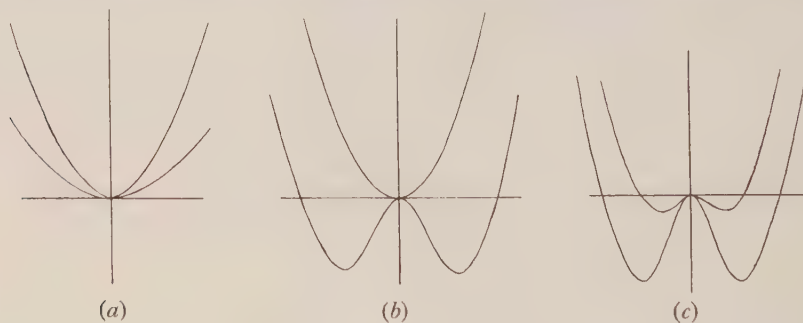


Figure 1.

both curves are parabolas of positive curvature; it is quite possible, however, for either or both curves to have negative curvature at the origin as indicated in figures 1 (b) and 1 (c).

The theoretical work of Walsh [5] and the experiments of Dressler and Ramsay, taken together, strongly suggest that the NH_2 radical is a case of the

type 1 (*b*). Walsh pointed out that according to molecular orbital theory the ground state of NH_2 should differ from that of OH_2 , which is bent, only in the absence of one of the $2p\pi$ electrons of the central atom, but that this would not affect the valency angle very much. As to the first excited state of NH_2 , Walsh's prediction was less definite, but the alternation of symmetry type for successive bands in the progression indicates, as Dressler and Ramsay point out, a change from a bent to a linear structure. In the absence of a theory of the Renner effect for case 1 (*b*), however, this argument is suggestive rather than conclusive, so we have undertaken a theoretical investigation of the type of spectrum to be expected in this case. We have found indeed that an effect of the type postulated by Dressler and Ramsay accounts very adequately for certain observed features of the NH_2 absorption spectrum.

2. THEORETICAL MODEL

We shall adopt a simplified theoretical model in order to set up the mathematical equations for the relevant vibronic levels. As will appear, this model incorporates the essential features of the situation in, for example, the NH_2 radical; that is to say, the resulting equations of motion are mathematically equivalent to those obtained by Renner from more sophisticated premisses.

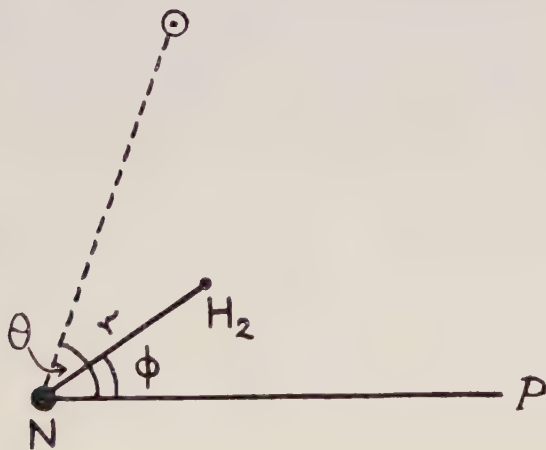


Figure 2.

We restrict consideration to three degrees of freedom of the radical. The first two of these are the two components of the doubly degenerate bending mode, with which may be associated two coordinates: the amplitude r of the distortion and the angle ϕ between the plane of bending and a fixed plane P through the axis of the unbent radical. The other degree of freedom may be described as the angular distance of the odd electron round the molecular axis, as measured from the plane P . This angle, to be denoted as θ , is more properly regarded as the coordinate conjugate to the axial angular momentum of all the electrons, but the simpler interpretation is physically more illuminating. Our notation is illustrated in figure 2. The coordinate r is positive or zero; ϕ and θ lie in the range 0 to 2π .

Our procedure is now as follows: first to determine the nature of the vibronic states when there is no coupling between θ and ϕ ; secondly, to discover how

these states are modified when such a coupling is introduced into the Hamiltonian; and thirdly, to see how far, in the case of NH_2 , it is possible to calculate the actual energies of the vibronic levels without introducing unknown parameters into the calculation.

In the absence of any coupling between θ and ϕ , each vibronic wave function may be separated into an electronic and a vibrational factor. The electronic factor is $\exp(i\Lambda\theta)$ where $\Lambda = \pm 1$ for an electronic Π state. The vibrational factor is determined by a potential which depends on r only and therefore takes the form

$$|n, l\rangle = \rho_{n|l|}(r) \exp(il\phi), \quad (2.1)$$

where l is the vibrational angular momentum quantum number. The quantum number n (often denoted by $v_2 + 1$) is assigned the values

$$n = |l| + 1, \quad |l| + 3, \dots \quad (2.2)$$

If the vibrational potential is harmonic, the wave functions (2.1) reduce to the well known form for the two-dimensional harmonic oscillator.

The vibronic wave functions can now be written

$$|\Lambda, n, l\rangle = \exp(i\Lambda\theta) \rho_{n|l|}(r) \exp(il\phi), \quad (2.3)$$

it being implied that they are eigenfunctions of both the electronic and the vibrational angular momentum about the molecular axis. Figure 3 shows the resulting scheme of energy levels when the bending vibration is harmonic; the energy is then proportional to n and independent of l and Λ . At the bottom of the figure are printed the symbols conventionally used for classifying the vibronic states according to the value of $|K|$, where $K = \Lambda + l$ and is proportional to the total angular momentum in the direction of the axis.

		$ 1, 4, -3\rangle$		$ 1, 4, -1\rangle$		$ 1, 4, 1\rangle$		$ 1, 4, 3\rangle$
$ -1, 4, -3\rangle$		$ -1, 4, -1\rangle$		$ 1, 4, 1\rangle$		$ -1, 4, 3\rangle$		
			$ 1, 3, -2\rangle$		$ 1, 3, 0\rangle$		$ 1, 3, 2\rangle$	
	$ -1, 3, -2\rangle$		$ -1, 3, 0\rangle$		$ -1, 3, 2\rangle$			
				$ 1, 2, -1\rangle$		$ 1, 2, 1\rangle$		
		$ -1, 2, -1\rangle$		$ -1, 2, 1\rangle$				
					$ 1, 1, 0\rangle$			
			$ -1, 1, 0\rangle$					
Γ ($K=4$)	Φ ($K=3$)	Δ ($K=2$)	Π ($K=1$)	Σ ($K=0$)	Π ($K=1$)	Δ ($K=2$)	Φ ($K=3$)	Γ ($K=4$)

Figure 3.

We now have to consider how this scheme will be modified by introducing into the Hamiltonian additional terms H' representing an angular coupling between the odd electron and the nuclear framework. In the first place we note that such coupling terms can only depend on the *relative* angle $\alpha = \theta - \phi$

and the amplitude r . Secondly, H' must be a symmetrical function of α and consequently can be expanded in the form

$$H' = V_0(r) + V_1(r)[\exp(i\alpha) + \exp(-i\alpha)] + V_2(r)[\exp(2i\alpha) + \exp(-2i\alpha)] + \dots, \quad (2.4)$$

where $V_m(r)$ is of order r^m at $r=0$. Further, reference to (2.3) shows that H' , depending only on $\theta - \phi$, can only mix together functions with the same value of the quantum number

$$K = A + l. \quad (2.5)$$

Thus K remains a good quantum number, as would be expected since it represents the total angular momentum about the axis. Hence within the electronic system $A = \pm 1$ (that is, within the components of the Π electronic state) the only non-vanishing matrix elements of H' are those of the form

$$\begin{aligned} \langle 1, n, K-1 | H' | 1, n', K-1 \rangle &= \langle n, K-1 | V_0 | n', K-1 \rangle, \\ \langle -1, n, K+1 | H' | -1, n', K+1 \rangle &= \langle n, K+1 | V_0 | n', K+1 \rangle, \\ \langle 1, n, K-1 | H' | -1, n', K+1 \rangle &= \langle n, K-1 | V_2 \exp(-2i\phi) | n', K+1 \rangle, \end{aligned}$$

and

$$\langle -1, n, K+1 | H' | 1, n', K-1 \rangle = \langle n, K+1 | V_2 \exp(2i\phi) | n', K-1 \rangle, \quad (2.6)$$

where on the right-hand side only the vibrational degrees of freedom enter into consideration. Since $V_1, V_3 \dots$ do not appear in (2.6), one may, provided mixing with other electronic states is unimportant, take H' in the simpler form

$$H' = V_0 + V_2[\exp(2i\alpha) + \exp(-2i\alpha)] \quad (2.7)$$

without making any difference at all to the results.

In order to understand the separation of the pairs of curves in figure 1 it is necessary to investigate the effect of the perturbation (2.7) on the electronic potential function, which in the unperturbed situation we may take to be $U^0(r)$. If the nuclei are held in a non-linear configuration the perturbation H' causes the electronic sub-levels $\exp(\pm i\theta)$ to interact and resolves their degeneracy in the first order. For given r and ϕ the matrix of H' between the functions $\exp(i\theta)$ and $\exp(-i\theta)$ is immediately seen to be

$$\begin{bmatrix} V_0 & V_2 \exp(-2i\phi) \\ V_2 \exp(2i\phi) & V_0 \end{bmatrix} \quad (2.8)$$

and diagonalization of this matrix leads at once to the zeroth-order wave functions $\cos(\theta - \phi)$ and $\sin(\theta - \phi)$, with which are associated the first-order energies $V_0 + V_2$ and $V_0 - V_2$ respectively. Hence, as remarked earlier, the Born-Oppenheimer electronic wave function is split into two real components by the distortion, the associated bending potentials being

$$\begin{aligned} U^+ &= U^0 + V_0 + V_2, \\ U^- &= U^0 + V_0 - V_2, \end{aligned} \quad (2.9)$$

according as the electronic wave function is symmetric or antisymmetric about the plane of the distortion. In the next section we shall assume that V_2 is positive, so that U^+ is the potential for the upper surface. If V_2 is negative a corresponding theory is easily developed with some change of notation.

3. THE UPPER VIBRONIC LEVELS

Since we are primarily interested in the upper vibronic levels of NH_2 , we shall begin by taking the unperturbed situation to be one in which $U^0(r)$ is identical with $U^+(r)$, the potential for the upper curve in figure 1 (b). From this point of view the lower curve is regarded as diverging from the upper curve as a consequence of the perturbation

$$H' = V_0[1 - \exp(2i\alpha) - \exp(-2i\alpha)] \quad (3.1)$$

in which V_2 has been set equal to $-V_0$, so that by (2.9) the upper curve is not affected in any way. Our reason for adopting this standpoint, rather than setting $U^0 = \frac{1}{2}(U^+ + U^-)$ as Renner did, is that we may hope, by sacrificing accuracy in our treatment of the lower levels, to gain accuracy in our quantitative calculations on the upper ones. There is also a point of convenience, namely that the upper curve is more nearly parabolic than the lower, so that we can make full use of the specially simple properties of the harmonic oscillator.

Before discussing arbitrary values of K we must, however, draw attention to an important property, first pointed out by Renner, of the levels for which $K=0$. Considerations of symmetry alone show that these levels, the Σ levels, must fall into two classes, Σ^+ and Σ^- , according as the vibronic wave function is unchanged or changes sign when the signs of θ and ϕ are simultaneously reversed. Now the functions $|1, n, -1\rangle$ and $|-1, n, 1\rangle$ taken separately do not have this property, but their sum is a Σ^+ function and their difference a Σ^- function. It is obvious on grounds of symmetry that the matrix elements between Σ^+ and Σ^- functions of any perturbation must vanish; it is also true, as will immediately be shown, that the perturbation (3.1) has vanishing matrix elements between all pairs of Σ^+ functions. For by (2.6)

$$\langle 1, n, -1 | H' | 1, n', -1 \rangle = 2\pi \int_0^\infty \rho_{n1} V_0 \rho_{n'1} r \, dr = \langle -1, n, 1 | H' | -1, n', 1 \rangle, \quad (3.2)$$

$$\langle 1, n, -1 | H' | -1, n', 1 \rangle = 2\pi \int_0^\infty \rho_{n1} V_2 \rho_{n'1} r \, dr = \langle -1, n, 1 | H' | 1, n', -1 \rangle. \quad (3.3)$$

Hence the matrix element of H' between the combinations

$$[|1, n, -1\rangle + |-1, n, 1\rangle]/\sqrt{2} \text{ and } [|1, n', -1\rangle + |-1, n', 1\rangle]/\sqrt{2}$$

reduces to

$$2\pi \int_0^\infty \rho_{n1} (V_0 + V_2) \rho_{n'1} r \, dr; \quad (3.4)$$

and if $V_0 + V_2 = 0$ this vanishes. Therefore the Σ^+ functions are unaffected either in form or in energy by any perturbation of the type (3.1) which alters the lower curve only, and are determined entirely by the form of the upper curve $U^+(r)$. By an exactly analogous argument one may show that the Σ^- levels are determined solely by the form of the function $U^-(r)$. These statements hold, furthermore, to all orders in the perturbation (3.1).

The Π , Δ , Φ , Γ , ... levels, with $K=1, 2, 3, 4, \dots$ respectively, present a more complicated situation. As Renner showed, a small *quadratic* perturbation of the form

$$H' = fr^2 \cos 2\alpha \quad (3.5)$$

splits each pair of degenerate functions in figure 3 into their sum and their difference, *in the first order*, and we shall see that the same is true of the perturbation

$$H' = \frac{1}{2}fr^2[1 - \exp(2i\alpha) - \exp(-2i\alpha)]. \quad (3.6)$$

By analogy with the behaviour of the Σ functions one might therefore speak of the combination

$$[|1, 3, 0\rangle + |-1, 3, 2\rangle]/\sqrt{2}$$

as a Π^+ function, and a combination of the type

$$[|1, 3, 0\rangle - |-1, 3, 2\rangle]/\sqrt{2}$$

as a Π^- function. Closer examination reveals, however, that the perturbation (3.6), and the more general perturbation (3.1), has non-vanishing matrix elements between, for example, different Π^+ functions, and also between Π^+ and Π^- , or Δ^+ and Δ^- functions. As a consequence, every vibronic level with $|K| \geq 1$ is determined by both the upper and lower potential energy curves. It is for this reason, as Renner showed, that the vibronic wave function can no longer be factorized into an electronic and a vibrational term. Nevertheless, in calculating the energies of the upper vibronic levels we shall make the simplifying assumption that their wave functions are adequately represented by the combinations which we have called Π^+ , Δ^+ , Φ^+ , Γ^+ etc., at least for large values of $n - |K|$. This assumption is admittedly somewhat questionable, but we think it sufficiently near the truth to yield results which are at least approximately correct.

4. CALCULATION OF ENERGY LEVELS FOR QUARTIC POTENTIAL SURFACES

We shall now apply the theory of the previous sections to the calculation of the upper vibronic energy levels when the potentials U^+ and U^- are of the type $\alpha r^2 + \beta r^4$. Such functions can give a reasonable representation of the situation illustrated by figure 1(b). In view of the simple properties of the harmonic oscillator, we shall adopt a slightly different procedure in which U^0 will be taken as the *parabola* which closely approximates to U^+ (the upper Born-Oppenheimer potential curve) for small r . It is convenient to adopt units of energy and distance such that

$$h\nu = 1, \quad \kappa = 1 \quad (4.1)$$

where ν and κ are the classical frequency and force constant of the bending vibration in the upper state. Thus, in these units,

$$U^0 = \frac{1}{2}r^2 \quad (4.2)$$

and the upper curve will be

$$U^+ = U^0 + hr^4, \quad (4.3)$$

h being a constant allowing for anharmonicity. The presence of this effect in NH_2 is indicated by the unequal spacing in the Σ^+ levels. We must also include a quartic term in the expression for the lower curve; this we write as

$$U^- = (\frac{1}{2} - f)r^2 + gr^4, \quad (4.4)$$

where $f > \frac{1}{2}$ and $g > 0$. By equation (2.9), therefore,

$$V_0 = -\frac{1}{2}fr^2 + \frac{1}{2}(g + h)r^4 \quad (4.5)$$

and

$$V_2 = +\frac{1}{2}fr^2 - \frac{1}{2}(g - h)r^4, \quad (4.6)$$

The energy of one of the upper vibronic levels is then given by

$$E^+(n, K) = n + \frac{1}{2} \langle (1, n, K-1) + (-1, n, K+1) | V_0 + 2V_2 \cos 2\alpha | (1, n, K-1) + (-1, n, K+1) \rangle, \quad (4.7)$$

where we have made the assumption, discussed in §3, that its wave function is the sum (here unnormalized) of two degenerate eigenfunctions of the unperturbed Hamiltonian.

In order to evaluate the vibronic energy given by (4.7) we require the matrix elements of r^2 , r^4 , $r^2 \cos 2\alpha$ and $r^4 \cos 2\alpha$ within the pair of functions $|1, n, K-1\rangle$ and $|-1, n, K+1\rangle$. According to (2.6) this amounts to finding the matrix elements of r^2 , r^4 , $r^2 \exp(2i\phi)$ and $r^4 \exp(2i\phi)$ between the vibrational wave functions $|n, K-1\rangle$ and $|n, K+1\rangle$. These matrix elements are determined as follows. Setting

$$r \exp(i\phi) = z \quad (4.8)$$

we observe that the four operators in question may be written as $z\bar{z}$, $(z\bar{z})^2$, z^2 and $z^2(z\bar{z})$, where \bar{z} is the complex conjugate of z . If, then, we can find the matrix elements of z and \bar{z} within the system of functions of $|n, l\rangle$, we can obtain those of $z\bar{z}$, $(z\bar{z})^2$, z^2 and $z^2(z\bar{z})$ from them by the ordinary rules of matrix multiplication. But it has been shown by various authors (Moffitt and Liehr [3], Longuet-Higgins *et al.* [4]) that all the matrix elements of z and \bar{z} in the system $|n, l\rangle$ vanish except those of the two types

$$\langle n, l | z | n+1, l-1 \rangle = \langle n+1, l-1 | \bar{z} | n, l \rangle = \sqrt{[\frac{1}{2}(n-l+1)]} \quad (4.9)$$

and

$$\langle n+1, l+1 | z | n, l \rangle = \langle n, l | \bar{z} | n+1, l+1 \rangle = \sqrt{[\frac{1}{2}(n+l+1)]}. \quad (4.10)$$

Hence the required matrix elements may be evaluated without further ado. As an example of our procedure, consider the matrix of the quadratic part of H' , namely

$$-\frac{1}{2}fr^2 + \frac{1}{2}fr^2(2\cos 2\alpha) = \frac{1}{2}f[r^2 \exp(2i\alpha) - r^2 + r^2 \exp(-2i\alpha)]. \quad (4.11)$$

The three terms on the right-hand side are treated separately, as follows :

$$\begin{aligned} \langle 1, n, K-1 | r^2 \exp(2i\alpha) | -1, n, K+1 \rangle &= \langle n, K-1 | (\bar{z})^2 | n, K+1 \rangle \\ &= \langle n, K-1 | \bar{z} | n+1, K \rangle \langle n+1, K | \bar{z} | n, K+1 \rangle \\ &\quad + \langle n, K-1 | \bar{z} | n-1, K \rangle \langle n-1, K | \bar{z} | n, K+1 \rangle \\ &= \sqrt{[\frac{1}{2}(n+K)]} \sqrt{[\frac{1}{2}(n-K)]} + \sqrt{[\frac{1}{2}(n-K)]} \sqrt{[\frac{1}{2}(n+K)]} = \sqrt{(n^2 - K^2)}; \end{aligned} \quad (4.12)$$

$$\begin{aligned} \langle -1, n, K+1 | r^2 | -1, n, K+1 \rangle &= \langle n, K+1 | z\bar{z} | n, K+1 \rangle \\ &= \langle n, K+1 | z | n+1, K \rangle \langle n+1, K | \bar{z} | n, K+1 \rangle \\ &\quad + \langle n, K+1 | z | n-1, K \rangle \langle n-1, K | \bar{z} | n, K+1 \rangle \\ &= \sqrt{[\frac{1}{2}(n-K)]} \sqrt{[\frac{1}{2}(n-K)]} + \sqrt{[\frac{1}{2}(n+K)]} \sqrt{[\frac{1}{2}(n+K)]} = n. \end{aligned} \quad (4.13)$$

Similarly,

$$\langle -1, n, K+1 | r^2 \exp(-2i\alpha) | 1, n, K-1 \rangle = \langle n, K+1 | z^2 | n, K-1 \rangle = \sqrt{(n^2 - K^2)} \quad (4.14)$$

and

$$\langle 1, n, K-1 | r^2 | 1, n, K-1 \rangle = \langle n, K-1 | z\bar{z} | n, K-1 \rangle = n. \quad (4.15)$$

Hence the matrix of (4.11) within the system $|1, n, K-1\rangle$, $|-1, n, K+1\rangle$ is

simply

$$\frac{1}{2}f \begin{bmatrix} -n & \sqrt{(n^2 - K^2)} \\ \sqrt{(n^2 - K^2)} & -n \end{bmatrix}. \quad (4.16)$$

The symmetry of this matrix substantiates our earlier statement that the quadratic perturbation (3.6) splits each such pair of degenerate functions into their sum and difference; the energies of these two combinations are seen to be, in the quadratic approximation,

$$n - \frac{1}{2}f[n - \sqrt{(n^2 - K^2)}] \quad \text{and} \quad n - \frac{1}{2}f[n + \sqrt{(n^2 - K^2)}] \quad (4.17)$$

respectively. Two things will be noted: first, that the energy of the sum is invariably higher than that of the difference, the correction to the energy of the former being relatively slight; and secondly, that if $K=0$ the perturbation (3.6) has no effect on the energy of the combination, as our more general argument has already established.

The matrices of r^4 and $r^4 \cdot 2 \cos 2\alpha$ within the pair of functions may be evaluated in an exactly similar manner. They are, respectively,

$$\begin{bmatrix} \frac{3}{2}n^2 - \frac{1}{2}K(K-2) & 0 \\ 0 & \frac{3}{2}n^2 - \frac{1}{2}K(K+2) \end{bmatrix} \quad (4.18)$$

and

$$\begin{bmatrix} 0 & \frac{3}{2}n\sqrt{(n^2 - K^2)} \\ \frac{3}{2}n\sqrt{(n^2 - K^2)} & 0 \end{bmatrix}. \quad (4.19)$$

Hence the complete matrix of H' , with V_0 and V_2 given by (4.5) and (4.6), is

$$\begin{bmatrix} -\frac{1}{2}fn + \frac{1}{2}(g+h)\{\frac{3}{2}n^2 - \frac{1}{2}K(K-2)\}, \frac{1}{2}f\sqrt{(n^2 - K^2)} - \frac{1}{2}(g-h)\frac{3}{2}n\sqrt{(n^2 - K^2)} \\ \frac{1}{2}f\sqrt{(n^2 - K^2)} - \frac{1}{2}(g-h)\frac{3}{2}n\sqrt{(n^2 - K^2)}, -\frac{1}{2}fn + \frac{1}{2}(g+h)\{\frac{3}{2}n^2 - \frac{1}{2}K(K+2)\} \end{bmatrix}. \quad (4.20)$$

The approximate energy of an upper vibronic level, is therefore, by (4.7)

$$E^+(n, K) = n - \frac{1}{2}f[n - \sqrt{(n^2 - K^2)}] + \frac{1}{4}(g+h)(3n^2 - K^2) - \frac{3}{4}(g-h)n\sqrt{(n^2 - K^2)}. \quad (4.21)$$

For small values of K ($K \ll n$) an expansion to order K^2 gives

$$E^+(n, K) = n + \frac{3}{2}hn^2 - \frac{1}{8}K^2[2fn^{-1} - g + 5h]. \quad (4.22)$$

Two points about this expression are worth noting. In the first place, for the Σ^+ levels ($K=0$) the energy reduces to $n + \frac{3}{2}hn^2$ confirming once again that these levels are independent of the lower energy curve $U^-(r)$. Secondly, the coefficient in square brackets will probably be positive so that a lowering of levels with $K > 0$ is predicted, approximately proportional to K^2 .

In the absence of angular coupling between the odd electron and the bending mode, the surfaces coincide ($f=0$, $g=h$) and (4.22) reduces to

$$E^+(n, K) = n + \frac{1}{2}h(3n^2 - K^2), \quad (4.23)$$

a formula which applies also, of course, if the molecule is in a Σ electronic state ($\Lambda=0$) and the bending vibration is anharmonic. Thus a Renner effect is only indicated if the K -dependence of the energy levels is greater than that predicted by (4.23).

5. APPLICATION TO NH_2

Before applying the theory quantitatively, some remarks should be made about the relevance of the simple one-electron model to a radical such as NH_2 .

In its linear form, the $^2\Pi$ state of NH_2 has the electronic configuration

$$K\sigma_g^2\sigma_u^2\pi^3$$

where the π molecular orbitals are approximately $2p\pi$ atomic orbitals of the nitrogen atom. There are two such orbitals π_x and π_y possessing a degeneracy which is removed when the nuclear framework is bent. The one with a node in the plane of the bent molecule (π_y say) will have the higher energy so that the configuration corresponding to the lower curve of figure 1(b) will be $K\sigma_g^2\sigma_u^2\pi_y^2\pi_x$ and for the upper curve it will be $K\sigma_g^2\sigma_u^2\pi_y\pi_x^2$. In absorption from the ground state, therefore, an electron is transferred from π_y to π_x , that is from a symmetric orbital into one with a node in the molecular plane. This is opposite to the convention adopted at the end of §2. Nevertheless this convention is appropriate in the case of NH_2 for the total (rather than orbital) symmetry, since the lower *state* has a node in the molecular plane. We may think, if we like, of the angle θ as the angular coordinate of the missing electron.

In order to apply equation (4.21) to the NH_2 radical, it is necessary to have some means of finding the quantities f , g and h . Of these the upper surface anharmonicity h is obtained by fitting the observed energies of the Σ^+ levels to the formula with $K=0$. Dressler and Ramsay find that these levels have energies which can be represented numerically by

$$9650 + 597n + 11.5n^2 \quad (5.1)$$

in wave numbers above the ground state. The unit of energy is therefore 597 cm^{-1} and the value of h (from equation (4.22) with $K=0$) is found to be

$$h = 0.01284. \quad (5.2)$$

We determine f and g from the valency angle in the ground state and the height of the barrier. If the valency angle is denoted as $(\pi - 2\chi)$ in radians, then the mean value of χ^2 would be given by

$$\overline{\chi^2} = \frac{h}{4\pi^2\nu MR^2} \quad (5.3)$$

in the lowest state if both surfaces were coincident parabola, where ν and M are the frequency and reduced mass associated with the bending mode, and R the NH bond length. Setting

$$M = 2M_N M_H / (M_N + 2M_H),$$

$$\nu/c = 597\text{ cm}^{-1}$$

and

$$R = 1.02\text{ \AA} \text{ (as given by Dressler and Ramsay)}$$

we obtain

$$\overline{\chi^2} = 3.077 \times 10^{-2} \text{ radian}^2.$$

Hence the root mean square value of χ would be 10.03° . But in the natural units which we have adopted the mean square value of the amplitude would be unity in this state; hence our natural unit for NH_2 must be taken as 10.03° . The value of χ in the ground state, given by Dressler and Ramsay as 38.5° , is therefore 3.84 of our units.

The height of the ground state barrier is close to 9650 cm^{-1} , but must be slightly greater than this because of the zero-point energy of the ground state. Adopting the value 10000 cm^{-1} , which equals 16.75 natural units, and noting

n	Σ^+	Π	Δ	Φ	Γ
4	12,220 (12,280)				
5		12,840			
6	13,650 (13,620)		13,420		
7		14,340 (14,360)			
8	15,160 (15,120)		14,960 (15,030)		14,310
9		15,910 (15,890)		15,540 (15,690)	
10	16,770 (16,740)		16,610 (16,620)		16,110 (16,290)
11		17,570 (17,550)		17,280 (17,290)	
12	18,470 (18,430)		18,340 (18,270)		17,920 (18,060)
13		19,320 (19,380)		19,070 (19,150)	
14	20,260 (20,310)		20,150 (20,190)		19,800 (19,900)
15		21,170 (21,210)		20,950 (20,980)	
16	22,150 (22,180)		22,050 (22,020)		21,750 (21,760)
17		23,100 (23,080)		22,910	
18	24,120 (24,090)				
19		25,120 (25,050)			

Table 1. Calculated and (in brackets) observed vibronic term values in NH_2 . Observed band origins are quoted to the nearest 10 cm^{-1} since the upper state levels are split slightly both by spin-orbit coupling and by the slight dynamical asymmetry produced by the bending vibration.

that $dU^-/dr=0$ for $r=3.84$, we obtain the following two equations for f and g :

$$\left. \begin{aligned} (\tfrac{1}{2}-f)+gr^2 &= -16.75/r^2 \\ (\tfrac{1}{2}-f)+2gr^2 &= 0 \end{aligned} \right\} r=3.84. \quad (5.4)$$

Solution of these equations yields

$$f=2.770, \quad g=0.07695. \quad (5.5)$$

It then only remains to insert these values of f , g and h into equations (4.21), multiply by 597 to convert to wave numbers and add 9650 cm^{-1} , which is the gap between the ground state and the top of the barrier, since the energy in (4.21) is measured from this point. The resulting theoretical frequencies, and their experimental counterparts, are given in Table 1.

6. DISCUSSION

The general agreement in Table 1 between the observed frequencies and those calculated from equation (4.21) leaves little doubt that Dressler and Ramsay were right in attributing the absorption spectrum of NH_2 to transitions between two real components of an electronic Π state which is split in the manner indicated in figure 1 (*b*) by electronic-vibrational coupling, for the reasons given by Renner. The corresponding calculation for a Σ electronic state using (4.23) yields a variation of $E^+(n, K)$ with K which is too small by an order of magnitude.

The near coincidence between the experimental and theoretical energies of the Σ^+ levels in Table 1 is not, of course, particularly significant, as the coefficient h in (4.3) was chosen to fit these levels as well as possible. It is, however, interesting to note that the value of h is positive, and that the upper potential curve shows no trace of a shallow maximum at $r=0$. As to the other levels, the agreement with experiment is clearly best for $K=1$ and worst for $K=4$. The reason for this is not, perhaps, difficult to appreciate; the larger the value of K , the more strongly will the energy of an upper vibronic level be affected by the form of the lower potential energy curve, and errors as to its precise shape will therefore be most apparent at high K values.

In conclusion it should perhaps be stressed that our theory is limited by a number of severe approximations. An exact calculation along the lines laid down by Renner would necessitate the diagonalization of an infinite matrix, whose rows and columns correspond to the members of a complete orthonormal set of functions with a given value of K , and whose matrix elements include contributions from all powers of r in $U^+(r)$ and $U^-(r)$. What we have done is to ignore all matrix elements except those between functions which are degenerate in the harmonic zeroth approximation, and to neglect all powers of r higher than the fourth. Not only this, but we have neglected all interactions between the bending mode and other modes, and have treated the bending mode as though its effective mass were independent of its amplitude, even at the very large amplitudes which are actually reached. Nevertheless, it appears from our results that these approximations are not so serious as might have been feared, and that the perturbation techniques similar to that which we have here adopted may be helpful in interpreting other instances of the Renner effect.

We are indebted to Dr. D. A. Ramsay for kindly drawing our attention to this problem, and to him and Dr. K. Dressler for making their results available

before publication. We would also like to thank Mr. A. D. McLachlan for assistance with the calculations.

On interprete quantitativement, par l'effet Renner, les observations de Dressler et Ramsay (1958) sur le spectre d'absorption vibronique du radical NH_2 . L'emploi d'une méthode de perturbation mène à la prédiction de fréquences en bon accord avec l'expérience, et confirme l'opinion des auteurs cités que la bande d'absorption est associée à des transitions entre les composantes, largement séparées par l'interaction électronique-vibrationnelle, d'un état électronique Π .

Die Beobachtungen von Dressler und Ramsay (1958) über das Absorptionsspektrum des NH_2 -Radikals werden als Folge des Renner-Effekts gedeutet. Die Anwendung einer Störungsrechnung gestattet es, die Frequenzen in guter Uebereinstimmung mit dem Experiment vorauszusagen. Hierdurch wird die Ansicht der genannten Autoren bestätigt, dass die Absorptionsbande durch Uebergänge zwischen den Komponenten eines elektronischen Π -Zustandes zustande komme, wobei diese Komponenten infolge einer Elektronen-Schwingungs-Wechselwirkung, weit voneinander entfernt seien.

REFERENCES

- [1] DRESSLER, K., and RAMSAY, D. A., 1958, *Proc. roy. Soc.* (in press); also 1957, *J. chem. Phys.*, **27**, 971.
- [2] RENNER, E., 1934, *Z. Phys.*, **92**, 172.
- [3] MOFFITT, W., and LIEHR, A., 1957, *Phys. Rev.*, **106**, 1195.
- [4] LONGUET-HIGGINS, H. C., ÖPIK, U., PRYCE, M. H. L., and SACK, R., 1958, *Proc. roy. Soc. A*, **244**, 1.
- [5] WALSH, A. D., 1953, *J. chem. Soc.*, 2260.

The π -electron spectra of the benzene N-heterocyclics

by J. N. MURRELL

Department of Theoretical Chemistry, Cambridge University

(Received 12 May, 1958)

The π -electron spectra of the nitrogen heterocyclics are discussed on the basis of a perturbation applied to the spectra of the corresponding aromatic hydrocarbons. The frequency of the first $\pi \rightarrow \pi$ band in pyridine is the same as that of the corresponding band in benzene, because of the accidental cancellation of a first-order blue shift by a second-order red shift. The first- and second-order shifts are related to two perturbation parameters, and these are obtained from experiment by examining the spectra of the benzene heterocyclics. These parameters can then be satisfactorily related to one another by assuming a perturbation field of the form $\exp(-2\eta r)/r$ and by allowing for the C-N bond being shorter than the C-C bond in benzene.

1. INTRODUCTION

The electronic spectra of the nitrogen heterocyclics are very similar to those of the corresponding aromatic hydrocarbons. The principal difference lies in the appearance of weak bands with sharp vibrational structure on the long wavelength side of the $\pi \rightarrow \pi$ bands. These so-called $n \rightarrow \pi$ bands arise from the transfer of an electron from the nitrogen lone-pair to a vacant π orbital: they will not be discussed further in this paper.

One might hope to explain the differences between the electronic states of a nitrogen heterocyclic and those of the corresponding hydrocarbon by a first order perturbation theory. The perturbation term in the Hamiltonian would involve the change in the electrostatic field arising from the replacement of C-H by N. The first order change in energy of an electronic transition would be given by the interaction of this field with an electron distribution which is equal to the difference in the electron densities of the ground and the excited state.

The frequency of the first $\pi \rightarrow \pi$ band in pyridine is almost exactly the same as that in benzene. One is tempted to conclude that there is no first order change in energy of this band on replacing CH by N. However, the predominant feature which does change is the intensity. The benzene 2600 Å band arises from an $A_{1g} \rightarrow B_{2u}$ symmetry-forbidden transition, and has an oscillator strength of about 0.0014. The corresponding band in pyridine is $A_1 \rightarrow B_1$. This is allowed by symmetry, and has an oscillator strength of about 0.03. To explain the increase in intensity on going from benzene to pyridine, one must allow for the changes in the wave functions of the ground and the excited states, and this would be accompanied by a change in energy which is of second order in the perturbation term.

By far the most important second-order interaction will be that between the B_{2u} and the E_{1u} state, the latter giving rise to the intense 1850 Å band of benzene. This interaction will depress the B_{2u} state and would tend to give a red shift to the 2600 Å band. It therefore follows that the position of the first $\pi \rightarrow \pi$ band is the same in pyridine and in benzene only because of an accidental cancellation of the

second-order red shift by an equal first-order blue shift. This cancellation must also extend to the pyridinium cation, for adding mineral acid to pyridine in solution produces no shift in the position of the first $\pi \rightarrow \pi$ band, but increases its intensity by a factor of 2.5.

It is then necessary to ask why the first order energy changes are so small. Now molecular orbital theory, including the zero-overlap approximation, predicts that the ground and first excited states of benzenoid hydrocarbons should have identical electron densities [1, 2]. It therefore follows that any difference in their densities must be of first order in the overlap integral between adjacent $2p\pi$ atomic orbitals, and the interaction of this overlap density with the perturbing field will necessarily be rather small. However, the transition densities between two different electronic states can have a contribution which is of zeroth order in the overlap integral, and it is the interaction of these transition densities with the perturbing field which determines the second-order energy terms.

In this paper it is proposed to examine the dependence of the first- and second-order energies on the form of the electronic wave functions, and the nature of the perturbing field for the simplest of the nitrogen heterocyclics, namely those derived from benzene.

2. THEORY

The wave functions and molecular orbitals of benzene must transform as some representation of the D_{6h} symmetry group. The B_{2u} state which gives rise to the 2600 Å band is usually assumed to have the wave function [3]

$$\chi_1 = \sqrt{\frac{1}{2}}(\psi_3^{-1}\psi_5 - \psi_2^{-1}\psi_4),$$

where the symbol $\psi_r^{-1}\psi_s$ is used to denote a singlet state which is derived from the ground state wave function by replacing the orbital ψ_r by the orbital ψ_s . The benzene molecular orbitals are taken as linear combinations of $2p\pi$ atomic orbitals, ϕ , in their real forms as follows:

$$\begin{aligned}\psi_2 &= N_2 \sum_{\nu=1}^6 \phi_\nu \cos \frac{1}{3}\nu\pi; & \psi_3 &= N_3 \sum_{\nu=1}^6 \phi_\nu \sin \frac{1}{3}\nu\pi \\ \psi_5 &= N_5 \sum_{\nu=1}^6 \phi_\nu \cos \frac{2}{3}\nu\pi; & \psi_4 &= N_4 \sum_{\nu=1}^6 \phi_\nu \sin \frac{2}{3}\nu\pi\end{aligned}$$

where the N 's are normalizing factors. If we write the overlap integral between the atomic orbitals on adjacent carbon atoms as

$$S = \int \phi_\nu(1)\phi_{\nu+1}(1)d\tau_1$$

and neglect all other overlap integrals, then the normalizing factors are found to be

$$N_2 = N_3 = (1 + S)^{-1/2}; \quad N_4 = N_5 = (1 - S)^{-1/2}.$$

The electron density in the excited state less that in the ground state is given by

$$\rho_{11} - \rho_{00} = \frac{1}{2}(\psi_5^2 - \psi_3^2 + \psi_4^2 - \psi_2^2),$$

and expanding in terms of atomic orbitals this is equal to

$$\frac{1}{3(1-S^2)} \sum_{\nu} (S\phi_\nu^2 - \phi_\nu\phi_{\nu+1}).$$

In other words, on going from the ground to the excited state, electrons are withdrawn from the bonds and placed on the carbon atoms. This is in accordance

with our expectation that the bond strengths in the excited state are less than in the ground state.

We now have to consider the form of the perturbing field. It is to be expected that the largest contribution to the first-order energy will arise from the part of the electron density which is near the nucleus of atom 1, for it is in this region that the perturbing field is largest. We will therefore make the assumption that only the terms $S\phi^2$, $\phi_1\phi_2$ and $\phi_1\phi_6$ (that is the electron density on atom 1 and in the bonds emanating from 1), make a significant contribution to the first order energy. If we write

$$\alpha' = \langle \phi_1 | H' | \phi_1 \rangle$$

and

$$\beta' = \langle \phi_1 | H' | \phi_2 \rangle$$

then the first-order energy E' is given by

$$E' = \frac{\alpha' S - 2\beta'}{3(1 - S^2)},$$

β' will be considerably smaller than α' , but will be of the same order as $S\alpha'$.

Two simple forms for the potential field which may prove useful are

$$H_1' = Z/r_1 \quad \text{and} \quad H_1' = \frac{\exp(-2\eta r_1)}{r_1}.$$

The first of these gives the field due to an effective charge Z at atom 1, and the second allows for the Coulombic field becoming zero at large r . If the carbon $2p\pi$ orbitals have the form

$$\phi = (\zeta^5/\pi)^{1/2} r \exp(-\zeta r) \sin \theta \cos \varphi$$

then $-\alpha'$ is given by

$$Z \langle \phi_1 | 1/r_1 | \phi_1 \rangle = \frac{1}{2} Z \zeta$$

or

$$\langle \phi_1 | \exp(-2\eta r_1)/r_1 | \phi_1 \rangle = \zeta^5/2(\zeta + \eta)^4$$

and $-\beta'$ by

$$Z \langle \phi_1 | 1/r_1 | \phi_2 \rangle = \frac{1}{2} Z \zeta (1 + \rho_1 + \rho_1^2/3) \exp(-\rho_1)$$

or

$$\langle \phi_1 | \exp(-2\eta r_1)/r_1 | \phi_2 \rangle = \zeta^2 \eta^{-1} (\zeta + 2\eta)^{-2} (\zeta + \eta)^{-1} R^3 [(1 + \kappa)\{6(1 + \kappa)^2(1 + \rho_1) + 4(1 - \kappa)\rho_1^2 + \rho_1^3\} \exp(-\rho_1) - (1 - \kappa)^2\{6(1 + \kappa)(1 + \rho_2) + 2\rho_2^2\} \exp(-\rho_2)]$$

where

$$\rho_1 = \zeta R, \quad \rho_2 = (\zeta + 2\eta) R$$

R being the bond length, and

$$\kappa = [\eta^2 + \zeta\eta + \zeta^2/2]/\eta(3 + \eta).$$

We will defer further examination of these integrals until we have looked at the second-order terms.

The second order change in energy of a state χ_1 is given by

$$E_1'' = \sum_r \langle \chi_1 | H' | \chi_r \rangle^2 / (E_1 - E_r).$$

The transition densities between the states χ_1 and χ_r , defined by

$$\rho_{1r} = i \int \chi_1 \chi_r \prod_{j \neq 1} d\tau_j,$$

where the integration is over the coordinates of all the i electrons except one, can contain contributions from the densities ϕ_v^2 , even in the zero-overlap approximation. It follows that the second-order energies will be expressible as a function of α' , the contribution from the terms containing β' being relatively small.

If more than one heteroatom is introduced into the benzene nucleus, then the net perturbation term in the Hamiltonian can be written as a sum of terms, one for each heteroatom as follows:

$$H' = \sum_{\mu} H'_{\mu}.$$

It follows that the first order contribution to the energy will be proportional to the number of nitrogen atoms introduced, but that the second order terms, which can be expanded to give

$$E_1'' = \sum_r \left\{ \sum_{\mu} \langle \chi_1 | H'_{\mu} | \chi_r \rangle \right\}^2 / (E_1 - E_r)$$

will not follow this simple relationship (although a simple non-additive, rule can be found for each pair of states χ_1 and χ_r), and must be evaluated for each molecule under consideration. The behaviour of the second order terms as a function of the different positions of substitution in the benzene nucleus is discussed by Murrell and Longuet-Higgins [4] and by Murrell and McEwen [5], and the reader is referred to these papers for more details.

In short, the change in energy of the 2600 Å band of benzene on introducing n nitrogen atoms, should follow a relationship

$$\begin{aligned} E_{\text{obs}} &= E' + E'' \\ &= n(\alpha' S - 2\beta')/3(1 - S^2) + I\alpha'^2 \end{aligned}$$

where I is a coefficient which depends on the energies and wave functions of the electronic states of benzene, and also on the relative positions of the substituents, but which is independent of the type of substituent introduced into the molecule.

	Ref.	ν (cm ⁻¹)	$\Delta\nu$	$\Delta\nu/n$	I/n (10 ⁻⁸ (cm))	ϵ
Benzene		39400				110
Pyridine (1)	[6]	40000	600	600	-244	1700
Pyridazine (1, 2)	[6]	40400	1000	500	-271	1100
Pyrimidine (1, 3)	[6]	41400	2000	1000	-68	2600
Pyrazine (1, 4)	[6]	38900 (37600)	-500 (-1800)	-250 (-900)	-796	6500
s-Triazine (1, 3, 5)	[7]	45000	5600	1870	+232	150
Tetrazine (1, 2, 4, 5)	[8]	39700	300	75	-398	2200

Table 1. The observed frequencies and intensities of the first $\pi \rightarrow \pi$ absorption band in the nitrogen heterocyclics derived from benzene.

Table 1 gives the observed energies of the first $\pi \rightarrow \pi$ band in the benzene heterocyclics, and the values of the coefficient I which have been taken from [5]. In figure 1 the change in energy of this band per heteroatom is plotted against I/n . In the absence of information on the frequency of the zero-zero transition, the observed frequencies have been taken from the absorption maxima. The points all lie on a straight line except in the case of pyrazine. However, taking the frequency of a vibrational peak at longer wavelengths for this molecule, complete agreement is obtained†. From the intercept on the 'observed' axis,

† If the frequencies of the smoothed absorption maxima are taken, the points are more scattered, but still lie quite close to the line drawn in figure 1,

one can calculate $(\alpha'S - 2\beta')/3(1 - S^2)$; it has the value 1220 cm^{-1} . From the slope of the line α'^2 is obtained directly to be $\alpha' = -17500 \text{ cm}^{-1}$. Assuming a value for S of 0.25, this then gives $\beta' = -3900 \text{ cm}^{-1}$.

Returning now to the suggested expressions for α' : taking Slater's value for the atomic orbital exponent ($\zeta = 1.625$), one finds that our experimentally deduced α' can be obtained using a value $Z = 0.098$ or $\eta = 1.278$. Calculating β' using these values one obtains $\beta' = -2770 \text{ cm}^{-1}$ or -906 cm^{-1} . Both approximations to the perturbing field underestimate the value of β' . However,

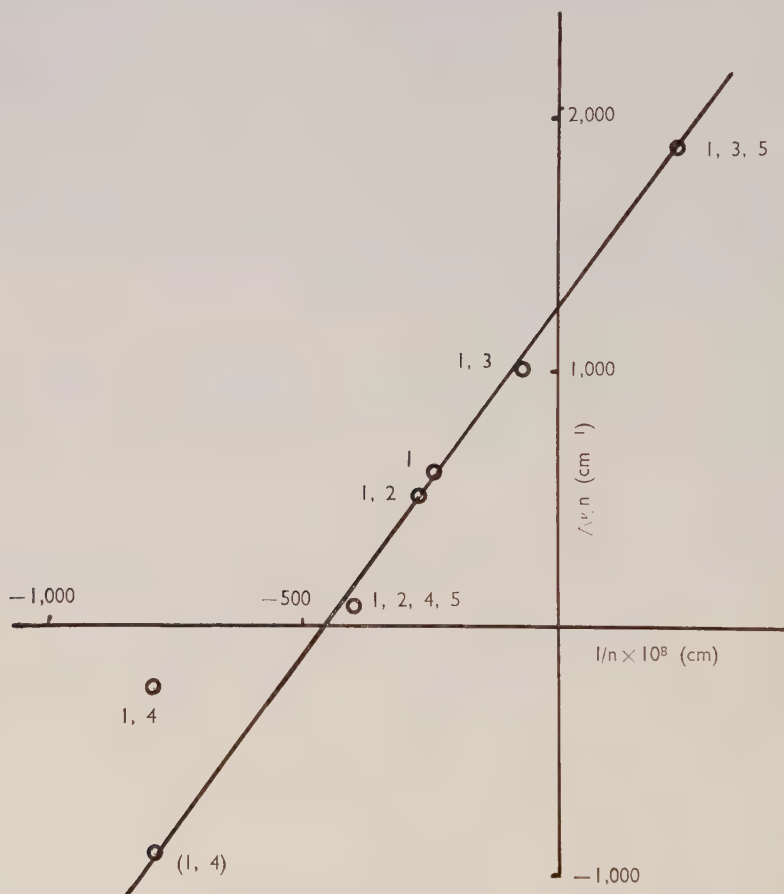


Figure 1.

we have assumed that the substitution of CH by N does not change the geometry of the molecule. In fact Schomaker and Pauling [9] have obtained a C-N bond length for pyridine of 1.37 \AA compared with the C-C bond length of 1.39 \AA in benzene. The difference appears small, but will lead to a significant change in the resonance integral β , since this varies inverse exponentially with the bond length. Pariser and Parr [10] have proposed an expression for the resonance integral of a C-C bond which has the form

$$\beta(r) = -5.197 \times 10^7 \exp(-5.6864r) \quad (\text{cm}^{-1})$$

where r is measured in angstroms. This gives a value for β' ($\beta(1.37) - \beta(1.39)$) equal to -2240 cm^{-1} . Adding this to the value of β' which has been calculated

to be due to the perturbation field, we obtain for $Z=0.098$, $\beta' = -5010 \text{ cm}^{-1}$; and for $\eta=1.279$, $\beta' = 3140 \text{ cm}^{-1}$. This latter is in quite good agreement with the observed value of -3900 cm^{-1} , when one considers the approximations which have been made.

Allowing for the contribution to β' due to the change in bond length means however that the first-order energy change is not strictly additive in the number of substituents, some correction being necessary when ortho substituents are present. The points in figure 1 suggest that this is not serious, the change in β due to the N-N bond shortening being about equal to the changes arising from the shortening of two C-N bonds. Strictly speaking there are other terms which would also contribute to the first order energy when one allows for the contraction of the C-N bond. However, the other integrals which are involved will either change very little, or if they do change appreciably will not contribute much to the energy of the electronic states.

It is interesting to note that the value of α' ($-17\,500 \text{ cm}^{-1}$) is quite close to the resonance integral for the C-C bond in benzene ($-19\,300 \text{ cm}^{-1}$). This would appear to add weight to the practice in simple molecular orbital theory of writing $\alpha_N = \alpha_C + \beta_{C-C}$.

The increase in intensity of the 2600 Å band on introducing a nitrogen atom, will be due to the change of the ground and excited state wave functions. Either the ground state taking some E_{2g} character, or the excited state some E_{1u} character will increase the intensity of this band. If we neglect changes in the ground state, then the increase in intensity should be in the ratio 1:1:1:4:0:4 for mono:ortho:meta:para:1,3,5:1,2,4,5, substitution. These ratios have been noted before [11, 12], and are seen to be in rough agreement with the observed extinction coefficients (see Table 1), except for tetrazine, where the band is much weaker than is theoretically expected. To be more exact, one should compare the above ratios with the observed oscillator strengths, but these are difficult to estimate because of the overlapping of neighbouring bands.

3. DISCUSSION

It is hoped that the parameters α' and β' which have been evaluated in this paper should carry over to other nitrogen heterocyclics. The difficult problem is to evaluate the wave functions for the parent hydrocarbon to the first order in the overlap integral. No theoretical treatment so far would claim this accuracy. Moreover, there has not yet been a satisfactory evaluation of the inductive parameters I for hydrocarbons other than benzene, although only the zero-overlap wave functions are required in this case. Lastly the bond contraction which occurs on replacing CH by N might vary a great deal on going from one molecule to another, and even from one band to another in the same molecule; hence β' might not in fact be a constant parameter. At the moment the prospects for a detailed understanding of the π -electron spectra of N-heterocyclics in general, are not bright.

On discute les spectres des électrons π des hétérocycles azotés au moyen d'une perturbation appliquée aux spectres des hydrocarbures aromatiques correspondants. La longueur d'onde de la première bande $\pi \rightarrow \pi$ de la pyridine est la même que celle de la bande correspondante du benzène parce qu'un déplacement hypsochrome du premier ordre et un déplacement bathochrome du second ordre s'annulent fortuitement. Les déplacements du

premier et du second ordre sont liés à deux paramètres perturbatifs, et ceux-ci s'obtiennent expérimentalement en examinant les spectres des hétérocycles benzéniques. On peut ensuite relier de façon satisfaisante ces paramètres en supposant que le champ de perturbation est de la forme $\exp(-2\eta r)/r$, et en tenant compte du fait que la liaison C-N est plus courte que la liaison C-C.

Für einige heterozyklische Stickstoffverbindungen werden die π -Elektronenspektren mit denen der entsprechenden aromatischen Kohlenwasserstoffe verglichen und als Störung dieser Aromatspektren behandelt. Die Frequenz der ersten $\pi \rightarrow \pi$ Bande im Pyridin fällt mit der entsprechenden Benzolbande zusammen, da sich hier zufällig eine Blauverschiebung erster Ordnung und eine Rotverschiebung zweiter Ordnung gegenseitig aufheben. Die Verschiebungen erster bzw. zweiter Ordnung lassen sich in Beziehung setzen zu zwei Störungsparametern, die aus den beobachteten Spektren der Benzol-Heterozyklen ermittelt werden. Die Beziehung der beiden Parameter zueinander lässt sich befriedigend ausdrücken, wenn man ein Störfeld von der Form $\exp(-2\eta r)/r$ ansetzt und ausserdem berücksichtigt, dass die C-N-Bindung kürzer ist als die C-C-Bindung.

REFERENCES

- [1] DEWAR, M. J. S., and LONGUET-HIGGINS, H. C., 1954, *Proc. phys. Soc. Lond.*, A, **67**, 795.
- [2] POPL, J. A., 1955, *Proc. phys. Soc. Lond.*, A, **68**, 81.
- [3] GÖPPERT-MAYER, M., and SKLAR, A. L., 1938, *J. chem. Phys.*, **6**, 645.
- [4] MURRELL, J. N., and LONGUET-HIGGINS, H. C., 1955, *Proc. phys. Soc. Lond.*, A, **68**, 329.
- [5] MURRELL, J. N., and MCEWEN, K. L., 1956, *J. chem. Phys.*, **25**, 1143.
- [6] KLEVENS, H. B., and PLATT, J. R., 1954, *Technical Report of the Laboratory of Molecular Structure*, (Department of Physics, University of Chicago).
- [7] HIRT, R. C., HALVERSON, F., and SCHMITT, R. G., 1954, *J. chem. Phys.*, **22**, 1148.
- [8] MASON, S., Private communication.
- [9] SCHOMAKER, V., and PAULING, L. 1939, *J. Amer. chem. Soc.*, **61**, 1769.
- [10] PARISER, R., and PARR, R. G., 1953, *J. chem. Phys.*, **21**, 767.
- [11] SKLAR, A. L., 1942, *J. chem. Phys.*, **10**, 135.
- [12] FÖRSTER, T., 1947, *Z. Naturf.*, A2, 149.

The infra-red spectra of some ferroelectric compounds with short hydrogen bonds

by R. BLINC† and D. HADŽI

University Chemical Laboratory and Institute
Boris Kidrič, Ljubljana

(Received 5 August 1958)

The infra-red spectra of KH_2PO_4 , $\text{NH}_4\text{H}_2\text{PO}_4$, NaH_2PO_4 , KH_2AsO_4 , $\text{NH}_4\text{H}_2\text{AsO}_4$, $\text{Ag}_3\text{H}_3\text{IO}_6$ and $(\text{NH}_4)_2\text{H}_3\text{IO}_6$ and of their deuterated analogues have been recorded at room temperature and some of them also at low temperature in the ferroelectric phase. The interpretation of the particularly interesting spectral region between 3000 and 1500 cm^{-1} , containing several OH bands, has been made in terms of the tunnelling of the protons between two minima of potential energy. These were taken to be of equal depth in the non-ferroelectric phase and unsymmetrical in the ferroelectric form. A quantum-mechanical treatment of the vibrational problem of the latter type has been carried out and is presented in the Appendix. Good agreement has been found between the theoretically predicted energy levels and the experimental data.

1. INTRODUCTION

The vibrational spectra of potassium dihydrogen phosphate and of related compounds exhibiting ferroelectric or antiferroelectric properties at certain temperatures and containing short hydrogen bonds present a very interesting problem in view of the possibility of detecting the spectroscopic effects of the tunnelling of the protons and relating this to the phenomenon of spontaneous polarization. When mentioning the tunnelling, we mean by it not only the penetration of the potential barrier by the particles, but primarily the resonance splitting of the vibrational levels which takes place even if the barrier is actually lower than the zero vibrational level. So far, there has been only one experimental proof of the existence of tunnelling in the phosphates and arsenates, and this is from proton magnetic resonance work [1]. From the neutron diffraction work of Bacon and Pease [2] it appears very probable that the protons participating in the strong hydrogen bonds of the tetragonal (non-ferroelectric) form are evenly distributed among two positions on the line connecting two oxygen atoms, indicating a potential field with two equally deep minima of energy and the possibility of tunnelling. The alternative interpretation of the results by assuming a potential field with a broad central trough and the protons exhibiting a large anisotropic thermal motion cannot be eliminated on the grounds of the diffraction data only. The diffraction data of the single domain crystals of the ferroelectric phase indicate clearly an uneven distribution of the protons along the line connecting the oxygens, and hence a potential field with two unequal potential minima, or a single one. The spectral consequences of potential fields with a single minimum or two minima respectively are different, and therefore the spectra should help in deciding about the form of the potential function

† Present address : Institute J. Stefan, Ljubljana.

governing the motions of the protons. Although vibrational spectra of phosphates and arsenates have been studied by several authors, the tunnel effect has been either disregarded or rejected in the interpretation of the spectra. Only in a very recent paper by Lazarev [3] which came to our attention during the preparation of this manuscript, is the interpretation of some bands in the spectrum of potassium dihydrogen phosphate in the non-ferroelectric phase based on the tunnel effect.

In this paper some new experimental data on the infra-red absorption of potassium, ammonium and sodium dihydrogen phosphates, potassium and ammonium dihydrogen arsenates, and of ammonium and silver trihydrogen periodates will be presented. For sake of brevity, these compounds will be henceforth designated in respect KHP, AHP, NaHP, KHAs, AHAs, AHIO, AgHIO. Some of the deuterated analogues were prepared and their spectra studied (H replaced by the D in the designations). The spectra of the compounds were recorded both at room temperature and below the Curie points, as far as this was possible. The assignments of the important bands will be made in terms of the proton tunnelling between two minima of potential energy. A comparison between the measured frequencies and the energy levels predicted by a quantum-mechanical treatment of the problem will be made.

2. EXPERIMENTAL DATA

Infra-red spectra of KHP, KDP [3, 13, 14, 15] and AHP have been already published, some in absorption and some in reflection [15]. Raman spectra have also been published in several instances [16, 17, 18]. The presently measured band frequencies are collected in Table 1 and supplemented by Raman data from other authors. The spectra are reproduced in figures 1-7.

The structure of potassium dihydrogen phosphate, the best-known representative of this group of compounds, is well known from the x-ray [4] and neutron diffraction analysis [2]. The structure of ammonium dihydrogen phosphate has been studied by both techniques [5]. For ammonium and potassium dihydrogen arsenate crystals only the symmetry and the cell dimensions are known [6]. All these crystals are isomorphous, belonging to the tetragonal symmetry at room temperature. Below the Curie point, which has been determined for all these compounds, a transition to the orthorhombic symmetry takes place. The O . . . O distance in KHAs has been quoted in connection with other work [7]. The ammonium and silver periodates are rhombohedral. The structure of the first compound has been determined by Helmholtz [8], but this was questioned by Gränicher *et al.* [9] who have studied also the structure of AgHIO. The crystals of sodium dihydrogen phosphate (NaHP) have monoclinic symmetry [10, 11], and they are not known to exhibit either ferro- or antiferroelectric properties. This compound has been included in the present study because of the spectral similarities with KHP and particularly with KDP which crystallizes from heavy water at first in the monoclinic symmetry, changing later to the tetragonal symmetry [12].

3. RESULTS AND DISCUSSION

3.1. The region 3000 to 1500 cm^{-1}

All the substances investigated show at least three bands in this region; the change of frequency of these bands upon deuteration proves that they are due

	KHP	KDP	AHP	ADP	NaHP	NaDP	KHAs	KDAs	AHAs	AHl _o	AgHl _o	AgDl _o
ν_3 NH ₄ (ND ₄)	—	—	3210	2350	—	—	—	—	3200	3140	—	—
ν_1 NH ₄ (ND ₄)	—	—	3080	2250	—	—	—	—	2820(?)	3040	—	—
ν OH(OD)	2750	2050	2850	1950	2900	2100	2700	—	2200(?)	2650	2560	1980
ν' OH(OD)	2400	1770	2350	1750	2400	1780	2350	—	1940	2300	2150	1690
ν_2 NH ₄ (ND ₄)	—	—	—	—	—	—	—	—	1720	1750	—	—
δ OH(OD)	1580	1200	~1600	1280	1650	1200	1680	—	1540	—	1540	1370
ν_4 NH ₄ (ND ₄)	—	—	1440	1155	—	—	—	—	1460	1420	—	—
			1440						1400			
γ OH(OD)	1300	942	1280	940	1300	910	1290	—	1175	1170	1160	805
ν_3 XO ₄ (IO ₆)	{ 1118 1080 1040 }	{ 1118 1080 1041 }	{ — 1090 1030 }	{ — 1100 — }	{ 1160 1040 975 }	{ 1140 1040 975 }	{ — 862 — }	{ 873 862 837 }	{ 870 840 810 }	{ 700 580 — }	{ 700 596 — }	{ 805 690 — }
ν_1 XO ₄	{ 920 490 }	{ 912 500 }	{ 890 — }	880	930	930	734	—	740	—	—	—
ν_2 XO ₄	{ 465 450 }	{ 490 490 445 }	r.n.i.†	r.n.i	r.n.i	r.n.i	415	410	r.n.i	—	—	r.n.i
ν_4 XO ₄ (IO ₆)	526	524	—	—	—	—	375	365	—	{ 468 427 413 }	{ 458 420 ? }	—

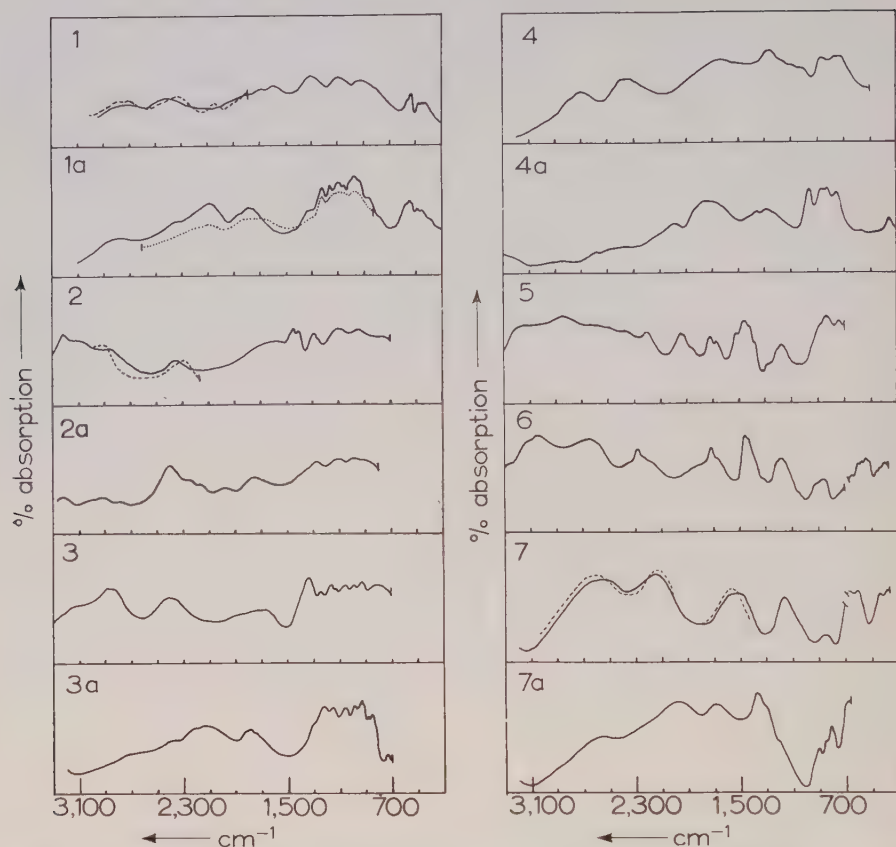
† Region not investigated.

Table 1 (a). The absorption frequencies and proposed assignments for the infra-red bands of dihydrogenphosphates, dihydrogenarsenates, and trihydrogenperiodates.

ν OH	KHP		AHP		ν' OH	KHP		AHP	
	{ 2500 [16, 17]		2600 [16]	2650 [18]		2700 [16]	2800 [17]	2800 [16]	2840 [18]

Table 1 (b). Raman frequencies of OH stretching bands.

The substances investigated were either good commercial samples or were prepared by standard methods. The deuterated analogues were prepared by recrystallization from 99.6 per cent deuterium oxide, except for the AgDl_o. This was prepared by precipitation of a solution of AgNO₃ in D₂O with a similar solution of previously deuterated periodic acid. Most of the spectra were recorded with a Perkin Elmer Mod. 21 infra-red spectrophotometer, equipped with a NaCl prism. The substances were milled with paraffin oil and hexachlorobutadiene respectively. The low temperature runs were made using a vacuum-jacketed cell of conventional design and liquid nitrogen as coolant. The temperatures were measured with a copper-constantan thermocouple inserted close to the AgCl plates which served as a support for the mulls.



Figures 1-7. Infra-red spectra of some ferroelectric and related compounds (drawings combined from original records of samples mulled with Nujol and hexachlorobutadiene, respectively. Region 3300 to 700 cm^{-1} recorded with a NaCl prism, region 700 to 300 cm^{-1} with KBr and CsI prisms). 1. KH_2PO_4 (full line : room temperature, dashed : cooled with liquid N_2); 1a. KD_2PO_4 (full line : monoclinic, dotted : tetragonal); 2. $\text{NH}_4\text{H}_2\text{PO}_4$ (full line : room temperature, dashed : cooled with liquid N_2); 2a. $\text{ND}_4\text{D}_2\text{PO}_4$; 3. NaH_2PO_4 ; 3a. NaD_2PO_4 ; 4. KH_2AsO_4 ; 4a. KD_2AsO_4 ; 5. NH_4AsO_4 ; 6. $(\text{NH}_4)_2\text{H}_3\text{IO}_6$; 7. $\text{Ag}_2\text{H}_3\text{IO}_6$ (full line : room temperature, dashed : cooled with liquid N_2); 7a. $\text{Ag}_2\text{D}_3\text{IO}_6$.

to vibrations involving the protons. The additional bands at 3000–3200 cm^{-1} and 1690 cm^{-1} in the compounds containing the ammonium ion can immediately be assigned to its vibrations and are without further interest. The present results are only in limited agreement with the ones reached by previous authors. Thus La Lau [13] does not mention the band at 2360 cm^{-1} in the spectrum of KHP. Rundle and Parasol [14] and Murphy and Weiner [15] list the latter band whereas they do not seem to have noted the band at 2793 cm^{-1} . With KDP and some other substances the situation is similar : the present investigation has revealed bands which were previously not described.

Of particular interest are the changes accompanying the transition below the Curie point. They consist in relatively small shifts of the bands without pronounced narrowing. There are indications of some bands being split up—e.g. the former band near 2800 cm^{-1} in KHP now shows maxima at 2800 and 2750 cm^{-1}

—but it is not certain whether this splitting is introduced by the transition or whether it was present also in the tetragonal form and became more pronounced on cooling owing to some narrowing of the components. The second alternative is more plausible in view of the fact that two components of the absorption band near 2340 cm^{-1} were observable in the reflection spectra [15].

The following discussion of the hydroxyl vibrations has to be necessarily based on a very simple model in order to enable us to do some quantitative theoretical calculations and to compare them subsequently with the spectroscopic results. The model is that of an isolated oscillator, consisting of a proton on the line connecting two oxygen atoms. For the case of a single symmetric potential minimum, there is a single infra-red OH band to be expected in this region, corresponding to an asymmetric stretching motion. This vibration is Raman inactive. For the case of a double minimum and a large separating barrier, the effective symmetry would be C_{2v} , allowing for a single vibration active both in Raman and infra-red. With a sufficiently small potential barrier the influence of the tunnelling of the proton becomes perceptible by causing a splitting of the vibrational levels. This gives rise to two infra-red and two Raman active bands, as will be shown later. The splitting depends on the mass of the tunnelling particle and on the area under the potential barrier and can be obtained by solving the Schrödinger equation for the general case and inserting appropriate parameters. The treatment is different according as the minima of potential energy are equal or unequal. The equations for the case of two equally deep minima have been already developed and the numerical values for the splitting of the vibrational energy levels have been given for nearly all the physically probable parameters [19]. However, the selection rules were not given in that paper and this will be done here. Table 2 presents the matrix of dipole transitions for a double minimum potential field. Here M_{mn} is equal to $\int \phi_m M \phi_n d\tau$, M being the dipole moment operator of the whole system and ϕ a linear combination of wave functions for the case of the single minimum field.

$$||M|| = \begin{vmatrix} 0 & M_{12}e^{-i\omega_{12}t} & 0 & M_{14}e^{-i\omega_{14}t} & \vdots \\ M_{21}e^{i\omega_{21}t} & 0 & M_{23}e^{-i\omega_{23}t} & 0 & \vdots \\ 0 & M_{32}e^{i\omega_{32}t} & 0 & M_{34}e^{-i\omega_{34}t} & \vdots \\ M_{41}e^{i\omega_{41}t} & 0 & M_{43}e^{i\omega_{43}t} & 0 & \vdots \\ \dots & \dots & \dots & \dots & \vdots \end{vmatrix}$$

Table 2. Matrix of dipole transitions for a double minimum potential field.

Transitions M_{13} , M_{24} , M_{14} and M_{23} are expected in the region between 3000 and 1800 cm^{-1} . In the case of a symmetrical, isolated system the transitions M_{23} and M_{14} are allowed in absorption, but forbidden in scattering, whereas the opposite is true for the transitions M_{13} and M_{24} . This is shown schematically in figure 8. These selection rules are valid only for the case of the isolated symmetrical oscillator. Vibrational coupling may lead to a violation of the rules and the subsequent appearance of all four bands. With the minima unequally

deep, the four transitions become allowed in absorption. The general solutions and the numerical calculations for this case are given in the Appendix.

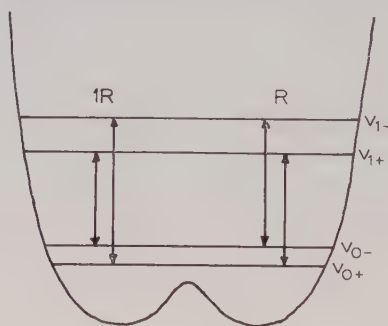


Figure 8. Schematic representation of infra-red and Raman-active transitions in a symmetric double minimum potential field.

Our task is now to analyse the multiple OH bands observed in the light of the foregoing predictions. First of all, it should be emphasized that the diffraction data show the equality of all hydrogen bonds and therefore the multiple OH bands cannot be due to different types of bond. Assuming a potential field with one symmetric minimum, some of the bands might be due to overtones or to combinations. As to the latter, difference tones especially may be excluded at once by the results of cooling of the samples: this did not cause any notable reduction in the relative intensity of one of the bands. In general, it is very unlikely that different substances with different symmetries and large variations in the frequencies of the XO_4 and IO_6 ions and also of the OH deformation vibrations could have so similar combination frequencies. The next possibility of accounting for the multiple bands is the coupling of OH vibrators. The lowest frequency band (near 1600 cm^{-1}) seems to be too far removed from the others to be accounted for by this mechanism, but anyway this band probably belongs to an OH deformation vibration, as will be shown later. Even so, the splitting shown by the remaining two bands seems to be too large to be caused by the vibrational coupling of the two OH and three OH groups in a phosphate or arsenate and periodate molecule respectively. Again, it is hardly possible that the splitting would be so similar in compounds differing in as much molecular and crystal structure as the phosphates and arsenates on one hand and the periodates on the other. Similar arguments may be advanced against the supposition that the splitting is caused by interactions in the unit cell of the crystals. Some other arguments against these possible origins of the multiple OH bands will be found later on amongst the arguments favouring the tunnel effect as the probable cause.

The tunnel effect, on the other hand, offers a good explanation for the appearance of two pairs of both infra-red and Raman frequencies. In particular, the Raman lines should show the same type of polarization and this is borne out by experiment [17]. Data for the infra-red absorption dichroism are unfortunately lacking and the reflection data [15] are of no help as the band near 2800 is missing from them. A good argument is offered by the comparison of the splitting in the infra-red and Raman spectra, respectively, the latter being consistently smaller in all cases observed, as required by theory.

In Table 3 the calculated band positions and splittings are compared with the spectroscopically determined ones. The agreement is good for the undeuterated compounds and also the expected reduction of the splitting due to the increase of mass of the tunnelling atom is borne out. The general trends

	KHP	KDP	KHAs	KDAs
q	2.23	2.27	2.27	2.32
$E_{1-}(\text{cm}^{-1})$	4090	2986	3966	3863
$E_{1+}(\text{cm}^{-1})$	3710	2756	3606	2693
$E_{0-}(\text{cm}^{-1})$	1326	975	1287	943
$E_{0+}(\text{cm}^{-1})$	1274	938	1237	909
$\Delta\nu$ (meas.)	382	273	410	204
$\Delta\nu$ (calc.)	400	270	360	226

Table 3. Calculated OH and OD vibrational levels.

of these splittings certainly favour the tunnel effect as the cause of splitting, but the numerical agreements, although good, are not a proof by themselves. The splitting is a function of the dimensionless parameter q [19], equal to $\sqrt{4\pi^2 m \nu l^2 / h}$, where m is the mass of the vibrator, ν the mean frequency, and $2l$ the distance between the two minima. The error in the calculation of the splitting falls approximately with $\exp(-q^2)$. The uncertainties in the position of the proton give rise to rather a large latitude in the splittings.

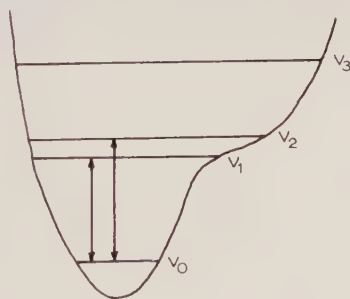


Figure 9. Anharmonic potential function exhibiting an apparent doubling of the ν OH bands.

Dr. Bratož (Centre de Chimie Théorique, Paris) has drawn our attention to a special case of an anharmonic potential function which is shown schematically in figure 9. It can be seen from the vibrational levels indicated there that the $v_0 \rightarrow v_1$ and $v_0 \rightarrow v_2$ transitions are close together and might give rise to two bands in the fundamental stretching region, giving the impression of a splitting. Calculations with this model give the proper frequencies using reasonable parameters, but show that the increase in the mass of the vibrator leads to an increase of the apparent splitting if the difference between v_1 and v_2 does not exceed 1000 cm^{-1} . Hence this type of potential function does not fit the present experimental facts.

The assumption of a single minimum potential function implies a fair amount of lengthening of the OH bonds (up to 0.2 \AA [3]) at the transition to the low

temperature form. According to the bond length-vibration frequency relation of Badger [20] the OH stretching frequency would have to increase as much as 60 per cent because of this lengthening. Similarly, Lippincott and Schroeder's [21] model yields a frequency increase of 400 cm^{-1} . No such changes, but only much smaller shifts were in fact observed. On the other hand, no significant change in the bond distances is implied by the double minimum model. The main change results from imposing an asymmetry on the depth of the minima. Following the theoretical treatment of this model, given in the Appendix, we have calculated the matrix elements and the energy levels taking $q=2.273$, $\nu_0=2600\text{ cm}^{-1}$, and $B=100\text{ cm}^{-1}$. The asymmetry parameter B is equal to $2elF \cos \theta$ and its assumed value has been obtained by considering both the geometrical arrangement of the atoms in KHP combined with dielectric data, and also the neutron diffraction intensity data. The estimate of the distribution of the protons between the two unequally deep minima of potential energy ($N_2/N_1=\exp(B/kT)=9:1$ at 77°K) has been communicated to us by Dr. G. E. Bacon (Harwell), to whom our thanks are due. The results are summarized in Tables 4 and 5. For comparison, the results obtained with $B=0$, i.e. the symmetrical double minimum, have been added.

$v=0$		$v=1$	
$B=100\text{ cm}^{-1}$	$B=0$	$B=100\text{ cm}^{-1}$	$B=0$
$H_{11}^0 = 0.49946\text{ }h\nu_0$	$0.49944\text{ }h\nu_0$	$H_{11}^1 = 1.49217\text{ }h\nu_0$	$1.49212\text{ }h\nu_0$
$H_{22}^0 = 0.53787\text{ }h\nu_0$	$0.49944\text{ }h\nu_0$	$H_{22}^1 = 1.53053\text{ }h\nu_0$	$1.49212\text{ }h\nu_0$
$\beta^0 = -0.00435\text{ }h\nu_0$	$-0.00446\text{ }h\nu_0$	$\beta^1 = -0.01788\text{ }h\nu_0$	$-0.01890\text{ }h\nu_0$
$S^0 = 0.00570$	0.00570	$S^1 = -0.05324$	-0.05324

Table 4.

We see that even for a relatively large value of the asymmetry parameter B the changes produced in the ν_{OH} bands (Table 3) in going from the non-symmetrical ferroelectric to the symmetrical form of the potential field are small and in view of the broadness of ν_{OH} bands ($\sim 300\text{ cm}^{-1}$ in strongly H-bonded crystals) hardly recognizable. It follows from this calculation that the mean frequency of the two bands does not change significantly on going from the symmetrical double minimum potential to the asymmetrical one. This is borne out by experiment and appears particularly clearly in the case of AgHfO where the higher frequency band shifts by 40 cm^{-1} to still higher frequencies on cooling, and the other band by 50 cm^{-1} to lower frequencies, the mean value being thus practically unchanged.

So far, it has been assumed that the band appearing between 1550 and 1700 cm^{-1} was due to the OH bending vibration. An alternative to this assignment would be to consider it as one of the four OH stretching bands, two other ones being those discussed previously and the fourth missing for some reason. Four bands could be infra-red active if the selection rules valid for the isolated tunnelling system were broken. The large splitting (1225 cm^{-1}) would be possible if the O...O distance and the O-H bond length are such that $2l$ is 0.30 \AA which is still within the limits given by the neutron diffraction work [2]. A strong argument against this possibility is the fact that there should be Raman lines

near 2050 and 2400 cm^{-1} , which is contrary to observation. Also, there should be a band at 400 cm^{-1} corresponding to the $\nu_{0+} \leftrightarrow \nu_{0-}$ transition and this is also not borne out by the experimental results. On the other hand, the deuteration shift from 1540 to 1370 cm^{-1} , which is particularly clearly observed with AgHIO and AgDIO respectively, is in good agreement with the assignment to the OH and OD bending modes. The splitting of the OH bending modes due to the tunnelling is expected to be very small as the vibration is nearly perpendicular to the O . . . O line and thus may escape observation.

Transition type	Frequency	
	$B = 0$	$B = 100 \text{ cm}^{-1}$
$\nu_{0-} \leftrightarrow \nu_{1+}$	2405 cm^{-1}	2360 cm^{-1}
$\nu_{0+} \leftrightarrow \nu_{1-}$	2761 cm^{-1}	2810 cm^{-1}

Table 5.

In some cases, e.g. the spectrum of KHAs, the band near 1600 cm^{-1} is strongly broadened out and gives the impression of being actually coincident with the beginning of a strong background absorption which is extending out to about 600 cm^{-1} and which is interrupted by bands of greater transmission close to the distinct absorption bands, as in the Christiansen effect. This background interrupted by transmission bands has been observed in this laboratory in the spectra of several substances containing extremely strong hydrogen bonds. We shall reserve the discussion of the origin of this absorption for a separate paper as it is of a more general character.

3.2. The region below 1500 cm^{-1}

3.2.1. The phosphates and the arsenates

This region contains a few very broad bands some of which are affected by deuteration proving thus their relationship with the OH and NH_4 vibrations, respectively. The frequencies of these bands are reproduced in Table 1. The correlation of the OH and OD bands seems to be straightforward, one exception being perhaps the bands near 1300 cm^{-1} in the spectra of KHAs and KDAs. It might be assumed that deuteration does not cause the band at 1290 to shift at all. However, besides putting this substance in a very special position in relation to the others in this group, this hypothesis leaves the band at 942 cm^{-1} without any analogue in the spectrum of the undeuterated substance. Therefore it is assumed that the δ OH band shifts from 1575 cm^{-1} to 1295 cm^{-1} on deuteration whereas the former 1295 cm^{-1} band appears at 942 cm^{-1} after deuteration. The deformation frequencies appear to be high, in general, but this is not unexpected in view of the strong hydrogen bonding.

The remaining bands must be due to the vibrations of the XO_4 ions ($\text{X} = \text{P}$ and As , respectively). The selection rules for these ions, having approximately the symmetry T_d and occupying S_4 sites, have been discussed by Murphy *et al.* [15] and the proposed assignments of the bands are given in Table 1 with the presently measured frequencies. The selection rules valid for the proposed site group S_4 are, of course, valid if no distortion of the XO_4 tetrahedra by the

protons occurred. Such slight distortions are, however, apparent from the diffraction measurements [2, 3] and this may explain the indicated splitting of the band at 1100 cm^{-1} , the degeneracy of the ν_3 vibration being lifted. This may also be the cause of the very slight change on going to the low temperature monoclinic form of KHP and AHP. Here, the molecular and the site groups are C_{2v} and C_2 respectively, with all degeneracies lifted. In this connection it is interesting to note that the band near 1100 cm^{-1} in the monoclinic form of KDP (obtained immediately after crystallization from D_2O and without seeding with crystals of the tetragonal form) and in NaHP shows three distinct peaks. They are evidently due to the removal of the degeneracy of the ν_3 vibration.

When the same sample of KDP was examined a week later, the spectrum had reverted to the shape characteristic of the tetragonal form, the three peaks near 1100 cm^{-1} being smoothed out to a single band. There is a band in the spectra of the phosphates and the arsenates at slightly lower frequencies than the OH deformation band (near 1240 cm^{-1}) which shows up more distinctly after deuteration as well as in reflection spectra [15], but its origin is not clear. The assignment (Table 1) of the ν_2 and ν_4 modes of the XO_4 ions has been made according to Kohlrausch (quoted by Herzberg [22, p. 167]). The frequencies have been recalculated and a satisfactory agreement found with the observed ones, whereas Murphy *et al.* [15] do not give any particular reason for their assignment.

3.2.2. The periodates

The bands due to the OH bending motions are well pronounced here and have been already mentioned in connection with the previous group. We cannot discuss in detail the bands due to the IO_6 ion because no Raman data are available. The free ion belongs to the O_h point group and has 15 normal modes. Two of them are allowed in absorption, both being of the F_{1u} type and are triply degenerate [22]. We identify tentatively the broad band with several peaks extending between 700 and 590 cm^{-1} in the spectra of AgHIO and AHIO with the ν_3 vibration. The spectrum of AgHIO shows another complex band with peaks at 458 and 420 cm^{-1} (probably one more peak at still lower frequencies) and similarly AHIO ($468, 427, 412\text{ cm}^{-1}$). It is suggested that these bands are due to the ν_4 vibration, the separate peaks arising from the lifted degeneracy. The weak band at 830 cm^{-1} of AgHIO and at 850 cm^{-1} in AHIO may be due to some combination frequency.

Some comments have to be made on the individual compounds and their spectra. There is a band appearing at 2050 cm^{-1} in the spectrum of the orthorhombic form of KHP. It might be supposed that this is one of the OH transitions becoming allowed in the lower symmetry form. If this were true, it should be observed also in the Raman spectrum and probably also with other compounds. However, this is not the case and therefore we believe rather that this band is due to some combination tone and becomes better pronounced at low temperatures.

The absorption at 2280 cm^{-1} in the spectrum of AHIO seems to be composed of two bands, a broader one underlying a sharper peak with the frequency quoted. The broader band is probably one of the ν OH frequencies, the sharper one being due either to the NH_4 ion or to a combination frequency.

The OH bands of AHAs fall somewhat out of the region occupied by the other compounds, their frequencies being 1950 and 2200 cm^{-1} . The broad

band extending from 2400 to 3200 cm^{-1} probably contains the NH_4 stretching modes. It is possible that the broadness and composite character of this absorption is due to some particular hydrogen bonds between the hydrogens of the NH_4 ion and the arsenate group. This assignment is tentative only in view of the lack of Raman and precise structural data. The unusually low frequency of the OH bands might be connected with the large difference in Curie points of KHAs and AHAs. Whereas there is not a great difference in the Curie points of KHP and AHP, the latter being 25° higher, KHAs and AHAs differ by as much as 120° . This indicates that the hydrogen bond system in AHAs must be somewhat different from the rest of the compounds. It is also interesting to note that the ν_2 vibration of the NH_4 ion appears in absorption in the spectra of AHAs and of AHIO whereas this does not happen with AHP. The appearance of the band at 1690 cm^{-1} indicates some departure from the T_d symmetry of the ammonium ion.

For the calculation of the energy level splittings reliable geometrical parameters are required. Unfortunately, they seem to be available only for KHP. The O...O distances given for AHP [5] and also for KHAs [7] seem to be too long in view of the low OH frequencies. For this distance in AHIO a value of 2.6 Å has been advanced [8] but this seems to be definitely too large.

4. CONCLUSIONS

The problem upon which this investigation is mainly centred is the type of the potential field determining the behaviour of the protons. The fact that the low temperature transition causes but a very small change in the OH stretching bands can be explained only by the existence of the double minimum potential, symmetric at temperatures above the Curie point and becoming unsymmetric below the transition temperature. The quantitative agreement between the calculated and the observed energy level splittings is of minor importance as it can be achieved by the selection of geometrical parameters within the limits set by the diffraction data.

A knowledge of the nature of the potential function in the hydrogen bonded ferroelectrics enables one to calculate in several ways by quantum-mechanical methods the polarization properties of hydrogen bonded systems. Each of these ways leads to the result that the Curie point depends on a certain power of the mass of the moving particle. The power itself depends on the anharmonicity of the hydrogen bond system. The details of these calculations will be published in a subsequent paper.

The authors are grateful to the Boris Kidrič Fund for some financial assistance, to M. Jean Lecomte (Paris) and Mr. D. Jeremic (Beograd) for having recorded the spectra in the low frequency region, and to Mr. L. Golič for the preparation of the arsenates and the periodates.

APPENDIX

The quantum-mechanical problem in which the potential field possesses two symmetrical minima has been treated by various authors; but the case of two unequally deep valleys has been treated only once [23] by the WKB method, which is not appropriate for the case of relatively small energy barriers.

For the one-dimensional case the Hamiltonian is

$$H = -\frac{\hbar^2}{2m} \frac{d^2}{dx^2} + V,$$

where the potential energy operator V is given by $V = V_1 = \frac{1}{2}k_1(x+l)^2$, for $-\infty < x < b$ and $V = V_2 = \frac{1}{2}k_2(x-l)^2 + B$, for $b < x < \infty$ with $b = B/2kl$.

$2l$ is the distance between the two minima and k is a force constant. For convenience and because we were primarily interested in O-H . . . O bonds we have put k_1 equal to k_2 . The coordinates of the point of intersection of V_1 and V_2 are:

$$[B/2kl, \frac{1}{2}k(B/2kl+l)^2].$$

Acceptable wave functions are constructed by linear combination of ψ_1^0 and ψ_2^0 , where ψ_1^0 and ψ_2^0 are normalized solutions of wave equations for V_1 and V_2 separately. With the help of the variation principle we obtain:

$$\begin{vmatrix} H_{11} - E & H_{12} - ES \\ H_{21} - ES & H_{22} - E \end{vmatrix} = 0. \quad (1)$$

The symbols used for the matrix components have their usual significance:

$$\begin{aligned} H_{11} &= \int_{-\infty}^{+\infty} \psi_1^0 H \psi_1^0 dx, \quad H_{22} = \int_{-\infty}^{+\infty} \psi_2^0 H \psi_2^0 dx \\ \beta &= H_{21} = H_{12} = \int_{-\infty}^{+\infty} \psi_2^0 H \psi_1^0 dx \\ S &= S_{21} = S_{12} = \int_{-\infty}^{+\infty} \psi_1^0 \psi_2^0 dx. \end{aligned}$$

The rigorous solution of (1) may be found by expanding the secular determinant and solving the resulting quadratic equation:

$$\begin{aligned} E_{\pm} &= \frac{1}{2(1-S)^2} [(H_{11} + H_{22} - 2\beta S) \\ &\quad \pm \sqrt{(H_{11} + H_{22} - 2\beta S)^2 - 4(1-S)^2(H_{11}H_{22} - \beta^2)}]. \end{aligned} \quad (2)$$

The matrix components for the ground ($v=0$) and the first excited vibrational level ($v=1$) are calculated as functions of two parameters q and $B/h\nu_0$ and are summarized below:

$$\begin{aligned} H_{11}^0 &= \frac{1}{2}h\nu_0 \left\{ 1 + \frac{B}{h\nu_0} \left[1 - \phi \left(q + \frac{B}{h\nu_0} \cdot \frac{1}{2q} \right) \right] + 2q^2 \left[1 - \phi \left(q + \frac{B}{h\nu_0} \cdot \frac{1}{2q} \right) \right] \right. \\ &\quad \left. - \frac{2q}{\sqrt{\pi}} \exp \left[- \left(q + \frac{B}{h\nu_0} \cdot \frac{1}{2q} \right)^2 \right] \right\}, \\ H_{22}^0 &= \frac{1}{2}h\nu_0 \left\{ 1 + \frac{B}{h\nu_0} \left[1 + \phi \left(q - \frac{B}{h\nu_0} \cdot \frac{1}{2q} \right) \right] + 2q^2 \left[1 - \phi \left(q - \frac{B}{h\nu_0} \cdot \frac{1}{2q} \right) \right] \right. \\ &\quad \left. - \frac{2q}{\sqrt{\pi}} \exp \left[- \left(q - \frac{B}{h\nu_0} \cdot \frac{1}{2q} \right)^2 \right] \right\}, \\ H_{11}^1 &= \frac{1}{2}h\nu_0 \left\{ 3 + 2q^2 \left[1 - \phi \left(q + \frac{B}{h\nu_0} \cdot \frac{1}{2q} \right) \right] + \frac{B}{h\nu_0} \left[1 - \phi \left(q + \frac{B}{h\nu_0} \cdot \frac{1}{2q} \right) \right] \right. \\ &\quad \left. - \frac{4q}{\sqrt{\pi}} \exp \left[- \left(q + \frac{B}{h\nu_0} \cdot \frac{1}{2q} \right)^2 \right] \right\}, \\ H_{22}^1 &= \frac{1}{2}h\nu_0 \left\{ 3 + 2q^2 \left[1 - \phi \left(q - \frac{B}{h\nu_0} \cdot \frac{1}{2q} \right) \right] + \frac{B}{h\nu_0} \left[1 + \phi \left(q - \frac{B}{h\nu_0} \cdot \frac{1}{2q} \right) \right] \right. \\ &\quad \left. - \frac{4q}{\sqrt{\pi}} \exp \left[- \left(q - \frac{B}{h\nu_0} \cdot \frac{1}{2q} \right)^2 \right] \right\}, \end{aligned}$$

$$\begin{aligned}\beta^0 &= \frac{1}{2} h\nu_0 \left\{ 1 + \frac{B}{h\nu_0} \left[1 - \phi \left(\frac{B}{h\nu_0} \cdot \frac{1}{2q} \right) \right] \right. \\ &\quad \left. - \frac{2q}{\sqrt{\pi}} \exp \left[- \left(\frac{B}{h\nu_0} \cdot \frac{1}{2q} \right)^2 \right] \right\} \exp(-q^2), \\ \beta^1 &= \frac{1}{2} h\nu_0 \left\{ 3(1-2q^2) - \frac{B}{h\nu_0} (1-2q^2) \left[1 - \phi \left(\frac{B}{h\nu_0} \cdot \frac{1}{2q} \right) \right] \right. \\ &\quad \left. - \frac{4q}{\sqrt{\pi}} (1-2q^2) \exp \left[- \left(\frac{B}{h\nu_0} \cdot \frac{1}{2q} \right)^2 \right] \right\} \exp(-q^2), \\ S^0 &= \exp(-q^2), \\ S^1 &= (1-2q^2) \exp(-q^2),\end{aligned}$$

$$\phi(q) = \frac{2}{\sqrt{\pi}} \int_0^q \exp(-t^2) dt, \quad q^2 = \frac{4\pi^2 m\nu_0 l^2}{h}.$$

For the case of the symmetrical double minimum ($B=0$) the rather complicated energy level expression (2) goes over into simpler ones, which have been obtained and calculated for several values of the parameter q in a preceding paper [19].

In the case of high potential barriers we may put for a qualitative discussion the overlap integral $S=0$ and $H_{11}=E_1^0$, $H_{22}=E_2^0$, where E_1^0 and E_2^0 are unperturbed energy level values.

The secular determinant (1) reduces to

$$\begin{vmatrix} E_1^0 - E & \beta \\ \beta & E_2^0 - E \end{vmatrix} = 0.$$

From this we obtain for the perturbed energy levels:

$$E_{\pm} = \bar{E} \pm \frac{1}{2} \sqrt{(4\beta^2 + B^2)} \quad (3)$$

where $\bar{E} = \frac{1}{2}(E_1^0 + E_2^0)$ is the mean of the unperturbed levels and $B = E_1^0 - E_2^0$ is the separation of the unperturbed levels. It may be noted that equation (3) is formally the same as that obtained in the case of Fermi resonance, where the perturbations are due to the anharmonic terms in the potential energy function. Formula (3) shows that there is no perturbation and hence no splitting if the exchange integral β is 0 or $\ll B$. In this case we have two different chemical species with separated sets of energy levels. If $B=0$, the splitting of the energy levels is in this approximation equal to twice the value of the exchange integral.

If we plot the position of the perturbed levels for a constant β and \bar{E} as a function of B (the separation of the unperturbed levels) we obtain a hyperbolic curve. The shift produced by the perturbation is given by the vertical distance between two points at $B = \text{const.}$, one being on the full heavy curve and the other on the broken line asymptote, which represents the unperturbed level. We see that the shift caused by the perturbation (but not the total splitting) is the largest for $B=0$.

The eigenfunctions of the two resulting states E_{\pm} are mixtures of the zero order eigenfunctions ψ_1^0 and ψ_2^0 :

$$\begin{aligned}\phi_1 &= C_1 \psi_1^0 - C_2 \psi_2^0 \\ \phi_2 &= C_2 \psi_1^0 + C_1 \psi_2^0\end{aligned}$$

where

$$C_1 = \left[\frac{\sqrt{4(\beta^2 + B^2)} + B}{2\sqrt{4(\beta^2 + B^2)}} \right]^{1/2} \quad \text{and} \quad C_2 = \left[\frac{\sqrt{4(\beta^2 + B^2)} - B}{2\sqrt{4(\beta^2 + B^2)}} \right]^{1/2}. \quad (4)$$

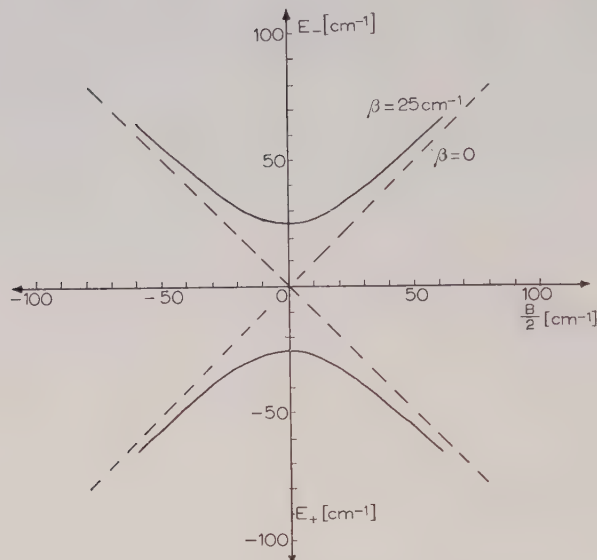


Figure 10. Energy level splitting as a function of the unsymmetry parameter B for $\bar{E}_0=0$ and $\beta=25\text{ cm}^{-1}$.

If $B=0$ or small as compared to β we obtain from (4) a 1:1 mixture ($C_1=C_2=1/\sqrt{2}$). If B is large as compared to β there is no mixing any more: ($C_1\rightarrow 1$, $C_2\rightarrow 0$) and $\phi_1\rightarrow\psi_1^0$ as well as $\phi_2\rightarrow\psi_2^0$.

In this approximation neglecting interactions, which are the reason for additional splitting of energy levels, we may expect from the selection rules in the case $B=0$ two, and in the case $B\neq 0$ four, infra-red absorption bands in the 3μ region due to proton vibrations. In the non-symmetrical case in which $B\gg\beta$ we may expect that the molecules behave as belonging to two different chemical species. Only if the separation of energy levels is equal in both minima or if the proportion of the protons or deuterons transferred to the higher minima is not large enough to give rise to another absorption band, we may expect in this case only one ν_{OH} band.

Nous avons étudié les spectres infrarouges des biphosphates potassique, ammonié et sodique, des bisarsénates potassique et ammonié, ainsi que des periodates diargenté et diammonié. L'étude est complétée par les spectres des analogues deutérés et des spectres de quelques de ces substances prises à basse température, sous le point de transition en phase ferroélectrique. L'interprétation des spectres dans la région entre 3000 et 1500 cm^{-1} , particulièrement intéressante à cause des bandes OH multiples lesquelles y apparaissent, a été faite à la base du tounellement des protons entre deux minima de l'énergie potentielle. La fonction potentielle serait symétrique pour la phase non-ferroélectrique tandis qu'elle se présenterait sous forme non-symétrique pour la modifications à basse température. Un traitement quantique du problème vibrationnel concernant la fonction potentielle assymétrique est présenté dans l'Appendice. La comparaison des fréquences calculés et mesurés des bandes ν_{OH} est satisfaisante.

Die Infrarotspektren von Kalium und Ammoniumdihydrogen- und Natriumdihydrogenphosphat, Kalium- und Ammoniumdihydrogenarsenat, sowie von Silber- und Ammoniumtrihydrogenperiodat wurden untersucht und die Studie erweitert durch einige Deuteriumanalogen von den genannten Salzen. Einige von den Substanzen wurden auch in der

ferroelektrischen Phase aufgenommen. Die Deutung der Spektren im Gebiet zwischen 3000 und 1500 cm^{-1} , dass mehrere OH Valenzbanden enthält, wurde unter der Annahme des Tunnelierens vom Proton zwischen zwei Minima der potentiellen Energie durchgeführt. Es wurde angenommen, dass die beiden Minima in der nichtferroelektrischen Phase symmetrisch sind und unsymmetrisch in der ferroelektrischen Phase. Im Appendix wird eine quantenmechanische Berechnung des Schwingungsproblems für den Fall der unsymmetrischen Potentialfunktion wiedergegeben. Eine gute Übereinstimmung zwischen den berechneten und den gefundenen OH Valenzbanden wurde festgestellt.

REFERENCES

- [1] NEWMANN, R., 1950, *J. chem. Phys.*, **18**, 669.
- [2] BACON, G. E., and PEASE, R. S., 1953, *Proc. roy. Soc. A*, **220**, 397 ; 1955, *Ibid.*, **230**, 359.
- [3] LAZAREV, A. N., 1957, *Izv. Akad. Nauk SSSR*, Ser. Fiz., **21**, 320.
- [4] WEST, J., 1930, *Z. Kristallogr.*, **74**, 306.
- [5] PEPINSKY, R., 1955, *Proc. Inst. Radio Engrs*, N.Y., **43**, 1772.
- [6] BAERTSCHI, P., 1945, *Helv. phys. acta*, **18**, 267.
- [7] GARRET, B. S., 1954, *Oak Ridge Natl. Lab. Rept.* No. 1745, 144.
- [8] HELMHOLTZ, L., 1937, *J. Amer. chem. Soc.*, **59**, 2036.
- [9] GRÄNICH, H., MEIER, W. M., and PETTER, W., 1954, *Helv. phys. acta*, **27**, 216.
- [10] ABOAV, D., GRÄNICH, H., and PETTER, W., 1955, *Helv. phys. acta*, **28**, 299.
- [11] MEGAW, H. D., 1957, *Ferroelectricity in Crystals* (London : Methuen), p. 46.
- [12] ÜBBELOHDE, A. R., and WOODWARD, I., 1943, *Proc. roy. Soc. A*, **179**, 1942.
- [13] LA LAU, C., 1947, *Thesis*, Amsterdam.
- [14] RUNDLE, R. E., and PARASOL, M., 1952, *J. chem. Phys.*, **20**, 1487.
- [15] MURPHY, G. M., WEINER, G., and OBERLEY, J. J., 1954, *J. chem. Phys.*, **22**, 1322.
- [16] NARAYANAN, P. S., 1951, *Proc. Indian Acad. Sci. A*, **33**, 240 ; 1948, *Ibid.*, **28**, 469.
- [17] LANDSBERG, G. S., and BARYSHANSKAYA, F. S., 1948, *Dokl. Akad. Nauk SSSR*, **61**, 1027.
- [18] STEKHANOV, A. J., 1957, *Izv. Akad. Nauk SSSR*, Ser. Fiz., **21**, 311.
- [19] BLINC, R., and HADŽI, D., 1958, *Hydrogen Bonding*, Pergamon Press (in preparation).
- [20] BADGER, R. M., 1934, *J. chem. Phys.*, **2**, 128.
- [21] LIPPINCOTT, E. R., and SCHROEDER, R., 1955, *J. chem. Phys.*, **23**, 1099.
- [22] HERZBERG, G., 1949, *Infra-red and Raman Spectra* (New York : D. Van Nostrand).
- [23] TA-YOU-WU, 1933, *Phys. Rev.*, **44**, 727.

Structure of the methyl radical

by T. COLE, H. O. PRITCHARD, N. R. DAVIDSON and
H. M. McCONNELL

Gates and Crellin Laboratories of Chemistry, California Institute of Technology,
Pasadena 4, California

(Received 26 August 1958)

Carbon-13 hyperfine splittings equal to 41 ± 3 gauss have been observed in the paramagnetic resonance of a mixture of C^{12}H_3 and C^{13}H_3 radicals produced by x-irradiation of CH_3I at 77°K . The observed splitting provides strong evidence that CH_3 is a planar molecule.

Several investigators [1, 2, 3] have observed the paramagnetic resonance of the methyl radical at low temperatures in various matrices. The observed proton hyperfine splittings do not depend significantly on the temperature, or matrix, and are in the range 25 ± 2 gauss. It is now rather well established on both theoretical and experimental grounds [4, 5, 6] that in planar π -electron radicals the in-plane or σ -proton hyperfine splittings a_N can be used to measure unpaired electron spin densities ρ_N on adjacent carbon atoms. These quantities are related through the equation [4],

$$a_N = Q\rho_N \quad (1)$$

where Q has the semiempirical value, -22.5 gauss. A planar CH_3 radical is a prototype of π -electron radicals. From (1) a splitting of 22.5 gauss for planar CH_3 is predicted. The close agreement between the predicted (22.5 gauss) and observed splittings (25 ± 2 gauss) does in fact support the idea that CH_3 is planar. Unfortunately it is difficult to say on simple theoretical grounds just how large the proton hyperfine splittings would be if CH_3 were *not* planar, and so the observed splittings are not proof positive of the planarity of CH_3 . On the other hand, as indicated below, one can make reasonable theoretical estimates of C^{13} hyperfine splittings in planar, and non-planar, C^{13}H_3 . For this reason we undertook an experiment on the spin resonance of C^{13}H_3 .

Methyl radicals were produced by x-irradiation of 0.1 c.c. of CH_3I (53% C^{13}) in the bottom of a 3 cm microwave cavity maintained at 77°K ; the dosage was approximately 10^6 r at 50 k.v. Figure 1 (*b*) shows the spectrum of the C^{12}H_3 - C^{13}H_3 radical mixture produced by this irradiation, and a comparison spectrum is given for C^{12}H_3 alone in figure 1 (*a*). Figure 2 shows how the composite spectrum in figure 1 (*b*) may be interpreted as the superposition of the C^{12}H_3 spectrum and the proposed C^{13}H_3 spectrum. The absolute value of the C^{13} hyperfine splitting constant, $|A|$, is equal to the separation of the outermost peaks in figure 1 (*b*) minus the separation of the outermost peaks in figure 1 (*a*), namely $116 - 75 = 41 \pm 3$ gauss. (Note that $|A| = 1.68 |a_H|$.) This observed splitting may be compared with several theoretical estimates given below.

Assumption (a).—Assume that methyl is planar and that the radicals undergo isotropic reorientations in the CH_3I matrix at 77°K with a frequency large compared

to the expected C^{13} anisotropic hyperfine interaction, i.e., 78 Mc (see below). If we assume equation (1) to be valid for C^{13} hyperfine splittings, then Q for planar C^{13} can be estimated from the known isotropic C^{13} splittings in naphthalene

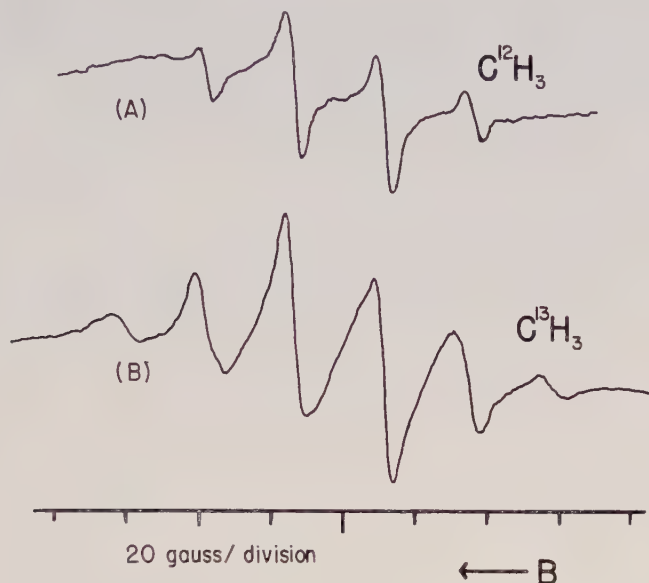


Figure 1. Paramagnetic resonance of $C^{12}H_3$ at $77^\circ K$ in CH_3I (a) and of a 47% $C^{12}H_3$ -53% $C^{13}H_3$ mixture at $77^\circ K$ in CH_3I (b).

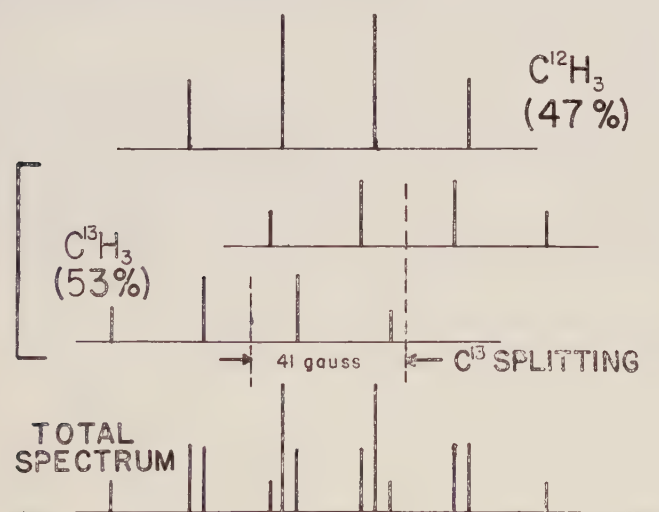


Figure 2. Theoretical analysis of observed spectrum of $C^{12}H_3$ - $C^{13}H_3$ mixture (bottom) in terms of the $C^{12}H_3$ and $C^{13}H_3$ spectra.

negative ion (7.1 gauss for an α -carbon atom [7]) and in triphenylmethyl (26 gauss for the central carbon atom [6]). The known α -proton hyperfine splitting in naphthalene negative ion (5.01 gauss [5]) and equation (1) gives a spin density

$\rho = 0.223$ for the α -carbon atom. (Simple molecular orbital theory gives $\rho = 0.18$.) Thus, the calculated Q for planar C^{13} is $(7.1/0.23) = 32$ gauss. The observed C^{13} splitting in triphenylmethyl is 26 gauss [6] and the spin density deduced from the hyperfine anisotropy is 0.68. This leads to a C^{13} Q of $(26/0.68) = 38$ gauss. (Simple valence bond theory yields a spin density on the central atom of 0.6 [6].) Both of these estimated C^{13} Q values, 32 and 38 gauss, are in good semiquantitative agreement with the observed 41 gauss splitting in $C^{13}H_3$.

Assumption (b).—Assume that methyl is planar but undergoes reorientation only about its symmetry axis in the CH_3I matrix, or not at all. In this case we have in addition to the 32–38 gauss C^{13} isotropic splitting estimated above, an additional anisotropic splitting of 28 gauss which has been calculated by Adam and Weissman [6] from the 2p atomic Hartree function given by Torrance [8]. These C^{13} splittings could have the same or opposite signs, leading to a total splitting (anisotropic + isotropic) of 60–66 gauss, or 4–10 gauss. These calculated C^{13} splittings for planar but nonrotating CH_3 are only in order of magnitude agreement with the observed splittings. Assumption (a) is also to be preferred over assumption (b) in that there is additional evidence for rotational freedom for $C^{13}H_3$ in CH_3I at 77°K.

The $C^{12}H_3$ spectrum in figure 1 (a) and the $C^{12}H_3$ – $C^{13}H_3$ spectra in figure 1 (b) were obtained with identical radiation dosages, sample volumes, and spectrometer sensitivity settings. They are of comparable intensity. An anisotropic coupling of 28 gauss would cause strongly asymmetric lines and would greatly lower peak intensities [9]. Since the lines appear rather symmetric after making correction for background (compare figure 1 (a) and figure 1 (b)), and are of full intensity, it is probable that the radicals are isotropically tumbling at a sufficiently high rate to average out the anisotropic coupling. It should be emphasized that either with or without the anisotropic terms, the predicted C^{13} splitting in the planar radical is of the order of magnitude of that observed.

Assumption (c).—Assume that CH_3 is non-planar, and consider a tetrahedral structure in which the odd electron occupies an sp^3 hybrid orbital. For this one predicts an isotropic splitting $1/4$ as large as that due to an odd electron in a 2s atomic orbital of carbon, i.e., $1/4 \times 1200 = 300$ gauss. (The 2s hyperfine splitting of 1200 gauss was obtained from the Hartree wave functions of Torrance [8].) This calculated isotropic splitting is so much larger than the observed splitting that we may conclude that the methyl radical does not have the sp^3 tetrahedral structure. In fact, the odd electron in CH_3 could be in a 2s orbital only (40/1200) or 0.03 of the time. Since any methyl structure deviating significantly from planarity would be expected to have significant 2s character in the odd electron distribution, this is very strong evidence that CH_3 is planar. A non-planar tunnelling radical would also show a large hyperfine interaction, and is excluded. On the other hand, the observed splitting is of just the order of magnitude that one would expect from a straight-forward extension of previous calculations of σ – π configuration interaction in planar π -electron radicals [4, 10, 11].

We are indebted to Professor J. D. Roberts for the $C^{13}H_3I$. This research has been supported by the O.O.R., O.N.R. and the N.S.F. One of us (H.M.McC.) is indebted for an Alfred P. Sloan Fellowship and another of us (H.O.P.) is the recipient of a Fulbright travel grant.

On a observé, pour le Carbone 13, un dédoublement hyperfin de 41 ± 3 Gauss dans la résonance paramagnétique d'un mélange de radicaux $C^{12}H_3$ et $C^{13}H_3$, obtenu en soumettant CH_3I au rayonnement x à 77 K. Le dédoublement observé suggère fortement que CH_3 est une molécule plane.

Mit Hilfe paramagnetischer Resonanz wurden für eine Mischung von $C^{12}H_3$ - und $C^{13}H_3$ -Radikalen, die durch Röntgenbestrahlung von CH_3I bei 77°K erzeugt wurden, vom Kohlenstoffisotop C^{13} herrührende Hyperfein-Aufspaltungen von 41 ± 3 Gauss beobachtet. Diese Aufspaltung spricht deutlich dafür, dass die Atome in CH_3 in einer Ebene liegen.

REFERENCES

- [1] LUCK, C. F., and GORDY, W., 1956, *J. Amer. chem. Soc.*, **78**, 3240.
GORDY, W., and McCORMICK, C. G., 1956, *J. Amer. chem. Soc.*, **78**, 3243.
- [2] SMALLER, B., and MATHESON, M. S., 1958, *J. chem. Phys.*, **28**, 1169.
- [3] JEN, C. K., FONER, S. N., COCHRAN, E. L., and BOWERS, V. A., *Phys. Rev.*, to be published.
- [4] McCONNELL, H. M., 1956, *J. chem. Phys.*, **24**, 632; 1956, *Ibid.*, **24**, 764; McCONNELL, H. M., and CHESNUT, D. B., 1957, *J. chem. Phys.*, **27**, 984; 1958, *Ibid.*, **28**, 107; McCONNELL, H. M., 1957, *Proc. Nat. acad. Sci. U.S.*, **43**, 721; 1958, *J. chem. Phys.*, **28**, 51; 1958, *Ibid.*, **28**, 1188; 1958, *Ibid.*, **29**, 244.
- [5] WEISSMAN, S. I., 1956, *J. chem. Phys.*, **25**, 890; WEISSMAN, S. I., TUTTLE, T., and DE BOER, E., 1957, *J. phys. Chem.*, **61**, 28; DE BOER, E., 1956, *J. chem. Phys.*, **25**, 190.
- [6] ADAM, F. C., and WEISSMAN, S. I., 1958, *J. Amer. chem. Soc.*, **80**, 2057.
- [7] TUTTLE, T. R., WARD, R., and WEISSMAN, S. I., 1956, *J. chem. Phys.*, **25**, 189.
- [8] TORRANCE, C. C., 1934, *Phys. Rev.*, **46**, 388.
- [9] A good example of a precisely analogous effect can be seen in figure 1 in the work of COLE, T., and McCONNELL, H. M., "Zero Field Splittings in Atomic Nitrogen at 4·2°K," *J. chem. Phys.*, in the press.
- [10] BERSOHN, R., 1956, *J. chem. Phys.*, **24**, 1006.
- [11] JARRETT, H. S., 1956, *J. chem. Phys.*, **25**, 1289.

RESEARCH NOTES

Ligand field bands of four-coordinated paramagnetic nickel (II) complexes

by CHR. KLIXBULL JØRGENSEN

Department of Theoretical Chemistry, University of Cambridge†

[Received 24 May 1958]

Although octahedrally six-coordinated nickel (II) complexes have been studied extensively, and their weak, Laporte-forbidden absorption bands interpreted by ligand field theory [1-5], it has generally been supposed that tetrahedrally coordinated complexes of paramagnetic nickel (II) must be exceedingly rare. However, Venanzi [6] has demonstrated that the complexes NiR_2X_2 with $\text{R} = \text{P}(\text{C}_6\text{H}_5)_3$ and $\text{X} = \text{NO}_3^-$, Cl^- , Br^- , I^- are paramagnetic, and are four-coordinated in the crystalline state. Recently, moreover, Boston and Smith [7] and Gruen [8] have reported the absorption spectra of Ni(II) in salt melts, containing KCl or other chlorides. The present note will draw attention to the fact that the spectrum of one of the species occurring in these salt melts can be interpreted by assuming the first coordination sphere of Ni (II) to contain four tetrahedrally arranged chloride ions. The transition ${}^3\text{A}_2(\text{F}) \rightarrow {}^3\text{T}_1(\text{P})$ (or in Bethe's notation, ${}^3\Gamma_2(\text{F}) \rightarrow {}^3\Gamma_4(\text{P})$) occurs [1-5] in $\text{Ni}(\text{H}_2\text{O})_6^{++}$ at $395 \text{ m}\mu$ ($= 25\,300 \text{ cm}^{-1}$). In the six-coordinated Perovskite-type chlorides MNiCl_3 , this band occurs in the reflection spectrum [9] at $21\,300$ – $21\,600 \text{ cm}^{-1}$. This shift towards lower wave numbers is partly caused by decreased values of the ligand field parameter Δ (8500 cm^{-1} in the hexa-aquo ion and about 7100 cm^{-1} in the chlorides) and partly by the decreased interelectronic repulsion parameters [5, 10]. In analogy to the bands at $23\,350 \text{ cm}^{-1}$ of Ni(II) in concentrated sulphuric acid [3] and at $22\,700 \text{ cm}^{-1}$ in molten potassium nitrate [8], the band near $500 \text{ m}\mu$ observed in molten chlorides [7] can be ascribed to an octahedrally coordinated ion NiCl_6^{-4} .

When the contribution of this species to the light absorption is subtracted, a spectrum remains, which is rather constant in the range of temperature studied by Boston and Smith [7]. This spectrum consists of the following features:—

III a shoulder near $570 \text{ m}\mu$ ($= 17\,500 \text{ cm}^{-1}$)

IV a maximum at $625 \text{ m}\mu$ ($= 16\,000 \text{ cm}^{-1}$)

V a narrow band at $695 \text{ m}\mu$ ($= 14\,400 \text{ cm}^{-1}$).

It is remarkable that no absorption band of this species is observed in the range 350 – $480 \text{ m}\mu$, indicating a much smaller Δ than usually encountered. The spectrum resembles closely that [11] of CoCl_4^{-} , which has [1] $\Delta = -3750 \text{ cm}^{-1}$ and in which the term distances of gaseous Co^{++} have been reduced by a factor $\beta \sim 0.72$. It has generally been verified [12] that values of Δ for tetrahedral complexes are about $-4/9$ times those of the corresponding octahedral complexes, as predicted by electrostatic perturbation theory [13]. Thus, it would be expected

† Visitor May, 1958 from Chemistry Department A, Technical University of Denmark, Copenhagen,

that NiCl_4^{--} would have $\Delta \sim 3200 \text{ cm}^{-1}$ and the distance $^3\text{F} \rightarrow ^3\text{P}$ decreased from $16\,000 \text{ cm}^{-1}$ in gaseous Ni^{++} (when corrected for spin-orbit coupling [5]) to $11\,500 \text{ cm}^{-1}$ (the same value as found [9] for MnCl_3). With these assumptions the predicted levels are:—

$^3\Gamma_4(\text{F})$	0 cm^{-1}
$^3\Gamma_5(\text{F})$	2600
$^3\Gamma_2(\text{F})$	5800
$^1\Gamma_5(\text{D})$	10300
$^1\Gamma_3(\text{D})$	11000
$^3\Gamma_4(\text{P})$	13600

with ^1G levels distributed in the range $16\text{--}17\,000 \text{ cm}^{-1}$. It seems most reasonable to identify the bands III and IV as transitions to $^3\Gamma_4(\text{P})$. The splitting of this level is too large to be accounted for solely by first-order (L, S) coupling, but is rather connected with a loss of T_d symmetry due to the Jahn–Teller distortion. This effect, which is absent in CoCl_4^{--} , could account for the deviation of about 3000 cm^{-1} between the observed and calculated wave numbers. The narrow band V is probably the transition to one of the singlet levels $^1\Gamma_5(\text{D})$ or $^1\Gamma_3(\text{D})$, which has borrowed intensity from the adjacent spin-allowed band [3].

The position of the principal band $^3\Gamma_4(\text{F}) \rightarrow ^3\Gamma_4(\text{P})$ does not vary much in the available tetrahedral nickel (II) complexes, the wave number being about $(^3\text{P} \rightarrow ^3\text{F}) + 0.8\Delta$. Thus, Venanzi's complex [6] with $\text{X} = \text{Cl}^-$ is blue and with $\text{X} = \text{Br}^-$ dark green. The same colours are observed [14] in the hot, violet-blue chloride and dark green bromide melts. Asmussen and Bostrup [15] report bands of $\text{Ni}(\text{P}(\text{C}_2\text{H}_5)_3)_2(\text{NO}_3)_2$ at 1060 and $660 \text{ m}\mu$.

An analogous situation occurs in tetrahedral cobalt (II) complexes, where the known cases [16] with four I^- , Br^- , Cl^- , SCN^- and OH^- ligands have the same type of spectrum. The conspicuous fine structure of the principal band $^4\Gamma_2(\text{F}) \rightarrow ^4\Gamma_4(\text{P})$ is probably caused by intermixing with doublet levels such as $^2\Gamma_3$ or $^2\Gamma_4$ and not by first-order (L, S) coupling alone. It has not been possible to find weak bands at lower wave numbers than the principal band, except in the case of $\text{Co}(\text{P}(\text{C}_2\text{H}_5)_3)_2\text{Cl}_2$ (to be discussed later with Professor K. A. Jensen, University of Copenhagen) where a narrow band is observed at $750 \text{ m}\mu$. Here, the ratio [2] between Δ and the term distances is larger than in the other $\text{Co}(\text{II})$ cases, where accidentally, this ratio is nearly constant.

Finally, it is interesting to note that NiCl_4^{--} has a molar extinction coefficient ϵ of only 61 in the highest ligand field band, while the tetrahedral cobalt (II) complexes are known to have ϵ between 500 and 2000. This demonstrates that the absence of a centre of inversion in T_d does not necessarily produce high intensities; it is only when there are Laporte-allowed contributions to the transition probability matrix elements that the intensities increase above those produced by vibronic interactions in systems with a centre of inversion [2], e.g. O_h . Thus, the octahedral species [7] has $\epsilon = 60$ at $500 \text{ m}\mu$ compared to $\epsilon = 5$ for the corresponding band of $\text{Ni}(\text{H}_2\text{O})_6^{++}$. The electron transfer spectra are not very different in NiCl_4^{--} and CoCl_4^{--} : the former ion has a band with $\epsilon = 3600$ at $260 \text{ m}\mu$ (though one cannot exclude the hypothesis that it is mainly caused by the octahedral form) while CoCl_4^{--} has [17] $\epsilon \sim 2000$ at $235 \text{ m}\mu$. Undoubtedly, the cobalt (II) complex must have much stronger bands at higher wave numbers to explain the unusually high intensity of the visible, spin-allowed ligand field band.

Weyl [18] studied equilibria between yellow NiO_6 groups (with a band near $450 \text{ m}\mu$) and purple NiO_4 (with maxima at 650 and $560 \text{ m}\mu$ and perhaps at $500 \text{ m}\mu$) in glasses with alkali silicates. The latter ion can be assumed to have a distorted tetrahedral structure, as NiCl_4^{--} discussed here. Dunitz and Orgel [19] have studied the values of Δ for this type of oxide glass.

I wish to thank Dr. L. E. Orgel for many valuable and interesting discussions. I am also grateful to the British Council for the award of a Bursary.

REFERENCES

- [1] ORGEL, L. E., 1955, *J. chem. Phys.*, **23**, 1004.
- [2] TANABE, Y., and SUGANO, S., 1954, *J. Phys. Soc. Japan*, **9**, 766.
- [3] JØRGENSEN, C. K., 1955, *Acta chem. Scand.*, **9**, 1362.
- [4] JØRGENSEN, C. K., 1956, *Acta chem. Scand.*, **10**, 887.
- [5] BOSTRUP, O., and JØRGENSEN, C. K., 1957, *Acta chem. Scand.*, **11**, 1223.
- [6] VENANZI, L. M., 1958, *J. chem. Soc.*, 719.
- [7] BOSTON, C. R., and SMITH, G. P., 1958, *J. phys. Chem.*, **62**, 409.
- [8] GRUEN, D. M., 1957, *J. Inorg. Nucl. Chem.*, **4**, 74.
- [9] ASMUSSEN, R. W., and BOSTRUP, O., 1957, *Acta chem. Scand.*, **11**, 745.
- [10] JØRGENSEN, C. K., 1957, *Energy Levels of Complexes and Gaseous Ions*. Gjellerups Forlag, Copenhagen.
- [11] BALLHAUSEN, C. J., and JØRGENSEN, C. K., 1955, *Acta chem. Scand.*, **9**, 397.
- [12] JØRGENSEN, C. K., 1957, *Acta chem. Scand.*, **11**, 53.
- [13] BALLHAUSEN, C. J., 1954, *Kgl. Dansk Vidensk. Selskab, Mat. fys. Medd.*, **29**, No. 4.
- [14] HORNYAK, F. M., 1957, *J. Amer. chem. Soc.*, **79**, 5435.
- [15] ASMUSSEN, R. W. A., and BOSTRUP, O., 1957, *Acta chem. Scand.*, **11**, 1097.
- [16] SHIMURA, Y., and TSUCHIDA, R., 1957, *Bull. chem. Soc., Japan.*, **30**, 502.
- [17] KATZIN, L. I., 1952, *J. chem. Phys.*, **20**, 1165.
- [18] WEYL, W. A., and THÜMEN, E., 1933, *Glastech. Ber.*, **11**, 113, and *Quelques Problèmes de Chimie Minérale*, X Solvay Conseil de Chimie, Bruxelles, 1956, p. 420.
- [19] DUNITZ, J., and ORGEL, L. E., 1957, *J. Phys. chem. Solids*, **3**, 318.

Planarity of 1 : 2 : 4 : 5-tetrabromobenzene molecule

by G. GAFNER and F. H. HERBSTEIN

National Physical Research Laboratory,
Council for Scientific and Industrial Research, Pretoria, South Africa

(Received 25 July 1958)

We have recently completed a three-dimensional analysis of the crystal structure of that phase of 1 : 2 : 4 : 5-tetrabromobenzene which is stable at room temperature. The crystallographic constants of this phase are : $a = 10.323 \text{ \AA}$, $b = 10.705 \text{ \AA}$, $c = 4.018 \text{ \AA}$, $\beta = 102^\circ 22'$, $Z = 2$. Space group $P2_1/a$; molecular symmetry 1.

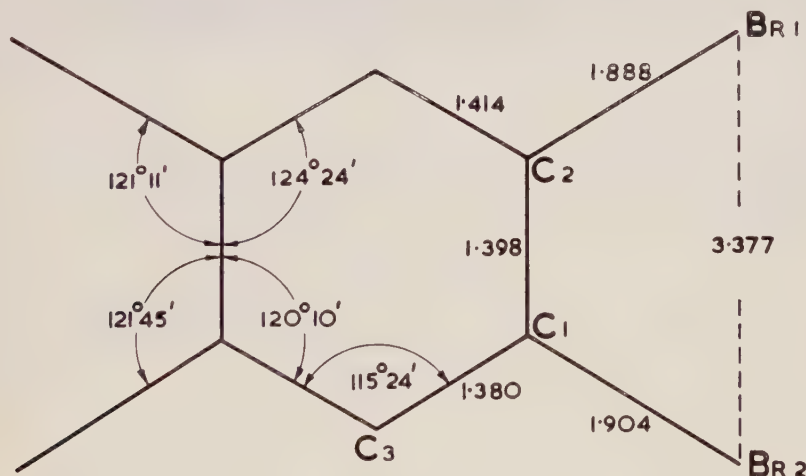
The initial coordinates of the bromine atoms were found by Patterson methods. A three-dimensional least-squares refinement of the carbon and bromine parameters, including separate isotropic temperature factors for each atom,

was then carried out on the IBM 704 computer, using the programme NYXR2 developed by Dr. D. Sayre. The final coordinates of the atoms and their perpendicular distances from the molecular plane are given in the Table. Within the limits of error the molecule is planar. The mean standard deviations of the atomic positions are $\sigma_C(x) = 0.026 \text{ \AA}$ and $\sigma_{Br}(x) = 0.0028 \text{ \AA}$. The molecular dimensions are given in the figure.

Atom	Fractional coordinates			Normal distance from molecular plane \AA
	<i>u</i>	<i>v</i>	<i>w</i>	
C 1	0.1229	0.0343	0.1680	-0.030
C 2	0.0376	0.1243	-0.0113	0.001
C 3	0.0900	-0.0897	0.1950	-0.0004
Br 1	0.0891	0.2930	-0.0272	-0.002
Br 2	0.2951	0.0784	0.4246	0.004

Atomic coordinates and normal distances from best molecular plane.

Hexachlorobenzene has also recently been shown to be planar in the solid state [1]. Hexachlorobenzene and hexabromobenzene are isomorphous [2], as are the room-temperature phases of 1:2:4:5-tetrachlorobenzene [3] and 1:2:4:5-tetrabromobenzene. Thus we may conclude that polychlorinated and polybrominated benzenes containing halogens ortho to one another are planar



Molecular dimensions of 1:2:4:5-tetrabromobenzene. The standard deviations of the interatomic distances and bond angles are: $\sigma(C-C) = 0.037 \text{ \AA}$; $\sigma(C\hat{C}C) = 3^\circ 23'$; $\sigma(C-Br) = 0.026 \text{ \AA}$; $\sigma(C\hat{C}Br) = 1^\circ 38'$; $\sigma(Br \dots Br) = 0.004 \text{ \AA}$.

despite the close approach distances between the ortho halogen atoms. This conclusion is contrary to assumptions made in recent discussions of the nuclear quadrupole resonance frequencies in polyhalogenated benzenes [4, 5], and to the results deduced from sector electron-diffraction measurements on various polyhalogenated benzenes in the vapour phase [6, 7]. Details of this work will be published later.

We are grateful to the South African Council for Scientific and Industrial Research for permission to publish this note, and to Dr. J. N. van Niekerk for his interest in this work.

REFERENCES

- [1] TULINSKY, A., and WHITE, J. G., 1958, *Acta Cryst.*, **11**, 7.
- [2] PLUMMER, W. G., 1925, *Phil. Mag.*, **50**, 1214.
- [3] Unpublished work in this laboratory.
- [4] DUCHESNE, J., and MONFILS, A., 1954, *J. chem. Phys.*, **22**, 562, 1275.
- [5] BRAY, P. J., BARNES, R. G., and BERSOHN, R., 1956, *J. chem. Phys.*, **25**, 813.
- [6] BASTIANSEN, O., and HASSEL, O., 1947, *Acta chem. Scand.*, **1**, 489.
- [7] HARNIK, E., HERBSTEIN, F. H., SCHMIDT, G. M. J., and HIRSHFELD, F. L., 1954, *J. chem. Soc.*, p. 3288.

Dipole interactions in fluids and fluid mixtures

by J. S. ROWLINSON

Department of Chemistry, The University, Manchester

(Received 31 July 1958)

The energy of interaction of two dipoles, μ_1 and μ_2 , at a separation r may be written

$$u(r, \omega) = \frac{\mu_1 \mu_2}{r^3} f(\omega)$$

where ω denotes the three angles needed to specify the mutual orientation, and where $f(\omega)$ lies between -2 and $+2$. The unweighted average of $f(\omega)$ is zero, and so

$$\int u(r, \omega) d\omega = 0.$$

The effect of weak dipoles on the thermodynamic properties of an assembly of molecules may be calculated by taking an average value of u over all angles, and using this average in the phase integral for a central potential. Such a preliminary averaging is not the most straightforward way of obtaining the effect of the dipole-dipole energy, but Rushbrooke [1] has shown that it is justified if the average is chosen to be an average free-energy given by

$$\overline{u(r, T)} = -kT \ln \left[\frac{\int \exp [-u(r, \omega)/kT] d\omega}{\int d\omega} \right].$$

This form of average was used by Cook and Rowlinson [2]. The more familiar canonical average

$$\overline{u(r, T)} = \frac{\int u(r, \omega) \exp [-u(r, \omega)/kT] d\omega}{\int \exp [-u(r, \omega)/kT] d\omega}$$

may not be used. To the order of the first non-vanishing terms of the exponential expansions, $\overline{u(r, T)}$ is twice $\overline{u(r, T)}$. The canonical average has, however,

been used recently by Balescu [3] and by Prigogine [4], and has led them to the conclusion that the excess free-energy and enthalpy of a mixture of chloroform and carbon tetrachloride are due almost entirely to the dipole-dipole interaction between the chloroform molecules. The maximum excess free energy at 25°C is 26 cal mole⁻¹. The average $\overline{u(r, T)}$ predicts a maximum of 17 cal mole⁻¹, but the correct average $\overline{u(r, T)}$ predicts a maximum of only 8.5 cal mole⁻¹. It is clear, therefore, that most of the excess free energy of this system is not accounted for by the dipole energy. Mixtures of carbon tetrachloride with non-polar liquids such as benzene and cyclohexane have excess free energies of about 20 cal mole⁻¹, and such 'non-polar' contributions are to be expected also in the system chloroform + carbon tetrachloride.

REFERENCES

- [1] RUSHBROOKE, G. S., 1940, *Trans. Faraday Soc.*, **36**, 1055.
- [2] COOK, D., and ROWLINSON, J. S., 1953, *Proc. roy. Soc. A*, **219**, 405.
- [3] BALESCU, R., 1955, *Bull. Acad. Belg. Cl. Sci.*, **41**, 1242.
- [4] PRIGOGINE, I., 1957, *Molecular Theory of Solutions* (Amsterdam : North-Holland), Chap. 14.

INDEX OF AUTHORS (WITH THE TITLES OF PAPERS)

- BALK, P., DE BRUIJN, S., and HOIJTINK, G. J.: Electronic spectra of alternant hydrocarbon di-negative ions, 151
- BARNETT, M. P., BIRSS, F. W., and COULSON, C. A.: Electron-electron separation in molecular hydrogen, 44
- BIRSS, F. W., *see* BARNETT, M. P.
- BLINC, R., and HADŽI, D.: The infra-red spectra of some ferroelectric compounds with short hydrogen bonds, 391
- BRIGMAN, G. H., *see* HURST, R. P.
- BROWN, R. D.: Evaluation of coulomb repulsion integrals from spectroscopic data, 304
- DE BRUIJN, S., *see* BALK, P.
- BUCK, H. M., LUPINSKI, J. H., and OOSTERHOFF, L. J.: Paramagnetism in molecular compounds, 196
- BYERS BROWN, W.: Constant pressure ensembles in statistical mechanics, 68
- CARRÁ, S., *see* SIMONETTA, M.
- COLE, T., PRITCHARD, H. O., DAVIDSON, N. R., and MCCONNELL, H. M.: Structure of the methyl radical, 406
- COLPA, J. P., and KETELAAR, J. A. A.: The pressure-induced rotational absorption spectrum of hydrogen: I, 14
- COLPA, J. P., and KETELAAR, J. A. A.: The pressure-induced rotational absorption spectrum of hydrogen: II, 343
- COULSON, C. A., *see* BARNETT, M. P.
- DALLINGA, G., MACKOR, E. L., and VERRIJN STUART, A. A.: The absorption spectra of aromatic carbonium ions in HF solution, 123
- DAMMERS-DE KLERK, A.: Concentration quenching in fluorescent acene solutions, 141
- DAVIDSON, N. R., *see* COLE, T.
- FAVINI, G., *see* SIMONETTA, M.
- GAFNER, G., and HERBSTEIN, F. H.: Planarity of 1:2-4:5-tetrabromobenzene molecule, 412
- GRAY, J. D., *see* HURST, R. P.
- HADŽI, D., *see* BLINC, R.
- HAMEKA, H. F.: On the nuclear magnetic shielding in the hydrogen molecule, 203
- HAMEKA, H. F., and LIQUORI, A. M.: Some considerations on the dipole moments of azines, 9
- HAMEKA, H. F., and OOSTERHOFF, L. J.: The probability of triplet-singlet transitions in aromatic hydrocarbons and ketones, 358
- HASSEL, O.: Structure of electron-transfer and related molecular complexes in the solid state, 241
- HERBSTEIN, F. H., *see* GAFNER, G.
- HIJMANS, J.: Application of Brønsted's principle of congruence to n-alkane mixtures, 307
- HOFFMAN, R. A.: Long range spin-spin interactions in high resolution nuclear magnetic resonance and the concept of hyperconjugation, 326
- HOIJTINK, G. J.: Electron spin densities in alternant hydrocarbon mono-negative and mono-positive ions and in odd alternant hydrocarbon radicals, 157
- HOIJTINK, G. J., *see* BALK, P.

- HURST, R. P., GRAY, J. D., BRIGMAN, G. H., and MATSEN, F. A.: Open shell calculations for the two- and three-electron ions, 189
- JØRGENSEN, C. K.: Ligand field bands of four-coordinated paramagnetic nickel (II) complexes, 410
- KETELAAR, J. A. A., *see* COLPA, J. P.
- LIQUORI, A. M., *see* HAMEKA, H. F.
- LONGUET-HIGGINS, H. C.: One-dimensional multicomponent mixtures, 83
- LONGUET-HIGGINS, H. C., and VALLEAU, J. P.: Transport coefficients of dense fluids of molecules interacting according to a square well potential, 284
- LONGUET-HIGGINS, H. C., *see* POPLE, J. A.
- LUPINSKI, J. H., *see* BUCK, H. M.
- McCONNELL, H. M., *see* COLE, T.
- MACKOR, E. L., *see* DALLINGA, G., *also* MACLEAN, C.
- McLACHLAN, A. D.: Hyperconjugation in the electron resonance spectra of free radicals, 233
- MACLEAN, C., VAN DER WAALS, J. H., and MACKOR, E. L.: Proton magnetic resonance of aromatic carbonium ions. I. Structure of the conjugate acid, 247
- McWEENY, R.: Ring currents and proton magnetic resonance in aromatic molecules, 311
- MARSHALL, T. W., and POPLE, J. A.: Nuclear magnetic shielding of a hydrogen atom in an electric field, 199
- MATSEN, F. A., *see* HURST, R. P.
- MILLS, IAN M.: Vibrational intensities in methane, 107
- MILLS, IAN M.: Wave functions for the methane molecule, 99
- MÜNSTER, A., and SAGEL, K.: Kritische Opaleszenz fester Lösungen, 23
- MURRELL, J. N.: The π -electron spectra of some benzene N-heterocyclics, 384
- NEDERBRAGT, G. W., and PELLE, J.: Dielectric properties of iodine in aromatic solvents at 9000 Mc/sec, 97
- OOSTERHOFF, L. J., *see* BUCK, H. M., *also* HAMEKA, H. F.
- ORGEL, L. E.: Nuclear magnetic resonance spectra of compounds of the B-subgroup metals, 322
- PELLE, J., *see* NEDERBRAGT, G. W.
- PISTORIUS, C. W. F. T.: A normal coordinate treatment of the plane symmetrical XY_4 molecule, 295
- PLATTEUW, J. C., and VAN DER WAALS, J. H.: Thermodynamic properties of gas hydrates, 91
- POPLE, J. A.: Molecular orbital theory of aromatic ring currents, 175
- POPLE, J. A.: Nuclear magnetic resonance and rotational isomerism in substituted ethanes, 1
- POPLE, J. A.: Nuclear spin coupling by electron orbital polarization, 216
- POPLE, J. A.: The effect of quadrupole relaxation on nuclear magnetic resonance multiplets, 168
- POPLE, J. A., and LONGUET-HIGGINS, H. C.: Theory of the Renner effect in the NH_2 radical, 372
- POPLE, J. A., *see* MARSHALL, T. W.
- PRIGOGINE, I., and TODA, M.: On irreversible processes in quantum mechanics, 49
- PRITCHARD, H. O., *see* COLE, T.
- RICHARDS, R. E., and SCHAEFER, T.: High resolution hydrogen resonance spectra of trisubstituted benzenes, 331

- ROWLINSON, J. S.: Dipole interactions in fluids and fluid mixtures, 414
- RUSHBROOKE, G. S., and WOOD, P. J.: On the Curie points and high temperature susceptibilities of Heisenberg model ferromagnetics, 257
- SACK, R. A.: A contribution to the theory of the exchange narrowing of spectral lines, 163
- SAGEL, K., *see* MÜNSTER, A.
- SCHAEFER, T., *see* RICHARDS, R. E.
- SIMONETTA, M., FAVINI, G., and CARRÁ, S.: A molecular orbital treatment of the vinyl chloride molecule, 181
- STEPHEN, M. J.: Rotary dispersion in hydrated cobaltous salts, 301
- STEPHEN, M. J.: The effect of molecular interaction on magnetic shielding constants, 223
- VALLEAU, J. P.: Transport of energy and momentum in a dense fluid of rough spheres, 63
- VALLEAU, J. P., *see* LONGUET-HIGGINS, H. C.
- VERRIJN STUART, A. A., *see* DALLINGA, G.
- VAN DER WAALS, J. H., *see* MACLEAN, C.
- VAN DER WAALS, J. H., *see* PLATTEUW, J. C.
- WOOD, P. J., *see* RUSHBROOKE, G. S.

CORRIGENDA

Page 313, Equation (3.3). Insert $\sum_{k,l}$ after $\sum_{i,j}$

Page 317, Equation (5.1). Insert asterisks above ω_{61} and $\omega_{10,5}$

Page 335, First line after equation (4.2), for J read J'